This Document Contains Page/s
Reproduced From
Best Available Copy

DEPARTMENT OF THE ARMY TECHNICAL MANUAL

DEPARTMENT OF THE NAVY PUBLICATION

DEPARTMENT OF THE AIR FORCE MANUAL

AD A951601

STRUCTURES TO
THE EFFECTS OF AC
EXPLOSION

DTIC FILE COPY

This document contains
blank pages that were
not filmed

DEPARTMENTS OF THE ARMY, THE NAVY, AN

JUNE 1969

This Document Contains Page/s
Reproduced From
Best Available Copy

TECHNICAL MANUAL

'BLICATION

E MANUAL

TM 5-1300

NAVFAC P-397

AFM 88-22

This document contains
blank pages that were
not filmed

'URES TO RESIST
;TS OF ACCIDENTAL
XPLOSIONS

DTIC
ELECTE
FEB 2 1982
H

DISTRIBUTION STATEMENT A
Approved for public release;
Distribution Unlimited

F THE ARMY, THE NAVY, AND THE AIR FORCE

JUNE 1969

82 02 01 003

This Document Contains Page/s
Reproduced From
Best Available Copy

FOREWORD

This manual is the result of a sustained long-term program of engineering analysis which was confirmed by an independent series of destructive proof tests.

The testing upon which this material is based involved both full-scale and model structures and component structural elements. Full-scale tests employed explosive charge weights as large a 7,500 pounds while model tests utilized various charge sizes representing up to 10,000 pounds at full scale.

The engineering effort presented herein represents the coordinated activity of many governmental agencies and private industrial and engineering organizations. Many individuals contributed extensively to the development of the manual and their efforts are appreciated.

The material in this manual is intended for the advice of individuals and organizations concerned with the design of protective construction to limit the effects of accidental explosions. It represents a significant advance in this design and provides a basis for greatly increased protection against propagation of explosions, damage to facilities, and loss of life.

Nevertheless, in a work of this magnitude it is expected that there may be points which require further verification or modification as a result of future tests and experience. Recommendations for such changes or comments with regard to the usefulness of the manual may be submitted through appropriate military channels to:

Chairman
Armed Services Explosives Safety Board
Nassif Building
Washington, D.C. 20315

For sale by the Superintendent of Documents, U.S. Government Printing Office
Washington, D.C. 20402 - Price $5.25.

This document contains
blank pages that were
not filmed

This Document Contains Page/s
Reproduced From
Best Available Copy

TECHNICAL MANUAL
No. 5-1300
NAVY PUBLICATION
NAVFAC P-397
AIR FORCE MANUAL
AFM 88-22

DEPARTMENT OF THE ARMY
THE NAVY, AND THE AIR FORCE
WASHINGTON, D.C., *15 June 1969*

STRUCTURES TO RESIST THE EFFECTS OF ACCIDENTAL EXPLOSIONS

			Paragraph	Page
CHAPTER	1.	INTRODUCTION		
		Purpose and objective	1-1	1-1
		Background	1-2	1-1
		Scope of manual	1-3	1-1
		Format of manual	1-4	1-1
		Safety factor and accuracy	1-5	1-1
CHAPTER	2.	EXPLOSION PROTECTIVE SYSTEM		
		System components	2-1	2-1
		Donor system	2-2	2-1
		Receiver system	2-3	2-1
		Protective structures	2-4	2-1
CHAPTER	3.	BASIS FOR STRUCTURAL DESIGN		
Section	I.	Structural Response		
		General	3-1	3-1
		Pressure design ranges	3-2	3-1
		Analyzing blast environment	3-3	3-1
	II.	Protection Categories		
		General	3-4	3-2
		Shelters	3-5	3-2
		Barriers	3-6	3-2
	III.	Receiver Sensitivity		
		Human tolerance	3-7	3-2
		Equipment	3-8	3-4
		Explosives	3-9	3-4
	IV.	Structural Behavior		
		Modes of structural behavior	3-10	3-5
		Structural behavior of reinforced concrete	3-11	3-5
CHAPTER	4.	EFFECTS OF EXPLOSIONS		
Section	I.	Introduction		
		Effects of explosive output	4-1	4-1
		Scope	4-2	4-1
	II.	Blast Pressure Output		
		Blast phenomena	4-3	4-1
		Blast-loading categories	4-4	4-1
		Blast-wave phenomena	4-5	4-2
	III.	Unconfined Explosions		
		Free-air burst	4-6	4-3
		Air burst	4-7	4-3
		Surface burst	4-8	4-7
	IV.	Partially Confined Explosions		
		Effects of confinement	4-9	4-9
		Fully vented explosions	4-10	4-9
		Partially vented explosions	4-11	4-59
	V.	External Blast Loads on Structures		
		General	4-12	4-60
		Forces acting on structures	4-13	4-60
		Above-ground rectangular structures	4-14	4-60
	VI.	Pressure Increase Within a Structure		
		General	4-15	4-64
		Method of calculation	4-16	4-65
	VII.	Multiple Explosions		
		General	4-17	4-65
		High-pressure range	4-18	4-65
		Intermediate- and low-pressure ranges	4-19	4-65

Accession For
NTIS GRA&I
DTIC TAB
Justification
By
Distribution/
Availability Codes
Dist | Avail and/or Special
A
UNANNOUNCED
DTIC COPY INSPECTED 2

OF THE ARMY

THE AIR FORCE

C., *15 June 1969*

APPENDI
CHAPTER
Section

SIONS

Paragraph	Page
1-1	1-1
1-2	1-1
1-3	1-1
1-4	1-1
1-5	1-1
2-1	2-1
2-2	2-1
2-3	2-1
2-4	2-1
3-1	3-1
3-2	3-1
3-3	3-1
3-4	3-2
3-5	3-2
3-6	3-2
3-7	3-2
3-8	3-4
3-9	3-4
3-10	3-5
3-11	3-5
4-1	4-1
4-2	4-1
4-3	4-1
4-4	4-1
4-5	4-2
4-6	4-3
4-7	4-3
4-8	4-7
4-9	4-9
4-10	4-9
4-11	4-59
4-12	4-60
4-13	4-60
4-14	4-60
4-15	4-64
4-16	4-65
4-17	4-65
4-18	4-65
4-19	4-65

APPENDIX
CHAPTER
Section

		Paragraph	Page
VIII.	Primary Fragments		
	General	4-20	4-66
	Initial fragment velocities (explosives with cylindrical containers)	4-21	4-66
	Number and weight of fragments (explosives with cylindrical containers)	4-22	4-66
	Initial fragment velocities (non-cylindrical containers)	4-23	4-67
	Number and weight of fragments (noncylindrical containers)	4-24	4-67
	Variation of fragment velocity with distance	4-25	4-67
APPENDIX 4A.	Explosive Effects—Illustrative Examples		4-69
CHAPTER 5.	STRUCTURAL BEHAVIOR OF REINFORCED CONCRETE		
Section I.	Ultimate Strength		
	General	5-1	5-1
	Ultimate static moment capacity	5-2	5-1
	Ultimate static shear capacity	5-3	5-2
	Ultimate static bond capacity and anchorage	5-4	5-3
	Dynamic strengths	5-5	5-3
	Allowable stresses	5-6	5-4
II.	Static Properties		
	Modulus of elasticity	5-7	5-5
	Moment of inertia	5-8	5-5
III.	Resistance-Deflection Functions		
	General	5-9	5-6
	Ultimate resistance	5-10	5-6
	Post-ultimate resistance	5-11	5-12
	Partial failure and ultimate deflections	5-12	5-13
	Elasto-plastic resistance	5-13	5-14
	Elasto-plastic stiffnesses and deflections	5-14	5-14
IV.	Resistance-Deflection Functions for Design		
	General	5-15	5-19
	Limited deflections	5-16	5-19
	Large deflections	5-17	5-20
V.	Ultimate Shears and Shear Stresses		
	General	5-18	5-20
	One-way elements	5-19	5-21
	Two-way elements	5-20	5-21
APPENDIX 5A.	Structural Behavior of Reinforced Concrete Illustrative Examples		5-25
CHAPTER 6.	STRUCTURAL ANALYSIS AND DESIGN FOR DUCTILE MODE RESPONSE		
Section I.	Design Parameters and General Procedure		
	General	6-1	6-1
	Interrelationship of design parameter	6-2	6-1
II.	Principles of Dynamic Analysis		
	Basic principles	6-3	6-3
	Dynamically equivalent systems	6-4	6-4
	Dynamic analysis and design	6-5	6-4
	Effective mass	6-6	6-4
III.	Design for Flexure		
	General	6-7	6-7
	Elements which respond to pressure only and pressure-time relationship	6-8	6-7
	Elements which respond to impulse	6-9	6-10
IV.	Design for Shear		
	General	6-10	6-21
	Elements which respond to pressure only and pressure-time relationship	6-11	6-21
	Elements which respond to impulse	6-12	6-21
V.	Composite Construction		
	General	6-13	6-40
	Analysis of composite elements	6-14	6-40
APPENDIX 6A.	Structural Design in the Ductile Mode Illustrative Examples		6-42
CHAPTER 7.	STRUCTURAL ANALYSIS AND DESIGN FOR BRITTLE MODE RESPONSE		
Section I.	Introduction		
	Types of fragmentation	7-1	7-1
	Design considerations	7-2	7-1
II.	Spalling of Concrete		
	Direct spalling	7-3	7-1
	Scabbing	7-4	7-2
	Minimization of effects of spalling	7-5	7-2

DISTRIBUTION STATEMENT A
Approved for public release;
Distribution Unlimited

		Paragraph	Page
Section III.	Post-Failure Concrete Fragments		
	General	7-6	7-4
	Fragment velocities	7-7	7-4
	Post-fragment impulse capacity	7-8	7-6
APPENDIX 7A.	Structural Design in the Brittle Mode		
	Illustrative Examples		7-9
CHAPTER 8.	STRUCTURAL BEHAVIOR TO PRIMARY FRAGMENT IMPACT		
Section I.	Introduction		
	Fragment characteristics	8-1	8-1
	Velocity and impact limitations	8-2	8-1
II.	Fragment Impact on Concrete		
	General	8-3	8-1
	Penetration of armor-piercing fragments	8-4	8-1
	Penetration of fragments other than armor-piercing	8-5	8-3
	Spalling due to fragment impact	8-6	8-3
III.	Composite Construction		
	General	8-7	8-3
	Penetration of composite barriers	8-8	8-3
APPENDIX 8A.	Primary Fragments		
	Illustrative Examples		8-5
CHAPTER 9.	CONSTRUCTION DETAILS AND PROCEDURES		
Section I.	Laced Reinforced Concrete Construction		
	General	9-1	9-1
	Concrete	9-2	9-1
	Flexural reinforcement	9-3	9-1
	Lacing reinforcement	9-4	9-1
	Corner details	9-5	9-5
II.	Detailing and Construction of Laced Structures		
	Laced elements	9-6	9-6
	Composite construction	9-7	9-8
	Single and multicubicle structures	9-8	9-10
	Sequence of construction	9-9	9-10
III.	Unlaced Reinforced Concrete Construction		
	General	9-10	9-12
	Differences from conventional construction	9-11	9-12
	Details of unlaced elements	9-12	9-12
CHAPTER 10.	OTHER FACTORS CONSIDERED IN EXPLOSIVE FACILITY DESIGN		
Section I.	Introduction		
	Scope	10-1	10-1
II.	Site Planning		
	Guide lines	10-2	10-1
	Typical case study	10-3	10-2
III.	Cost Effectiveness		
	General	10-4	10-4
	Cost comparison for laced concrete elements	10-5	10-5
IV.	Protective Closure Systems for Shelters		
	General	10-6	10-8
	Blast doors	10-7	10-8
	Blast valves and shields	10 8	10-10
V.	Protection Against Structure Motions		
	Structure motions	10-9	10-15
	Isolation systems	10-10	10-16
	Protective material, clothing, and restraining devices	10-11	10-17
VI.	Earth-Covered Steel-Arch Magazines		
	General	10-12	10-18
	Description of earth-covered steel-arch magazine	10-13	10-19
	Investigations performed	10-14	10-19
	Design	10-15	10-19
	Construction	10-16	10-19
	Standard design	10-17	10-19
APPENDIX A.	LIST OF SYMBOLS		A-1
B.	BIBLIOGRAPHY		B-1
GLOSSARY			GLOSSARY-1
INDEX			INDEX-1

Number	
2-1.	Exp
3-1.	Var
3-2.	Par
3-3.	Dee
3-4.	Bou
3-5.	Bou
3-6.	Ter
3-7.	Fra
3-8.	Lac
3-9.	Ty
3-10.	Res
3-11.	Sup
3-12.	Fai
3-13.	Fai
3-14.	Ele
4-1.	Bla
4-2.	Fre
4-3.	Fre
4-4.	Pre
4-5.	Sh
4-6.	Re
4-7.	Air
4-8.	Pre
4-9.	Sc
4-10.	Su
4-11.	In
4-12.	Sh
4-13.	Cu
4-14.	Pa
4-15.	Ba
4-16.	Li
4-17.	Sc
4-18.	Sc
4-19.	Sc
4-20.	Sc
4-21.	Sc
4-22.	Sc
4-23.	Sc
4-24.	Sc
4-25.	Sc
4-26.	Sc
4-27.	Sc
4-28.	Sc
4-29.	Sc
4-30.	Sc
4-31.	Sc
4-32.	Sc
4-33.	Sc
4-34.	Sc
4-35.	Sc
4-36.	Sc
4-37.	Sc
4-38.	Sc
4-39.	Sc
4-40.	Sc
4-41.	Sc
4-42.	Sc
4-43.	Sc
4-44.	Sc
4-45.	Sc
4-46.	Sc
4-47.	Sc
4-48.	Sc
4-49.	Sc
4-50.	Sc

LIST OF ILLUSTRATIONS

Number	Title	Page
2-1.	Explosion protective system	2-1
3-1.	Variation of structural response and blast loads	3-1
3-2.	Parameters defining pressure design ranges	3-2
3-3.	Design ranges corresponding to location of the structural element relative to an explosion	3-3
3-4.	Boundary velocity curve for uncased pentolite	3-4
3-5.	Boundary velocity curve for uncased cyclotol	3-5
3-6.	Tension cracks	3-5
3-7.	Fragmentation	3-5
3-8.	Lacing reinforcement	3-6
3-9.	Typical laced wall	3-6
3-10.	Resistance-deflection curve	3-6
3-11.	Support rotation	3-7
3-12.	Failure at plastic hinges of laced element	3-7
3-13.	Failure of an unlaced element	3-8
3-14.	Element at the verge of incipient failure	3-8
4-1.	Blast-loading categories	4-2
4-2.	Free field pressure time variation	4-2
4-3.	Free-air-burst blast environment	4-3
4-4.	Pressure-time variation for free air burst	4-3
4-5.	Shock-wave parameters for spherical TNT explosion in free air at sea level	4-4
4-6.	Reflected pressure coefficient vs. angle of incidence	4-5
4-7.	Air burst blast environment	4-5
4-8.	Pressure-time variation for air burst	4-6
4-9.	Scaled height of triple point	4-6
4-10.	Surface burst blast environment	4-7
4-11.	Incident pressure and scaled incident impulse vs. scaled distance for surface burst (hemispherical charges)	4-7
4-12.	Shock-wave parameters for hemispherical TNT surface explosion at sea level	4-8
4-13.	Cubicle structure	4-9
4-14.	Partially confined explosion blast environment	4-10
4-15.	Barrier and cubicle configurations and parameters	4-11
4-16.	List of illustrations for scaled average unit impulse loads	4-12
4-17.	Scaled average unit blast impulse ($N = 1$, $l/L = 0.10$, $h/H = 0.15$)	4-13
4-18.	Scaled average unit blast impulse ($N = 1$, $l/L = 0.25$ and 0.75, $h/H = 0.15$)	4-14
4-19.	Scaled average unit blast impulse ($N = 1$, $l/L = 0.50$, $h/H = 0.15$)	4-15
4-20.	Scaled average unit blast impulse ($N = 1$, $l/L = 0.10$, $h/H = 0.25$)	4-16
4-21.	Scaled average unit blast impulse ($N = 1$, $l/L = 0.25$ and 0.75, $h/H = 0.25$)	4-17
4-22.	Scaled average unit blast impulse ($N = 1$, $l/L = 0.50$, $h/H = 0.25$)	4-18
4-23.	Scaled average unit blast impulse ($N = 1$, $l/L = 0.10$, $h/H = 0.50$)	4-19
4-24.	Scaled average unit blast impulse ($N = 1$, $l/L = 0.25$ and 0.75, $h/H = 0.50$)	4-20
4-25.	Scaled average unit blast impulse ($N = 1$, $l/L = 0.50$, $h/H = 0.50$)	4-21
4-26.	Scaled average unit blast impulse ($N = 1$, $l/L = 0.25$ and 0.75, $h/H = 0.75$)	4-22
4-27.	Scaled average unit blast impulse ($N = 1$, $l/L = 0.50$, $h/H = 0.75$)	4-23
4-28.	Scaled average unit blast impulse ($N = 2$, $l/L = 0.10$, $h/H = 0.15$)	4-24
4-29.	Scaled average unit blast impulse ($N = 2$, $l/L = 0.25$, $h/H = 0.15$)	4-25
4-30.	Scaled average unit blast impulse ($N = 2$, $l/L = 0.50$, $h/H = 0.15$)	4-26
4-31.	Scaled average unit blast impulse ($N = 2$, $l/L = 0.75$, $h/H = 0.15$)	4-27
4-32.	Scaled average unit blast impulse ($N = 2$, $l/L = 0.10$, $h/H = 0.25$)	4-28
4-33.	Scaled average unit blast impulse ($N = 2$, $l/L = 0.25$, $h/H = 0.25$)	4-29
4-34.	Scaled average unit blast impulse ($N = 2$, $l/L = 0.50$, $h/H = 0.25$)	4-30
4-35.	Scaled average unit blast impulse ($N = 2$, $l/L = 0.75$, $h/H = 0.25$)	4-31
4-36.	Scaled average unit blast impulse ($N = 2$, $l/L = 0.10$, $h/H = 0.50$)	4-32
4-37.	Scaled average unit blast impulse ($N = 2$, $l/L = 0.25$, $h/H = 0.50$)	4-33
4-38.	Scaled average unit blast impulse ($N = 2$, $l/L = 0.50$, $h/H = 0.50$)	4-34
4-39.	Scaled average unit blast impulse ($N = 2$, $l/L = 0.75$, $h/H = 0.50$)	4-35
4-40.	Scaled average unit blast impulse ($N = 2$, $l/L = 0.25$, $h/H = 0.75$)	4-36
4-41.	Scaled average unit blast impulse ($N = 2$, $l/L = 0.50$, $h/H = 0.75$)	4-37
4-42.	Scaled average unit blast impulse ($N = 2$, $l/L = 0.75$, $h/H = 0.75$)	4-38
4-43.	Scaled average unit blast impulse ($N = 3$, $l/L = 0.10$, $h/H = 0.15$)	4-39
4-44.	Scaled average unit blast impulse ($N = 3$, $l/L = 0.25$ and 0.75, $h/H = 0.15$)	4-40
4-45.	Scaled average unit blast impulse ($N = 3$, $l/L = 0.50$, $h/H = 0.15$)	4-41
4-46.	Scaled average unit blast impulse ($N = 3$, $l/L = 0.10$, $h/H = 0.25$)	4-42
4-47.	Scaled average unit blast impulse ($N = 3$, $l/L = 0.25$ and 0.75, $h/H = 0.25$)	4-43
4-48.	Scaled average unit blast impulse ($N = 3$, $l/L = 0.50$, $h/H = 0.25$)	4-44
4-49.	Scaled average unit blast impulse ($N = 3$, $l/L = 0.10$, $h/H = 0.50$)	4-45
4-50.	Scaled average unit blast impulse ($N = 3$, $l/L = 0.25$ and 0.75, $h/H = 0.50$)	4-46

Number	Title	Page	Num
4-51.	Scaled average unit blast impulse ($N = 3$, $l/L = 0.50$, $h/H = 0.50$)	4-47	6-26
4-52.	Scaled average unit blast impulse ($N = 3$, $l/L = 0.25$ and 0.75, $h/H = 0.75$)	4-48	6-27
4-53.	Scaled average unit blast impulse ($N = 3$, $l/L = 0.50$, $h/H = 0.75$)	4-49	6-28
4-54.	Scaled average unit blast impulse ($N = 4$, $l/L = 0.10$, $h/H = 0.15$)	4-50	6-29
4-55.	Scaled average unit blast impulse ($N = 4$, $l/L = 0.25$ and 0.75, $h/H = 0.15$)	4-51	6-30
4-56.	Scaled average unit blast impulse ($N = 4$, $l/L = 0.50$, $h/H = 0.15$)	4-52	6-31
4-57.	Scaled average unit blast impulse ($N = 4$, $l/L = 0.10$, $h/H = 0.25$ and 0.75)	4-53	6-32
4-58.	Scaled average unit blast impulse ($N = 4$, $l/L = 0.25$ and 0.75, $h/H = 0.25$ and 0.75)	4-54	6-33
4-59.	Scaled average unit blast impulse ($N = 4$, $l/L = 0.50$, $h/H = 0.25$ and 0.75)	4-55	6-34
4-60.	Scaled average unit blast impulse ($N = 4$, $l/L = 0.10$, $h/H = 0.50$)	4-56	6-35
4-61.	Scaled average unit blast impulse ($N = 4$, $l/L = 0.25$ and 0.75, $h/H = 0.50$)	4-57	
4-62.	Scaled average unit blast impulse ($N = 4$, $l/L = 0.50$, $h/H = 0.50$)	4-58	6-36
4-63.	Exterior leakage pressure vs. ground scaled distance	4-59	6-37
4-64.	Pressure-time variation for a partially vented explosion	4-60	6-38
4-65.	Maximum mean pressure in a partially vented chamber	4-60	6-39
4-66.	Peak incident pressure vs. peak dynamic pressure	4-61	
4-67.	Front wall loading	4-61	6-40
4-68.	Roof and side wall loading (span direction perpendicular to shock front)	4-62	
4-69.	Equivalent load factor and blast wave location ratio vs. wave length-span ratio	4-63	6-41
4-70.	Roof and side wall loading (span direction parallel to shock front)	4-63	6-42
4-71.	Rear wall loading	4-64	6-43
4-72.	Leakage pressure coefficient vs. pressure differential	4-64	
4-73.	Initial velocity of primary fragments vs. charge weight	4-66	6-44
4-74.	Variation of primary fragment velocities with distance	4-67	6-45
5-1.	Typical reinforced concrete cross sections	5-1	7-1
5-2.	Moment capacity of rectangular sections without compression reinforcement	5-2	7-2
5-3.	Stress-strain curves for concrete and reinforcing bars	5-3	7-3
5-4.	Recommended dynamic yield stresses for reinforcing steels	5-4	7-4
5-5.	Coefficients for moment of inertia of cracked sections with tension reinforcement only	5-5	7-5
5-6.	Typical resistance-deflection function for two-way element	5-6	7-6
5-7.	Idealized yield-line locations for several two-way elements	5-7	7-7
5-8.	Determination of ultimate unit resistance	5-7	7-8
5-9.	Yield line location for two-way element with two adjacent edges supported and two edges free	5-9	7-9
5-10.	Yield line location for two-way element with three edges supported and one edge free	5-10	7-10
5-11.	Yield line location for two-way element with four edges supported	5-11	7-11
5-12.	Effects of openings on yield line locations	5-12	7-12
5-13.	Deflection of two-way element	5-14	8-1
5-14.	Deflection and moments for uniformly loaded two-way element with three edges fixed and one edge free	5-14	8-2
5-15.	Deflection and moments for uniformly loaded two-way element with two opposite edges simply-supported, one edge free, and one edge fixed	5-17	8-3 8-4
5-16.	Deflection and moments for uniformly loaded two-way element with three edges simply-supported and one edge free	5-17	8-5
5-17.	Deflection and moments for uniformly loaded two-way element with all edges fixed	5-18	8-6
5-18.	Deflection and moments for uniformly loaded two-way element with two opposite edges fixed and two edges fixed and two edges simply-supported	5-18	9-1 9-2
5-19.	Deflection and moments for uniformly loaded two-way element with all edges simply-supported	5-19	9-3
5-20.	Resistance-deflection functions for limited deflections ($\theta_m \leq 5°$)	5-20	9-4
5-21.	Resistance-deflection functions for large deflections ($\theta_m > 5°$)	5-20	9-5
5-22.	Determination of ultimate shears	5-21	9-6
6-1.	Design procedure for explosive protective structures	6-1	9-7
6-2.	Relationships between design parameters	6-2	9-8
6-3.	Typical single-degree-of-freedom system	6-4	9-9
6-4.	Determination of load-mass factor in the plastic range	6-5	9-1
6-5.	Load-mass factors in plastic range for two-way elements	6-5	9-1
6-6.	Idealization of pressure-time functions	6-7	9-1
6-7.	Maximum response of simple spring-mass system to initially peaked triangular pressure pulse	6-8	9-1
6-8.	Elastic rebound of simple spring-mass system	6-9	9-1
6-9.	Pressure time and resistance-time curves for elements which respond to impulse	6-10	9-1
6-10.	Impulse coefficient C_1 for an element with two adjacent edges fixed and two edges free	6-14	10-
6-11.	Impulse coefficient C_1 for an element with three edges fixed and one edge free	6-15	10-
6-12.	Impulse coefficient C_1 for an element with four edges fixed	6-16	10
6-13.	Impulse coefficient C_u for an element with two adjacent edges fixed and two edges free	6-17	10-
6-14.	Impulse coefficient C_u for an element with three edges fixed and one edge free	6-18	10-
6-15.	Impulse coefficient C_u for an element with four edges fixed	6-19	10-
6-16.	Determination of optimum ratio of p_V/p_H for maximum impulse capacity	6-20	10-
6-17.	Optimum ratio of p_V/p_H for maximum impulse capacity at partial failure deflection X_1	6-20	10-
6-18.	Optimum ratio of p_V/p_H for maximum impulse capacity at incipient failure deflection X_u	6-21	10-
6-19.	Angle of inclination of lacing bars	6-22	10-

Number	Title	Page
6-20.	Shear coefficients for ultimate support shear (cross section type II and III)	6-25
6-21.	Shear coefficients for ultimate support shear (cross section type II and III)	6-25
6-22.	Shear coefficients for ultimate support shear (cross section type II and III)	6-26
6-23.	Shear coefficients for ultimate support shear (cross section type II and III)	6-26
6-24.	Vertical shear coefficients for ultimate shear stress at distance d_e from the support (cross section type II and III)	6-27
6-25.	Horizontal shear coefficients for ultimate shear stress at distance d_e from the support (cross section type II and III)	6-27
6-26.	Vertical shear parameters for ultimate shear stress at distance d_e from the support (cross section type II and III)	6-28
6-27.	Vertical shear coefficient ratios for ultimate shear stress at distance d_e from the support (cross section type II and III)	6-29
6-28.	Horizontal shear parameters for ultimate shear stress at distance d_e from the support (cross section type II and III)	6-30
6-29.	Horizontal shear coefficient ratios for ultimate shear stress at distance d_e from the support (cross section type II and III)	6-31
6-30.	Vertical shear parameters for ultimate shear stress at distance d_e from the support (cross section type II and III)	6-32
6-31.	Vertical shear coefficient ratios for ultimate shear stress at distance d_e from the support (cross section type II and III)	6-33
6-32.	Horizontal shear parameters for ultimate shear stress at distance d_e from the support (cross section type II and III)	6-34
6-33.	Horizontal shear coefficient ratios for ultimate shear stress at distance d_e from the support (cross section type II and III)	6-35
6-34.	Vertical shear parameters for ultimate shear stress at distance d_e from the support (cross section type II and III)	6-36
6-35.	Vertical shear coefficient ratios for ultimate shear stress at distance d_e from the support (cross section type II and III)	6-37
6-36.	Horizontal shear parameters for ultimate shear stress at distance d_e from the support (cross section type II and III)	6-38
6-37.	Horizontal shear coefficient ratios for ultimate shear stress at distance d_e from the support (cross section type II and III)	6-39
6-38.	Attenuation of blast impulse in sand and concrete	6-40
6-39.	Attenuation of blast impulse in sand and concrete	6-40
7-1.	Direct spalled element	7-1
7-2.	Scabbed element	7-2
7-3.	Unspalled receiver panel of composite panel	7-3
7-4.	Shielding systems for protection against concrete fragments	7-3
7-5.	Rigid attachment of fragment shield to barrier	7-4
7-6.	Failure of an unlaced element	7-4
7-7.	Failure at plastic hinges of laced element	7-5
7-8.	Backwall failure of cubicle with laced reinforcement	7-5
7-9.	Idealized curves for determination of post-failure fragment velocities	7-6
7-10.	Post-failure fragment coefficient C_f for an element fixed on two adjacent sides and two sides free	7-7
7-11.	Post-failure fragment coefficient C_f for an element fixed on three sides and one side free	7-7
7-12.	Post-failure fragment coefficient C_f for an element fixed on four sides	7-8
8-1.	Perforation and spalling of concrete due to primary fragments	8-1
8-2.	Shape of primary fragment	8-1
8-3.	Fragment penetration through concrete	8-2
8-4.	Limits of concrete spalling and perforation	8-2
8-5.	Residual velocity of primary fragment after perforation	8-3
8-6.	Fragment penetration through sand	8-4
9-1.	Laced reinforced element	9-1
9-2.	Typical flexural reinforcement splice patterns	9-2
9-3.	Typical lacing bend details	9-2
9-4.	Typical methods of lacing	9-3
9-5.	Typical location of continuous and discontinuous lacing	9-4
9-6.	Typical details for splicing of lacing bars	9-5
9-7.	Length of lacing bar	9-5
9-8.	Reinforcement details of laced concrete walls	9-7
9-9.	Typical detail at intersection of two continuous walls	9-8
9-10.	Typical detail at intersection of continuous and discontinuous walls	9-8
9-11.	Typical detail at corner	9-9
9-12.	Typical composite wall details	9-10
9-13.	Typical single-cell structures	9-10
9-14.	Typical multicubicle structures	9-11
9-15.	Pouring sequence	9-11
10-1.	Control of debris by proper design	10-1
10-2.	Site planning of typical ammunition maintenance facility	10-2
10-3.	Off-site separation distances (typical ammunition maintenance facility)	10-3
10-4.	Ammunition maintenance building	10-3
10-5.	Surface pressure vs. distance for 5,000-pound charge in cubicle	10-4
10-6.	Cost effectiveness system	10-4
10-7.	Cost analysis of laced cantilever wall	10-5
10-8.	Variation of optimum reinforcement with unit price of concrete and steel	10-5
10-9.	Comparison of cost and thickness of laced and standard walls	10-6
10-10.	Variation of cost and thickness with percent reinforcement	10-6

Number	Title	Page
10-11.	Variation of cost with separation distance	10-7
10-12.	Variation of cost with wall length to height ratios	10-7
10-13.	Proportioning of reinforcement in two-way elements	10-8
10-14.	Steel-plate doors	10-9
10-15.	Vault-type door	10-9
10-16.	Welded-beam door	10-10
10-17.	Built-up steel door	10-10
10-18.	Airtight door	10-11
10-19.	Steel-arch doors	10-11
10-20.	Tension-arch door	10-12
10-21.	Dome-plate door	10-12
10-22.	Leakage pressures into a structure	10-13
10-23.	Peak incident pressure vs. time of arrival (surface burst)	10-14
10-24.	Air intake system	10-14
10-25.	Time-delay path	10-15
10-26.	Helical compression spring mounts	10-15
10-27.	Typical suspended platform isolation system	10-17
10-28.	Minimum magazine separation distances	10-18
10-29.	Typical earth covered steel-arch magazine	10-18

LIST OF TABLES

3-1	Tentative criteria for primary-blast effects in man applicable to fast-rising air blasts of short duration (3 ms)	3-3
3-2	Examples of equipment shock tolerances	3-4
3-3	Impact sensitivity constant	3-5
4-1	Equivalent weight ratios for free-air effects	4-1
4-2	Constants for primary fragment calculations	4-67
4-3	Initial velocity of primary fragments	4-68
5-1	Minimum area of flexural reinforcement	5-2
5-2	Allowable bond stresses (nonlaced sections)	5-4
5-3	Dynamic increase factors (DIF)	5-4
5-4	Minimum static design stresses	5-4
5-5	Ultimate unit resistances for one-way elements	5-8
5-6	Ultimate unit resistances for two-way elements	5-12
5-7	Post-ultimate unit resistances for two-way elements	5-13
5-8	General and ultimate deflections for one-way elements	5-13
5-9	General, partial failure, and ultimate deflections for two-way elements	5-15
5-10	Elasto-plastic unit resistances for one-way elements	5-16
5-11	Elasto-plastic stiffnesses for one-way elements	5-19
5-12	Ultimate support shears for one-way elements	5-21
5-13	Ultimate shear stress at distance d_s from face of support for one-way elements	5-21
5-14	Ultimate support shears for two-way elements	5-23
5-15	Ultimate shear stresses at distance d_s from the supports for two-way elements	5-24
6-1	Load-mass factors K_{LM} for one- and two-way elements with uniform loading	6-6
6-2	Impulse coefficient C_s for one-way elements	6-11
6-3	Impulse coefficients C_1 and C_s for two-way elements	6-12
6-4	Design equations for elements which respond to impulse	6-13
6-5	Shear coefficients for ultimate support shear for one-way elements (cross sections type II and III)	6-23
6-6	Shear coefficients for ultimate shear stress at distance d_s from the support for one-way elements (cross sections type II and III)	6-23
6-7	Shear coefficients for ultimate support shear for two-way elements (cross sections type II and III)	6-23
6-8	Shear coefficients for ultimate shear stress at distance d_s from the support for two-way elements (cross sections type II and III)	6-24
10-1	Standard drawings for blast doors	10-13
10-2	Blast valves	10-15
10-3	Safe impact velocities of the human head using protective cushioning materials	10-17
10-4	Required steel thicknesses for various magazine widths	10-19

Page

10-7
10-7
10-8
10-9
10-9
10-10
10-10
10-11
10-11
10-12
10-12
10-13
10-14
10-14
10-15
10-15
10-17
10-18
10-18

3-3
3-4
3-5
4-1
4-67
4-68
5-2
5-4
5-4
5-4
5-8
5-12
5-13
5-13
5-15
5-16
5-19
5-21
5-21
5-23
5-24
6-6
6-11
6-12
6-13
6-23

6-23
6-23

6-24
10-13
10-15
10-17
10-19

CHAPTER 1

INTRODUCTION

1–1. Purpose and Objective

a. This manual presents methods of design for protective construction used in facilities for the manufacture, maintenance, modification, inspection, and storage of explosive materials.

b. The primary objectives are to establish design procedures and construction techniques whereby propagation of explosions (from one building or part of a building to another) or mass detonations will be prevented and protection for personnel and valuable equipment will be provided.

c. The secondary objectives are: (1) Establish blast load parameters required for design of protective structures; (2) Provide methods for calculating the dynamic response of reinforced concrete and other materials; (3) Establish construction details necessary to afford the required strength to resist the applied blast loads; (4) Establish guide lines for siting explosive facilities to obtain maximum cost effectiveness in both site planning and structural arrangement, providing closures, and preventing damage to interior portions of structures due to structural motion and shock.

1–2. Background

a. Over the last 60 years criteria and methods based upon results of catastrophic events have been used for the design of explosive facilities. The criteria and methods did not include a detailed or reliable quantitative basis for assessing the degree of protection afforded by the protective facility. Recently, extensive research and development programs have been undertaken to establish procedures which permit a more sound and scientifically based approach to current and future design requirements. The results of this research to date are embodied in this manual.

b. Modern methods for the manufacture and storage of explosive materials, which include many exotic chemicals, fuels, and propellants, allow less space for a given quantity of explosive material than previously permitted. Such concentrations of explosives increase the possibility of the propagation of accidental explosions (one accidental explosion causing the detonation of other explosive materials). It is evident that a requirement for more accurate design techniques has become essential. This manual describes a rational design method to provide the required structural protection.

c. This design method accounts for the close-in effects of a detonation, including associated high pressures and nonuniformity of the blast loading on protective structures or barriers. The dynamic response of structures can now be calculated, and details have been developed to provide the properties necessary to supply the required strength and ductility specified by the design. Development of these procedures has been directed primarily towards blast load analysis of protective barriers for explosive systems contained within structures. However, this approach is general and is applicable to the design of other explosive environments as well.

d. The design techniques set forth in this manual are based upon the results of numerous full- and small-scale structural response and explosive effects tests conducted in conjunction with the Establishment of Safety Design Criteria Program.

1–3. Scope of Manual

a. This manual is limited only by variety and range of the assumed design situations. An effort has been made to cover the more probable situations. However, sufficient general information on protective design techniques has been included in order that applications of the basic theory can be made to situations other than those which were fully considered.

b. Although many of the charts included in the explosive effects and structural response portions of this manual are applicable to detonations of the order of hundreds of thousands of pounds of high explosives, the usual design situation, where this manual will generally apply, is for explosive quantities less than 25,000 pounds.

c. Because the tests conducted so far in connection with the Safety Design Criteria Program have been directed primarily towards the response of reinforced concrete elements to blast overpressures, this manual concentrates on the procedures and techniques required for the design of reinforced concrete protective structures. However, this does not imply that concrete is the only useful material for protective construction. Tests to establish the response of structural steel and other materials to the effects of explosions are either under-

way or contemplated. The results of these tests will be used to establish design methods for these materials and, at a later date, will supplement this manual.

d. Other manuals are available which enable one to design protective structures against the effects of nuclear detonations. These procedures are also applicable to the design of protective structures at considerable distance from very large quantities of explosives and, therefore, have only been qualitatively discussed. The primary concern of this manual is the design of structural elements or structures located close to a potential high-explosive hazard.

1–4. Format of Manual

a. Chapters of this manual are divided into three main categories, as follows: (1) chapters 1, 2, and 3 which contain a qualitative description of both the explosive effects and the structure's response, (2) chapters 4 through 8 which present the quantitative procedures for computing the blast output and structural behavior, and (3) chapters 9 and 10 which discuss methods of detailing and construction and other features of protective construction such as site planning, closure systems, cost effectiveness, and the effect of structural motions. Appendixes pertinent to a particular chapter and containing illustrative examples of explosive effects and structural response problems, appear at the end of the chapter to which they pertain.

b. Commonly accepted symbols have been used as much as possible. However, protective design involves many different scientific and engineering fields, and therefore, no attempt has been made to standardize completely all of the symbols used. Each symbol has been defined where it is first introduced, and a list of the symbols, with their definitions and units, is contained in appendix A. The symbols along with their units also have been indicated on all appropriate tables and charts.

c. Appendixes A and B appear in the back of the manual.

1–5. Safety Factor and Accuracy

a. Certain simplifications have been made in the development of the design procedures presented in this manual. As a result, an analysis of a structure using these procedures will generally result in a conservative estimate of the structure's capacity and, consequently, structures designed using these procedures will generally be adequate for the blast load exceeding the assumed loading conditions.

b. Certain unknown factors can result in an overestimate of the protective structure's capability to resist the effects of an explosion. These factors, reflections of the shock waves, structural response, construction methods, quality of construction materials, workmanship, etc., vary for each facility design. To compensate for weaknesses resulting from these factors, it is recommended that the "effective charge weight" or the actual charge weight, depending upon the method used to determine the TNT equivalent, be increased by 20 percent for design purposes. Modification of this increased "effective charge weight" in a particular design situation may only be made for those cases which are sufficiently simple and well tried to justify this action. Such modifications must be approved by the cognizant military construction agency.

CHAPTER 2

EXPLOSION PROTECTIVE SYSTEM

2–1. System Components

Explosive storage and operating facilities which are to be constructed so that they provide a predetermined level of protection against the hazards of accidental explosions can be thought of as a problem consisting of three broad components: (1) the donor system (amount, type, and location of the potentially detonating explosive) which produces the damaging output, (2) the receiver system (personnel, equipment, and "acceptor" explosives) which requires a level of protection, and (3) the protective structure or structural elements (or distance) necessary to shield against or attenuate the hazardous effects to levels which are tolerable to the receiver system. The flow chart in figure 2–1 briefly summarizes the protective system and relates the individual components to each other.

2–2. Donor System

a. The donor system includes the type and amount of the donor explosive as well as its location relative to the components of the protective facility. The output of the donor explosive includes blast overpressures (hereafter referred to as blast pressures or pressures) and, in the case of cased explosives, primary fragments. Other effects from the donor include ground shock, fire, heat, dust, etc. For the quantities of explosives considered in this manual (say up to 25,000 pounds) blast pressures are normally the principal parameter governing the design of protective structures. However, in some situations, primary fragments from cased explosives may assume equal importance in the planning of the protective system. The other effects enumerated (except ground shock) are usually specific to certain types of facilities, and their influence on the overall design can usually be met with the use of standard engineering design procedures. Except for very large quantities of explosives (far above the upper limit considered in this manual), ground shock effects will usually be small and, therefore, may generally be disregarded.

b. The chemical and physical properties of the donor explosive determine the magnitude of the blast pressure whereas the distribution of the pressure patterns is primarily a function of the location of the donor explosive relative to the components of the protective facility. The mass-velocity characteristics of the primary fragments also depend upon the properties of the donor explosive

c. The explosive properties, including the molecular structure (monomolecular, bimolecular, etc.) of the explosive, shape and dimensional characteristics, and physical makeup (solid, liquid, gas) of the charge, determine the limitation of the detonation process and thereby result in either high- or low-order detonation. With high-order detonation, the process is generally complete and results in the maximum pressure output for the given type and amount of material. On the other hand, if the detonation is incomplete with the initial reaction not proceeding throughout the material mass, then a large quantity of the explosive is consumed by deflagration and the blast pressure is reduced.

d. Heavy, high-velocity, primary fragments may penetrate a protective element depending upon its thickness and other characteristics, while lightweight fragments seldom achieve penetration. However, both light and heavy fragments may richochet into the protected area and cause injury to personnel, damage to equipment, or the detonation of acceptor explosives. For protection against primary fragments, sufficient structural thickness must be provided to prevent full penetration, and the configuration of the components of the protective facility must be such as to prevent fragments from richocheting in the direction of the protected area.

2–3. Receiver System

The second component of the problem is the receiver, which is the personnel, equipment, or explosives that require protection. Acceptable injury to personnel or damage to equipment, and the sensitivity of the protected explosive(s), establishes the degree of protection for which the protective structure is designed. For a given yield and location of the donor, the type and capacity of the protective structure are selected to produce a balanced design with respect to the degree of protection required by the receiver. Full protection is usually required for personnel and equipment, while the degree of protection required for explosives ranges from full protection to allowable partial or total collapse of the protective structure.

2–4.

a. I
and b
are us
age t
sensit
betwe
b.
tranc
upon
(two
openi
latior

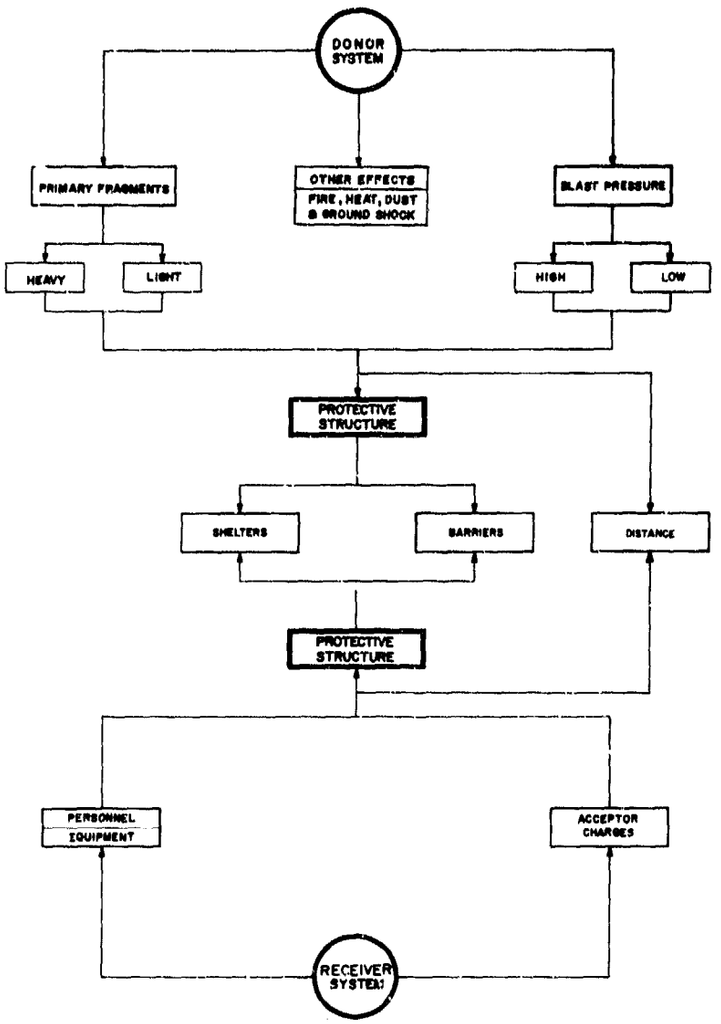


Figure 2–1. Explosion protective system.

2–4. Protective Structures

a. Protective structures can be classified as shelters and barriers. Shelters are fully enclosed structures and are used to protect personnel from injury, prevent damage to valuable equipment, and prevent detonation of sensitive explosives, while barriers are used as a shield between two or more potentially detonating explosives.

b. Because shelters are fully enclosed structures, entrances must be sealed with blast doors and, depending upon the traffic flow, may also require blast locks (two blast doors, one of which is always closed). Other openings required for facility operations, such as ventilation passages, equipment access openings, etc., may be sealed with blast valves or blast shields. Design criteria for these protective closures are governed by the magnitude of the blast pressures acting on them, their size and location, the magnitude and rate of pressure buildup within the structure when partial openings are permitted, and the sensitivity of the occupants and contents to the internal pressure buildup. Special provisions may also be necessary to insure that interior mechanical and electrical fixtures, piping, and conduits are not displaced as a result of movement of the structure.

c. Barriers can be either barricades (revetted or unrevetted earth barricades, simple cantilever walls, etc.) or cubicle-type structures where one or more sides

and/or the roof of the structure are of frangible construction or open to the atmosphere. Igloos (earth covered magazines), below-ground silos, and other similar structures with open or frangible surfaces can also be classified as barriers. Because these structures are usually used in the storage, manufacture, or processing of explosives or explosive materials, the explosives will be located close to the protective elements of the structures and, therefore, will be subjected to high-intensity blast loadings.

CHAPTER 3

BASIS FOR STRUCTURAL DESIGN

Section I. STRUCTURAL RESPONSE

3–1. General

The selection of the dynamic response for use in the design of a protective structure and its elements to the output of an explosion is governed by: (1) the properties (type, weight, shape, etc.) and location of the donor explosive, (2) the sensitivity of the receiver system, and (3) the physical properties and configuration of the structure itself. However, the response of the selected structure depends only upon the donor system and the properties of the structure.

3–2. Pressure Design Ranges

a. General. An engineering analysis of the blast pressures on structures can be made to describe the response of protective structures to these pressures. This response is expressed in terms of design ranges according to pressure intensity, namely: (1) high, (2) intermediate, and (3) low. As subsequently shown, these design ranges are related to the relative location of the protective structure to the explosion.

b. High-Pressure Design Range. At the high-pressure design range, the initial pressures acting on the protective structure are usually extremely high and further amplified by their reflections from the structure. Also, the durations of the applied loads are short in comparison to the response time (time to reach maximum deflection) of the individual elements of the structure. Therefore, structures subjected to blast effects at the high-pressure range are designed for the impulse (area under the pressure-time curve (chap. 4)) rather than for the peak pressures associated with longer duration blast pressures.

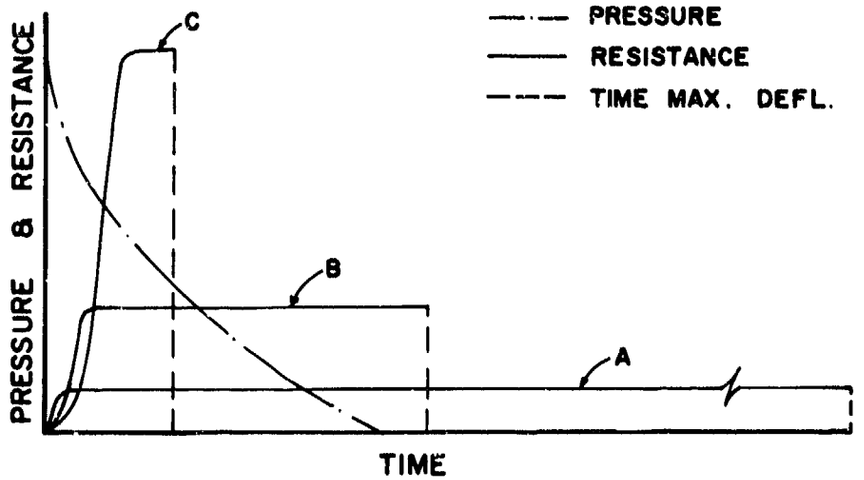
c. Intermediate-Pressure Design Range. Structures subjected to blast pressures associated with the intermediate-pressure design range sustain blast pressures of smaller intensity than those associated with the high-pressure range. However, because the duration of these pressures (which are long in comparison to those for the high-pressure range) are in the order of magnitude of the response time of the structure, structural elements designed for the intermediate range respond to the combined effects of both the pressure and impulse associated with the blast output.

d. Low-Pressure Design Range. Durations of blast loads acting on protective structures designed using the low-pressure design range are extremely long in comparison to those associated with the other two ranges. Here the structure responds primarily to the peak pressure in a manner similar to those structures designed to resist the effects of nuclear detonations.

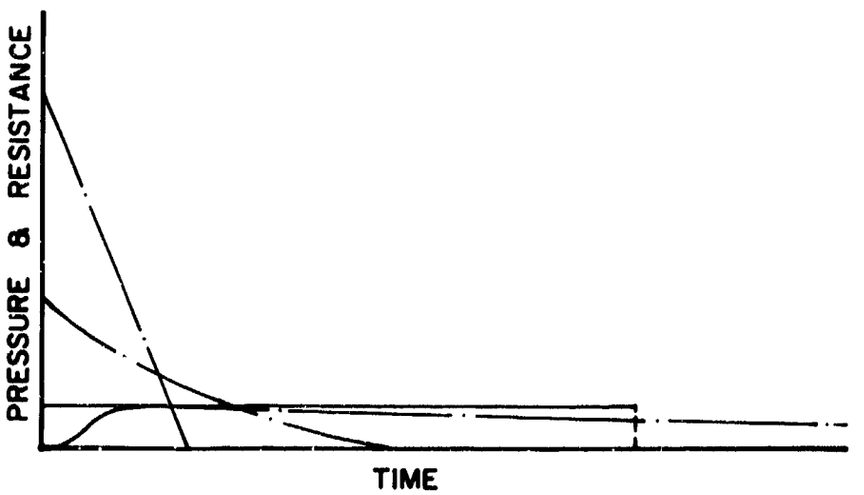
3–3. Analyzing Blast Environment

a. Although each design range is distinct in itself, no clear-cut divisions between the three ranges exist; therefore, each protective structure must be analyzed for its own blast environment to determine its response.

b. Depending on the type of protective structure being considered and its location relative to the explosion, multiple solutions of the structural response can exist, particularly near the fringe areas between the design ranges. To illustrate these fringe areas, consider the three theoretically possible response (resistance-time) curves of an element subjected to a given pressure-time loading (a, fig. 3–1). Curve A represents the resistance-time function of an element which responds to the impulse (high-pressure range); the time to reach maximum deflection is very long in comparison to the load duration. The intermediate range is represented by curve B where the duration of the load is in the order of magnitude of the response time. In other design cases, the response time of an element subjected to intermediate-range blast loads can be less than, equal to, or greater than the load duration (fig. 3–2). This variation depends upon the parameters of the blast (pressure and duration), the physical properties (strength and period of vibration) of the element, and the maximum deflection permitted. Curve C illustrates the low-pressure design range of an element. The required peak resistance is in the order of magnitude of the peak pressure while the duration of the load is extremely long compared to the time to reach maximum deflection. Although the required maximum resistance will vary in comparison to the peak pressure, the variation will be slight, and in general the required maximum resistance of an element to resist long duration



a) VARIABLE RESISTANCE – TIME CURVES



b) VARIABLE PRESSURE – TIME CURVES

Figure 3–1. Variation of structural response and blast loads.

loads will be only slightly larger (5 to 10 percent) than the peak pressure.

c. Multiple solutions of the structural response near the fringe areas are illustrated in b, figure 3-1. The magnitude of both the peak pressure and duration of each curve has been selected so that the areas under the individual curves are equal to one another. Also, the area under the resistance-time curve is equal to the area under each pressure-time curve, resulting in a situation where the response of the element can be solved by any one of the three design-range methods (chap. 6), thereby obtaining the same response for all three. Figure 3–2 indicates semiquantitatively the parameters which define the three design ranges of an element including the appropriate relationship between the time to reach maximum deflection and the load duration.

d. It was indicated earlier that the design range of an element is related to the location of the element relative to the explosion. For the quantity of explosives considered in this manual, an element designed for the

2

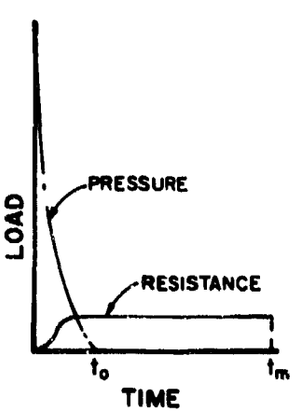
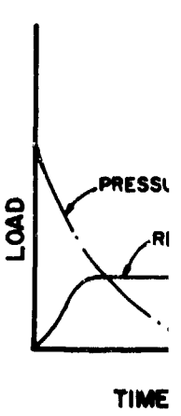
		
PRESSURE DESIGN RANGE	HIGH	INTERMED
DESIGN LOAD	IMPULSE	PRESSURE
PRESSURE LEVEL	$\gg$ 200 psi	<200p
PRESSURE DURATION	SHORT	INTERME
RESPONSE TIME	LONG	INTERME
RELATIONSHIP OF t_m/t_o	$t_m/t_o > 3$	$3 > t_m/t_$

Figure 3–2. Parameters defining pressure design ran

high-pressure range is usually situated immediately adjacent to the explosion, and its exposed surface facing the explosion is oriented normal or nearly normal to the propagation of the initial pressure wave (fig. 3–3, cases I and II). On the other hand, elements which are located close to the explosion and are positioned parallel to the path of the wave propagation may respond to the blast effects associated with the intermediate-pressure design range. Elements located close to a detonation seldom respond solely to a peak pressure.

e. Certain elements of a protective structure located a distance from the explosion may respond to the impulse (high-pressure range) while other elements respond to the blast loads of either the intermediate- or low-pressure range (fig. 3–3, case III). In most cases, those elements facing the explosion will be sensitive either to the high- or intermediate-pressure range blast loads while other elements will respond to the blast parameters associated with either the intermediate- or low-pressure ranges.

extremely se
plished by n
ter, providi
structure, a
the structur
of fragments
the uncontr
vided by co
the explosio
the material
areas.

Section II. PROTECTION CATEGORIES

3–4. General

For the purpose of analysis, the protection afforded by a facility or its components can be subdivided into four protection categories as described below.

a. Protect personnel from fragments, falling portions of the structure and/or equipment, and attenuation of blast pressures and structural motion to a level consistent with safety requirements.

b. Protect equipment and supplies from fragment impact, blast pressures, and structural motions; and/or protect against the uncontrolled release of hazardous materials, including toxic chemicals, active radiological or biological materials, etc.

c. Prevent communication of detonation by fragments and high-blast pressures.

d. Prevent mass detonation of explosives as a result of subsequent detonations produced by communication of detonation between two adjoining areas.

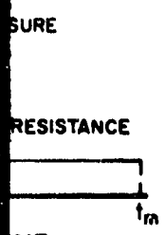
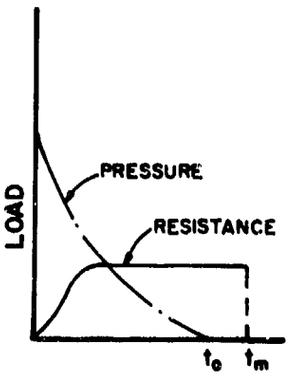
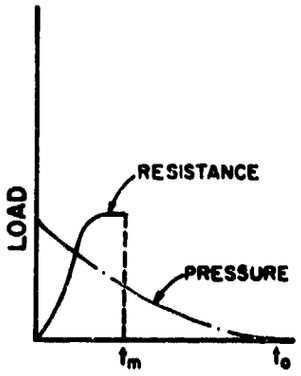
3–5. Shelters

The first two categories (para 3–4*a* and *b*) apply to protective structures classified as shelters which provide protection for personnel, valuable equipment, and/or

3–7. Hum

a. Blast

(1) Hu
explosion is
of a person
to the pressu
shape of the

		
ME	INTERMEDIATE	LOW
GH	PRESSURE-TIME	PRESSURE
LSE	<200psi	< 10 psi
00 psi	INTERMEDIATE	LONG
ORT	INTERMEDIATE	SHORT
NG	$3 > t_m/t_o > 0.1$	$t_m/t_o < 0.1$
> 3		

2. Parameters defining pressure design ranges.

extremely sensitive explosives. This protection is accomplished by minimizing the pressure leakage into a shelter, providing adequate support for the contents of the structure, and preventing penetration to the interior of the structure by primary fragments and/or formation of fragments from the structure itself. Protection against the uncontrolled spread of hazardous materials is provided by confining materials within the structure where the explosion takes place or by permitting spreading of the materials by controlled means to controlled (safe) areas.

3–6. Barriers

The last two protection categories (para 3–4*c* and *d*) pertain to the design of barriers where protection of explosives from the effects of blast pressures and impact of primary fragments must be provided. For the third protection category (para 3–4*c*), the explosion must be confined to a donor cell, whereas in the fourth protection category (para 3–4*d*), propagation between two adjacent areas is permitted. However, this communication of detonation must not extend to other areas of the facility. This situation may arise in the event of the dissimilarity of construction and/or explosive contents of adjacent areas.

Section III. RECEIVER SENSITIVITY

3–7. Human Tolerance

a. Blast Pressures.

(1) Human tolerance to the blast output of an explosion is relatively high. However, the orientation of a person (standing, sitting, prone, face-on or side-on to the pressure front) relative to the blast, as well as the shape of the pressure front (fast or slow rise, stepped loading), are significant factors in determining the amount of injury sustained. Shock tube and explosive tests have indicated that human blast tolerance varies with the duration of the applied loading, i.e., the pressure tolerance for short-duration blast loads is significantly higher than that for long-duration blast loads.

(2) Recent tests have indicated that the lungs can be considered as the critical target organs in blast-

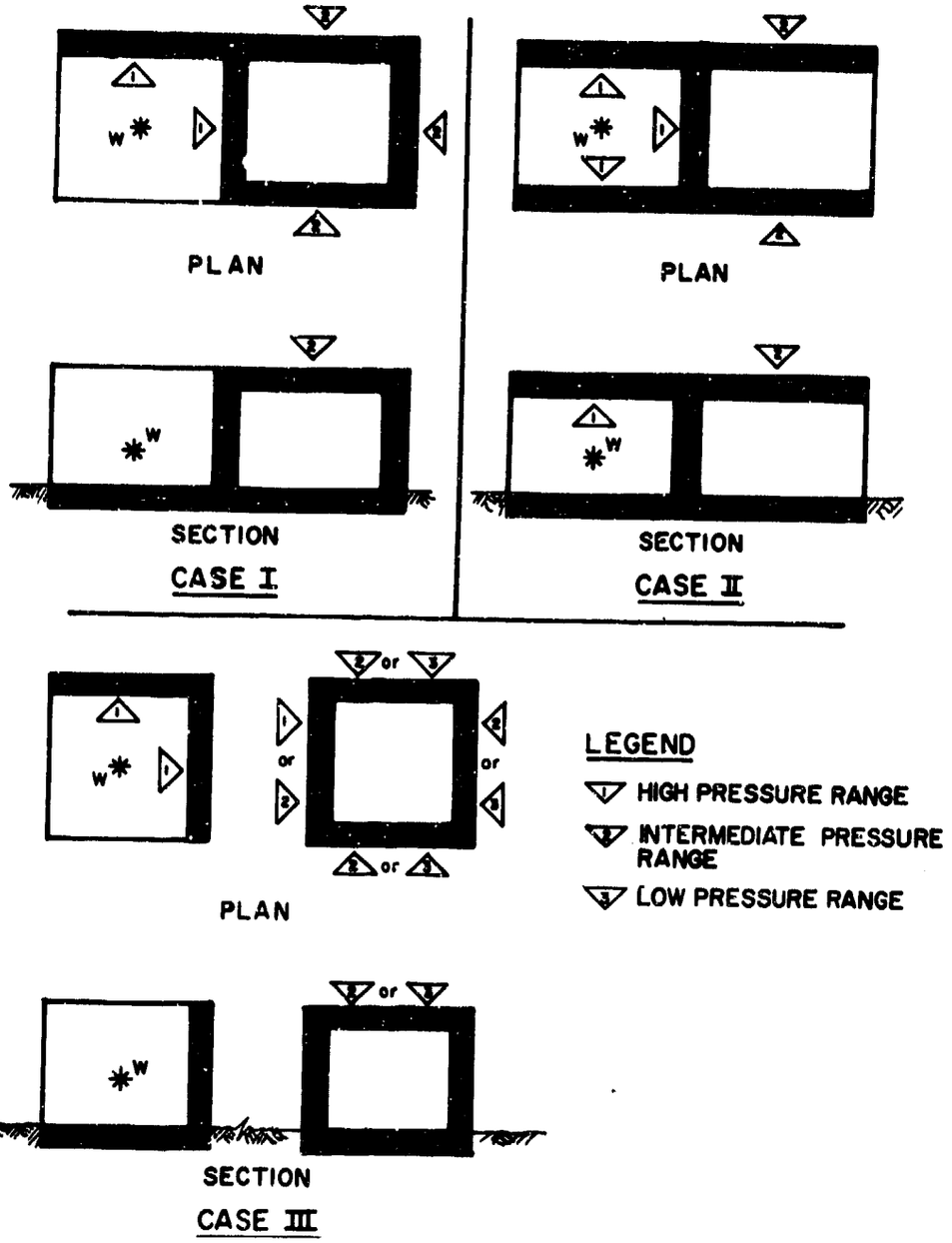


Figure 3–3. Design ranges corresponding to location of the structural element relative to an explosion.

pressure injuries. The release of air bubbles from disrupted alveoli of the lungs into the vascular system probably accounts for most deaths. Based on present data, a tentative estimate of man's response to fast-rise pressures of short duration (3 to 5 ms) is given in table 3–1. The threshold and severe lung-hemorrhage pressure levels are 30 to 40 psi and above 80 psi, respectively, while the threshold for lethality due to lung damage is approximately 100 to 120 psi. On the other hand, the threshold pressure level for petechial hemorrhage resulting from long-duration loads may be as low as 10 to 15 psi or approximately one-third that for short-duration blast loads. The time-honored estimate for human eardrum rupture is 5 and 15 psi for threshold and 50 percent chance of casualty, respectively.

(3) The pressures referred to in (2) above are the maximal effective pressures, that is, the highest of either the incident pressure, the incident plus the dynamic

Table 3–1. Tentative Criteria for Primary-Blast Effects in Ma- Applicable to Fast-Rising Air Blasts of Short Duration (3 ms)

Critical organs or event	Maximal effective pressure[1] (psi)
Eardrum Rupture:	
Threshold	5
50 percent	15
Lung Damage:	
Threshold	30–40
Severe	80 and above
Lethality:	
Threshold	100–120
50 percent	130–180
Near 100 percent	200–250

[1] The maximal effective pressure may be either the incident pressure, the incident plus dynamic pressures, or the reflected pressure (para 3–7*a*(2)).

pressures, or the reflected pressure. The type of pressure which will be the maximal effective depends upon the orientation of the individual relative to the blast as well as the proximity of reflecting surfaces. As an example, consider the pressure level which will cause the onset of lung injury to personnel in various positions and locations. The threshold would be 30 to 40 psi reflected pressure for personnel against a reflector (any position), 30 to 40 psi incident plus dynamic pressure (20 to 25 psi would be the incident pressure plus 10 to 15 psi dynamic pressure) for personnel in the open either standing or prone-side-on, and 30 to 40 psi incident pressure for personnel in the open in a prone-end-on position.

(4) Based upon the above tolerances, shelters containing personnel may be permitted to have some interior pressure buildup as a result of pressure leakage through small openings. However, this buildup in pressure should be controlled both in magnitude and duration, and provisions should be made in the design to insure that the leakage pressures do not produce internal damage to the structure or its contents. Direct exposure to the pressures entering the structure should be minimized. The jetting effects produced by the pressures passing through an opening can result in amplification of the pressures at the interior side of the opening. The magnitude of this increased pressure can be several times as large as the maximum average pressure acting on the interior of the structure during the passage of the blast wave.

b. Structural Motions.

(1) Because the structural motions associated with high-explosive detonations are transient in nature and can possibly impart an abrupt velocity change to the body either in stopping or starting, in addition to shaking or vibrating of the body, it is necessary that human tolerance to two types of shock exposures be considered:

(*a*) Impacts involving velocity shocks causing body acceleration or deceleration.

(*b*) Body vibration as a result of the vibratory motion of the structure.

(2) If a subject is not attached to the structure, he may be vulnerable to impact resulting from collision with the floor due to the structure dropping out beneath him and/or the structure rebounding upward towards him. However, the more plausible means of impact injury results from the subject being thrown off balance because of the horizontal motions of the structure, causing him to be thrown bodily against other persons, equipment, walls, and hard surfaces.

(3) A recent study has indicated that a probable safe impact tolerance velocity is 10 fps. This applies to impact with hard, flat surfaces in various body postures and to impact of the head. If the line of thrust for head impact with a hard surface is directly along the longitudinal axis of the body (a subject falling head first), the 10 fps value does not apply since the head would receive the total kinetic energy of the entire mass of the body. Impacts with corners or edges are also extremely critical, even at velocities less than 10 fps. An impact velocity of 10 fps is considered to be generally safe for personnel who are in a fairly rigid posture; therefore, greater impact velocities can be tolerated if the body is in a more flexible position or if the area of impact is large.

(4) The effects of horizontal motion on the stability of personnel (throwing them off balance or hurling them laterally) depends on the body stance and position, the acceleration intensity and duration, and the rate of onset of the acceleration (jolt). An investigation of data concerning sudden stops in automobiles and passenger trains indicates that personnel can (depending on stance and jolt) sustain horizontal accelerations less than 0.4 g without being thrown off balance. These accelerations have durations of several seconds; hence the accelerations considered in this manual required to throw personnel off balance are probably greater because of their shorter durations and associated jolts. Therefore, the tolerable horizontal acceleration of 0.50 g required to provide protection against ground-shock effects resulting from nuclear detonations is recommended for nonrestrained personnel (standing, sitting, or reclining).

(5) If the vertical downward acceleration of the structure is greater than 1 g, relative movement between the subject and the structure is produced. As the structure drops beneath him, the subject begins to fall until such time that the structure slows down and the free falling subject overtakes and impacts with the structure. The impact velocity is equal to the relative velocity between the structure and the subject at the time of impact, and to assure safety it should not exceed 10 fps.

(6) To illustrate this vertical impact, a body which free falls for a distance equal to approximately 1½ feet has a terminal or impact velocity of 10 fps against another stationary body. If the second body had a downward velocity of 2 fps at the time of impact, then the impact velocity between the two bodies would be 8 fps.

(7) Because of the general activity required in

most manufacturing processes, attaching personnel to a structure to prevent displacement is not usually practical. However, in certain testing and other facility operations, this method of protection against structural motion may be useful. Although the possibility of the occurrence of impact associated with nonrestrained personnel is not a factor in protecting restrained subjects, the harmful effects associated with restraining can be more severe than for nonattached personnel. In addition to the direct interference with physical activity, discomfort, pain, trauma and, depending on the severity of the motion and the physical condition of the subject, mortality can occur. Other effects associated with long-duration vibrations, such as irritation and fatigue, are not likely because of the transient nature of the motions.

(8) Based on the available personnel vibration data, the following vibrational tolerances for restrained personnel were considered: 2 g for less than 10 cps, 5 g for 10–20 cps, 7 g for 20–40 cps, and 10 g above 40 cps. However, the use of acceleration tolerances greater than 2 g usually requires restraining devices too elaborate for most explosive handling or testing facilities.

c. Fragments. Human tolerance to fragment impact is very low. As mentioned in *b*(5) above, the impact of a relatively large mass with a velocity less than 10 fps against a subject can result in serious bodily injury. Also the impact of smaller masses with higher velocities can result in injuries as severe as those produced by larger masses. In general, complete protection must be afforded personnel from all falling and/or flying objects.

3–8. Equipment

a. Blast Pressures. Unless the equipment is of the heavy-duty type (motors, generators, etc.), equipment to be protected from blast pressures must be housed in shelter-type structures similar to those required for the protection of personnel. Under these circumstances, the equipment will be subjected to the blast pressures which are permitted to leak into the shelter through small openings. If the magnitude of these leakage pressures is minimized to a level consistent with that required for personnel protection, then in most cases protection from the direct effects of the pressures is afforded to the equipment. However, in some instances, damage to the equipment supports may occur which, in turn, can result in damage to the equipment as a result of falling. Also, if the equipment is located adjacent to the shelter openings, the jetting effects of the pressures entering the structure can have adverse effects on the equipment. In general, equipment should be positioned away from openings and securely supported.

b. Structural Motion and Shock.

(1) Damage to equipment can result in failures which can be divided into two classes: temporary and permanent. Temporary failures, often called "malfunctions", are characterized by temporary disruption of normal operation, whereas permanent failures are characterized by breakage, resulting in damage so severe that the ability of the equipment to perform its intended function is impaired permanently.

(2) The capacity of an item of equipment to withstand shock and vibration is conventionally expressed in terms of its "fragility level" which is defined as the magnitude of shock (acceleration) that the equipment can tolerate and still remain operational. The fragility level for a particular equipment item is dependent upon the strength of the item (frame, housing, and components) and, to some extent, the nature of the excitation to which it is subjected. An equipment item may sustain a single peak acceleration due to a transient input load, but may fail under a vibration-type input having the same peak acceleration amplitude. For this reason, fragility data should be considered in conjunction with such factors as the natural frequencies and damping characteristics of the equipment and its components, as well as the characteristics of the input used to determine the tolerance as compared to the motion of the structure which will house the equipment.

(3) The maximum shock tolerances for equipment vary considerably more than those for personnel. To establish the maximum shock tolerance for a particular item, it is necessary to perform tests or analyses. Only selected items of equipment have been tested to determine shock tolerances applicable for protection from the damage which may be caused by structural motions, with most of this data resulting from tests to sustain ground-shock motions due to a nuclear environment. However, data is available concerning general shock effects, indicating strength and ruggedness or sensitivity of equipment. This data, which is based primarily on transportation and conventional operational shock requirements, indicates that most commercial mechanical and electrical equipment items are able to sustain at least 3 g while fragile equipment (such as electronic equipment) can generally sustain 1.5 g.

(4) The above tolerances are safe values, and actual tolerances are in many cases higher than 3 g as indicated in table 3–2. However, the use of such acceleration values requires verification by shock testing with the induced motions (input) consistent with expected structural motions.

Table 3–2. Examples of Equipment Shock Tolerances

Equipment	*Peak acceleration*
Fluorescent light fixtures (with lamps)	20 to 30 g
Heavy machinery (motors, generators, transformers, etc. > 4,000 lbs)	10 to 30 g
Medium-weight machinery (pumps, condensers, AC equip. 1,000 to 4,000 lbs)	15 to 45 g
Light machinery (small motors < 1,000 lbs)	30 to 70 g

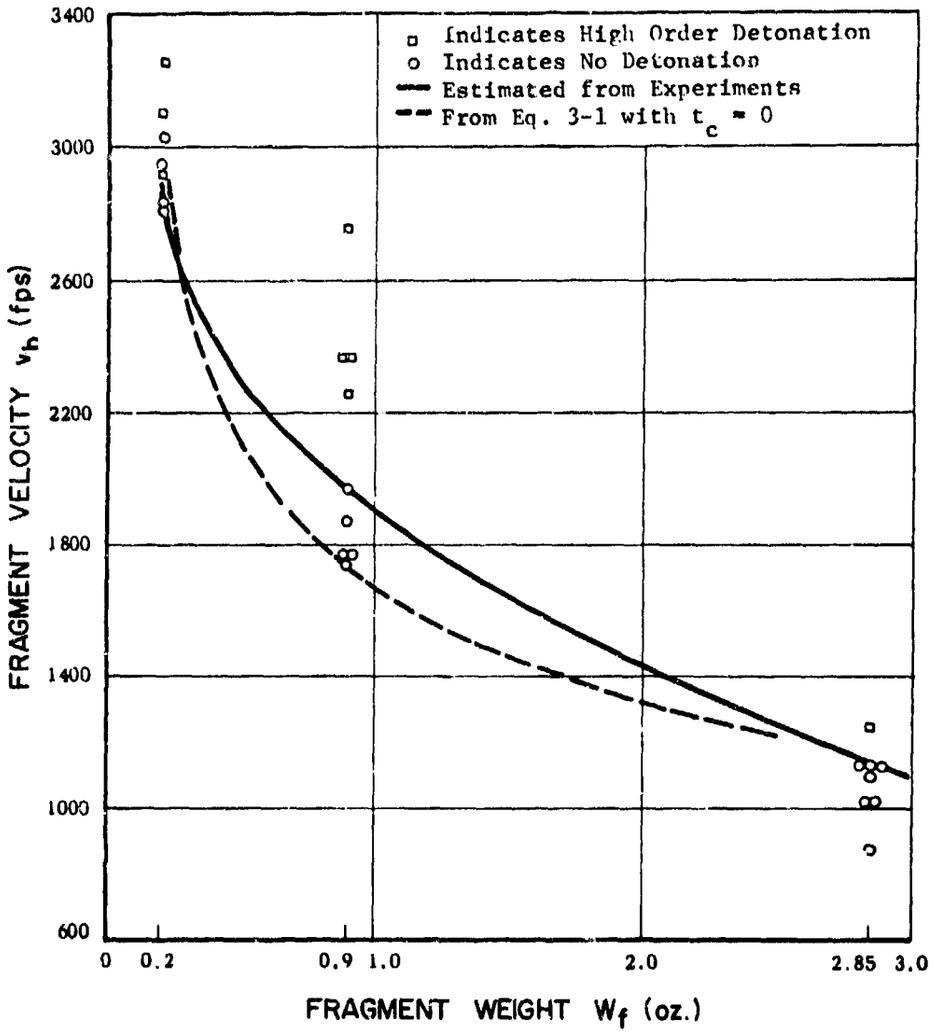


Figure 3-4. Boundary velocity curve for uncased pentolite.

c. Fragments.

(1) Susceptibility of an item of equipment to damage from fragment impact depends upon the ruggedness of its components, its container, if any, and upon the size and velocity of the fragment at the time of impact.

(2) Some heavy equipment (motors, generators, etc.) may sustain malfunctions as a result of the severing of electrical connections, etc., but seldom is destroyed as the result of the impact. On the other hand, more fragile equipment (electronic equipment, etc.) will generally be rendered inoperable due to the impact effects of large masses (of either low or high velocities). Light fragments with high velocities may also completely destroy fragile equipment. The impact force and penetration capability of the fragment may be such as to cause perforation of the equipment container and damage to the interior contents. Low-velocity, light fragments seldom result in severe damage. These fragments usually richochet beyond the equipment unless the component part of the equipment it strikes is glass or other fragile material, in which case, some damage may be inflicted.

(3) Although the damage to the equipment of a structure can be great as a result of falling or flying debris, the increased cost of strengthening walls and other portions of the protective structure is usually not justified unless personnel or acceptor charge protection is also required and/or the cost of the equipment item being protected exceeds the increased construction costs.

3-9. Explosives

a. General. The tolerances of explosives to blast pressure, structural motion, and impact differ for each type

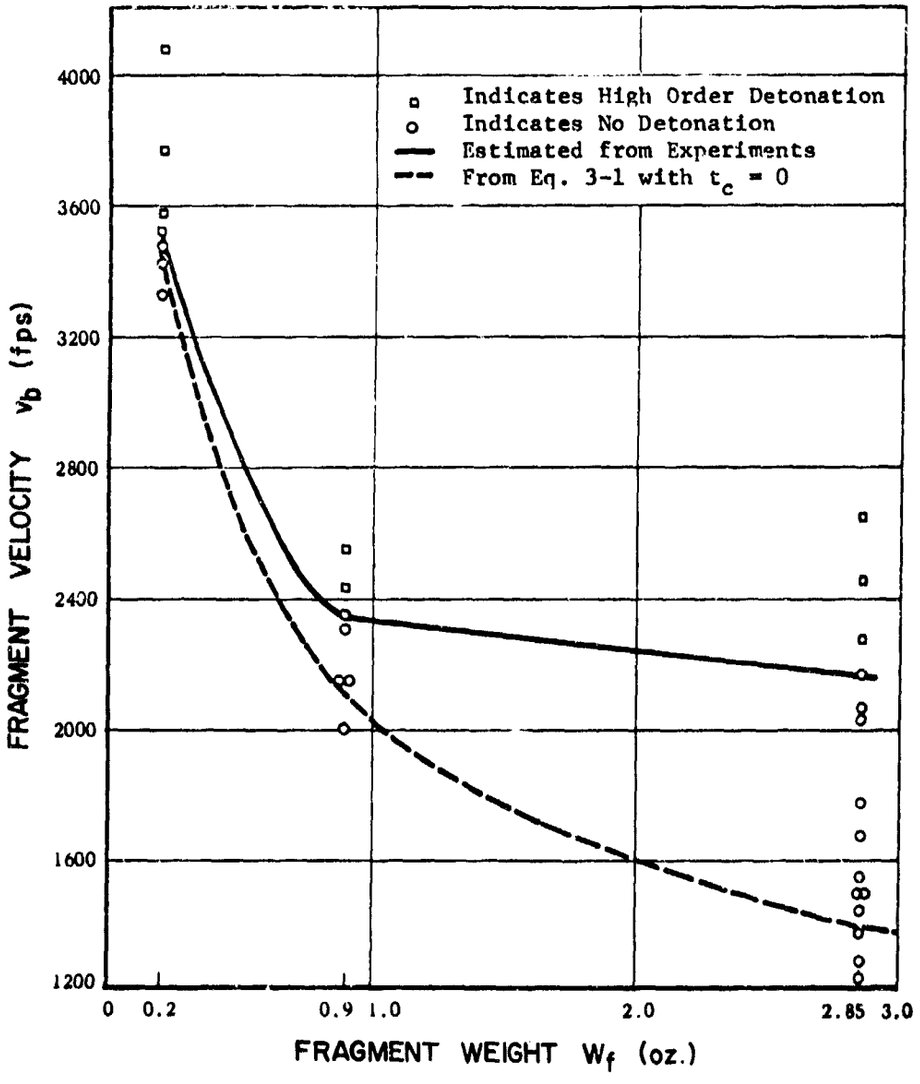


Figure 3-5. Boundary velocity curve for uncased cyclotol.

of explosive material with pressure and motion being the least cause of propagation.

b. Blast Pressures. Except in the region of extremely high pressures, most explosive materials are insensitive to the effects of blast pressures. In many instances, however, the secondary effects, such as dislodgment of the explosive from its support and propulsion of the explosive against hard surfaces, can result in a possible detonation depending upon the tolerance of the explosive to impact. Results of several different types of sensitivity tests (drop tests, card gap tests, friction tests, etc.) are presently available which aid in the establishment of the tolerance of most explosive materials to impact.

c. Structural Motions. Structural motion effects on explosives are similar to the impact effects produced by blast pressures. The movement of the structure tends to dislodge the explosive from its support resulting in an impact of the explosive with the floor or other parts of the structure. The distance the explosive falls and its sensitivity to impact and friction determine whether or not propagation occurs.

d. Fragments.

(1) Although blast pressure and structural motions can produce explosive propagation, the main source of communication of explosions is by primary fragments from the breakup of the donor casing, fragments produced by the fracture of a portion of the structure,

or disengagement of interior equipment. Only a smattering of information is available pertaining to the tolerance of explosives to fragment impact.

(2) A theoretical relationship has been established between the weight of a primary fragment W_f and the thickness of the acceptor casing t_c which defines the minimum or boundary velocity v_b at which propagation of an explosion occurs as a result of primary fragment impact:

$$v_b^2 = \frac{Ke^{(5.37 t_c/W_f^{1/3})}}{W_f^{2/3}(1+3.3t_c/W_f^{1/3})} \qquad \textbf{Equation 3-1}$$

where K is a constant that depends upon the sensitivity of the explosive material contained in the acceptor charge. The values of K have been derived from a number of experiments and are listed in table 3-3.

(3) Although the above relationship has not been verified for cased acceptor explosives, recent tests have indicated that equation 3-1 will give conservative estimates of the boundary velocities of uncased pentolite (fig. 3-4) and cyclotol (fig. 3-5) when impacted by light metal fragments.

Table 3-3. Impact Sensitivity Constant

Type of explosive	Impact sensitivity constant K
Amatol	14.50×10^6
Cyclotol (60/40)	4.10×10^6
Pentolite	2.78×10^6
RDX/TNT (70/30)	3.24×10^6
RDX/TNT (60/40)	4.15×10^6
TNT	16.30×10^6
Torpex	3.55×10^6

(4) Several testing methods have been developed to determine the sensitivity of explosives to impact by fragments. Although the number of tests performed has been small and only the impact effects of small quantities (maximum weight of 70 pounds) of concrete fragments or sand and gravel rubble have been investigated, the results do indicate that the boundary velocity for lightly cased composition B acceptor explosives for the conditions investigated is in the order of approximately 400 fps. Additional tests are required to determine if variation of the fragment mass and shape will affect the magnitude of the boundary velocity established to date.

Section IV. STRUCTURAL BEHAVIOR

3-10. Modes of Structural Behavior

The response of a structural element can be expressed in terms of two modes of structural behavior: (1) the *ductile mode* in which the element attains large inelastic deflections without complete collapse and (2) the *brittle mode* in which partial failure or total collapse of the element occurs. The selected behavior of an element for a particular design is governed by (1) the magnitude and duration of the blast output, (2) the occurrence of primary fragments, and (3) the function of the protective structure, i.e., shelter or barrier depending upon the protection level required.

3-11. Structural Behavior of Reinforced Concrete

a. General. As a reinforced-concrete element is dynamically loaded, the element deflects (with well-defined cracking (fig. 3-6)) until such time that: (1) the strain energy of the element is developed sufficiently to balance the kinetic energy produced by the applied loads and the element comes to rest, or (2) fragmentation of the concrete (fig. 3-7) occurs resulting in either partial or total collapse of the element. The maximum deflection attainable is a function of the span concrete dimensions and the type, amount, and details of the reinforcement used in a particular design.

b. Ductile Mode of Behavior of Laced Elements.

(1) To insure ductile behavior and to optimize the development of the available strain energy of reinforced



Figure 3-6. Tension cracks.



Figure 3-7. Fragmentation.

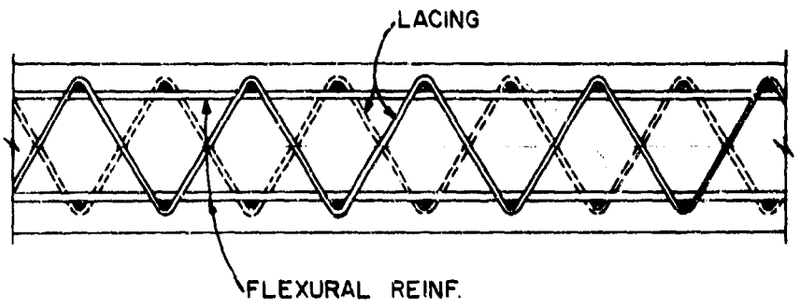


Figure 3-8. Lacing reinforcement.

concrete elements, it is often nesecsary to make basic changes in the reinforcement details in concrete elements used in blast-resistant design as compared to those utilized in conventional design. The element is reinforced symmetrically, i.e., the compression reinforcement is the same as the tension reinforcement. Also the straight flexural reinforcing bars on each face of the element and the intervening concrete are laced together (figs. 3-8 and 3-9) with continuous bent diagonal bars. This system of lacing contributes to the integrity of the protective element in the following several ways.

(*a*) Ductility of the flexural steel, including the strain hardening region, is fully developed.

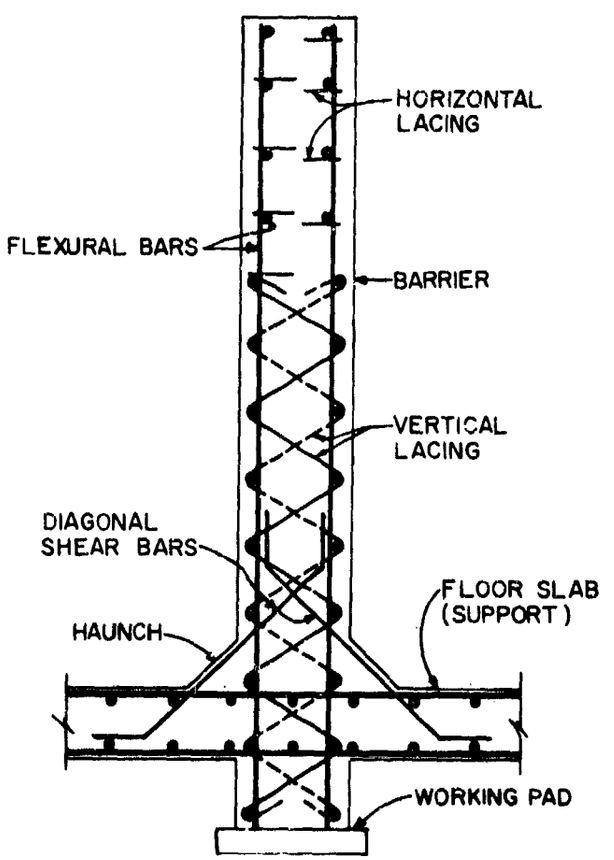


Figure 3-9. Typical laced wall.

(*b*) Integrity
layers of flexural r
massive cracking.

(*c*) Compres
buckling.

(*d*) High sh
sisted.

(*e*) Local sh
intensity of the pe

(*f*) Quantity
ments produced d
are reduced.

(2) The resis
demonstrates the
elements. The lacin
the strain hardenin
strain curve beyon
increases with inc
developed and ten
standard reinforcin
of the concrete fro
and buckling of th
failure long before
ment and the maxi

(3) Even witl
tion in strength (fig
or spalling of the
the element. The
stresses are transf
pression reinforcer
reduction is in pa
concrete cover.

(4) Lacing
strength to resist
the supports and i
by the strength

RESISTANCE

(*b*) Integrity of the concrete between the two layers of flexural reinforcement is maintained despite massive cracking.

(*c*) Compression reinforcement is restrained from buckling.

(*d*) High shear stresses at the supports are resisted.

(*e*) Local shear failure produced by the high intensity of the peak blast pressures is prevented.

(*f*) Quantity and velocity of post-failure fragments produced during the brittle mode of behavior are reduced.

(2) The resistance-deflection curve (fig. 3–10) demonstrates the action of laced reinforced concrete elements. The lacing enables the element to deflect until the strain hardening region (that portion of the stress-strain curve beyond the yield point where the strength increases with increasing strain) of the steel is fully developed and tension failure of the steel occurs. With standard reinforcing details, cracking and dislodgment of the concrete from between the reinforcement layers and buckling of the compression steel usually produce failure long before the ultimate strain of the reinforcement and the maximum energy absorption are attained.

(3) Even with laced reinforcement, a small reduction in strength (fig. 3-10) occurs because of the crushing or spalling of the concrete in the compression region of the element. The concrete fails and the compression stresses are transferred from the concrete to the compression reinforcement. The magnitude of the strength reduction is in part a function of the thickness of the concrete cover.

(4) Lacing reinforcement provides adequate strength to resist high shear stresses in the region of the supports and in the interior portions of the element by the strength of the lacing, by the development of dowel action of the flexural steel, and by developing the shear strength of the concrete remaining between the layers of reinforcement. Extension of the lacing and flexural reinforcement into the supports provides the required anchorage to assure full development of the flexural strength, and continuity of the lacing throughout the element prevents direct (pure) shear and diagonal tension failures.

(5) The need for high strength and large deflection capability requires the use of lacing in the design of some portions of structures located close to the detonation. Because blast loads associated with the blast effects of a close-in detonation are nonuniform and of high intensity, extremely high-pressure concentrations are developed which, in turn, can produce local (punching) failure of an element. With the use of lacing, however, the high shears produced in the vicinity of the concentrated loads are transferred to other areas of the element where the applied blast loads are less severe. In effect, the lacing tends to spread out the effects of non-uniformity of the loading. Lacing is also useful in those elements where large deflections are desirable. In these cases, the lacing not only resists the high shears but also maintains the integrity of the severely cracked concrete between the compression and tension reinforcement during the latter stages of deflection.

c. Ductile Mode of Behavior of Unlaced Elements.

(1) Structures located outside the immediate area of high blast intensity (high-pressure design range) can be designed without lacing. In the intermediate- and low-pressure design ranges, the distribution of the applied loads is fairly uniform and the deflections required to absorb the loading are considerably smaller than the deflections which can be realized with laced concrete elements.

(2) Results of high-explosive structura response

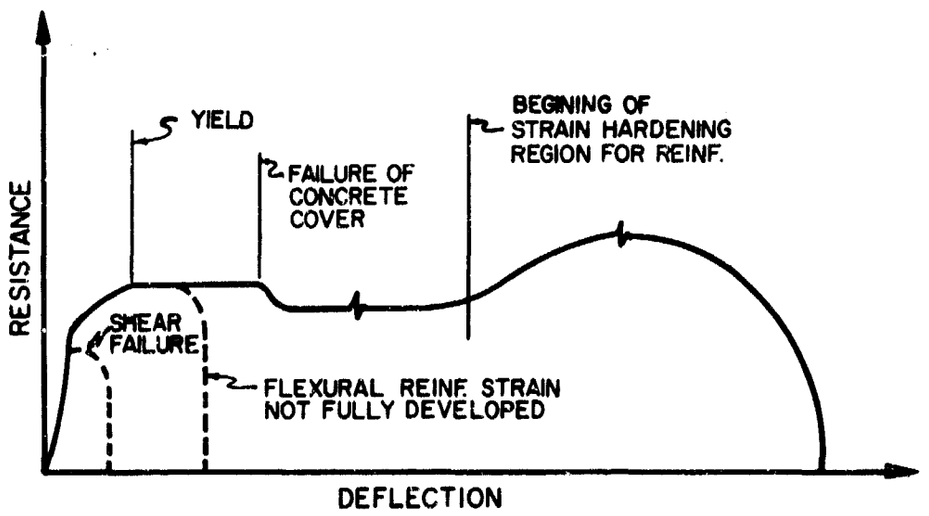


Figure 3–10. Resistance-deflection curve.

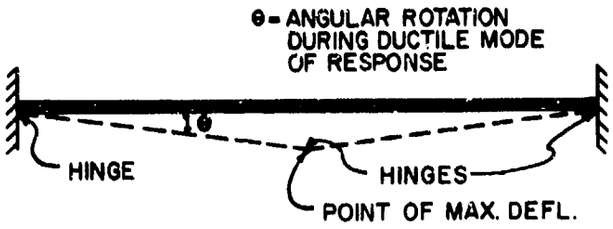


Figure 3–11. Support rotation.

tests have indicated that unlaced concrete elements, which do not fail because of insufficient shear capacity, begin to lose their structura' integrity after support rotations (fig. 3–11) in the order of 2 degrees are achieved. If additional shear strength above that afforded by the concrete is required in unlaced elements, then discontinuous loop stirrups or other conventional types of shear reinforcement may be used to fully develop the ultimate strength of the element.

d. Brittle Mode of Behavior.

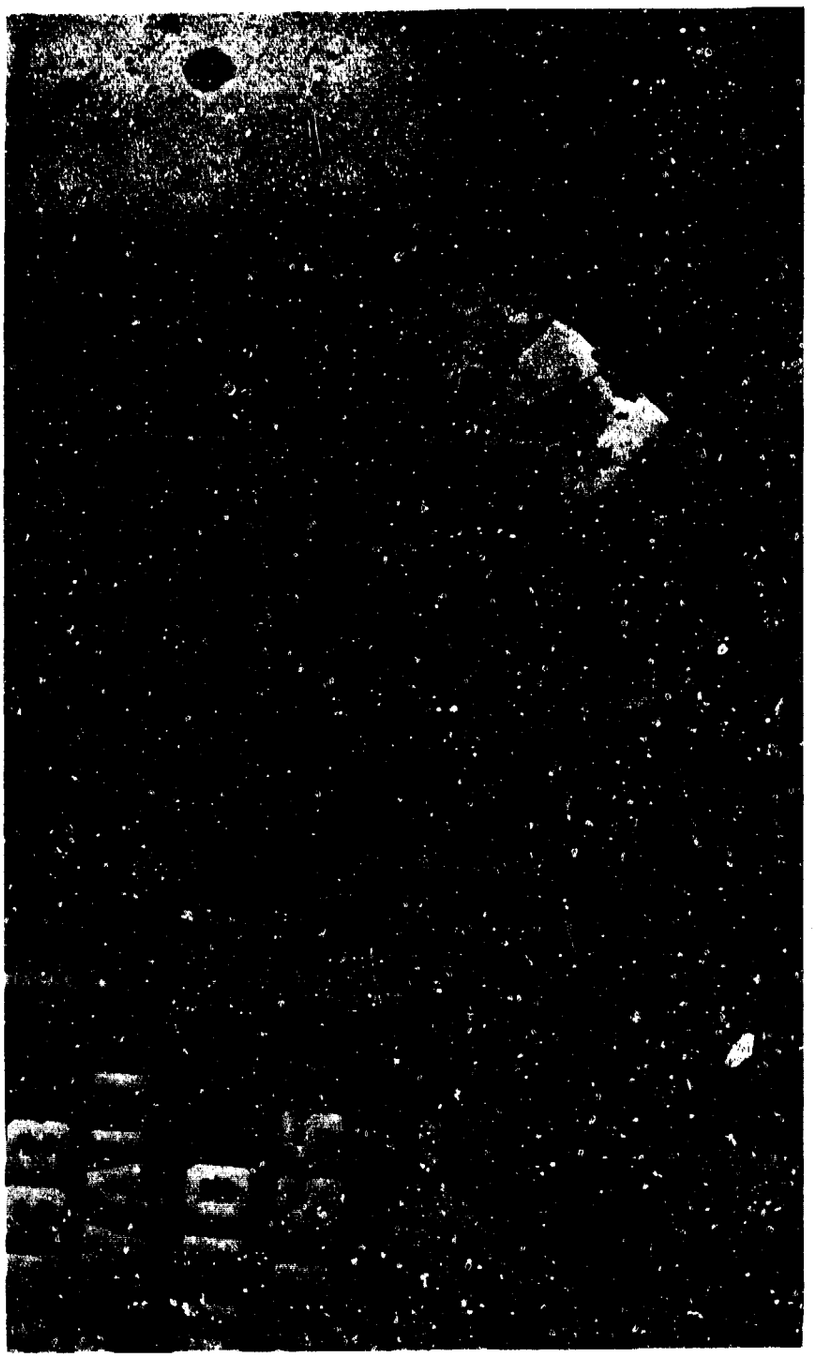
(1) The brittle behavior of reinforced concrete is composed of two types of concrete failure: (1) spalling which consists of the dynamic disengagement of the concrete cover over the flexural reinforcement, and (2) post-failure fragments which are formed by the collapse of the structure. The latter is usually the more serious. Post-failure fragments are generally large in number and/or size with velocities which can result in propagation of explosion. Spalling is usually only of concern in those protective structures where personnel, equipment, or sensitive explosives require protection, while controlled post-failure fragments are permitted where the receiver system consists of less sensitive explosives.

(2) Two types of spalling may occur: (1) direct spalling, at the free surfaces of the concrete, resulting from the reflection of high shock pressures of the blast wave being transmitted through the concrete, and (2) scabbing produced by large strains in the flexural reinforcement. Both direct spalling and scabbing will occur during the ductile mode of behavior. Because direct spalling is dependent upon the transmission of shock pressures, fragments formed from this type of spalling will be produced immediately after the blast pressures. Scabbing, on the other hand, will occur during the later stages of the flexural (ductile mode) action of the element. Both type of spalls will affect the capacity of the element to resist the applied blast loads.

(3) The failure characteristics of an element with laced reinforcement differ from those of other concrete elements. The size of failed sections of laced elements is fixed by the regions of maximum stress in the element where hinges form during the plastic (post-yield) range of response (fig. 3–11). After failure, the element between the hinges usually remains intact (fig. 3–12) whereas in unlaced elements, fragments are usually in the form of concrete rubble (fig. 3–13). Tests have shown that support rotations (fig. 3–14) of laced elements can reach or exceed 12° before failure occurs with resultant fragment velocities as low as 30 percent of the maximum velocity of the rubble formed from similarly loaded unlaced elements.

, and (2)
ural rein-
will occur
se direct
of shock
f spalling
ressures.
the later
f the ele-
ity of the

ent with
concrete
elements
e element
ld) range
ment be-
g. 3–12)
sually in
ests have
aced ele-
curs with
ent of the
similarly



2



Figure 3-13. Failure of an unlaced element.



Figure 3–14. Element at the verge of incipient failure.

CHAPTER 4

EFFECTS OF EXPLOSIONS

Section I. INTRODUCTION

4–1. Effects of Explosive Output

In the design of protective structures to resist the effects of accidental explosions, the principal effects of the explosive output to be considered are blast pressures and primary fragments. Of these two parameters, the blast pressures are usually the governing factor in the determination of the structure's response. However, in some situations, primary fragments from the explosive container may be just as important as the pressures in determining the configuration of the protective facility.

4–2. Scope

This chapter deals primarily with the blast pressures and associated structure loadings produced by explosions. Both unconfined explosions (air and surface bursts) and explosions which are confined or partially confined by surrounding structures or walls are considered. Although the quantitative data presented pertains to the blast output of bare TNT spherical or hemispherical charges considered as point source explosions, the data can be extended by appropriate means to include other potentially mass-detonating materials (solid, liquid, or gas) of varying shapes. In addition, this chapter discusses the velocity, weight, and number of primary fragments produced by the shattering of the metal container of cased explosives.

Section II. BLAST PRESSURE OUTPUT

4–3. Blast Phenomena

a. The blast effects of an explosion are in the form of a shock wave composed of a high-pressure shock front which expands outward from the center of the detonation with intensity of the pressures decaying with distance and as a function of time. As the wave front impinges on a protective structure, a portion of the structure or the structure as a whole will be engulfed by the shock pressures. The magnitude and distribution of the blast loads on the structure arising from these pressures are a function of the following factors: (1) explosive properties, namely, type of explosive material, energy output (high or low order detonation) and weight of explosive; (2) the location of the explosion relative to the protective structure; and (3) the magnitude and reinforcement of the pressure by its interaction with the ground, barrier, or the protective structure itself. The first of these three factors is discussed in *b* and *c* below and the latter two factors are discussed throughout the remainder of this chapter.

b. Explosive Materials.

(1) Explosive materials may be classified according to their physical state: (*a*) solids, (*b*) liquids, and (*c*) gases. Solid explosives are primarily high explosives; however, other materials such as chemicals and propellants may also be classified as potentially explosive materials. Liquid and gaseous explosives encompass a wide variety of substances used in the manufacture of chemicals, fuels, propellants, etc. The blast pressure environment produced will vary not only among the different materials but may also differ for a particular material. Such factors as methods and procedures used in manufacturing, storage, and handling, in addition to specific individual physical and chemical characteristics, may alter the blast effects of an explosive material.

(2) The blast effects of solid materials are best known. This is particularly true for high-explosive materials. The blast pressures, impulse, durations, and other blast effects of an explosion have been well established. These effects are contained in this chapter.

(3) Unlike high-explosive materials, other solid, liquid, and gaseous explosive materials will exhibit a variation of their blast pressure output. An explosion of these materials is in many cases incomplete, and only a portion of the total mass of the explosive (effective charge weight) is involved in the detonation process. The remainder of the mass is usually consumed by deflagration resulting in a large amount of the material's chemical energy being dissipated as thermal energy which, in turn, may cause fires. The discontinuance in the detonation process is produced by the physical and chemical properties of the material including its bimolecular structure, combining of the various physical

states, ineffective combining of the fuel and oxidizer, and other similar related factors.

c. *TNT Equivalent.*

(1) The major quantity of blast effects data presented in this manual pertains to the blast pressure output of TNT explosions. This data can be extended to include other potentially mass-detonating materials and explosives whose shapes differ from those considered in the manual by relating the explosive energy of the "effective charge weight" of these materials to that of an equivalent weight of TNT. The explosive energy of the effective charge weight is also equal to that of the total mass of the material. No clear-cut high-explosive equivalent may be utilized to define the blast effects of explosive materials other than high-explosives themselves. The blast effects of other materials in the anticipated environments must be analyzed and then related to the blast effects produced by the TNT explosion at the range of interest to obtain their equivalencies. To illustrate a typical analysis, explosive tests of certain propellant liquids and hydrocarbon mixtures have indicated that the explosive equivalent of these materials which relate both the peak blast pressures and impulse is constant over the entire intermediate- and low-pressure ranges. At higher pressures, the TNT equivalent will vary for each pressure level and will be different than the TNT equivalent which relates the impulse.

(2) For blast-resistant design in general, the TNT equivalent should be based upon a pressure and/or impulse relationship depending upon the anticipated pressure-design range. In addition to being a function of the comparable blast effects themselves, the equivalent will also be dependent upon the anticipated structural response. For the lower pressure ranges where structures respond to either the peak pressure or pressure pulse of the shock wave, the ratio of the weights of given explosives to that of TNT is given in table 4–1 for both peak pressure and impulse in pressure levels varying between 2 and 50 psi.

Table 4–1. Equivalent Weight Ratios for Free-Air Effects

Material	Peak pressure P_{so}	Impulse i_s
Comp A-3	1.09	1.07
Comp B	1.10	1.06
Comp B/TiH_2 (70/30)	1.13	1.13
Cyclotol (70/30)	1.14	1.09
Explosive D	0.85	0.81
HBX-1	1.21	1.21
HBX-3	1.16	1.25
H-6	1.27	1.38
Minol II	1.19	1.17
Pentolite	1.17	1.15
Picratol	0.90	0.93
RDX/Wax (98/2)	1.19	1.16
RDX/Wax (95/5)	1.19	1.16
TNT	1.00	1.00
TNETB	1.13	0.96
Torpex II	1.24	1.20
Tritonal (80/20)	1.07	1.11

Note. Data is applicable for pressure levels between 2 and 50 psi range for shock overpressure.

4–4. Blast-Loading Categories

a. The blast loading on structures can be divided into two main groups ((1) and (2) below) based upon the confinement of the explosive charge (unconfined and partially confined explosions) and further subdivided into blast-loading categories based upon the relative charge location and the blast loading produced on the structure. The relative charge locations are illustrated in figure 4–1.

(1) *Unconfined explosions.*

(*a*) *Free-air-burst loads.* The blast wave propagates away from the center of the explosion striking the structure without intermediate amplification of the initial shock wave.

(*b*) *Air-burst loads.* The explosion is located at a distance away from and above the structure so that ground reflections of the initial wave occur before the blast wave reaches the structure.

(*c*) *Surface-burst loads.* The explosion is located close to or on the ground so that the shock wave is amplified at the point of detonation due to ground reflections.

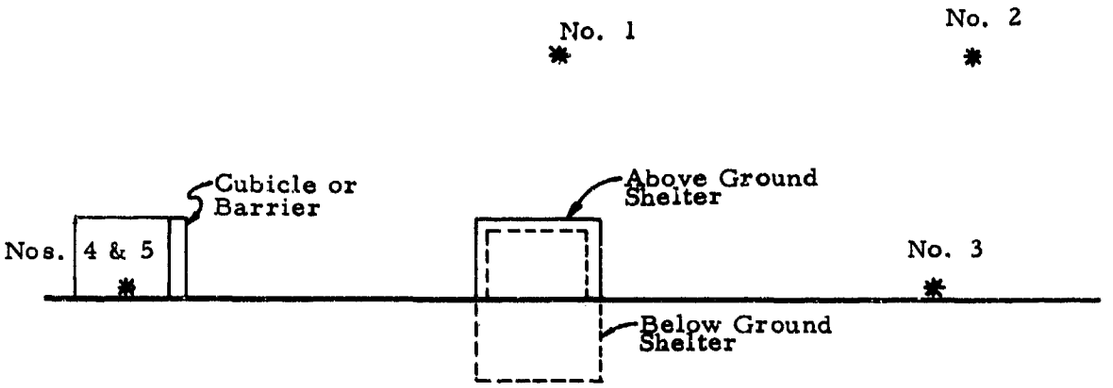
(2) *Partially confined explosions.*

(*a*) *Exterior or leakage-pressure loads.* The detonation occurs near the ground surface and behind an obstruction (barrier or within a cubicle) so that the shock wave is interfered with before reaching the structure.

(*b*) *Interior or high-pressure loads.* The detonation is located within or immediately adjacent to barrier-type structures and the blast pressures are amplified due to their multiple reflections by the structure as a result of the closeness of the structure to the explosion.

b. Protection of personnel and valuable equipment (receiver system) will usually involve protective shelters located away from the detonation. Their design may involve one or more of the following blast-loading categories: (1) free-air burst, (2) air burst, (3) surface burst, and (4) exterior or leakage pressure. These shelters are usually completely enclosed buildings located at pressure ranges of a few hundred psi or less. Depending on the design pressures, these structures can be either above, below, or at ground surface. For the fifth blast-loading category (interior or high pressure), protection is required immediately adjacent to the protective structure or barrier confining the explosion. The receiver portion of such an explosive system may include other explosive materials and/or personnel.

c. Of the five defined categories, those for air bursts



BLAST LOADING CATEGORIES		
Charge Confinement	Category	Protective Structure
Unconfined	1. Free Air Burst Loads 2. Air Burst Loads 3. Surface Burst Loads	Shelter
Partially Confined	4. Exterior or Leakage Pressure Loads	Shelter
	5. Interior or High Pressure Loads	Cubicle or Barrier

Figure 4–1. Blast-loading categories.

are seldom encountered and the free-air burst is the least likely to occur. The possibility of such blast environments exist where potentially explosive materials are stored at heights adjacent to, or away from, protective structures, such as in manufacturing (storage tanks, etc.) or missile sites. In the latter, the rocket propellant would be a source of explosive danger to the ground crew and control facilities.

d. The other three blast-loading categories can occur in most explosive manufacturing and storage facilities. In such installations, transportation of explosive materials between buildings either by rail, vehicle or, in the case of liquid or gases, through piping, is a requirement. Also storage and handling of explosives within a building is a requirement.

e. Although the blast-loading categories can be separated and classified individually, no clear-cut limits differentiate each category. In most explosive facilities the various blast environments will overlap, and judgment should be used in the application of the following recommendations for determining the blast parameters consistent with the various blast-loading categories.

4–5. Blast-Wave Phenomena

a. The violent release of energy from a detonation in a gaseous medium gives rise to a sudden pressure increase in that medium. The pressure disturbance, termed the blast wave, is characterized by an almost instantaneous rise from the ambient pressure to a peak incident pressure P_{so}. This pressure increase or shock front travels radially from the burst point with a diminishing velocity U which is always in excess of the sonic velocity of the medium. Gas molecules, making up the front, move at lower velocities u. This latter particle velocity is associated with a dynamic pressure or the pressure formed by the winds produced by the shock fronts. As the shock front expands into increasingly larger volumes of the medium, the peak incident pressure at the front decreases and the duration of the pressures increases.

b. At any point away from the burst, the pressure disturbance has the shape shown in figure 4–2. The shock front arrives at time t_A and, after the rise to the peak value, the incident pressure decays to the ambient

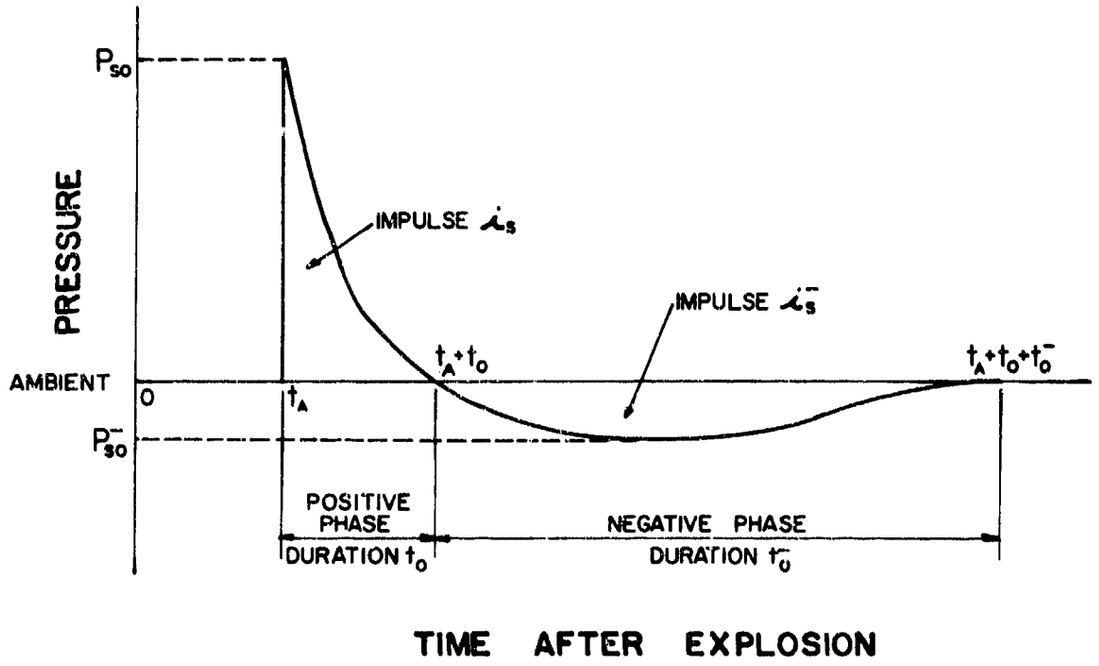


Figure 4-2. Free field pressure time variation.

value in the time t_o which is the positive phase duration. This is followed by a negative phase with a duration t_o^- longer than the positive phase and characterized by a pressure below the pre-shot ambient pressure (maximum value of P_{so}^-) and a reversal of the particle flow. The negative phase is usually less important in a design than is the positive phase. The incident impulse density (hereafter referred to as unit incident impulse) associated with the blast wave is the integrated area under the pressure-time curve and is denoted as i_s for the positive phase and i_s^- for the negative phase.

c. If the shock wave impinges on a rigid surface oriented at an angle to the direction of propagation of the wave, a reflected pressure is instantly developed on the surface, and the pressure is raised to a value in excess of the incident pressure. The reflected pressure is a function of the pressure in the incident wave and the angle formed between the rigid surface and the plane of the shock front. For a reflector, where flow around an edge or edges occurs, the duration of the reflected pressures is controlled by the size of the reflecting surface. The high reflected pressure seeks relief toward the lower pressure regions, and this tendency is satisfied by the propagation of rarefaction waves from the low- to the high-pressure region. These waves, traveling at the velocity of sound in the reflected pressure region, reduce the reflected pressures to the stagnation pressure which is the value that is in equilibrium with the high-velocity air stream associated with the incident pressure wave. When such a relief is not possible, for example when an incident wave strikes an infinite surface, the incident pressure at every point in the wave will be reflected, and these reflected pressures will last for the duration of the wave.

d. The peak positive reflected pressure is designated P_r, the peak negative reflected pressure P_r^-, and the unit impulses associated with a completely reflected incident wave are i_r for the positive phase and i_r^- for the negative phase.

e. An additional parameter of the blast wave, the wave length, is sometimes required in the analysis of structures. The positive phase wave length L_w is that length at a given distance from the detonation which, at a particular instant of time, is experiencing positive pressures. The negative wave length L_w^- is similarly defined for negative pressures.

f. The above treatment of the blast wave phenomena is general. In subsequent sections of this chapter, the magnitudes of the various parameters are presented depending upon the category of the detonation as previously described: free-air burst, air burst, surface burst, exterior or leakage pressure, or interior or high-pressure blast loading.

Section III. UNCONFINED EXPLOSIONS

4–6. Free-Air Burst

a. When a detonation occurs adjacent to and above a protective structure such that no amplification of the initial shock wave occurs between the explosion source and the protective structure, then the blast loadings acting on the structure are free-air-burst blast pressures (fig. 4–3).

b. As the incident pressure wave moves radially away from the center of the explosion, it will come in contact with the structure, and, upon contact, the initial wave pressures and impulse are reinforced and reflected (fig. 4–4). typic

c. orien trave point (nor phas vary dista the p the sl and sphe the s

d. on tl value angle dista struc

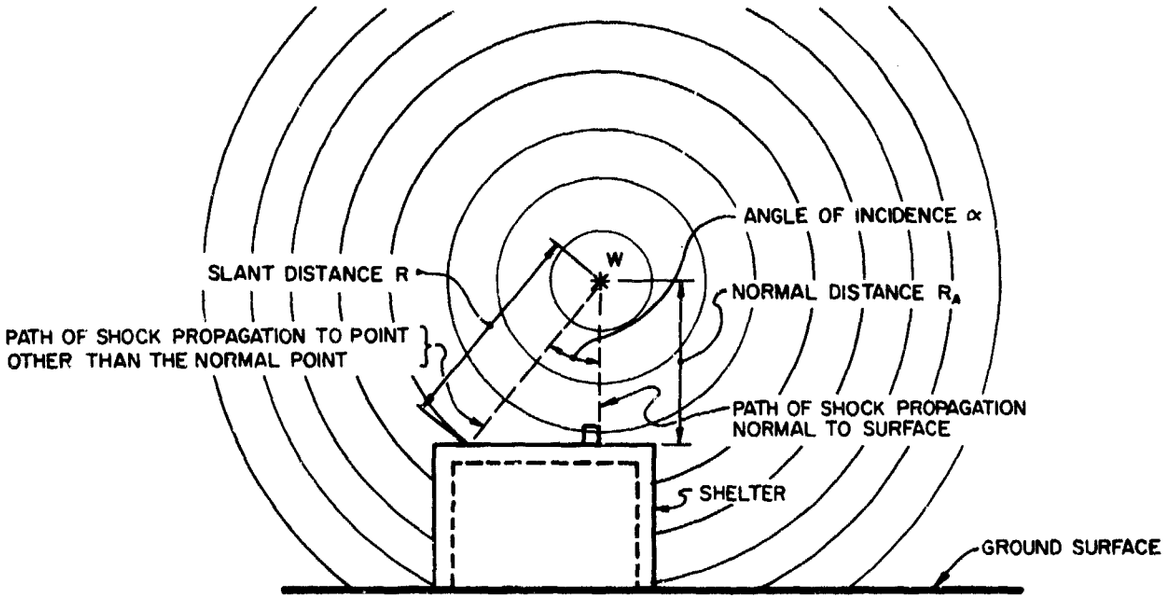


Figure 4–3. Free-air-burst blast environment.

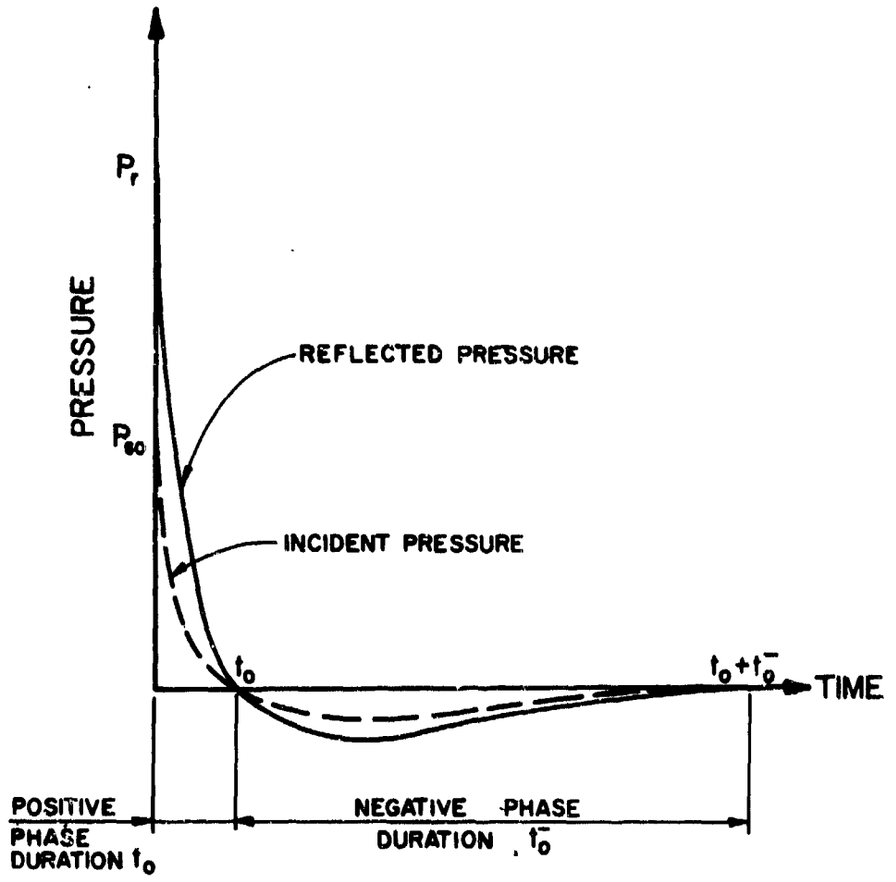


Figure 4–4. Pressure-time variation for free air burst.

4–4). The reflected pressure pulse of figure 4–4 is typical for infinite plane reflectors.

c. When the shock wave impinges on a surface oriented so that a line which describes the path of travel of the wave is normal to the surface, then the point of initial contact is said to sustain the maximum (normal reflected) pressure and impulse. The positive phase pressure and impulse patterns on the structure vary with distance from a maximum at this normal distance R_A to a minimum (incident pressure) where the plane of the structure's surface is perpendicular to the shock front. The peak pressures, impulses, velocities, and other parameters of this shock environment for a spherical TNT explosion are given in figure 4–5 versus the scaled distance ($Z = R_A/W^{1/3}$).

d. The variation of the pressure and impulse patterns on the surface between the maximum and minimum values is a function of the angle of incidence α. This angle is formed by the line which defines the normal distance R_A between the point of detonation and the structure and the line R which defines the path of shock propagation between the center of the explosion and any other point in question.

e. The effect of the angle of incidence on the peak reflected pressures is shown in figure 4–6 which is a plot of the angle of incidence versus the peak reflected pressure coefficient as a function of the peak incident pressure. The peak reflected pressure $P_{r\alpha}$ is obtained by multiplying the peak reflected pressure coefficient $C_{r\alpha}$ by the peak incident pressure P_{so}. For design purposes, the other blast parameters except the duration of the wave may be taken as those corresponding to the reflected pressure $P_{r\alpha}$ and are obtained from figure 4–5. The duration of the blast wave corresponds to the duration of the free air pressures.

4–7. Air Burst

a. The air burst blast environment is produced by detonations which occur above the ground surface and at some distance away from the protective structure so that the initial shock wave, propagating away from the explosion, impinges on the ground surface prior to

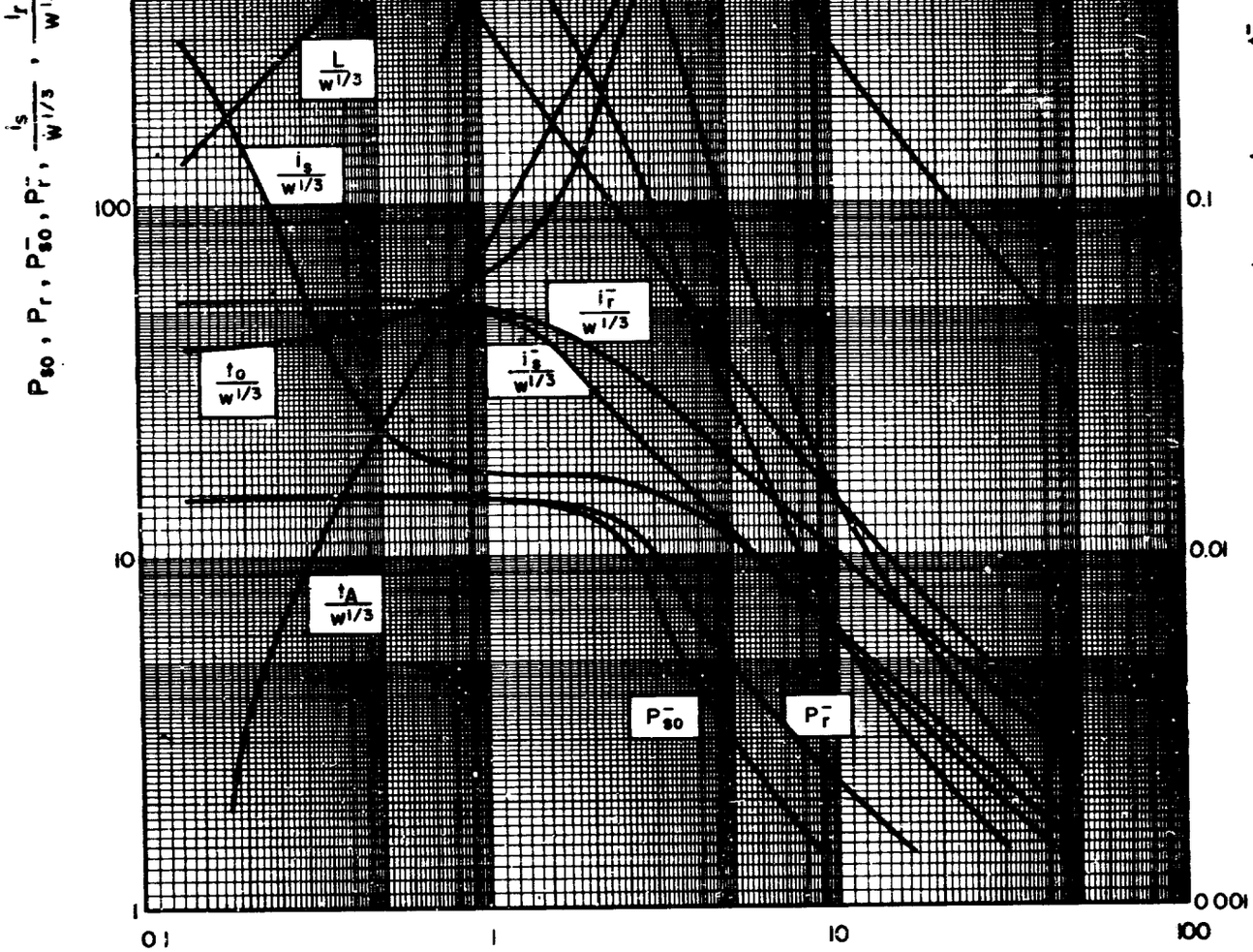
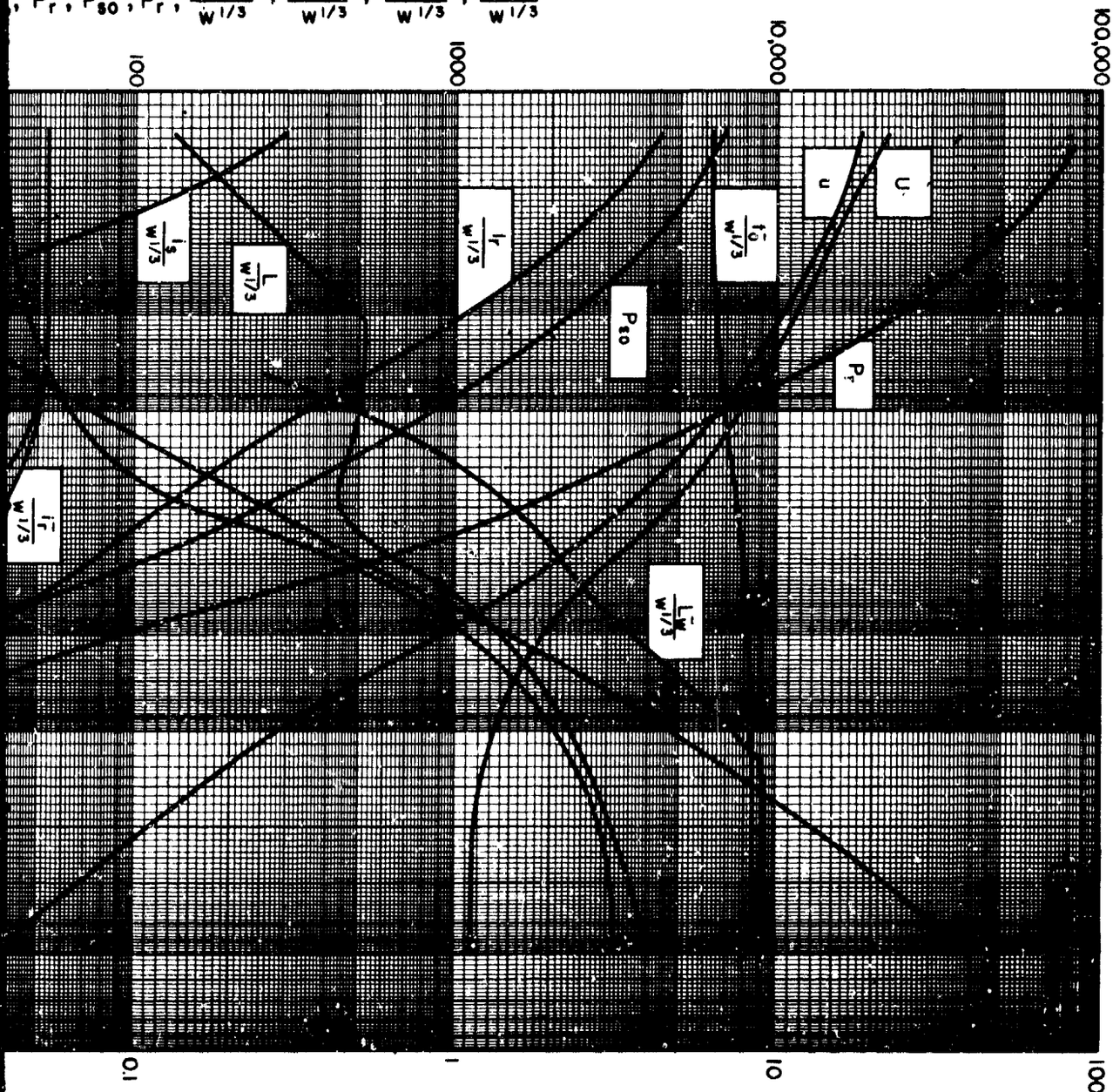


Figure 1-6. Shock-wave parameters for spherical TNT explosion in free air

P_{so} = Peak Positive Incident Pressure, psi
P_{so}^- = Peak Negative Incident Pressure, psi
P_r = Peak Positive Normal Reflected Pressure, psi
P_r^- = Peak Negative Normal Reflected Pressure, psi
$i_s/W^{1/3}$ = Scaled Unit Positive Incident Impulse, psi-ms/lb$^{1/3}$
$i_s^-/W^{1/3}$ = Scaled Unit Negative Incident Impulse, psi-ms/lb$^{1/3}$
$i_r/W^{1/3}$ = Scaled Unit Positive Normal Reflected Impulse, psi-ms/lb$^{1/3}$
$i_r^-/W^{1/3}$ = Scaled Unit Negative Normal Reflected Impulse, psi-ms/lb$^{1/3}$
$t_A/W^{1/3}$ = Scaled Time of Arrival of Blast Wave, ms/lb$^{1/3}$
$t_o/W^{1/3}$ = Scaled Positive Duration of Positive Phase, ms/lb$^{1/3}$
$t_o^-/W^{1/3}$ = Scaled Negative Duration of Positive Phase, ms/lb$^{1/3}$
$L_w/W^{1/3}$ = Scaled Wave Length of Positive Phase, ft/lb$^{1/3}$
$L_w^-/W^{1/3}$ = Scaled Wave Length of Negative Phase, ft/lb$^{1/3}$
U = Shock Front Velocity, ft/ms
u = Particle Velocity, ft/ms
W = Charge Weight, lbs
R = Radial Distance from Charge, ft
Z = Scaled Distance, ft/lb$^{1/3}$

$, P_r, P_{so}^-, P_r^-, \frac{i_s}{W^{1/3}}, \frac{i_r}{W^{1/3}}, \frac{i_s^-}{W^{1/3}}, \frac{i_r^-}{W^{1/3}}$



$\frac{t_A}{W^{1/3}}, \frac{t_o}{W^{1/3}}, \frac{t_o^-}{W^{1/3}}, \frac{L_w}{W^{1/3}}, \frac{L_w^-}{W^{1/3}}, U, u$

ameters for spherical TNT explosion in free air at sea level.

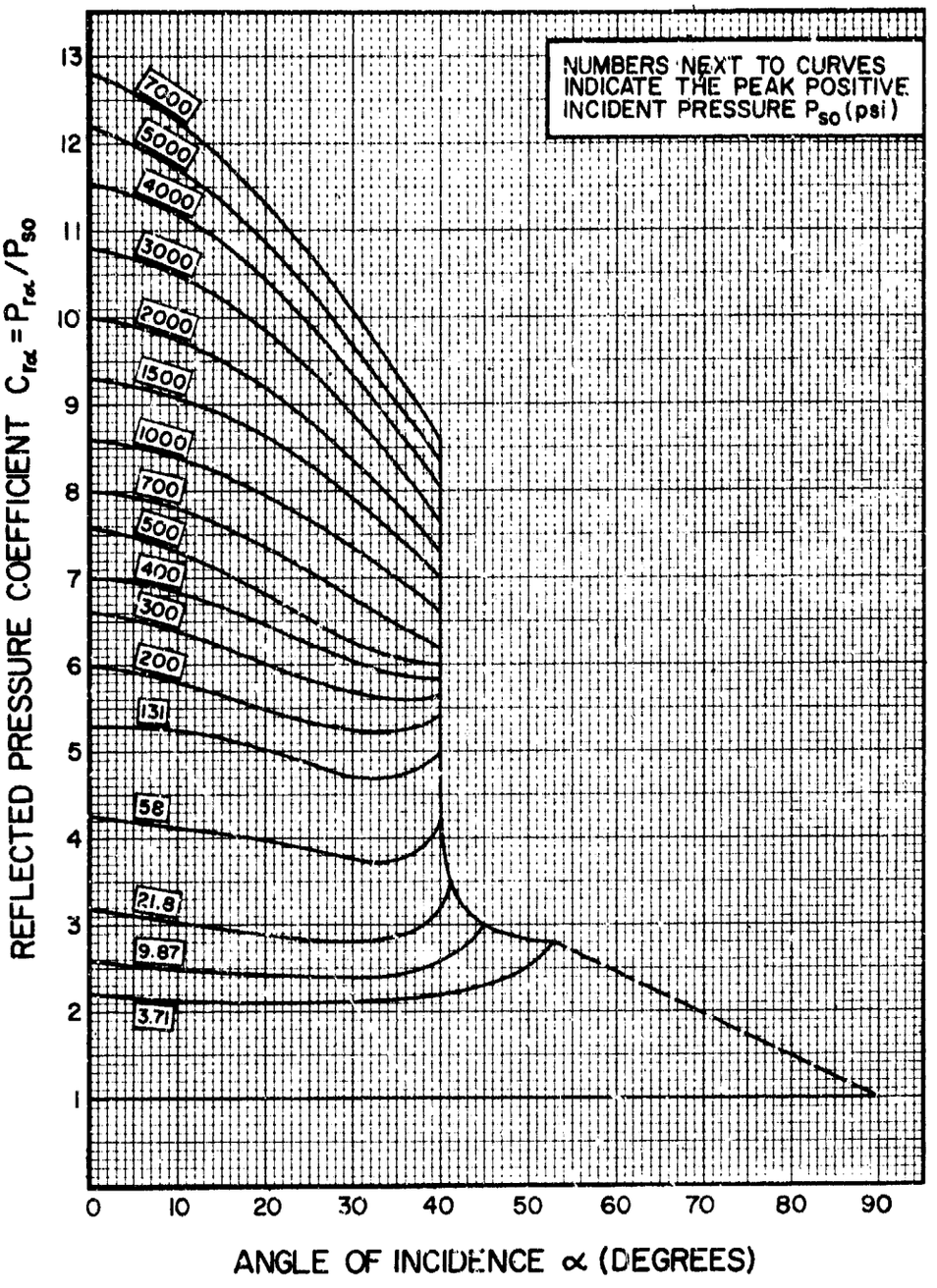


Figure 4–6. Reflected pressure coefficient vs. angle of incidence.

arrival at the structure. As the blast wave continues to propagate outward, a front known as the Mach front (fig. 4–7) is formed by the interaction of the initial wave (incident wave) and the reflected wave which is the result of the reinforcement of the incident wave by the ground.

b. Some variation of the pressures over the height of the Mach front occurs but, for design purposes, this variation can be neglected and the shock considered as a plane wave over the full height of the front. The pressure-time variation of the Mach front (a, fig. 4–8) is similar to that of the incident wave except that the magnitude of the pressure is somewhat larger.

c. The height of the Mach front increases as the

wave propagates away from the center of the detonation. This increase in height is referred to as the path of the triple point and is formed by the intersection of the initial, reflected, and Mach waves. A protective structure is subjected to a plane wave (uniform pressure) when the height of the triple point exceeds the height of the structure. The scaled height of the triple point H_T versus scaled distance Z and scaled charge height H_C is plotted in figure 4–9.

d. If the height of the triple point does not extend above the height of the structure, then the magnitude of the applied loads will vary with the height of the point considered. Above the triple point, the pressure-time variation consists of an interaction of the incident

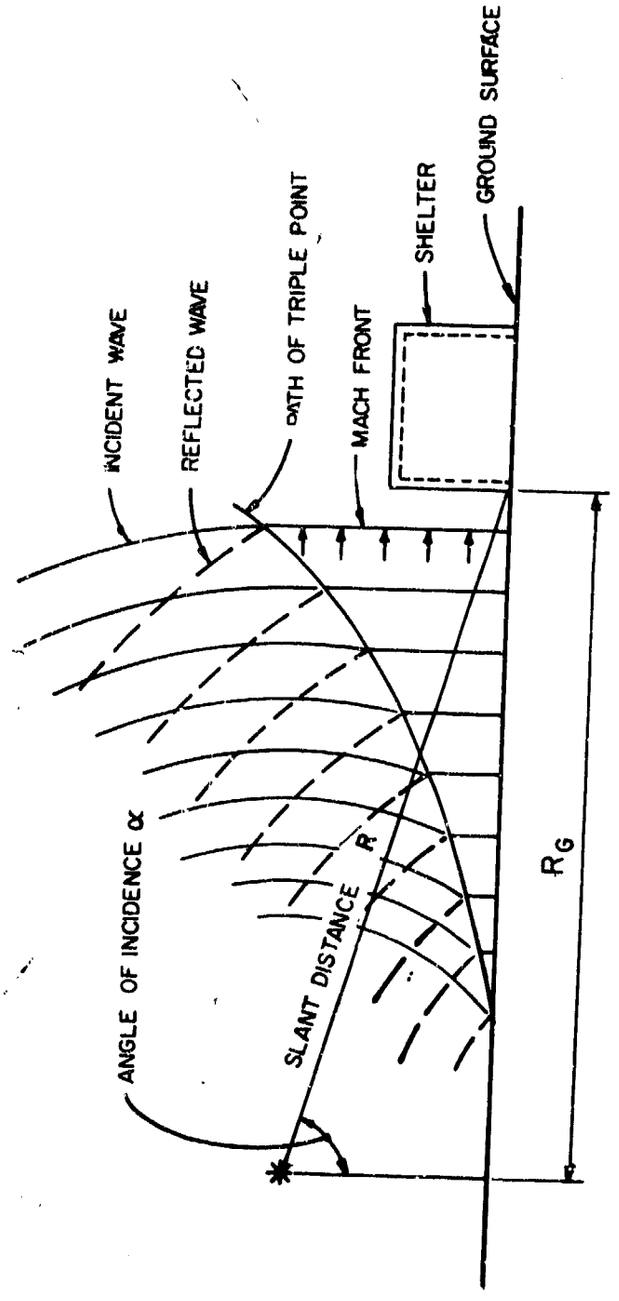


Figure 4–7. Air burst blast environment.

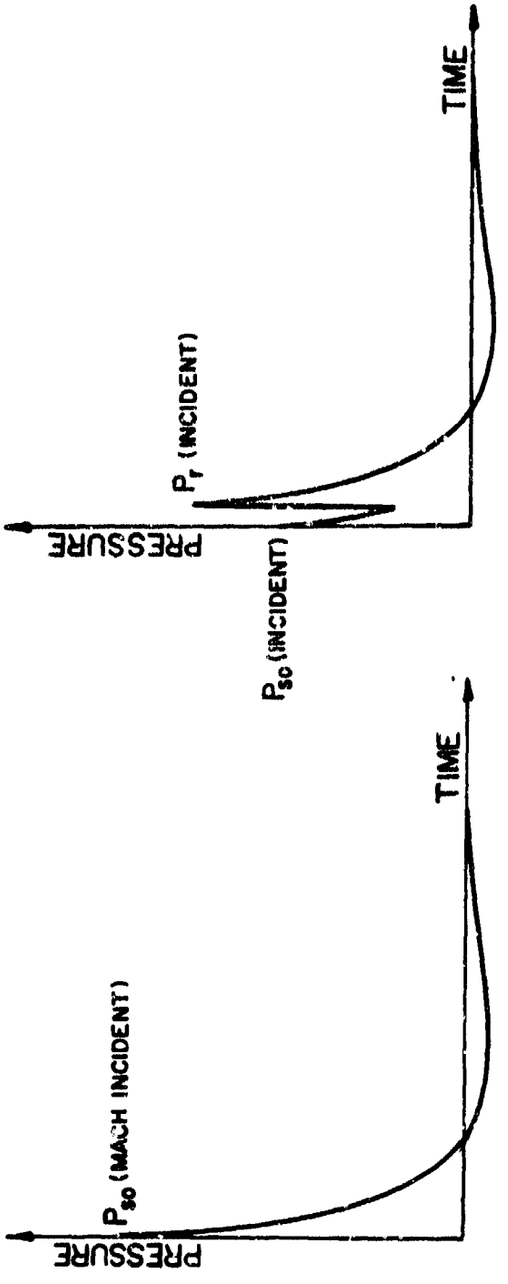


Figure 4-8. Pressure-time variation for air burst.

and reflected incident wave pressures resulting in a pressure-time variation (b, fig. 4–8) different from that of the Mach incident wave pressures. The magnitude of pressures above the triple point is smaller than that of the Mach front. In most practical design situations, the location of the detonation will be far enough away from the structure so as not to produce this pressure variation. An exception may exist for multi-story buildings although these buildings are usually located at very low-pressure ranges where the triple point is high.

e. For determining the magnitude of the blast loads acting on the surface of an above-ground protective structure, the peak incident blast pressures in the Mach

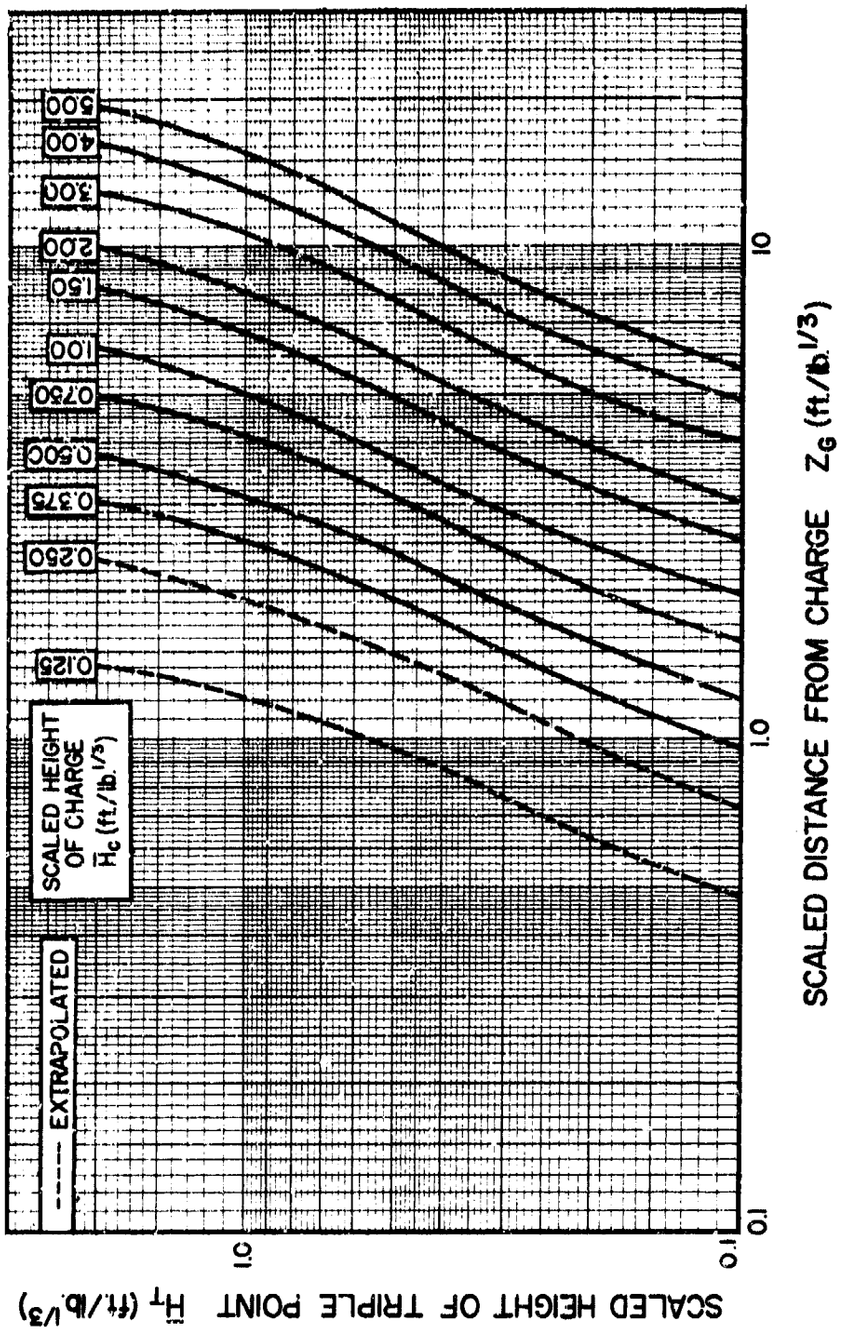


Figure 4–9. Scaled height of triple point.

wave acting on the ground surface immediately before the structure are calculated first. The peak incident free-air pressure is determined for this point from figure 4–5 using the distance R (fig. 4–7) which corresponds to the path of the initial shock wave between the explosive source and any point on the ground surface beyond the point at which the Mach wave is formed.

Once the incident free-air pressure is obtained, then the peak incident pressure P_m in the Mach wave is computed from figure 4–6, using the predetermined values of the angle of incidence α and the peak incident free-air pressure. Other blast parameters of the Mach wave are determined from figure 4–5 in a manner similar to that used for reflected free-air pressures.

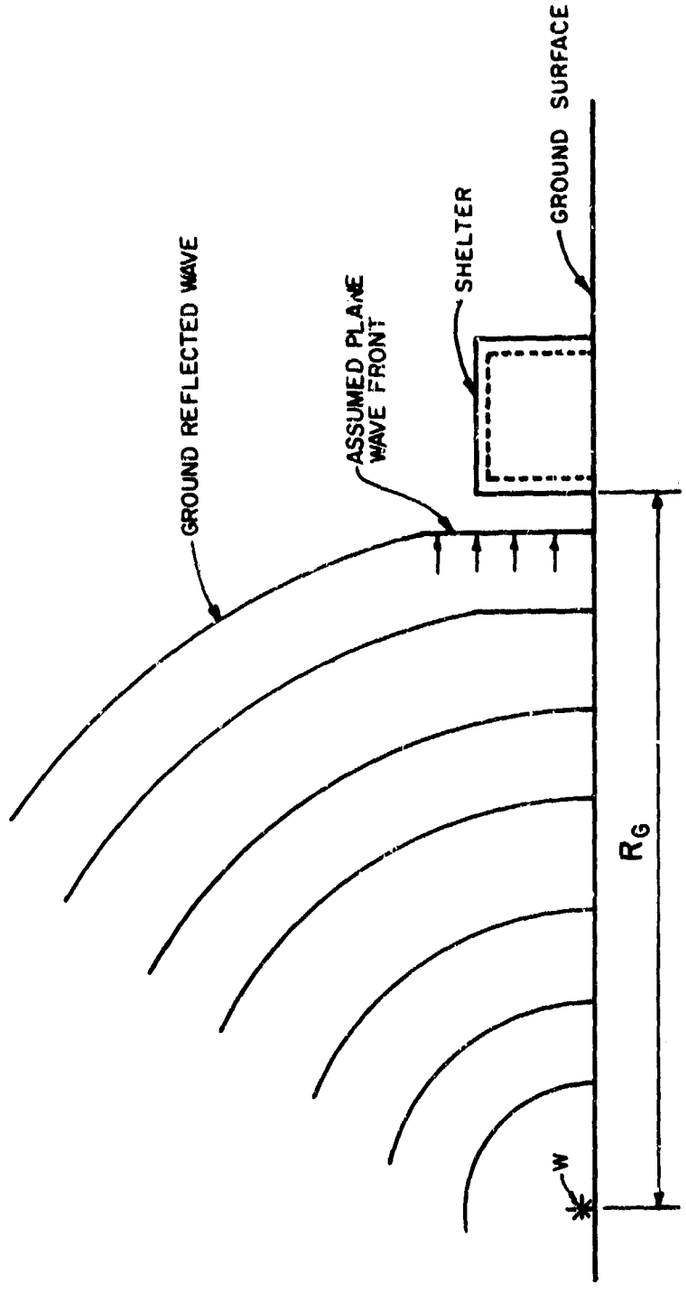


Figure 4–10. Surface burst blast environment.

4–8. Surface Burst

a. A charge located on or very near the ground surface is considered to be a surface burst. The initial wave of the explosion is reflected and reinforced by the ground surface to produce a reflected wave. Unlike the air burst, the reflected wave merges with the incident wave at the point of detonation to form a single wave similar in nature to the reflected wave of the air burst but essentially hemispherical in shape (fig. 4–10).

b. Quite often a theoretical procedure utilizing the charge reflection factor method is used to estimate the

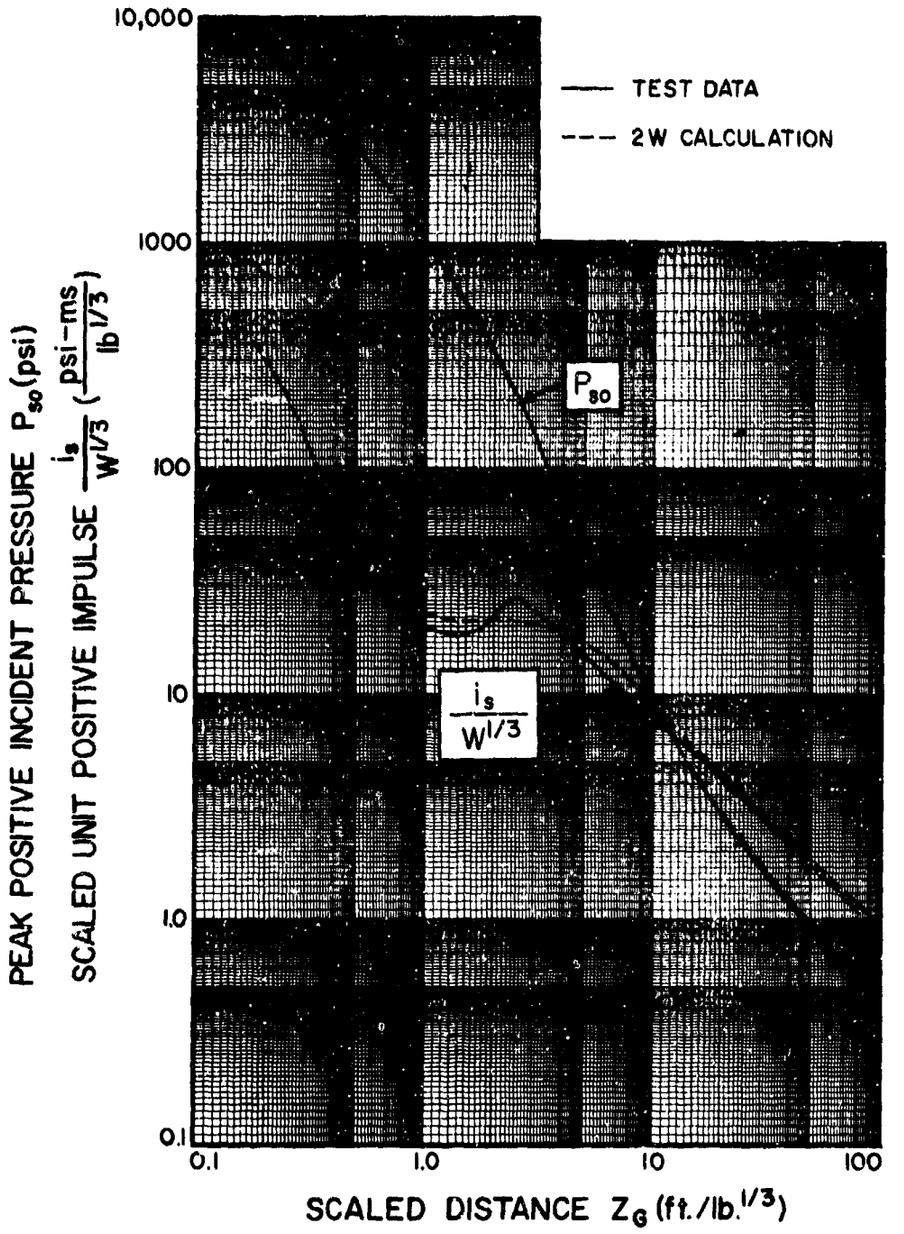


Figure 4–11. Incident pressure and scaled incident impulse vs. scaled distance for surface burst (hemispherical charges).

magnitude of the incident pressures, impulses, and other blast parameters resulting from surface bursts. This method assumes that the explosive output of a detonation on the ground is equivalent to that produced by a larger quantity of explosive detonated in free air. The use of this procedure is demonstrated by the comparison of the pressure-distance and impulse-distance data obtained from hemispherical TNT surface-burst tests and calculated by the theoretical method (fig. 4–11). Here the pressure-distance relationship, as predicted by the test data, can be duplicated by varying the value of the reflected charge from 1.3W at the 3,000 psi range to 2W at 10 psi. For pressure levels less than 10 psi, pressure values calculated using reflected charges less than 2W will correspond to those obtained from the test data. If the 2W reflected charge

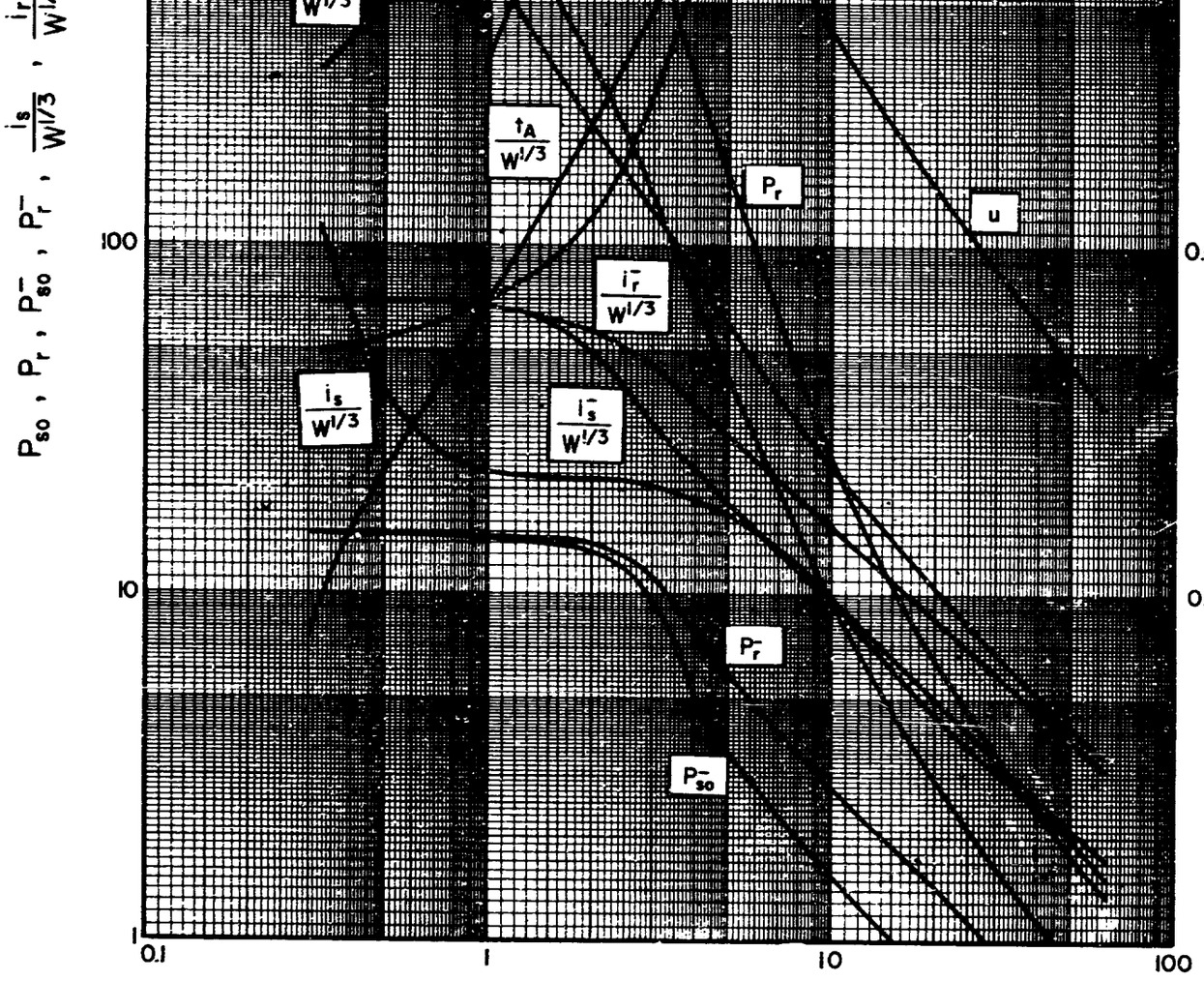
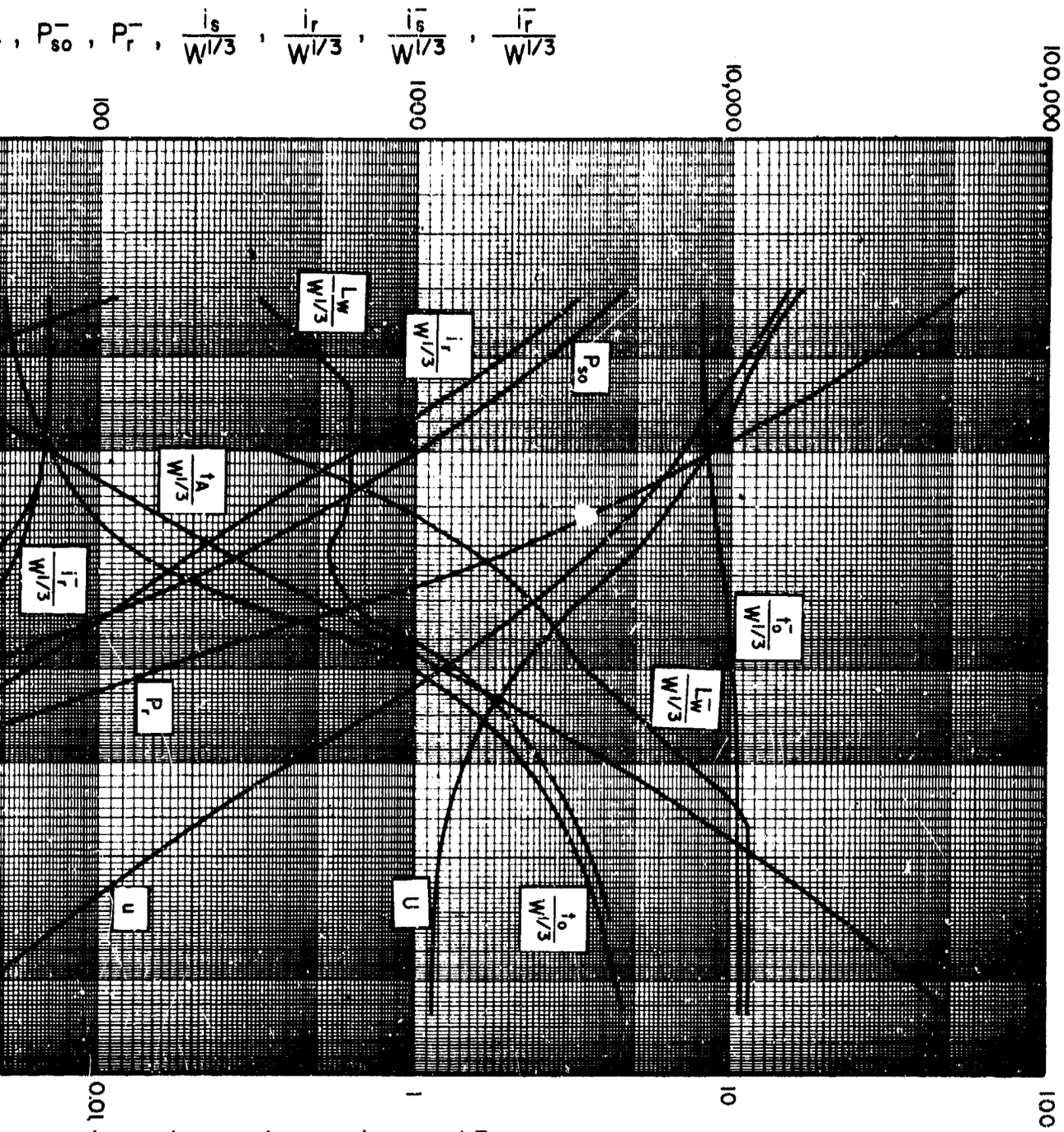


Figure 4-18. Shock-wave parameters for hemispherical TNT surface explosion

P_{so} = Peak Positive Incident Pressure, psi
P_{so}^- = Peak Negative Incident Pressure, psi
P_r = Peak Positive Normal Reflected Pressure, psi
P_r^- = Peak Negative Normal Reflected Pressure, psi
$i_s/W^{1/3}$ = Scaled Unit Positive Incident Impulse, psi-ms/lb$^{1/3}$
$i_s^-/W^{1/3}$ = Scaled Unit Negative Incident Impulse, psi-ms/lb$^{1/3}$
$i_r/W^{1/3}$ = Scaled Unit Positive Normal Reflected Impulse, psi-ms/lb$^{1/3}$
$i_r^-/W^{1/3}$ = Scaled Unit Negative Normal Reflected Impulse, psi-ms/lb$^{1/3}$
$t_A/W^{1/3}$ = Scaled Time of Arrival of Blast Wave, ms/lb$^{1/3}$

$t_o/W^{1/3}$ = Scaled Positive Duration of Positive Phase, ms/lb$^{1/3}$
$t_o^-/W^{1/3}$ = Scaled Negative Duration of Positive Phase, ms/lb$^{1/3}$
$L_w/W^{1/3}$ = Scaled Wave Length of Positive Phase, ft/lb$^{1/3}$
$L_w^-/W^{1/3}$ = Scaled Wave Length of Negative Phase, ft/lb$^{1/3}$
U = Shock Front Velocity, ft/ms
u = Particle Velocity, ft/ms
W = Charge Weight, lbs
R = Radial Distance from Charge, ft
Z_G = Scaled Ground Distance, ft/lb$^{1/3}$



ers for hemispherical TNT surface explosion at sea level.

is used to calculate pressure values less than 10 psi, then these values will differ from those pressures obtained from test data at corresponding ranges by approximately 10 percent (fig. 4–1). Test results of the scaled impulse show good agreement with those obtained by the application of the 2W reflected charge over the entire pressure range considered in the comparison. The impulse from the theoretical method, however, is generally conservative relative to the test results over the major portion of the range. Other blast parameters acquired from hemispherical surface burst tests were compared to those obtained using the theoretical method. Except for the durations of the positive phase pressures at the high-pressure levels, the comparison of the two methods showed good agreement. As will be shown later, the design of protective structures against the effects of surface bursts will not usually be required for high-pressure levels and, therefore, this variance may be neglected.

c. The parameters of the surface burst environment for TNT explosions are given in figure 4–12. A comparison of figures 4–5 and 4–12 shows that, at a given distance from a detonation of the same weight of explosive, all of the parameters of the surface burst environment are larger than those for the free-air environment.

d. As for the case of air bursts, protective structures subjected to the explosive output of a surface burst will usually be located in the pressure regions where the plane wave (fig. 4–10) concept can be applied. Therefore, for surface bursts, the blast loads acting on structure surfaces are calculated as described for the air burst, except that the incident pressures and other parameters of the free-field shock environment are obtained from figure 4–12.

Section IV. PARTIALLY CONFINED EXPLOSIONS

4–9. Effects of Confinement

a. When an explosion occurs within a structure, the peak pressures associated with the initial shock front (free-air pressures) will be extremely high and, in turn, will be amplified by their reflections within the structure. In addition, the accumulation of gases from the explosion will exert additional pressures and increase the load duration within the structure. The combined effects of both pressures may eventually destroy the structure unless venting for the gas and the shock pressures is provided. The use of a cubicle-type structure (fig. 4–13), or other similar barriers, with one or more surfaces either sufficiently frangible or open to the atmosphere, will provide adequate venting. This type of structure will permit the blast wave from an internal explosion to spill over onto the exterior ground surface. These pressures are referred to as exterior or leakage pressures. The pressures reflected and reinforced within the structure are referred to as interior shock front pressures, while those pressures produced by the accumulation of the gaseous products of the explosion are identified as gas pressures. Figure 4–14 is a schematic representation of a typical partially confined explosion.

b. It should be noted that the term "frangible" pertains to those elements of a protective structure whose strength and mass are such as to minimize the amplification of the shock-front pressures and reduce confinement of the explosive gases.

c. To minimize the amplification of the shock pressures, frangible elements must fail so as to relieve quickly the interior pressures acting on these surfaces and prevent their reflection to the nonfrangible elements of the structure. On the other hand, the buildup of the gas pressures is dependent upon the ratio of the weight of the charge to the volume of the confining structure and the size of the vents. This pressure buildup will not begin until sometime near the end of, or after, the positive phase of the shock pressures. Therefore, an element which is not considered frangible for the shock pressures may be frangible for gas accumulation. In addition to being dependent upon the physical properties of an element, frangibility will also be a function of the magnitude of the applied blast loads and, therefore, a function of the quantity of explosives being contained and the distance from the frangible element. Although frangibility is imperfectly understood and difficult to measure, it has been assumed that a material whose weight is 10 pounds per square foot of surface area or less may be considered frangible for both the shock-front pressures and gas pressures resulting from detonation of explosives greater than 100 pounds. Some materials which conform to the limitation of 10 psf are the following: lightweight steel joists and corrugated metal decking for roofs, insulated metal panels for walls, wooden frames with a plywood covering for roofs and walls, plexiglass panels in combination with either wooden or lightweight steel frames, etc. If a large portion (one or more surfaces) of a structure whose weight is greater than that specified above fails, then this section of the structure is considered frangible for the gas pressures. However, because the heavier sections will take longer to fail than the lighter elements, full reflection of the shock-front pressures will occur.

d. In the following paragraphs of this section, simple cantilever barriers as well as cubicle-type structures are considered. These cubicles are assumed to have one or more surfaces which are open or frangible. The

levels and, there-

ce burst environ-
in figure 4–12. A
shows that, at a
f the same weight
f the surface burst
or the free-air en-

otective structures
of a surface burst
ure regions where
t can be applied.
st loads acting on
described for the
ressures and other
environment are

on the ratio of the
e of the confining
his pressure build-
ar the end of, or
pressures. There-
lered frangible for
e for gas accumu-
t upon the physical
ty will also be a
pplied blast loads
ntity of explosives
rom the frangible
mperfectly under-
been assumed that
ds per square foot
dered frangible for
gas pressures re-
s greater than 100
m to the limitation
ght steel joists and
s, insulated metal
a plywood covering
els in combination
steel frames, etc.
ces) of a structure
ecified above fails,
onsidered frangible
ecause the heavier
an the lighter ele-
ront pressures will

this section, simple
cle-type structures
sumed to have one
or frangible. The

surface
comple
buildup

4–10.

a. In

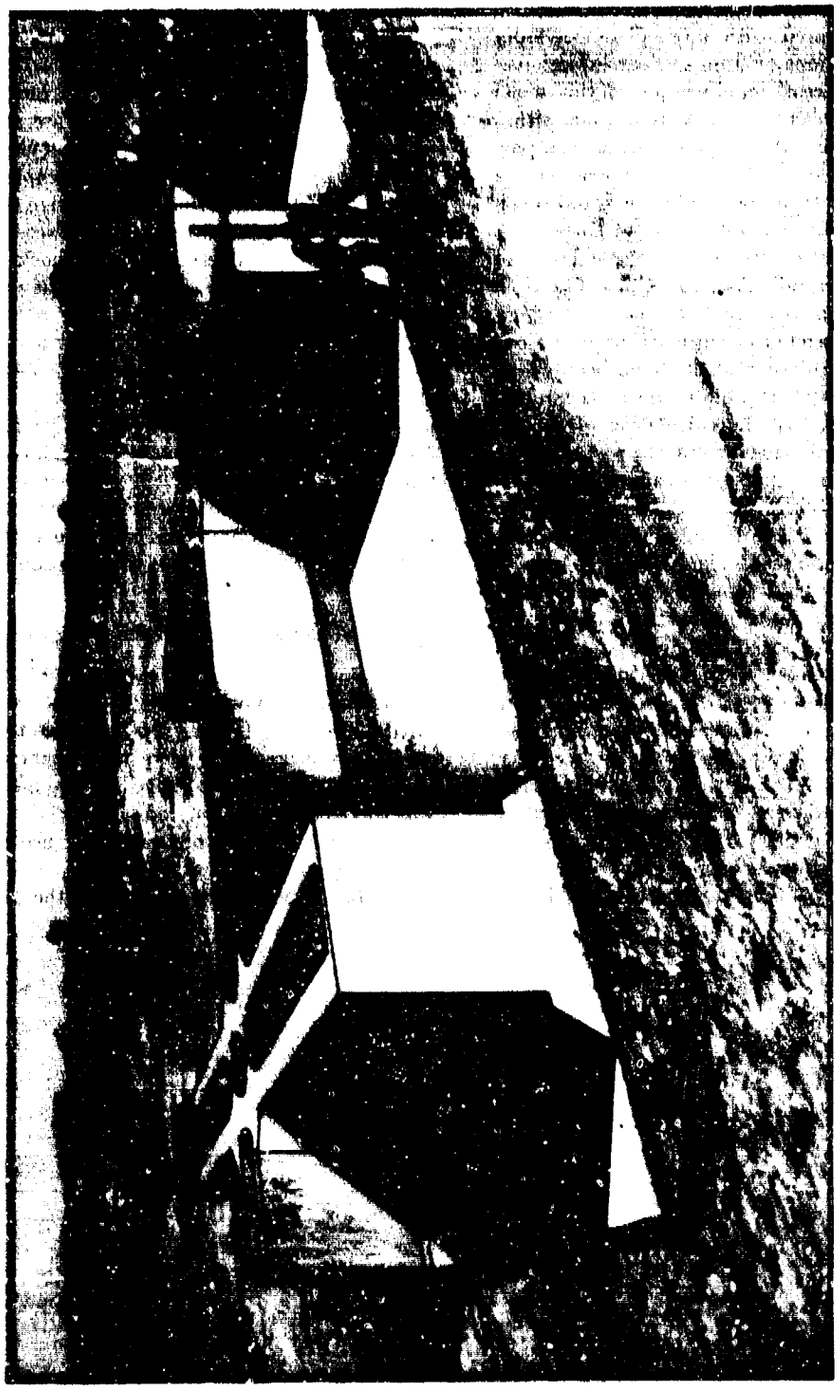


Figure 4–15. Cubicle structure.

surface area of the frangible elements is sufficient to completely vent the structure and prevent gas-pressure buildup.

4–10. Fully Vented Explosions

a. Interior Blast Loadings.

(1) When an explosion occurs within a cubicle, the peak pressures associated with the shock front will be extremely high. However, because of the short duration of the blast wave at close distances from high-explosive detonations, cubicle structures can usually be designed for the impulse loading rather than for the

2

peak pressures as required for the relatively long duration loadings associated with large distances from high-explosive detonations or from nuclear explosions.

(2) In confined areas, amplification of the initial shock front (free-air pressures) due to reflections within the structure will occur. At any given point on a particular reflecting surface, the total impulse loading is a combination of the contributions from the initial shock and from the shock reflected from adjacent surfaces.

(3) An approximate method for the calculation of the total impulse in a fully vented cubicle has been developed in connection with the Safety Design Criteria Program. The total reflected impulse acting on various points of each surface of the cubicle have been calculated and then integrated to obtain the total impulse loads. In order to simplify the calculation of the response of a protective barrier or cubicle wall to these applied loads, the total impulse is assumed to be distributed uniformly, giving an average value of the impulse acting on any one surface. The actual distribution of the blast impulses is highly irregular due to the multiple reflections and time phasing, and results in localized high shear stresses in the element. The use of average impulse loads when designing is predicated on the ability of the element to transfer these localized loads to regions of lower stress. Laced reinforced concrete and structural steel plates exhibit this characteristic.

(4) The method of calculating the average blast impulses was developed using a theoretical procedure based on semi-empirical blast data and on the results of response tests of reinforced concrete slabs. The calculated average impulse loads have been compared with those obtained from the results of tests of a scale-model steel cubicle and have shown good agreement for a wide range of cubicle arrangements.

(5) The parameters which are necessary to determine the average impulse loads are structure configuration and size, charge weight, and charge location. Figure 4–15 shows many possible simple barrier and cubicle configurations and the definition of the various parameters pertaining to each. Surfaces depicted are not frangible for determining the shock loadings but could be frangible when considering gas pressure build-up. For the four-wall cubicle with roof, one of the surfaces shown must be frangible for such gas pressures.

(6) Because of the wide range of required parameters, the procedure for the determination of the impulse loads was programmed for solution on a digital computer. The results of these calculations, presented in figures 4–17 through 4–62, give the scaled average unit blast impulse i_s as a function of the parameters defining the configurations presented in figure 4–15. Each illustration is for a particular combination of values of $\frac{h}{H}, \frac{l}{L}$, and the number N of reflecting surfaces adjacent to the surface for which the impulses are being calculated. The wall (if any) parallel to the surface in question was found to have a negligible contribution to the impulse for the range of parameters used and was therefore not considered.

(7) The general procedure for use of the above illustrations is as follows:

(*a*) From figure 4–15 select the particular sur-

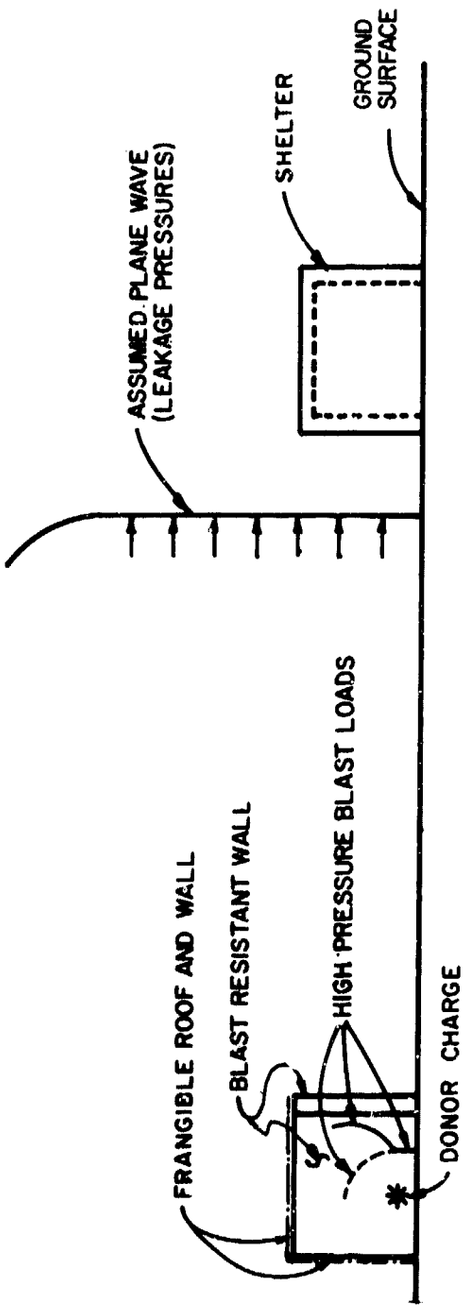


Figure 4–14. Partially confined explosion blast environment.

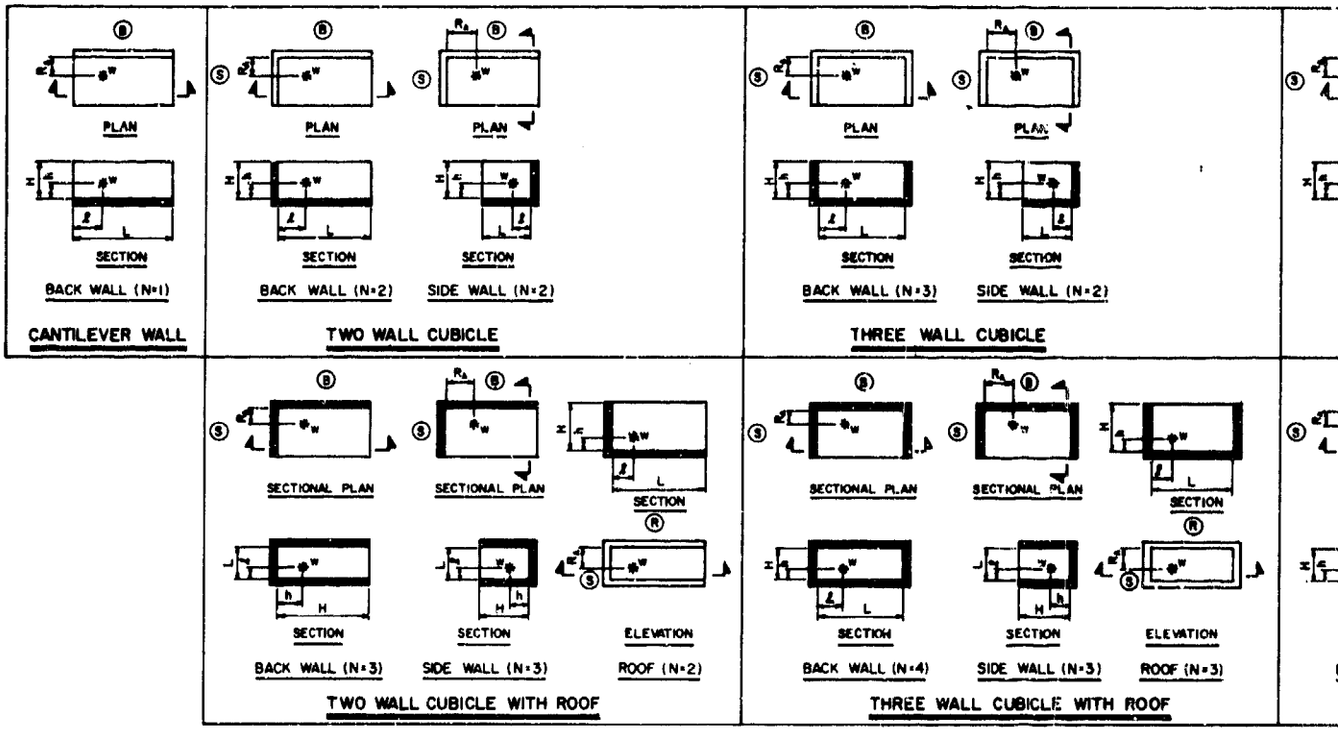


Figure 4-16. Barrier and cubicle configur

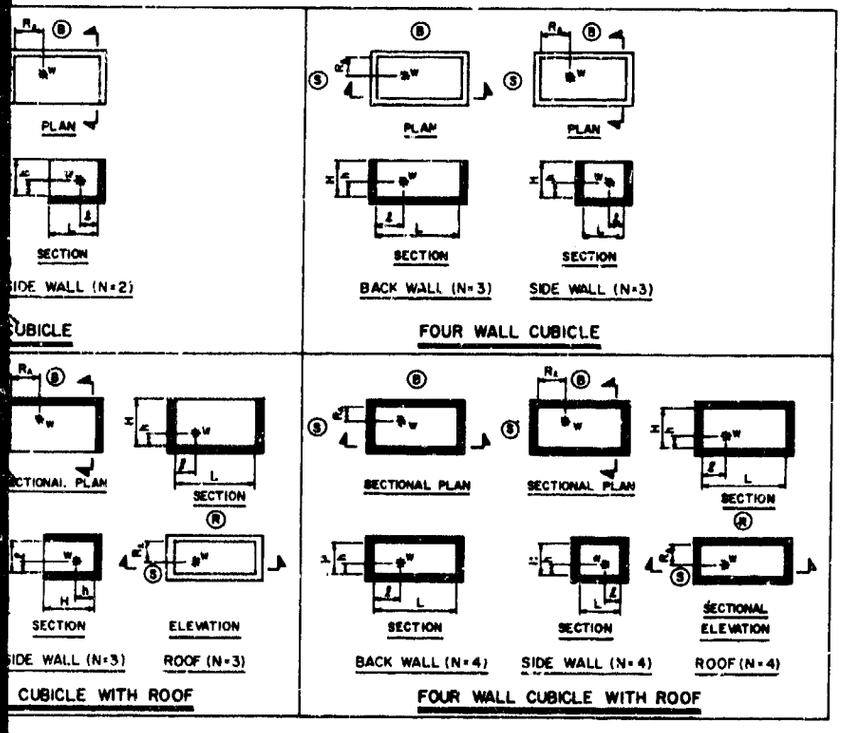


Figure 4-15. Barrier and cubicle configurations and parameters.

Notes

1. B denotes Back WAll, S Side Wall and R Roof

2. Numbers in parentheses indicate number N of reflecting surfaces adjacent to surface in question.

3. h is always measured to the nearest reflecting surface.

4. ℓ is always measured to the nearest reflecting surface except for the cantilever wall where it is measured to the nearest free edge.

5. For values of scaled average unit blast impulse I_b for barrier and cubicle arrangements shown see Figures 4-17 thru 4-62. Required parameters are:

$$\frac{\ell}{L},\ \frac{h}{H},\ \frac{L}{H},\ \frac{L}{R_A},\ \text{and}\ Z_A = \frac{R_A}{W^{1/3}}$$

For reference list of above figures for particular values of the parameters see Figure 4-16.

h/H	l/L	No. of Adjacent Reflecting Surfaces (N)			
		One	Two	Three	Four
0.15	0.10 0.25 0.50 0.75	4-17 4-18 4-19	4-28 4-29 4-30 4-31	4-43 4-44 4-45	4-54 4-55 4-56
0.25	0.10 0.25 0.50 0.75	4-20 4-21 4-22	4-32 4-33 4-34 4-35	4-46 4-47 4-48	4-57 4-58 4-59
0.50	0.10 0.25 0.50 0.75	4-23 4-24 4-25	4-36 4-37 4-38 4-39	4-49 4-50 4-51	4-60 4-61 4-62
0.75	0.25 0.50 0.75	4-26 4-27	4-40 4-41 4-42	4-52 4-53	

Figure 4–16. List of illustrations for scaled average unit impulse loads.

face of the barrier or cubicle configuration which conforms to the protective structure given and note the number N of adjacent reflecting surfaces as indicated in parentheses.

(*b*) Determine the values of the parameters indicated for the selected surface of the barrier or cubicle configuration in (*a*) above and calculate the following quantities:

$$\frac{h}{H}, \frac{l}{L}, \frac{L}{H}, \frac{L}{R_A}, \quad \text{and} \quad Z_A = R_A/W^{1/3}$$

(*c*) Refer to figure 4–16 for the proper impulse charts conforming to the number of adjacent reflecting surfaces and the values of l/L and h/H of (*b*) above, and enter these charts to determine the value of $\bar{i}_b$.

(8) In most cases the above procedure will require interpolation for one or more of the parameters which define a given situation, in order to obtain the correct average impulse load. Examples of this interpolation procedure are given in appendix 4A.

(9) Because of the limitation in the range of the test data and the limited number of values of the parameters given in the above impulse charts, extrapolation of the data given in figures 4–17 through 4–62 may be required for some of the parameters involved. On the other hand, the limiting values as given in the charts for other parameters will not require extrapolation. The values of the average impulse loads corresponding to the values of the parameters which exceed their limiting values (as defined by the charts), will be approximately equal to those corresponding to the limiting values. The following are recommended procedures which will be applicable in most cases for either extrapolation, or establishing the limits of impulse loads corresponding to values of the various parameter which exceed the limits of the charts:

(*a*) Plot curve of values of $\bar{i}_b$ versus Z_A for constant values of L/R_A, L/H, h/H, and l/L. Extrapolate curve to include value of $\bar{i}_b$ corresponding to the value of Z_A required.

(*b*) Extrapolate given curve for constant values of Z_A, L/H, h/H, and l/L, to include value of $\bar{i}_b$ corresponding to the value of L/R_A required.

(*c*) Values of $\bar{i}_b$ corresponding to values of L/H greater than 6 shall be taken as equal to those corresponding to $L/H=6$ for actual values of Z_A, h/H, and l/L but with a fictitious value of L/R_A in which R_A is the actual value and L is fictitious value equal to $6H$.

(*d*) Values of $\bar{i}_b$ corresponding to values of l/L less than 0.10 and greater than 0.75 shall be taken as equal to those corresponding to $l/L=0.10$ and 0.75, respectively.

(e) Values of i_s corresponding to values of h/H less than 0.15 and greater than 0.75 shall be taken as equal to those corresponding to $h/H = 0.15$ and 0.75, respectively.

(10) As previously mentioned, a protective element subjected to the high-pressure range effects of an explosion may be designed for the impulse rather than for the pressure pulse only if the duration of the applied pressures acting on the entire element is short in comparison to its response time. An estimate of this duration may be obtained by adding the time increments corresponding to the time required for the blast wave to fully engulf the element and the duration of the blast load at the section of the element furthest removed from the explosion. This relationship is represented by:

$$t_o = (t_A)_F - (t_A)_A + 1.5(t_o)_F \qquad \textbf{Equation 4–1}$$

where t_o = duration of load (ms)

$(t_A)_F$ = time of arrival of the blast wave at the point on the element furthest from the explosion; defined by the largest slant distance.

$(t_A)_F$ = time of arrival of the blast wave at the point on the element nearest to the explosion; defined by the normal distance.

$(t_o)_F$ = duration of the blast pressure at the point on the element furthest from the explosion.

The time of arrival of the blast wave for the two points of interest as well as the duration of the load at the furthest point on the element are obtained from figure 4–5. To account for the increased load duration due to the multiple reflections of the blast wave within the cubicle, the value of $(t_o)_F$ has been increased by 50 percent.

(11) A protective element subjected to the high-pressure range effects of an explosion may have to be designed for the pressure pulse rather than for the impulse effects if the duration of the applied pressures acting on the entire element is long in comparison to the response time of the element (t_m less than $3t_o$). For these cases, the actual pressure-time relationship resulting from a pressure distribution on the element, which is highly irregular due to the multiple reflections and time phasing, may be approximated by a fictitious peaked triangular pressure pulse. The duration t_o of this pulse is obtained from equation 4–1 and a fictitious peak pressure P_f is established as a function of this duration and the average blast impulse i_s (figs. 4–17 through 4–62) acting on the element.

$$P_f = \frac{2i_s}{t_o}$$

(12) The above solution for the average impulse load does not account for increased blast effects produced by contact charges. Therefore, if the values of the average impulse loads given in figures 4–17 through 4–62 are to be applicable, a separation distance between the element and explosive must be maintained. This separation is measured between the surface of the element and the surface of either the actual charge or the spherical equivalent; whichever results in the larger normal distance between the element's surface and the center of the explosive (the radius of a spherical TNT charge $r = 0.136W^{1/3}$). For purposes of design, the following separation distances are recommended for various charge weights:

Weight of explosive (lbs)	*Separation distance (ft)*
up to 500	1.0
500 to 1,000	1.5
1,001 to 2,000	2.0
2,001 to 3,000	2.5
above 3,000	3.0

(13) The above separation distances do not apply to floor slabs or other similar concrete elements poured on grade. However, a separation distance of at least 1 foot should be maintained to minimize the size of craters associated with contact explosions.

(14) It should be noted that these separation distances do not necessarily conform to those specified by other government regulations; their use in a particular design must be approved by the cognizant military construction agency.

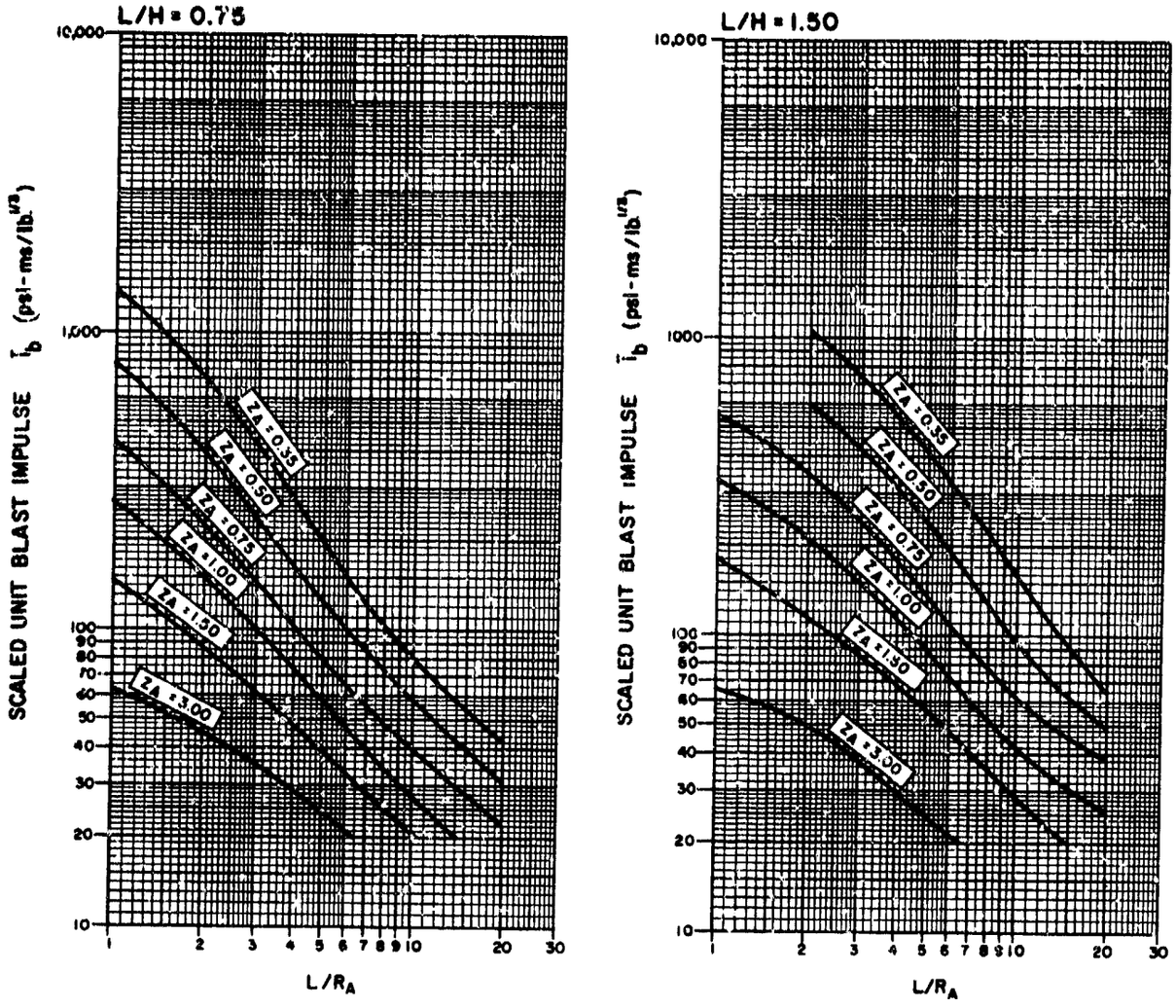
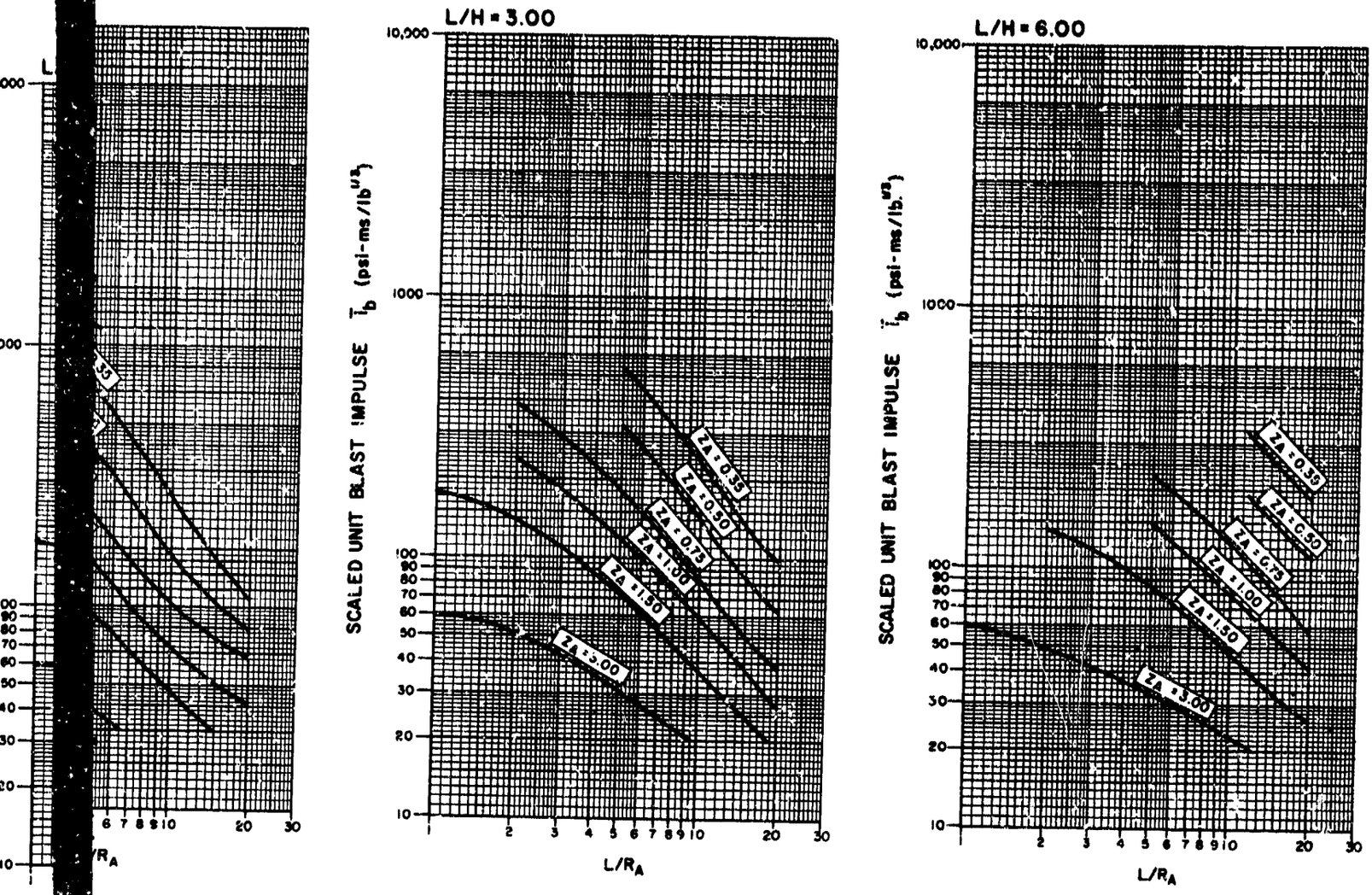
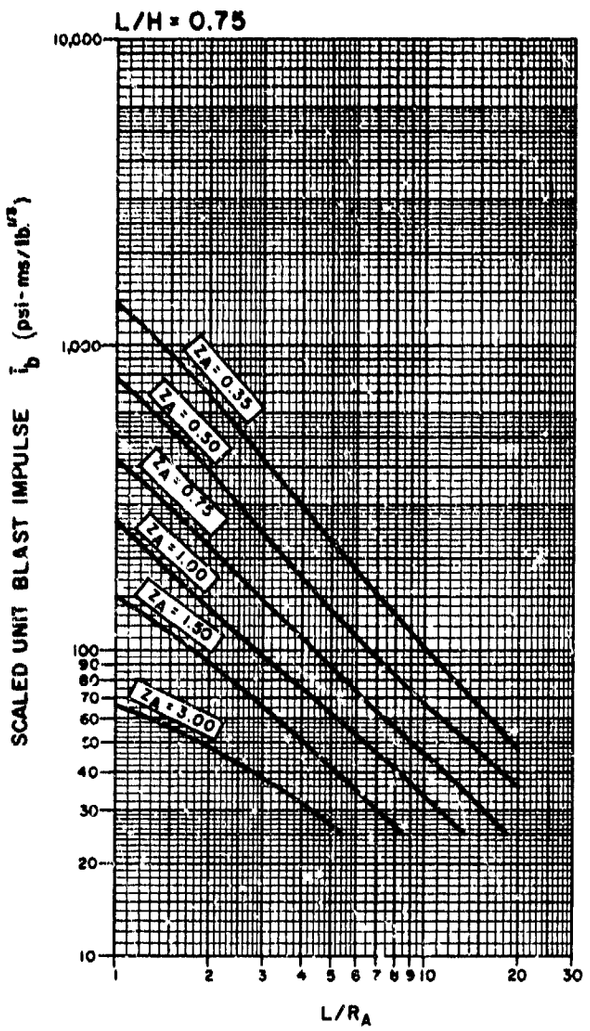


Figure 4-17. Scaled average unit blast impulse (N = 1, l/L =



17. Scaled average unit blast impulse ($N=1$, $l/L=0.10$, $h/H=0.15$).



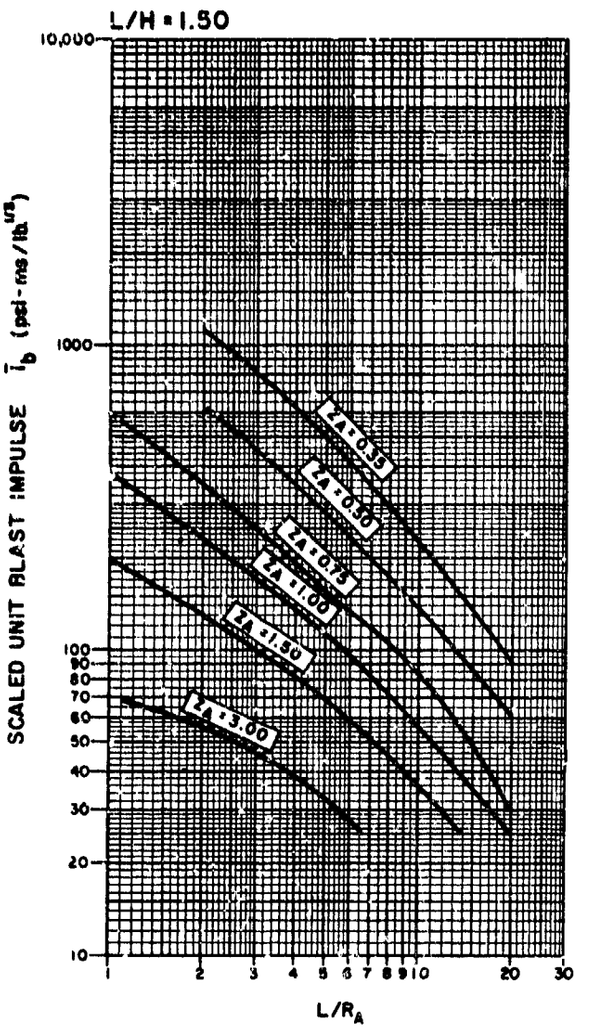
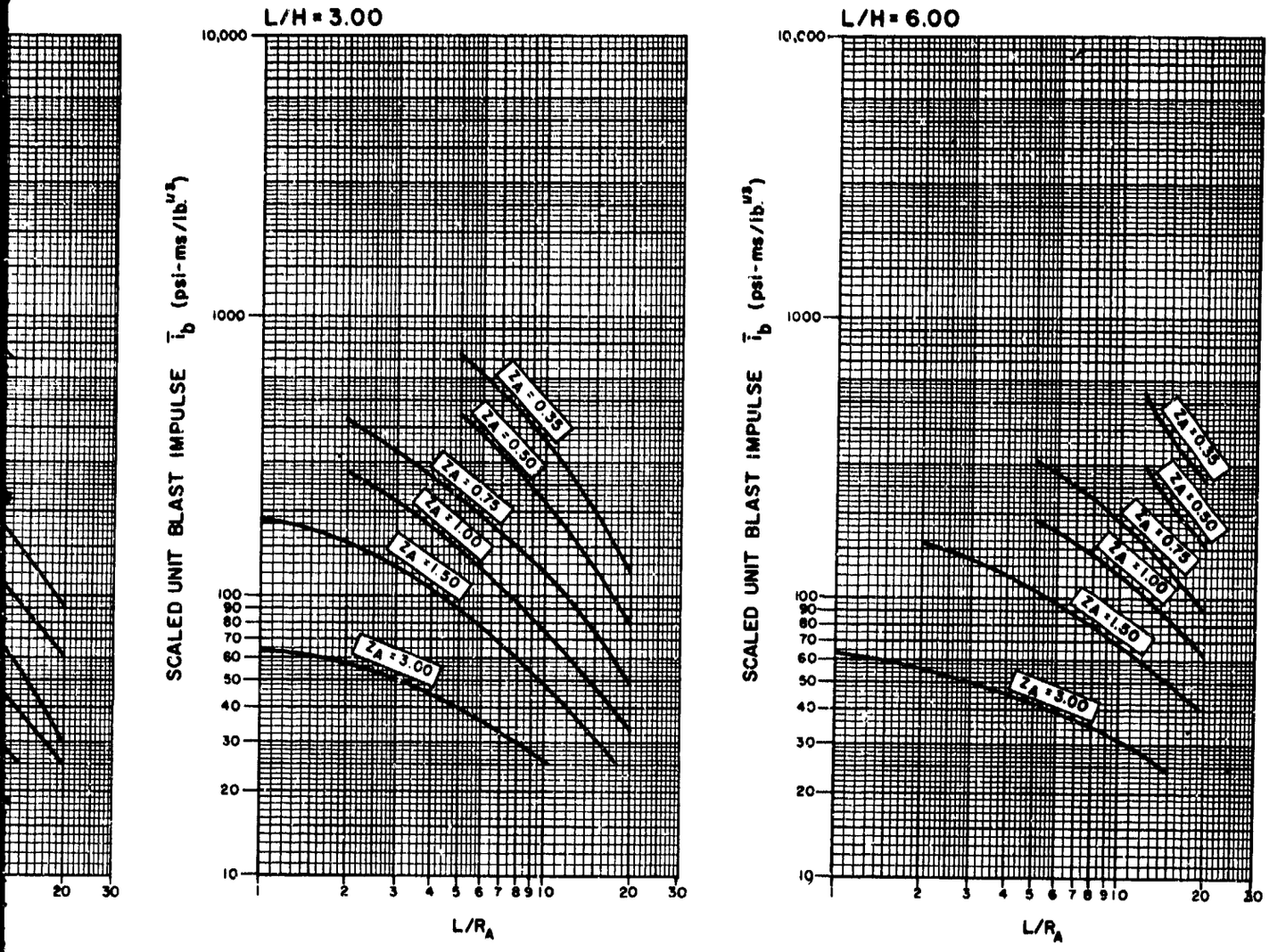
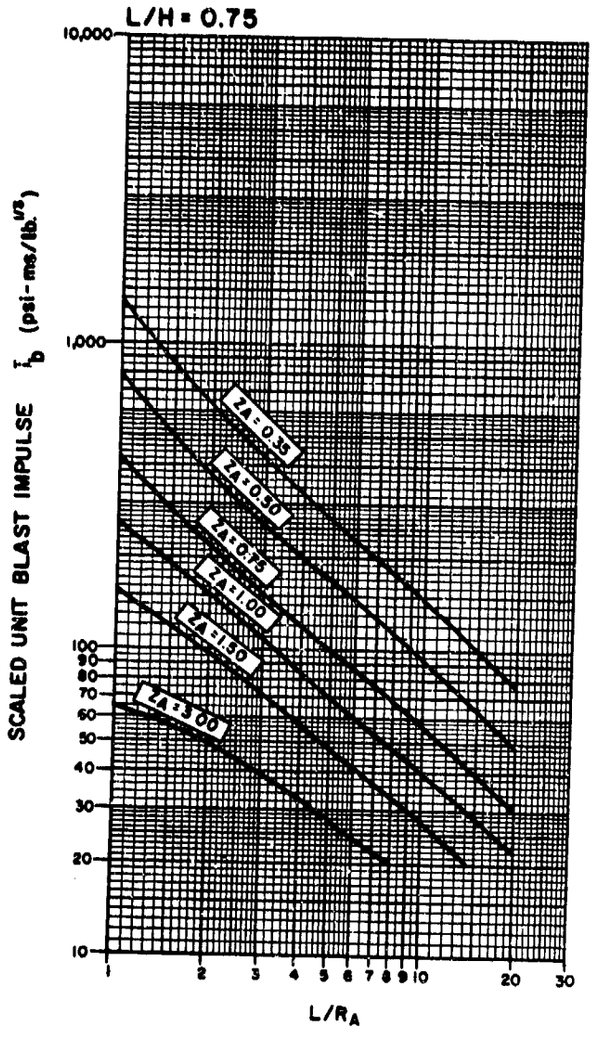




Figure 4–18. Scaled average unit blast impulse (N = 1, l/L = 0.25 and 0.75, I



unit blast impulse ($N=1$, $l/L=0.25$ and 0.75, $h/H=0.15$).



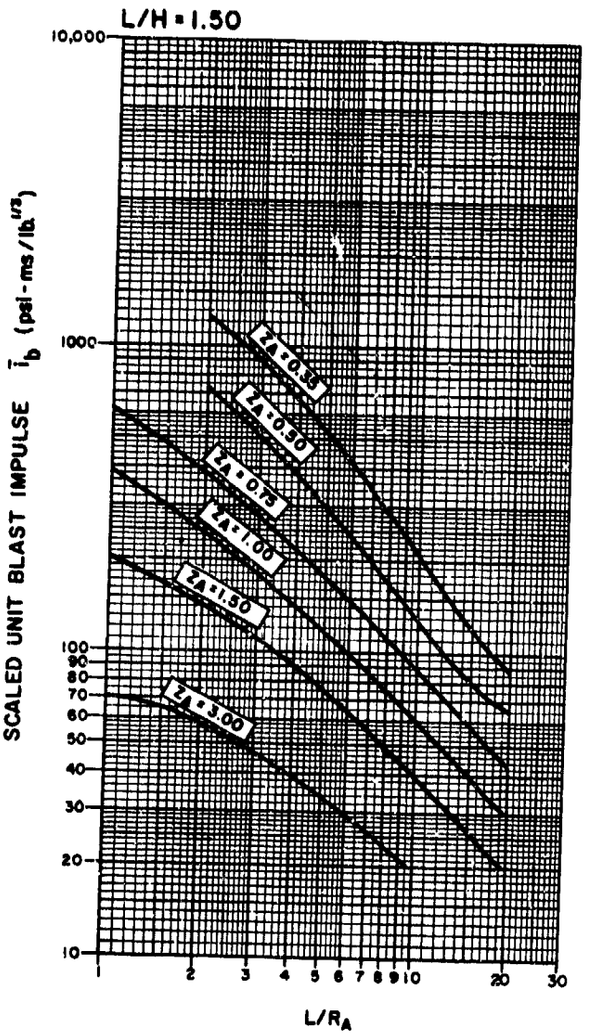


Figure 4-19. Scaled average unit blast impulse (N

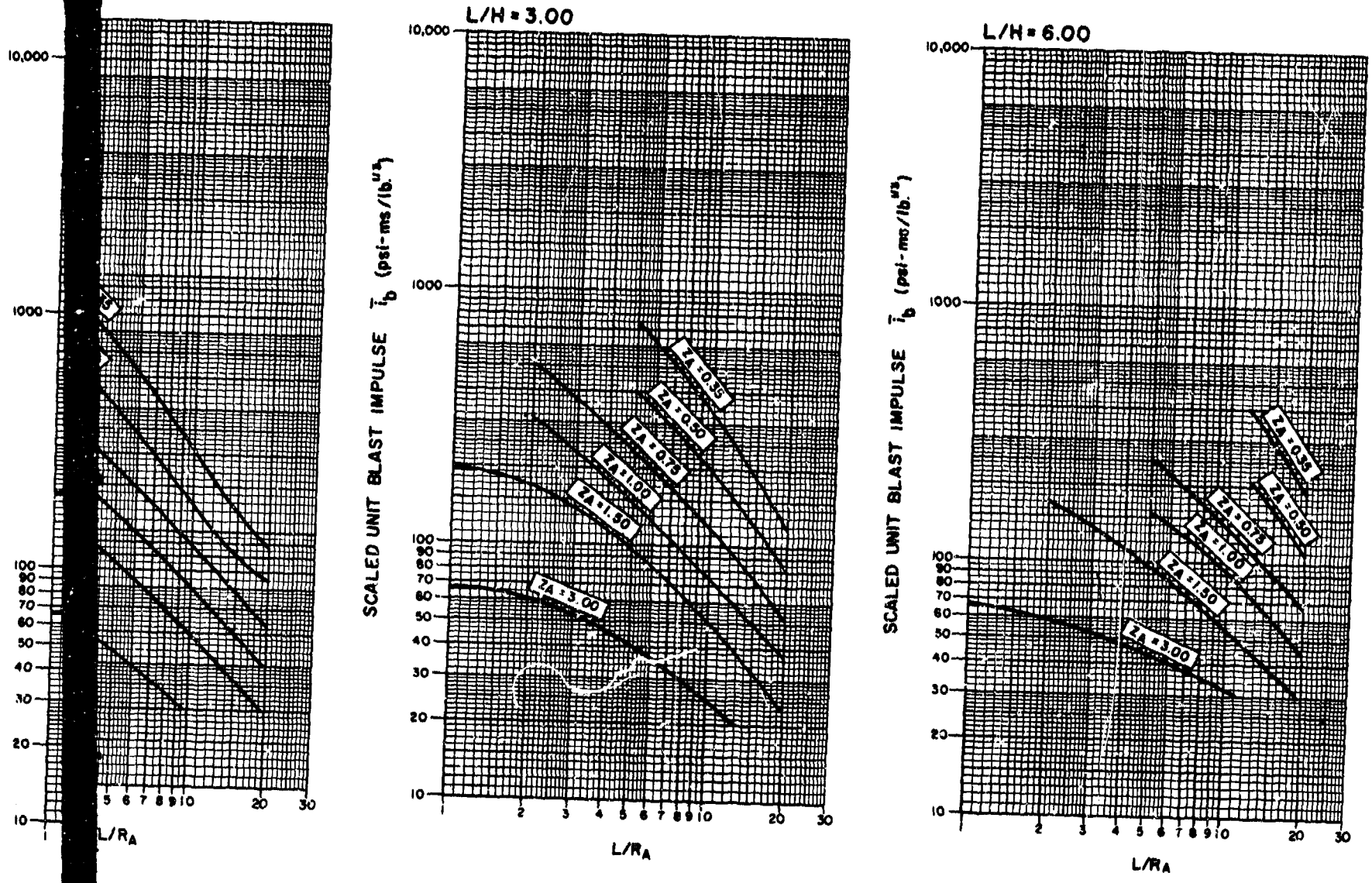
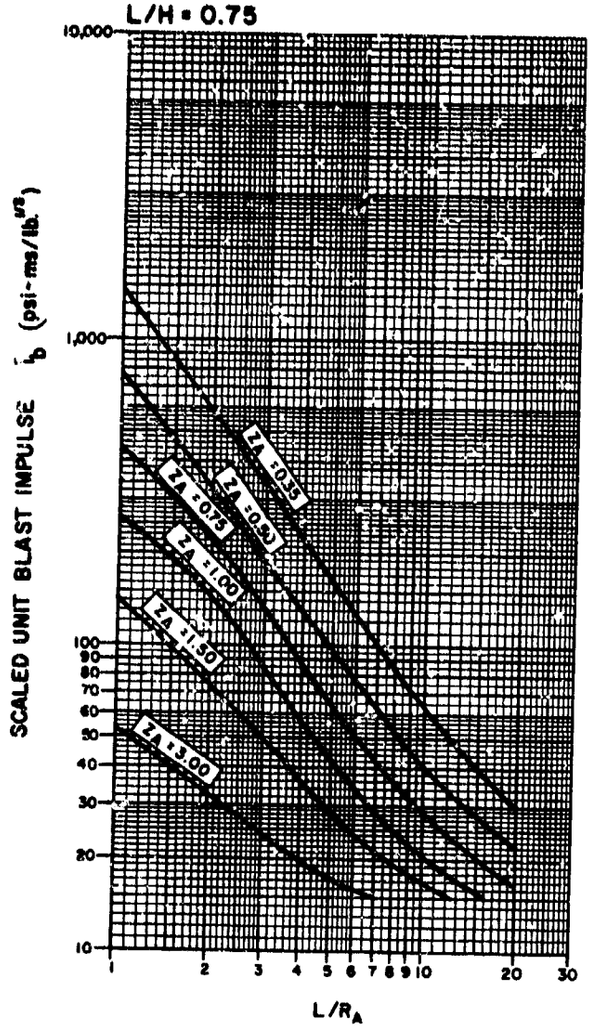


Figure 4–19. Scaled average unit blast impulse ($N = 1$, $l/L = 0.50$, $h/H = 0.15$).



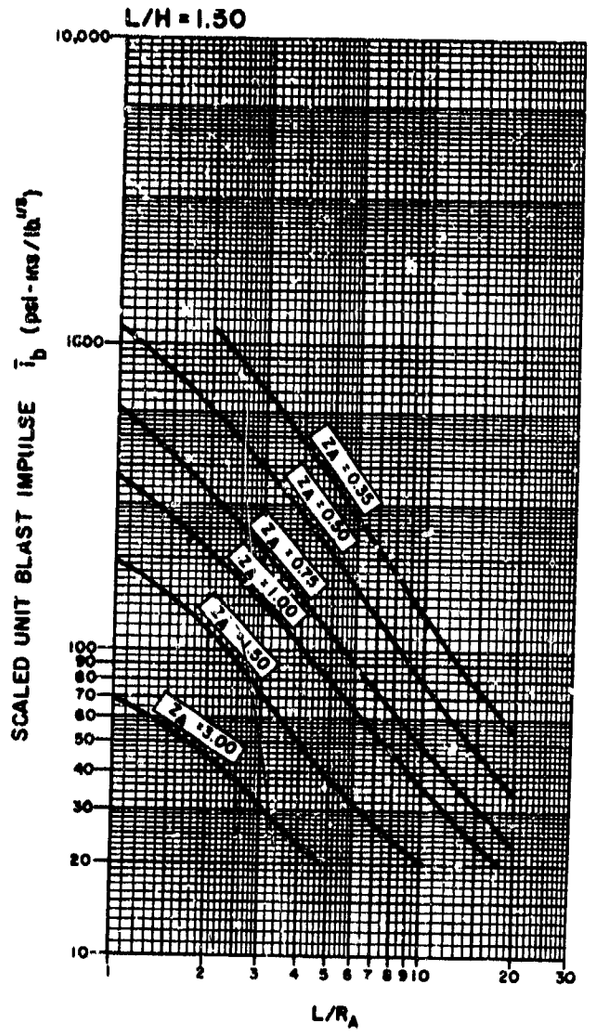
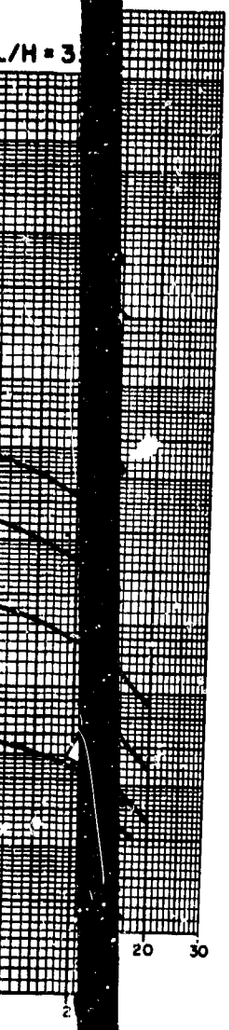
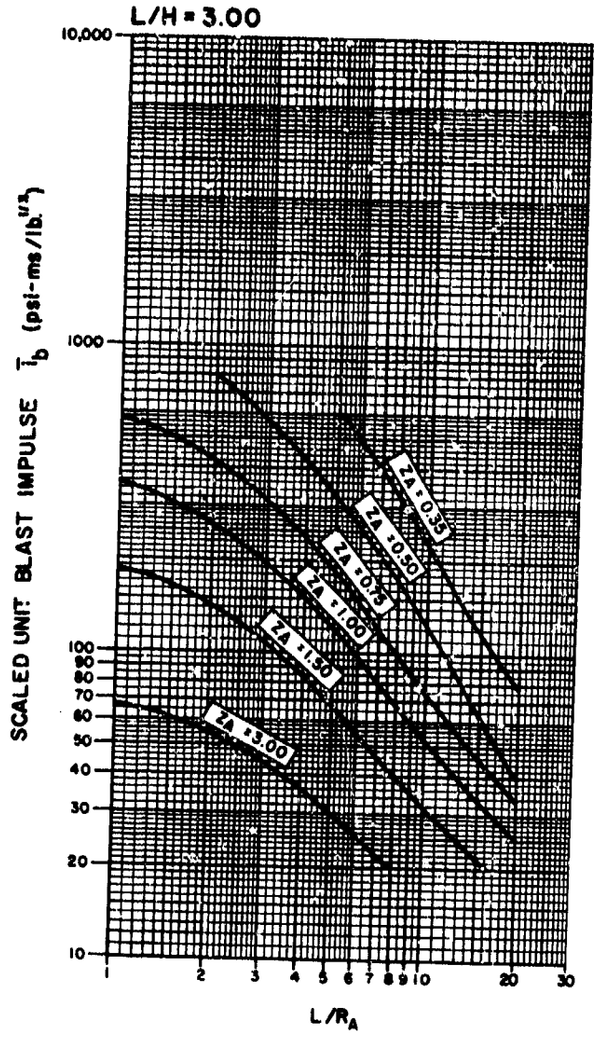
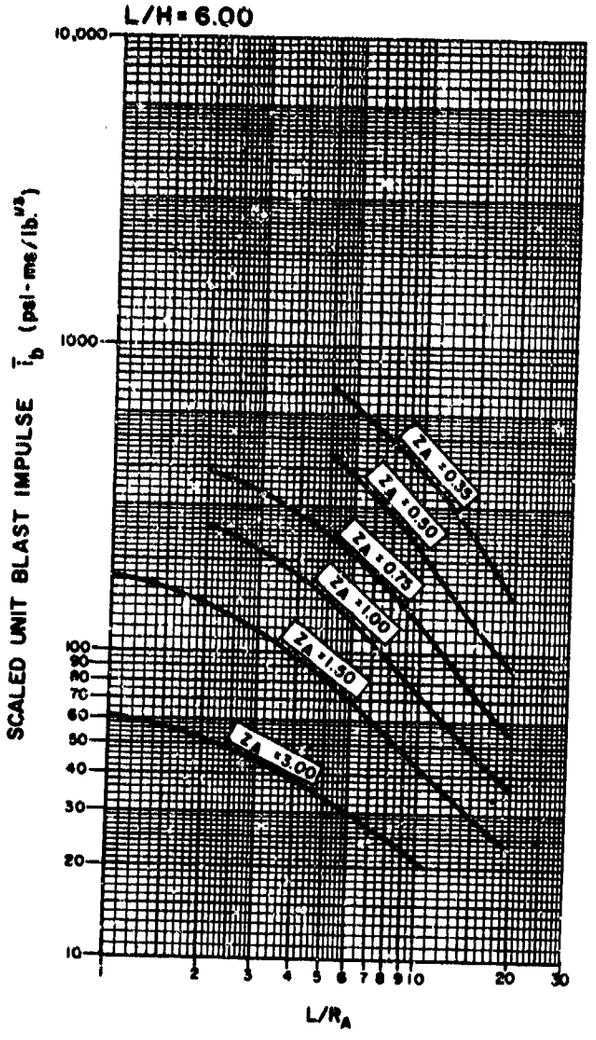




Figure 4-20. Scaled average unit blast impulse ($N = 1$, $l/L = 0.10$

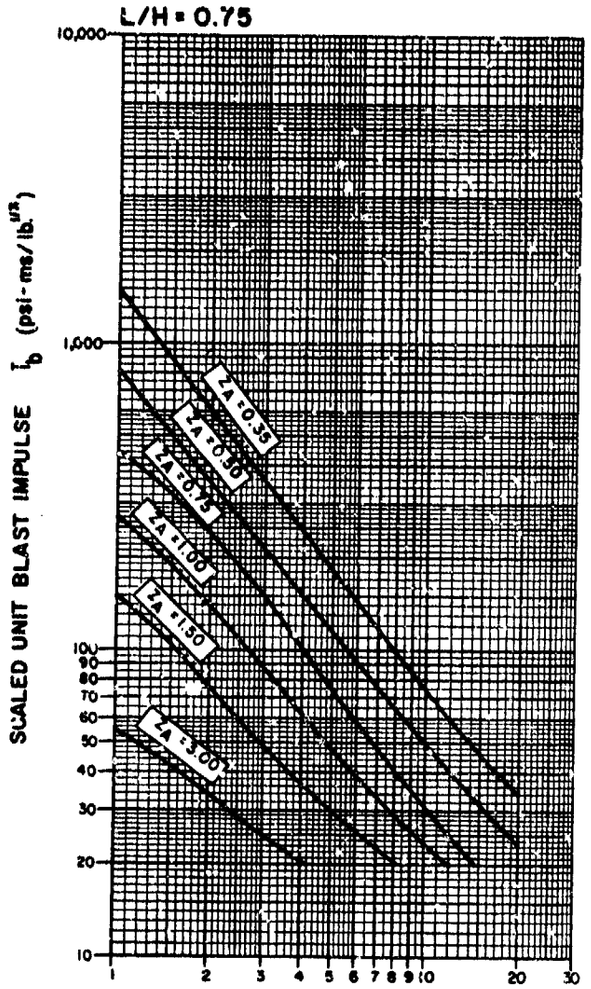






e unit blast impulse ($N = 1$, $l/L = 0.10$, $h/H = 0.25$).

$= 0.10$, $h/$



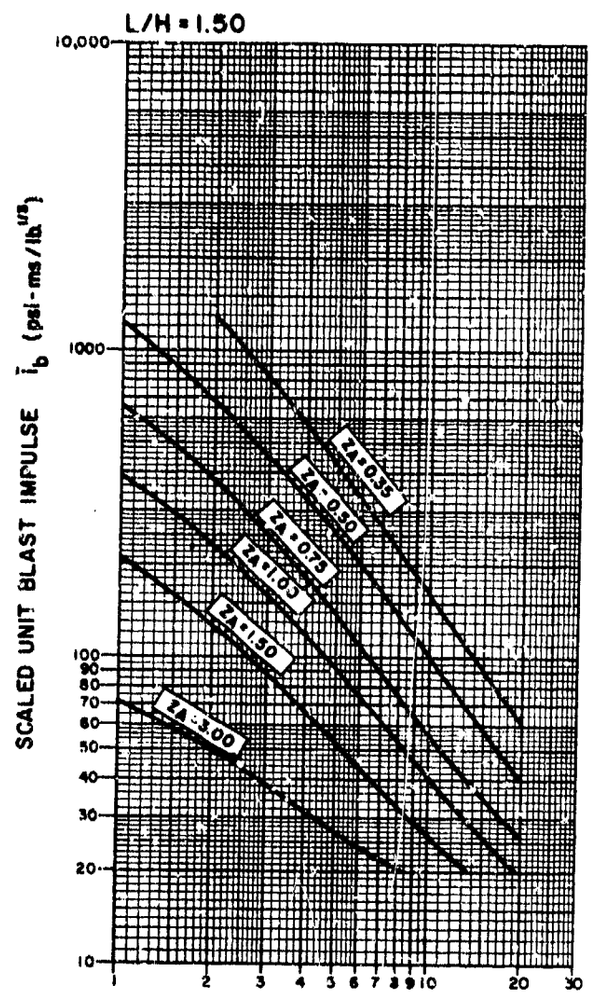
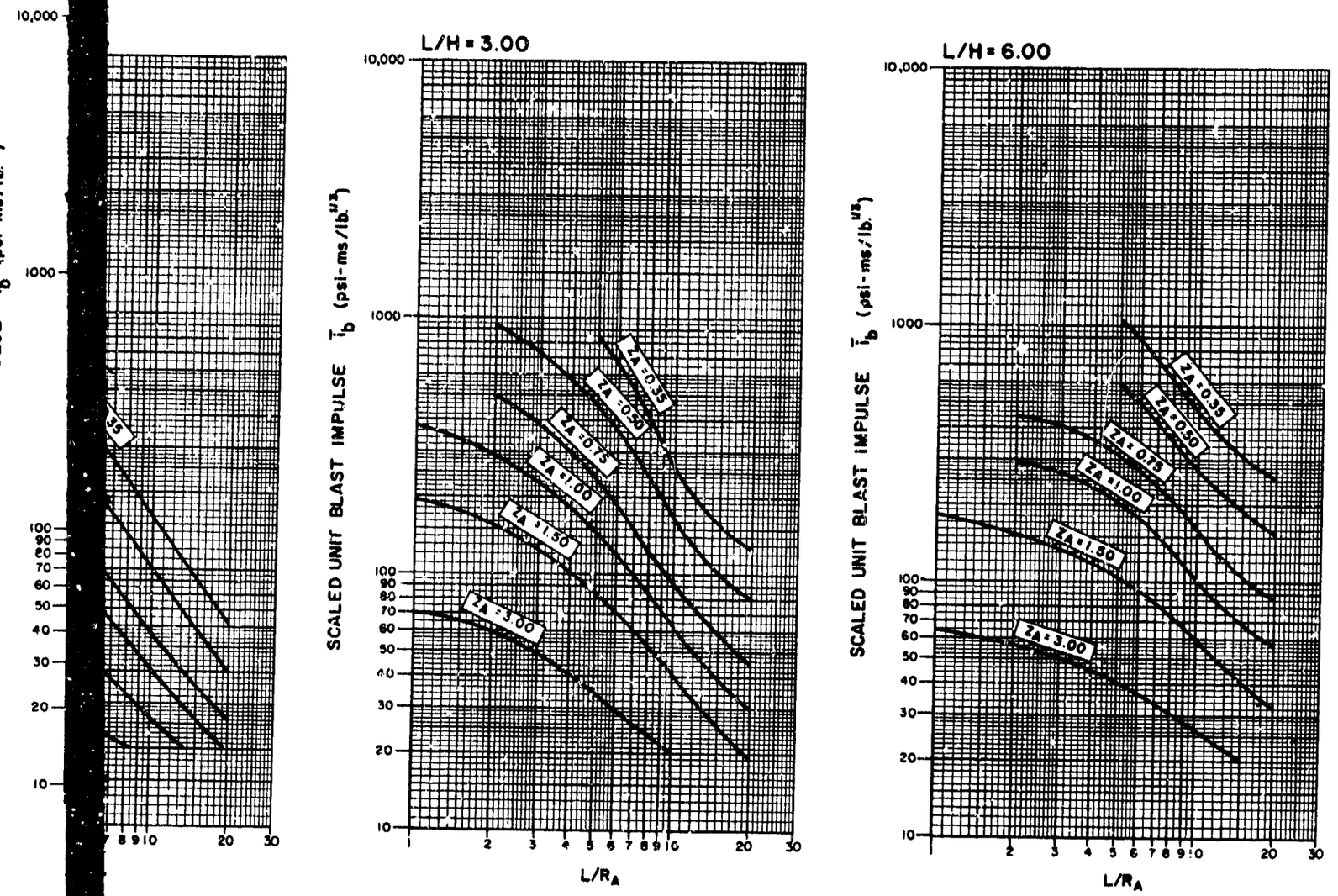




Figure 4-21. Scaled average unit blast impulse (N = 1, l/L



...led average unit blast impulse ($N = 1$, $l/L = 0.25$ and 0.75, $h/H = 0.25$).

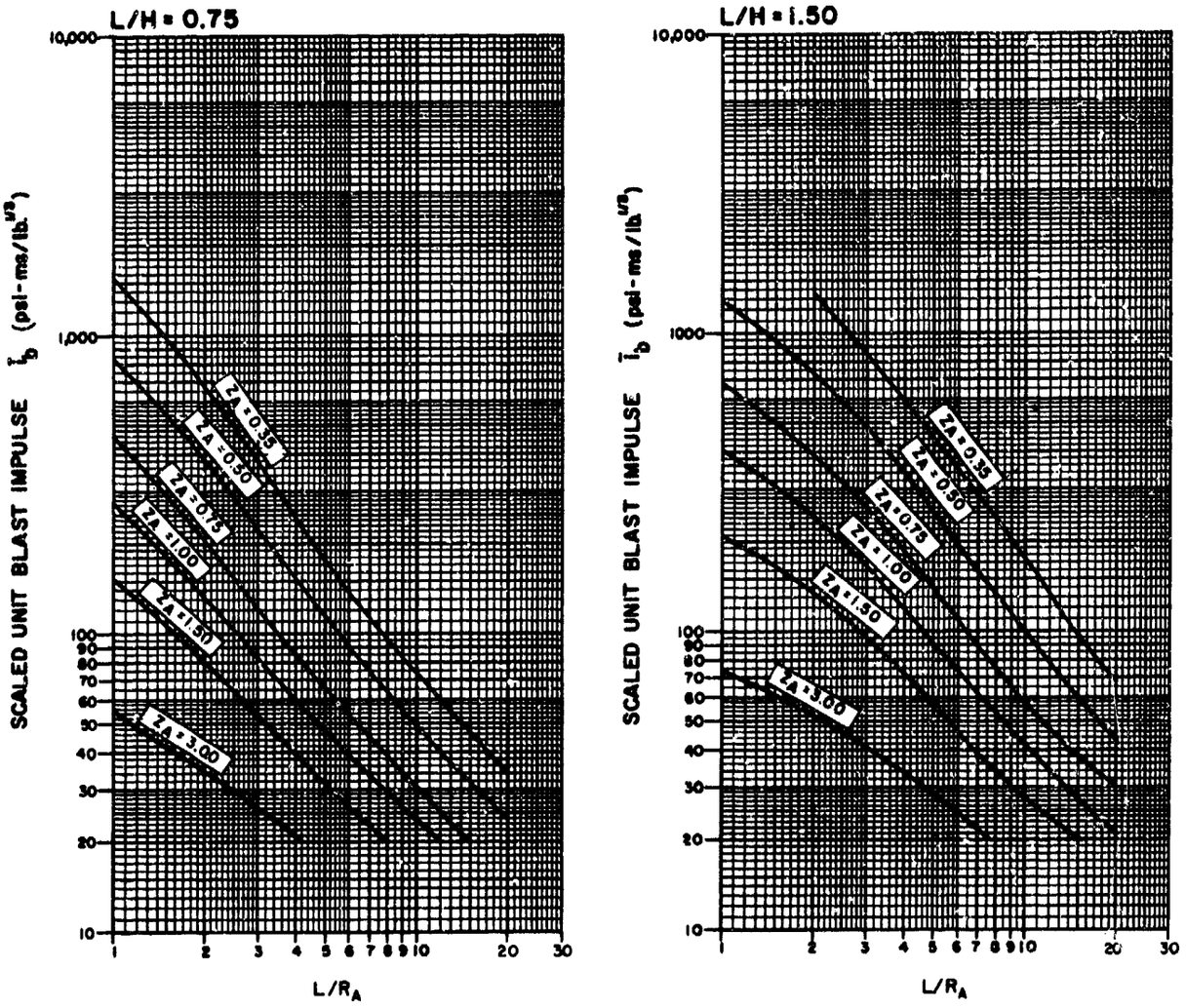
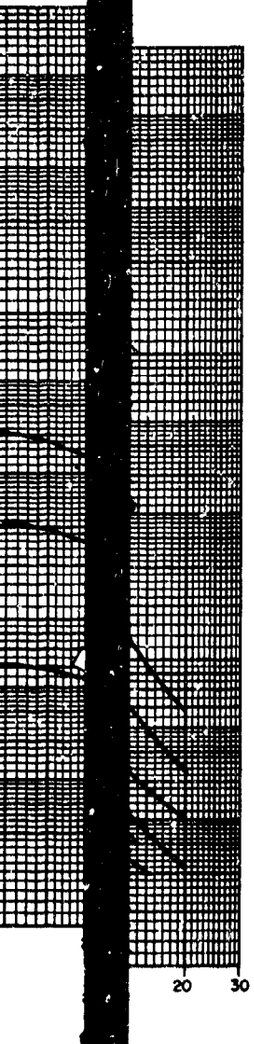
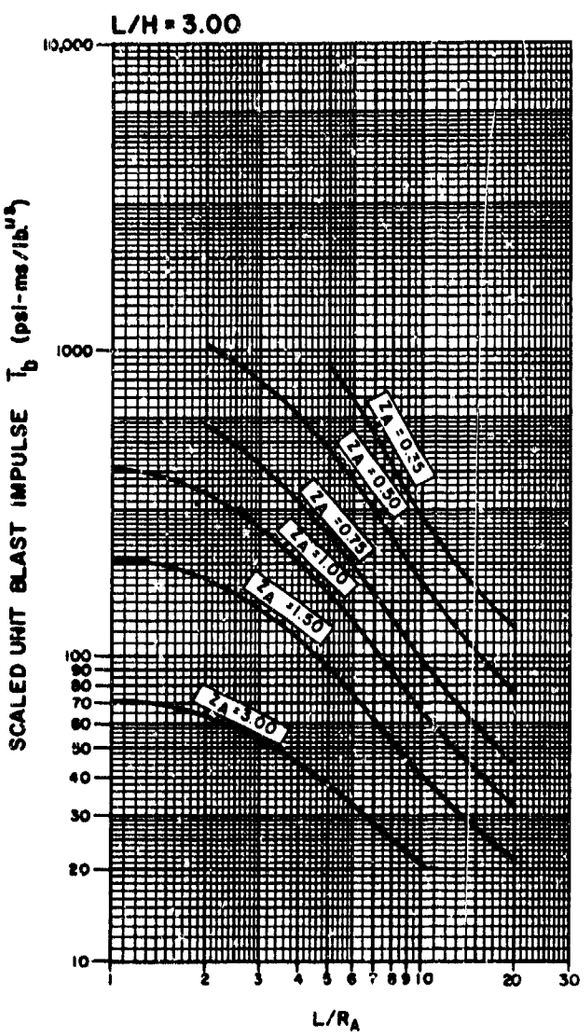
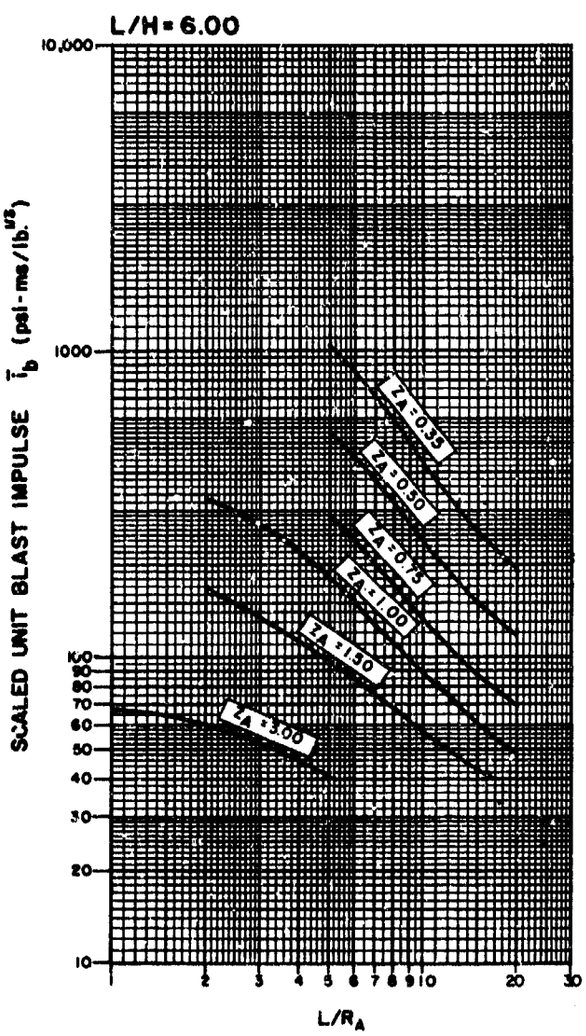


Figure 4-22. Scaled average unit blast impulse ($N = 1$, $l/L = 0$







/L = 0.50,

verage unit blast impulse ($N = 1$, $l/L = 0.50$, $h/H = 0.25$).

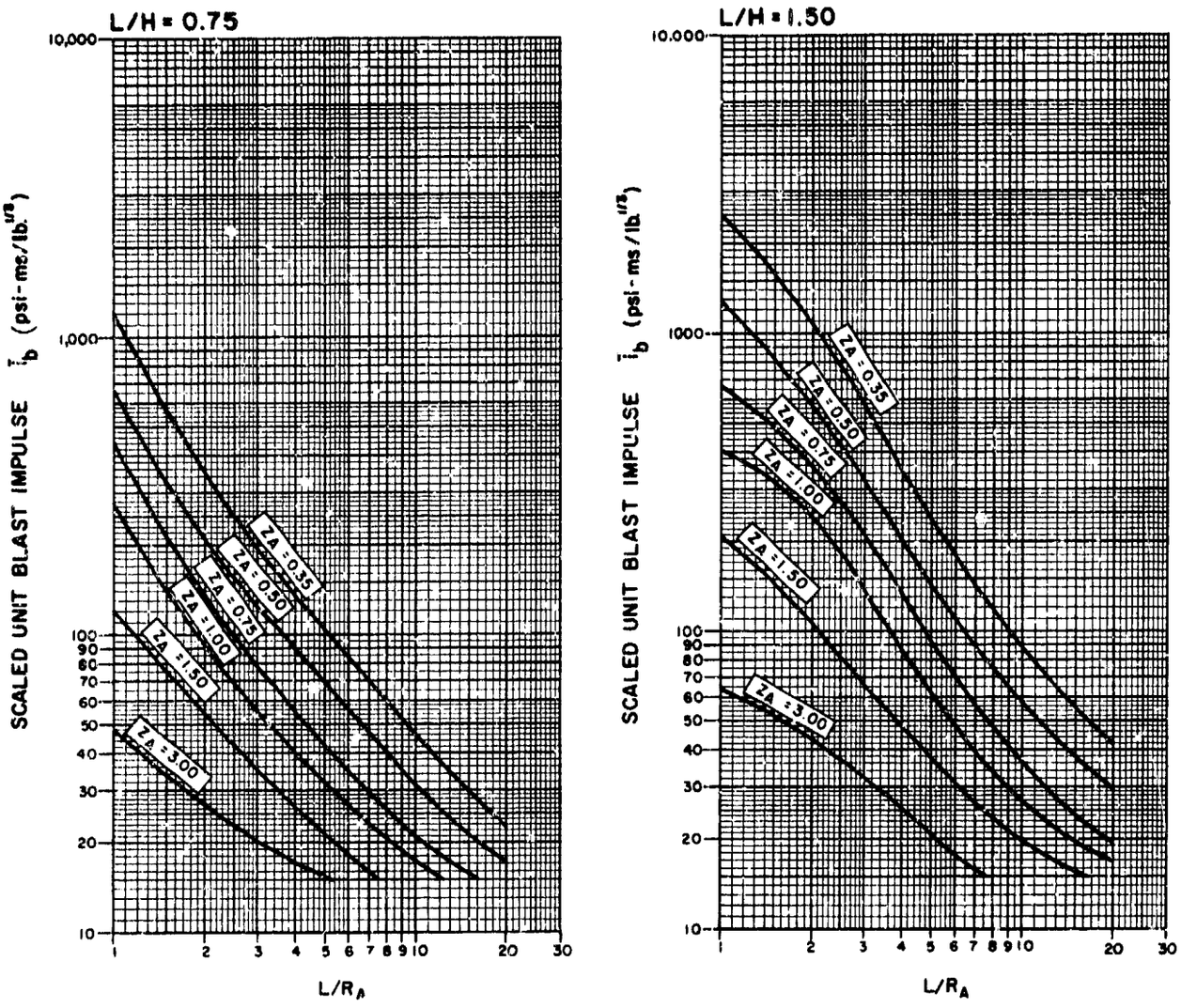
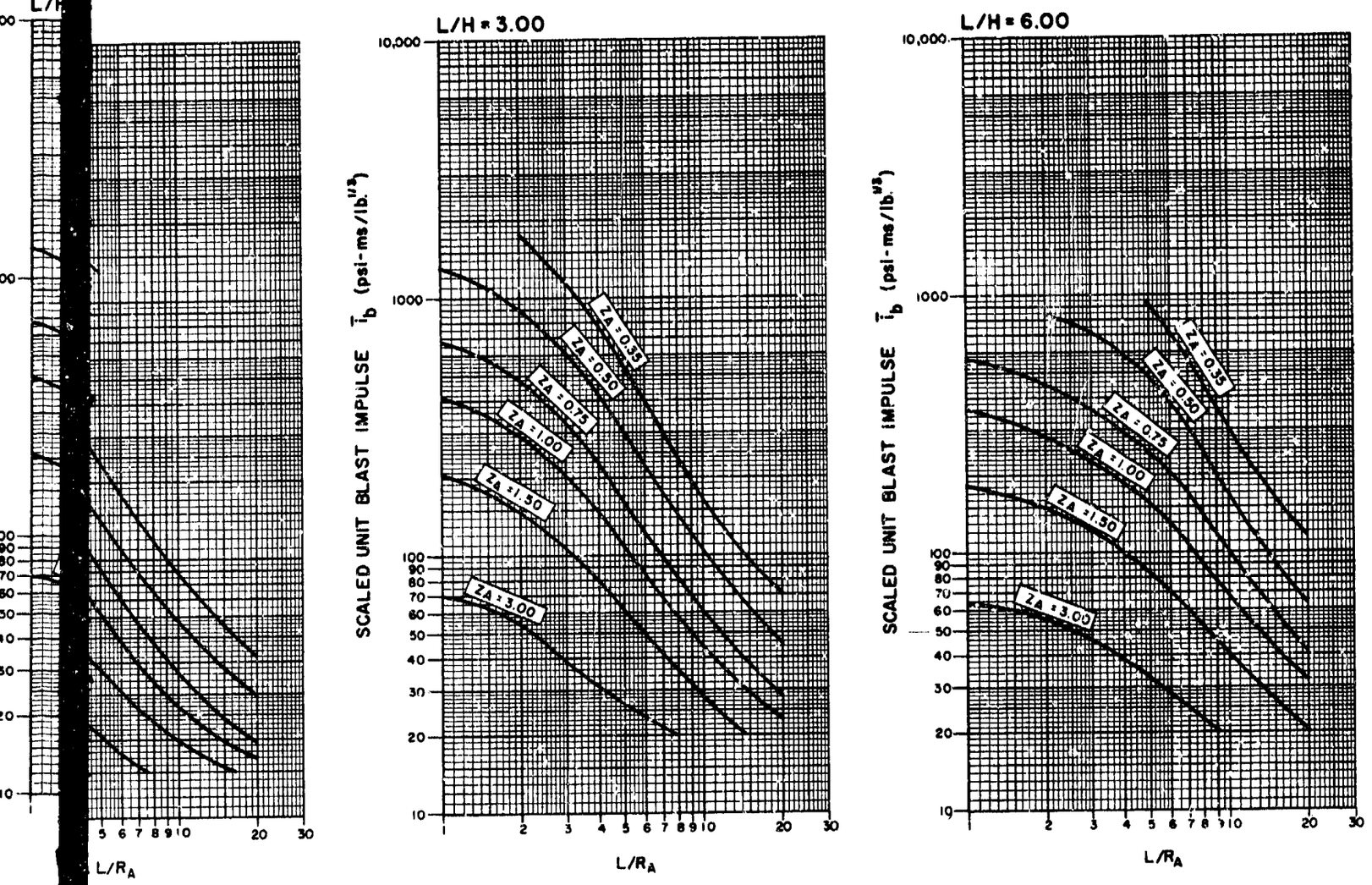


Figure 4–23. Scaled average unit blast impulse ($N = 1$, l/L



e 4-23. Scaled average unit blast impulse ($N = 1$, $l/L = 0.10$, $h/H = 0.60$).

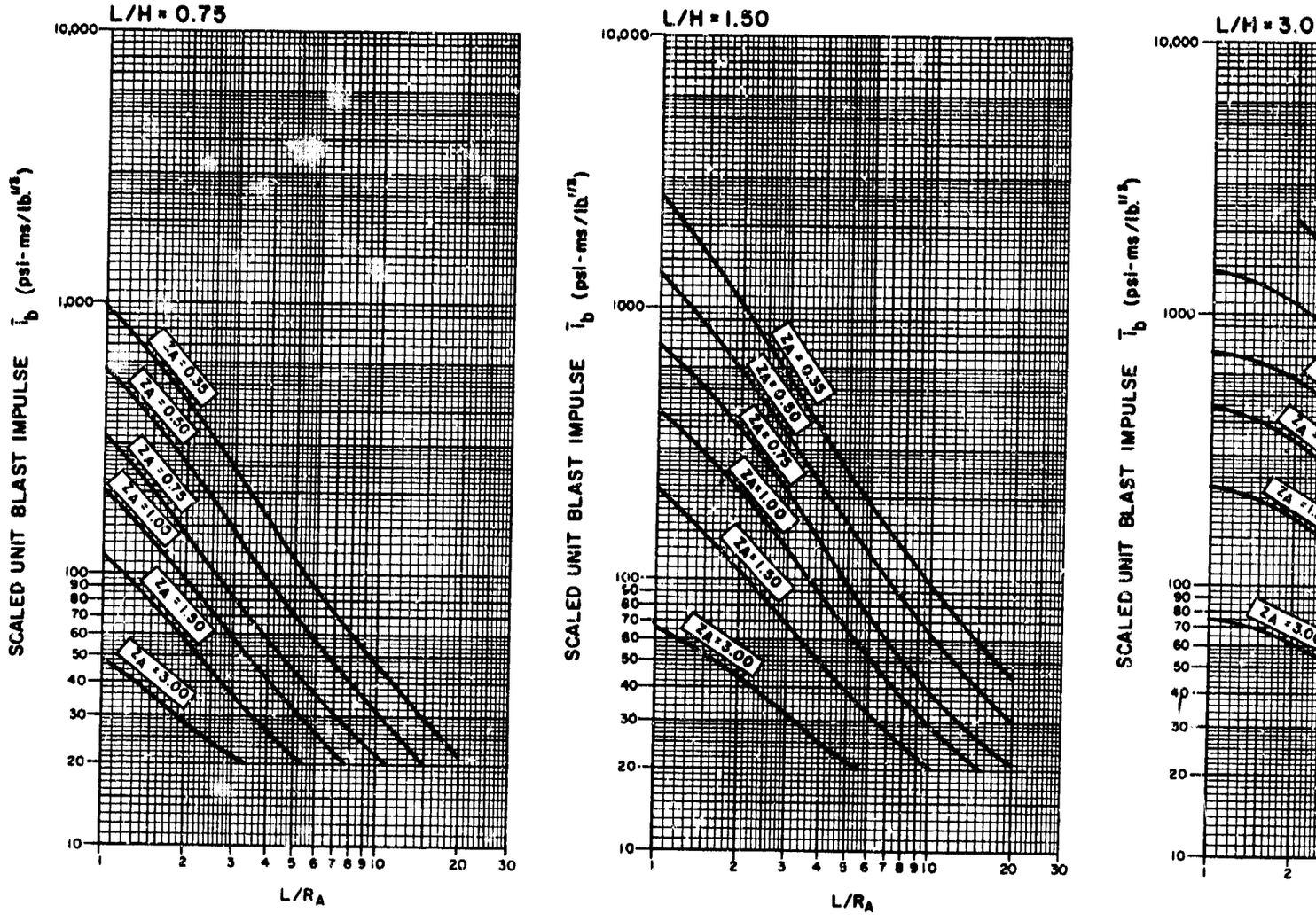
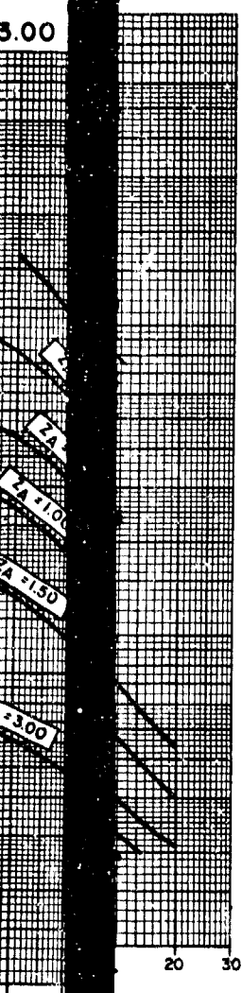
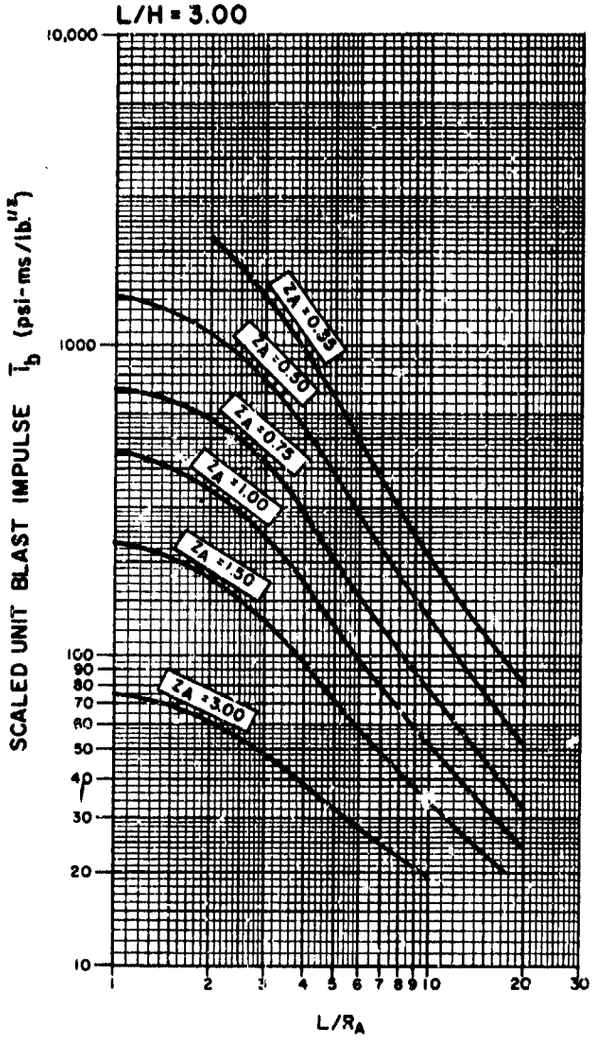
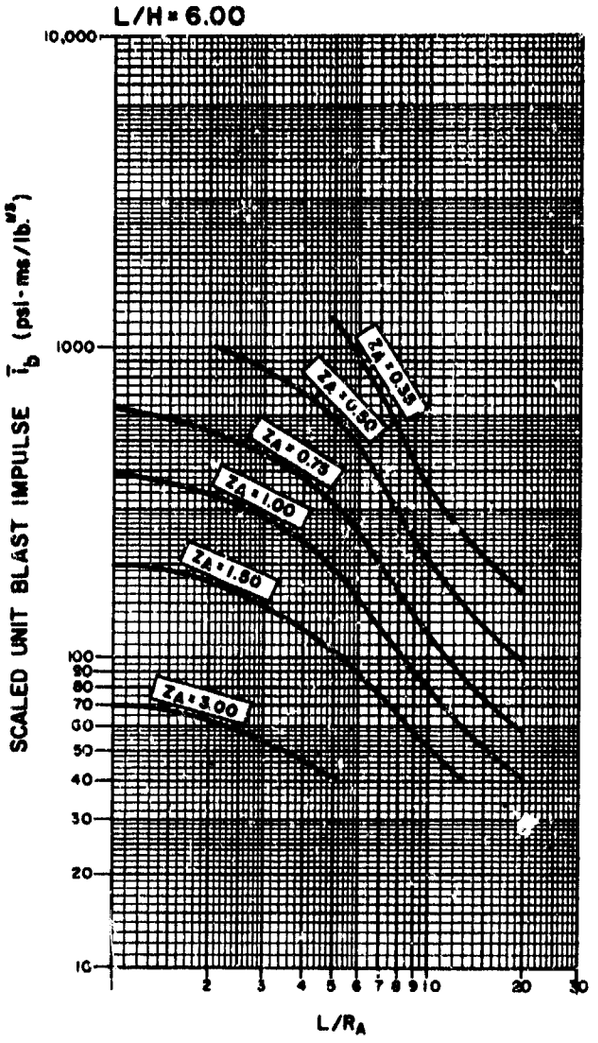


Figure 4-24. Scaled average unit blast impulse ($N = 1$, $l/L = 0.25$ and 0.75,







e unit blast impulse ($N = 1$, $l/L = 0.25$ and 0.75, $h/H = 0.50$).

0.75, h/

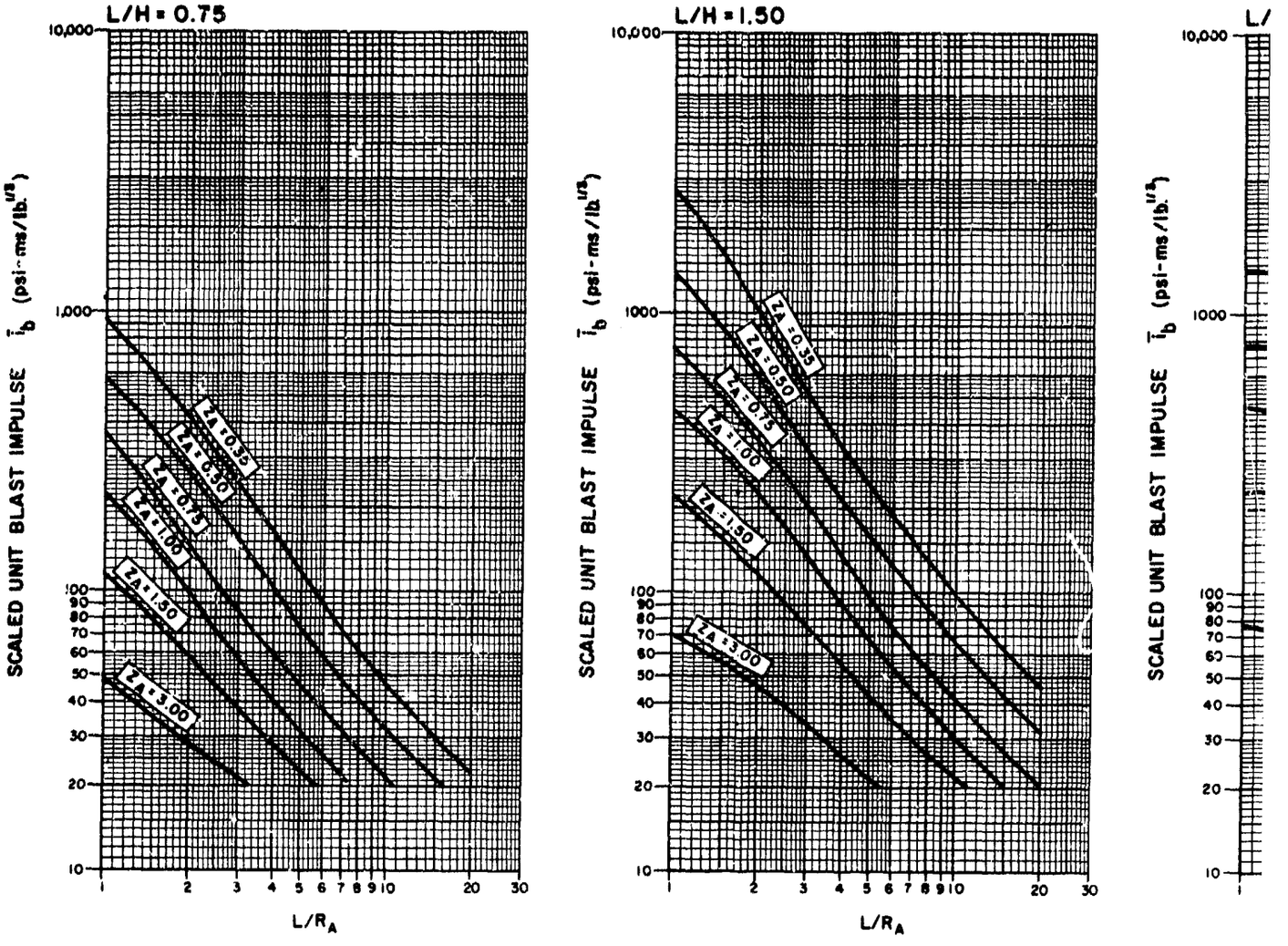
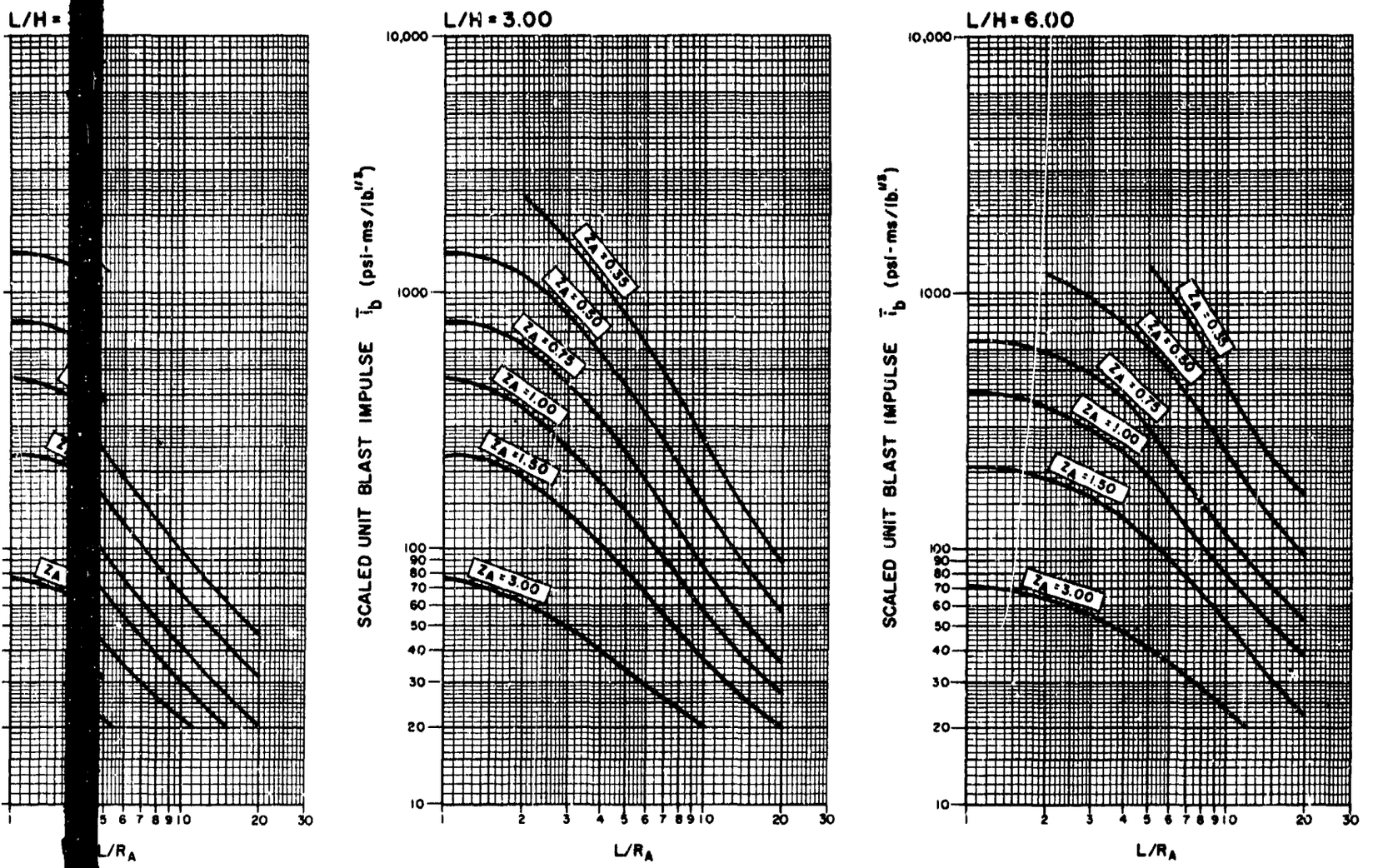


Figure 4-25. Scaled average unit blast impulse ($N = 1$, l/L



l/L=0.5 *4-25. Scaled average unit blast impulse (N=1, l/L=0.50, h/H=0.50).*

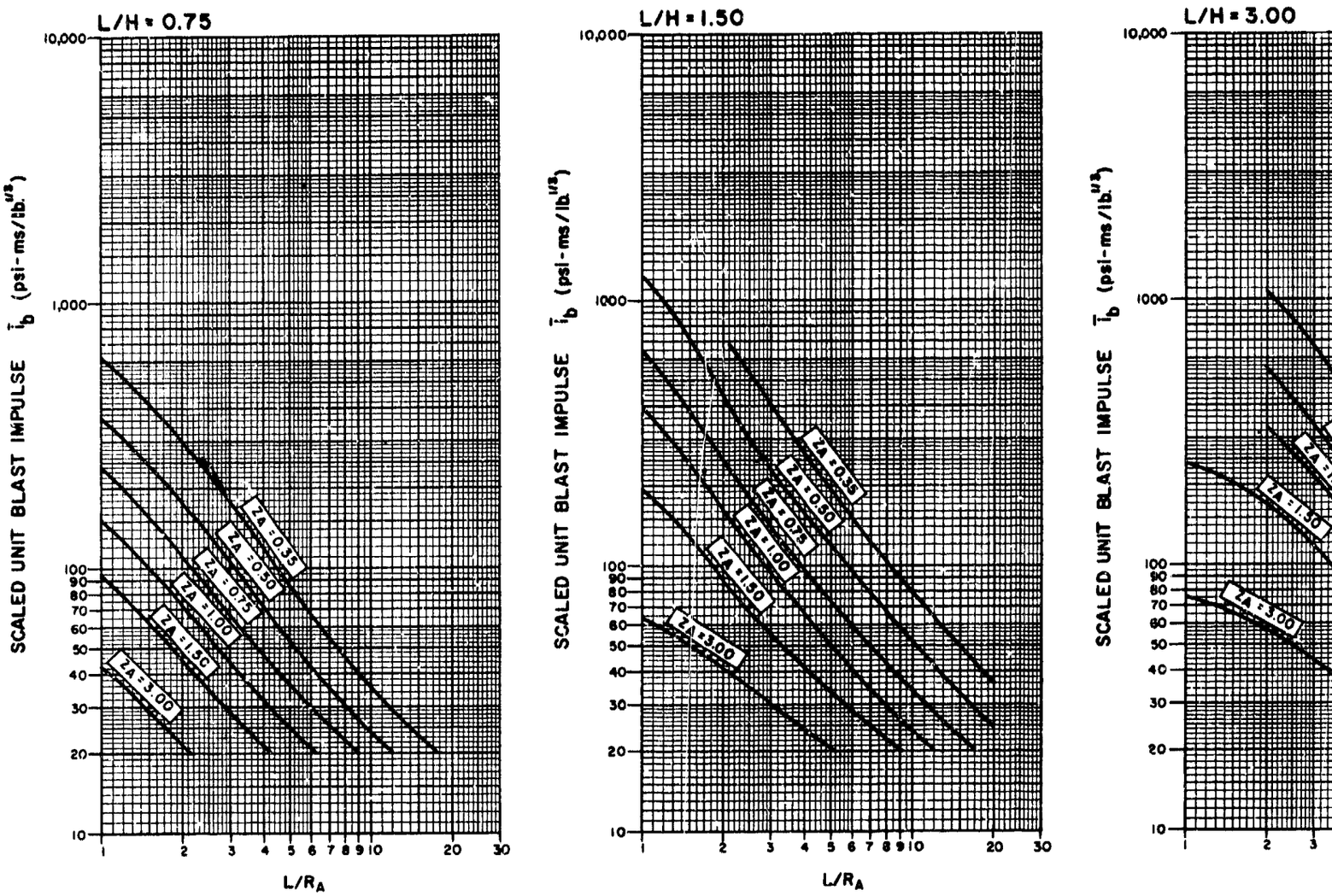
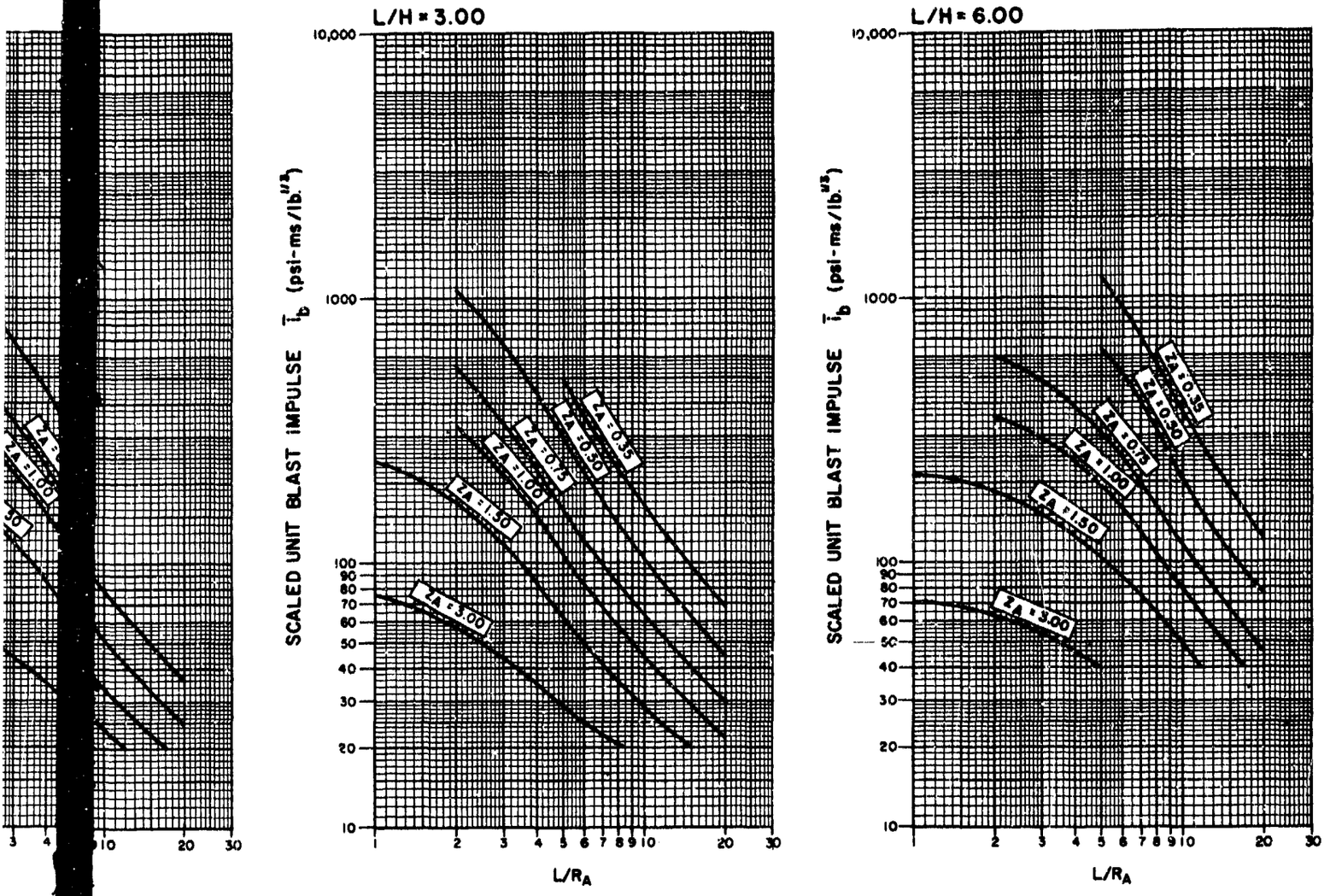


Figure 4–86. Scaled average unit blast impulse ($N = 1$, $l/L = 0.25$ and 0.75, h/H



h/H = 0. *average unit blast impulse (N = 1, l/L = 0.25 and 0.75, h/H = 0.75).*

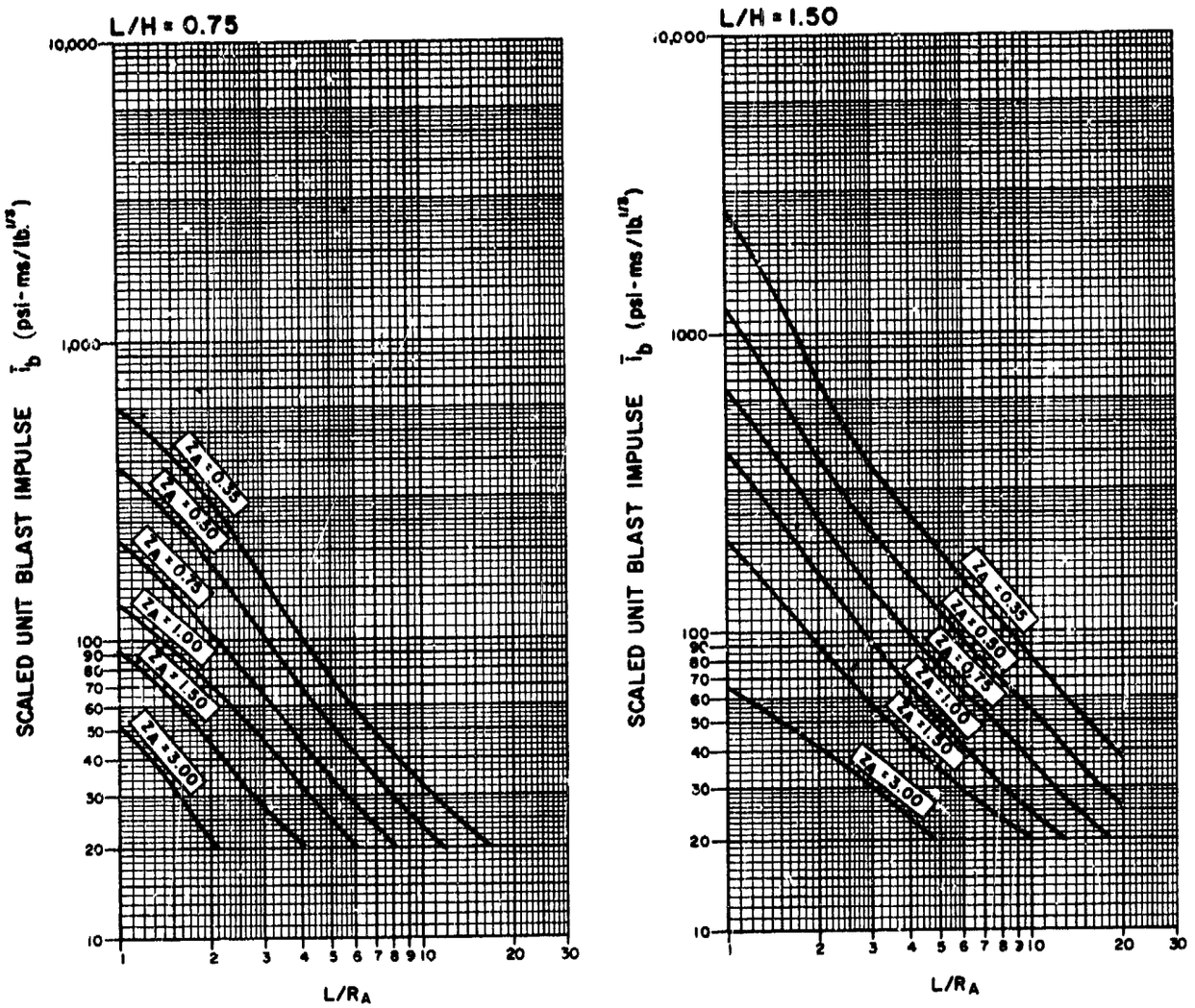
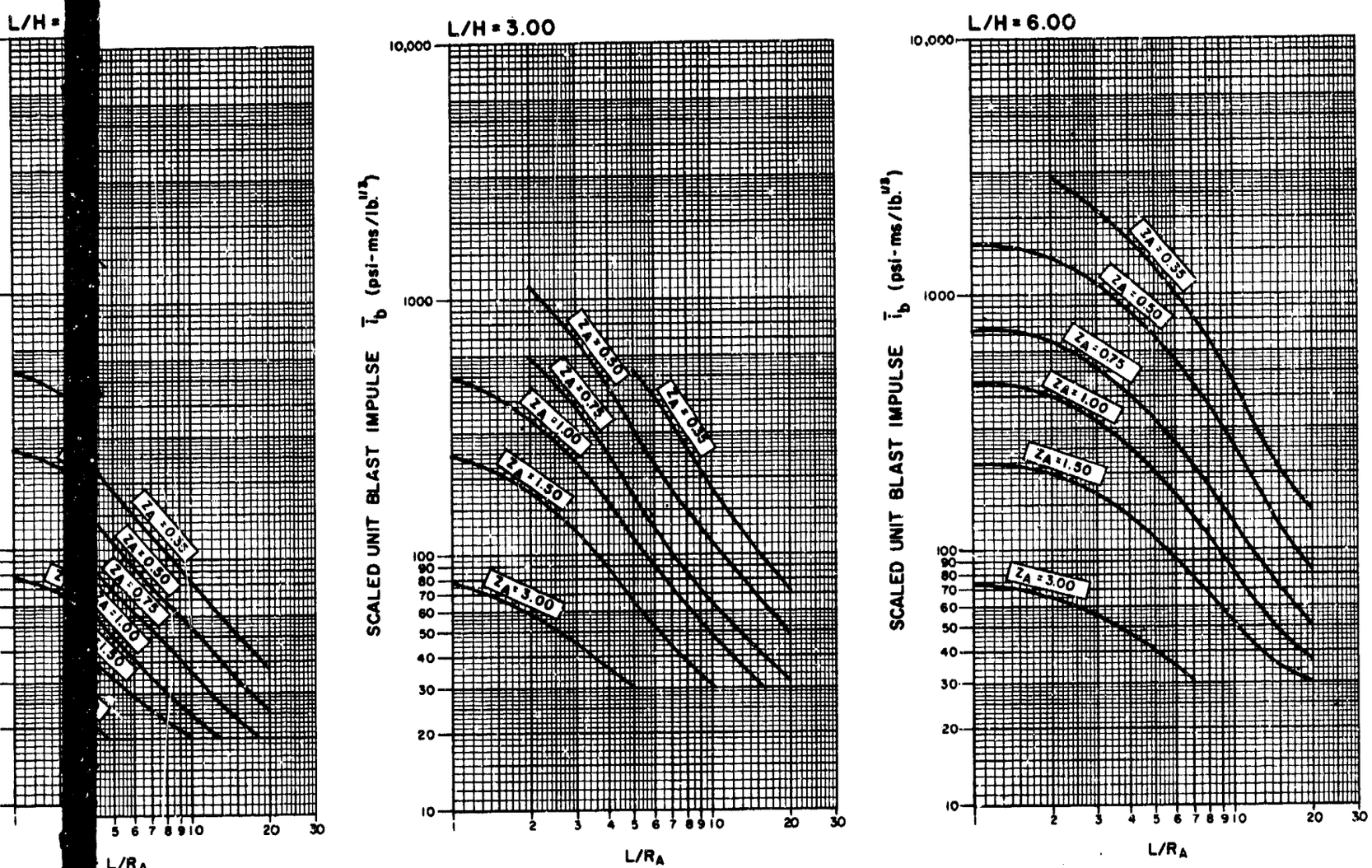


Figure 4-27. Scaled average unit blast impulse (N = 1, l/L = 0



L/L=0.50, h/H=0.75).

4-27. Scaled average unit blast impulse (N=1, l/L=0.50, h/H=0.75).

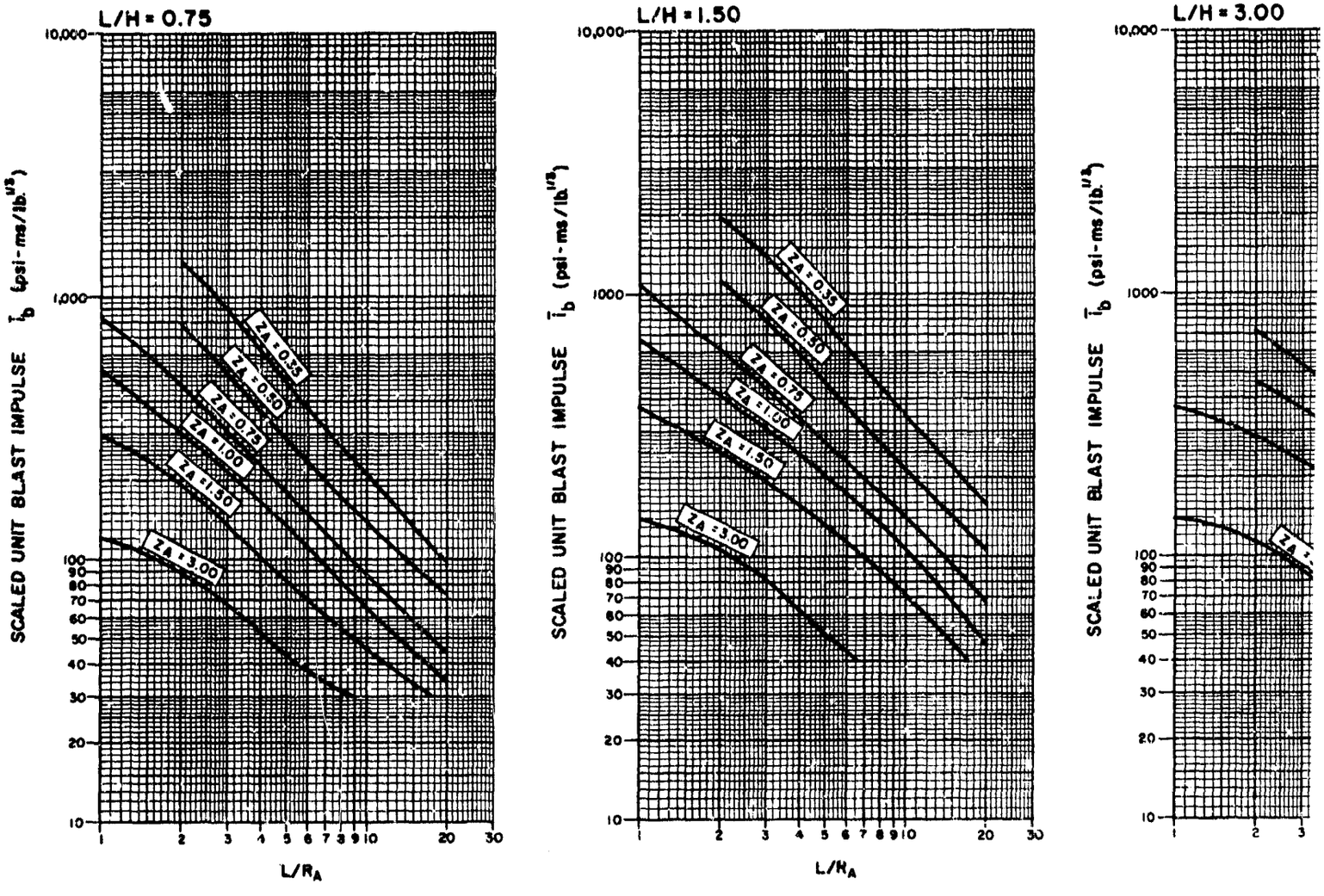
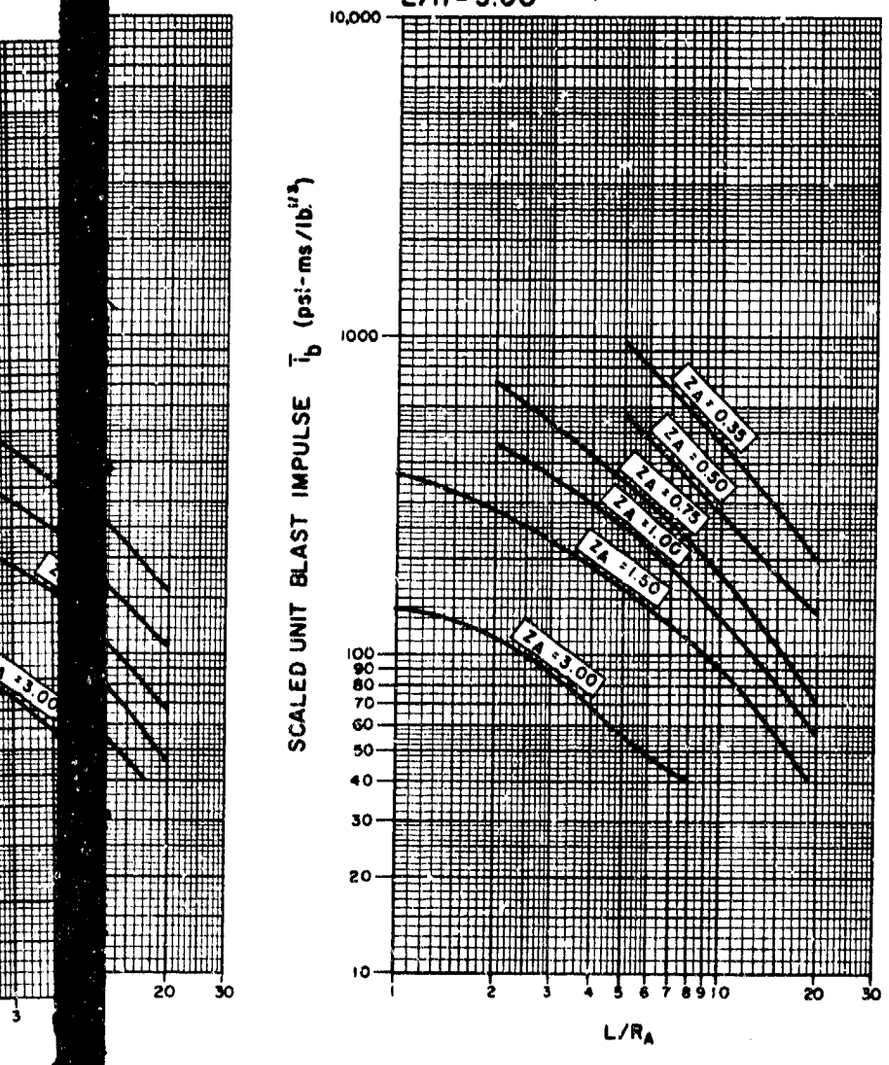
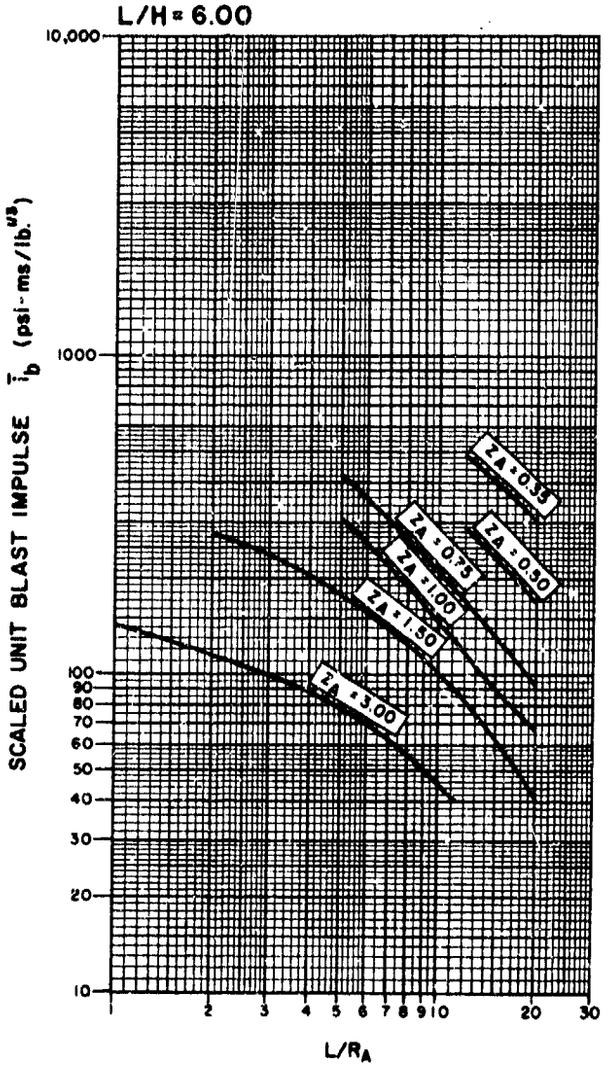
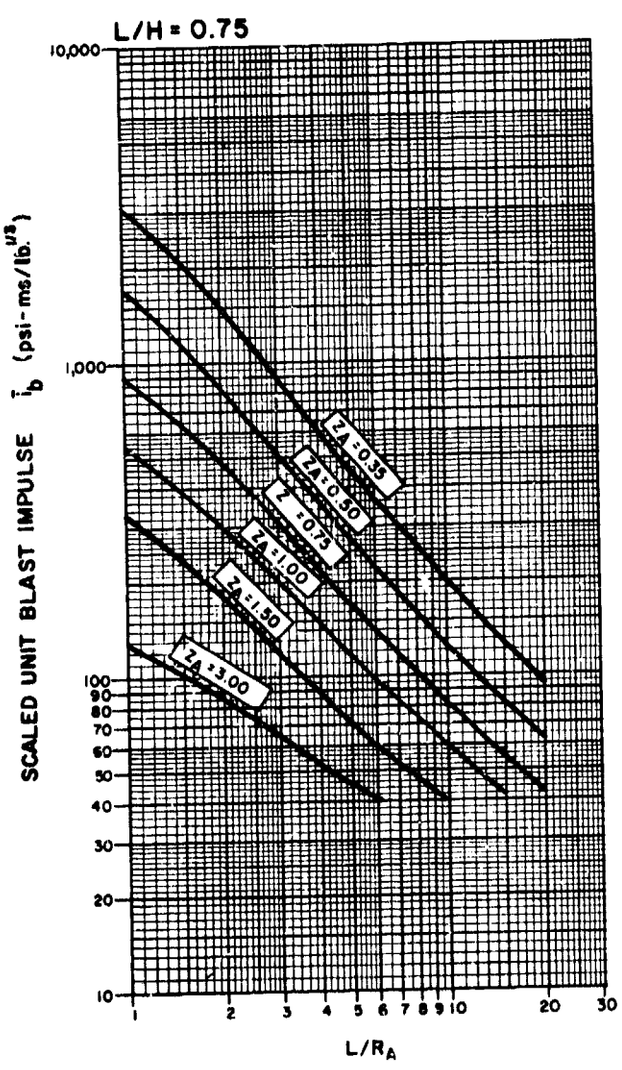


Figure 4-26. Scaled average unit blast impulse ($N = 2$, $l/L = 0.10$, $h/H = 0$.





erage unit blast impulse ($N = 2$, $l/L = 0.10$, $h/H = 0.15$).



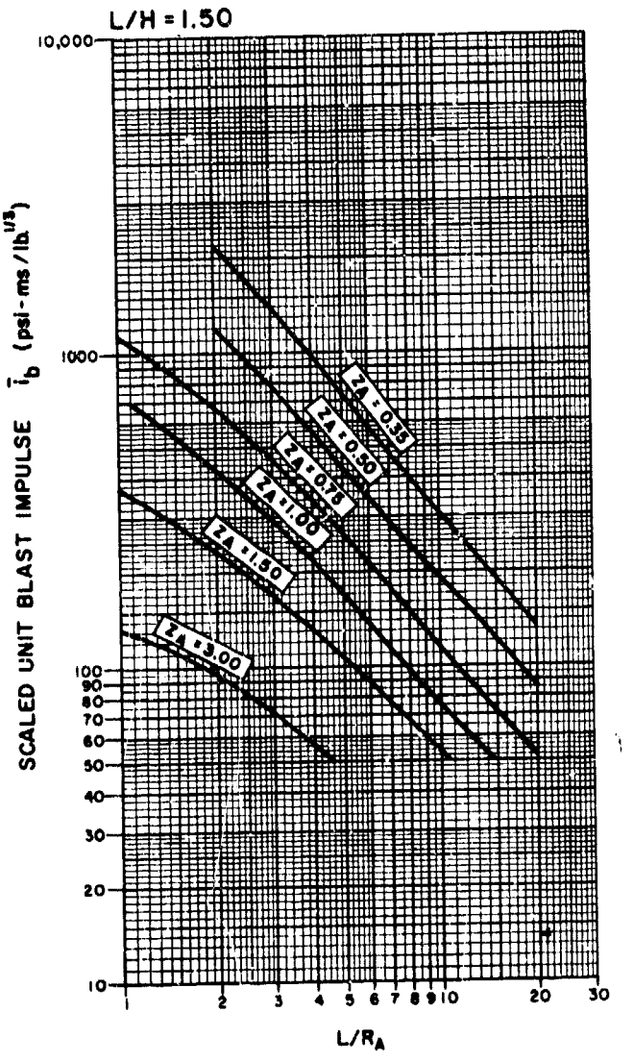
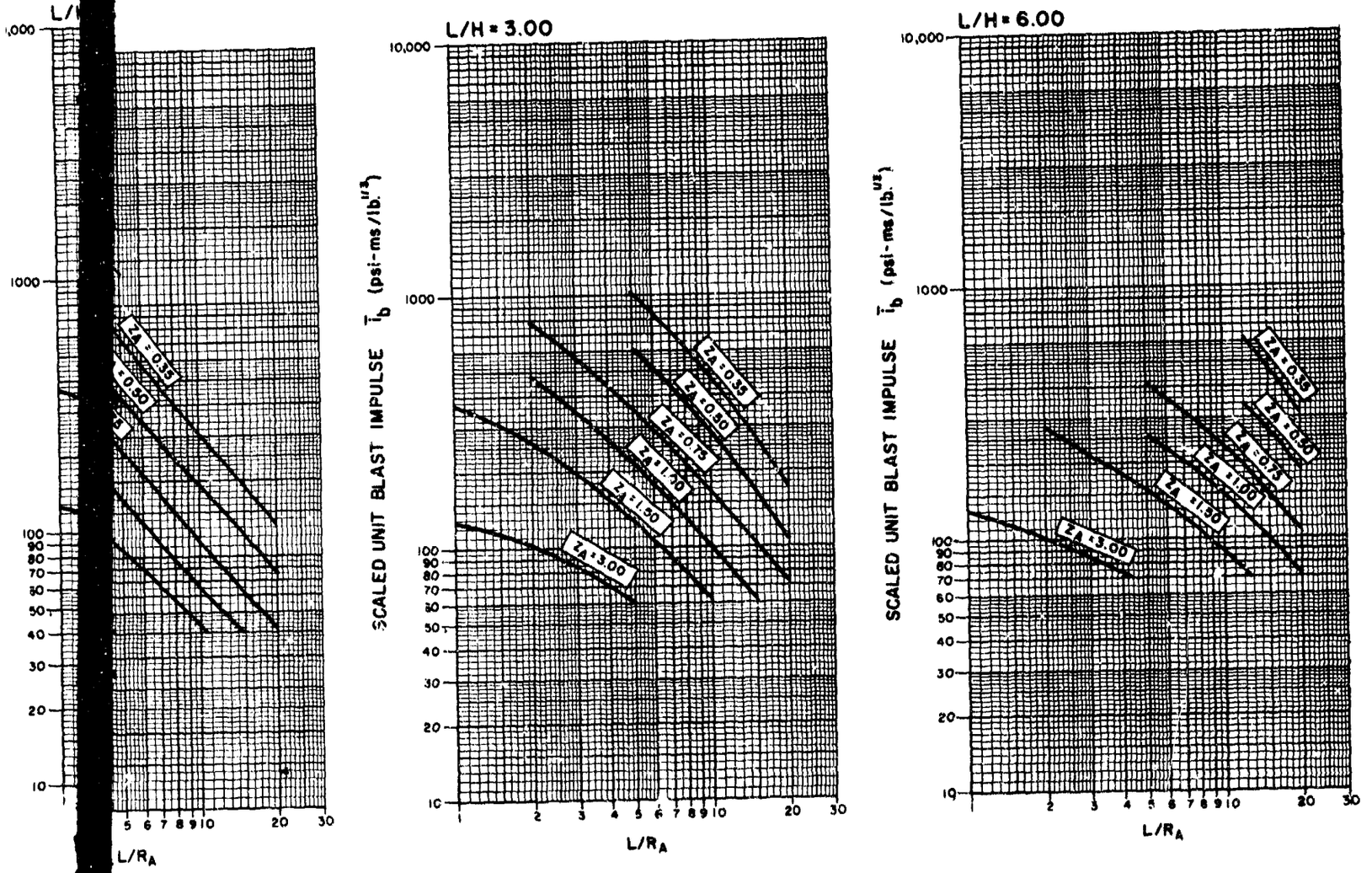




Figure 4-29. Scaled average unit blast impulse (N =



N = 2, l/L

4-29. Scaled average unit blast impulse (N = 2, l/L = 0.85, h/H = 0.15).

2

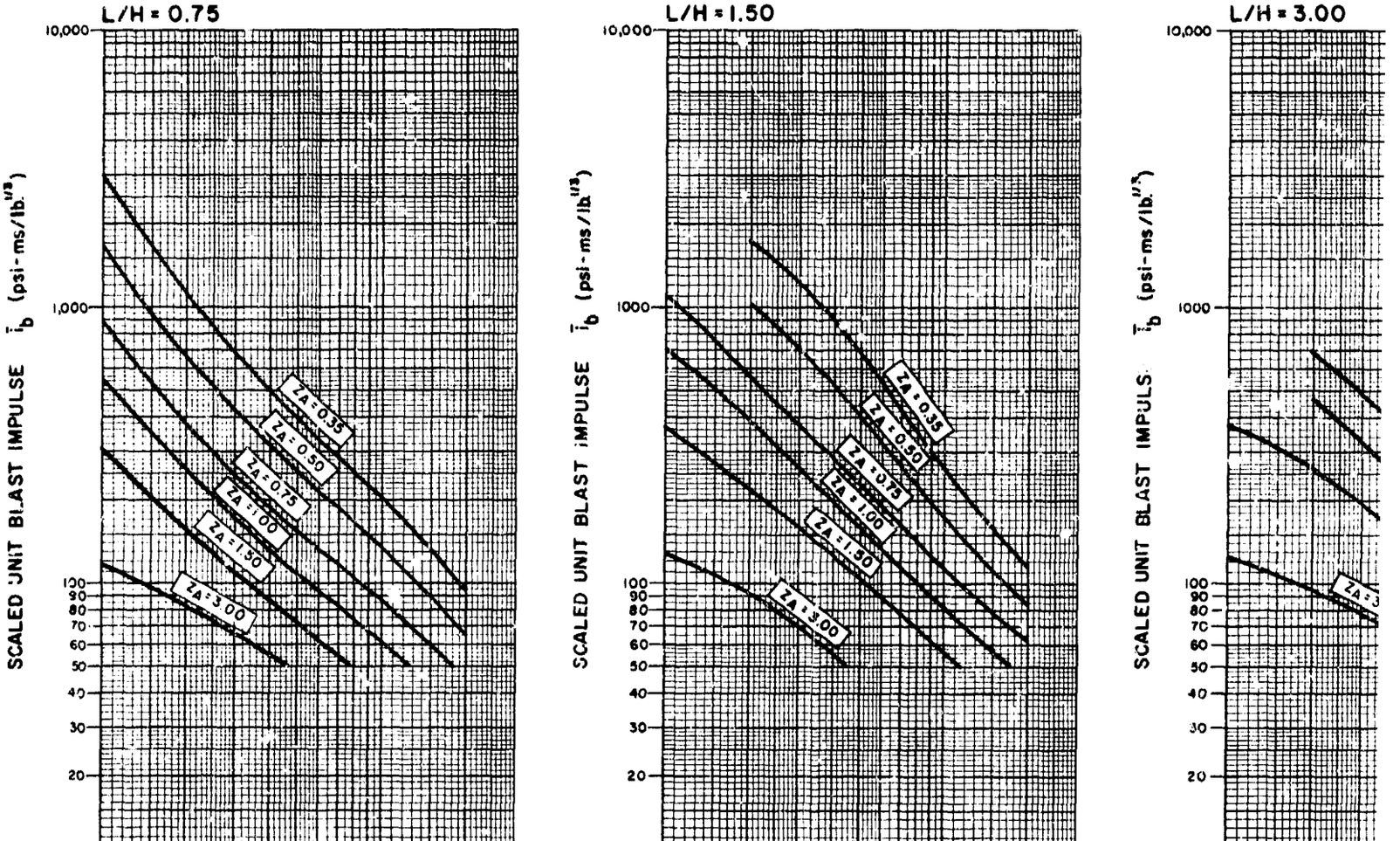
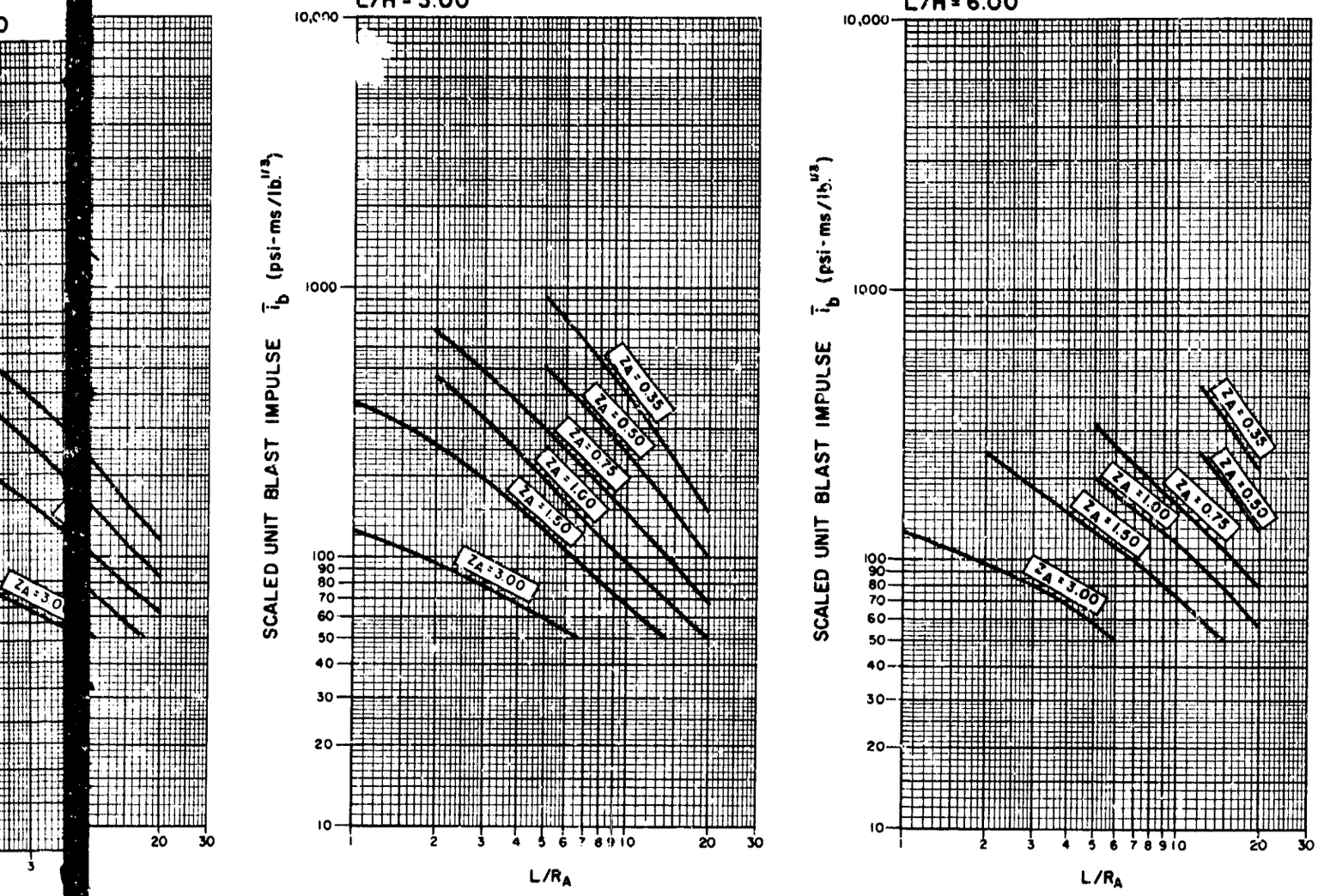


Figure 4-30. Scaled average unit blast impulse ($N = 2$, $l/L = 0.50$, $h/H = 0.1$



average unit blast impulse ($N=2$, $l/L=0.50$, $h/H=0.15$).

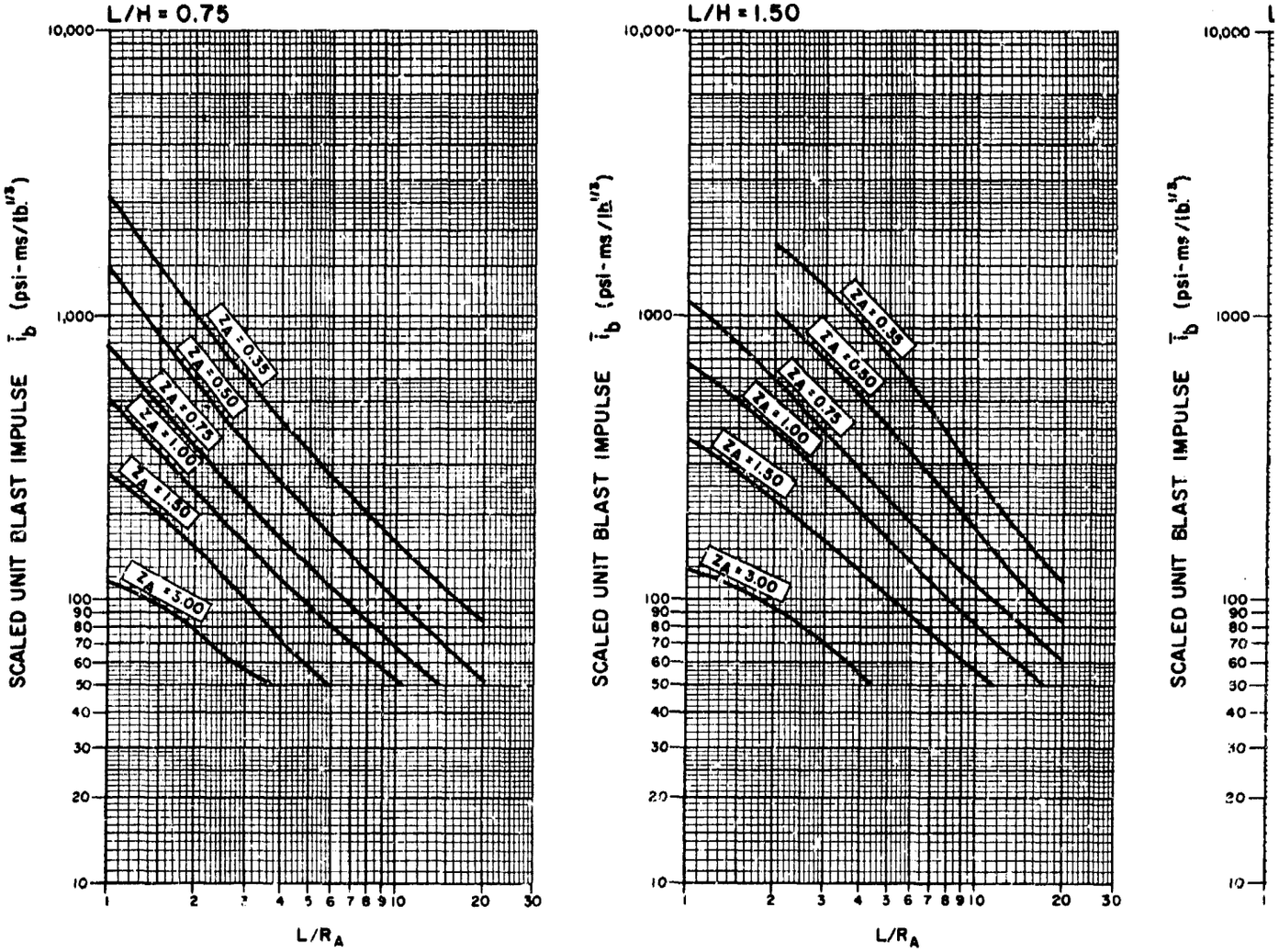


Figure 4-31. Scaled average unit blast impulse ($N = 2$,

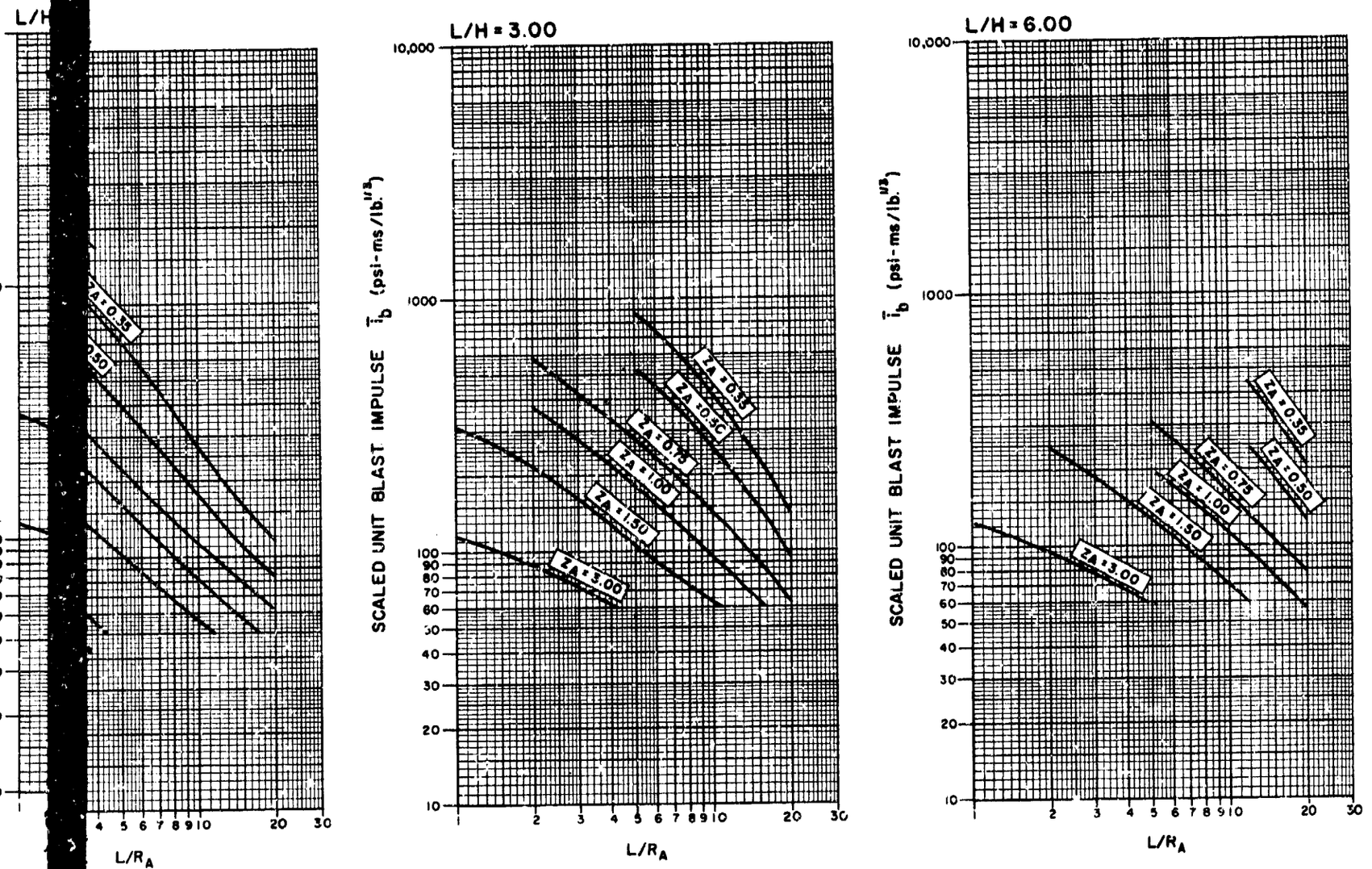
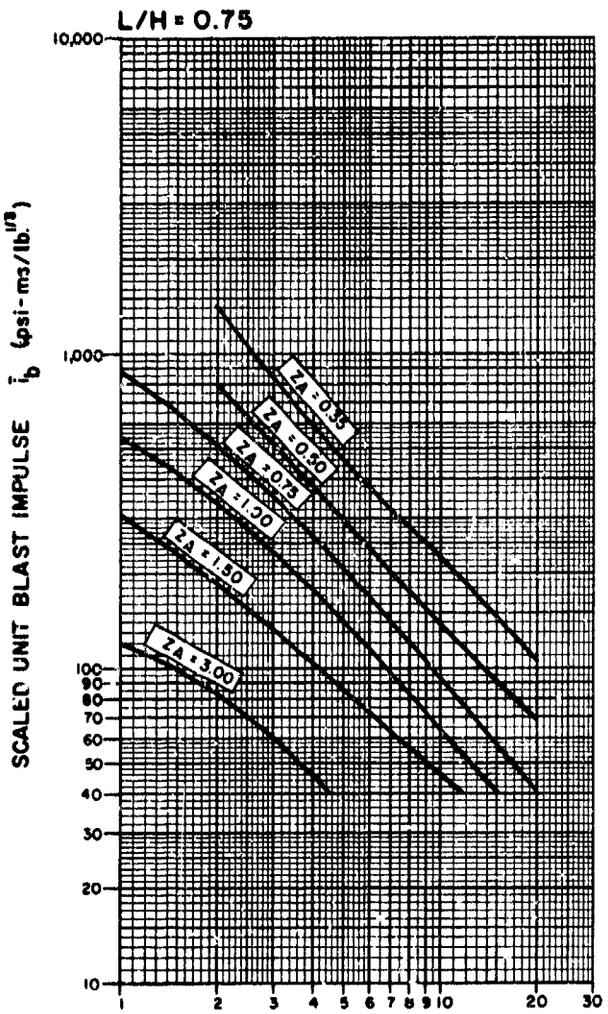
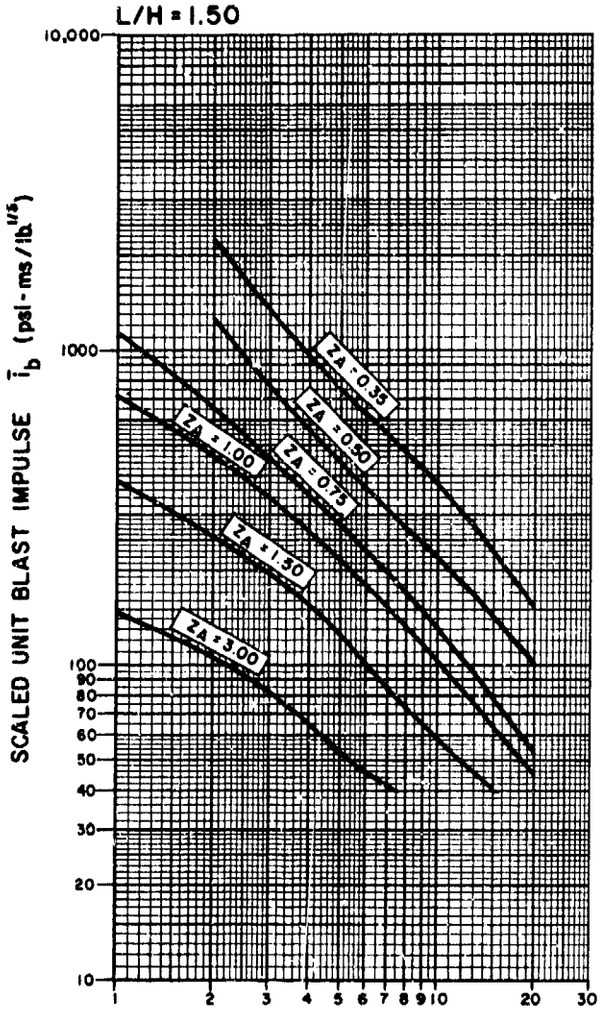


Figure 4-31. Scaled average unit blast impulse ($N=2$, $l'/L=0.75$, $h/H=0.15$).





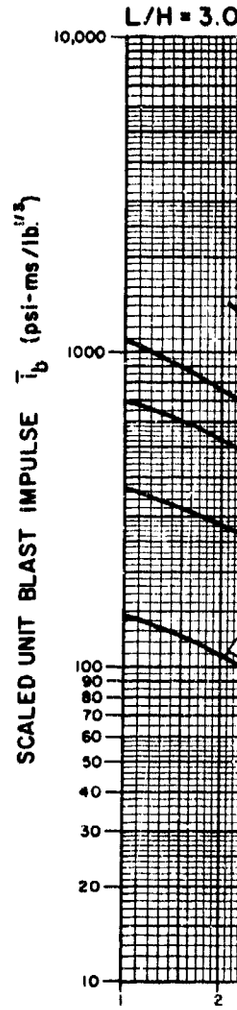
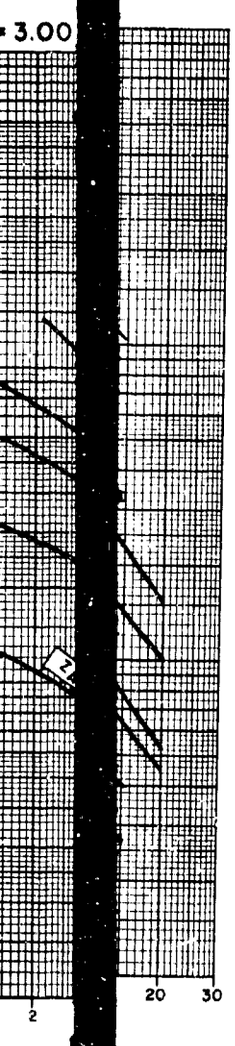
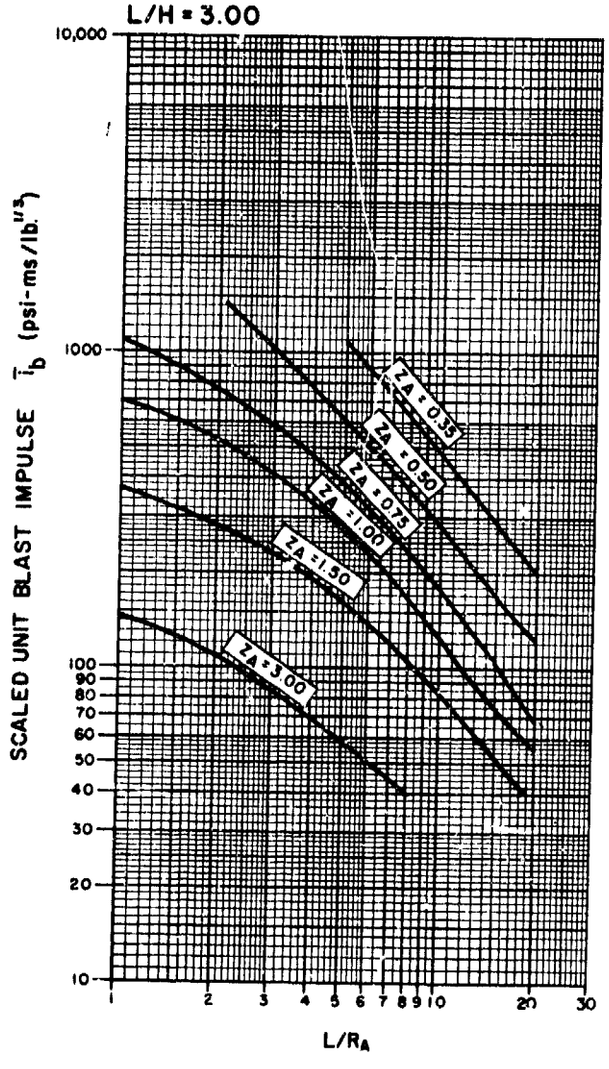
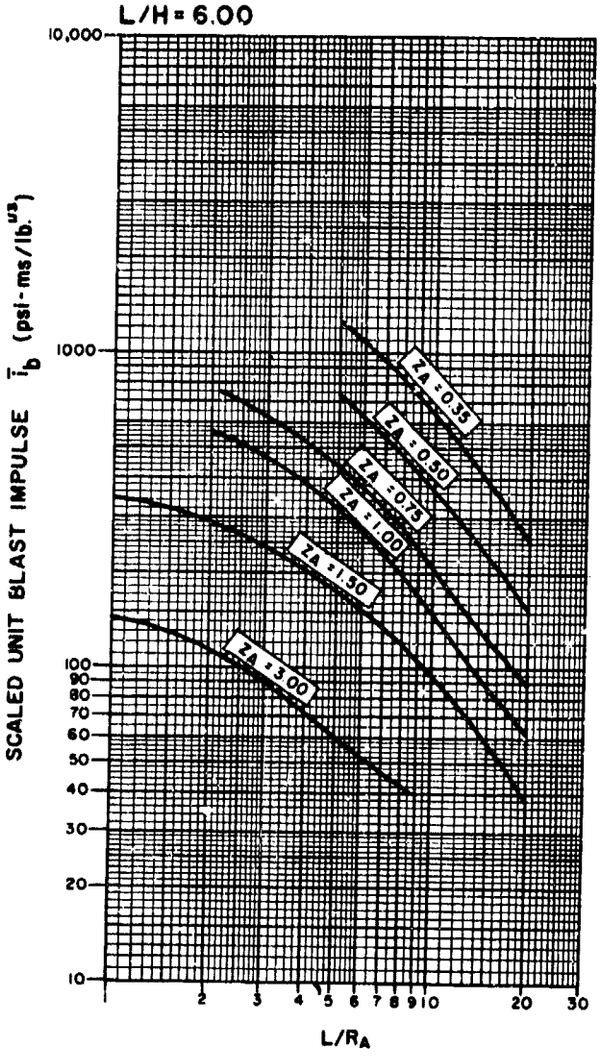


Figure 4-32. Scaled average unit blast impulse ($N = 2$, $l/L = 0.10$, $h/$







10, h/H = ...age unit blast impulse ($N = 2$, $l/L = 0.10$, $h/H = 0.25$).

2

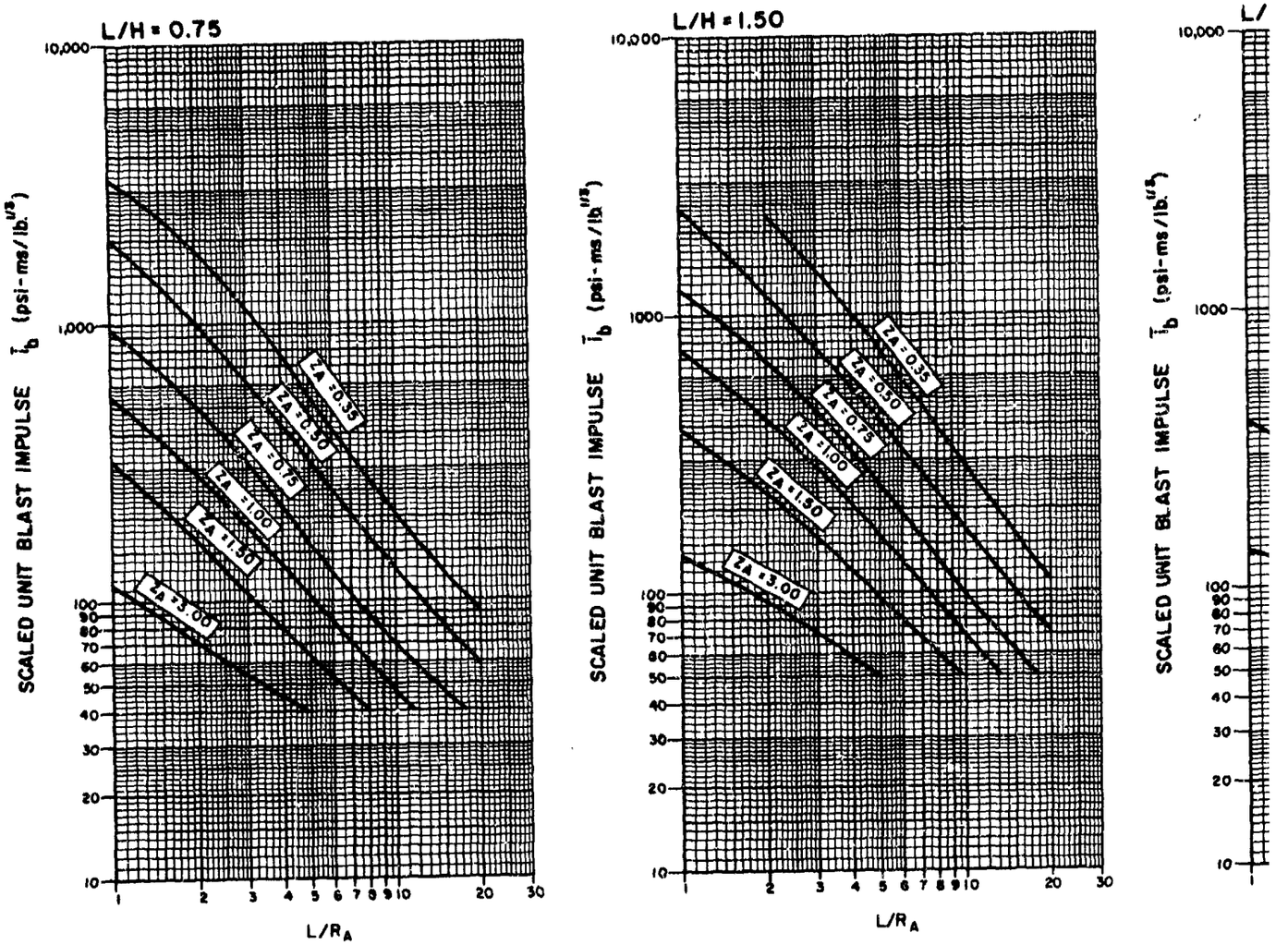


Figure 4-33. Scaled average unit blast impulse ($N = 2$, $1/1$

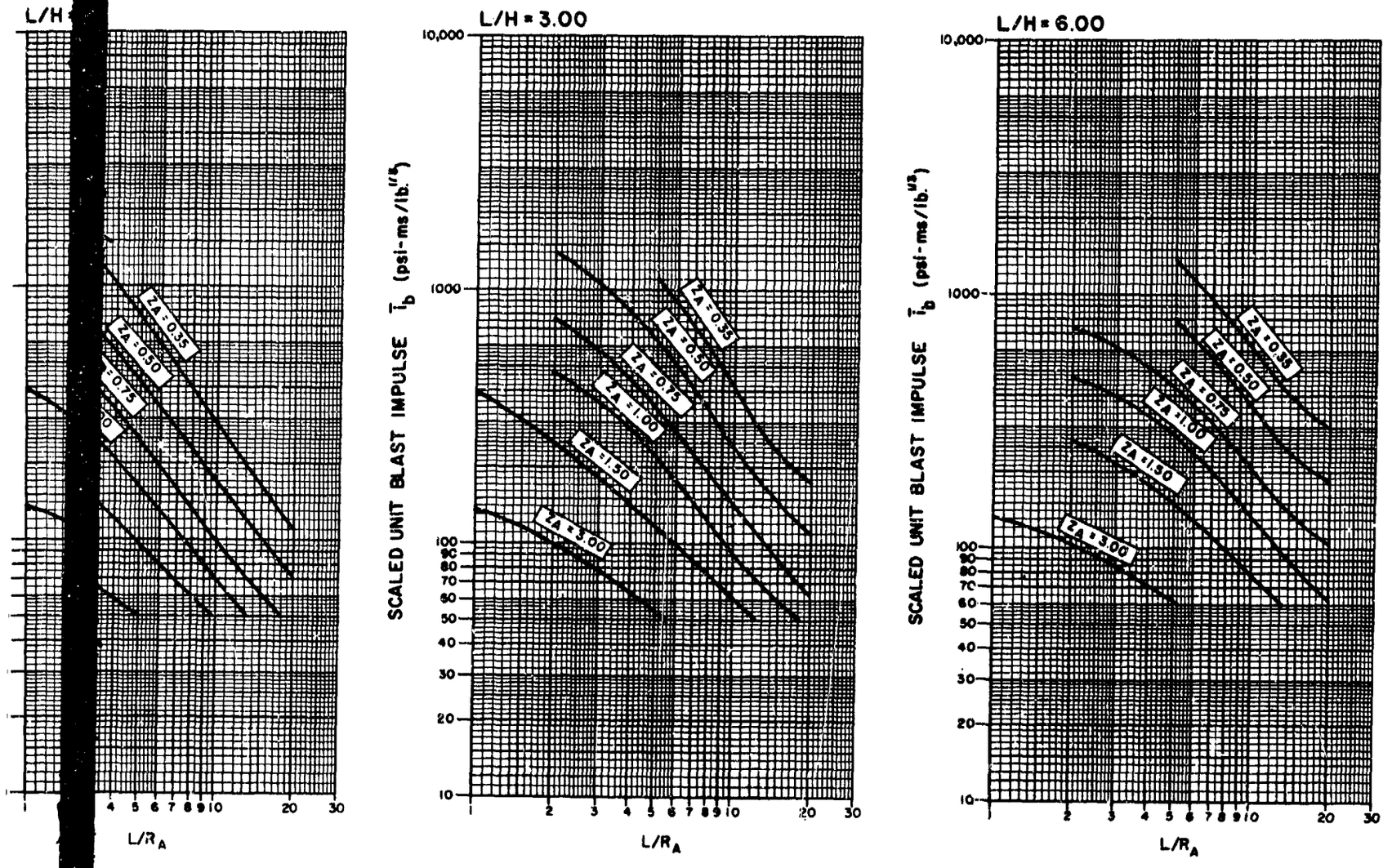
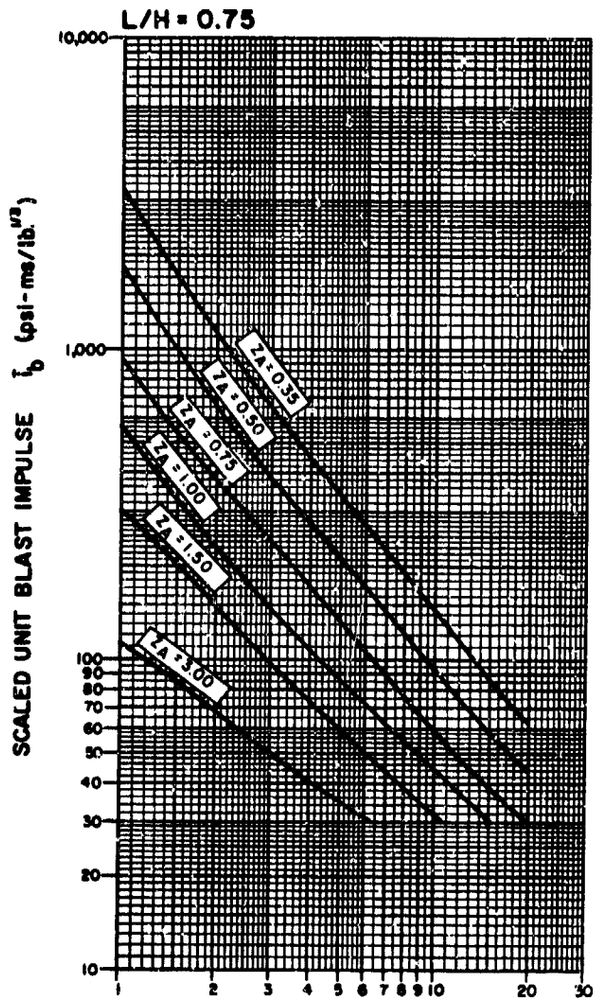
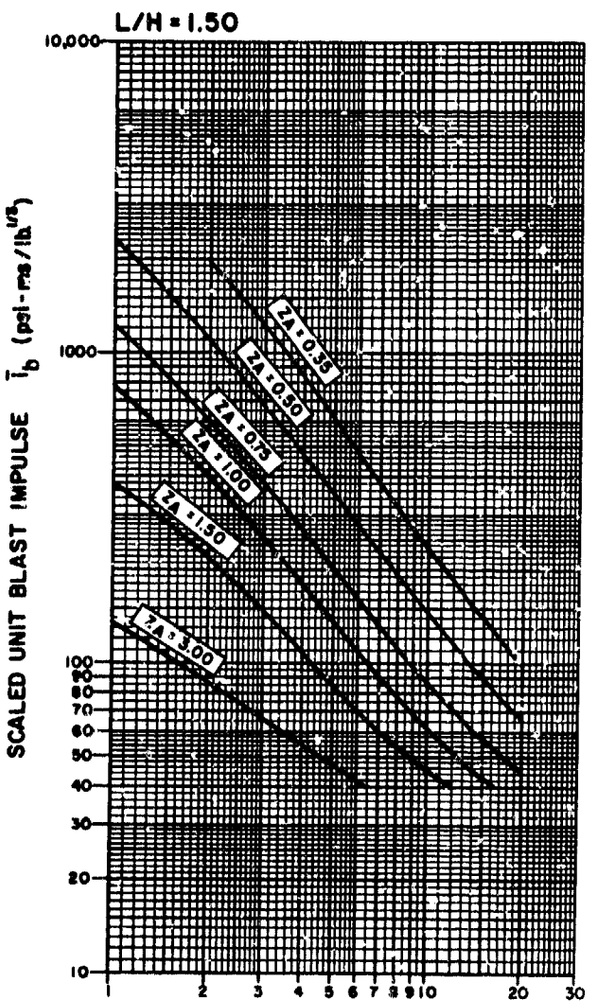


Figure 4-33. Scaled average unit blast impulse ($N = 2$, $l/L = 0.25$, $h/H = 0.25$).





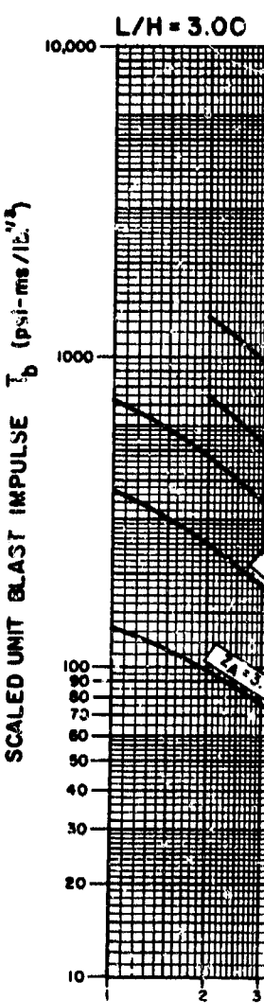
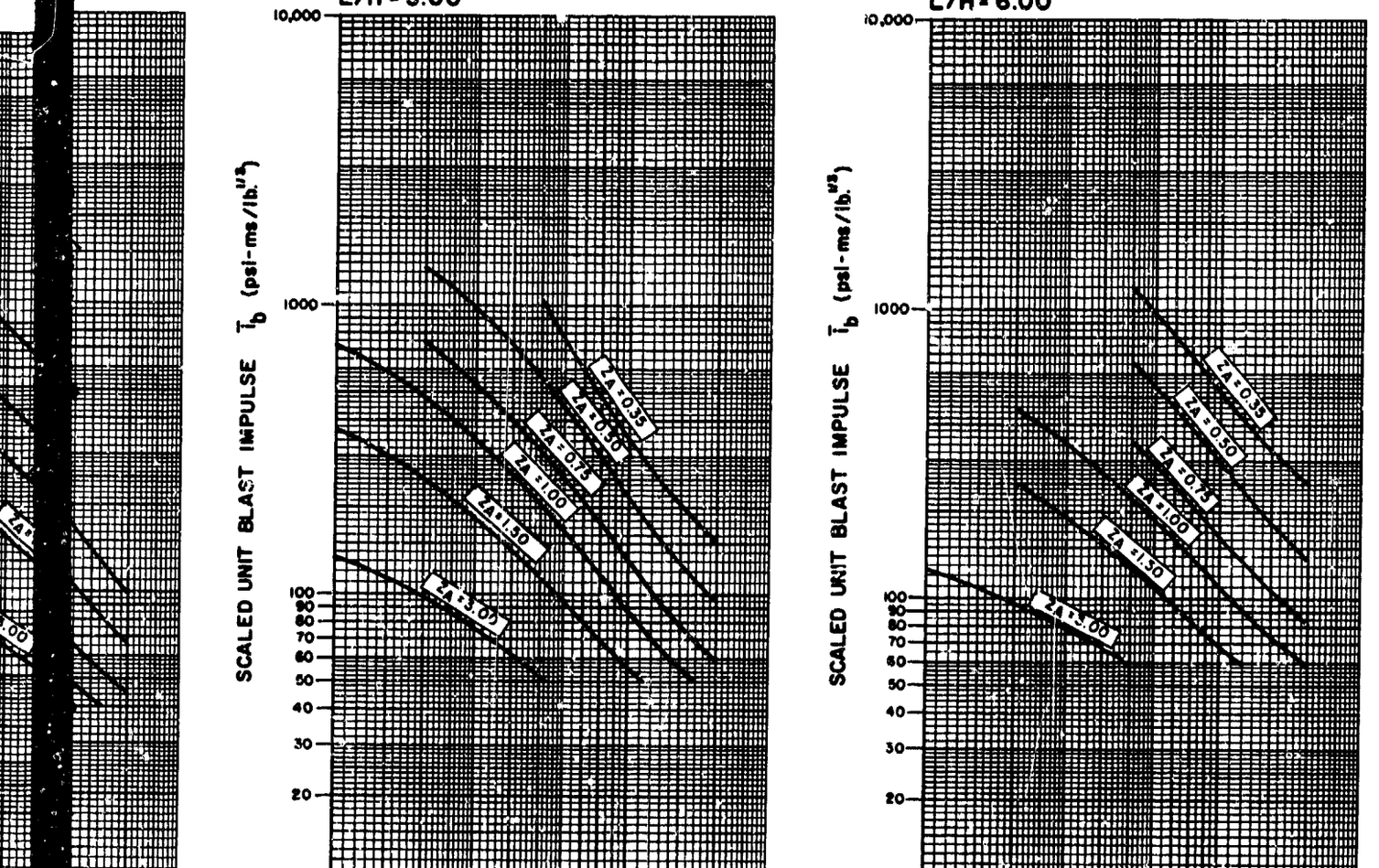


Figure 4–54. Scaled average unit blast impulse ($N = 2$, $l/L = 0.50$, $h/H = 0$



erage unit blast impulse ($N=2$, $l/L=0.50$, $h/H=0.35$).

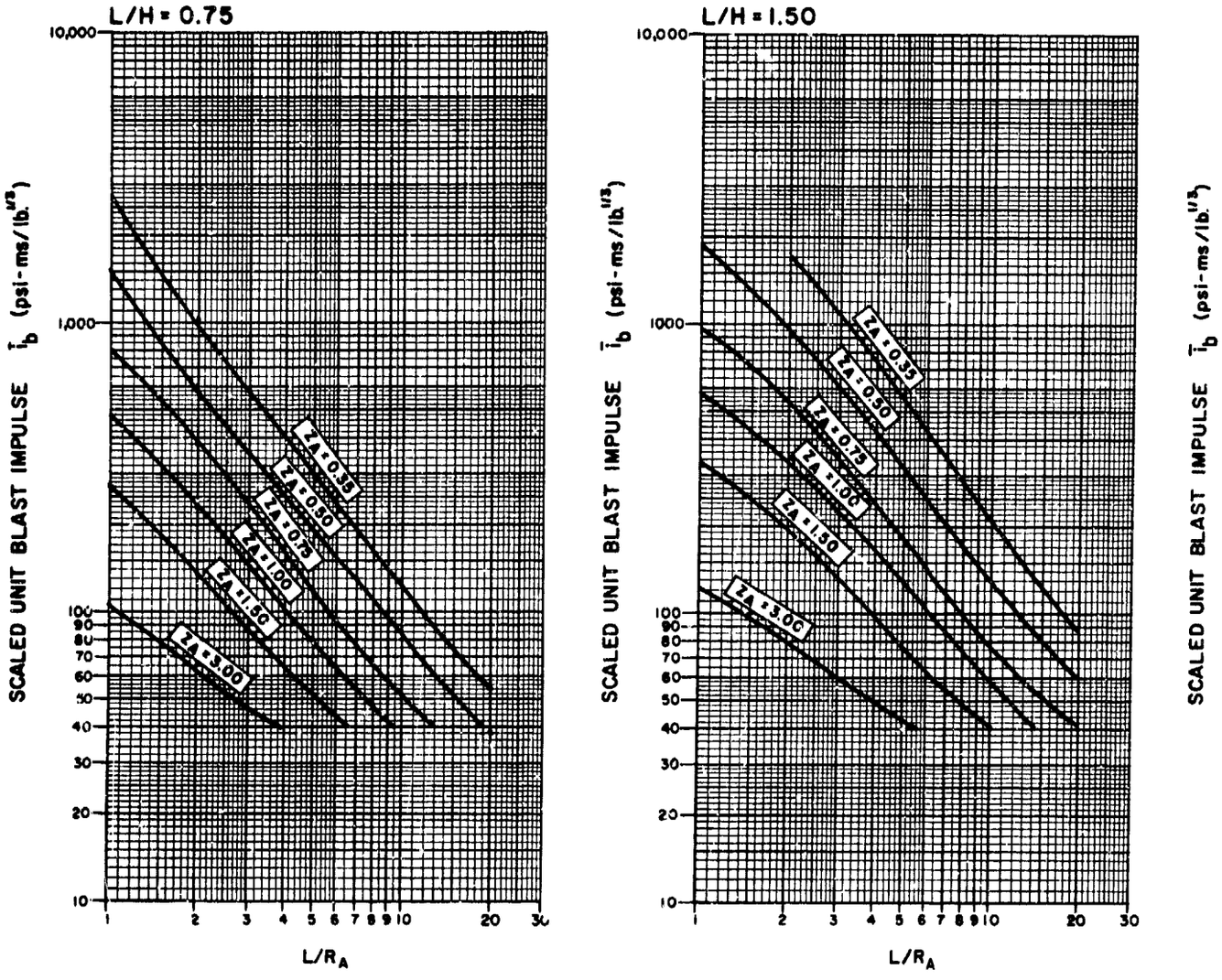
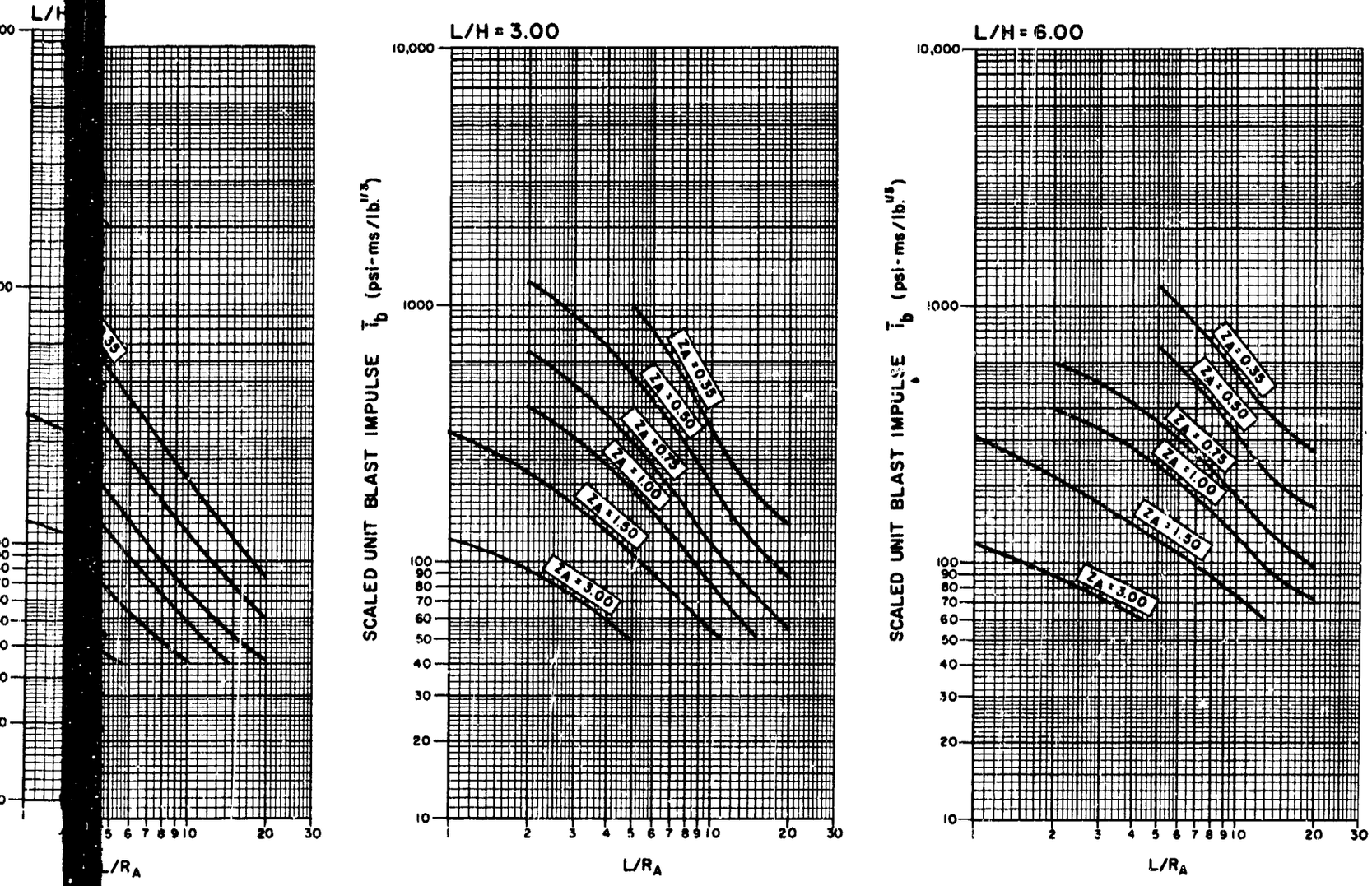
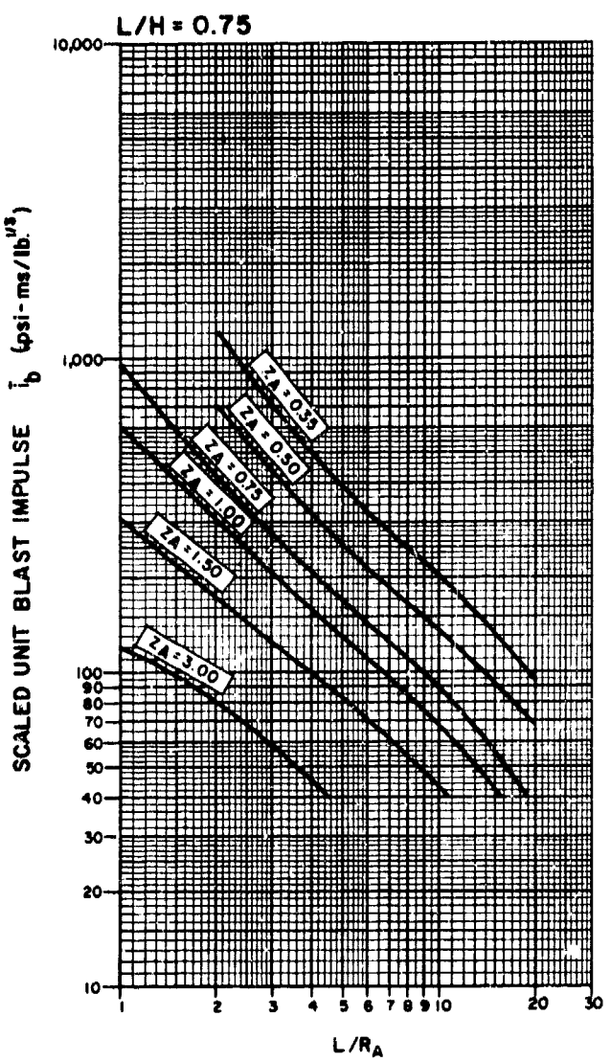


Figure 4-35. Scaled average unit blast impulse (N = 2,



4-35. Scaled average unit blast impulse ($N = 2$, $l/L = 0.75$, $h/H = 0.25$).



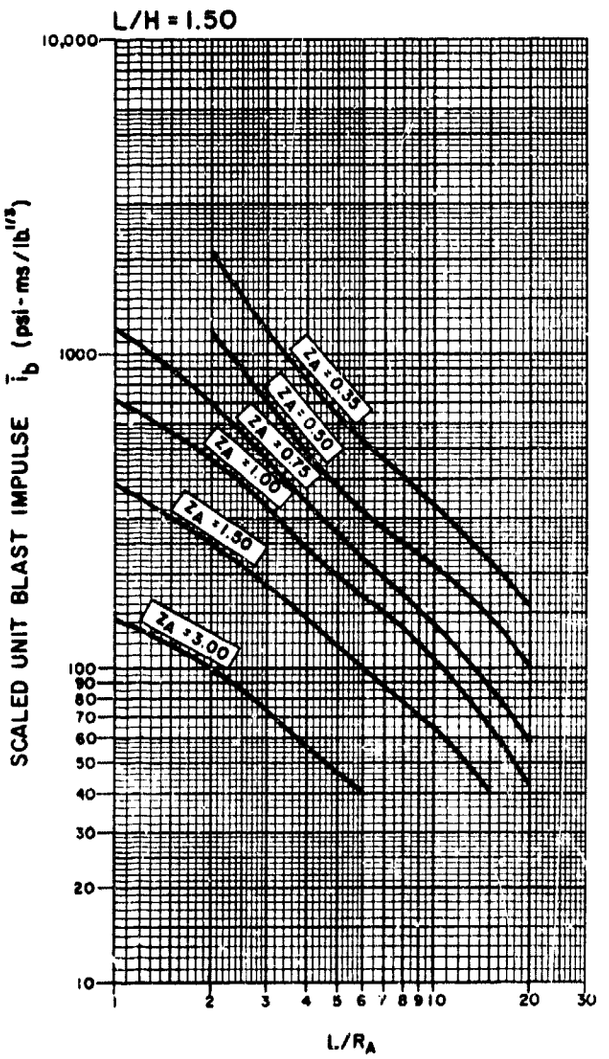
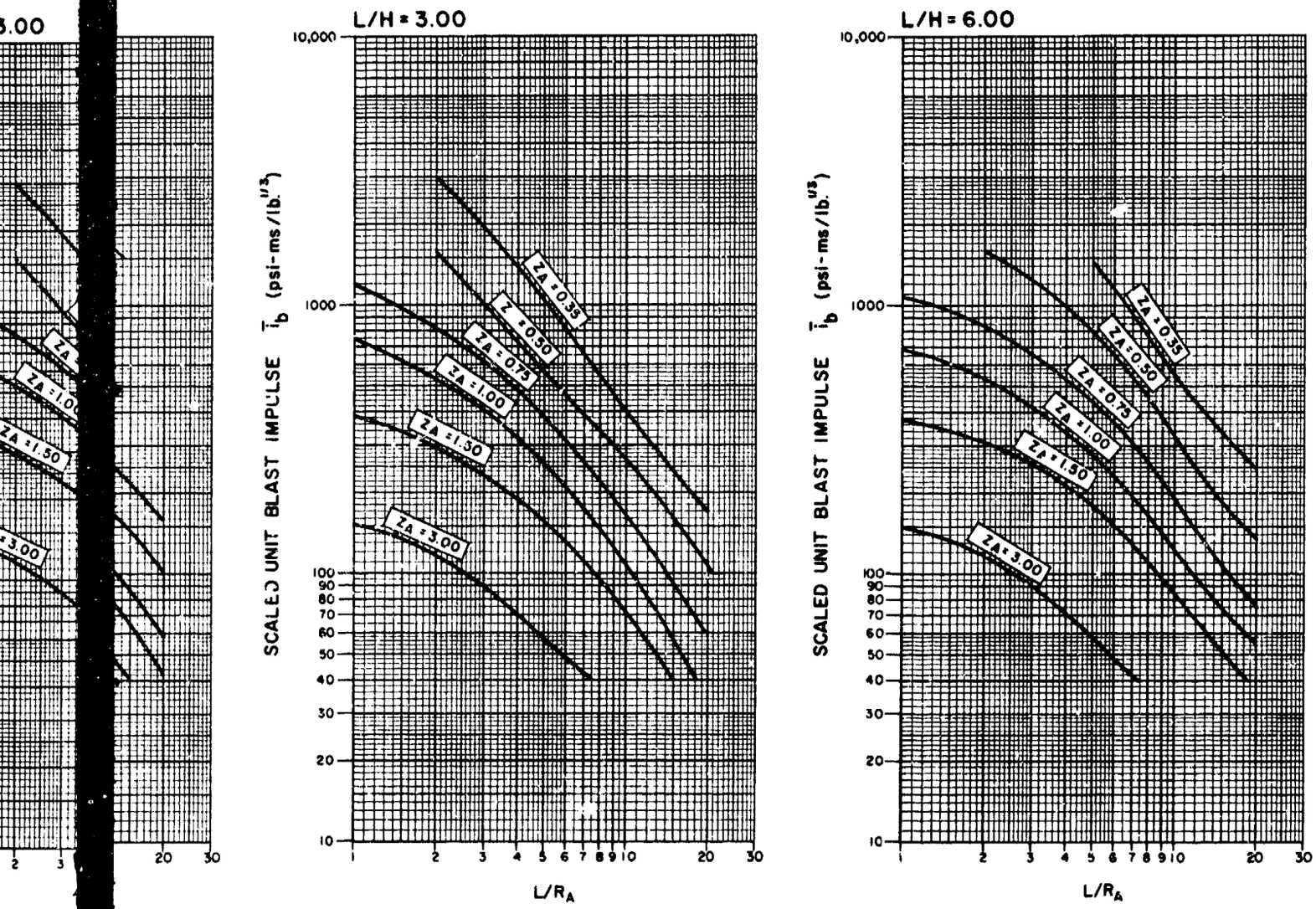




Figure 4-36. Scaled average unit blast impulse ($N = 2$, $l/L = 0.10$, $h/H =$



, h/H = 0.5 *erage unit blast impulse (N = 2, !/L = 0.10, h/H = 0.50).*

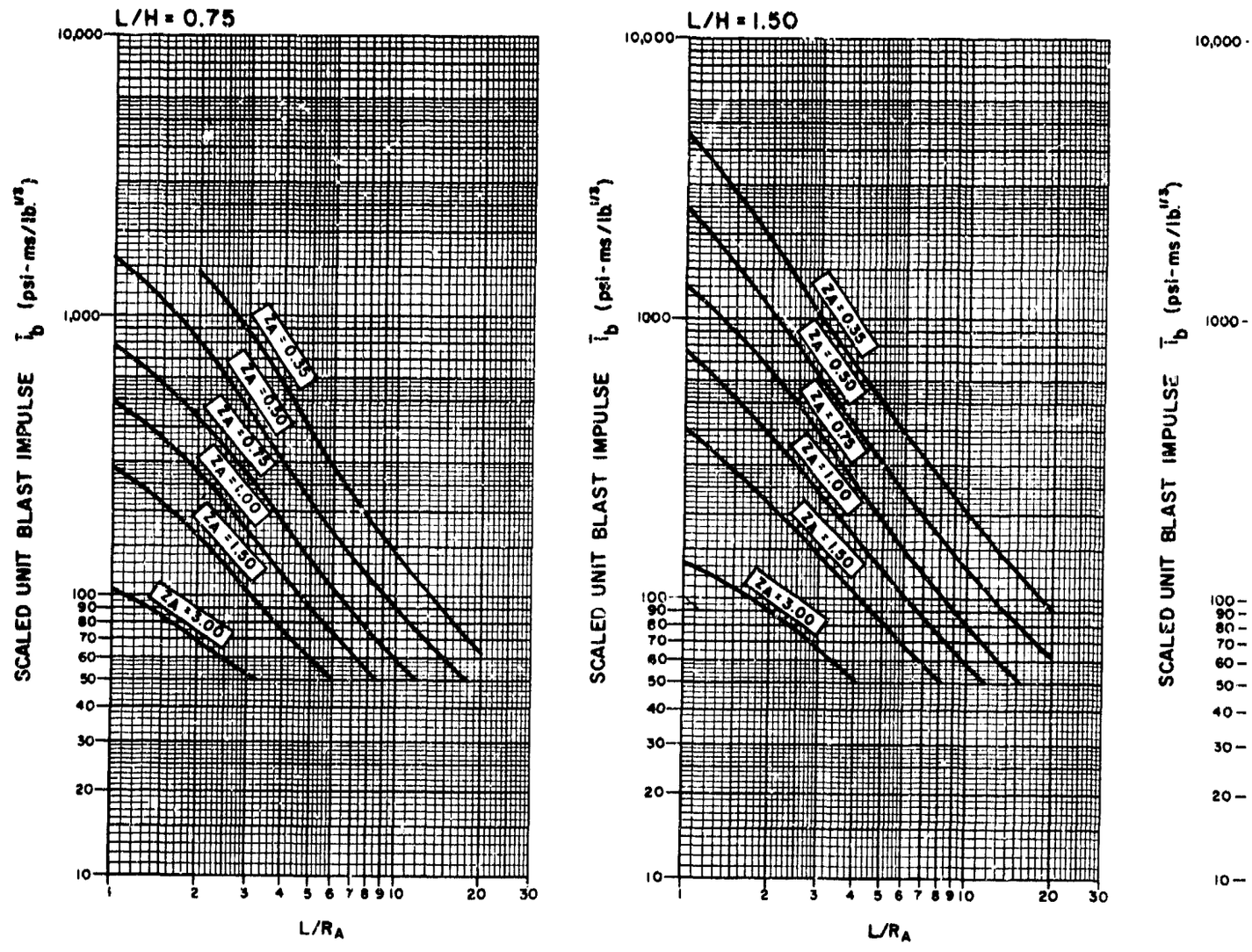
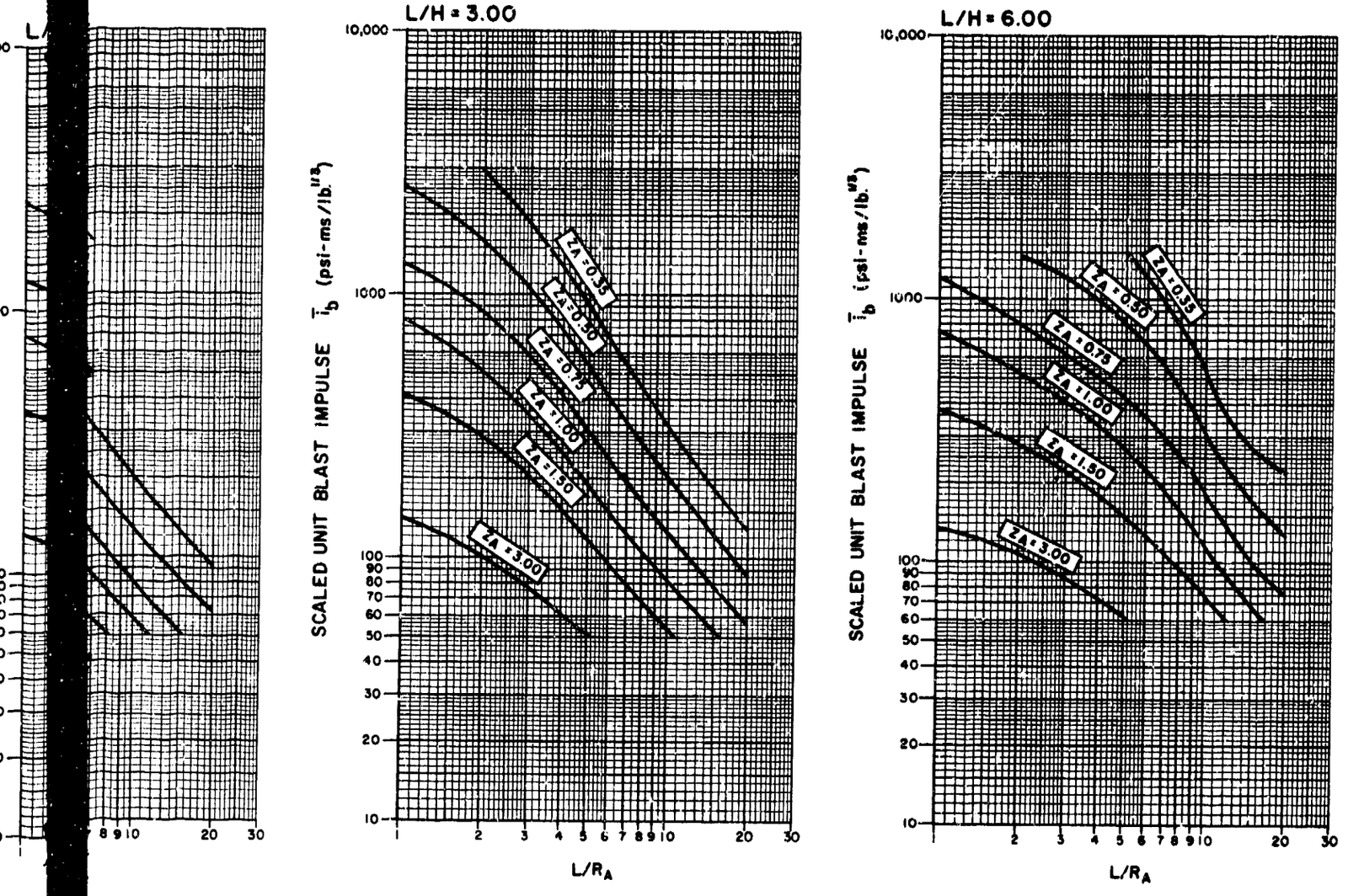


Figure 4-37. Scaled average unit blast impulse (N = 2, 1



Scaled average unit blast impulse ($N = 2$, $l/L = 0.25$, $h/H = 0.50$).

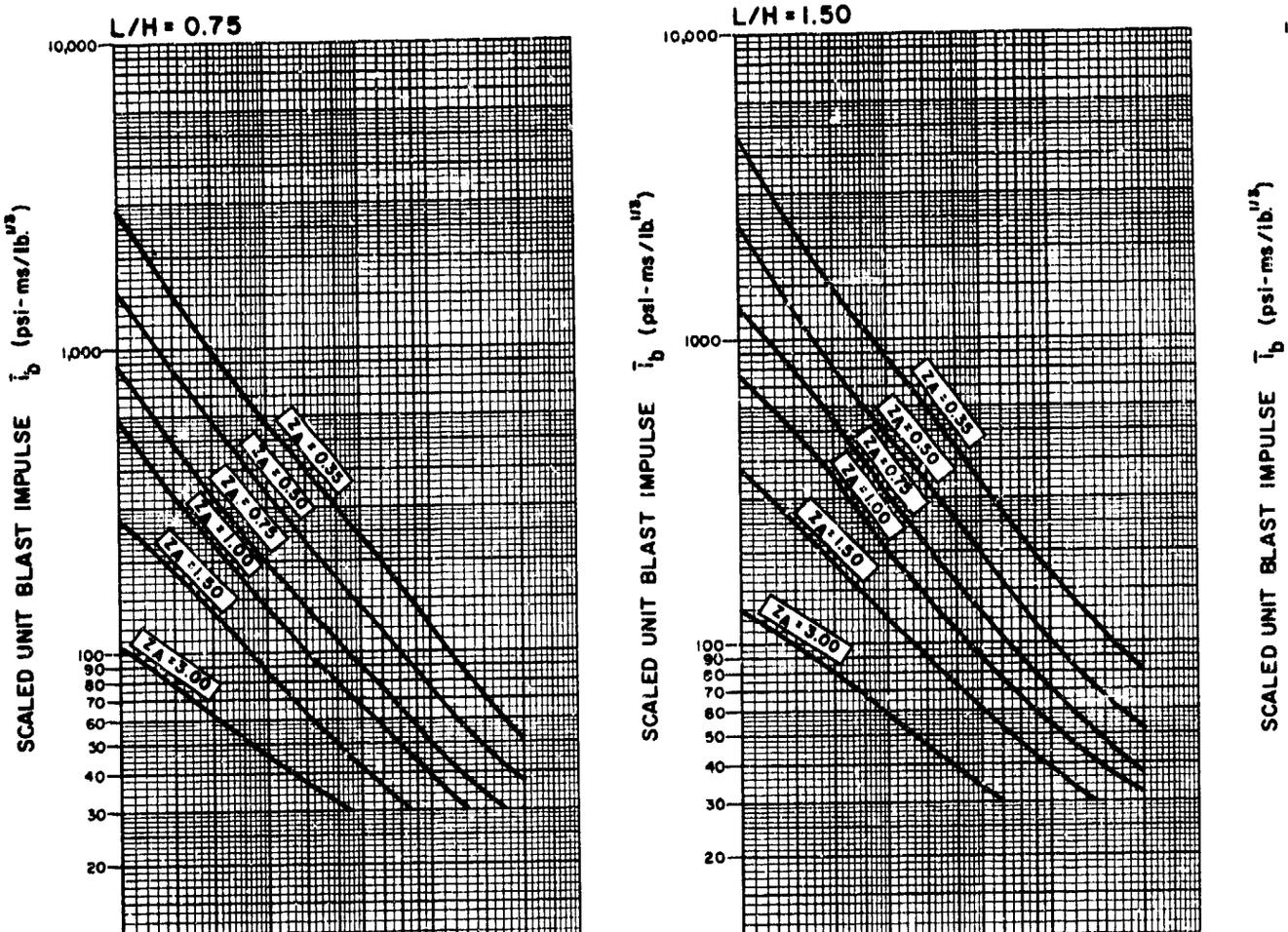
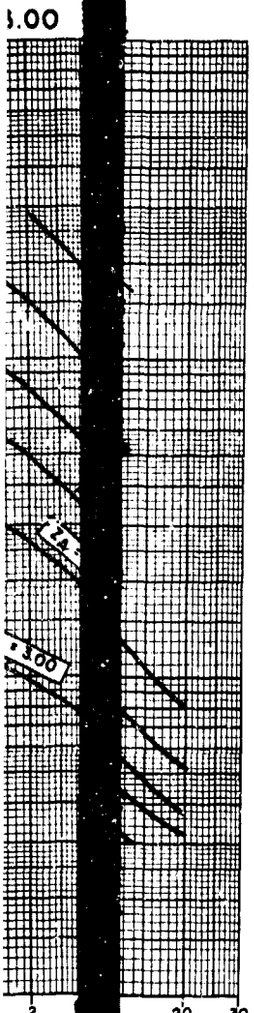
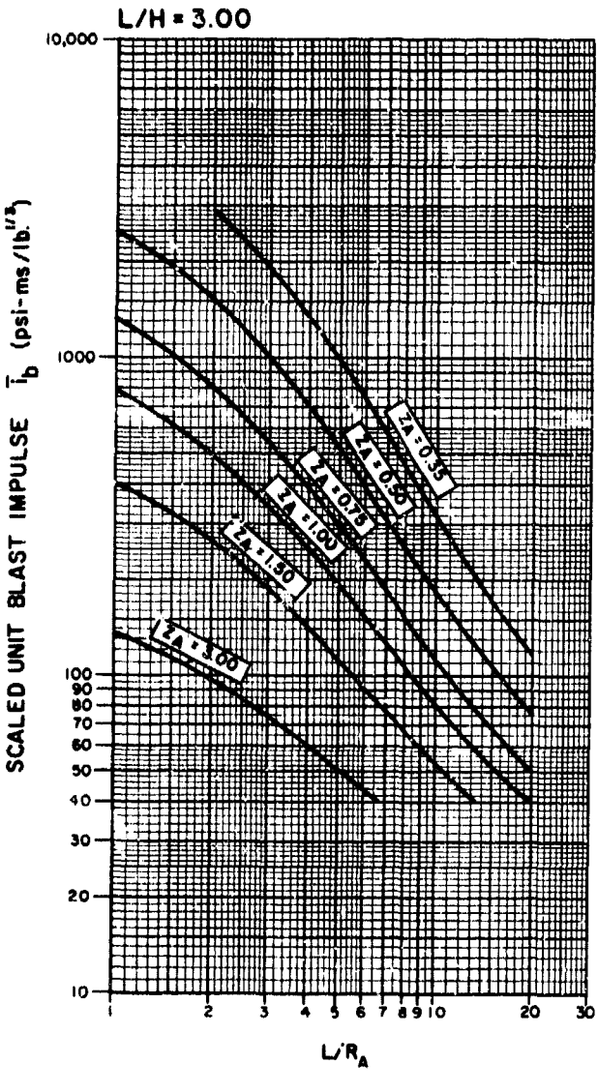
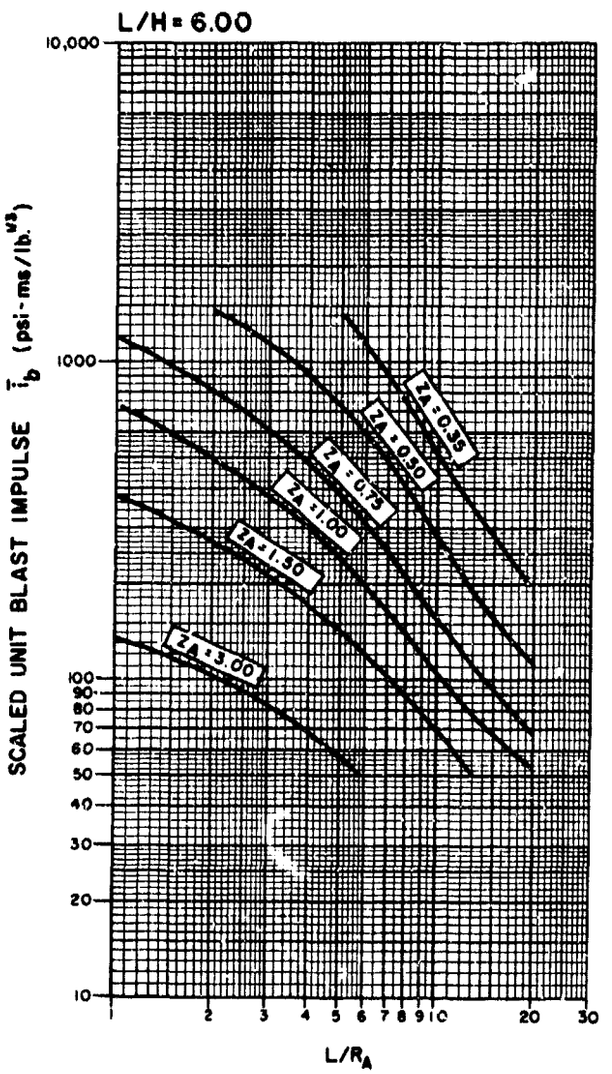


Figure 4-38. Scaled average unit blast impulse ($N = 2$, $l/L = 0.50$, h







50, h/H = ...verage unit blast impulse (N = 2, l/L = 0.50, h/H = 0.50).

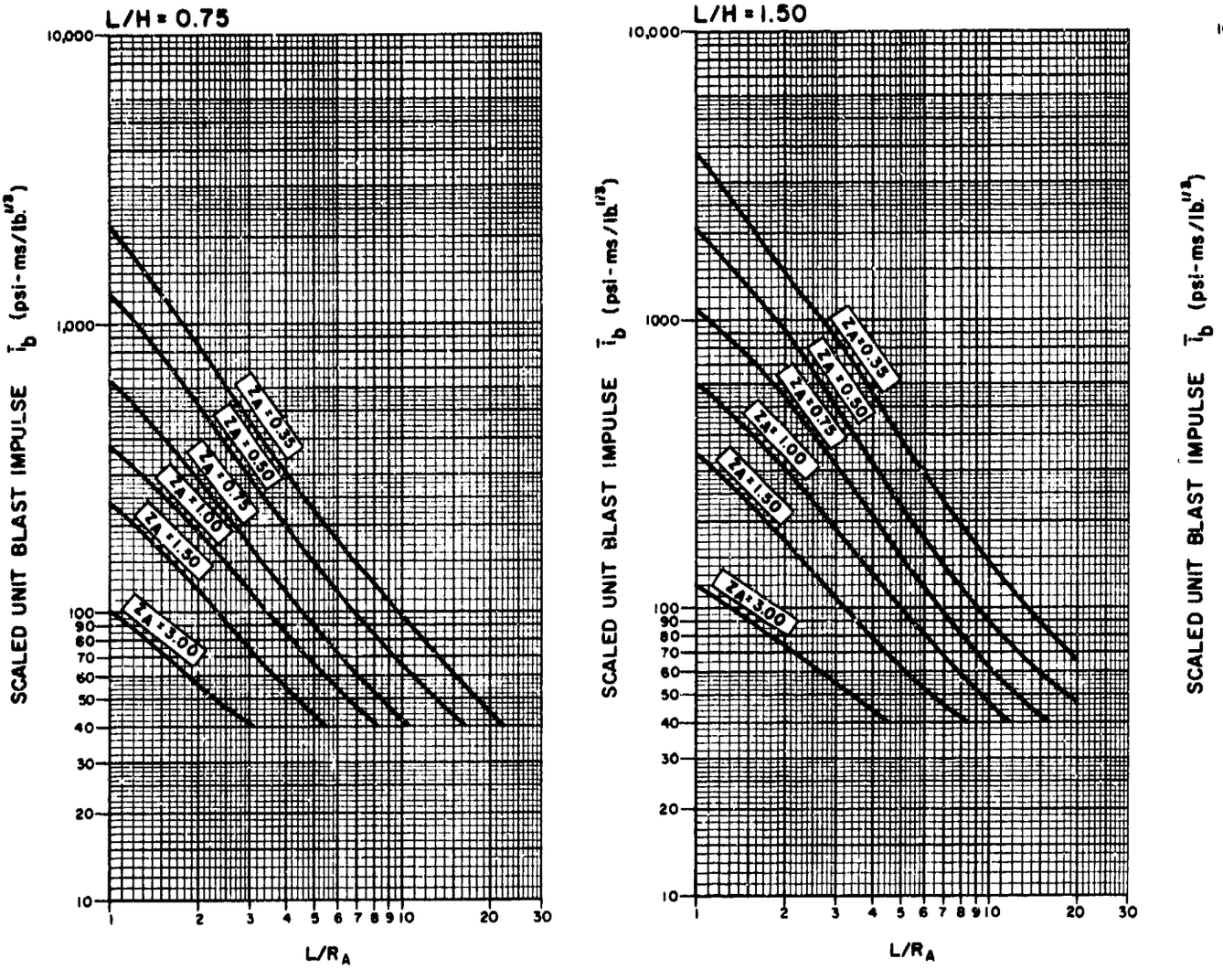
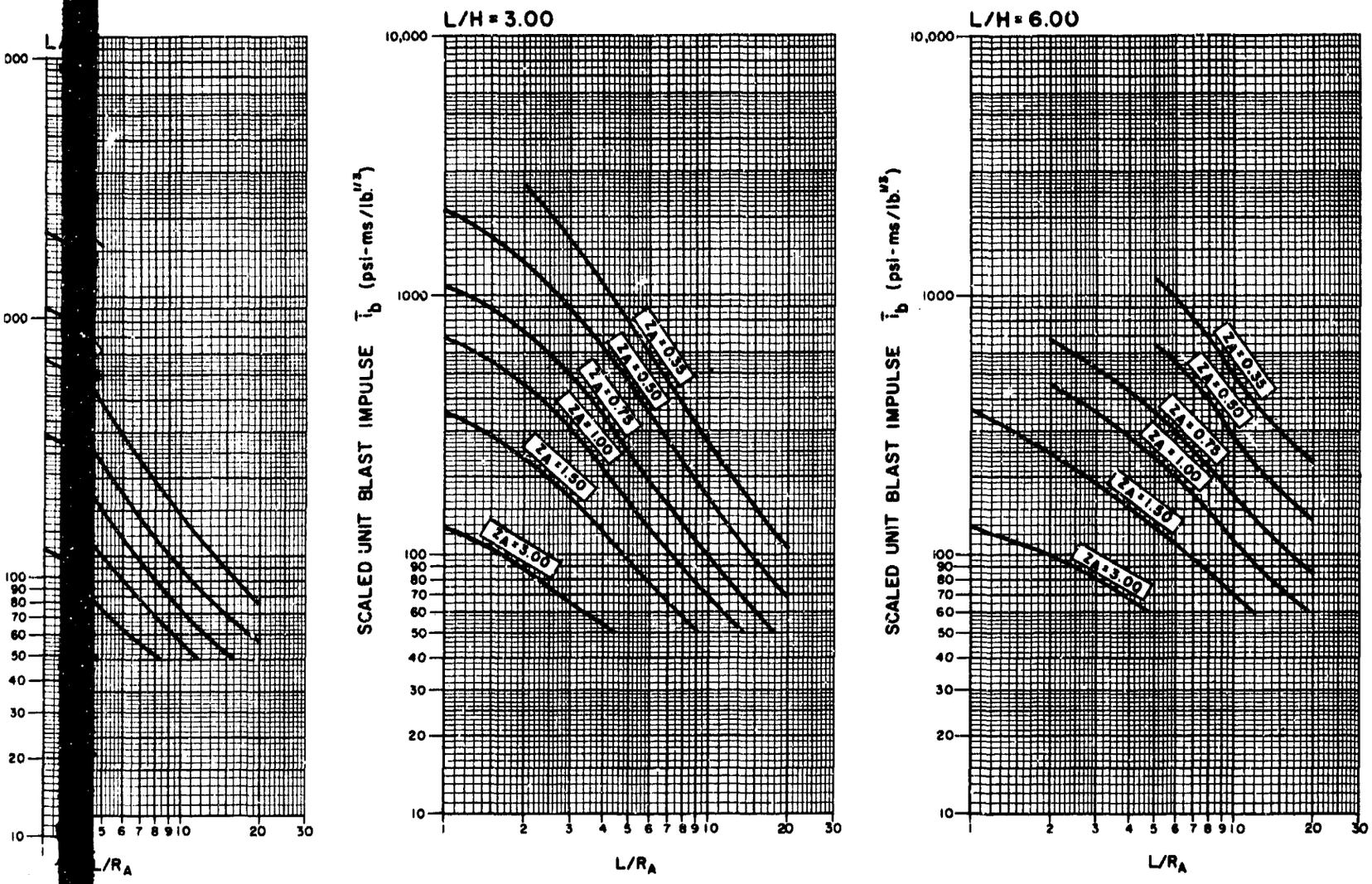


Figure 4–39. Scaled average unit blast impulse (N = 2



4–39. Scaled average unit blast impulse ($N = 2$, $l/L = 0.75$, $h/H = 0.50$).

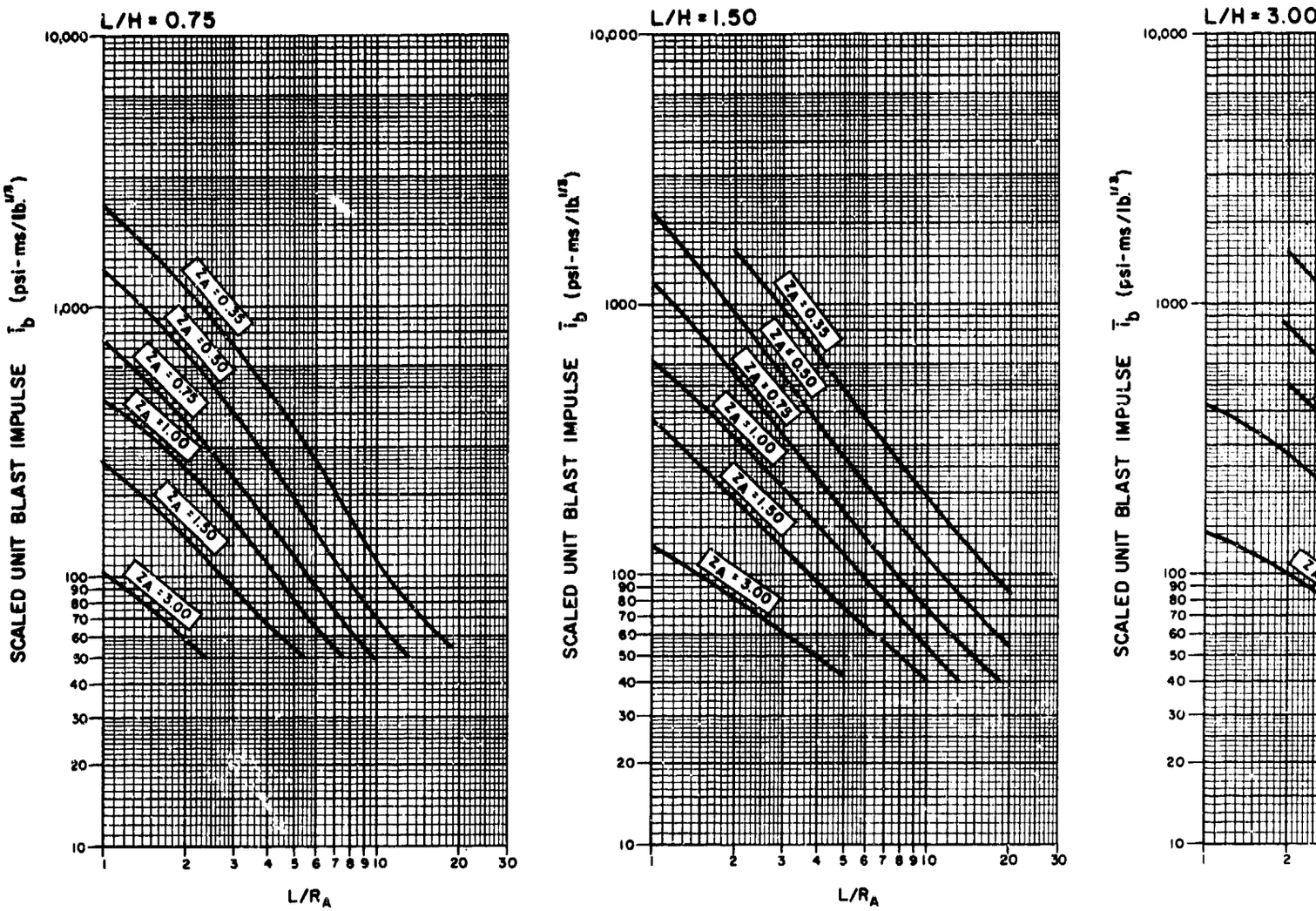
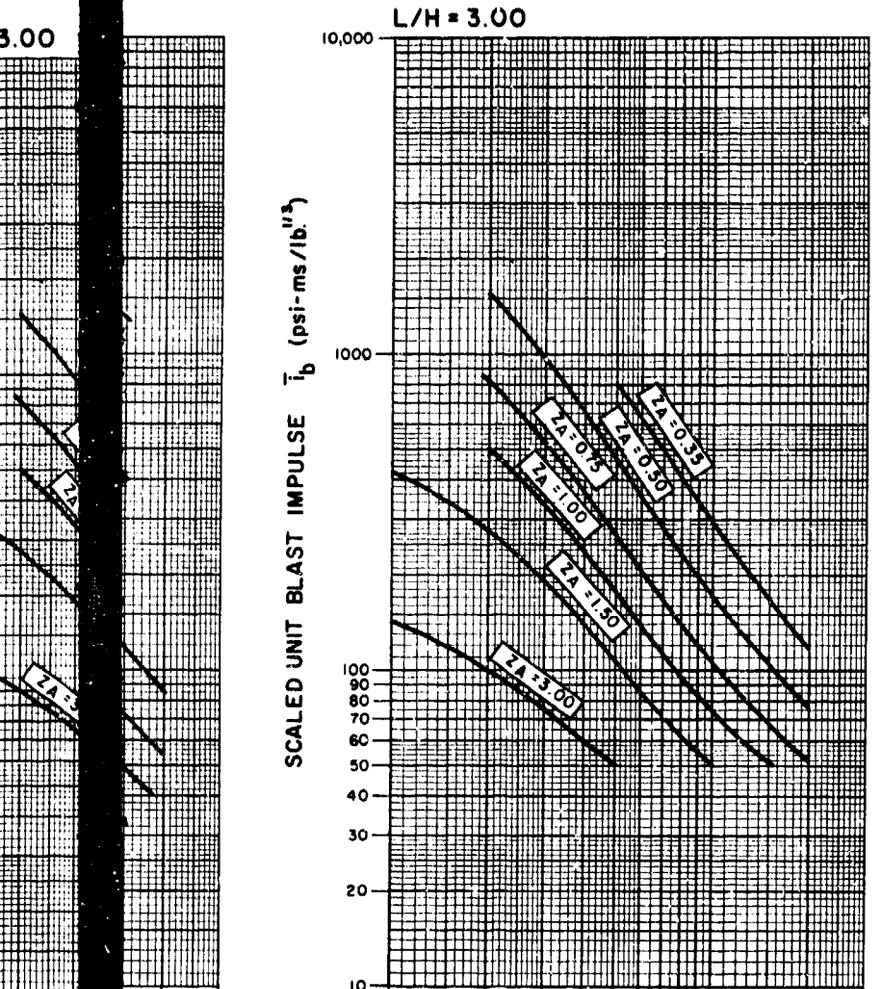
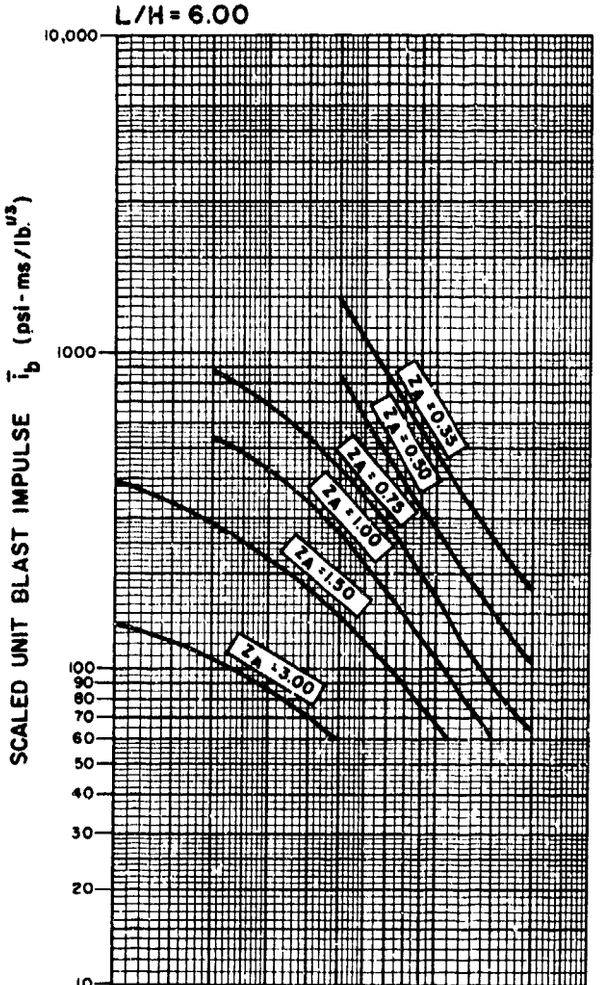


Figure 4-40. Scaled average unit blast impulse ($N = 2$, $l/L = 0.25$, h/H





ag: unit blast impulse ($N=2$, $l/L=0.25$, $h/H=0.75$).

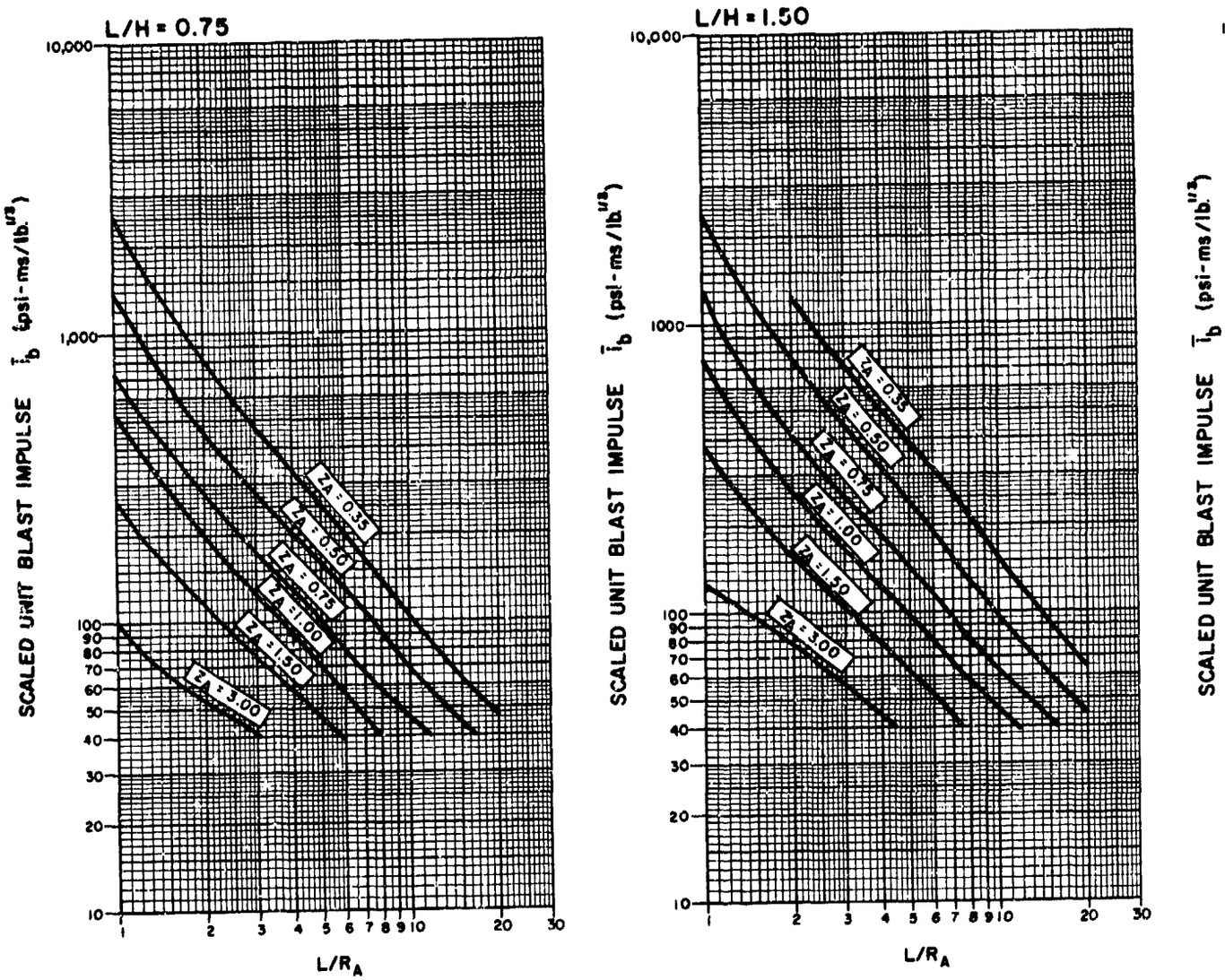
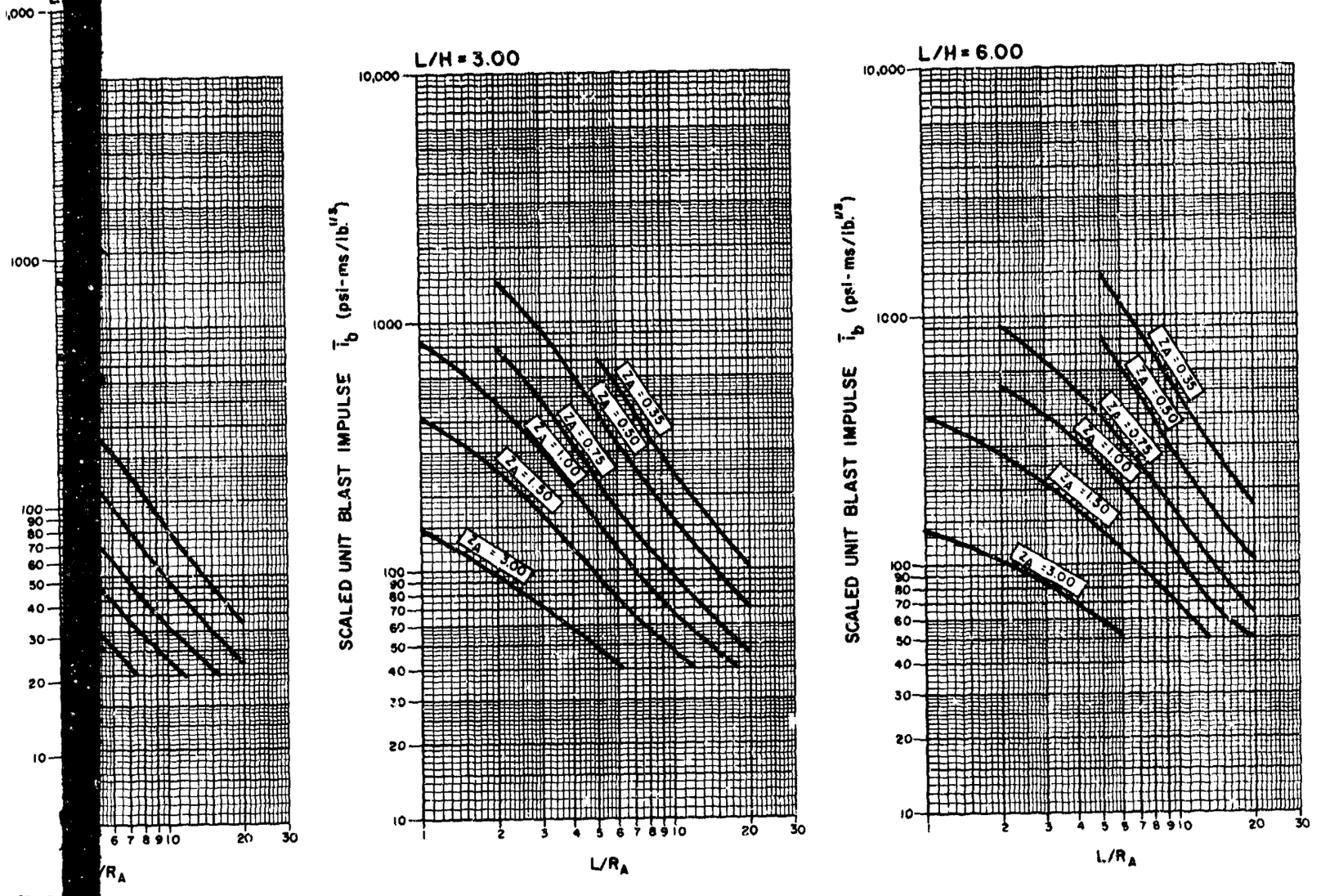
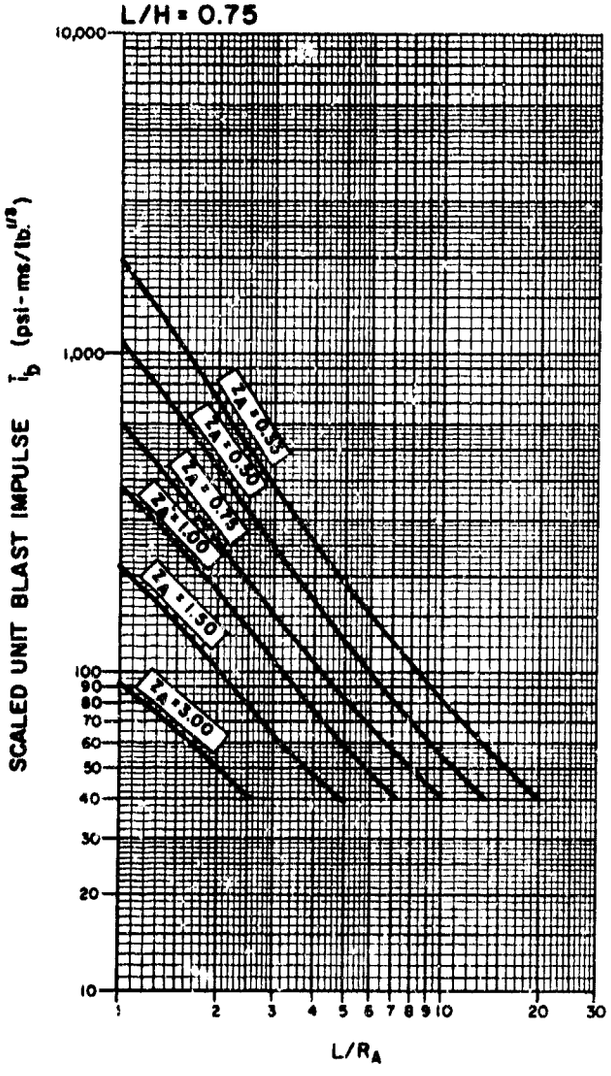


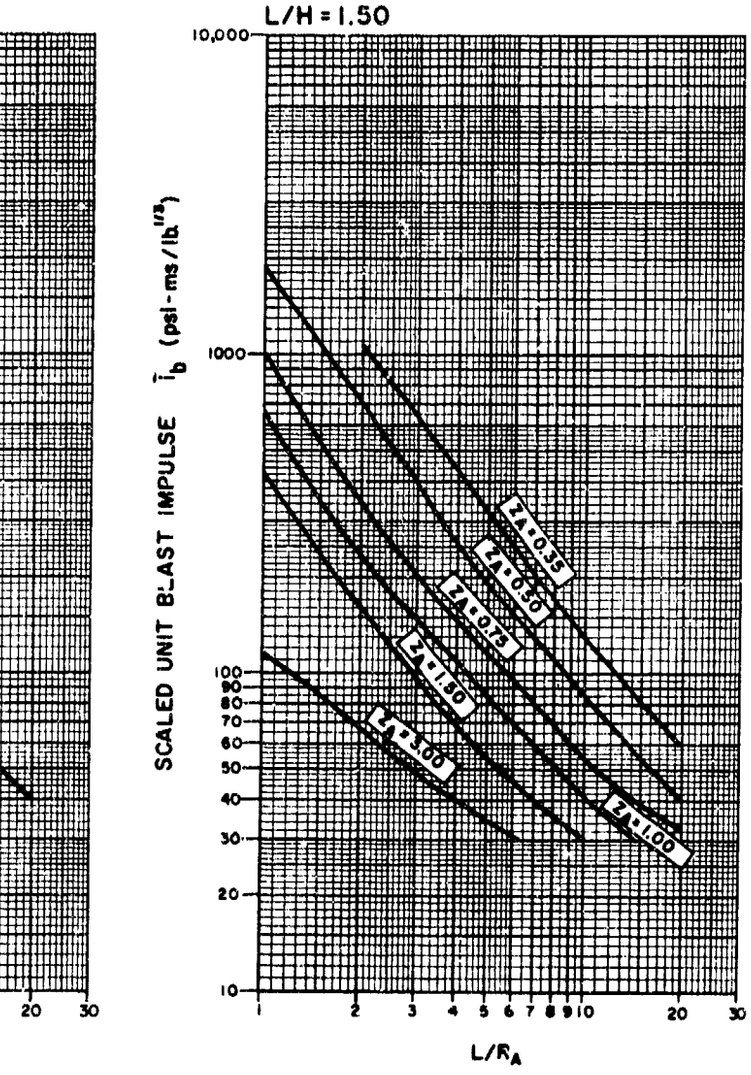
Figure 4–41. Scaled average unit blast impulse (N



(N = 2,

4-41. Scaled average unit blast impulse ($N = 2$, $l/L = 0.50$, $h/H = 0.75$).





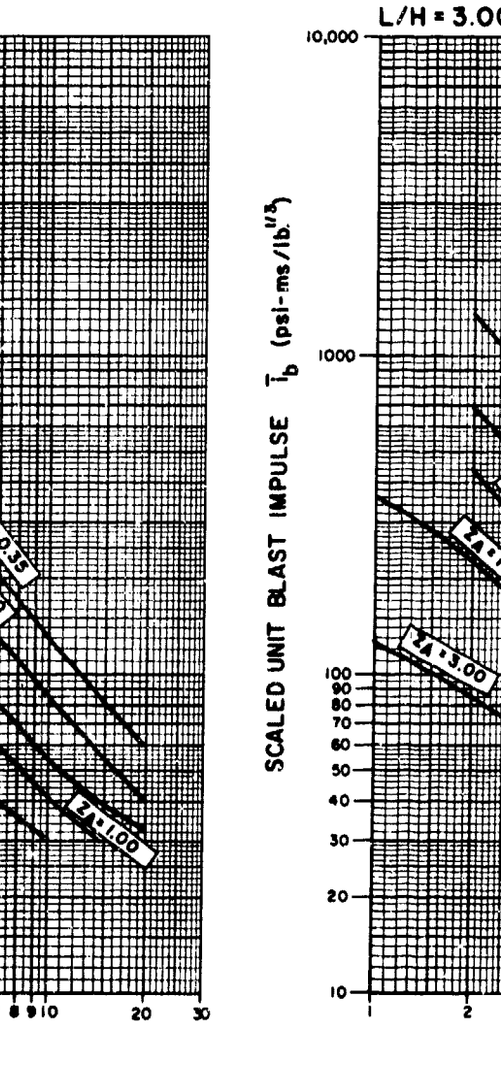
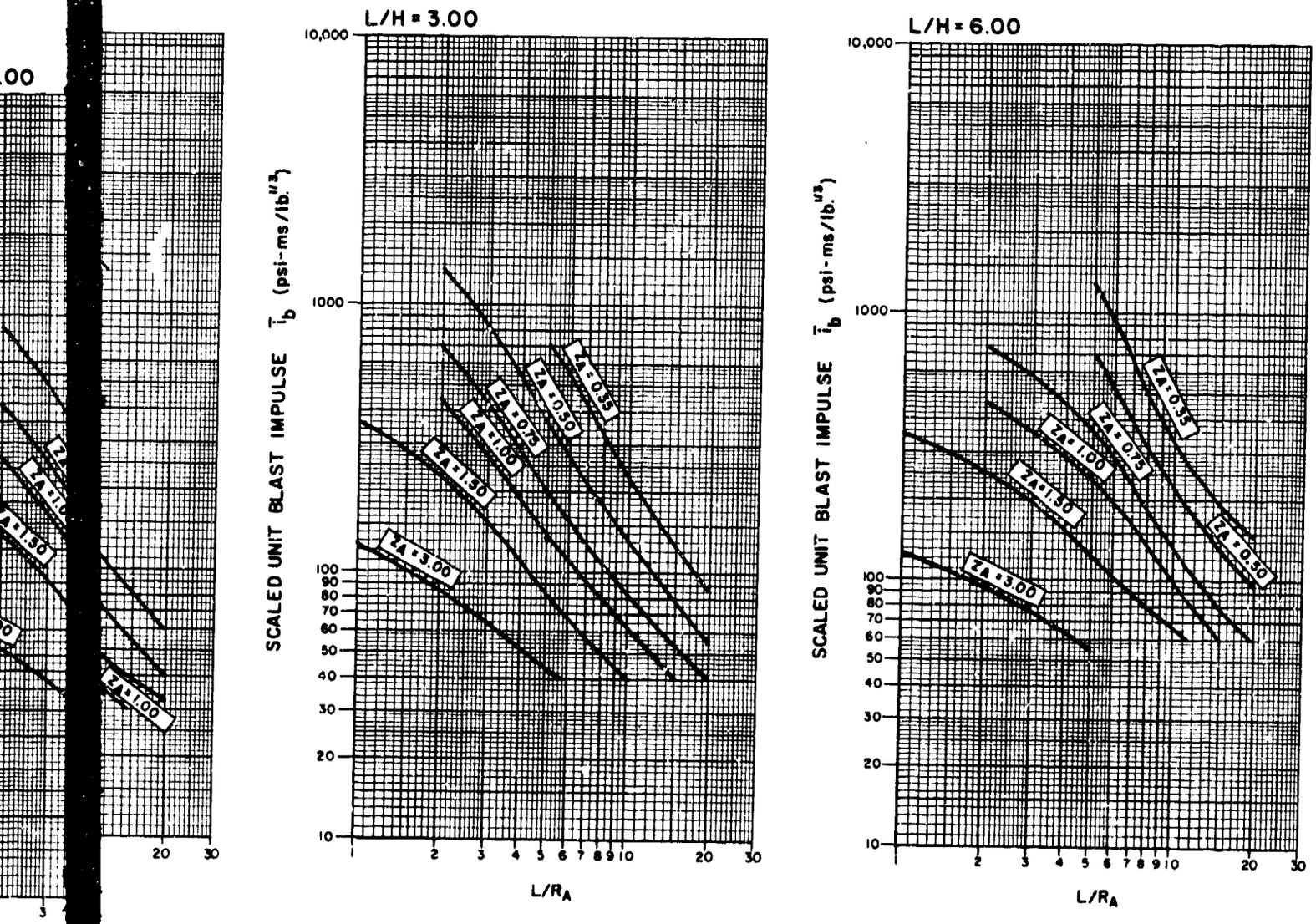
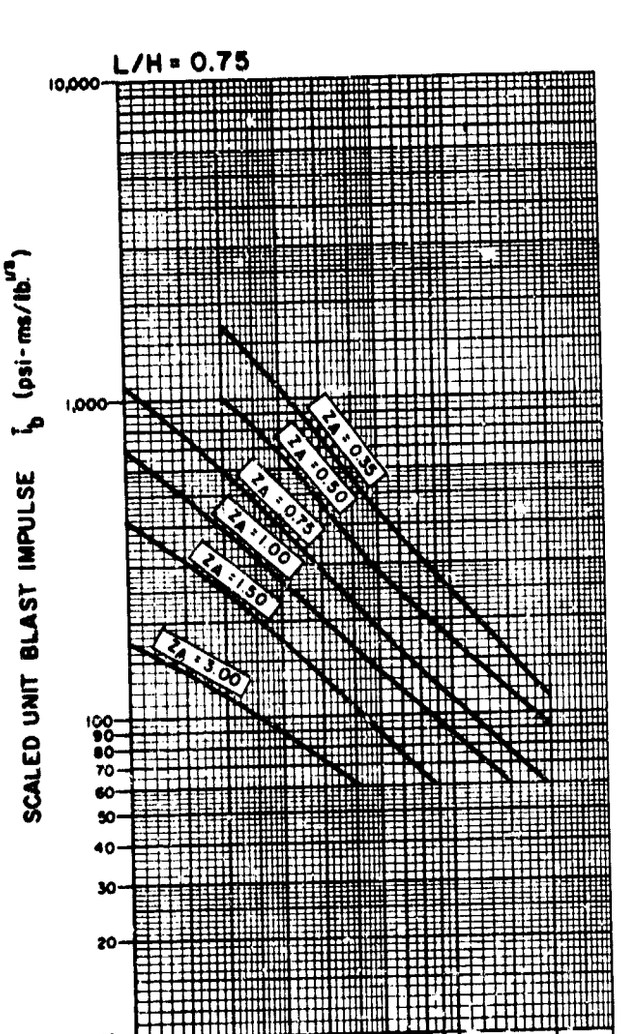


Figure 4-42. Scaled average unit blast impulse ($N = 2$, $l/L = 0.75$, h/H



Average unit blast impulse ($N = 2$, $l/L = 0.75$, $h/H = 0.75$).



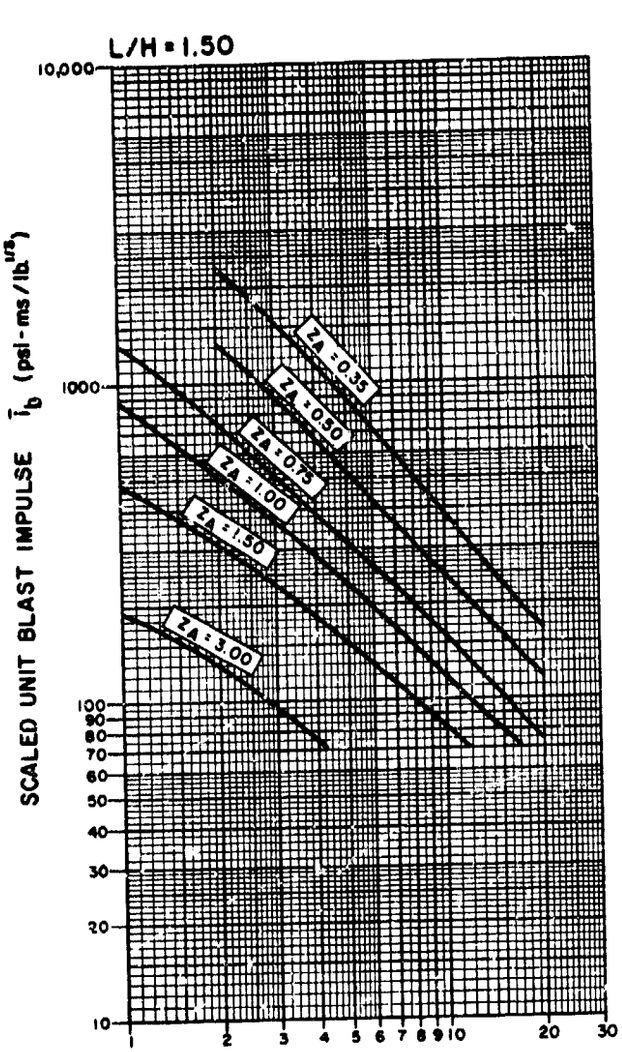
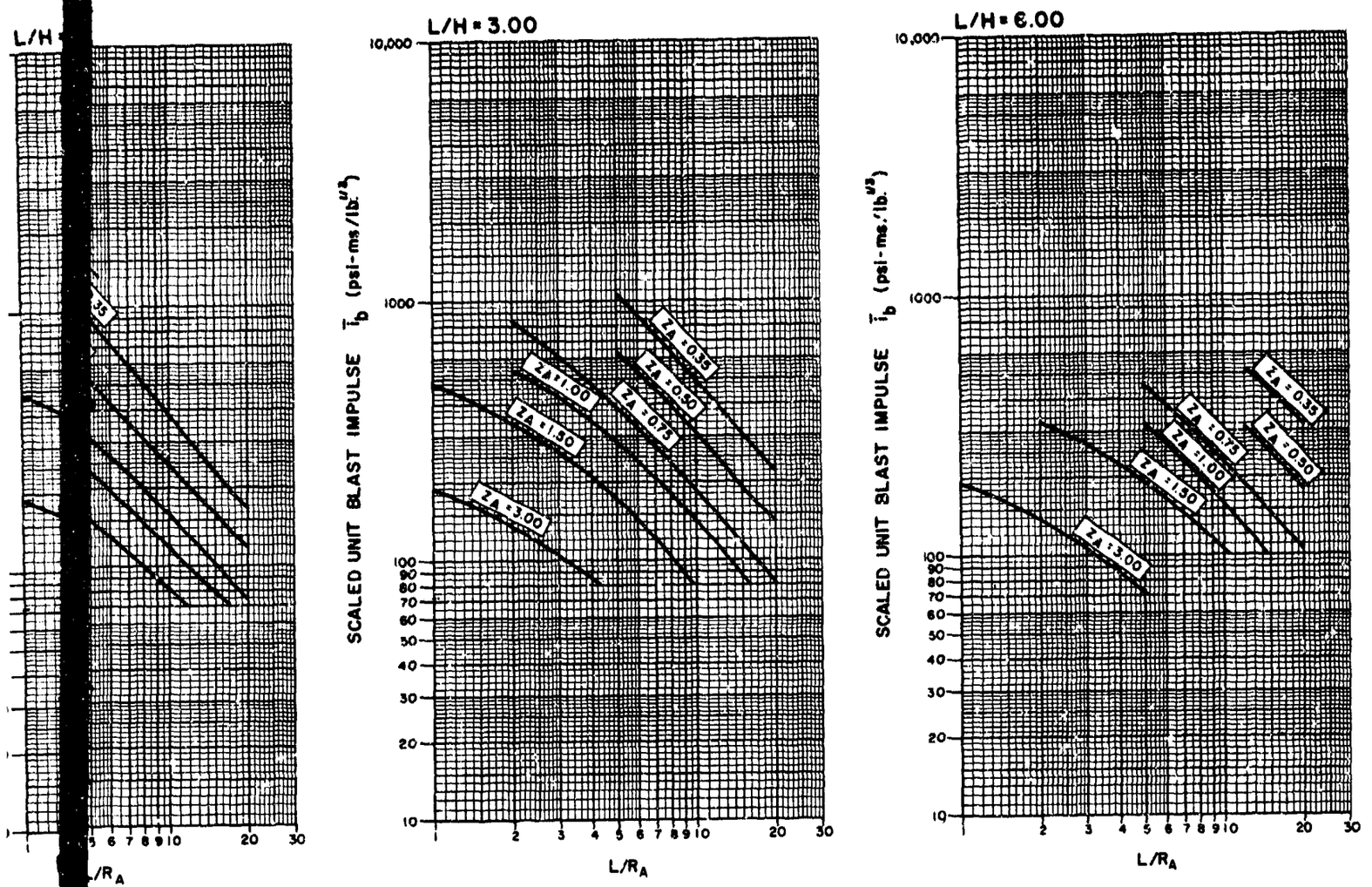




Figure 4-43. Scaled average unit blast impulse (N = 3, l/L



3, l/L = 0.10, h/H = 0.15).

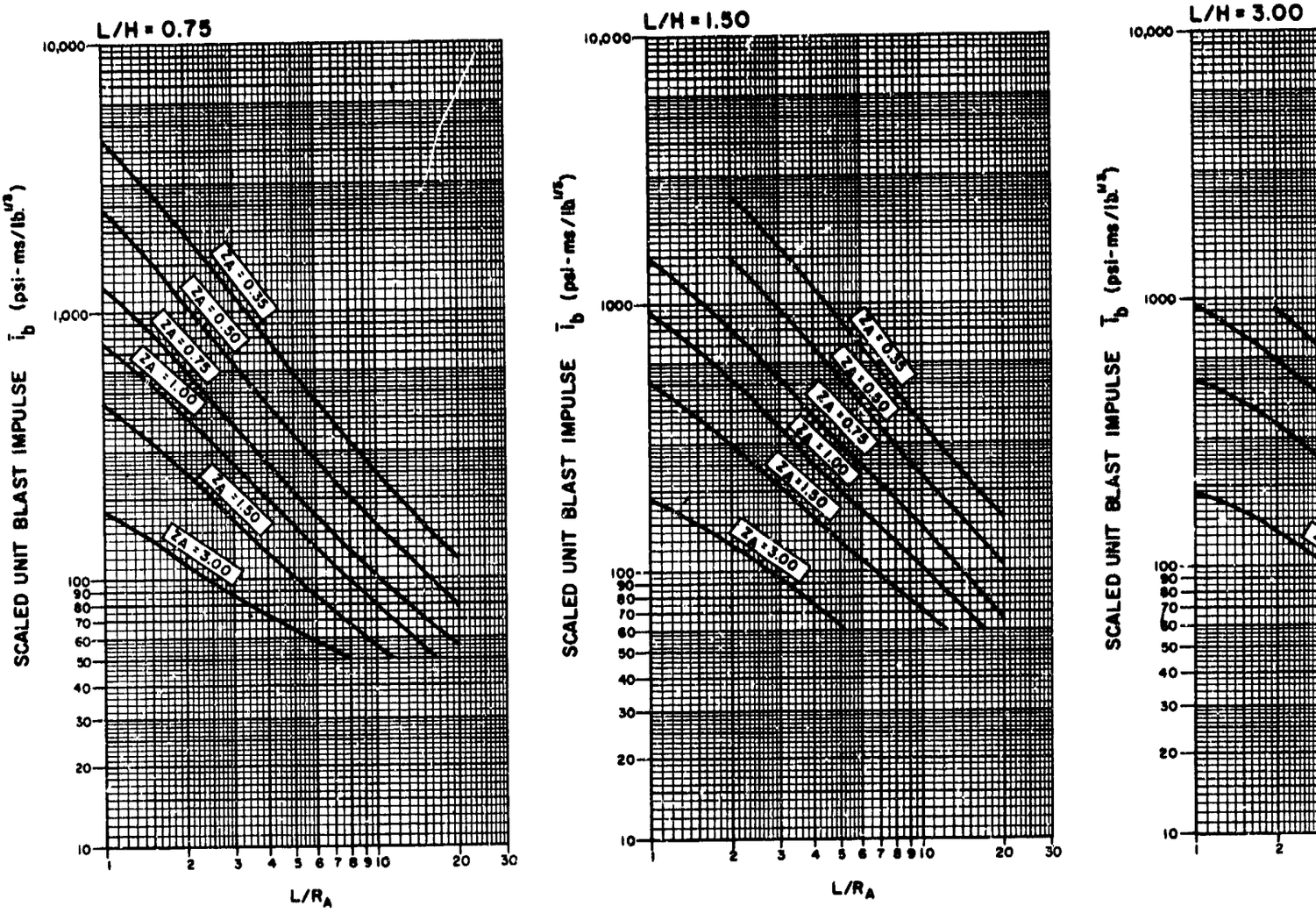
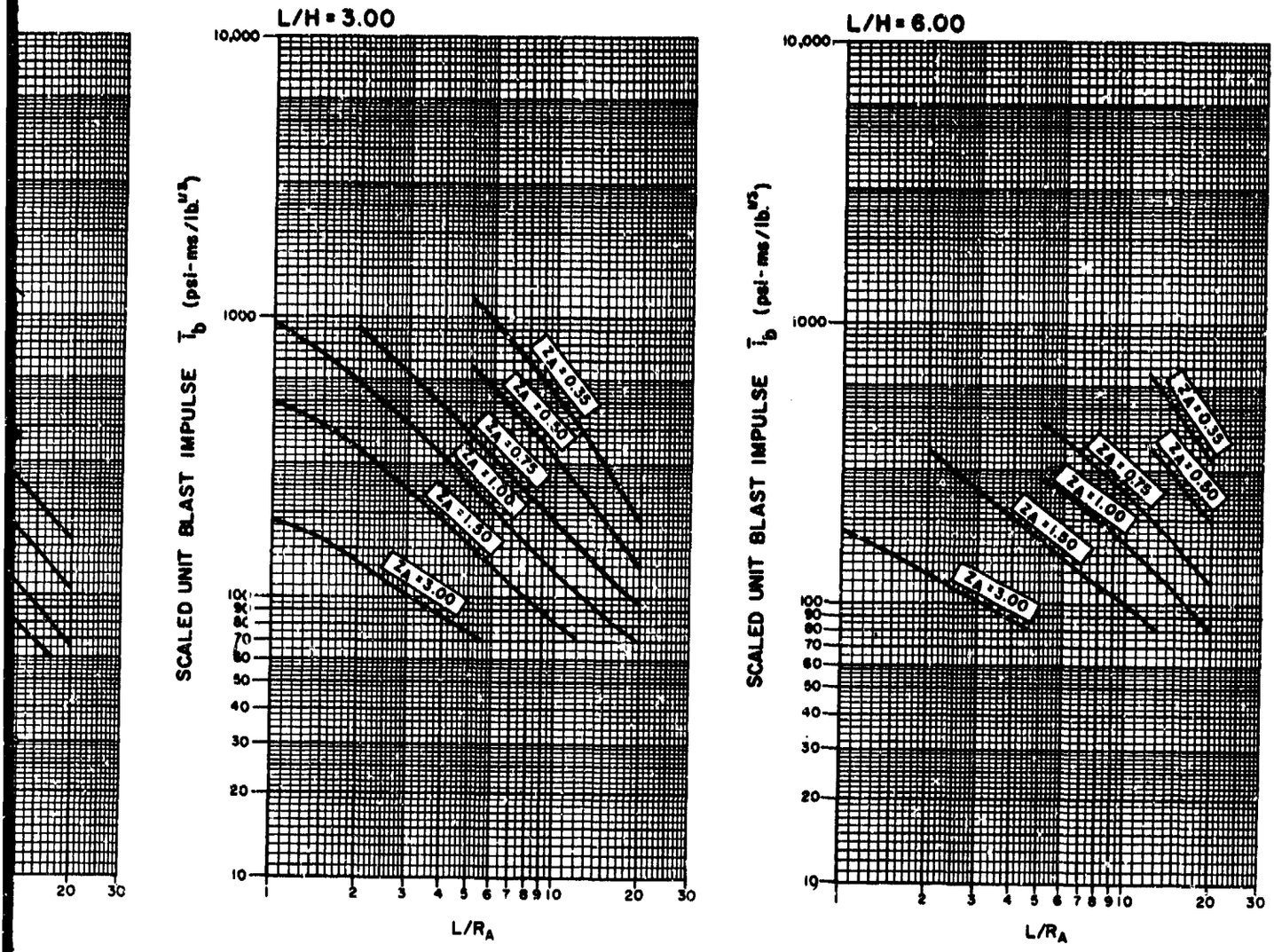
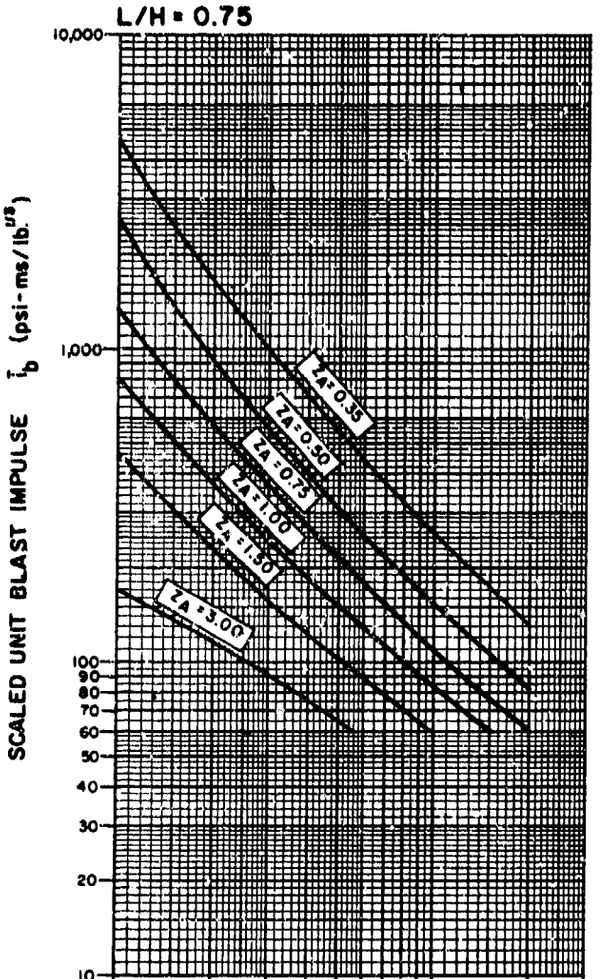


Figure 4-44. Scaled average unit blast impulse ($N = 3$, $1/L = 0.25$ and 0.75,



e unit blast impulse ($N=3$, $l/L=0.25$ and 0.75, $h/H=0.15$).



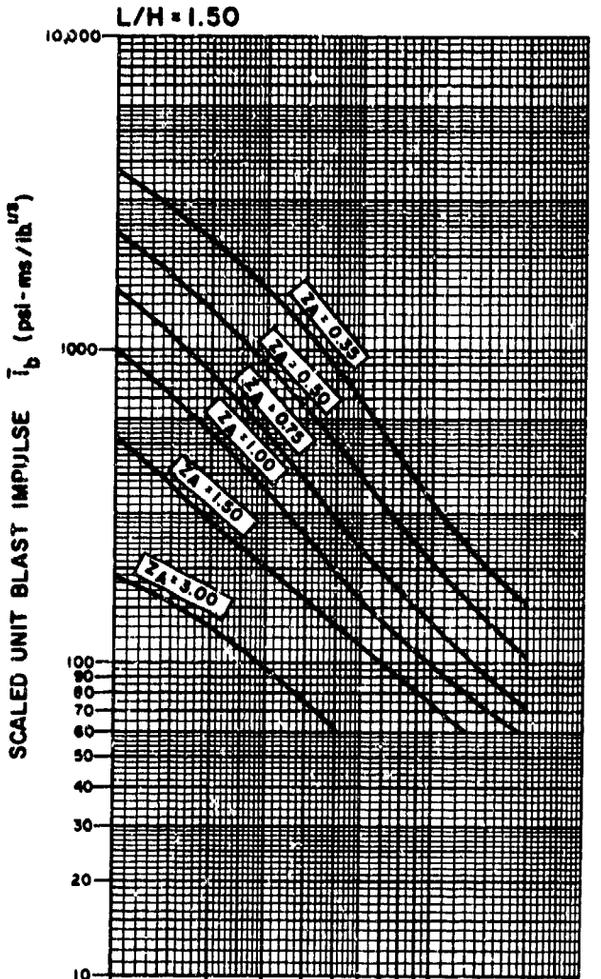
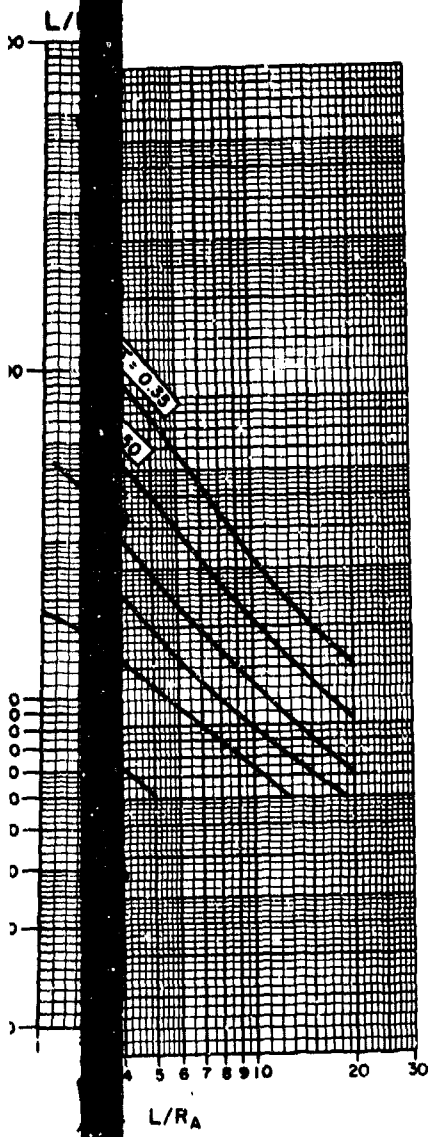
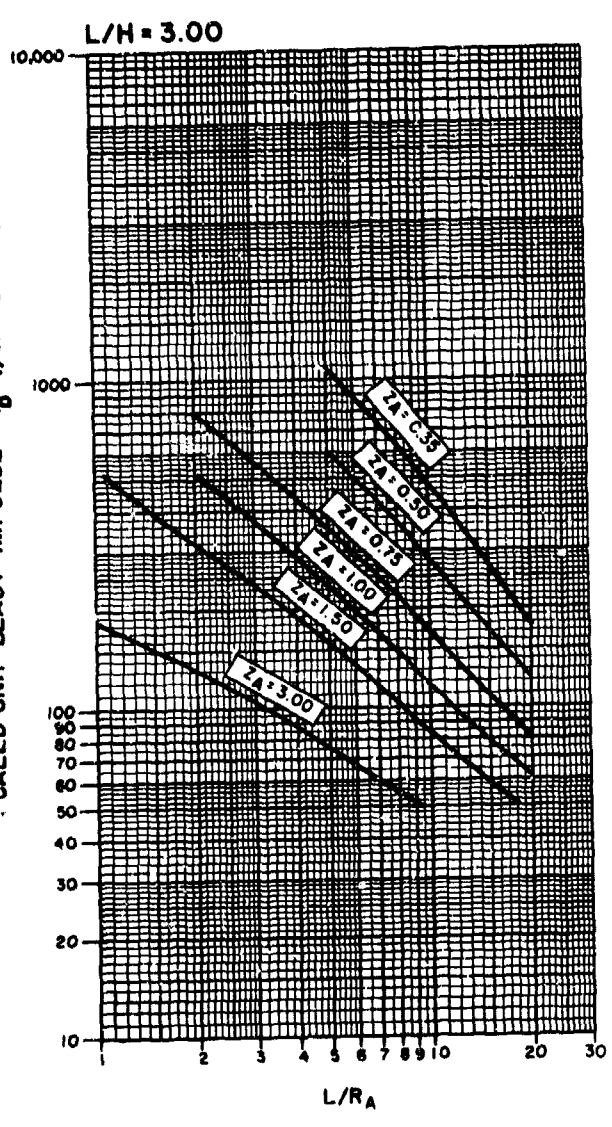
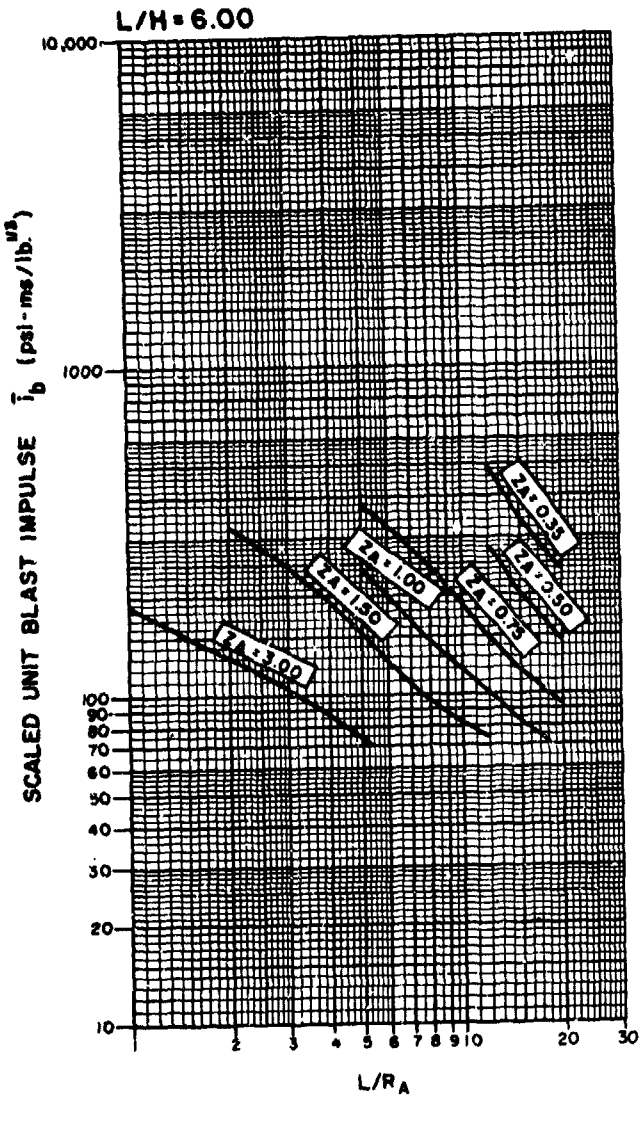




Figure 4-45. Scaled average unit blast impulse ($N = 3$, $l/L =$







, $l/L = 0$

re 4-45. Scaled average unit blast impulse ($N = 3$, $l/L = 0.50$, $h/H = 0.15$).

2

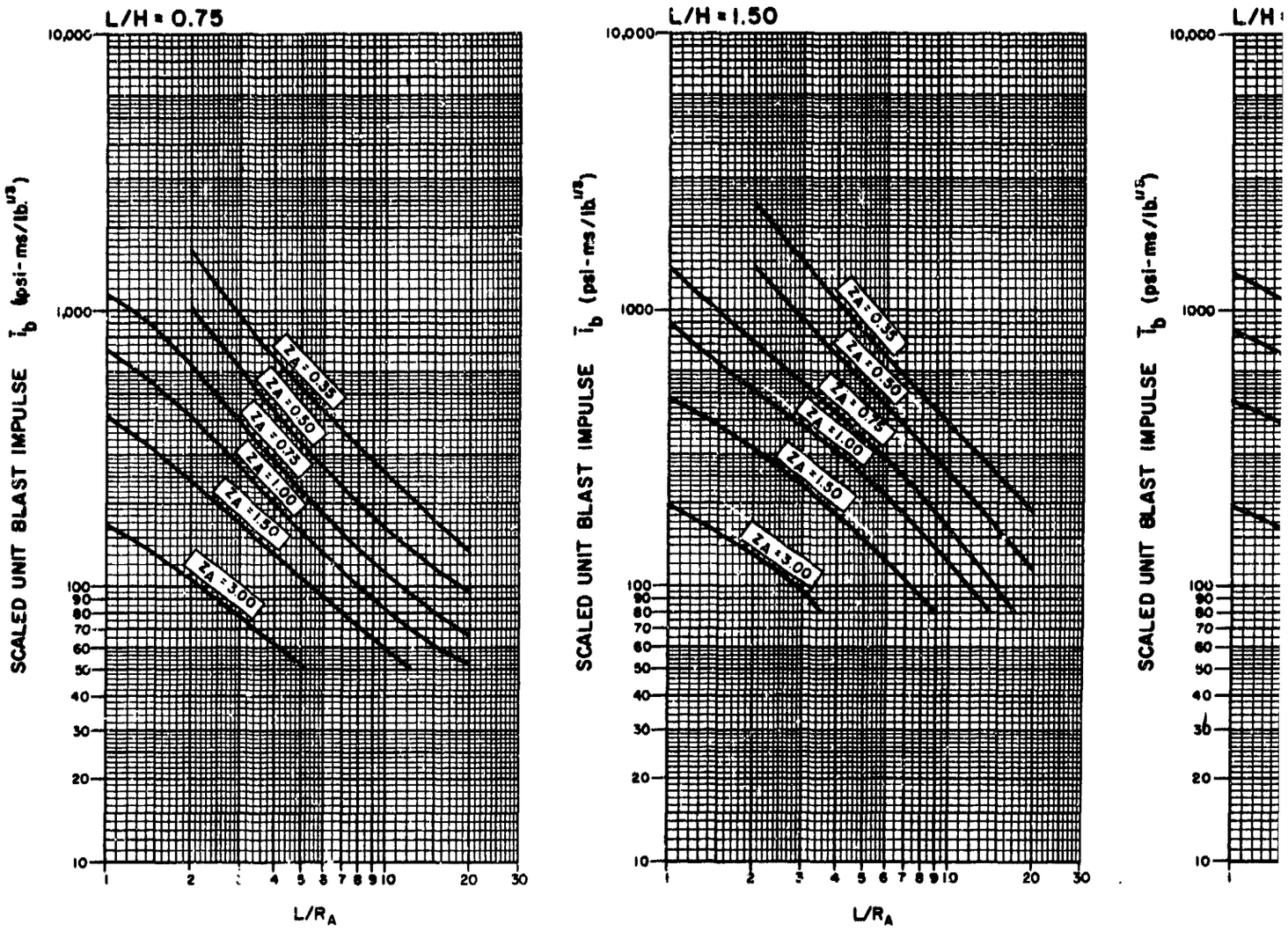
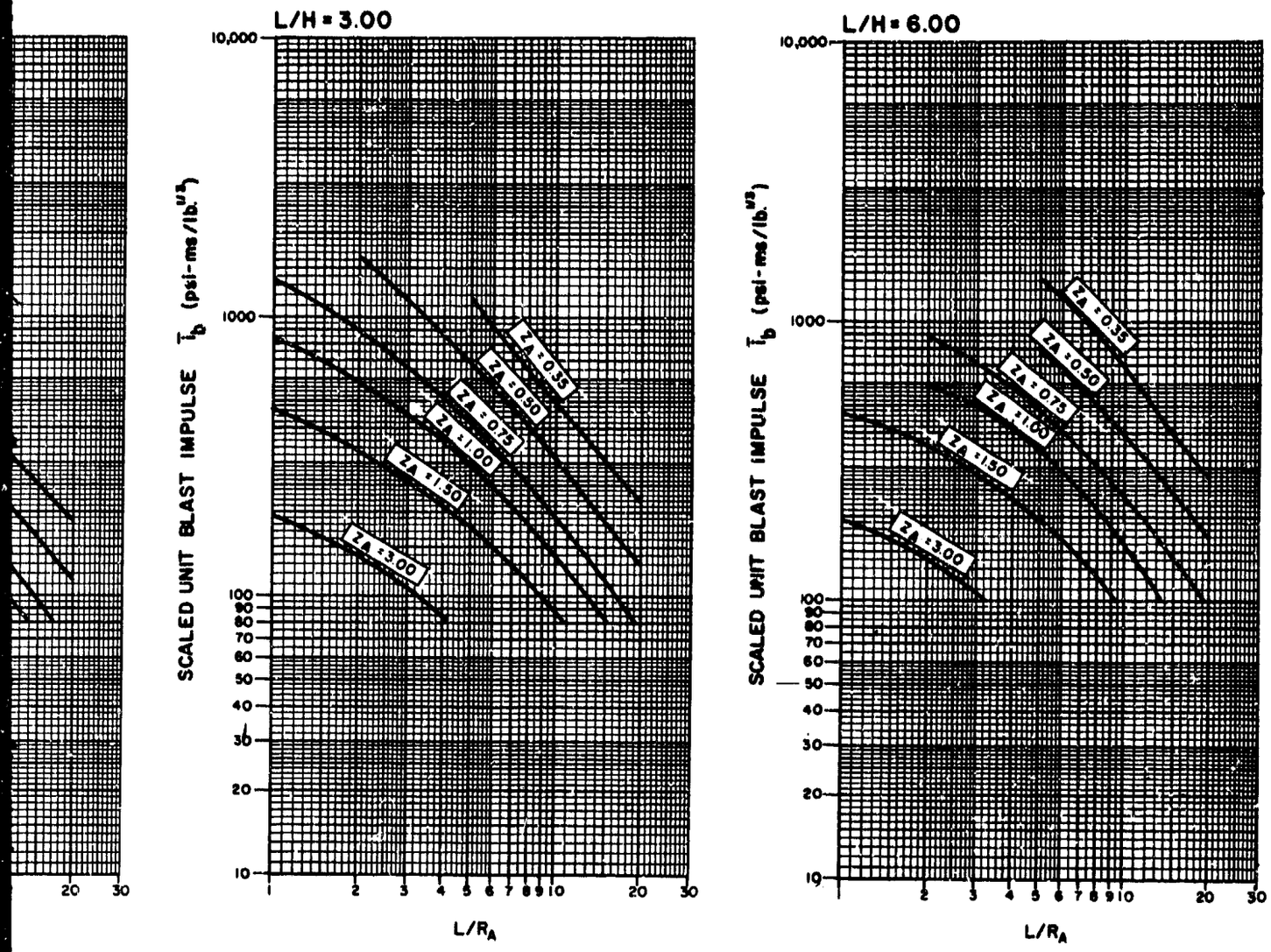


Figure 4-46. Scaled average unit blast impulse (N = 8, l/L = 0..



erage unit blast impulse ($N=8$, $l/L=0.10$, $h/H=0.25$).

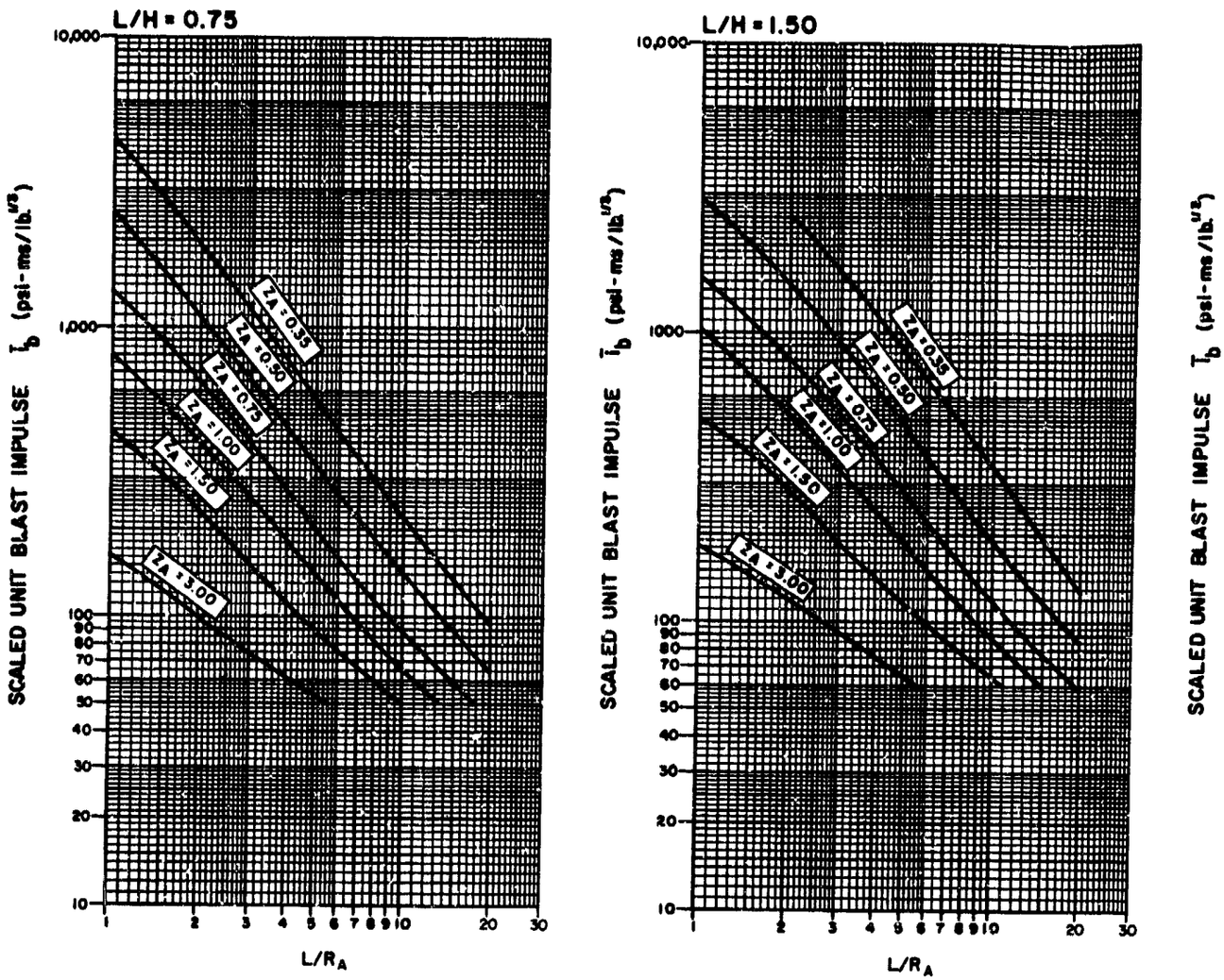
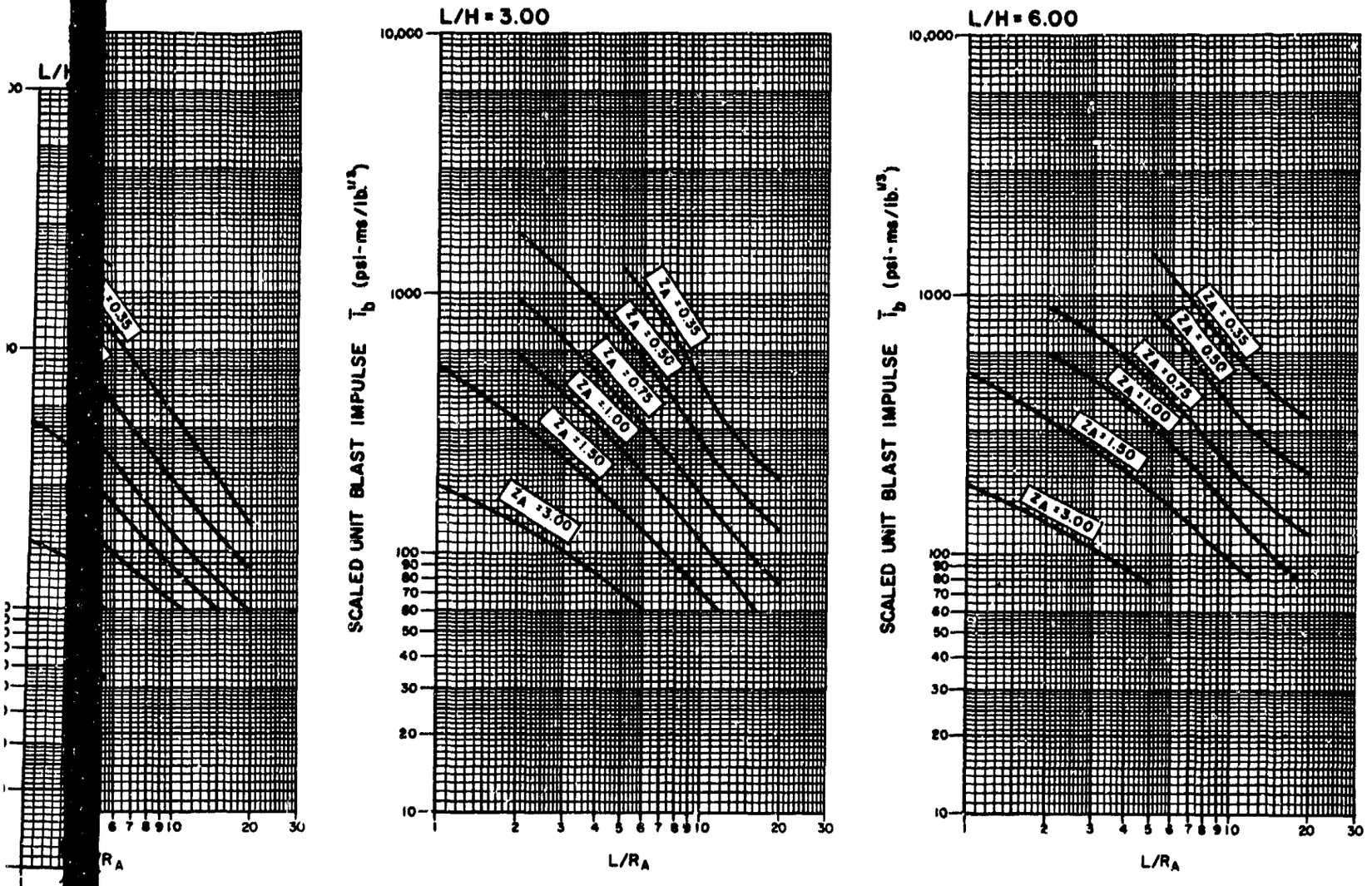


Figure 4-47. Scaled average unit blast impulse ($N = 3$, $l/L = 0.8$



Scaled average unit blast impulse ($N = 3$, $l/L = 0.25$ and 0.75, $h/H = 0.25$).

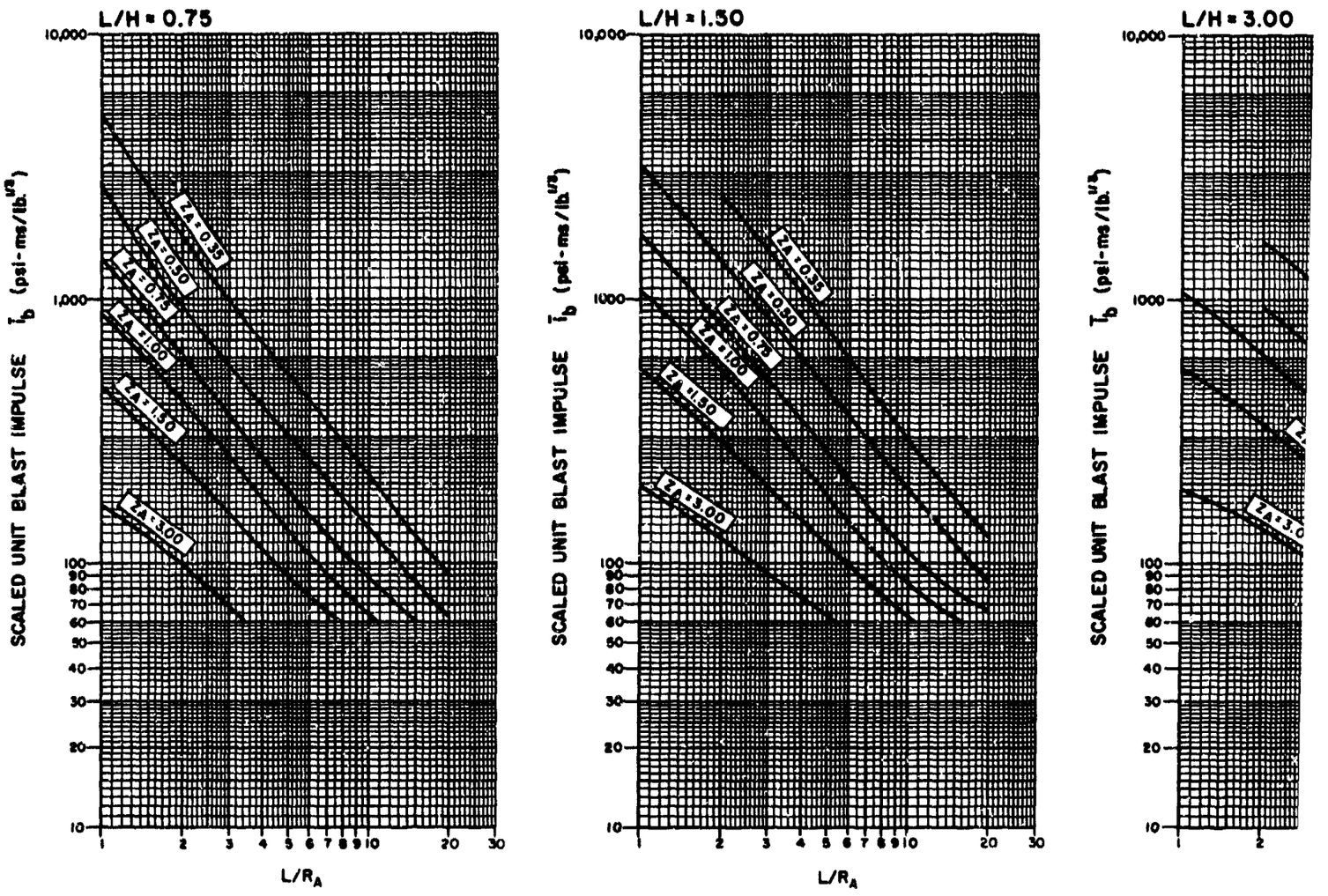
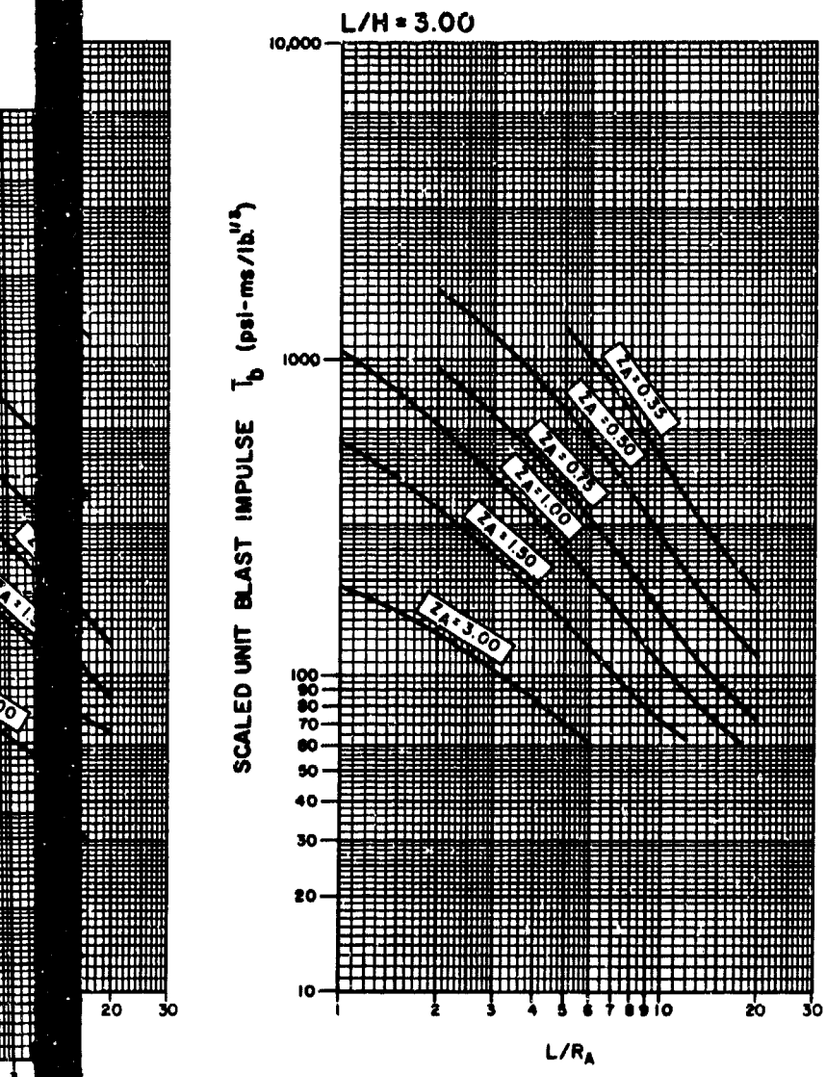
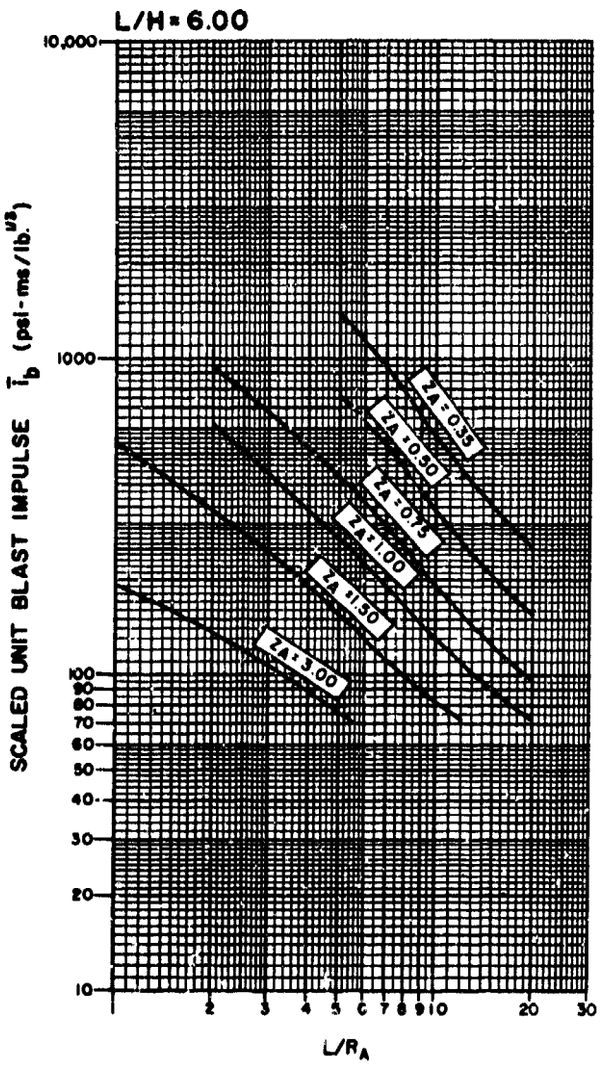
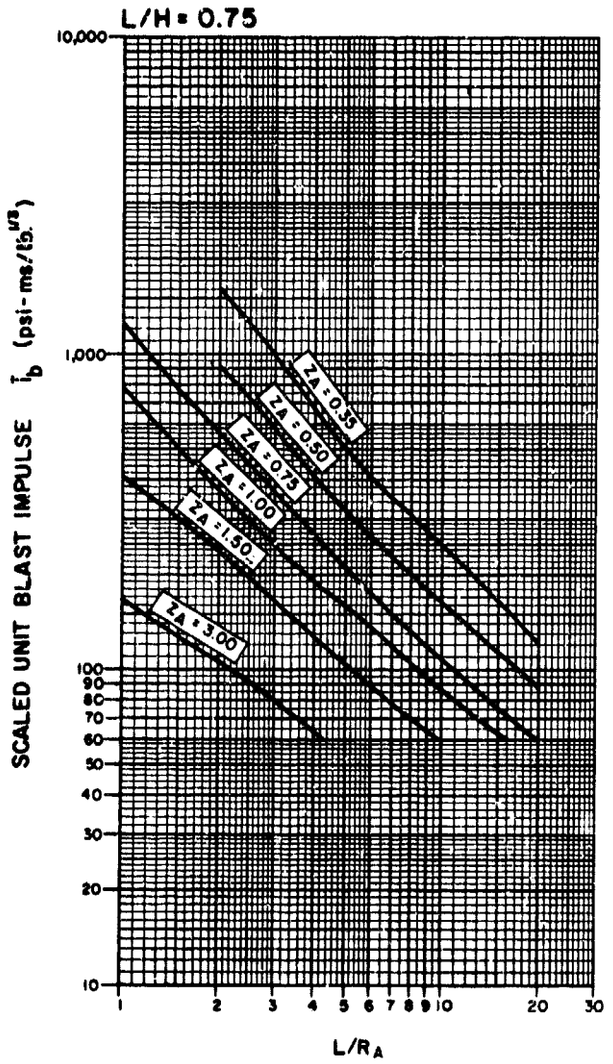


Figure 4–48. Scaled average unit blast impulse ($N = 3$, $l/L = 0.50$, $h/H =$





e unit blast impulse ($N = 3$, $l/L = 0.50$, $h/H = 0.25$).



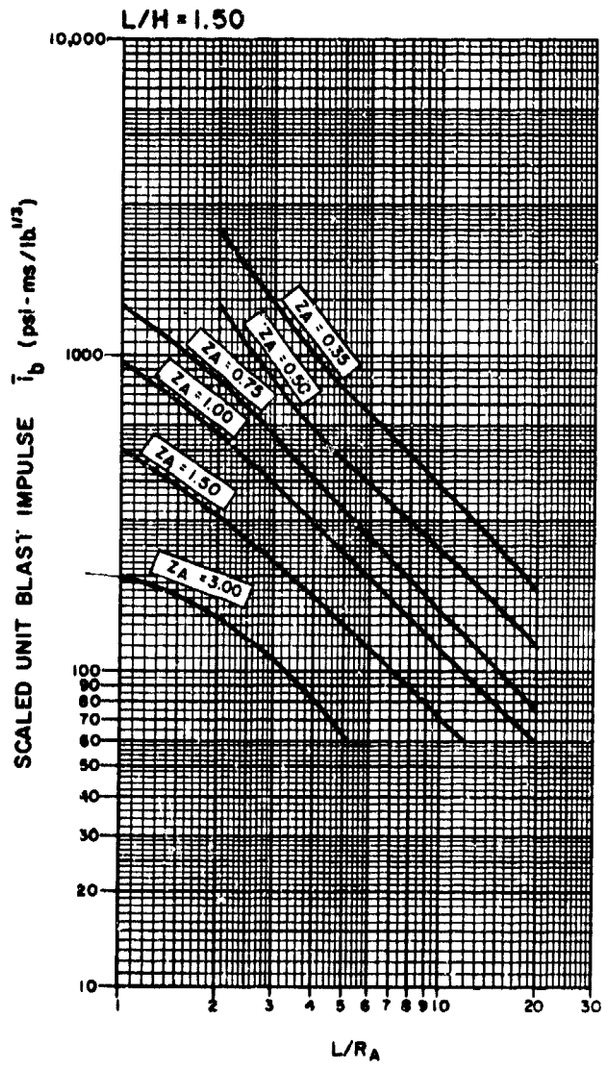
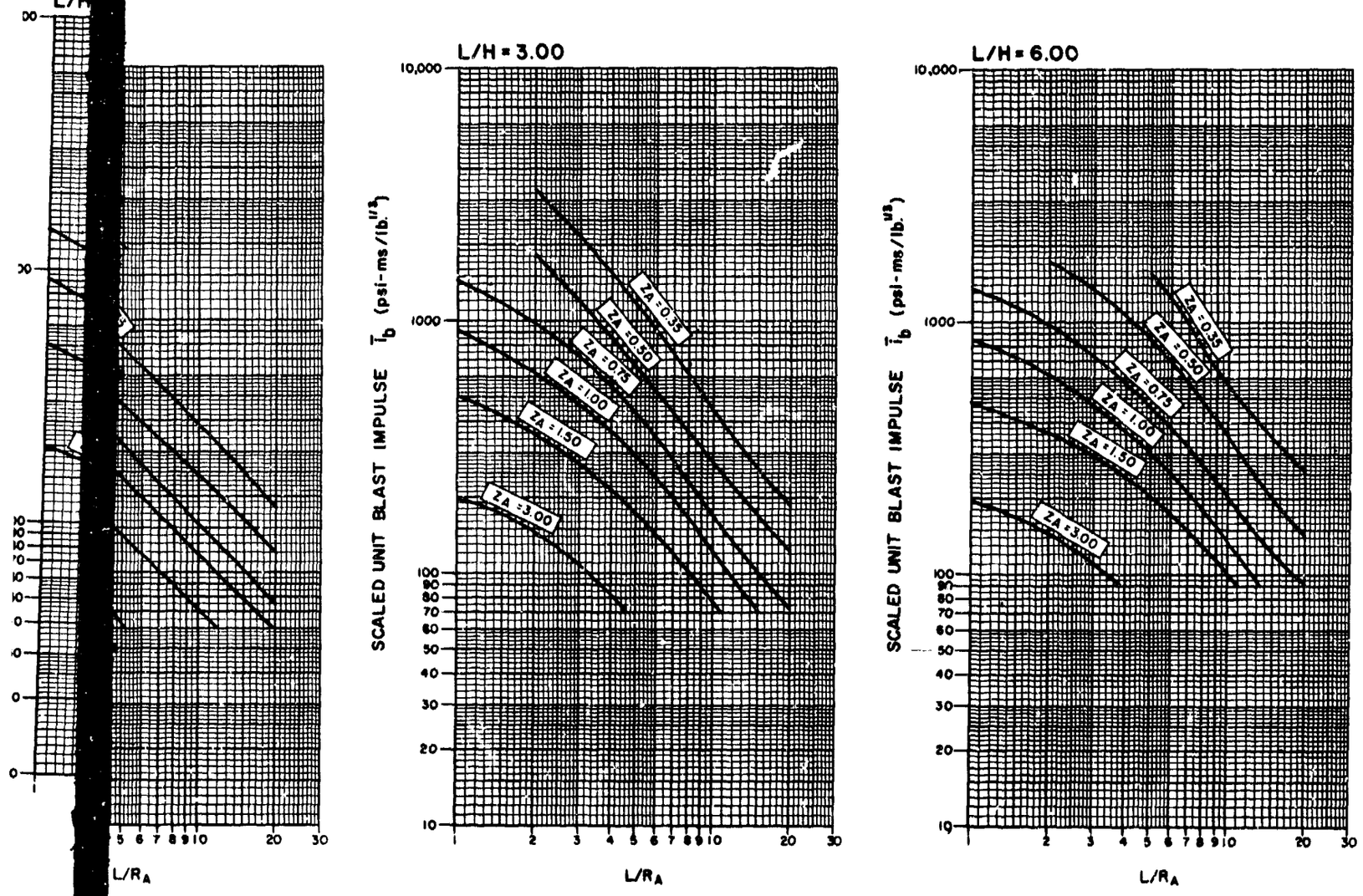




Figure 4-49. Scaled average unit blast impulse (N = 3, l



3, l/L = 0.

4–49. Scaled average unit blast impulse (N = 3, l/L = 0.10, h/H = 0.50).

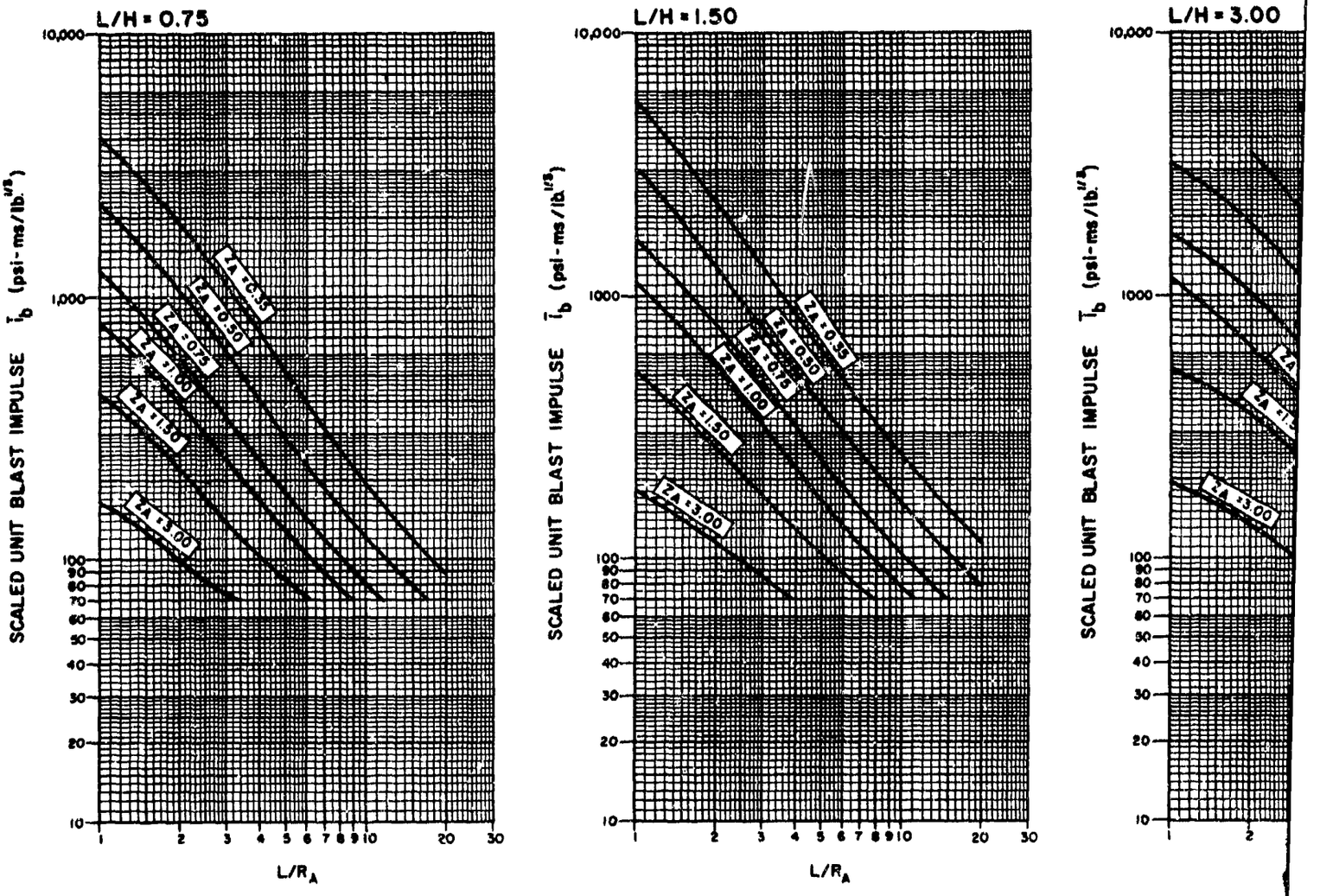
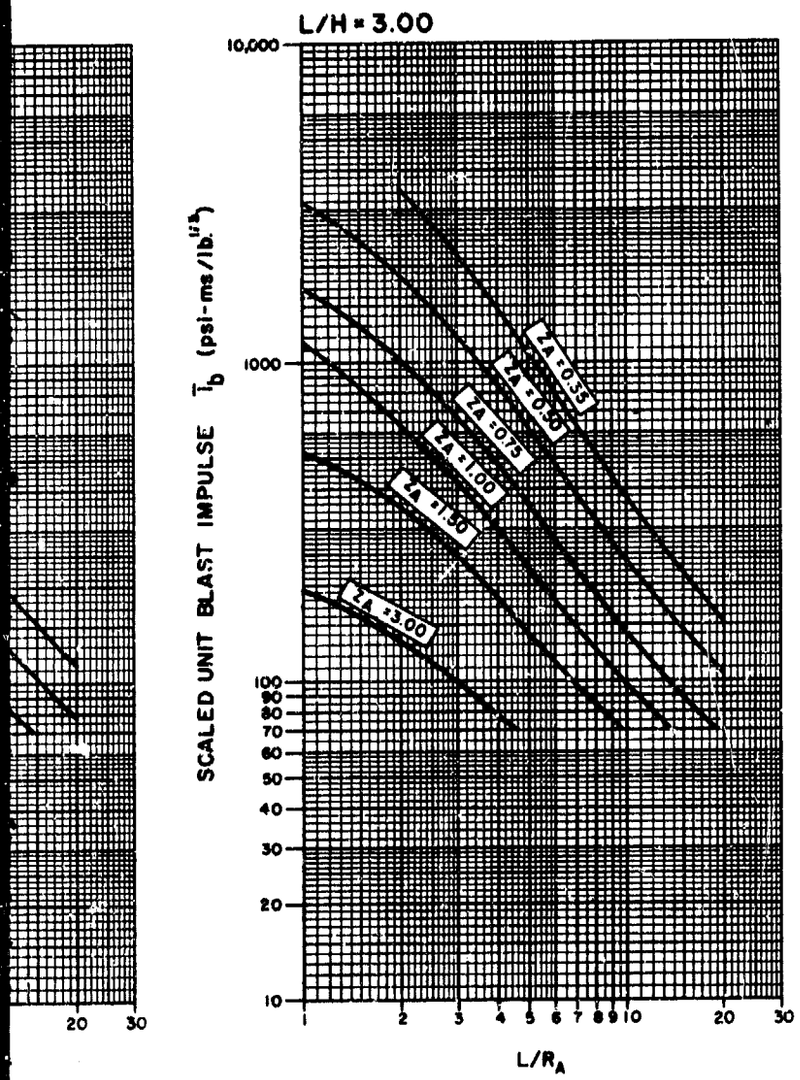
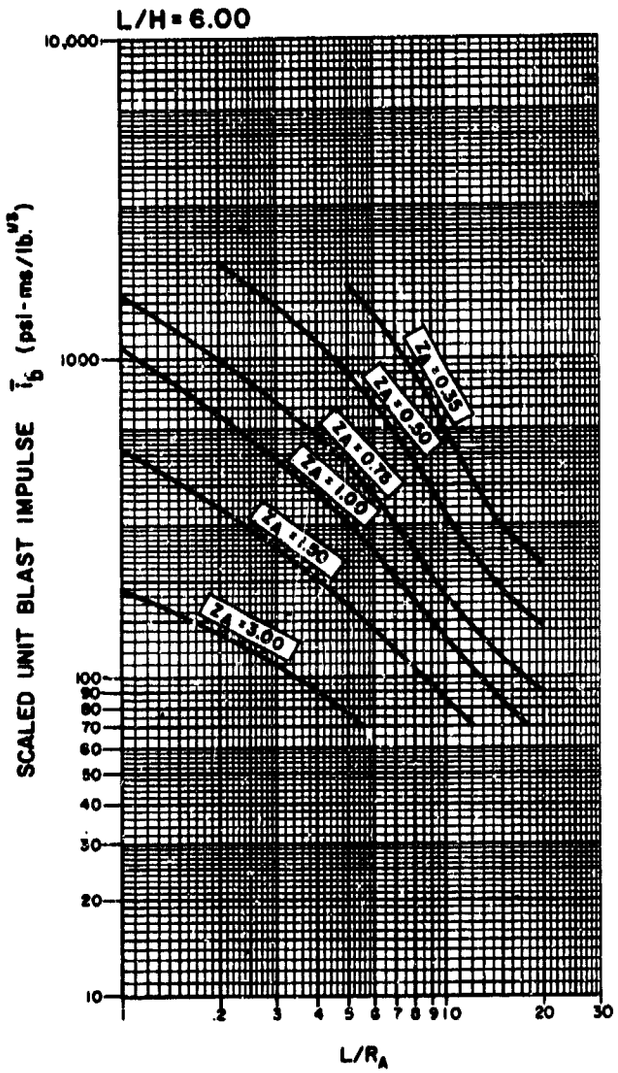


Figure 4-50. Scaled average unit blast impulse ($N = 3$, $l/L = 0.25$ and 0.75, h





e unit blast impulse ($N = 3$, $l/L = 0.25$ and 0.75, $h/H = 0.50$).

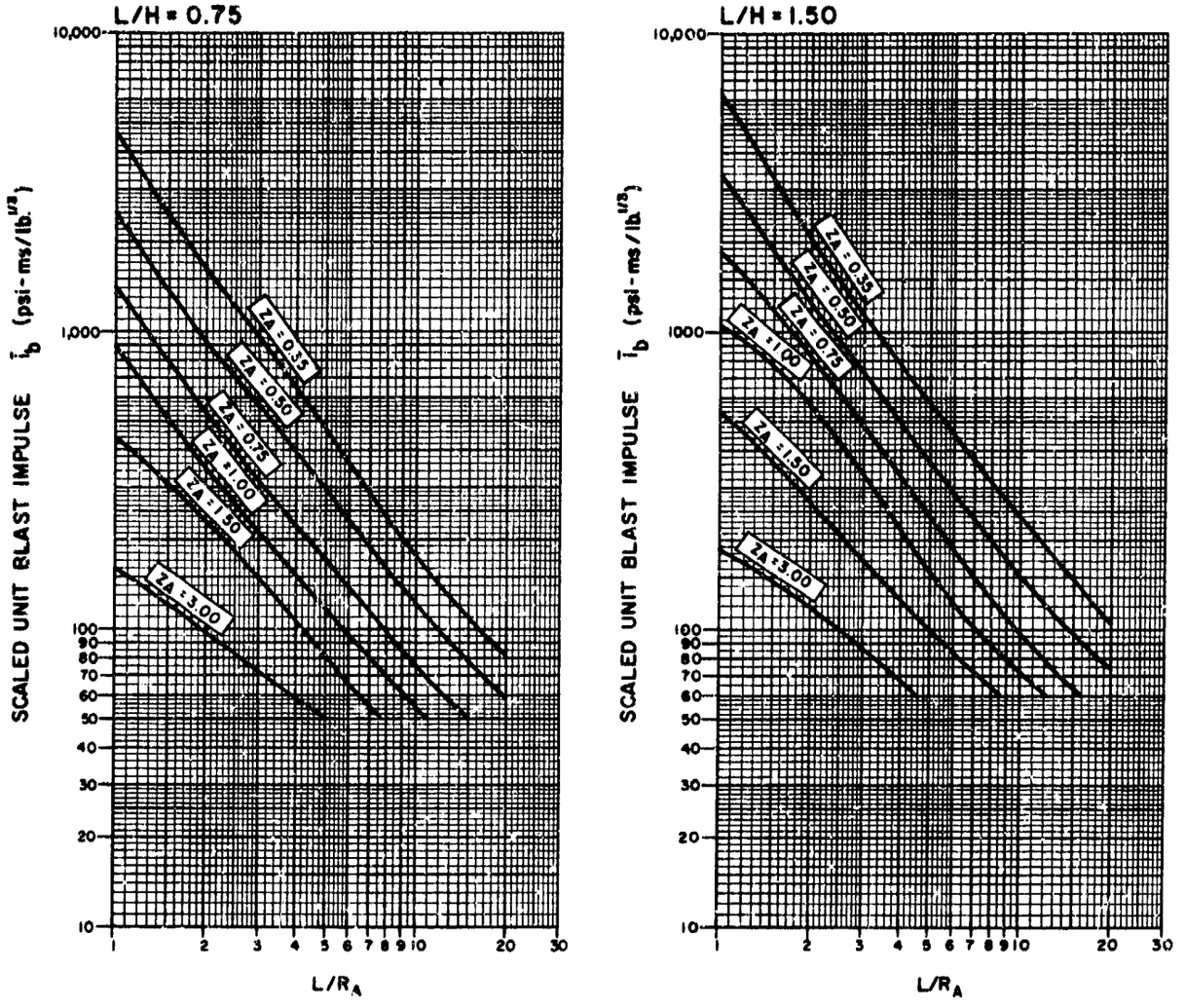
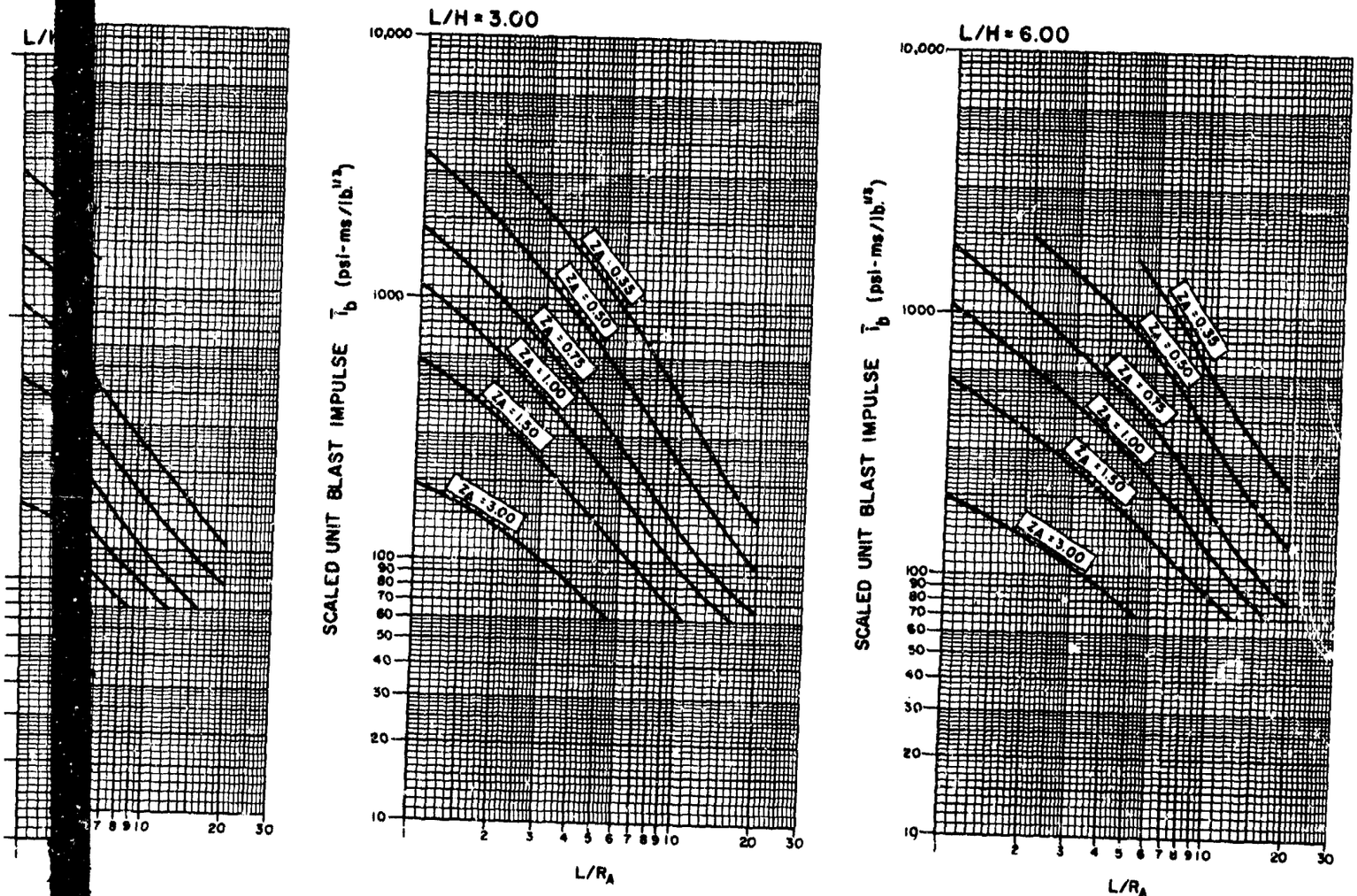


Figure 4-51. Scaled average unit blast impulse ($N = 3$, $l/L =$



Scaled average unit blast impulse ($N=3$, $l/L=0.50$, $h/H=0.50$).

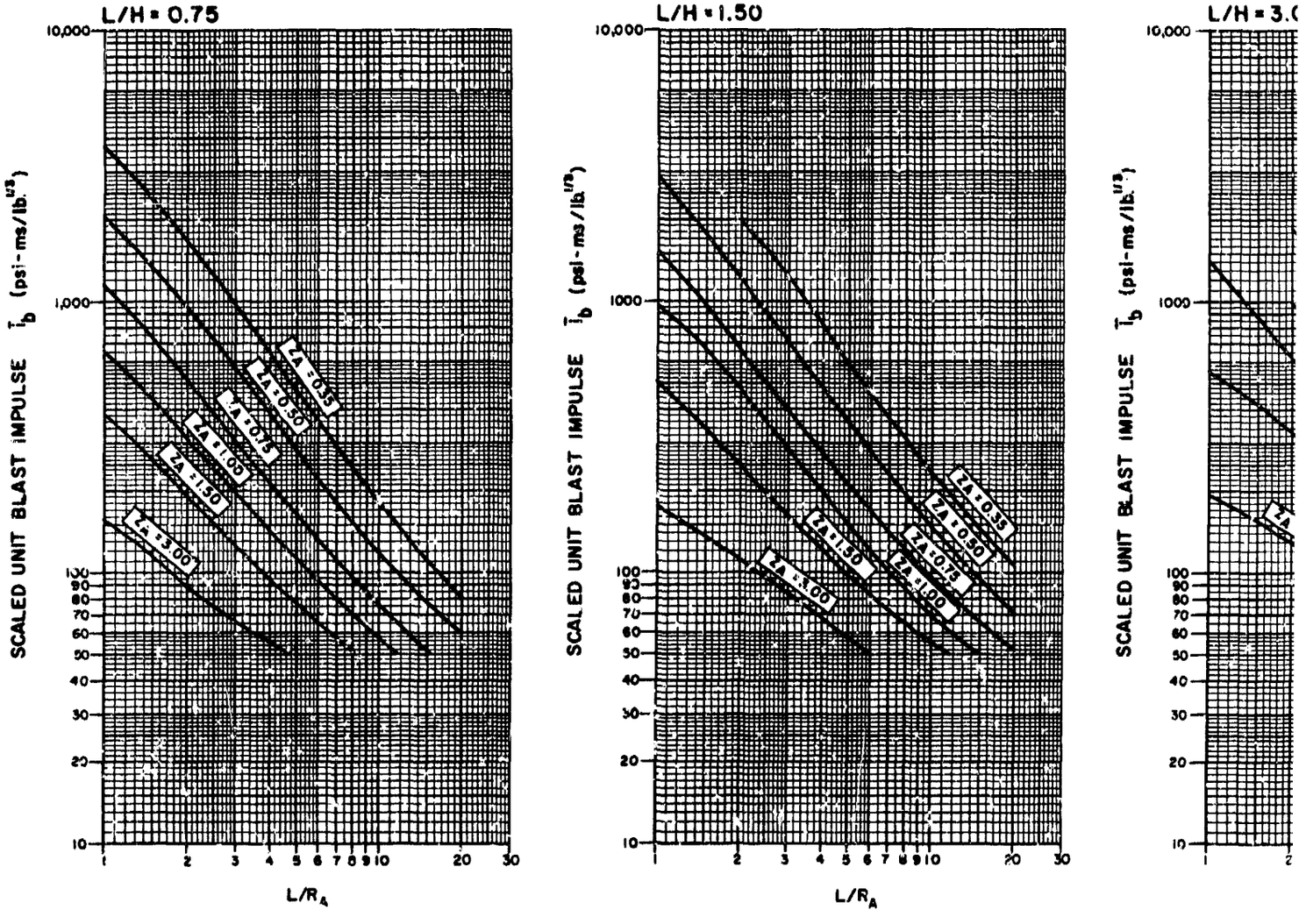
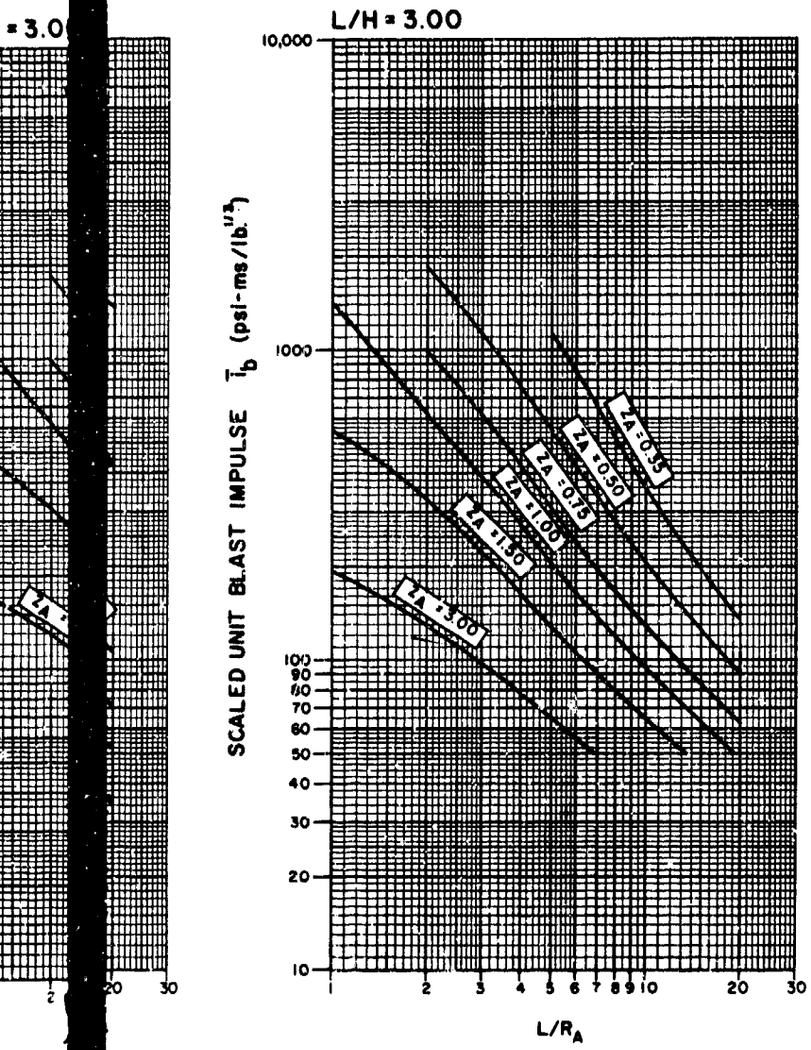
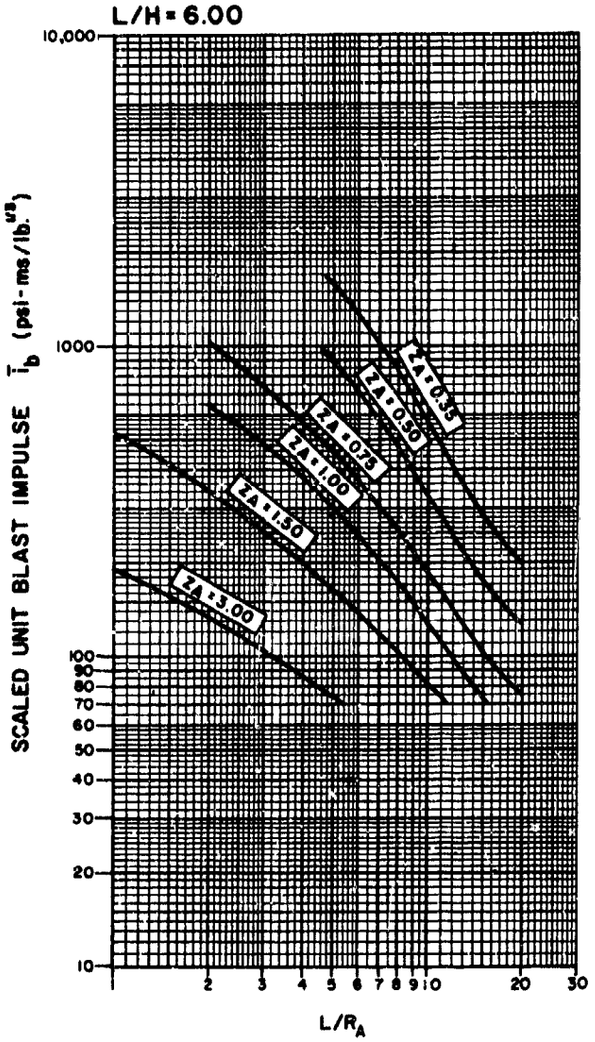
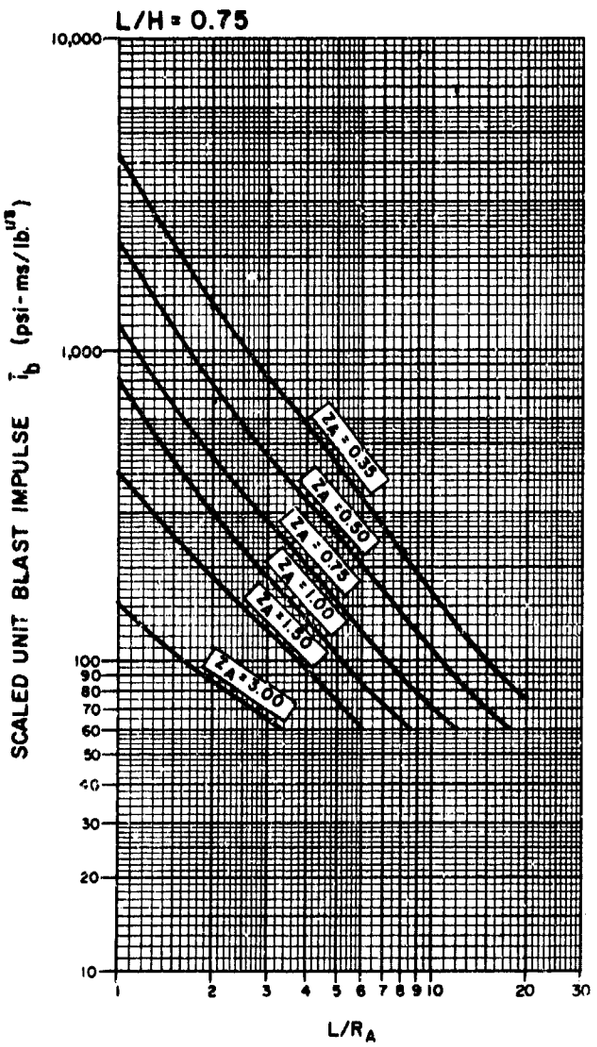


Figure 4-69. Scaled average unit blast impulse ($N = 3$, $l/L = 0.85$ and 0.





and 0.7 blast impulse ($N=3$, $l/L=0.25$ and 0.75, $h/H=0.75$).



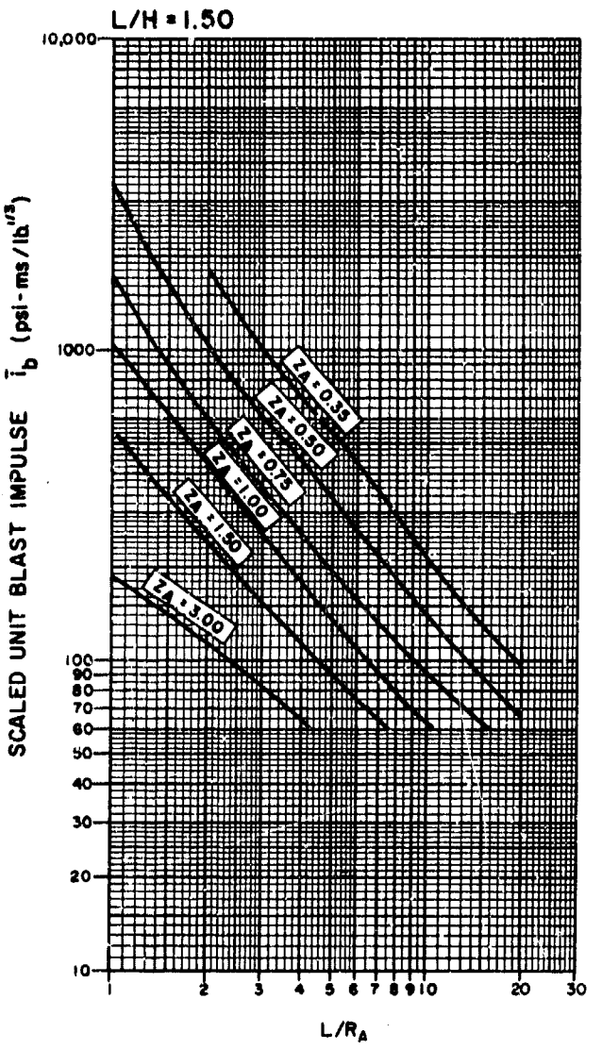
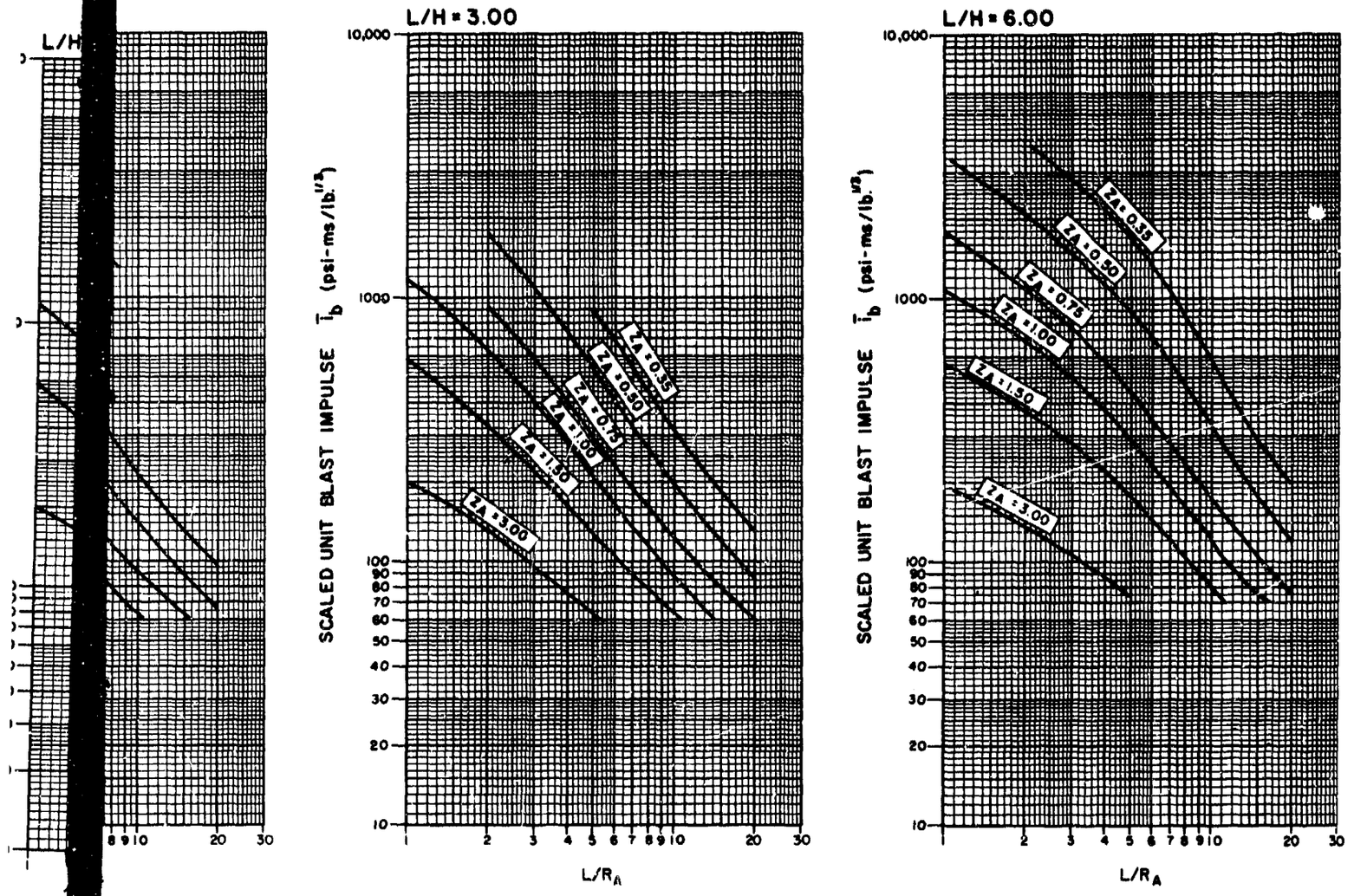




Figure 4-63. Scaled average unit blast impulse (N = 3, l/L =



Scaled average unit blast impulse ($N=3$, $l/L=0.50$, $h/H=0.75$).

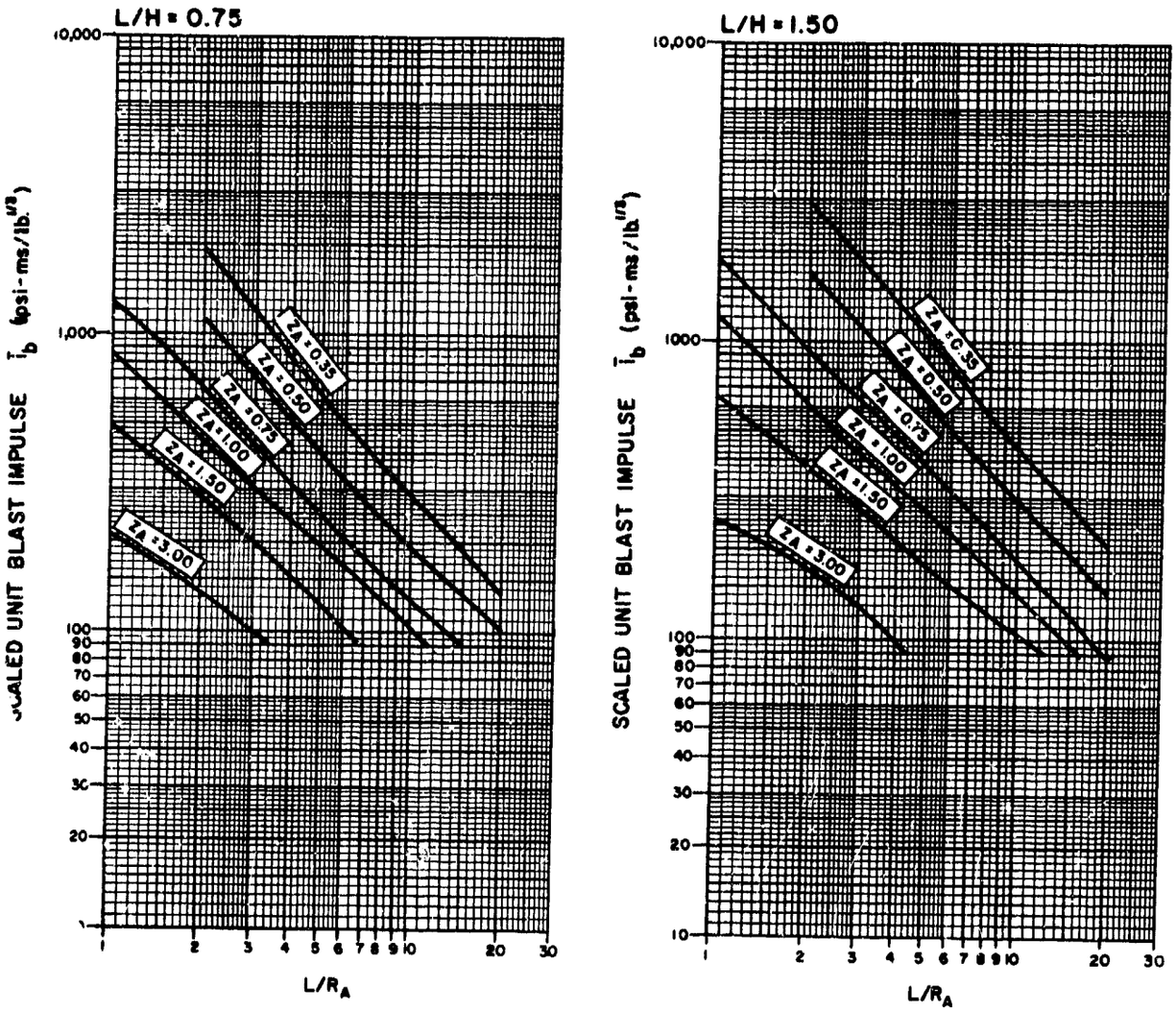
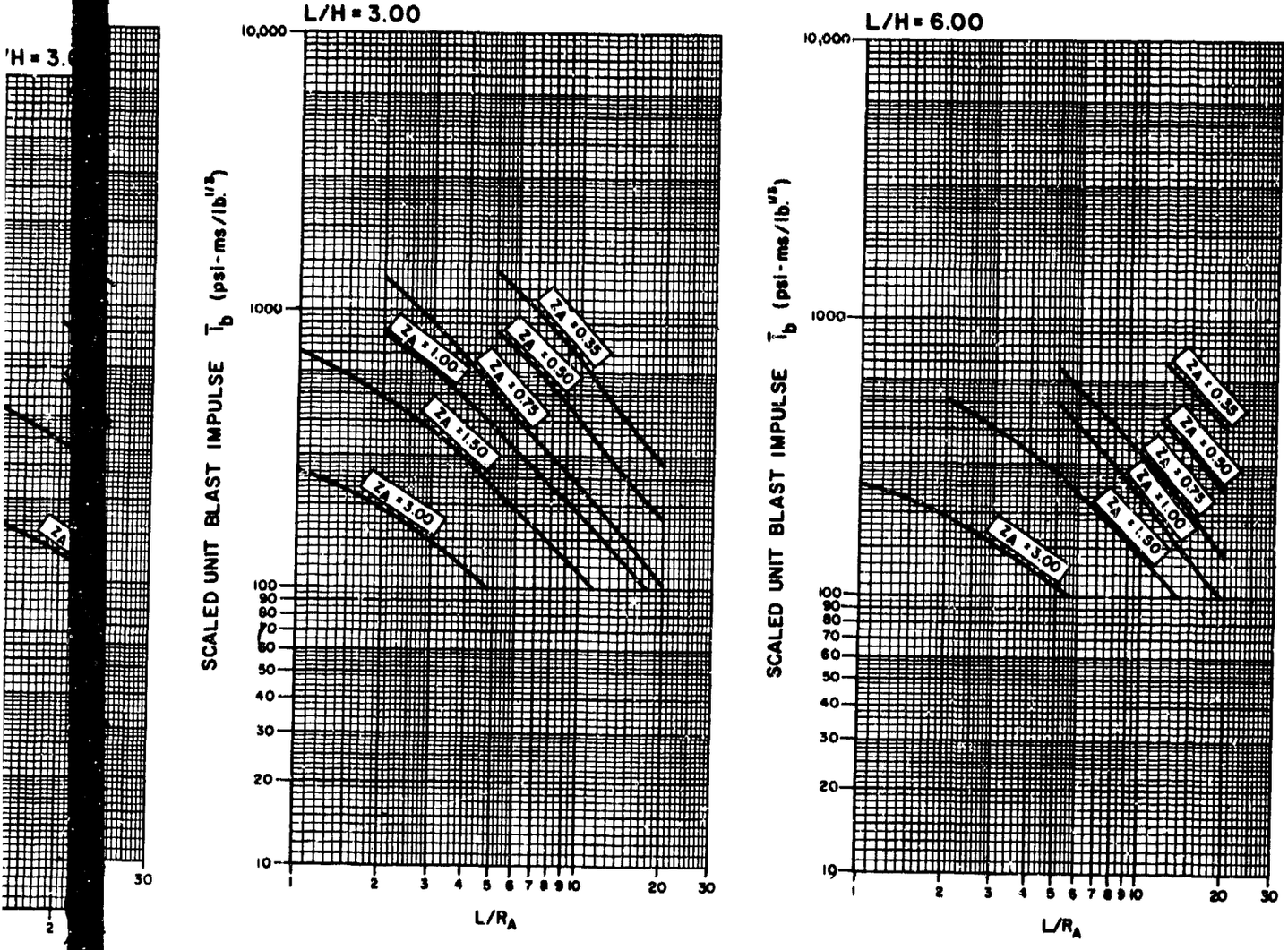
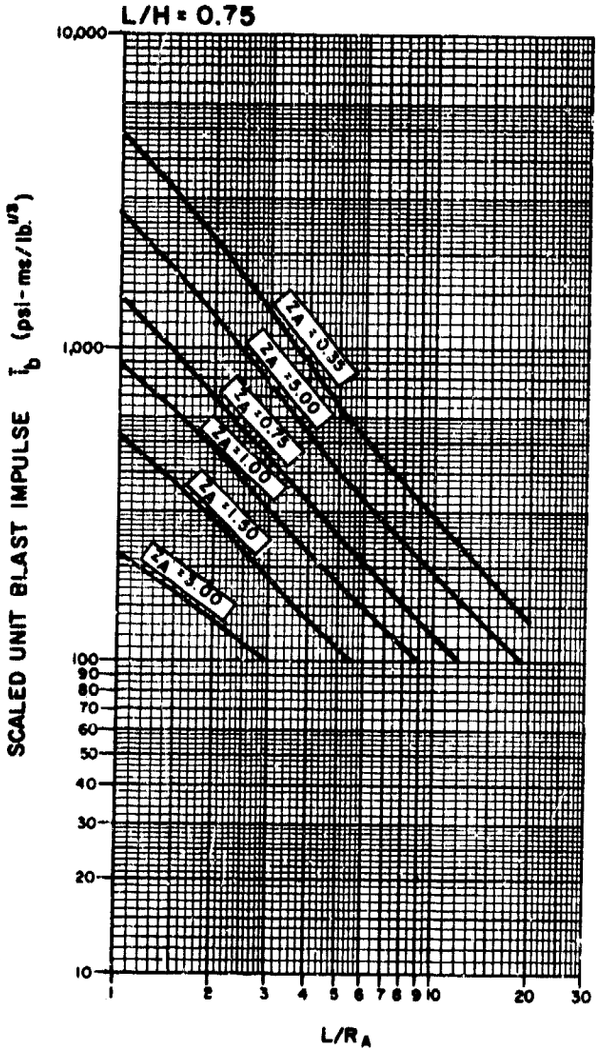


Figure 4-54. Scaled average unit blast impulse ($N = 4$, $l/L = 0.10$, h



t blast impulse ($N = 4$, $l/L = 0.10$, $h/H = 0.15$).

0.10, h/H



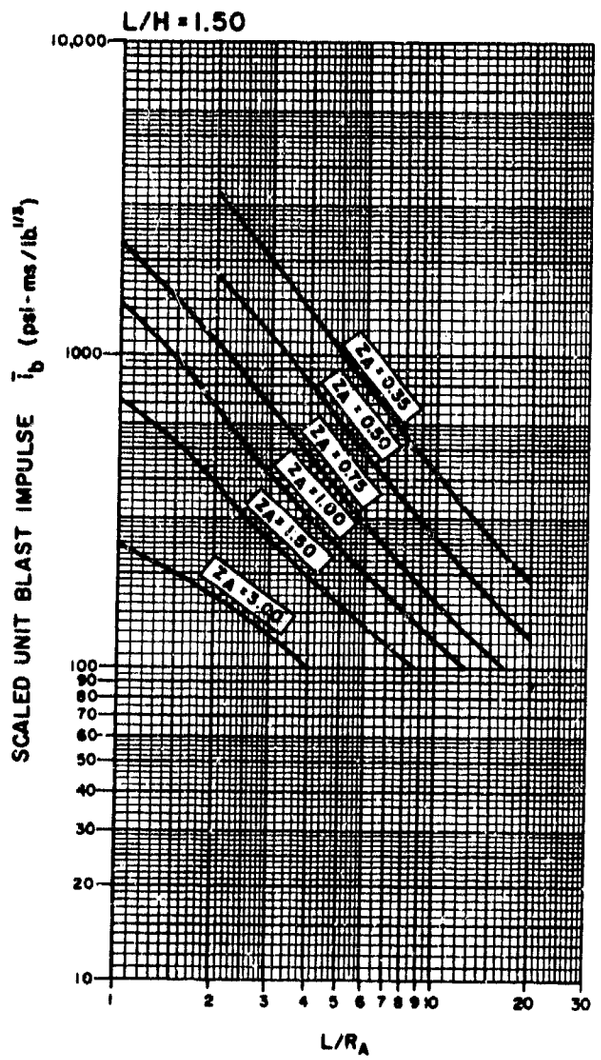
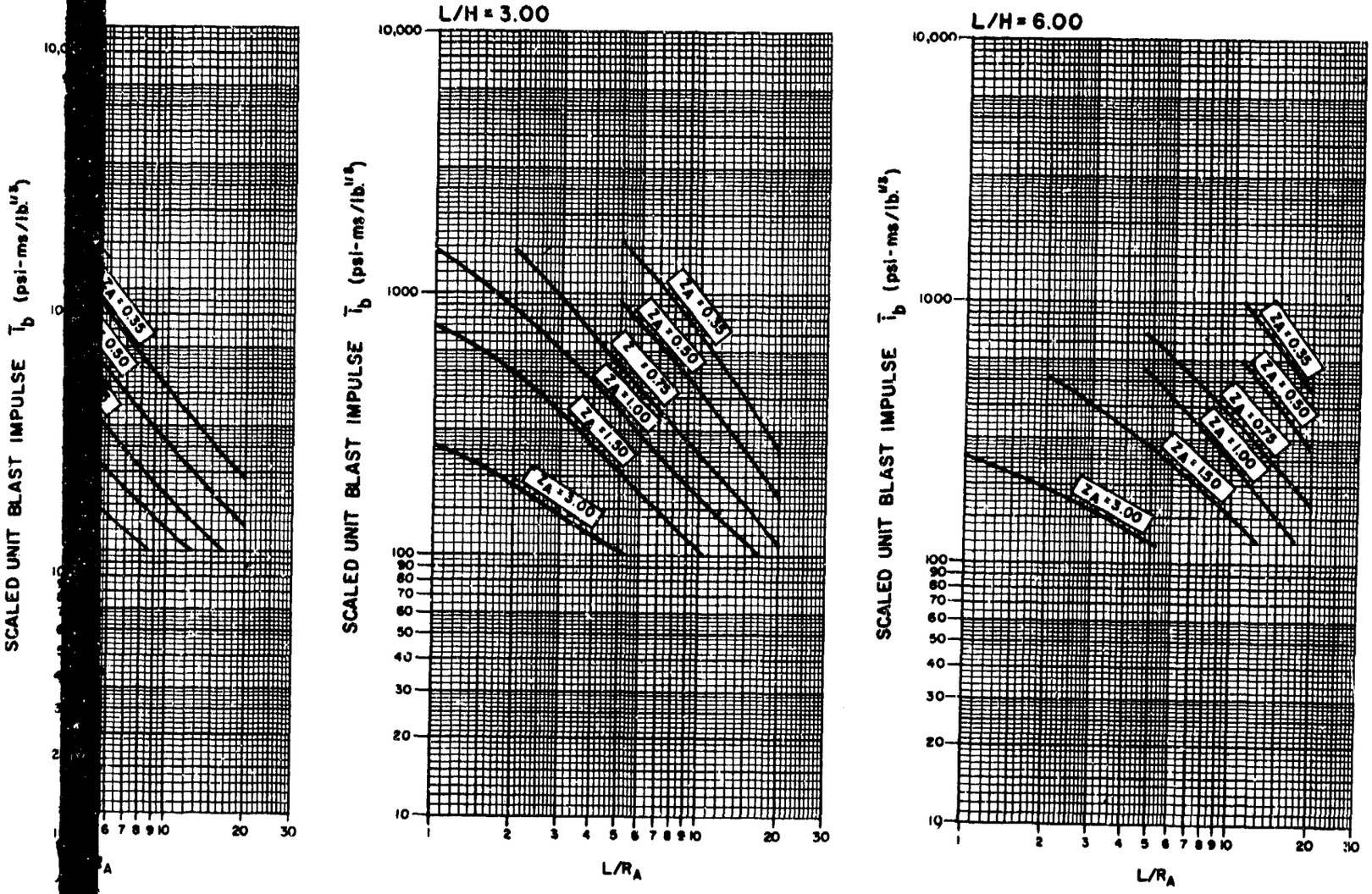


Figure 4-55. Scaled average unit blast impulse (N =



Scaled average unit blast impulse ($N = 4$, $l/L = 0.25$ and 0.75, $h/H = 0.15$).

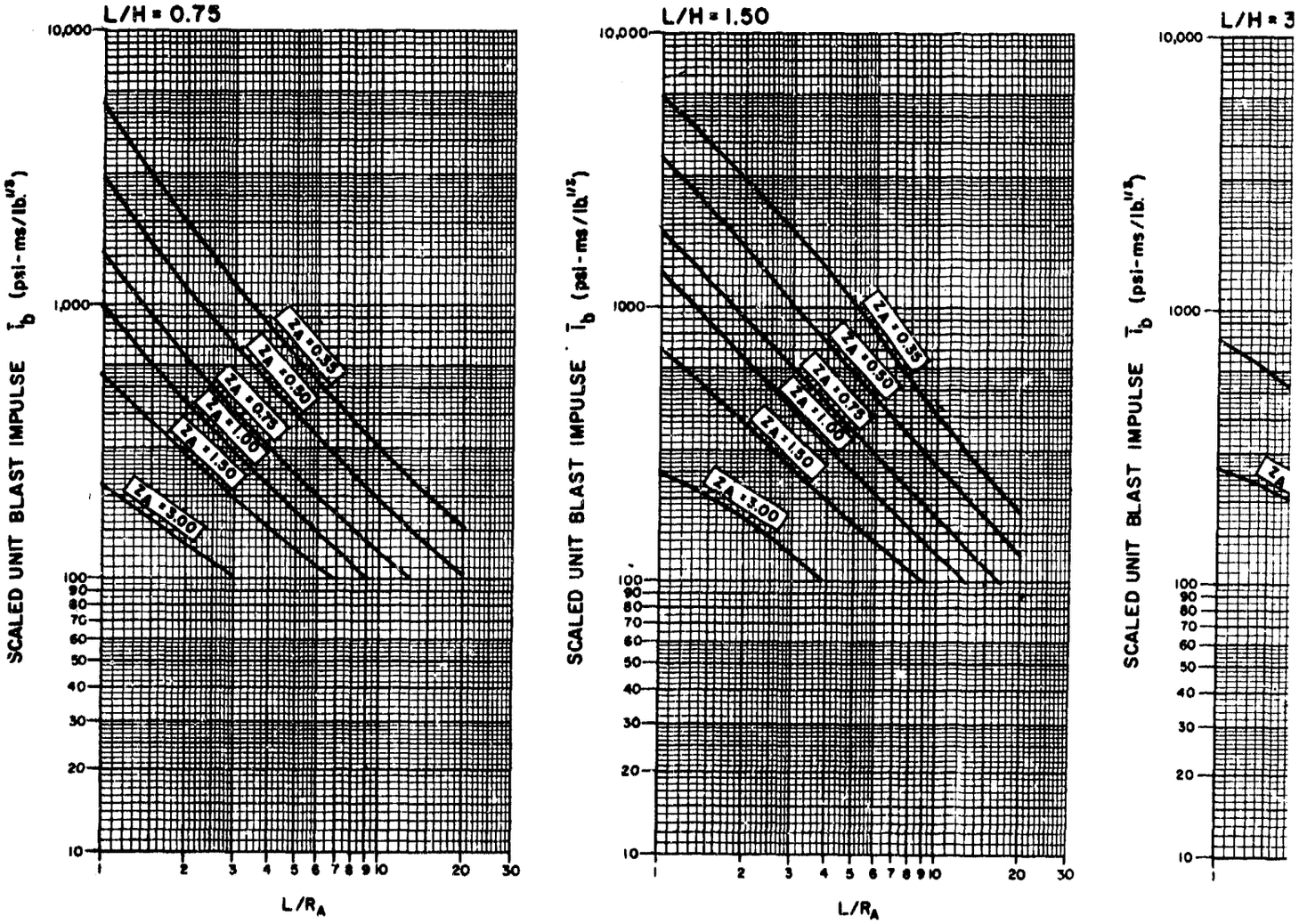
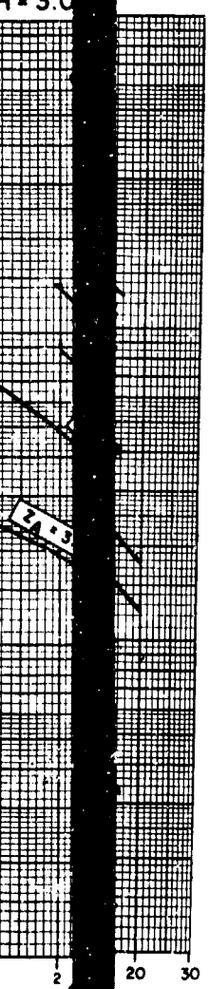
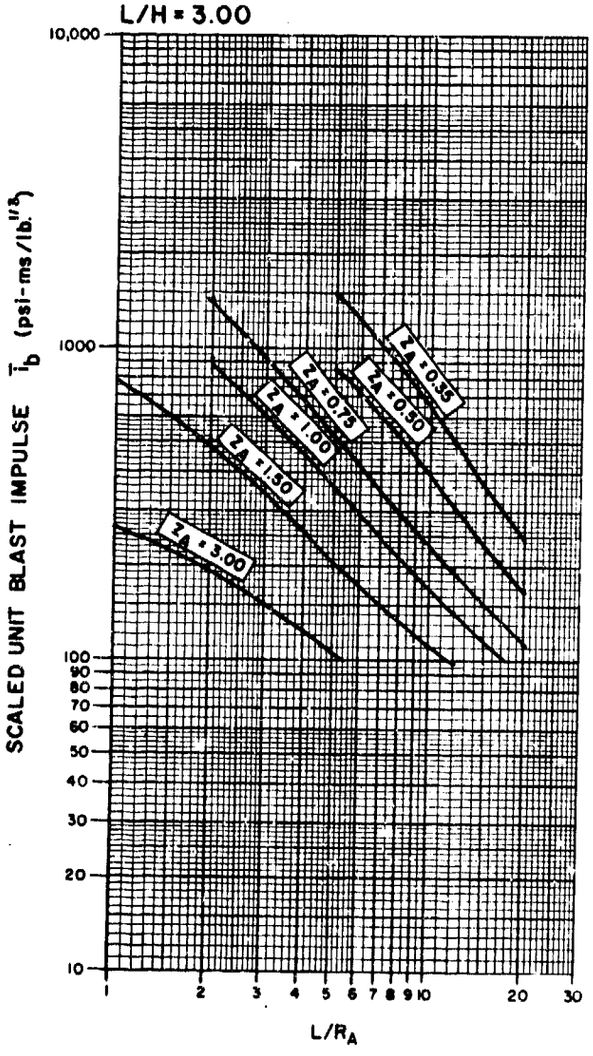
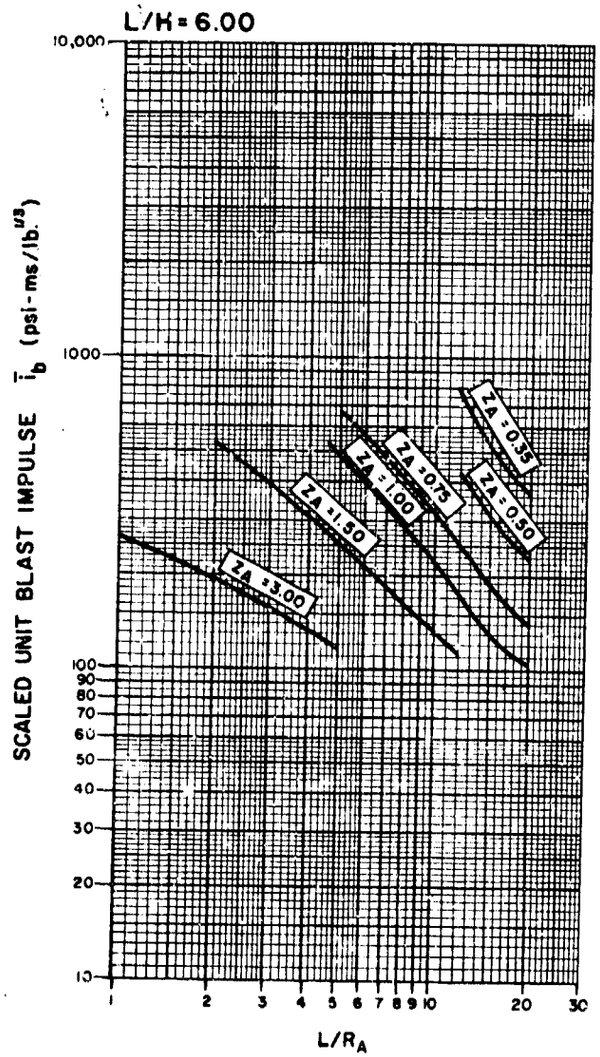


Figure 4-66. Scaled average unit blast impulse ($N = 4$, $l/L = 0.50$







=0.50, h/ e unit blast impulse ($N=4$, $l/L=0.50$, $h/H=0.15$).

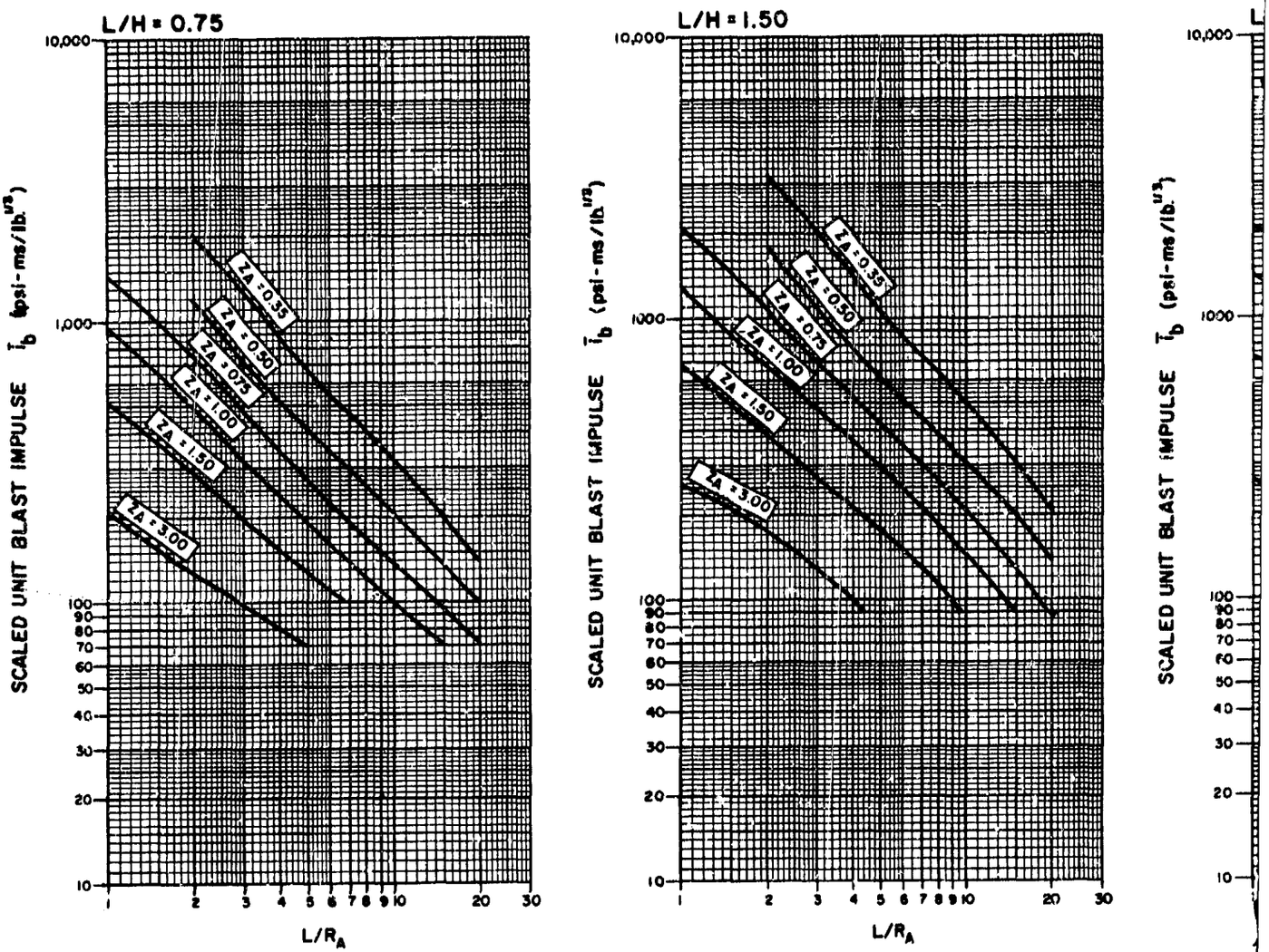
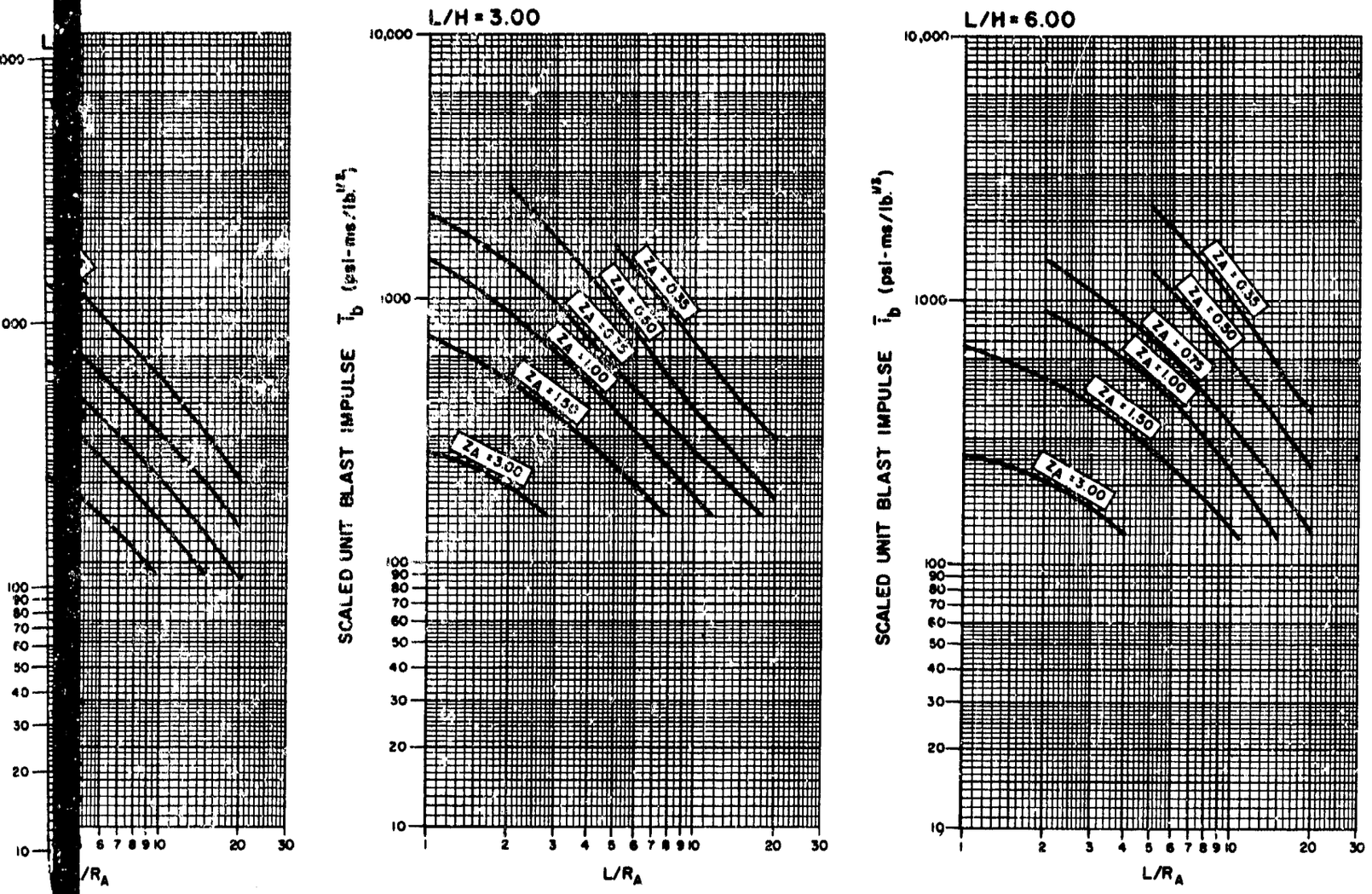


Figure 4-57. Scaled average unit blast impulse ($N = 4$, $l/L =$



Scaled average unit blast impulse ($N = 4$, $l/L = 0.10$, $h/H = 0.95$ *and* 0.75).

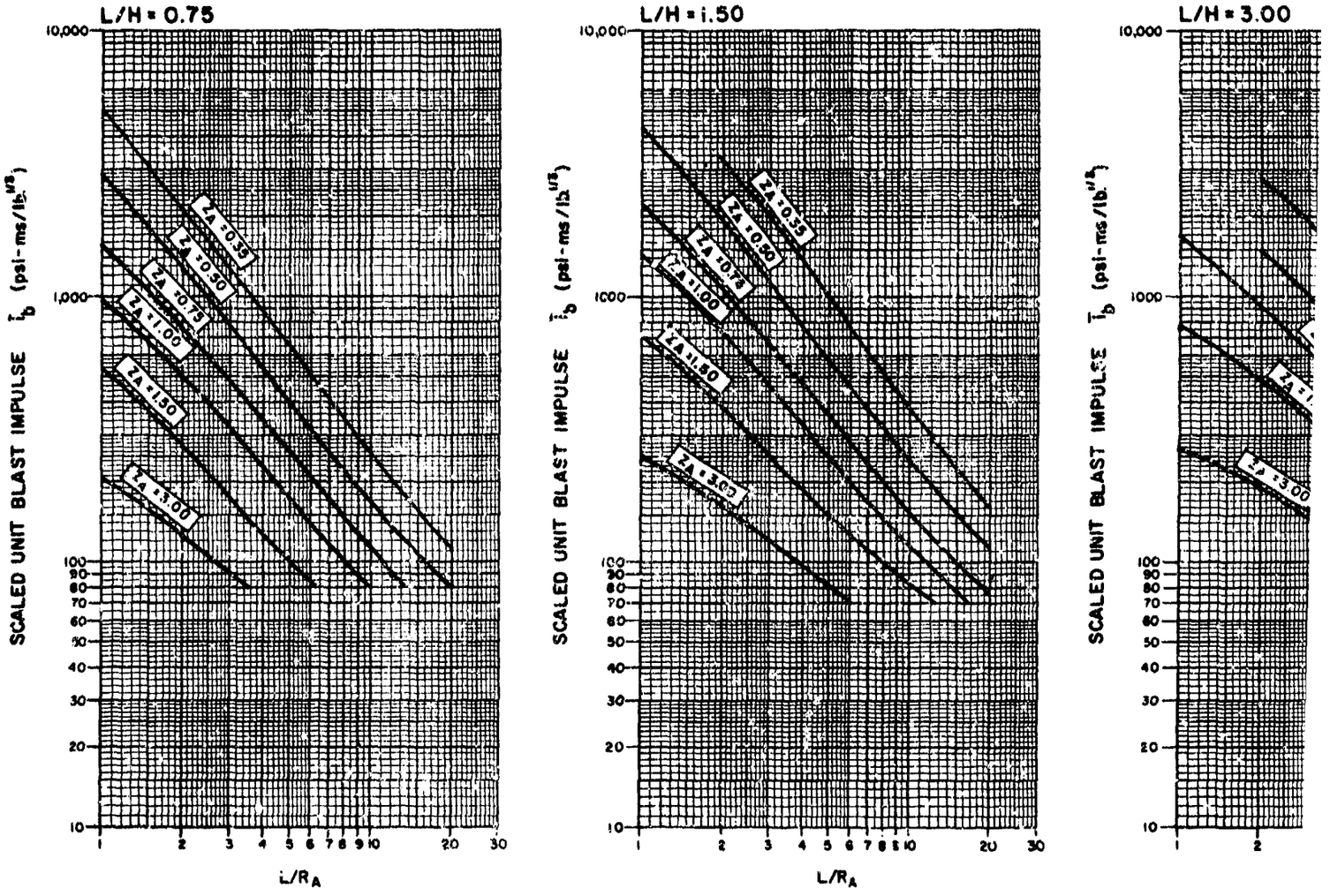
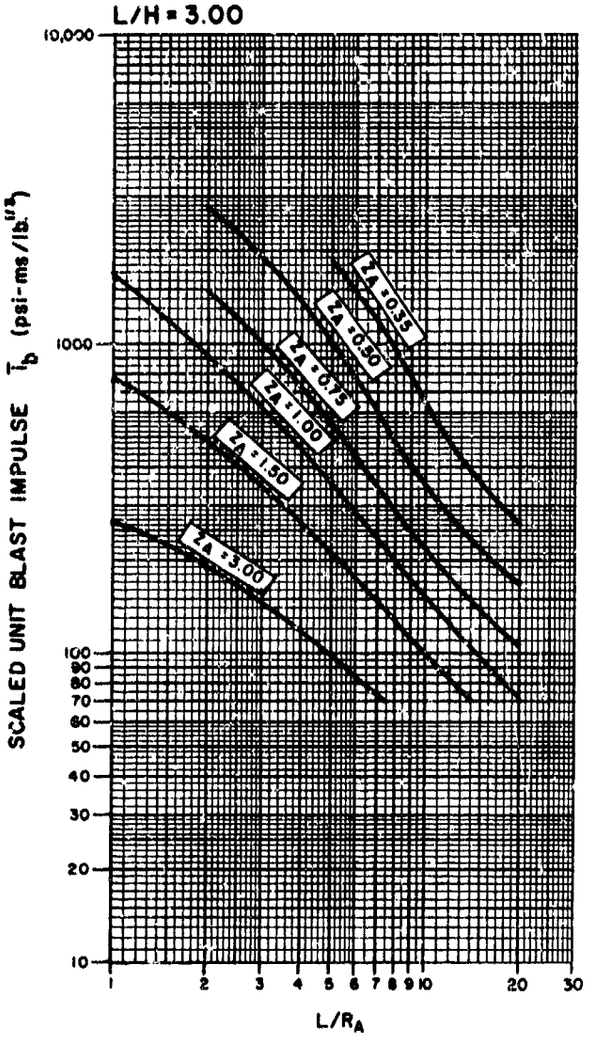
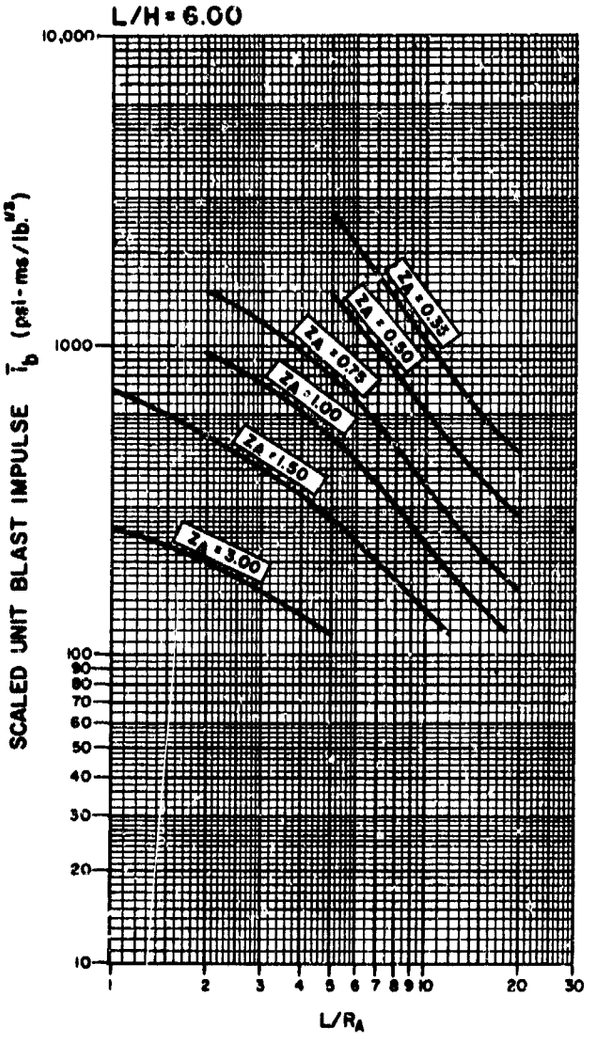
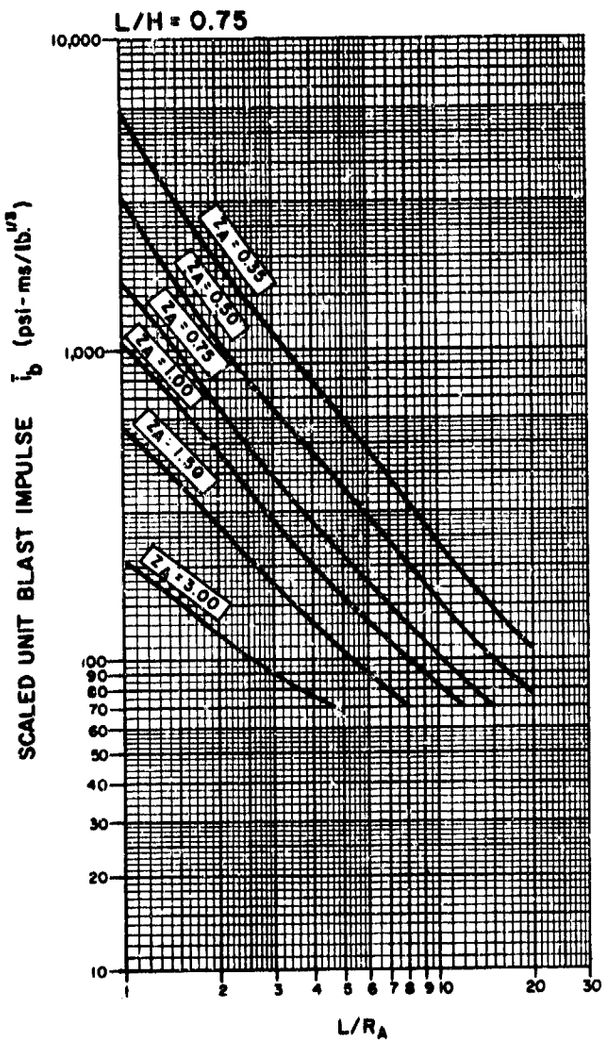


Figure 4–58. Scaled average unit blast impulse ($N = 4$, $l/L = 0.25$ and 0.75, $h/H =$





last impulse ($N = 4$, $l/L = 0.25$ and 0.75, $h/H = 0.25$ and 0.75).



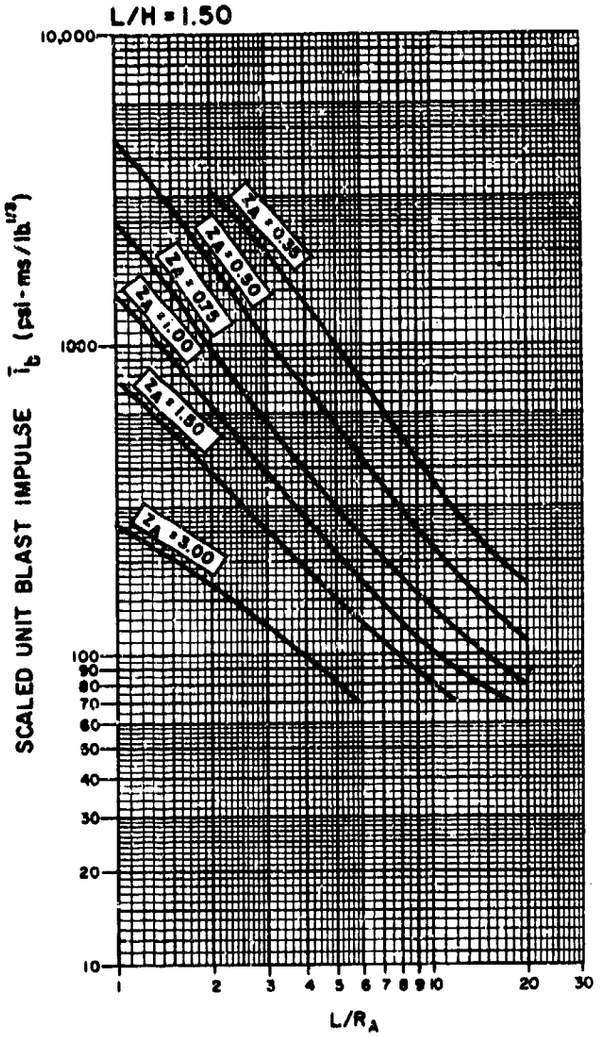
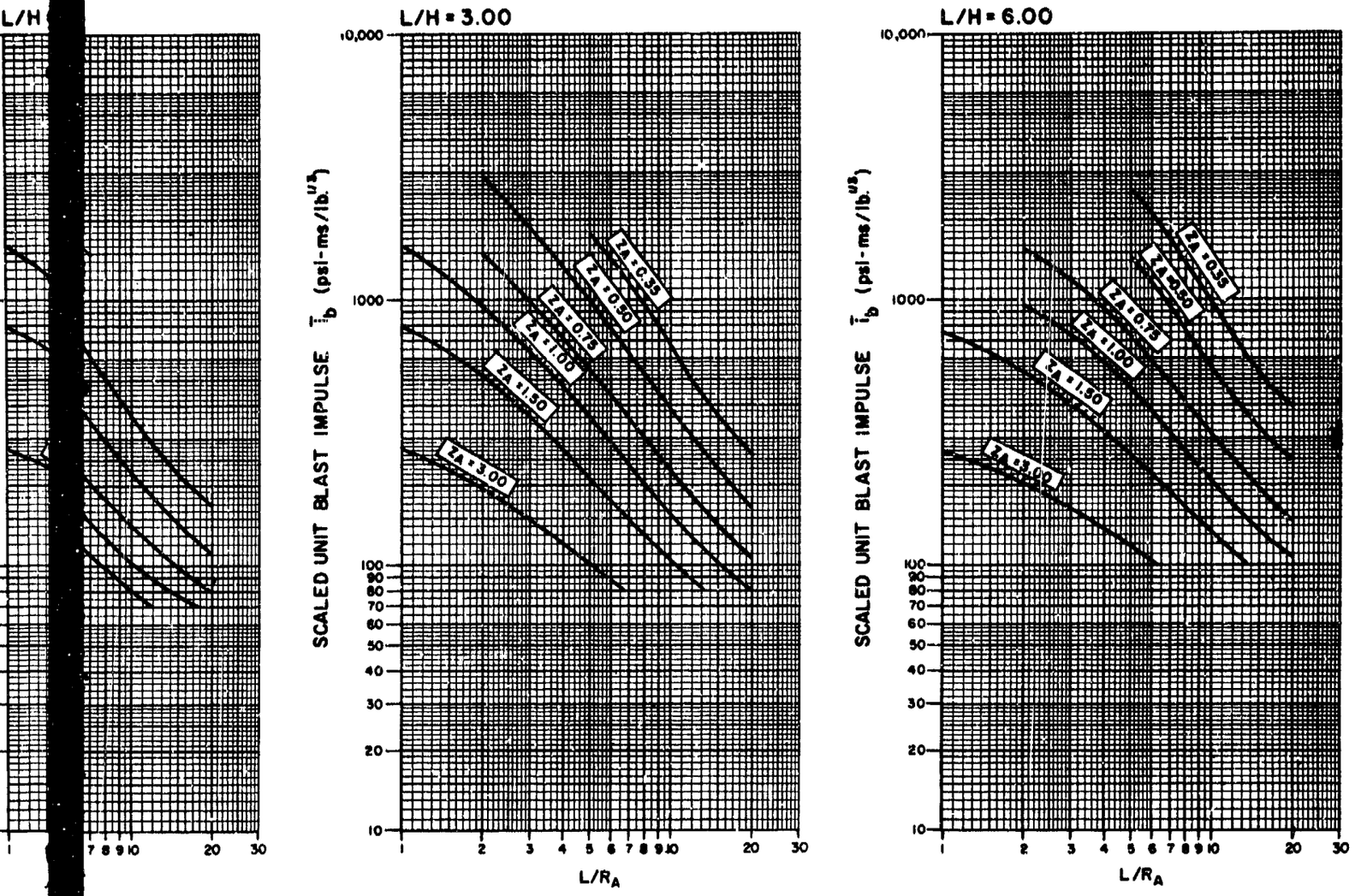
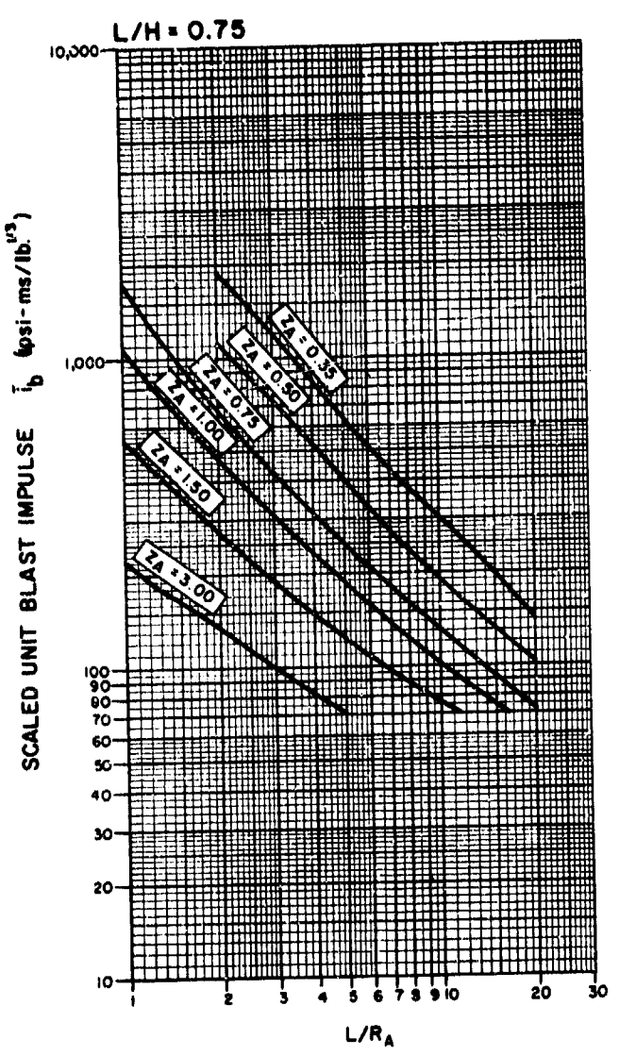


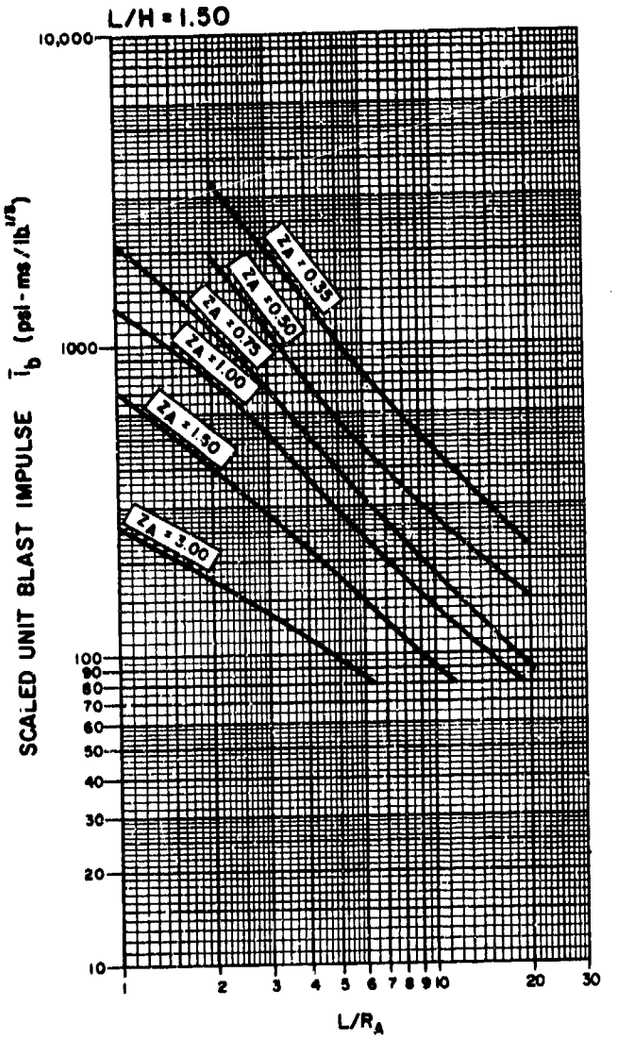


Figure 4-59. Scaled average unit blast impulse ($N = 4$, $i/L = 0.5$



...=0.50, ...aled average unit blast impulse (N = 4, l/L = 0.50, h/H = 0.25 and 0.75).





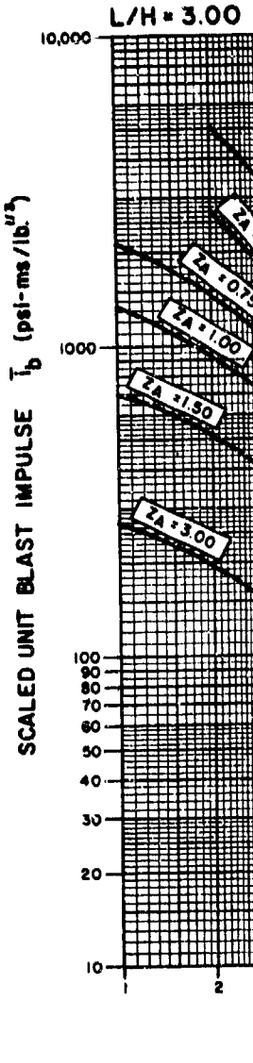
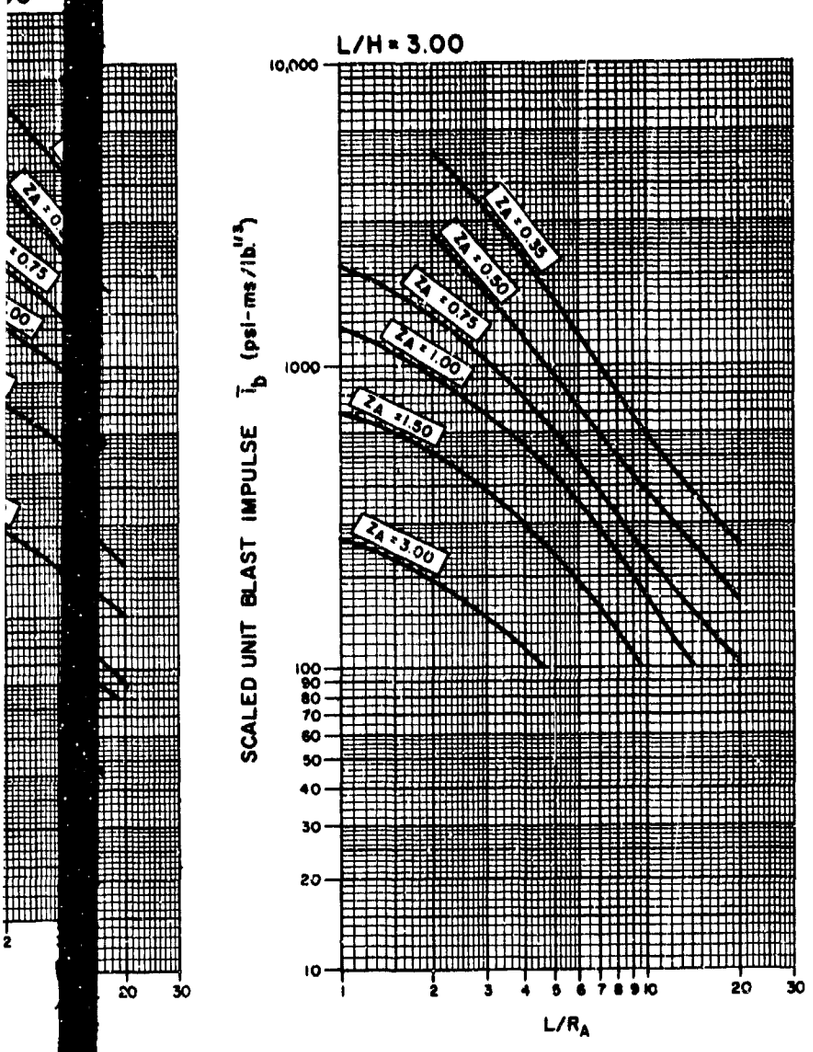
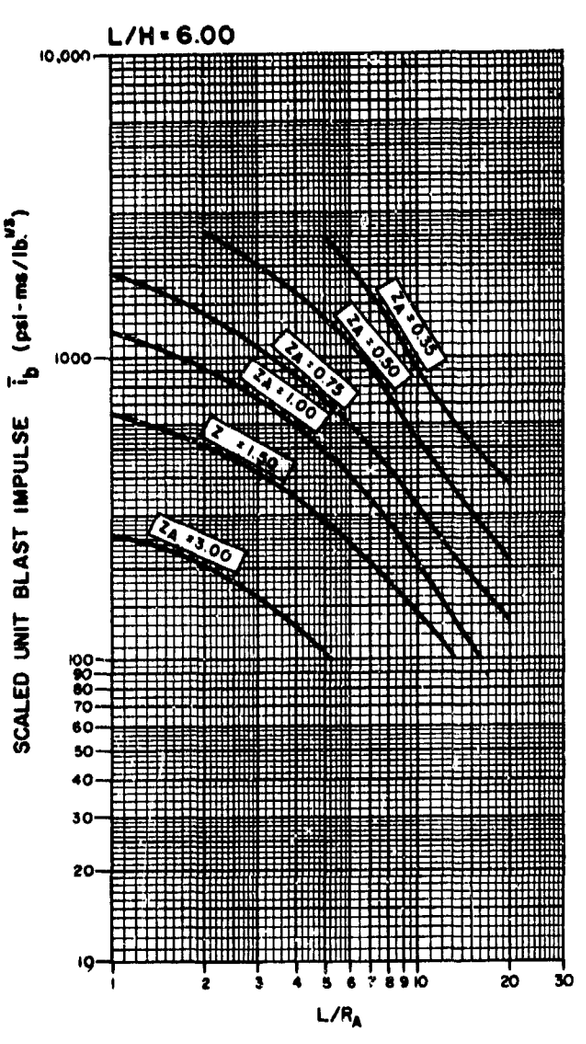


Figure 4-60. Scaled average unit blast impulse ($N = 4$, $l/L = 0.10$, h/H





ge unit blast impulse ($N = 4$, $l/L = 0.10$, $h/H = 0.50$).

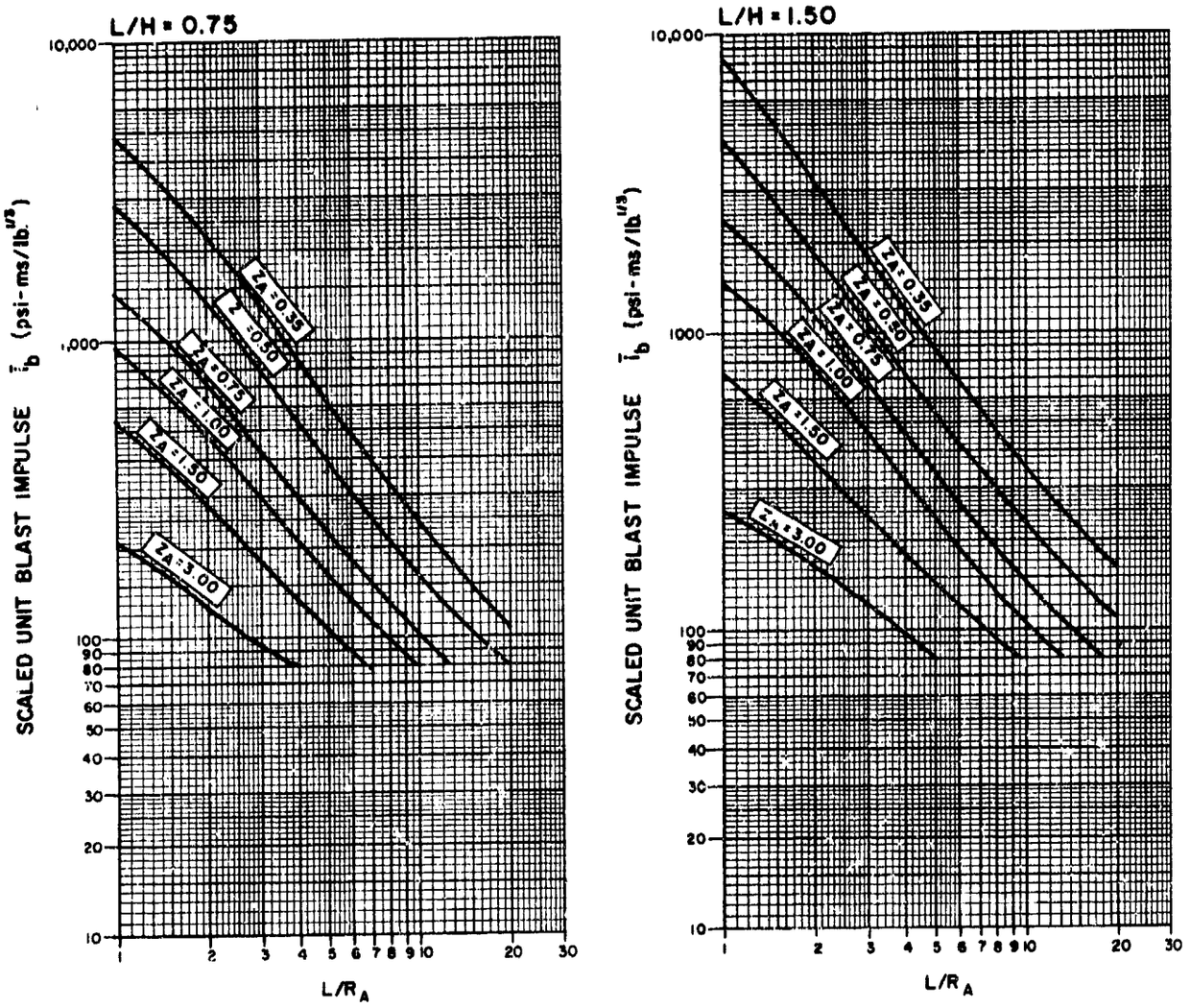
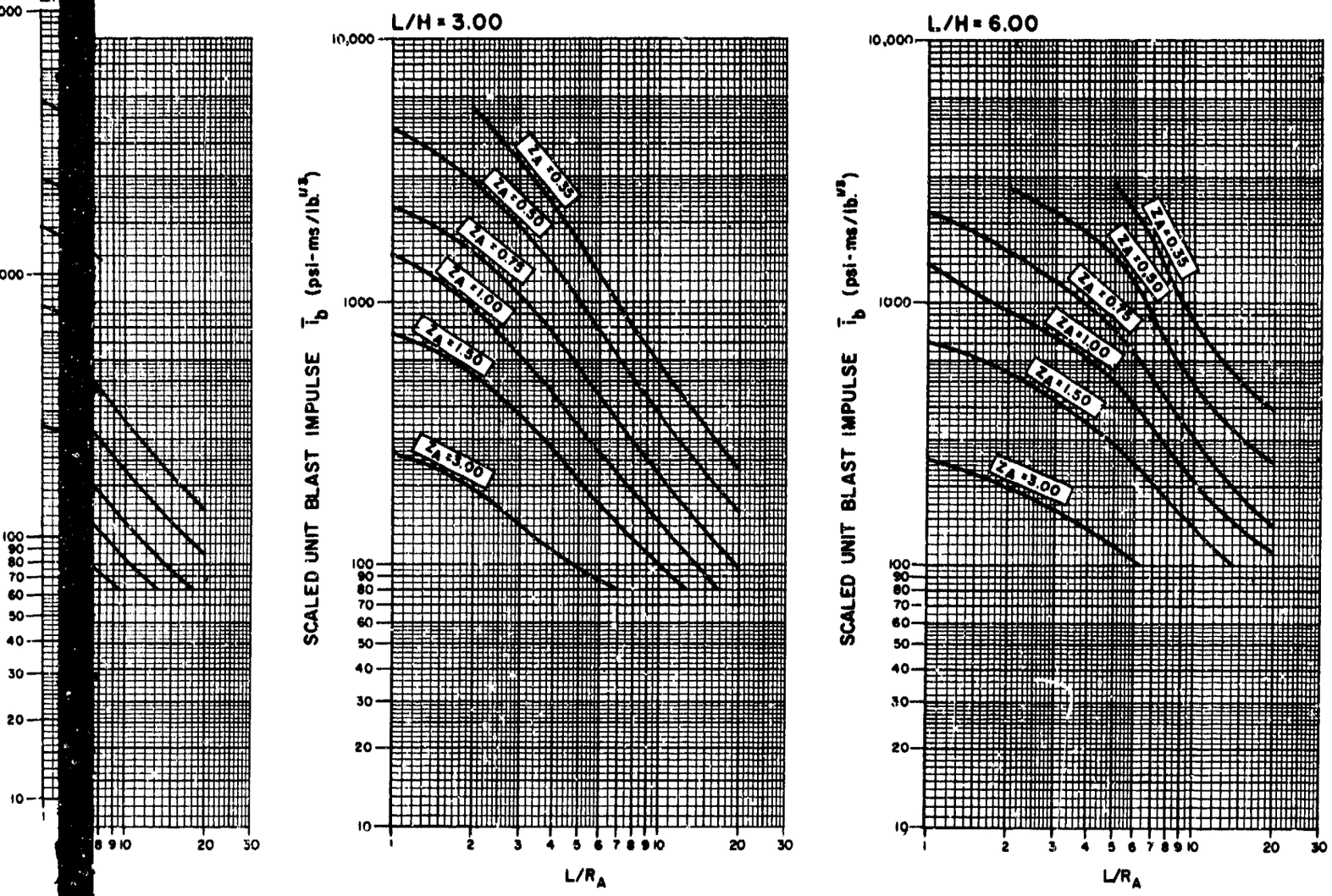


Figure 4-61. Scaled average unit blast impulse (N = 4, l/L =



average unit blast impulse ($N = 4$, $l/L = 0.85$ and 0.75, $h/H = 0.60$).

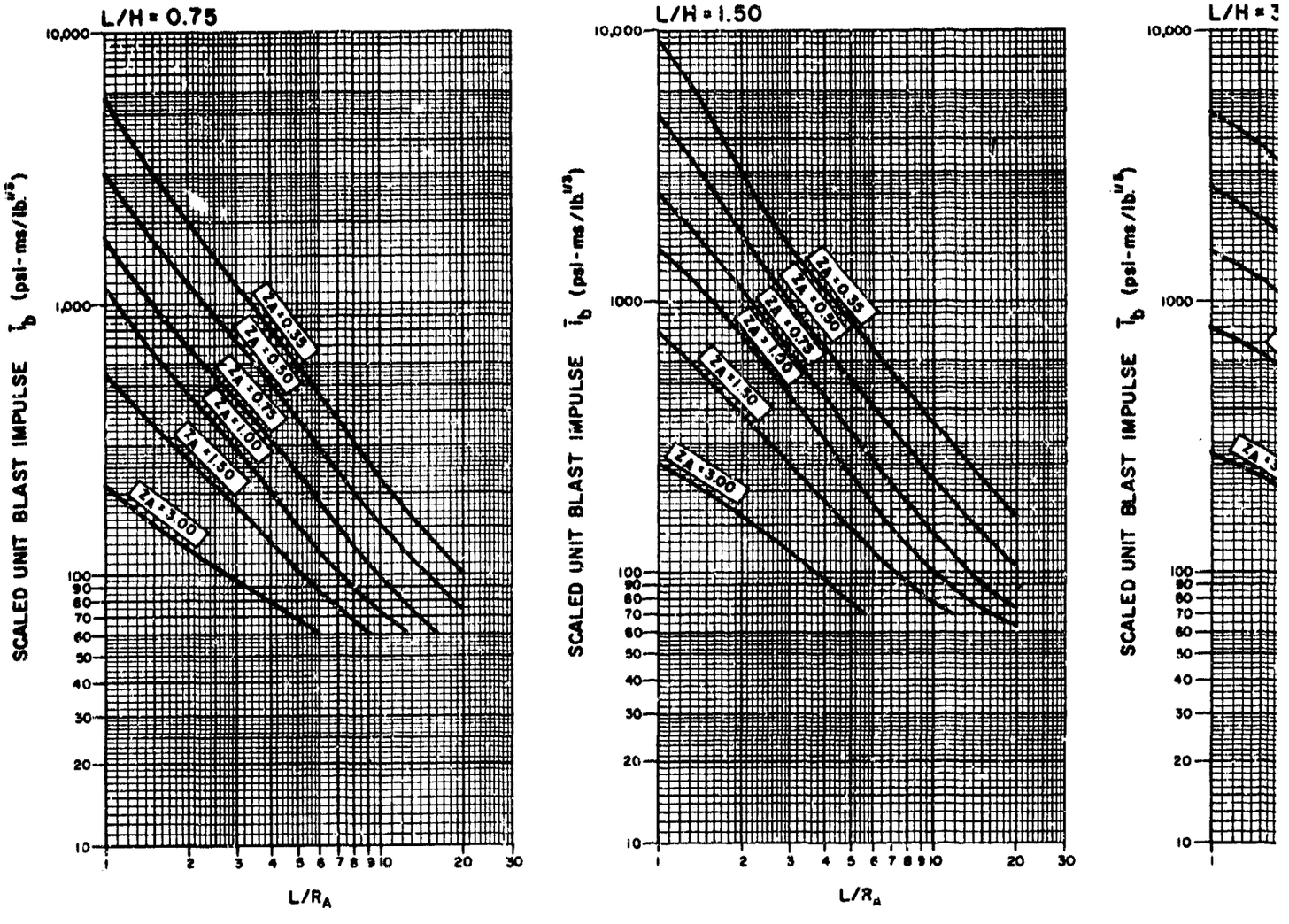
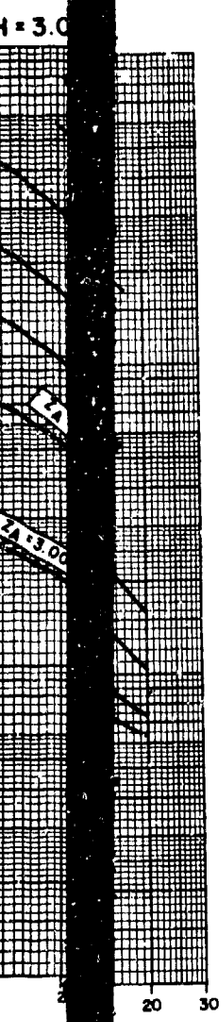
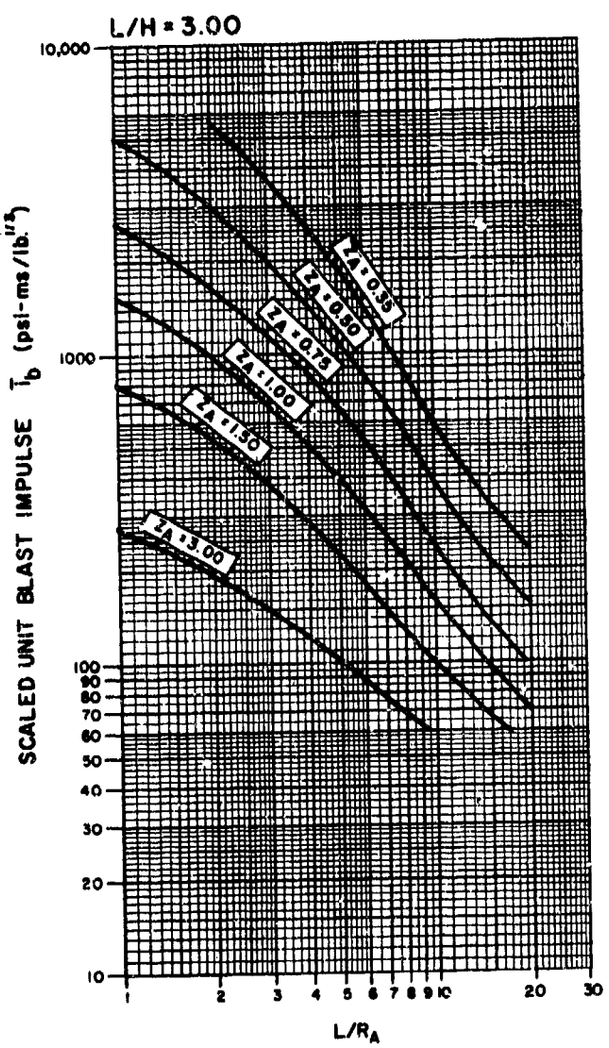
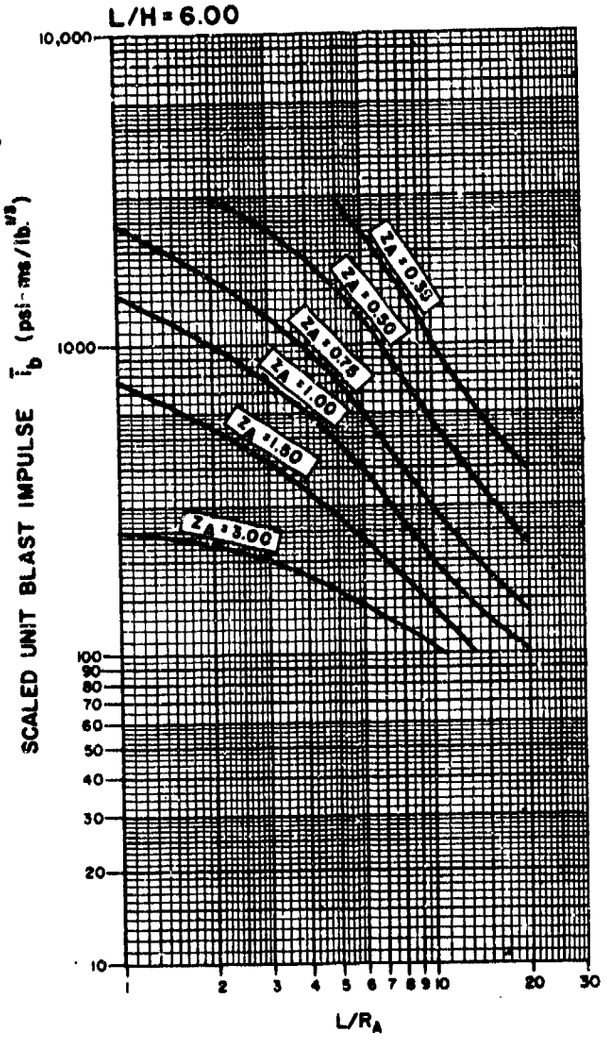


Figure 4-62. Scaled average unit blast impulse ($N = 4$, $l/L = 0.5$







=0.50, l/L=0.50, h/H=0.50) ...rage unit blast impulse (N=4, l/L=0.50, h/H=0.50).

b. Exterior or Leakage Pressure Loadings.

(1) For cubicle-type structures where full venting is provided through the frangible or open portion of the structure, the resulting blast wave exterior of the cubicle will be appreciably modified as compared to an unbarricaded detonation. As the blast wave propagates out from the center of the explosion, the shock front will collide with the interior surfaces of the structure. These collisions will reflect and reinforce the initial loads (pressures and impulse). Eventually these pressures will spill over, around, and, in the event of rapid collapse, through the structure to the surrounding area. The exterior pressures will not initially have a definite shock front but will, at some distance from the structure, shock-up with frontal pressures similar to those produced by a surface burst. The pressure-distance gradients away from the explosion will vary in all directions, this variation being defined by the con-

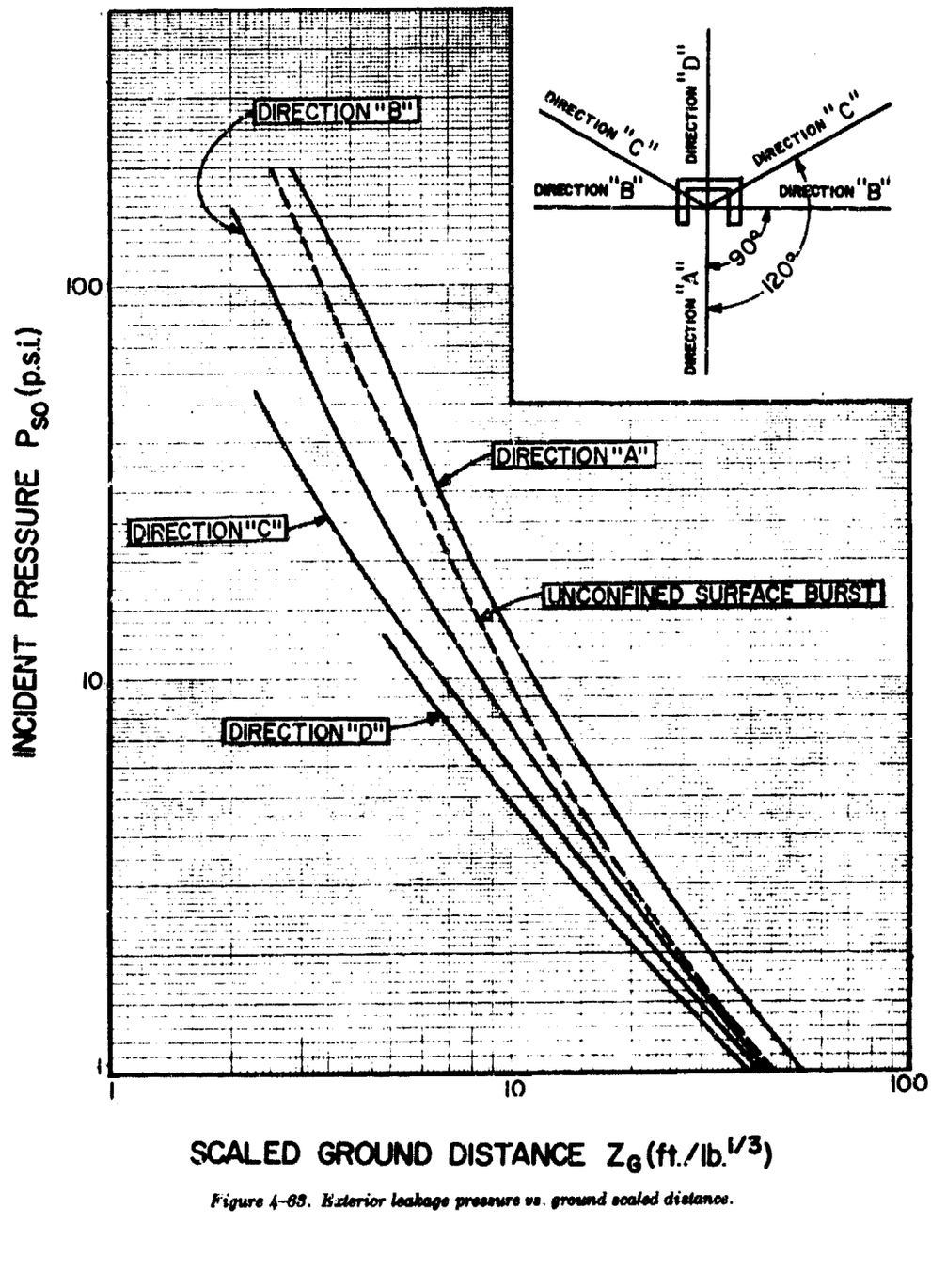


Figure 4-63. Exterior leakage pressure vs. ground scaled distance.

figuration (shape, openings, etc.) of the protective structure containing the explosion.

(2) A series of tests have been performed on cubicle-type reinforced concrete structures where the roof and one wall of each cubicle were open or frangible. Analysis of the test results indicated that the leakage pressures on the ground surface outside the structure vary in all directions for any particular scale distance.

(3) Figure 4-63 illustrates this variation as compared to an unconfined surface burst. Blast pressures propagating from the open end of the cubicle are higher than those resulting from the unconfined surface burst whereas all pressures exterior of the walls are equal to, or less than, the unconfined surface burst pressures. The relationship between the pressure-distance curves for confined explosions to that of the unconfined surface burst vary with the magnitude of the pressure. The difference between the curves is pronounced at a scale distance of 2 (limit of test data), although the curves for a confined explosion begin to merge with the unconfined surface burst curve at pressure levels of 1.0 psi and less. Except for the open end, the leakage pressures in all directions from a cubicle are equal to those of the unconfined surface burst for pressure levels below approximately 0.5 psi.

(4) The pressure-distance data of figure 4–63 is based upon those tests involving cubicle structures where the length (L) to height (H) ratio of the back walls was approximately equal to 1.0 while the charge weight to structure volume ratio varied between 0.2 and 2.0. The reflection (change in wave propagation direction) of the blast pressures off the back wall and focusing of these pressures by the side walls resulted in a shotgun effect which produced the larger pressures adjacent to the open end. On the other hand, pressures acting on the ground in other areas around the structure were reduced below those of an unconfined burst by the shielding afforded by the walls which focused the blast pressures upward resulting in an initial radial dispersion of the pressures at a higher altitude than would normally occur if the walls were not present. The degree of upward focusing is primarily a function of the height of the three walls and the distance between, and length of, the side walls.

(5) In another test series, a reinforced concrete cubicle structure with a back and two side walls was tested with donor charges as large as 5,000 pounds. The height of all walls and the length of the side walls were approximately the same as those of the test structures previously mentioned. However, the length to height ratio of the back wall of this cubicle was at least two times that of the structures of previous tests. Because of the increased width of this structure, the pressure-distance relationship of pressures acting on the ground surface in areas adjacent to the walls was significantly different from that indicated in figure 4–63, and was in the order of magnitude of the unconfined surface burst for scale distances equal to or larger than 10 (limit of test data). On the other hand, the pressures adjacent to the open end of the cubicle were the same as those previously indicated.

(6) The significance of the results of the later tests is that the primary factor affecting the pressure-distance relationship of the pressures adjacent to the open end of a cubicle is the presence of a back wall and not the relative dimensions of the structure, while the pressures in areas adjacent to the walls are affected by the structure geometry.

(7) It should be noted that the pressure-distance relationships discussed above are valid only for the structural arrangements and charge weights involved in the various tests. It is expected that for large charge weight to structure volume and large structure volume to charge weight ratios, the pressure-distance relationships in all directions from the structure will approach that for an unconfined surface explosion. An indication of this aspect may be seen from the results of mounded magazine tests, particularly for the test involving 100,000 pounds of TNT. Here, the peak ground pressures in all directions from the igloo were slightly less than the pressures produced by an unconfined explosion. In the case of the large structure volume to charge ratio, the cubicle walls simulate barricades located some distance from a confined explosion. Analysis of tests has indicated that, except in the immediate vicinity of the barricade, the pressures acting on the ground differ only slightly from those of the unconfined explosion.

(8) The blast wave parameters for the leakage pressure shock environment are obtained from figure 4–12 corresponding to the value of the peak incident pressure indicated in figure 4–63.

4–11. Partially Vented Explosions

a. Interior Blast Loadings.

(1) When the openings in a cubicle-type structure are small compared to the total surface area, full venting of a contained explosion will not occur. The effect of the reduction of the venting areas from a fully-vented configuration is an increase in the interior pressures, impulse, and duration. In addition to the initial shock wave and its reflections, the accumulation of gases from the explosion results in a pressure buildup, and since the venting area is limited, the duration of the pressure is prolonged.

(2) A typical pressure-time record at a point on the wall of a partially vented chamber is shown in figure 4–64. The high peaks are the multiple reflections of the initial shock wave. The mean pressure, denoted as p_m, has a long duration when compared to the duration of the shock wave pressures. The maximum mean pressure p_{m_s} is used as the basis for design and is a function of the charge weight, contained volume of the chamber, and venting area.

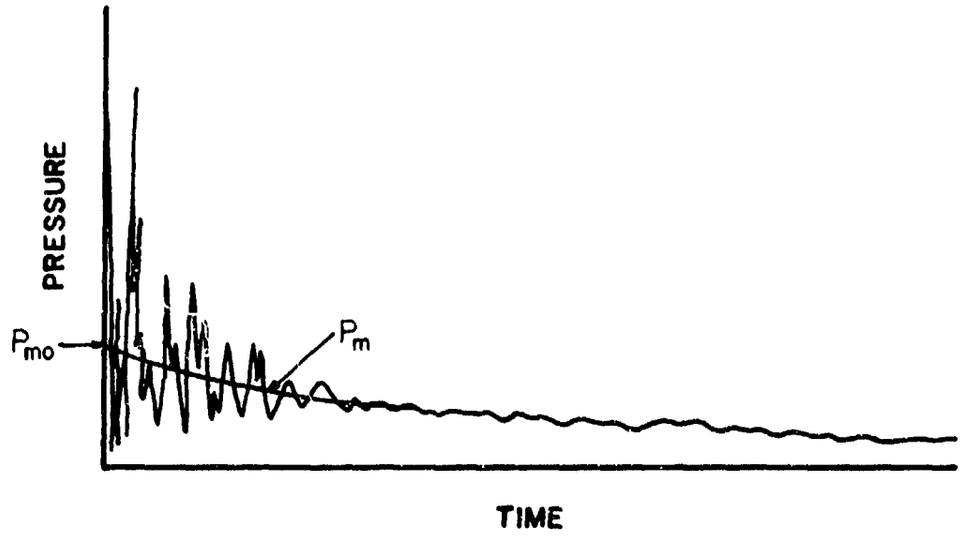


Figure 4–64. Pressure-time variation for a partially vented explosion.

(3) Figure 4–65 shows an experimentally fitted curve based upon test results of partially vented chambers with small venting areas. The maximum mean pressure is plotted against the charge-volume ratio. The sizes of the venting areas used in the individual tests were relatively small compared to the volume of the chambers and the quantities of explosive, and had no noticeable influence on the maximum pressures recorded.

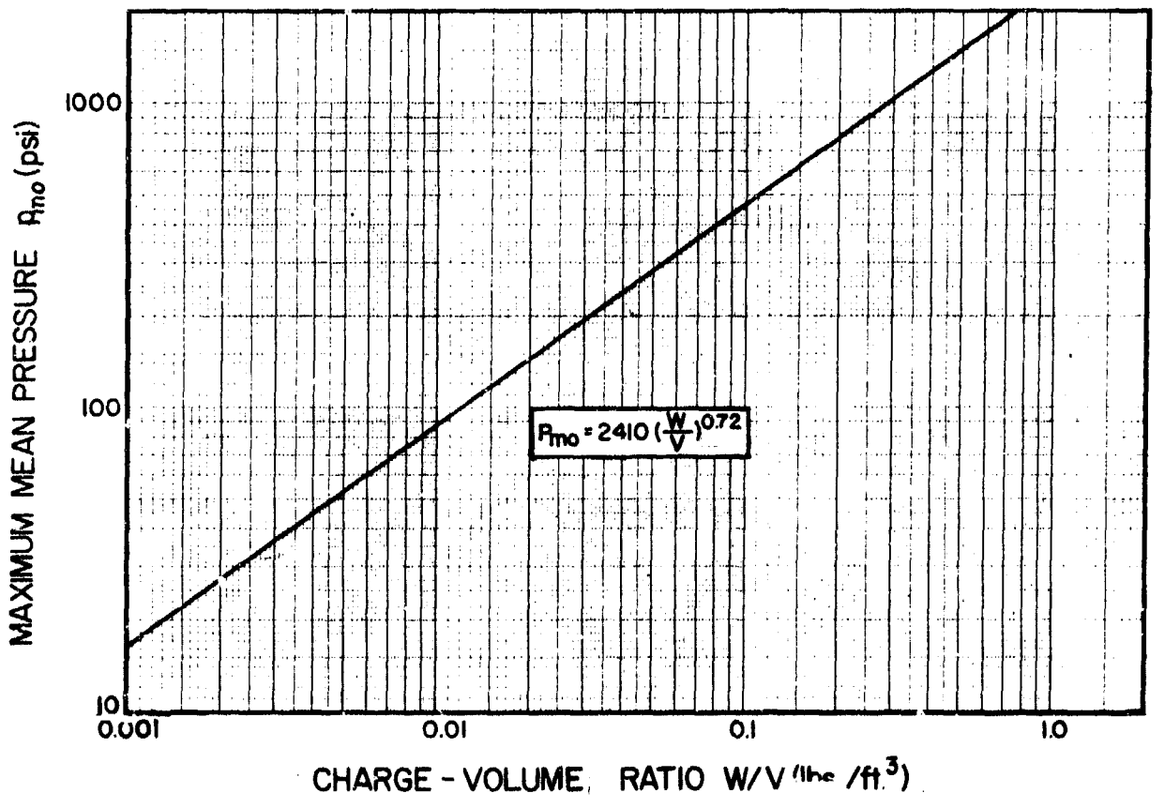


Figure 4–65. Maximum mean pressure in a partially vented chan

(4) Since no data is available concerning the duration of these pressures, it is suggested that for purposes of design, the pressures be assumed to have a very long duration and a constant magnitude insofar as the response of the structure is concerned. The total impulse used in the design of such a cubicle is a combination of the contributions from the initial shock wave, its reflections, and the pressures caused by the gas accumulations. Because of the long duration aspect of the gas accumulation pressures, the strength of the individual elements of the structure must be equal to, or greater than, the pressure p_{mo}, whereas the response of the elements to the initial blast wave and its reflections will be similar to the response of cubicles where full venting is achieved.

b. Exterior or Leakage Pressure Loadings. No data is currently available for the determination of leakage pressures from a partially vented explosion.

Section V. EXTERNAL BLAST LOADS ON STRUCTURES

4–12. General

a. The blast loading on a structure caused by a high-explosive detonation is dependent upon several factors: (1) the magnitude of the explosion, (2) location of the detonation relative to the ground surface and to the structure in question, (3) the geometrical configuration of the structure, and (4) the structure orientation with respect to the explosion and the ground surface (above, flush with, or below the ground).

b. The procedures presented here for the determination of the external blast loads on structures are restricted to rectangular structures and to structures located with respect to the detonation so that the shock front is normal to the ground surface (plane wave).

4–13. Forces Acting on Structures

a. The forces acting on a structure associated with a plane shock wave are dependent upon both the peak values and the pressure-time variation of the incident and dynamic pressures acting in the free-field. The peak values of the free-field incident pressures for the several blast loading categories were treated previously.

b. For each pressure range there is a particle or wind velocity associated with the blast wave that causes a dynamic pressure on objects in the path of the wave. In the free field, these dynamic pressures are essentially functions of the air density and particle velocity. For typical conditions, standard relationships have been established between the peak incident pressure P_{so} and the peak dynamic pressure q_o. The magnitude of the peak dynamic pressure is solely a function of the peak incident pressure, and therefore, independent of the size of the explosion. Figure 4–66 gives the values of the peak dynamic pressure versus peak incident pressure.

c. For design purposes, it is necessary to establish the variation or decay of both the incident and dynamic pressures with time since the effects on a structure subjected to a blast loading depend upon the intensity-time history of the loading as well as on the peak intensity. The idealized form of the incident blast wave (fig. 4–2) is characterized by an abrupt rise in pressure to a peak value, a period of decay to ambient pressure, and a period in which the pressure drops below ambient (negative pressure phase).

d. The rate of decay of the incident and dynamic pressures, after the passage of the shock front, is a function of the peak pressure and the size of the detonation. For design purposes, the actual decay of the incident pressure may be approximated by the use of an equivalent triangular pressure-time pulse. The actual duration of the positive pressure phase is replaced by a fictitious positive duration which is expressed as a function of the total positive impulse and the peak pressure:

$$t_{of} = \frac{2i}{P} \qquad \text{Equation 4–3}$$

The above relationship for the equivalent triangular pulse is applicable to the incident pressures as well as the reflected blast pressures; however, in the case of the latter, the value of the impulse used with equation 4–3 is equivalent to that associated with the reflected wave. The fictitious duration of the dynamic pressures may be assumed to be equal to that of the incident pressures.

e. For determining the pressure-time data for the negative phase, a similar procedure as used in the evaluation of the positive phase may be utilized. The equivalent negative pressure-time curve will have a time of rise equal to 0.125 t_o^- whereas the fictitious duration t_{of}^- is given by the triangular equivalent pulse equation.

$$t_{of}^- = \frac{2i^-}{P^-} \qquad \text{Equation 4–4}$$

where i^- and P^- are the total impulse and peak pressure of the negative phase and t_o^- is the actual negative phase duration.

4–14. Above-Ground Rectangular Structures

a. General.

(1) For any given set of free-field incident and dynamic pressure pulses, the forces imparted to an above-ground structure can be divided into three general components: (*a*) the force resulting from the inci-

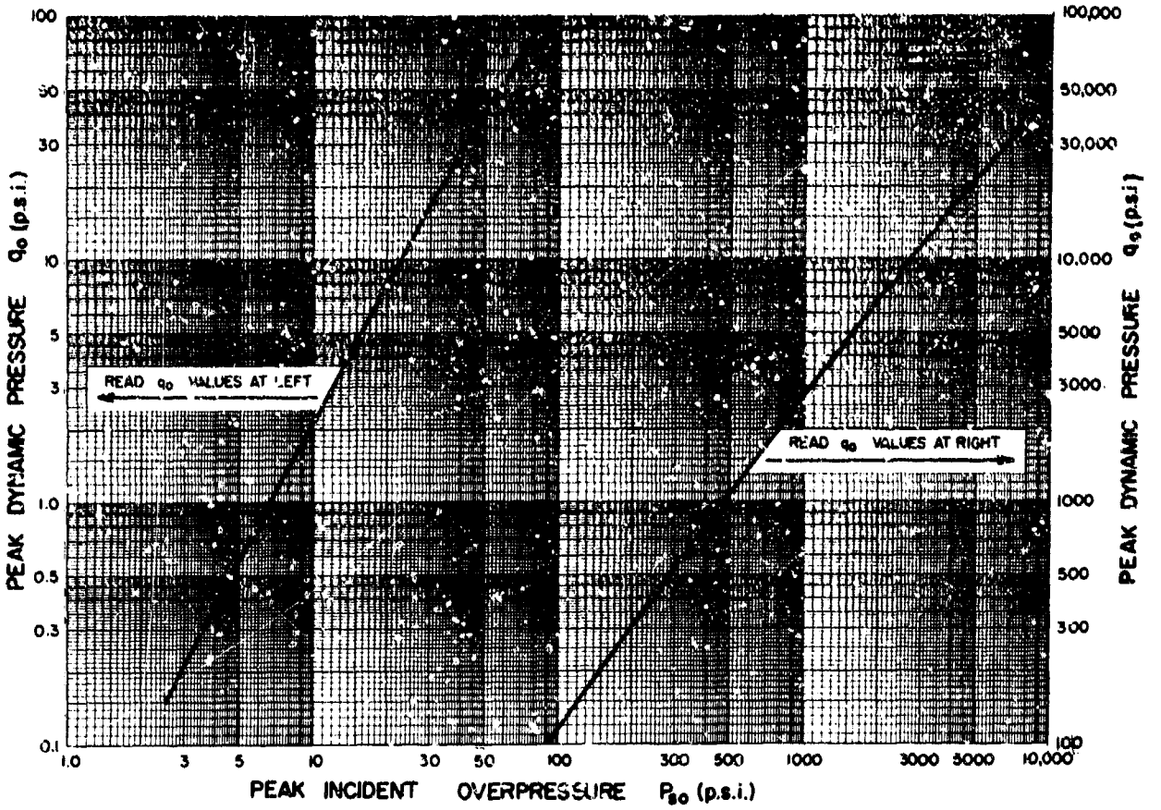


Figure 4–66. Peak incident pressure vs. peak dynamic pressure.

dent pressure, (*b*) the force resulting from the dynamic pressure, and (*c*) the reflected pressure resulting from the shock impinging upon an interfering surface. The relative significance of each of these components is dependent upon the geometrical configuration and size of the structure and the orientation of the structure relative to the shock wave.

(2) The interaction of the incident blast wave with an object is a complicated process. To reduce the complex problem of blast to reasonable terms, it will be assumed here that: (*a*) the structure is generally rectangular in shape, (*b*) the incident pressure of interest is in the order of 200 psi or less, and (*c*) the object being loaded is in the region of the Mach reflection.

b. Front Wall.

(1) For a rectangular above-ground structure at low pressure ranges, the variation of pressure with time on the side facing the detonation is illustrated in a, figure 4–67. At the moment the incident shock front strikes the wall, the pressure is immediately raised from zero to the reflected pressure P_r, which is a function of the incident pressure and the angle of incidence between the shock front and the structure face (fig. 4–6). The clearing time t_c required to relieve the reflected pressures is represented as

$$t_c = \frac{3S}{U} \qquad \textbf{Equation 4–5}$$

where U is the velocity of the shock front and S is equal to the height of the structure H_s or one-half its width W_s, whichever is smaller. The pressure P acting on the front wall after time t_c is the algebraic sum of the incident pressure P_s and the drag pressure $C_D q$.

$$P = P_s + C_D q \qquad \textbf{Equation 4–6}$$

The drag coefficient C_D gives the relationship between the dynamic pressure and the total translational pressure in the direction of the wind produced by the dynamic pressure and varies with the Mach number (or with the Reynold's number at low incident pressures) and the relative geometry of the structure. A value of $C_D = 1$ for the front wall is considered adequate for the pressure ranges considered in this manual.

(2) At higher pressure ranges, the above procedure may yield a fictitious pressure-time curve because of the extremely short pressure pulse durations involved.

Therefore,
be checked
is made by
as indicate
pressure i
depending
duration t_r

$$t_r = \frac{2i_r}{P_r}$$

where P_r is

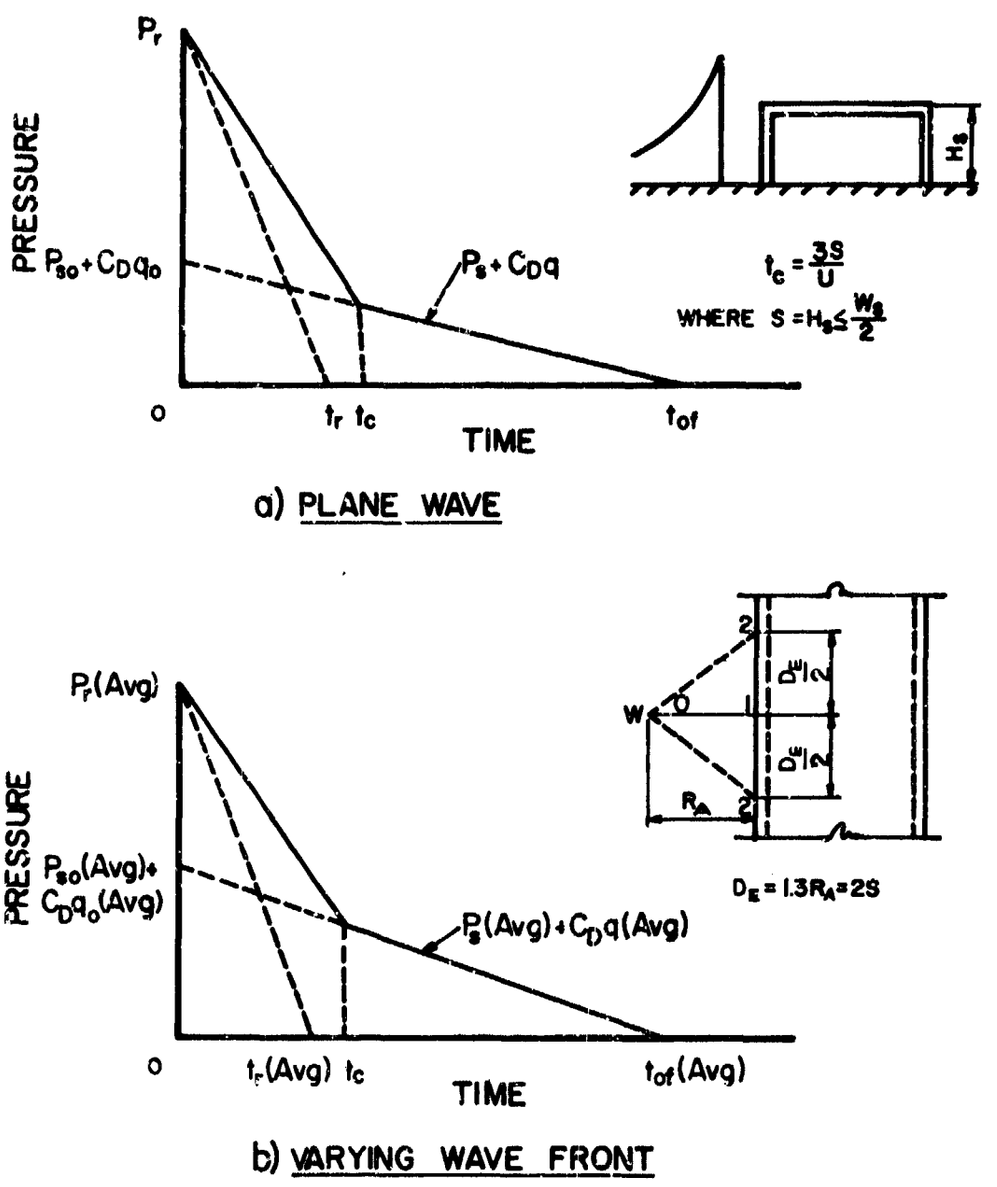


Figure 4-67. Front wall loading.

Therefore, the pressure-time curve construction must be checked to determine its accuracy. The comparison is made by constructing a second curve (dotted triangle as indicated in a, figure 4-67), using the total reflected pressure impulse i_r from either figure 4-5 or 4-12, depending upon the shock environment. The fictitious duration t_r of the reflected wave is calculated from

$$t_r=\frac{2i_r}{P_r} \qquad \textbf{Equation 4-7}$$

where P_r is the peak reflected pressure previously used. Whichever curve gives the smallest value of the impulse (area under curve), use that curve in calculating the wall loading. The reflected pressure impulse includes the effects of both the incident and dynamic pressures.

(3) The pressure-time curve (a, fig. 47) assumes that the shock front of the blast wave is essentially parallel to the front surface of the structure (plane wave shock front). In those cases where the detonation is located relatively close to the structure, the pressure and impulse patterns acting across the wall surface will vary. In these cases an average pressure-time curve

(b, fig. 4–67) may be constructed using average values of the loading acting over a length D_E of the structure where D_E is equal to $1.3R_A$ (R_A is the normal distance between the detonation and the front surface of the structure) but not greater than $2S$. In this solution both the pressures and the duration are average values of the loading acting on the wall between points 1 and 2.

(4) As in the case of the plane wave front, the calculations for the average loading on the front wall subjected to a varying shock wave front must consider the effect of extremely short pressure pulses. Here the values of P_r and t_r are taken as average values of the loading acting between points 1 and 2.

(5) In both the plane wave and varying wave front solutions, the height of the triple point (fig. 4–9) of the shock wave in an air burst shock environment is assumed to be above the top of the wall.

c. Roof and Side Walls.

(1) As the shock front traverses a structure, a pressure is imparted to the roof slab and side walls equal to the incident pressure at a given time at any specified point reduced by a negative drag pressure. The portion of the surface loaded at a particular time is dependent upon the location of the shock front and the wave lengths (L_w and L_w^-) of the positive and negative pulses.

(2) To determine accurately the overall loading on a surface where the span direction is perpendicular to the shock front, a step-by-step analysis of the wave propagation should be made. This analysis would include a simultaneous dynamic analysis of the stresses produced in the element at any given time. To simplify this procedure, an approximate method of calculating the pressure-time history has been developed where the actual loading on the surface has been replaced by an equivalent uniform loading, which will produce stresses in the element similar to those produced by the actual loading as the blast wave crosses the surface. For this analysis to be valid, it is assumed that the reinforcement on both faces is continuous across the span length.

(3) The peak value of the incident pressure decays and the wave length increases as the shock wave traverses the roof. As illustrated in a, figure 4–68. the maximum stress in the member occurs when the shock front is at point d although the point of maximum stress is located elsewhere. The equivalent uniform loading versus time is shown in b, figure 4–68 and, to simplify the calculations, has been taken as a function of the blast wave parameters at point b, the back end of the element being considered. The equivalent load factor C_E and the blast wave location ratio $\frac{D}{L}$ are obtained from figure 4–66 as a function of the wave length-span ratio $\frac{L_{wb}}{L}$. The pressure builds up linearly from the time t_f when the blast wave reaches the beginning of the element (point f) to time t_d when the blast wave reaches point d. The peak value P_e of the pressure is the sum of the contributions of the equivalent incident and drag pressures.

$$P_e = C_E P_{sob} + C_D q_{ob} \qquad \textbf{Equation 4–8}$$

where P_{sob} is the peak overpressure occurring at point b and q_{ob} corresponds to the value of $C_E P_{sob}$. Following the peak, the pressure decays linearly to zero at time $t_b + t_{of}$ where t_b is the time at which the blast wave reaches the end of the element (point b) and t_{of} is the fictitious duration of the positive phase. The negative phase of the equivalent uniform loading, if required, may conservatively be taken as that occurring at point b.

(4) The drag coefficient C_D for the roof and side walls is a function of the peak dynamic pressure. Recommended values are as follows:

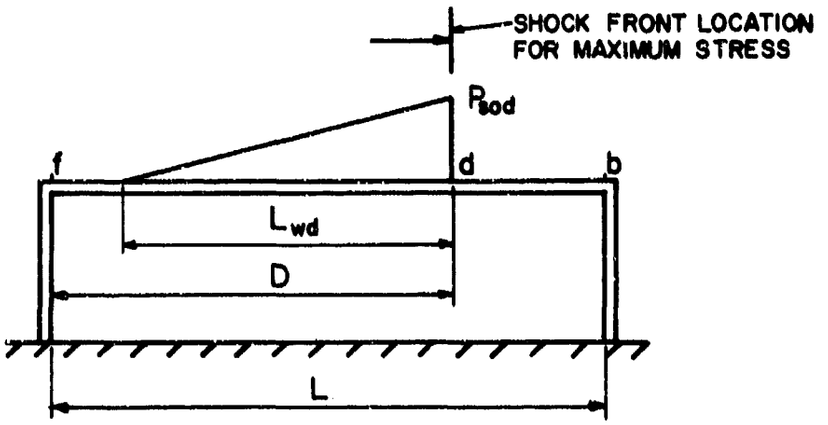
Peak dynamic pressure	*Drag coefficient*
0–25 psi	−0.40
25–50 psi	−0.30
50–130 psi	−0.20

(5) If the span direction of the member is parallel to the shock front, the pressure-time curve shown in figure 4–70 should be used where L is the width of the strip or element being considered.

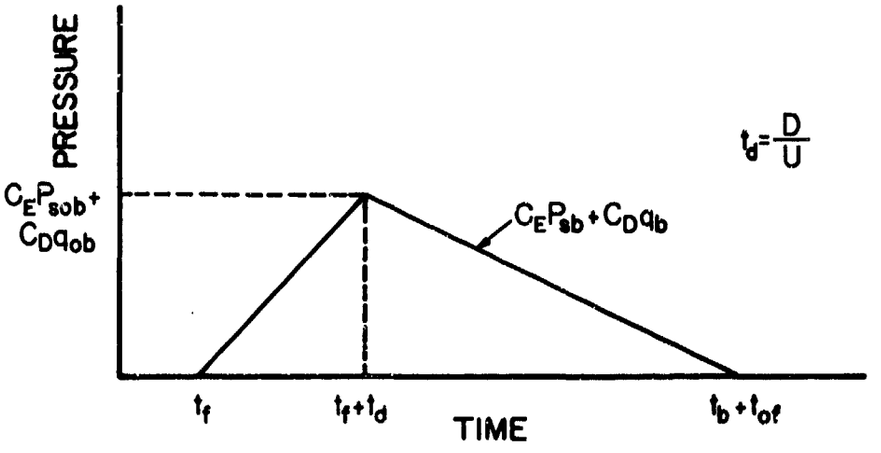
d. Rear Wall.

(1) As the shock front moves past the rear edges of the roof and/or side walls, the pressure front will expand forming secondary waves which propagate over the rear wall. In the case of long buildings, this secondary wave enveloping the back wall essentially results from the spillover from the roof, while in short buildings the wall loads arise from the interaction of the spillover both from the roof and the side walls. In both cases, the secondary waves are reinforced due to their impingement with reflecting surfaces. The reinforcement of the spillover wave from the roof is produced by its reflection from the ground surface at the base of the rear wall, whereas the reinforcement of the secondary waves from the side walls is produced by their collision near the center of the wall and/or their interaction with the wave from the roof. Little information is presently available on the overall effects on the rear wall loading produced by the reflections of the secondary waves.

(2) In most design cases, the primary reason for determining the blast loads acting on the rear wall is to determine the overall drag effects (both front and rear wall loadings) on the building. For this purpose,



a) SECTION THROUGH STRUCTURE



b) AVERAGE PRESSURE – TIME VARIATION

Figure 4–68. Roof and side wall loading (span direction perpendicular to shock front).

a procedure may be used where the blast loading on the wall is calculated using the equivalent uniform method utilized for computing the blast loads on the roof and side walls. Here the peak pressure of the pressure-time curve (b, fig. 4–71) is calculated using the peak pressure that would occur at distance H, (point e on a, fig. 4–71) past the rear edge of the roof slab. The equivalent load factor C_E is based on the wave length of the peak pressure above and the unsupported length of the rear wall as are the time of rise and duration.

(3) Like the roof and side walls, the blast loads acting on the rear wall are a function of the drag pressures in addition to the incident pressures. The dynamic pressure of the drag corresponds to that associated with the equivalent pressure, while the recommended drag coefficients are the same as used for the roof and side walls.

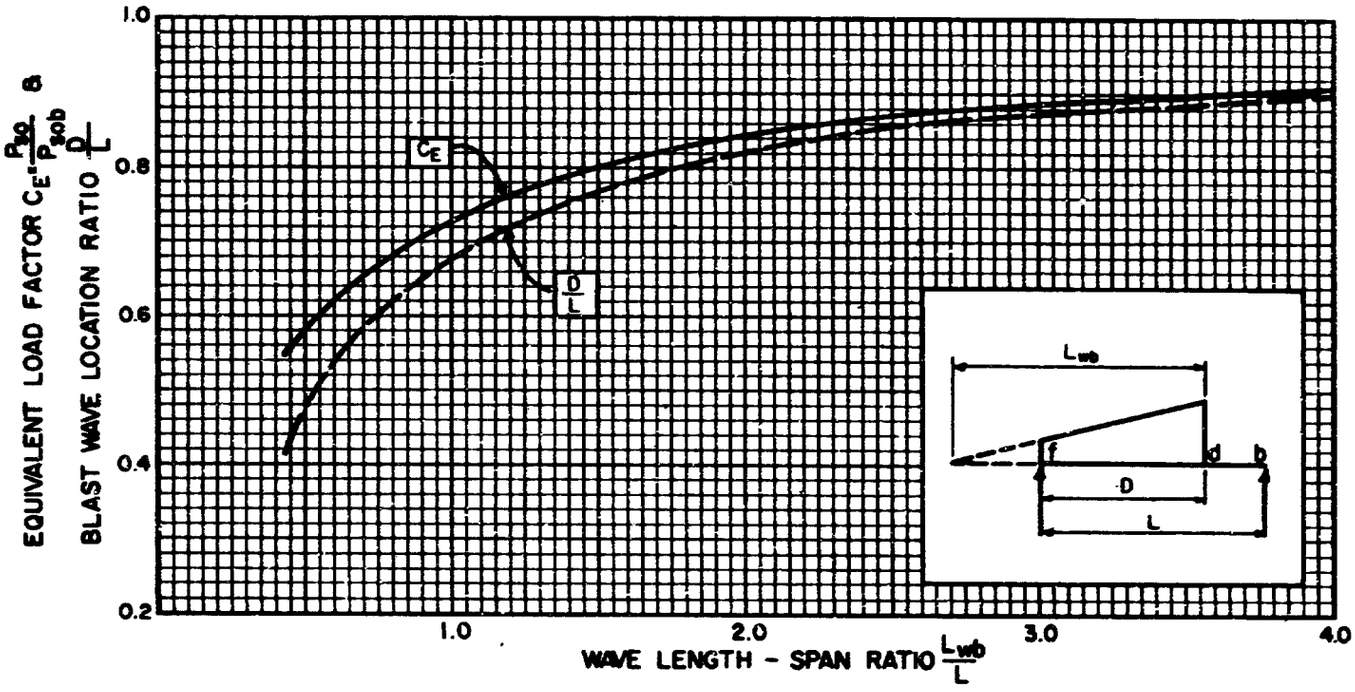


Figure 4-69. Equivalent load factor and blast wave location ratio vs. wave length-span ratio.

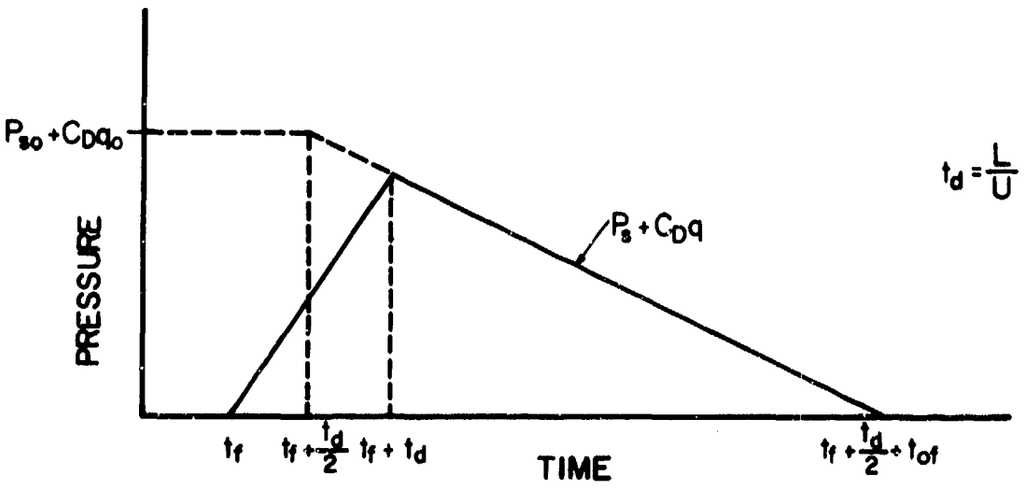
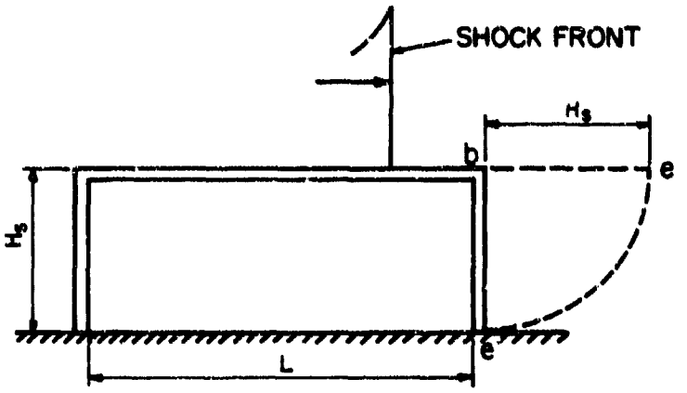
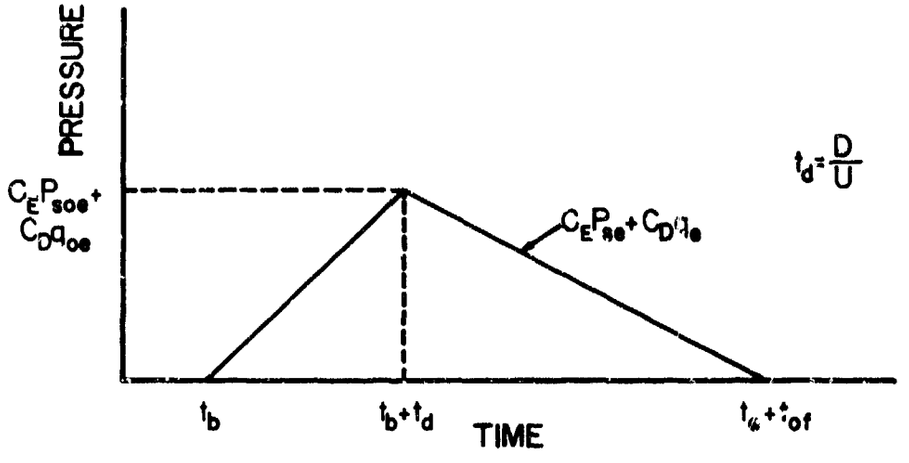


Figure 4-70. Roof and side wall loading (span direction parallel to shock front).



a) SECTION THROUGH STRUCTURE



b) AVERAGE PRESSURE – TIME VARIATION

Figure 4-71. Rear wall loading.

4-15. Ge

When a str
leakage of t
structure oc

LEAKAGE PRESSURE COEFFICIENT C_l ($\frac{psi-ft.}{}$)

Section VI. PRESSURE INCREASE WITHIN A STRUCTURE

4–15. General

When a structure is enveloped in a blast wave, a leakage of the pressures through any openings in the structure occurs. The interior of the structure experiences an increase in its ambient pressure in a time that is a function of the structure volume, area of openings, and applied exterior pressure and duration. Since personnel exhibit a tolerance limit to such pressure increases, a method of determining the average pressure

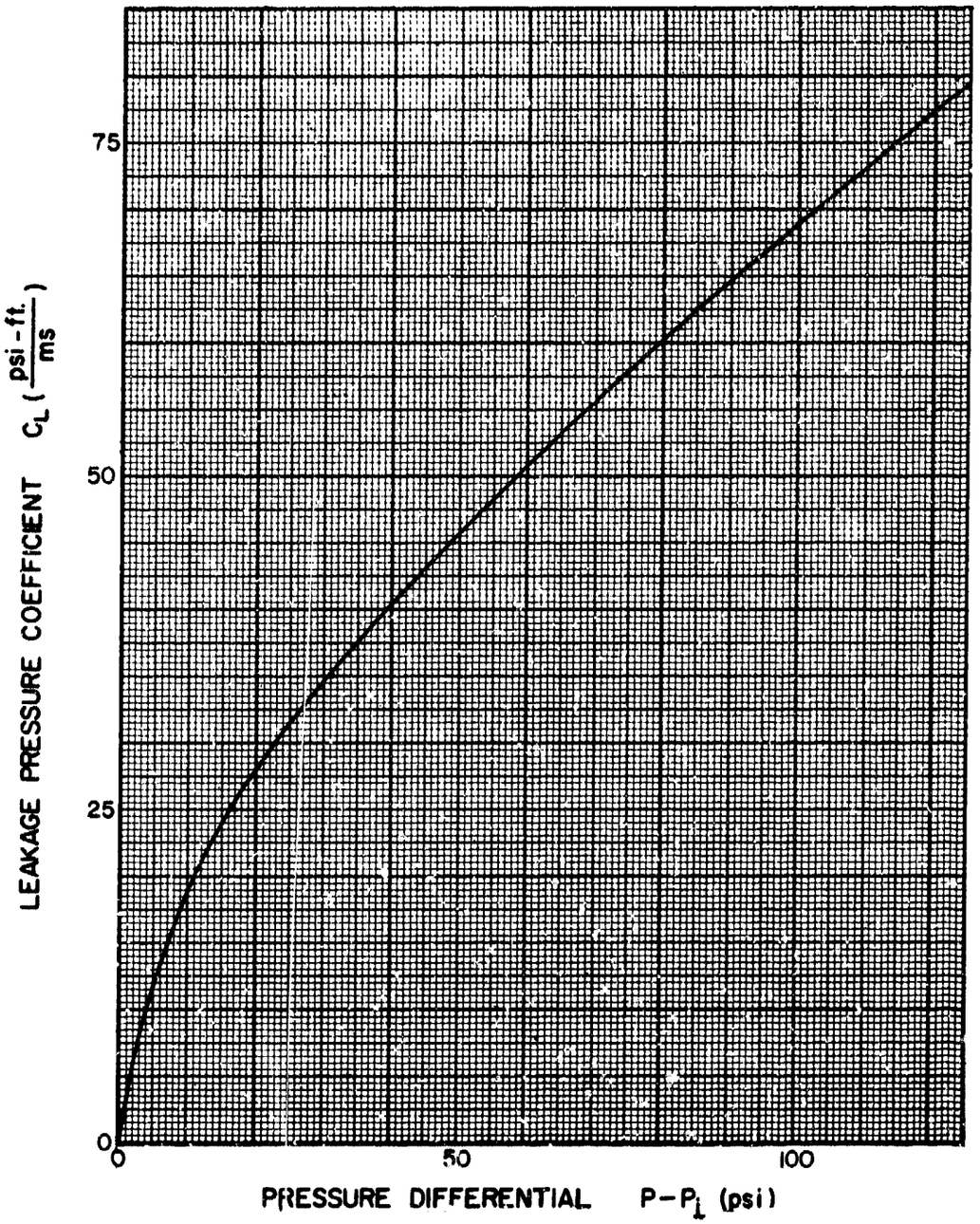


Figure 4–72. Leakage pressure coefficient vs. pressure differential.

inside the structure is needed. It should be noted that the interior pressures immediately adjacent to the openings will be higher than the average pressure.

4–16. Method of Calculation

a. The following treatment is applicable for structures with small area-volume ratios and applied blast pressures of less than 150 psi.

b. The change in pressure ΔP_i inside the structure within a time interval Δt is a function of the pressure difference at the openings $P-P_i$ and the area-volume ratio $\frac{A_o}{V_o}$:

$$\Delta P_i = C_L\left(\frac{A_o}{V_o}\right)\Delta t \qquad \text{Equation 4–9}$$

where C_L is the leakage pressure coefficient and a function of the pressure difference $P-P_i$
and P = applied pressure to the exterior of the structure
P_i = interior pressure
ΔP_i = interior pressure increment
A_o = area of openings
V_o = volume of structure
Δt = time increment
Figure 4–72 shows the variation of C_L versus $P-P_i$.

c. The interior pressure-time curve is calculated as follows:

(1) Determine the pressure-time history of the applied blast pressures P acting on the surface surrounding the opening as presented in section V of this chapter.

(2) Divide the duration t_o of the applied pressure into n equal intervals (Δt), each interval being approximately $\frac{t_o}{10}$ to $\frac{t_o}{20}$, and determine the pressures at the end of each interval.

(3) For each time interval, compute the pressure differential $P-P_i$, determine the corresponding value of C_L from figure 4–72, and calculate ΔP_i from equation 4–7 using the proper values of $\frac{A_o}{V_o}$ and Δt. Add ΔP_i to P_i for the interval being considered to obtain the new value of P_i for the next interval.

(4) Repeat for each interval using the proper values of P and P_i. Note that when $P-P_i$ becomes negative during the analysis, the value of C_L must be taken as negative also.

The above procedure is most easily accomplished by using a tabular arrangement for the computations, an illustrative example of which is presented in appendix 4A.

Section VII. MULTIPLE EXPLOSIONS

4–17. General

a. When two or more explosions of similar material occur several milliseconds apart, the blast wave of the initial explosion will propagate ahead of the waves resulting from the subsequent explosions, with the phasing of the propagation of these latter waves being governed by the initiation time and orientation of the individual explosives. If the time delay between explosions is not too large, the blast waves produced by the subsequent explosions will eventually overtake and merge with that of the initial detonation. The distance from the explosion at which this merger occurs will depend on: (1) the magnitude of the individual explosions, (2) the time delays between the initiation of explosions, (3) the separation distances between and orientation of the explosives, and (4) obstructions between the explosives themselves and other obstructions between the explosives and other parts of the facility (buildings, walls, barricades, terrain, etc.) which will distort, hinder, and generally interfere with wave propagation.

b. The pressure-time relationships associated with the wave propagation will depend upon the interaction of the individual waves themselves. After all the waves have merged, the pressures associated with the common or merged wave will have a pressure-time relationship which is similar to that produced by a single explosion (fig. 4–8). However, at closer distances to the explosion, the pressure-time relationship will be more closely represented by a pressure-time curve with multiple peak pressures (similar to that occurring above the triple point (fig. 4–8)). The multiple peak pressures represent the interaction as the various waves reach the point in question. At distances even closer to the explosion, the time history of the pressures acting on the ground surface may consist of a series of completely separate blast loads. This loading condition is a result of the arrival of the subsequent blast waves at a particular point during or after the occurrence of the negative phase pressures produced by the initial wave at that point.

c. The latter pressure-time relationship is probably most likely to occur at the high-pressure range while the multiple peak pressure pulse is normally associated with the intermediate-pressure range. However, in many instances, the multiple peak pressure pulse will occur at high pressures, in particular where the individual explosives are positioned close together, e.g.,

in a cubicle or other storage facilities. The pressure pulse associated with the merged shock wave is usually common to the low-pressure range but in some instances may occur at the lower pressure levels of the intermediate-pressure range.

4–18. High-Pressure Range

a. Partially Confined—Fully Vented Explosions.

(1) The blast pressures and impulse loads, acting on various elements of cubicle or other similar structures, which are produced by multiple explosions, will usually differ from those produced by a single explosion of the same amount of explosives.

(2) Although the magnitude of the total combined impulse produced by the multiple explosions will usually be larger than that produced by the single explosion, the damage to a protective element due to the impulse of the multiple detonation may be either greater, equal to, or less than that produced by the impulse of the single explosion. For a given total impulse, the degree of damage to a protective element will be defined by the duration of the entire load relative to the response time of the element (time to reach maximum deflection).

(3) A minimum amount of theoretical and experimental data is available concerning the degree of damage sustained by structural elements due to multiple explosions. However, results of response tests of reinforced concrete slabs have indicated that if the total combined duration of the blast loads produced by simultaneously or near simultaneously exploded charges is equal to or less than one-third the response time (time to reach maximum deflection) of the element, then the total combined impulse acting on the element can be estimated by numerically adding the impulse loads produced by the individual explosions. However, if the total combined duration of the blast loads is greater than one-third the response time, the actual pressure-time relationship of the combined loads approximated by a fictitious peaked triangular pressure pulse (similar to that of a single explosion) should be considered. The blast loads produced by charges that are not simultaneously or near simultaneously exploded may be considered as two or more impulse loads, two or more pressure-time loads, or a combination of impulse and pressure-time loads depending on the time delay and the duration of the individual loads compared to the response time of the element. A load or group of loads should be treated as an impulse load if the duration (one load or the combined duration of two or more loads) of the loading is less than one-third the time interval between the onset of the load or group of loads and the response time of the member.

(4) The duration of the blast loads due to multiple explosions may be approximated by considering the interrelationship between (*a*) the time intervals between individual explosions, (*b*) arrival times of the blast waves of the individual explosions at the element in question, (*c*) time required for the blast waves to fully engulf the element, and (*d*) the load duration at points on the element furthest from the individual explosions which should be increased by 50 percent in the calculations to account for the occurrence of multiple reflections of the blast pressures. Because of the many variables involved, a relationship cannot be given to obtain the duration of the blast loads due to multiple explosions. Each situation will require a series of computations involving the time increments outlined above.

b. Partially Confined—Partially Vented Explosions. The initial portion of the interior blast loads produced by multiple explosions in a partially vented chamber may be estimated by assuming their magnitude to be equal to those produced by similar explosions in fully vented structures. In addition to the initial blast wave and its reflections, the pressures produced by the release of the gaseous products of the multi-explosions is required to fully define the blast pressure environment within the chamber. An approximation of the value of the maximum mean pressure p_{mo} may be obtained by averaging upper and lower limits of the gas-pressure buildup. An upper limit of p_{mo} is obtained by considering the individual explosives as being detonated separately, and numerically summing the individual values of p_{mo} produced by the separate explosions. The lower limit of p_{mo} is determined by considering the explosion to be produced by a single explosive whose weight is equal to the combined weights of the individual charges. The values of p_{mo} for both the individual and combined charges are obtained from figure 4–64.

4–19. Intermediate- and Low-Pressure Ranges

a. As previously mentioned, the blast loads, produced by multiple explosions, acting on structures located at the intermediate-pressure range may consist of a series of separate pressure pulses rather than a single pulse blast load. However, the multiple pressure-pulse loading is usually associated with weights of explosives which are very small (several pounds) and, therefore, will not be the usual design situation. For large charge weights, however, the single pressure pulse loading with multiple peak pressures will occur. At the present time no specific method has been devised which will enable one to evaluate this type of blast loading. In the interim, it is suggested that the multiple peak pressure type loading be replaced by the pressure-pulse which is associated with the merged shock wave. The parameters of this shock wave and corresponding pressures are determined assuming a single explosion, the explosive weight of which is equal to the combined weight of the individual charges.

b. Because the individual blast waves produced by multiple explosions will merge either at the low-pressure levels of the intermediate-pressure range or at the low-pressure range, the determination of the blast loads on protective structures will be similar to that described above—a single explosion is considered.

Section VIII. PRIMARY FRAGMENTS

4–20. General

a. The explosion of a cased donor charge results in the formation of primary fragments which are produced by the shattering of the explosive container. The container may be the casing of conventional munitions, the kettles, hoppers, and other metal containers used in the manufacture of explosives, metal housing of rocket engines, etc.

b. Primary fragments are characterized by very high initial velocities (in the order of thousands of feet per second), a large number of fragments, and relatively small sizes in comparison to concrete fragments formed due to partial failure or total collapse of protective elements. The initial velocity and size of the fragments is a function of the thickness of the metal container, the shape of the explosive as a whole (spherical, cylindrical, prismatic) and the sections of the container (ends, middle, etc.) from which the fragments are formed.

c. When an explosion is located close to an object (acceptor explosive, barrier, etc.), the velocity v_s at which a fragment strikes the object is approximately equal to the initial velocity v_o. However, if the detonation is located at a relatively large distance from the object, then the impact or striking velocity of the fragment may be substantially less than its velocity immediately after the explosion. This variation in velocities, which is primarily a result of air resistance, is also a function of the physical properties of the casing and the distance between the donor explosive and object.

4–21. Initial Fragment Velocities (Explosives with Cyclindrical Containers)

a. Although only a minimum amount of work has been performed to date pertaining to the determination of initial velocities of large fragments, some work has been accomplished which permits the evaluation of the initial velocities of relatively small fragments (several ounces). A relationship has been developed for a charge which consists of an evenly distributed explosive in a cylindrical metal case of uniform thickness. The initial velocity v_o (ft/sec) is described in terms of the type of explosive, the amount of explosive W (lbs), and the weight of the cylindrical portion of the metal casing W_c (lbs) as follows:

$$v_o = (2E')^{1/2}\left[\frac{W/W_c}{1+W/2W_c}\right]^{1/2} \qquad \text{Equation 4–10}$$

where $(2E')^{1/2}$ is the Gurney Energy Constant which was developed from empirical data for various explosive materials contained in mild steel casings. Values of the Gurney Energy Constant for several different explosives are listed in table 4–3.

b. Figure 4–73 shows the variation of $v_o/(2E')^{1/2}$ versus the charge weight W for various container weights W_c. A maximum initial fragment velocity is obtained when the ratio of the container weight to the explosive weight (W_c/W) approaches zero. Therefore, the maximum initial velocity of primary fragments depends solely upon the Gurney Energy Constant and is given by:

$$v_o = 1.414(2E')^{1/2} \qquad \text{Equation 4–11}$$

4–22. Number and Weight of Fragments (Explosives with Cyclindrical Containers)

a. The explosion of a cased charge will produce a comparatively large number of primary fragments with varying weights. However, only the larger fragments are usually of concern in the design of a protective system since they may have the momentum necessary to perforate a barrier and/or cause propagation of explosions.

b. The fragmentation pattern and the weight of the largest fragment, resulting from the high-order detonation of an evenly distributed explosive in a cylindrical metal case of uniform thickness, were calculated according to relationships developed on the basis of theoretical considerations and confirmed with a large number of tests. The number of fragments produced is given by:

$$\ln N_f = \ln\left[\frac{8W_c}{M_A^2}\right] - \frac{W_f^{1/2}}{M_A} \qquad \text{Equation 4–12}$$

where N_f = the number of fragments larger than W_f
W_f = weight of primary fragment
W_c = total weight of the cylindrical portion of the metal casing
and the fragment distribution parameter M_A is defined by the equation

$$M_A = Bt_c^{5/6}d_i^{1/3}\left[1+\frac{t_{av}}{d_i}\right] \qquad \text{Equation 4–13}$$

where t_c = thickness of the metal casing
d_i = inside diameter of the casing
B = constant depending upon the explosive and casing material (table 4–2)
The largest fragment produced by an explosion can be found by setting $N_f = 1$, so that $\ln N_f = 0$ in equation 4–12. Thus the weight of the largest fragment is given by

$$W_f = \sqrt{M_A \ln\left[\frac{8W_c}{M_A^2}\right]} \qquad \text{Equation 4–14}$$

The symbol ln in equations 4–12 and 4–14 refers to the natural logarithmic function.

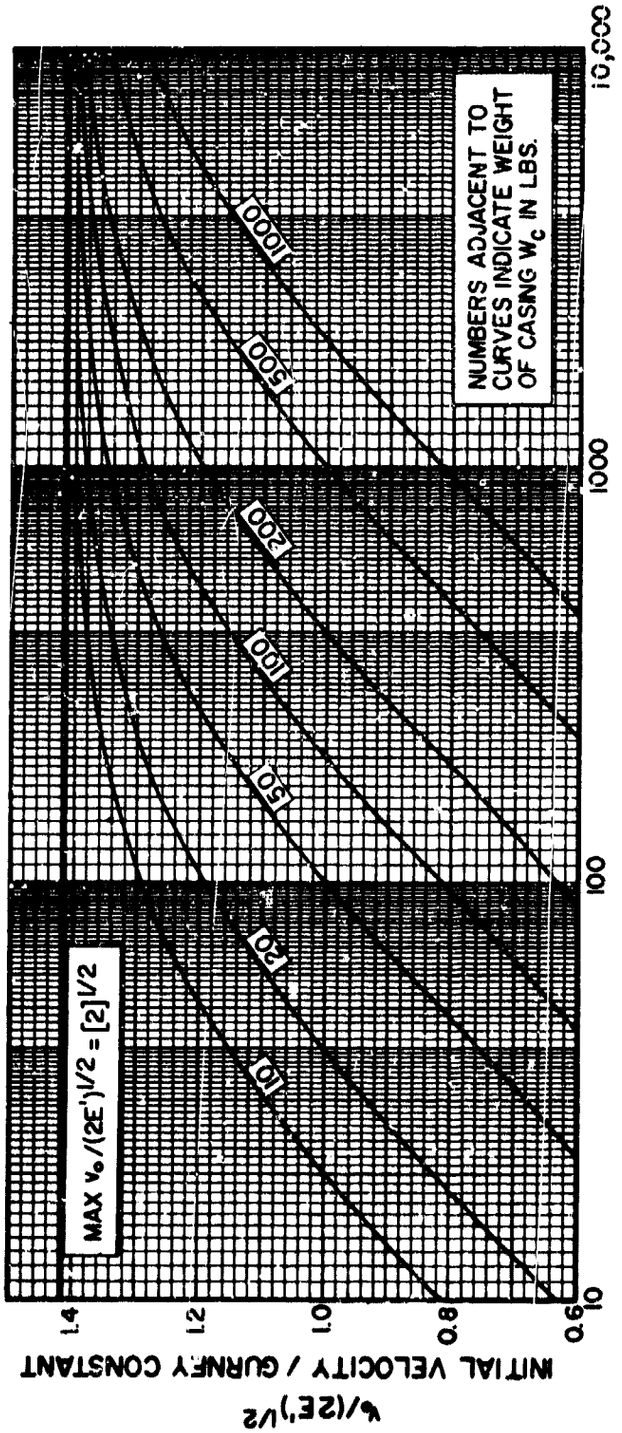


Figure 4-73. Initial velocity of primary fragments vs. charge weight.

f $v_o/(2E')^{1/2}$
us container
t velocity is
veight to the
. Therefore,
y fragments
onstant and

uation 4–11

ments (Ex-
Containers)

l produce a
gments with
r fragments
a protective
n necessary
pagation of

eight of the
order deto-
a cylindrical
lculated ac-
asis of theo-
large num-
produced is

uation 4–12

r than W_f

portion of

$_A$ is defined

uation 4–13

plosive and

sion can be
n equation
nt is given

uation 4–14

fers to the

4–23. Initial Fragment Velocities (Noncylindrical Containers)

a. By extension of the methods used to predict the initial velocities of small fragments from long cylindrical charges, expressions have been developed which permit the evaluation of the initial velocities of fragments from other simple combinations of metal and explosives. The expressions for the shapes considered are listed in table 4–3. Expressions are also listed in table 4–3 for the maximum initial fragment velocity which results when the ratio of the container (or plate) weight to the explosive weight (W_c/W) approaches zero.

b. The shapes considered in table 4–3 are assumed to have an evenly distributed explosive and also a uniform container (casing) or plate thickness. However, for those cases where the shape is slightly nonuniform, the initial velocity of the resulting fragments may be estimated by using the average cross-sectional dimensions.

Table 4–2. Constants for Primary Fragment Calculations

Explosive material	*Gurney Energy Constant* $(2E')^{1/2}$	*B*
Amatol		0.35
Comp. B	7880	
H-6	7710	
Hexanite		0.32
Pentolite	7550	
RDX/TNT (75/25)	7850	
RDX/TNT (70/30)	8380	
RDX/TNT (60/40)	7880	0.27
TNT	6940	0.30
Tetryl	7460	0.24
Torpex	7450	

Note. The above constants are for mild steel cylindrical containers of uniform thickness.

4–24. Number and Weight of Fragments (Noncylindrical Containers)

Information is not presently available which permits the evaluation of the number and weight of fragments from charges other than those having a cylindrical cross-section.

4–25. Variation of Fragment Velocity with Distance

a. As previously mentioned, the velocity of a fragment will decrease from its initial velocity with increasing distance. However, where the protective barriers are located 20 feet or less from a detonation, the variation between striking and initial velocities usually may be neglected. On the other hand, for determining the effects of primary fragment impact on structures further away from a detonation, the variation of fragment velocity with distance should be included in the design An estimate of this change in velocity with distance can be made using:

$$v_s = v_o e^{[-0.04R_f/W_f^{1/3}]} \qquad \textbf{Equation 4–15}$$

where v_s = the striking velocity
v_o = the initial fragment velocity
R_f = the distance traveled by the fragment
W_f = weight of primary fragment

b. The above relationship is applicable for small fragments up to several ounces in weight. No data is presently available for larger fragments. Figure 4–74 shows the variation of the ratio v_s/v_o versus the primary fragment weight W_f for various distances R_f.

oss-sectional dimen-

Fragments (Non-
)

lable which permits
weight of fragments
having a cylindrical

Velocity with Dis-

e velocity of a frag-
al velocity with in-
e the protective bar-
om a detonation, the
ial velocities usually
and, for determining
mpact on structures
he variation of frag-
d be included in the
ge in velocity with

Equation 4–15

locity
y the fragment
ment
applicable for small
weight. No data is
gments. Figure 4–74
v_o versus the primary
stances R_f.

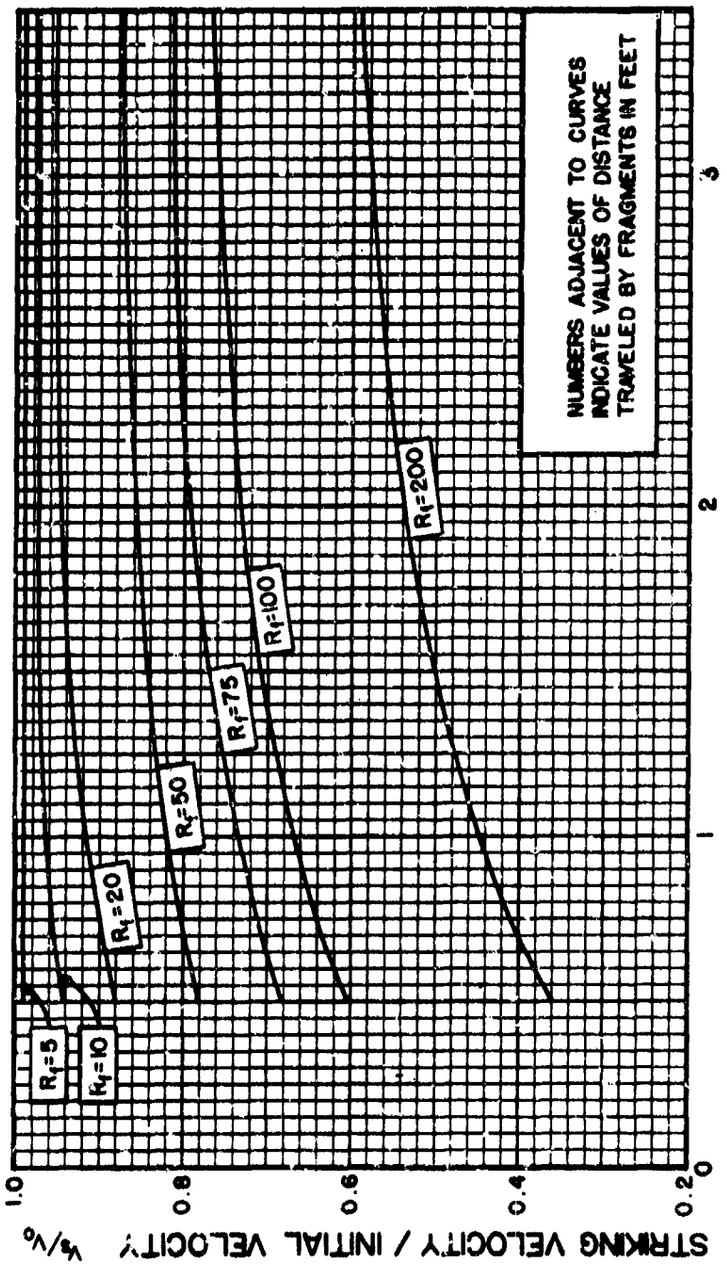
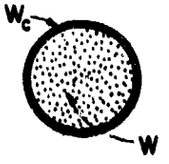
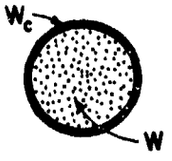
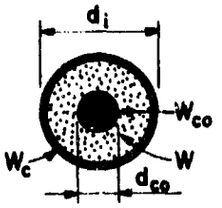
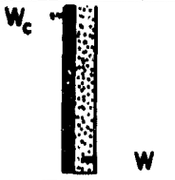
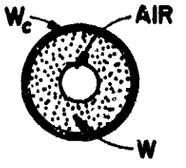
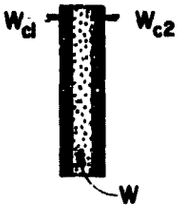


Figure 4-74. Variation of primary fragment velocities with distance.

2

Table 4-3. Initial Velocity of Primary Fragments

Type	Cross-sectional shape	Initial fragment velocity v_o	Maximum v_o	
Cylinder		$\sqrt{2E'}\left[\dfrac{\dfrac{W}{W_e}}{1+\dfrac{W}{2W_e}}\right]^{1/2}$	$\sqrt{2E'}\ \sqrt{2}$	See paragraph 4-
Sphere		$\sqrt{2E'}\left[\dfrac{\dfrac{W}{W_e}}{1+\dfrac{3W}{5W_e}}\right]^{1/2}$	$\sqrt{2E'}\ \sqrt{\frac{5}{3}}$	
Steel cored cylinder		$\sqrt{2E'}\left[\dfrac{\dfrac{W}{W_e}}{1+\dfrac{(3+a)W}{6(1+a)W_e}}\right]^{1/2}$ where $a=\dfrac{d_{co}}{1.6d_i}$	$\sqrt{2E'}\sqrt{\dfrac{6(1+a)}{(3+a)}}$	If the steel core for the initial where W_{co} is t
Plate		$\sqrt{2E'}\left[\dfrac{\dfrac{3W}{5W_e}}{1+\dfrac{W}{5W_c}+\dfrac{4W_c}{5W}}\right]^{1/2}$	$\sqrt{2E'}\ \sqrt{3}$	This expression having the sam in free air and resulting motic
Hollow cylinder		—	—	Although an ex an upper limit for a solid cyl The ratio of t cylindrical cha
Sandwich plates		if $W_{c1}\neq W_{c2}$ $\sqrt{2E'}\left[\dfrac{W}{W_{c1}+W_{c2}g+\dfrac{W}{3}(1-g+g^2)}\right]^{1/2}$ where $g=\dfrac{W_{c1}+\dfrac{W}{2}}{W_{c2}+\dfrac{W}{2}}$ if $W_{c1}=W_{c2}=W_c$ $\sqrt{2E'}\left[\dfrac{\dfrac{W}{2W_c}}{1+\dfrac{W}{6W_c}}\right]^{1/2}$	$\sqrt{2E'}\ \sqrt{3}$	This expression a plates having entire system i to its surface plane of the pl

W, W_c, W_{co}, W_{c1}, W_{c2} (lbs)
d_i, d_{co} (in.)
v_o, $\sqrt{2E'}$ (ft/sec)

4–3. Initial Velocity of Primary Fragments

	Maximum*	Remarks
	$\sqrt{2E'}\ \sqrt{2}$	See paragraph 4–21.
	$\sqrt{2E'}\ \sqrt{\frac{1}{}}$	
	$\sqrt{2E'}\sqrt{\frac{6(1+a)}{(3+a)}}$	If the steel core is many times more massive than the explosive, this expression for the initial velocity should be modified by multiplying it by the expression: $\sqrt{1-\frac{0.02W_c}{W}}$ where W_c is the weight of the steel core (lbs.).
	$\sqrt{2E'}\ \sqrt{3}$	This expression applies for a rectangular explosive in contact with a metal plate having the same surface area. It is assumed that the entire system is suspended in free air and its thickness is small in comparison to its surface area so that the resulting motions are essentially normal to the plane of the plate.
	—	Although an expression to predict the velocity of fragments is not available, an upper limit of the initial velocity may be obtained using the expression for a solid cylinder and a lower limit from the expression for a single plate. The ratio of the explosive weight to the casing weight (W/W_c) of the hollow cylindrical charge is used in both expressions.
	$\sqrt{2E'}\ \sqrt{3}$	This expression applies for a rectangular explosive sandwiched between two metal plates having the same surface area as the explosive. It is assumed that the entire system is suspended in free air and its thickness is small in comparison to its surface area so that the resulting motions are essentially normal to the plane of the plates.

APPENDIX 4A. EXPLOSIVE EFFECTS - ILLUSTRATIVE EXAMPLES

PROBLEM 4A-1. FREE-AIR BURST

Problem: Determine incident and reflected blast wave parameters on the roof of a structure for a free-air burst.

Procedure:

Step 1. Select several points of interest on the roof relative to the charge. Determine the charge weight, height of burst H_c, and several ground distances R_G.

Step 2. Apply a 20% safety factor to the charge weight.

Step 3. For each point, calculate slant distance R, scaled slant distance Z, and angle of incidence α :

$$R = \sqrt{R_G^2 + H_c^2}$$

$$Z = \frac{R}{W^{1/3}}$$

$$\alpha = \tan^{-1} \frac{R_G}{H_c}$$

Step 4. Determine incident blast wave parameters from figure 4-5 for corresponding scaled slant distance Z :

For each point read:

Peak positive incident pressure P_{so}

Shock front velocity U

Scaled unit positive incident impulse $i_s/W^{1/3}$

Scaled positive phase duration $t_o/W^{1/3}$

Scaled arrival time $t_A/W^{1/3}$

Multiply scaled values by $W^{1/3}$ to obtain absolute values.

Step 5. Determine peak reflected pressure P_r on the structure's roof for corresponding peak incident pressure P_{so} and angle of incidence α from figure 4-6:

For each point, read reflected pressure coefficient $C_{r\alpha}$:

$$P_r = C_{r\alpha} P_{so}$$

Step 6. Determine unit positive reflected impulse i_r from figure 4-5 for corresponding peak reflected pressure P_r:

For each point, read scaled unit positive reflected impulse

$$i_r/W^{1/3}$$

Multiply scaled value by $W^{1/3}$ to obtain absolute value.

EXAMPLE 4A-1. FREE-AIR BURST

Required: Incident blast wave parameters P_{so}, U, i_s, t_o, t_A and reflected blast wave parameters P_r, i_r at several points on a structure's roof below an air burst of 290 lbs at a height of burst of 30 ft above the roof.

Solution:

Step 1. Given: Charge weight = 290 lbs, H_c = 30 ft, R_{G2} = 20 ft, R_{G3} = 45 ft.

Step 2. W = 1.20 (290) = 350 lbs.

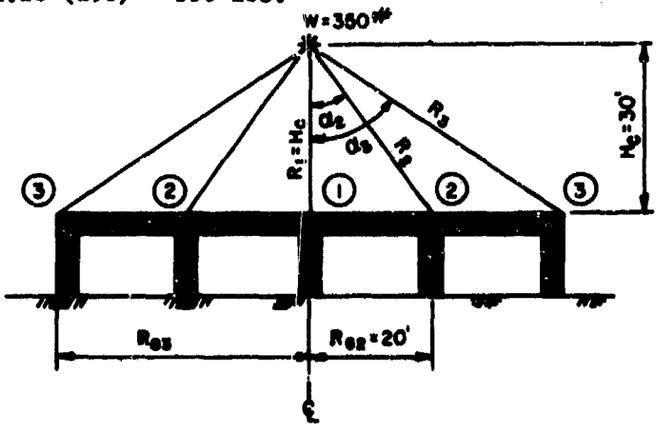


Figure 4A-1

Step 3. For point 3:

$$R_3 = \sqrt{R_{G3}^2 + H_c^2} = \sqrt{(45)^2 + (30)^2} = 54.1 \text{ ft}$$

$$Z_3 = \frac{R_3}{W^{1/3}} = \frac{54.1}{(350)^{1/3}} = 7.67 \text{ ft/lb}^{1/3}$$

$$\alpha_3 = \tan^{-1}\left[\frac{R_{G3}}{H_c}\right] = \tan^{-1}\left[\frac{45}{30}\right] = 56.3^{\circ}$$

Step 4. Determine incident blast wave parameters from figure 4-5 for $Z_3 = 7.67$ ft/lb$^{1/3}$:

$P_{so} = 10.3$ psi

$U = 1.48$ ft/ms

$\frac{i_s}{W^{1/3}} = 7.7$ psi-ms/lb$^{1/3}$ $\therefore i_s = 7.7\ (350)^{1/3} = 54.3$ psi-ms

$\frac{t_o}{W^{1/3}} = 1.70$ ms/lb$^{1/3}$ $\therefore t_o = 1.70\ (350)^{1/3} = 12.0$ ms

$\frac{t_A}{W^{1/3}} = 3.15$ ms/lb$^{1/3}$ $\therefore t_A = 3.15\ (350)^{1/3} = 22.2$ ms

Step 5. Determine reflected pressure on the roof from figure 4-6 for $P_{so} = 10.3$ psi and $\alpha = 56.3^{\circ}$:

$C_{r\alpha} = 2.65$

$P_r = C_{r\alpha} P_{so} = 2.65\ (10.3) = 27.3$ psi

Step 6. Determine reflected pressure impulse from figure 4-5. for $P_r = 27.3$ psi:

$\frac{i_r}{W^{1/3}} = 19.5$ psi-ms/lb$^{1/3}$ $\therefore i_r = 19.5\ (350)^{1/3} = 137.5$ psi-ms

Step 7. R
a

Poi

1
2
3

Step 7. Repeat steps 3 through 6 for points 1 and 2. The results are shown as follows:

Point	R_G (ft)	H_c (ft)	R (ft)	Z ($ft/lb^{1/3}$)	α (deg)
1	0	30	30	4.26	0
2	20	30	36.1	5.12	33.7
3	45	30	54.1	7.67	56.3

Point	P_{so} (psi)	U (ft/ms)	$i_s/W^{1/3}$ ($psi-ms/lb^{1/3}$)	i_s (psi-ms)	$t_o/W^{1/3}$ ($ms/lb^{1/3}$)	t_o (ms)
1	40.0	2.15	12.5	88.1	0.86	6.06
2	26.0	1.87	11.0	77.6	1.13	7.97
3	10.3	1.48	7.7	54.3	1.70	12.0

$t_A/W^{1/3}$ ($ms/lb^{1/3}$)	t_A (ms)	$C_{r\alpha}$	P_r (psi)	$i_r/W^{1/3}$ ($psi-ms/lb^{1/3}$)	i_r (psi-ms)	Point
1.07	7.54	3.75	150	43.0	303	1
1.54	10.9	3.00	78.0	33.5	236	2
3.15	22.0	2.65	27.3	19.5	137.5	3

PROBLEM 4A-2. AIR BURST

Problem: Determine free-field blast wave parameters at a point on the ground for an air burst.

Procedure:

Step 1. Select point of interest on the ground relative to the charge. Determine the charge weight, height of burst H_c, and ground distance R_G.

Step 2. Apply a 20% safety factor to the charge weight.

Step 3. Calculate slant distance R, scaled slant distance Z, and angle of incidence α :

$$R = \sqrt{R_G^2 + H_c^2}$$

$$Z = \frac{R}{W^{1/3}}$$

$$\alpha = \tan^{-1} \frac{R_G}{H_c}$$

Step 4. Determine peak free-air incident pressure P_{so}, scaled positive phase duration $t_o/W^{1/3}$, and scaled arrival time $t_A/W^{1/3}$ from figure 4-5 for value of Z.

Multiply scaled values by $W^{1/3}$ to obtain absolute values.

Step 5. Determine peak incident pressure P_{so} in the Mach front from figure 4-6 for corresponding free-air pressure P_{so} (incident) and angle of incidence α :

Read reflected pressure coefficient $C_{r\alpha}$

$$P_{so} = C_{r\alpha} P_{so} \text{ (free-air incident)}$$

Step 6. Determine shock front velocity U and scaled unit positive incident impulse $i_s/W^{1/3}$ from figure 4-5 for corresponding peak incident pressure P_{so} in the Mach front.

Multiply scaled value of $W^{1/3}$ to obtain absolute value.

EXAMPLE 4A-2. AIR BURST

Required: Free-field blast wave parameters P_{so}, U, i_s, t_o, t_A for an air burst of 20,800 lbs at a ground distance of 550 ft and a height of burst of 90 ft.

Solution:

Step 1. Given: Charge weight = 20,800 lb, R_G = 550 ft, H_c = 90 ft.

Step 2. W = 1.20 (20,800) = 25,000 lbs.

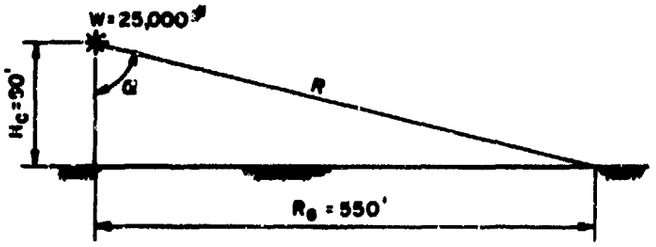


Figure 4A-2

Step 3. For point of interest:

$$R = \sqrt{R_G^2 + H_c^2} = \sqrt{(550)^2 + (90)^2} = 557 \text{ ft}$$

$$Z = \frac{R}{W^{1/3}} = \frac{557}{(25{,}000)^{1/3}} = 19.0 \text{ ft/lb}^{1/3}$$

$$\alpha = \tan^{-1}\left[\frac{R_G}{H_c}\right] = \tan^{-1}\left[\frac{550}{90}\right] = 80.7^{\circ}$$

Step 4. Determine free-air incident pressure, duration, and arrival time from figure 4-5 for $Z = 19.0$ ft/lb$^{1/3}$.

P_{so} (incident) = 2.40 psi

$\frac{t_o}{W^{1/3}} = 2.8$ ms/lb$^{1/3}$ $\quad \therefore t_o = 2.8\ (25{,}000)^{1/3} = 82$ ms

$\frac{t_A}{W^{1/3}} = 12.0$ ms/lb$^{1/3}$ $\quad \therefore t_A = 12.0\ (25{,}000)^{1/3} = 352$ ms

Step 5. Determine incident pressure P_{so} in the Mach front from figure 4-6 for P_{so} (free-air incident) = 2.40 psi and $\alpha = 80.7^{\circ}$:

$C_{r\alpha} = 1.43$

$P_{so} = C_{r\alpha} P_{so}$ (free-air incident) = 1.43(2.40) = 3.43 psi

Step 6. Determine other parameters from figure 4-5 corresponding to $P_{so} = 3.43$ psi.

$U = 1.22$ ft/ms

$\frac{i_s}{W^{1/3}} = 4.4$ psi-ms/lb$^{1/3}$ $\quad \therefore i_s = 4.4\ (25{,}000)^{1/3} = 129$ psi-ms

PROBLEM 4A-3. SURFACE BURST

Problem: Determine free-field blast wave parameters for a surface burst.

Procedure:

Step 1. Select point of interest on the ground relative to the charge. Determine the charge weight, and ground distance R_G.

Step 2. Apply a 20% safety factor to the charge weight.

Step 3.

Step 4.

Requir
surf

Soluti

Step 1

Step 2

Step 3

Step 3. Calculate scaled ground distance Z_G:

$$Z_G = \frac{R_G}{W^{1/3}}$$

Step 4. Determine free-field blast wave parameters from figure 4-12 for corresponding scaled ground distance Z_G:

Read:

Peak positive incident pressure P_{so}

Shock front velocity U

Scaled unit positive incident impulse $i_s/W^{1/3}$

Scaled positive phase duration $t_o/W^{1/3}$

Scaled arrival time $t_A/W^{1/3}$

Multiply scaled values by $W^{1/3}$ to obtain absolute values.

EXAMPLE 4A-3. SURFACE BURST

Required: Free-field blast wave parameters P_{so}, U, i_s, t_o, t_A for a surface burst of 20,800 lbs at a distance of 530 ft.

Solution:

Step 1. Given: Charge weight = 20,800 lbs, R_G = 530 ft.

Step 2. $W = 1.20\ (20{,}800) = 25{,}000$ lbs.

Step 3. For point of interest:

$$Z_G = \frac{R_G}{W^{1/3}} = \frac{530}{(25{,}000)^{1/3}} = 18.1\ \text{ft/lb}^{1/3}$$

Step 4. Determine blast wave parameters from figure 4-12 for $Z_G = 18.1$ ft/lb$^{1/3}$:

$$P_{so} = 3.50 \text{ psi}$$

$$U = 1.24 \text{ ft/ms}$$

$$\frac{i_s}{W^{1/3}} = 5.55 \text{ psi-ms/lb}^{1/3} \therefore i_s = 5.55(25{,}000)^{1/3} = 162.3 \text{ psi-ms}$$

$$\frac{t_o}{W^{1/3}} = 3.22 \text{ ms/lb}^{1/3} \therefore t_o = 3.22(25{,}000)^{1/3} = 94.2 \text{ ms}$$

$$\frac{t_A}{W^{1/3}} = 10.6 \text{ ms/lb}^{1/3} \therefore t_A = 10.6(25{,}000)^{1/3} = 310 \text{ ms}$$

PROBLEM 4A-4. LEAKAGE PRESSURES

Problem: Determine free-field blast wave parameters at a distance from a partially confined, fully vented explosion.

Procedure:

Step 1. Select point of interest on the ground relative to the charge. Determine the charge weight, ground distance R_G, and direction relative to cubicle (direction A,B,C, or D as shown in figure 4-63).

Step 2. Apply a 20% safety factor to the charge weight.

Step 3. Calculate scaled ground distance Z_G:

$$Z_G = \frac{R_G}{W^{1/3}}$$

Step 4. Determine peak incident pressure P_{so} from figure 4-63 for corresponding scaled distance Z_G and direction of interest.

Step 5. Determine free-field blast wave parameters from figure 4-12 for corresponding peak incident pressure P_{so}.

Read:

Shock front velocity U

Scaled unit positive incident impulse $i_s/W^{1/3}$

Scaled positive phase duration $t_o/W^{1/3}$

Scaled arrival time $t_A/W^{1/3}$

Multiply scaled values by $W^{1/3}$ to obtain absolute values.

EXAMPLE 4A-4. LEAKAGE PRESSURES

Required: Free-field blast wave parameters P_{so}, U, i_s, t_o, t_A for a partially confined explosion of 20,800 lbs at a distance of 400 ft behind the back wall of a three wall cubicle. The cubicle is fully vented, $\frac{L}{H} = 1$ for the backwall and $\frac{W}{V} = 1.5$.

Solution:

Step 1. Given: Charge weight = 20,800 lbs, R_G = 400 ft, Direction "D" (fig. 4-63).

Step 2. W = 1.20 (20,800) = 25,000 lbs.

Step 3. $Z_G = \frac{R_G}{W^{1/3}} = \frac{400}{(25,000)^{1/3}} = 13.7 \text{ ft/lb}^{1/3}$

Step 4. Determine P_{so} from figure 4-63 for $Z_G = 13.7 \text{ ft/lb}^{1/3}$ and Direction "D".

P_{so} = 3.25 psi

Step 5. Determine other parameters from figure 4-12 corresponding to P_{so} = 3.25 psi

Step 4.

$$U = 1.230 \text{ ft/ms}$$

$$\frac{i_s}{W^{1/3}} = 5.3 \text{ psi-ms/lb}^{1/3} \quad \therefore i_s = 5.3(25{,}000)^{1/3} = 155 \text{ psi-ms}$$

$$\frac{t_o}{W^{1/3}} = 3.25 \text{ ms/lb}^{1/3} \quad \therefore t_o = 3.25(25{,}000)^{1/3} = 95 \text{ ms}$$

$$\frac{t_A}{W^{1/3}} = 11.5 \text{ ms/lb}^{1/3} \quad \therefore t_A = 11.5(25{,}000)^{1/3} = 336 \text{ ms}$$

PROBLEM 4A-5. HIGH PRESSURE RANGE BLAST LOADS

Problem: Determine the average scaled impulse acting on the wall of a cubicle from a contained fully vented explosion.

Procedure:

Step 5.

Step 1. Select from figure 4-15 the structural configuration which will define the number N and location of effective reflecting surfaces for the wall of the structure in question. Determine the charge weight, and as defined by the structural configuration chosen above, the charge location parameters R_A, h, ℓ and the structural parameters L, H.

Step 2. Apply a 20% safety factor to the charge weight.

Step 3: Calculate the chart parameters $\frac{h}{H}$, $\frac{\ell}{L}$, $\frac{L}{R_A}$, $\frac{L}{H}$ and the scaled distance Z_A.

Note:

Use of the average impulse charts may require interpolation in many cases. Interpolation may be achieved by inspection for the scaled distance Z_A and by a graphical procedure for the chart parameters L/H, ℓ/L, and h/H using 2 cycle by 2 cycle logarithmic graph paper. The following procedure will illustrate the interpolation of all three chart parameters.

Step 4. From figure 4-16 determine the appropriate impulse charts for the number of adjacent reflecting surfaces N. Determine and tabulate the values of the average scaled impulse $\overline{i}_b$ from these charts for the required L/R_A and Z_A and the following variables:

L/H = 0.75, 1.50, 3.00, and 6.00

ℓ/L = 0.10, 0.25, 0.50, and 0.75

h/H = 0.15, 0.25, 0.50, and 0.75

FOR REQUIRED $\frac{L}{R_A}$ AND Z_A

h/H	0.15				0.25				0.50				0.75		
ℓ/L / L/H	0.10	0.25	0.50	0.75	0.10	0.25	0.50	0.75	0.10	0.25	0.50	0.75	0.25	0.50	0.75
0.75															
1.50															
3.00															
6.00															

Step 5. *a.* Prepare four 2-cycle log-log charts with $\frac{L}{H}$ as the lower abscissa, $\frac{\ell}{L}$ as the upper abscissa, and $\overline{i}_b$ as the ordinate (one chart for each of the $\frac{h}{H}$ ratios). On each chart for constant $\frac{h}{H}$ and Z_A, plot $\overline{i}_b$ versus $\frac{L}{H}$ for all $\frac{\ell}{L}$ values.

b. Using chart for $\frac{h}{H}$ = 0.15, read values of $\overline{i}_b$ versus $\frac{\ell}{L}$ for required $\frac{L}{H}$. Tabulated results.

FOR $\frac{h}{H}$ = 0.15 AND REQUIRED $\frac{L}{H}$

ℓ/L	$\overline{i}_b$
0.10	
0.25	
0.50	
0.75	

c. Repeat step 5*b* for charts $\frac{h}{H}$ = 0.25, 0.50, and 0.75. Tabulate results.

d. On each $\frac{h}{H}$ chart, plot $\bar{I}_b$ versus $\frac{\ell}{L}$ from steps 5*b* and 5*c*.

e. On each $\frac{h}{H}$ chart, read $\bar{I}_b$ for required $\frac{\ell}{L}$ ratio.

FOR CALCULATED $\frac{\ell}{L}$

h/H	$\bar{I}_b$
0.15	
0.25	
0.50	
0.75	

f. On a fifth chart, plot $\bar{I}_b$ from step 5*e* versus $\frac{h}{H}$.

Step 6. For required $\frac{h}{H}$ ratio, read $\bar{I}_b$ from chart of step 5*f*.

Step 7. Calculate duration of load on element.

a. For nearest point, determine the time of arrival of the blast from figure 4-5 for Z_A.

b. For furthest point, determine slant distance Z, and the time of arrival of the blast wave and duration of load from figure 4-5 for calculated slant distance.

c. Calculate duration of load using equation 4-1.

.75.

s 5b

io.

$\frac{h}{H}$.

5f.

of the

and the
f load

EXAMPLE 4A-5(A). HIGH PRESSURE RANGE BLAST LOADS

Required: Average scaled impulse on the side wall of a three-wall cubicle from an explosive charge of 205 lbs. The cubicle is fully vented.

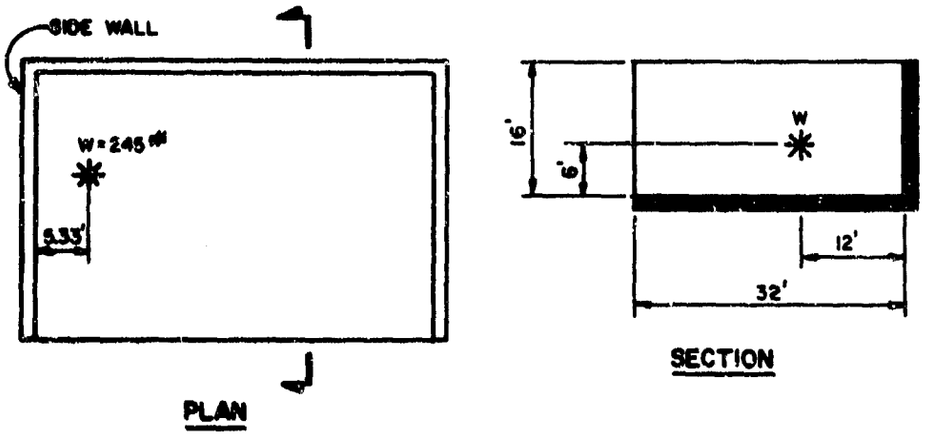


Figure 4A-3

Solution:

Step 1. H = 16 ft L = 32 ft Charge Weight = 205 lbs

h = 6 ft ℓ = 12 ft R_A = 5.33 ft

Note:

For definition of terms, see figure 4-15 (side wall of three wall cubicle, N = 2).

Step 2. W = 1.20 (205) = 245 lbs.

Step 3. $\frac{h}{H} = 0.375$ $\frac{\ell}{L} = 0.375$ $\frac{L}{R_A} = 6.00$ $\frac{L}{H} = 2.00$

$$Z_A = \frac{R_A}{W^{1/3}} = \frac{5.33}{(245)^{1/3}} = 0.85 \text{ ft/lb}^{1/3}$$

Interpolation is required for Z_A, $\frac{L}{H}$, $\frac{\ell}{L}$, and $\frac{h}{H}$.

Step 4. Determine and tabulate the values of $\bar{i}_b$ from figures 4-28 through 4-42 (see fig. 4-16 for N = 2) for: $L/R_A = 6.00$, $Z_A = 0.85$ (interpolate by inspection) and for values given for L/H, ℓ/L and h/H.

h/H	0.15				0.25				0.50				0.75		
ℓ/L / L/H	0.10	0.25	0.50	0.75	0.10	0.25	0.50	0.75	0.10	0.25	0.50	0.75	0.25	0.50	0.75
0.75	135	125	105	95	135	110	90	72	130	90	75	65	77	67	58
1.50	210	183	165	150	205	165	140	125	180	130	108	95	115	95	80
3.00	280	255	225	200	270	240	225	200	260	200	170	145	170	145	130
6.00	310	280	245	225	320	285	265	245	310	280	250	230	260	250	230
Figure	4-28	4-29	4-30	4-31	4-32	4-33	4-34	4-35	4-36	4-37	4-38	4-39	4-40	4-41	4-42

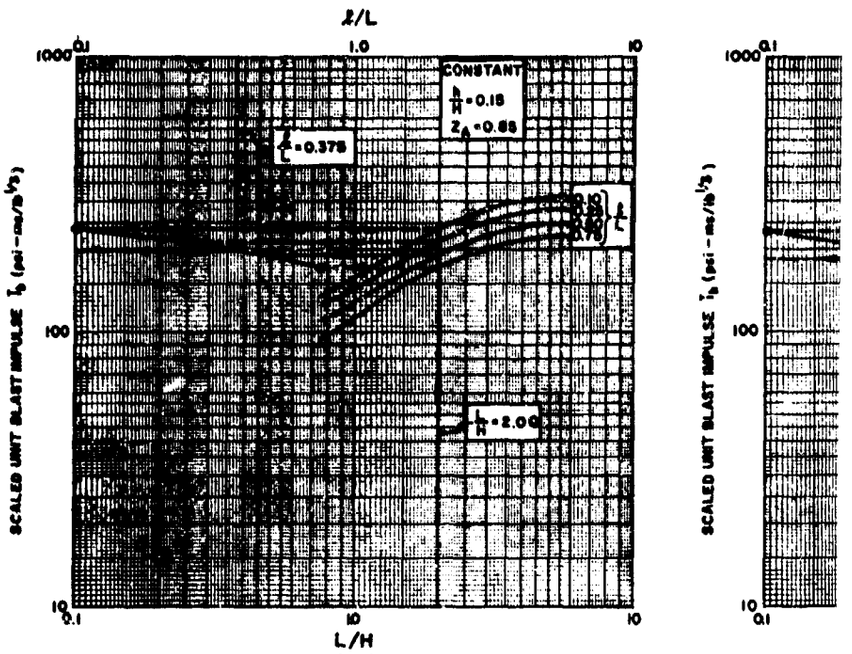
Step 5. *a.* Plot $\bar{i}_b$ versus $\frac{L}{H}$ for the values of ℓ/L and constant h/H (fig. 4A-4).

b. Determine $\bar{i}_b$ for $\frac{L}{H} = 2.00$, $\frac{h}{H} = 0.15$, and various $\frac{\ell}{L}$ ratios by entering figure 4A-4(a) with $\frac{L}{H} = 2.00$

$\frac{\ell}{L}$	$\bar{I}_b$
0.10	240
0.25	210
0.50	190
0.75	170

c. Repeat above step for $\frac{h}{H} = 0.25$, 0.50, and 0.75 by entering (b) through (d) of figure 4A-4 with $\frac{L}{H} = 2.00$ (tabulation of results not shown).

d. On each h/H chart, plot $\bar{i}_b$ (steps 5*b* and 5*c*) versus ℓ/L (upper abscissa of (a) through (d) of figure 4A-3).



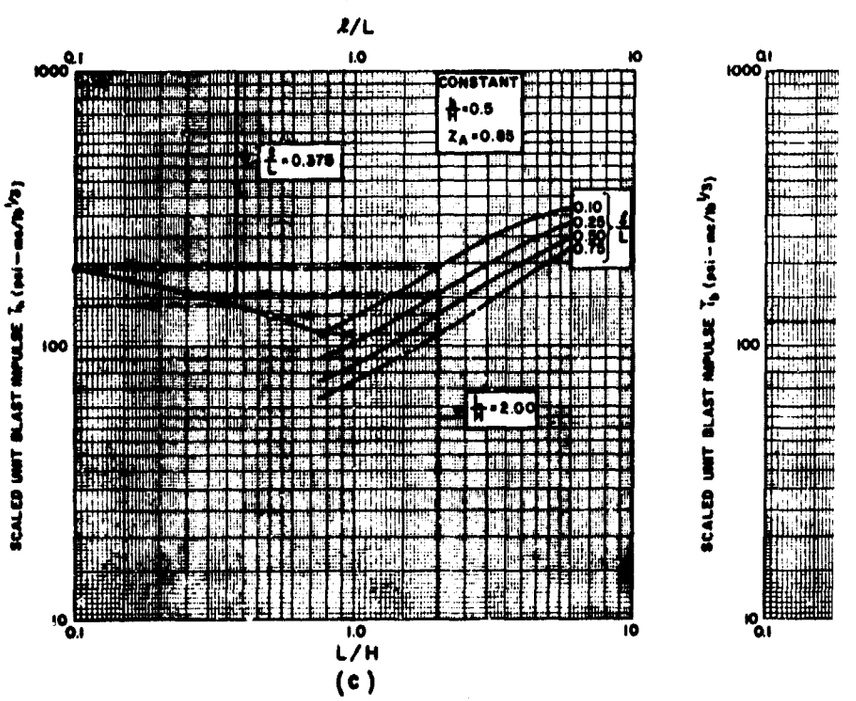
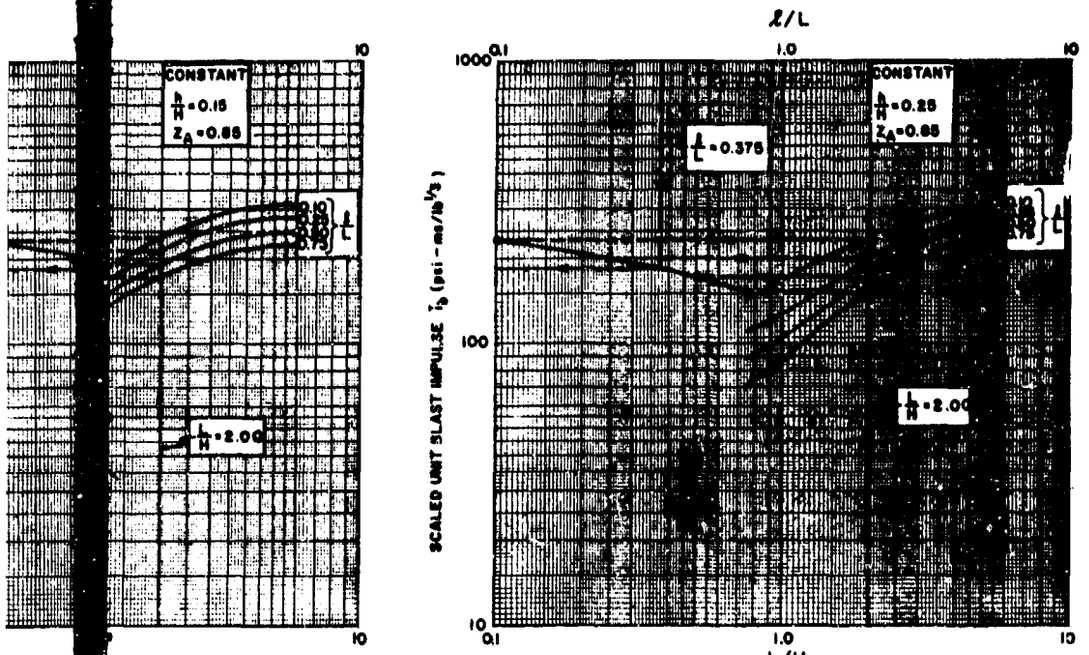
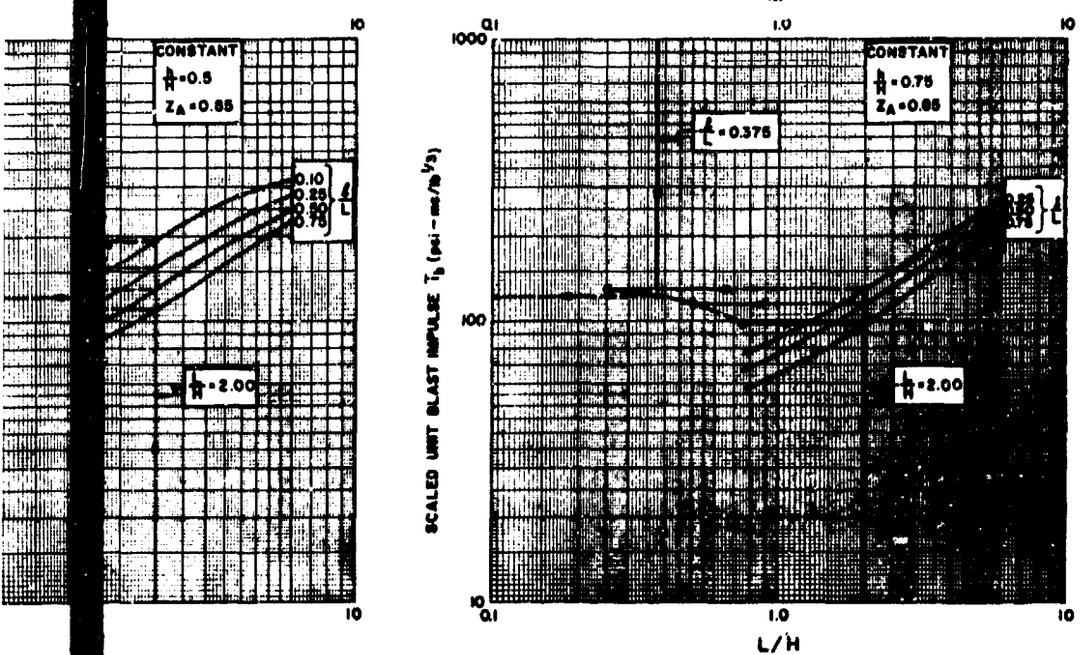


Figure 4A-4. Interpolation of scaled impulse f



(b)



(d)

se fo nterpolation of scaled impulse for L/H and ℓ/L ratios.

e. Determine $\bar{i}_b$ for $\frac{\ell}{L}$ = 0.375 on each h/H chart by entering (a) through (d) of figure 4A-4 with $\frac{\ell}{L}$ = 0.375 and reading curves plotted in step 5*d*.

$\frac{h}{H}$	$\bar{i}_b$	figure
0.15	197	4A-4(a)
0.25	185	4A-4(b)
0.50	140	4A-4(c)
0.75	123	4A-4(d)

f. Plot $\bar{i}_b$ (step 5*e*) versus $\frac{h}{H}$ (fig. 4A-5).

Step 6. For $\frac{h}{H}$ = 0.375 read $\bar{i}_b$ = 160 psi-ms/lb$^{1/3}$ on figure 4A-5.

Step 7. Calculate duration of load on wall.

a. For nearest point.

From figure 4-5 for Z_A = 0.85 ft/lb$^{1/3}$:

$$\frac{t_A}{W^{1/3}} = 0.057 \text{ ms/lb}^{1/3} \quad \therefore t_A = 0.057\ (245)^{1/3} = 0.36 \text{ ms}$$

b. For furthest point.

$$R = \sqrt{(5.33)^2 + (10)^2 + (20)^2} = 23 \text{ ft.}$$

$$Z = \frac{R}{W^{1/3}} = \frac{23}{(245)^{1/3}} = 3.67 \text{ ft/lb}^{1/3}$$

From figure 4-5 for Z = 3.67 ft/lb$^{1/3}$:

$$\frac{t_A}{W^{1/3}} = 0.79 \text{ ms/lb}^{1/3} \quad \therefore t_A = 0.79\ (245)^{1/3} = 4.95 \text{ ms}$$

$$\frac{t_o}{W^{1/3}} = 0.68 \text{ ms/lb}^{1/3} \quad \therefore t_o = 0.68\ (245)^{1/3} = 4.26 \text{ ms}$$

SCALED UNIT BLAST IMPULSE $\bar{i}_b$ (psi-ms/lb$^{1/3}$)

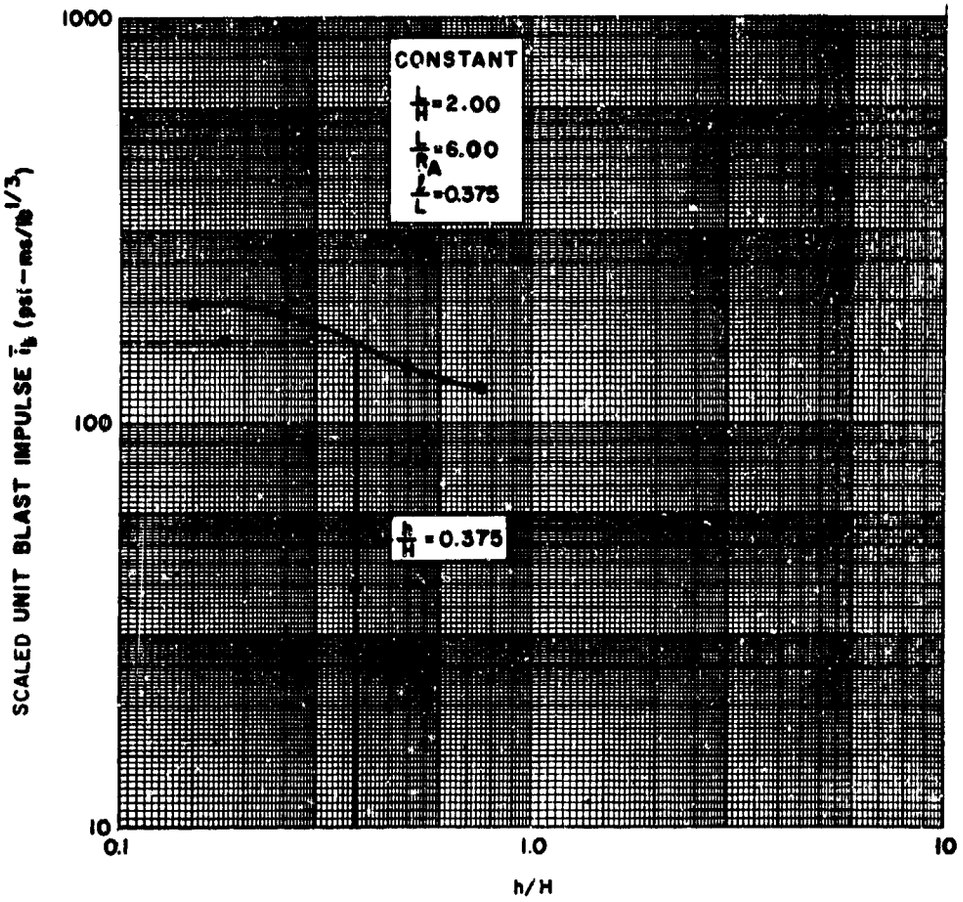


Figure 4A-5. Interpolation of scaled impulse for h/H ratios.

c. Duration of load on wall.

$$t_o = (t_A)_F - (t_A)_A + 1.5\,(t_o)_F \quad \text{(eq. 4-1)}$$

$$t_o = 4.95 - 0.36 + 1.5\,(4.26) = 10.98 \text{ ms.}$$

EXAMPLE 4A-5(B). HIGH PRESSURE RANGE BLAST LOADS

Required: Average scaled impulse on the back wall of a three-wall cubicle from an explosive charge of 3,750 lbs. The cubicle is fully vented.

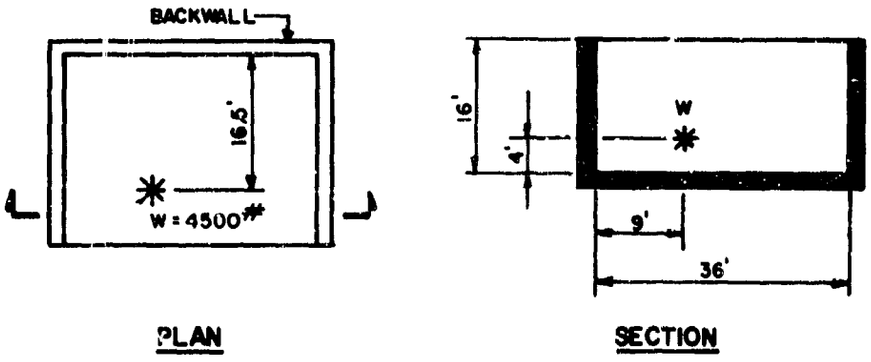


Figure 4A-6

Solution:

Step 1. H = 16 ft L = 36 ft Charge weight = 3,750 lbs

h = 4 ft ℓ = 9 ft R_A = 16.5 ft

Note:

For definition of terms, see figure 4-15 (back wall of three-wall cubicle, N = 3).

Step 2. $W = 1.20\ (3,750) = 4,500$ lbs

Step 3. $\frac{h}{H} = 0.25 \qquad \frac{\ell}{L} = 0.25 \qquad \frac{L}{R_A} = 2.18 \qquad \frac{L}{H} = 2.25$

$$Z_A = \frac{R_A}{W^{1/3}} = \frac{16.5}{(4,500)^{1/3}} = 1.00 \text{ ft/lb}^{1/3}$$

Interpolation is required for $\frac{L}{H}$

Step 4. Determine the values of $\bar{i}_b$ from figure 4-47 (determined from fig. 4-16 for $N = 3$, $h/H = 0.25$, $\ell/L = 0.25$) for $\frac{L}{H}$ ratios of 0.75, 1.50, 3.00, and 6.00.

$\frac{L}{H}$	$\bar{i}_b$
0.75	365
1.50	480
3.00	530
6.00	570

Step 5. Plot $\bar{i}_b$ versus $\frac{L}{H}$ (fig. 4A-7).

Step 6. For $\frac{L}{H} = 2.25$ read $\bar{i}_b = 515$ psi-ms/lb$^{1/3}$ on figure 4A-7.

Step 7. Calculate duration of load on wall.

a. For nearest point.

From figure 4A-7 for $Z_A = 1.00$ ft/lb$^{1/3}$:

$$\frac{t_A}{W^{1/3}} = 0.074 \text{ ms/lb}^{1/3} \quad \therefore t_A = 0.074\ (4500)^{1/3} = 1.22 \text{ ms}$$

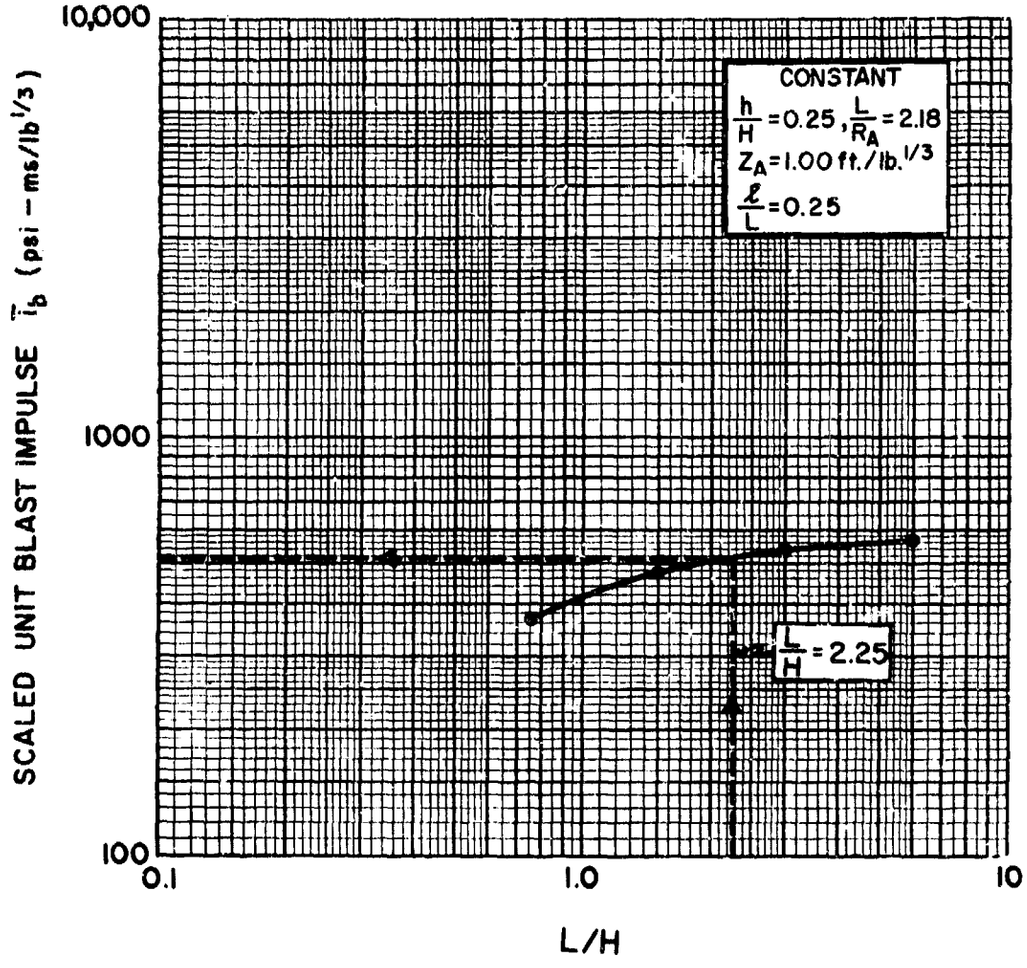


Figure 4A-7. Interpolation of scaled impulse for L/H ratios.

b. For furthest point.

$$R = \sqrt{(16.5)^2 + (27)^2 + (12)^2} = 33.8 \text{ ft}$$

$$Z = \frac{33.8}{(4500)^{1/3}} = 2.05 \text{ ft/lb}^{1/3}$$

From figure 4-5 for $Z = 2.05$ ft/lb$^{1/3}$:

$$\frac{t_A}{W^{1/3}} = 0.27 \text{ ms/lb}^{1/3} \quad \therefore t_A = 0.27\ (4500)^{1/3} = 4.46 \text{ ms}$$

$$\frac{t_o}{W^{1/3}} = 0.16 \text{ ms/lb}^{1/3} \quad \therefore t_o = 0.16\ (4500)^{1/3} = 2.64 \text{ ms}$$

c. Duration of load on wall.

$$t_o = (t_A)_F - (t_A)_A + 1.5\,(t_o)_F \quad \text{(eq. 4-1)}$$

$$t_o = 4.46 - 1.22 + 1.5\ (2.64) = 7.20 \text{ ms}$$

quired
explos

EXAMPLE 4A-5(C). HIGH PRESSURE RANGE BLAST LOADS

Required: Average scaled impulse on a cantilever barrier wall from an explosive charge of 6,250 lbs.

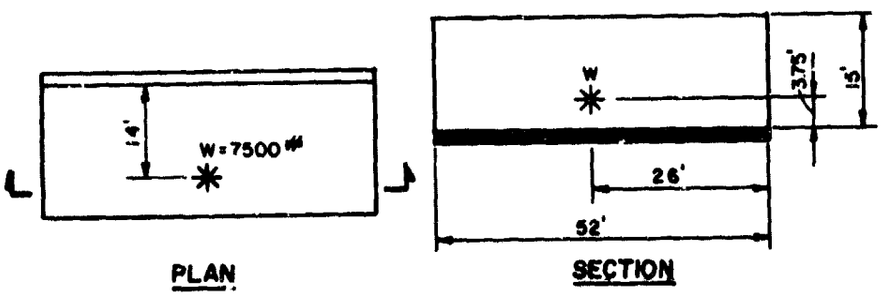


Figure 4A-8

Solution:

Step 1. H = 15 ft L = 52 ft Charge weight = 6,250 lbs

h = 3.75 ft ℓ = 26 ft R_A = 14 ft

Note:

For definition of terms, see figure 4-15 (cantilever wall. N = 1).

Step 2. W = 1.20 (6,250) = 7,500 lbs

Step 3. $\frac{h}{H} = 0.25$ $\frac{\ell}{L} = 0.50$ $\frac{L}{R_A} = 3.71$ $\frac{L}{H} = 3.47$

$$Z_A = \frac{R_A}{W^{1/3}} = \frac{14}{(7,500)^{1/3}} = 0.72 \text{ ft/lb}^{1/3}$$

Interpolation is required for $\frac{L}{H}$

Step 4. Determine the values of $\bar{i}_b$ from figure 4-22 (from fig. 4-1 for N = 1, h/H = 0.25, and ℓ/L = 0.50) for L/H ratios of 0.75, 1.50, 3.00, and 6.00.

$\frac{L}{H}$	$\bar{i}_b$
0.75	102
1.50	225
3.00	380
6.00	410

Step 5. Plot $\bar{i}_b$ versus $\frac{L}{H}$ (fig. 4A-9).

Step 6. For $\frac{L}{H} = 3.47$ read $\bar{i}_b = 390$ psi-ms/lb$^{1/3}$ on figure 4A-9.

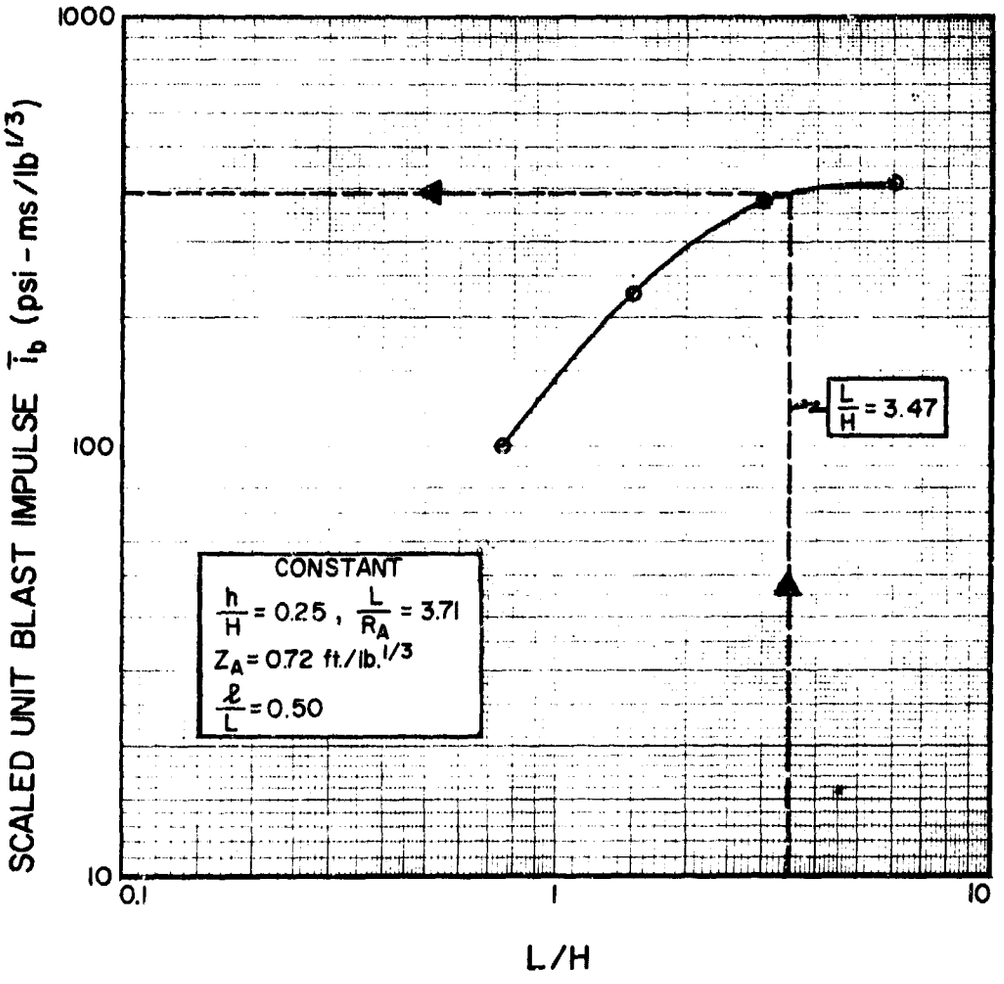


Figure 4A-9. Interpolation of scaled impulse for L/H ratios.

Step 7. Calculate duration of load on wall.

a. For nearest point.

From figure 4-5 for $Z_A = 0.72$ ft/lb$^{1/3}$:

$$\frac{t_A}{W^{1/3}} = 0.0435 \text{ ms/lb}^{1/3} \quad \therefore t_A = 0.0435\ (7500)^{1/3} = 0.85 \text{ ms}$$

b. For furthest point.

$$R = \sqrt{(14)^2 + (26)^2 + (11.25)^2} = 31.6 \text{ ft}$$

$$Z = \frac{31.6}{(7500)^{1/3}} = 1.61 \text{ ft/lb}^{1/3}$$

From figure 4-5 for $Z = 1.61$ ft/lb$^{1/3}$:

$$\frac{t_A}{W^{1/3}} = 0.175 \text{ ms/lb}^{1/3} \quad \therefore t_A = 0.175\ (7500)^{1/3} = 3.43 \text{ ms}$$

$$\frac{t_o}{W^{1/3}} = 0.100 \text{ ms/lb}^{1/3} \quad \therefore t_o = 0.100\ (7500)^{1/3} = 1.96 \text{ ms}$$

c. Duration of load on wall.

$$t_o = (t_A)_F - (t_A)_A + 1.5\ (t_o)_F \quad \text{(eq. 4-1)}$$

$$t_o = 3.43 - 0.85 + 1.5\ (1.96) = 5.52 \text{ ms}$$

PROBLEM 4A-6. HIGH PRESSURE RANGE BLAST LOADS

Problem: Determine the average scaled impulse and maximum mean pressure on the wall of an enclosed cubicle from a contained, partially vented explosion.

Procedure:

Step 1. Select from figure 4-15 the structural configuration which will define the number N and location of effective reflecting surfaces for the wall of the structure in question. Determine the charge weight, and as defined by the structural configuration chosen above, the charge location parameters R_A, h, ℓ, and the structural parameters L, H.

Step. 2 Apply a 20% safety factor to the charge weight.

Step 3. Calculate chart parameters $\frac{h}{H}$, $\frac{\ell}{L}$, $\frac{L}{R_A}$, $\frac{L}{H}$ and scaled distance Z_A.

$$Z_A = \frac{R_A}{W^{1/3}}$$

Steps 4,5,6. Following the procedure outlined in problem 4A-5, determine $\bar{i}_b$ conforming to the above parameters.

Step 7. Calculate charge-volume ratio $\frac{W}{V}$.

Step 8. For calculated $\frac{W}{V}$, read p_{mo} from figure 4-65.

EXAMPLE 4A-6. HIGH PRESSURE RANGE BLAST LOADS

Required: Average scaled impulse and maximum mean pressure on the roof slab of an enclosed cubicle with a small venting area from an explosive charge of 2.5 lbs.

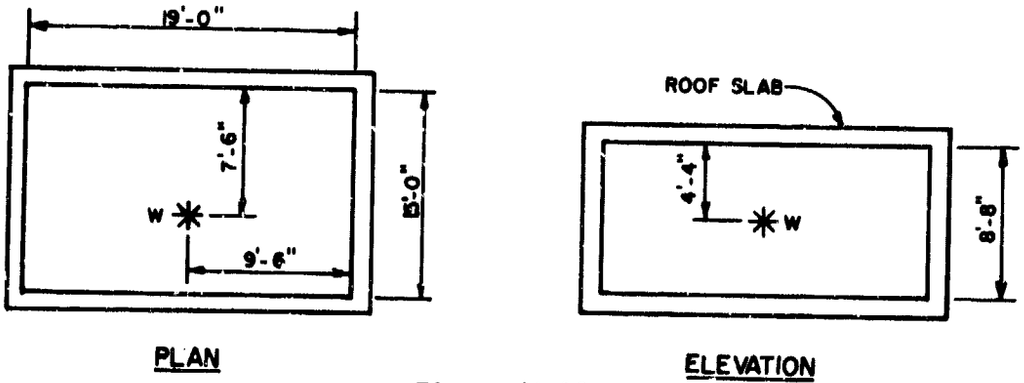


Figure 4A-10

Solution:

Step 1. H = 15 ft L = 19 ft Charge weight = 2.5 lb

h = 7.5 ft $\frac{\ell}{L}$ = 9.5 ft R_A = 4.33 ft

Note:

For definition of terms, see figure 4-15 (four wall cubicle with with roof, N = 4).

Step 2. W = 1.20 (2.5) = 3 lbs

Step 3. $\frac{h}{H}$ = 0.50 $\frac{\ell}{L}$ = 0.50 $\frac{L}{R_A}$ = 4.39 $\frac{L}{H}$ = 1.27

$$Z_A = \frac{R_A}{W^{1/3}} = \frac{4.33}{(3)^{1/3}} = 3.00 \text{ ft/lb}^{1/3}$$

Interpolation is required for $\frac{L}{H}$

Step 4. Determine the values of $\bar{i}_b$ from figure 4-62 (from fig. 4-16 for N = 4, h/H = 0.50, and ℓ/L = 0.50) for $\frac{L}{H}$ ratios of 0.75, 1.50, 3.00, and 6.00.

$\frac{L}{H}$	$\bar{i}_b$
0.75	74
1.50	87
3.00	112
6.00	171

Step 5. Plot $\bar{i}_b$ versus $\frac{L}{H}$ (fig. 4A-11).

Step 6. For $\frac{L}{H}$ = 1.27 read $\bar{i}_b$ = 81 psi-ms/lb$^{1/3}$ on figure 4A-11.

Step 7. Calculate charge-volume ratio $\frac{W}{V}$

$$\frac{W}{V} = \frac{3}{19(15)8.67} = 0.00121 \text{ lb/ft}^3$$

Step 8. For $\frac{W}{V}$ = 0.00121 lb/ft^3 read p_{mo} = 19 psi on figure 4-65.

hicle with

g. 4-16
os of

11.

4-65.

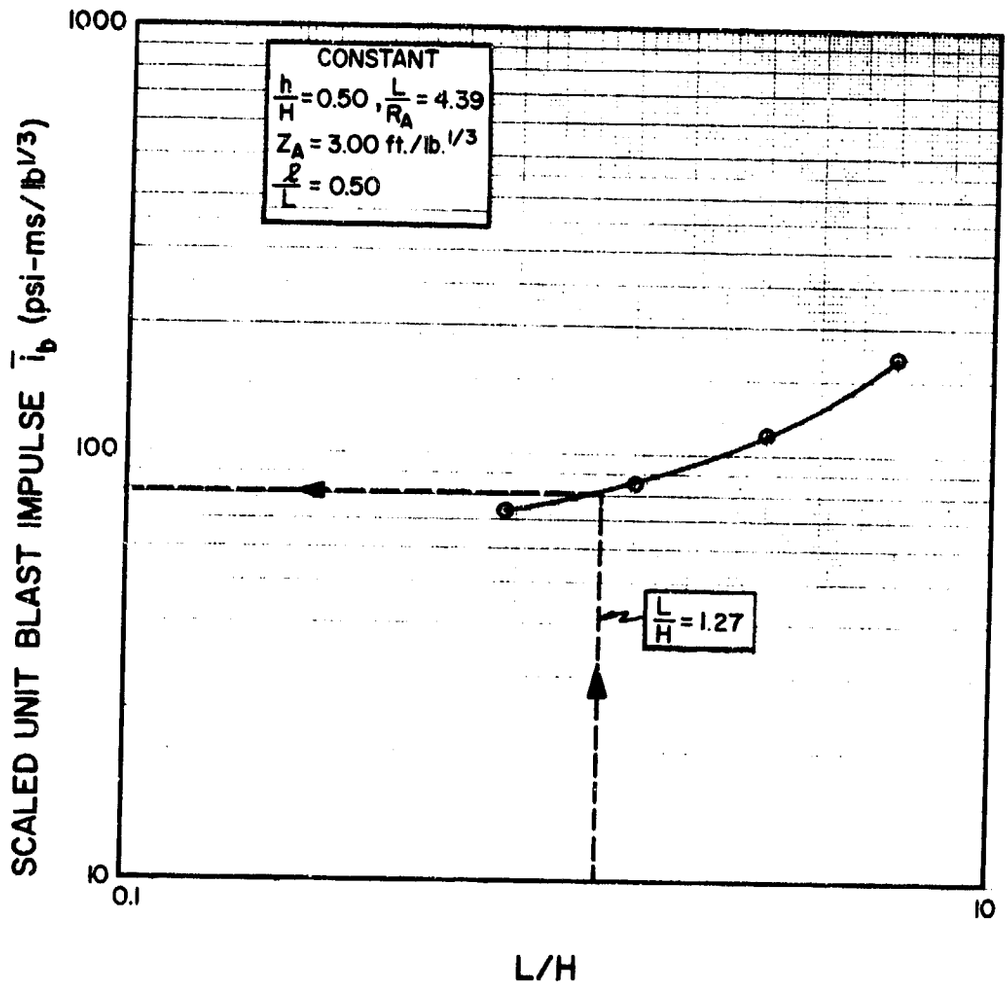


Figure 4A-11. Interpolation of scaled impulse for L/H ratios.

2

PROBLEM 4A-7. EXTERNAL BLAST LOADS ON STRUCTURES

Problem: Determine the pressure-time blast loading curves on a rectangular structure from an external explosion.

Procedure:

Step 1. Determine the charge weight, ground distance R_G, height of burst H_c, if any, and structure dimensions.

Step 2. Apply a 20% safety factor to the charge weight.

Step 3. Select several points on the structure (front wall, roof, rear wall, etc.) and determine free-field blast wave parameters (para. 4-12)for each point. For an air burst, follow the procedure outlined in problem 4A-2; a surface burst, problem 4A-3; leakage pressures, problem 4A-4.

For the front wall:

a. Calculate the scaled ground distance Z_G.

b. Determine free-field blast wave parameters for Z_G.

c. Determine reflected blast wave parameters from figure 4-5 or 4-12 for Z_G.

Read:

Peak positive normal reflected pressure P_r.

Scaled unit positive normal reflected impulse $i_r/W^{1/3}$.

Multiply scaled value by $W^{1/3}$ to obtain absolute value.

d. Repeat steps 3*a* and 3*b* for other points.

Step 4. Determine front wall loading.

If the wave front is not plane, use average values.

tep 5

a. Calculate clearing time t_c:

$$t_c = \frac{3S}{U} \quad \text{(eq. 4-5)}$$

where S = height of front wall or one-half its width, whichever is smaller

b. Calculate fictitious positive phase duration t_{of}:

$$t_{of} = \frac{2\, i_s}{P_{so}} \quad \text{(eq. 4-3)}$$

a. Determine peak dynamic pressure q_o from figure 4-66 for p_{so}.

d. Calculate $P_{so} + C_D q_o$. Obtain C_D from paragraph 4-14*b*.

e. Calculate fictitious reflected pressure duration t_r:

$$t_r = \frac{2\, i_r}{P_r} \quad \text{(eq. 4-7)}$$

f. Construct the pressure-time curves shown in either (a) or (b), figure 4-67. Whichever curve (reflected pressure or reflected pressure plus incident pressure) gives the smallest value of impulse (area under curve), that is the correct curve to use for the front wall.

tep 5. Determine side wall loading.

p 5.

a. Span Direction Parallel to Shock Front.

(1) Calculate rise time t_d :

$$t_d = \frac{L}{U}$$

where L is the width of the element being considered.

(2) Calculate fictitious positive phase duration t_{of} :

$$t_{of} = \frac{2\, i_s}{p_{so}} \quad \text{(eq. 4-3)}$$

(3) Determine dynamic pressure q_o from figure 4-66 for P_{so}.

(4) Calculate $P_{so} + C_D q_o$. Obtain C_D from paragraph 4-14*b*.

(5) Determine arrival time t_f.

(6) Construct the pressure-time curve shown in figure 4-70.

b. Span Direction Perpendicular to Shock Front.

(1) Calculate wave length-span ratio $\frac{L_{wb}}{L}$ and determine equivalent load factor C_E and blast wave location ratio $\frac{D}{L}$ from figure 4-69.

(2) Calculate equivalent uniform load $C_E P_{sob}$ and wave location D.

(3) Determine arrival times at front t_f and back t_b of span.

(4) Calculate rise time t_d :

$$t_d = \frac{D}{U}$$

(5) Calculate fictitious positive phase duration t_{of} :

$$t_{of} = \frac{2\, i_s}{P_{so}} \quad \text{(eq. 4-3)}$$

(6) Determine peak dynamic pressure q_{ob} from figure 4-66 for $C_E P_{sob}$.

(7) Calculate $C_E P_{sob} + C_D\, q_{ob}$. Obtain C_D from paragraph 4-14*a*.

(8) Construct the pressure-time curve shown in figure 4-68.

Step 6. Determine roof loading. Follow procedure outlined for side wall loading.

Step 7. Determine rear wall loading.

a. Calculate wave length-span ratio $\frac{L_{wb}}{L}$ and determine equivalent load factor C_E and blast wave location ratio $\frac{D}{L}$ from figure 4-69.

b. Calculate equivalent uniform load $C_E P_{soe}$ and wave location D.

c. Determine arrival times at bottom t_e and top t_b of span.

d. Calculate rise time t_d:

$$t_d = \frac{D}{U}$$

e. Calculate fictitious positive phase duration t_{of} :

$$t_{of} = \frac{2\, i_s}{P_{so}} \quad \text{(eq. 4-3)}$$

f. Determine peak dynamic pressure q_{oe} from figure 4-66 for $C_E P_{soe}$.

g. Calculate $C_E P_{soe} + C_D\, q_{oe}$. Obtain C_D from paragraph 4-14*c*.

h. Construct the pressure-time curve shown in figure 4-71.

EXAMPLE 4A-7. EXTERNAL BLAST LOADS ON STRUCTURES

Required: Pressure-time blast loading curves for the front wall, center roof span, side wall, and rear wall of the structure shown in figure 4A-12 for a surface burst of 4,170 lbs. at a distance from the front wall of 310 ft. Walls are one-way slabs spanning vertically, and roof is one-way slab spanning in the direction of the blast wave propagation. Structure width is 60 ft. Shock front is plane.

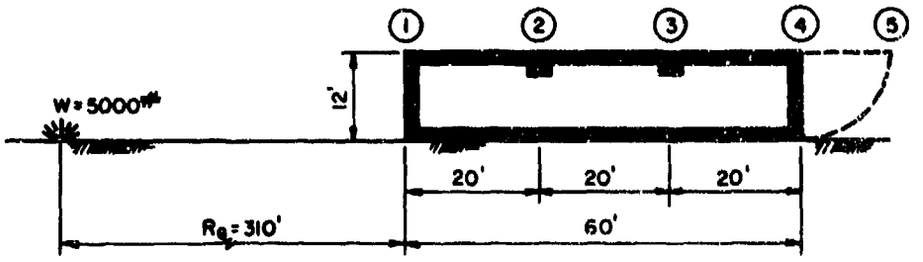


Figure 4A-12

Solution:

Step 1. Given: Charge weight = 4,170 lbs, R_G = 310 ft.

Step 2. W = 1.20 (4,170) ≈ 5,000 lbs.

Step 3. Determine free-field blast wave parameters P_{so}, U, i_s, t_o, t_A at points 1 through 5 and reflected blast wave parameters P_r, i_r at point 1. Following the procedure of problem 4A-3.

Point
1
2
3
4
5

For point 1:

a. $Z_G = \frac{R_G}{W^{1/3}} = \frac{310}{(5{,}000)^{1/3}} = 18.1 \text{ ft/lb}^{1/3}$

b. Determine free-field blast wave parameters from figure 4-12 for $Z_G = 18.1 \text{ ft/lb}^{1/3}$:

$P_{so} = 3.50$ psi

U = 1.24 ft/ms

$\frac{i_s}{W^{1/3}} = 5.55 \text{ psi-ms/lb}^{1/3} \therefore i_s = 5.55(5{,}000)^{1/3} = 94.9$ psi-ms

$\frac{t_o}{W^{1/3}} = 3.25 \text{ ms/lb}^{1/3} \quad \therefore t_o = 3.25(5{,}000)^{1/3} = 55.6$ ms

$\frac{t_A}{W^{1/3}} = 10.6 \text{ ms/lb}^{1/3} \quad \therefore t_A = 10.6(5{,}000)^{1/3} = 181$ ms

c. Determine reflected blast wave parameters from figure 4-12 for $Z_G = 18.1$ ft/lb$^{1/3}$.

$P_r = 7.80$ psi

$\frac{i_r}{W^{1/3}} = 11.8$ psi-ms/lb$^{1/3}$ $\therefore i_r = 11.8(5{,}000)^{1/3} = 202$ psi-ms

d. Repeat steps 3*a* and 3*b* for points 2 through 5. In addition, determine the wave length for these points. Results are tabulated below.

Point	R_G (ft)	Z_G (ft/lb$^{1/3}$)	P_{so} (psi)	U (ft/ms)	$i_s/W^{1/3}$ (psi-ms/lb$^{1/3}$)	i_s (psi-ms)	$t_o/W^{1/3}$ (ms/lb$^{1/3}$)	t_o (ms)
1	310	18.1	3.50	1.24	5.55	94.9	3.25	55.6
2	330	19.3	3.20	1.23	5.20	88.9	3.30	56.4
3	350	20.5	2.90	1.22	4.95	84.6	3.35	57.3
4	370	21.6	2.70	1.21	4.65	79.5	3.40	58.1
5	382	22.3	2.55	1.20	4.50	77.0	3.47	59.3

$t_A/W^{1/3}$ (ms/lb$^{1/3}$)	t_A (ms)	P_r (psi)	$i_r/W^{1/3}$ (psi-ms/lb$^{1/3}$)	i_r (psi-ms)	$L_w/W^{1/3}$ (ft/lb$^{1/3}$)	L_w (ft)	Point
10.6	181	7.80	11.8	202	—	—	1
11.7	200	—	—	—	3.60	61.6	2
12.7	217	—	—	—	3.68	62.9	3
13.5	231	—	—	—	3.75	64.1	4
14.3	245	—	—	—	3.80	65.0	5

Step 4. Determine front wall loading.

a. $t_c = \frac{3S}{U_1}$ (eq. 4-5)

where $S = 12 \text{ ft} < \frac{50}{2}$

$$t_c = \frac{3(12)}{1.24} = 29 \text{ ms}$$

b. $t_{of} = \frac{2\, i_{s1}}{P_{so1}}$ (eq. 4-3)

$$t_{of} = \frac{2(94.9)}{3.50} = 54.2 \text{ ms}$$

c. $q_o = 0.275$ psi for $P_{so} = 3.50$ psi (fig. 4-66)

d. $P_{so} + C_D\, q_o = 3.50 + 1\ (0.275) = 3.775$ psi

e. $t_r = \frac{2\, i_r}{P_r}$ (eq. 4-7)

$$t_r = \frac{2(202)}{7.80} = 51.8 \text{ ms}$$

f. Construct the pressure-time curves shown in figure 4-67(a). The construction is shown in figure 4A-13. Note that the curve using P_r and t_r to check the accuracy has a larger impulse and therefore is not used.

Note:

For the computation of the blast loading on the structure, the arrival times are taken from when the blast wave strikes the front wall, i.e., $t_A = 0$ at point 1.

Step 5. Determine side wall loading.

The side wall is a one-way slab spanning vertically. Thus, a 1-foot wide vertical strip is considered, and, since the rise time on such a strip $\frac{L}{U} = \frac{1}{U}$ is very small, it will be taken as zero. The loading curve thus becomes the free-field side-on pressure curve reduced by the drag pressures. The wall strip closest to the front wall will experience the highest pressures; therefore, the blast wave parameters for point 1 will be used.

PRESSURE (psi)

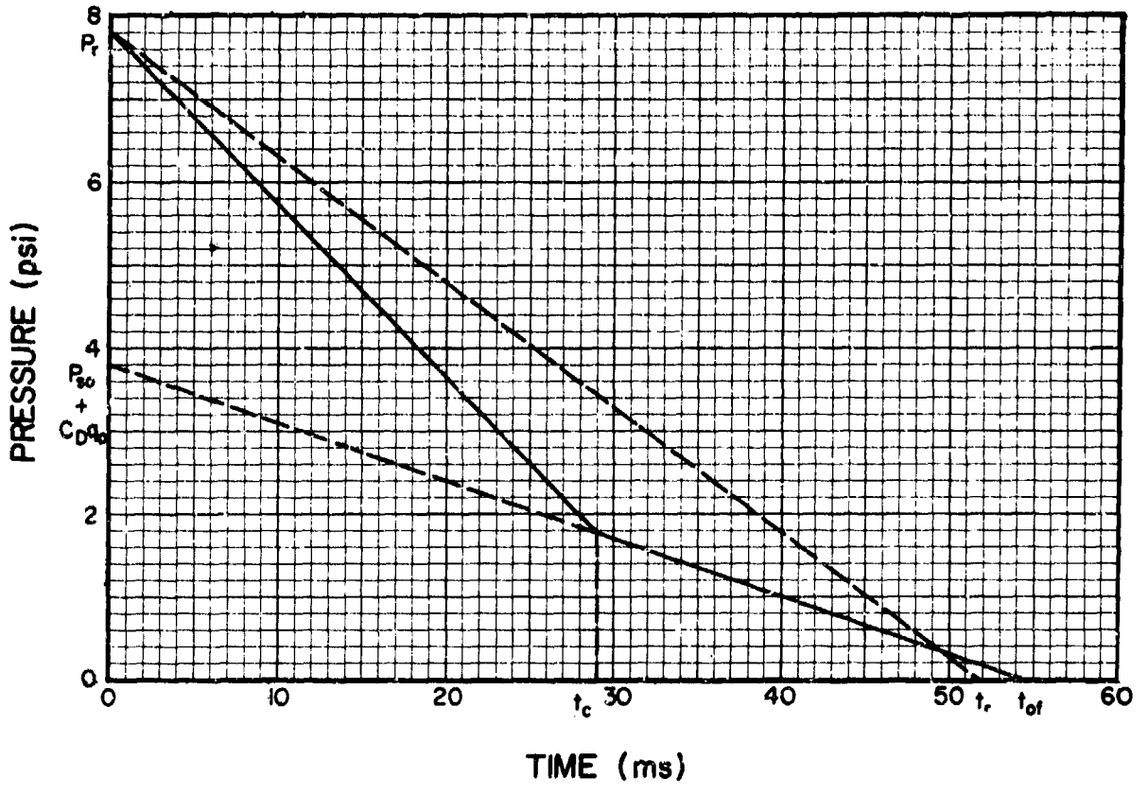


Figure 4A-13. Front wall loading.

e 4-67(a).
that the
a larger

tructure,
ve

Thus, a
he rise
taken as

ide-on
l strip
pressures;
be used.

2

a. $t_d = \frac{L}{U} = 0$

b. $t_{of} = \frac{2\, i_{sl}}{P_{sol}}$ (eq. 4-3)

$$t_{of} = \frac{2(94.9)}{3.50} = 54.2 \text{ ms}$$

c. $q_o = 0.275$ psi for $P_{so} = 3.50$ psi (fig. 4-66)

d. $P_{so} + C_D\, q_o = 3.50 - 0.40\ (0.275) = 3.39$ psi

where C_D is obtained from paragraph 4-14*d*.

e. Construct the pressure-time curve shown in figure 4-70. The construction is shown in figure 4A-14.

Step 6. Determine center roof span loading.

The roof is a one-way slab spanning in the direction of the blast wave propagation. Therefore, the equivalent uniform loading method will be used.

a. $\frac{L_{wb}}{L} = \frac{(L_{wb})\,3}{L}$ $\frac{62.9}{20} = 3.145$

$C_E = 0.890$ $\frac{D}{L} = 0.878$ (fig. 4-69)

b. $C_E P_{sob} = C_E P_{so3} = 0.890\ (2.90) = 2.58$ psi

$D = 0.878\ (20) = 17.56$ ft

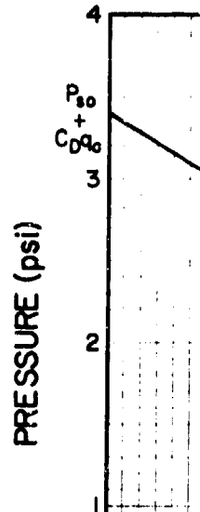
c. Denoting $t = 0$ as the instant that the shock front reaches the front wall:

$t_f = t_{A2} - t_{A1} = 200 - 181 = 19$ ms

$t_b = t_{A3} - t_{A1} = 217 - 181 = 36$ ms

d. $t_d = \frac{D}{U_2}$

$$t_d = \frac{17.56}{1.23} = 14.3 \text{ ms}$$



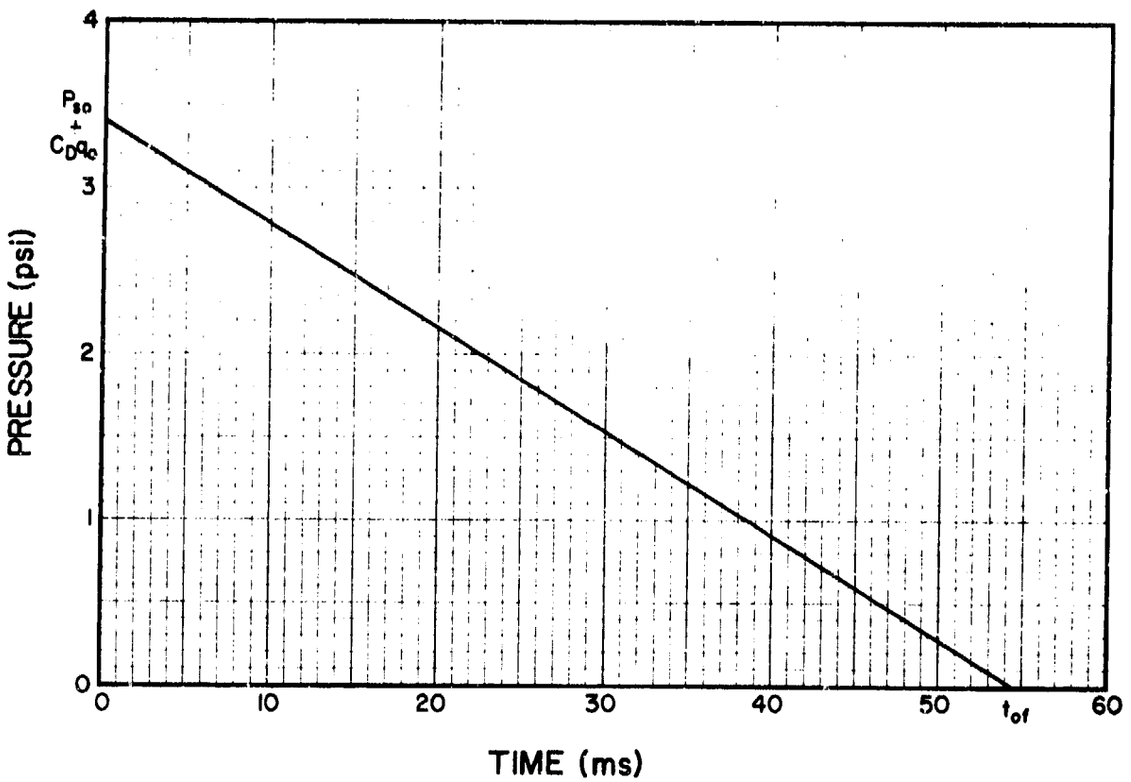


Figure 4A-14. Side wall loading.

e. $t_{of} = \frac{2\, i_{s3}}{P_{so3}}$ (eq. 4-3)

$$t_{of} = \frac{2(84.6)}{2.90} = 58.3 \text{ ms}$$

f. $q_{ob} = 0.158$ psi for $C_E P_{sob} = 2.58$ psi (fig. 4-66)

g. $C_E P_{sob} + C_D\, q_{ob} = 2.58 - 0.40\ (0.158) = 2.52$ psi (eq. 4-8)

where C_D is obtained from paragraph 4-14*c*.

h. Construct the pressure-time curve shown in figure 4-68. The construction is shown in figure 4A-15.

Step 7. Determine rear wall loading.

a. $\frac{L_{wb}}{L} = \frac{(L_{wb})\,5}{L} = \frac{65}{12} = 5.42$

$C_E = 0.940$ $\frac{D}{L} = 0.930$ (fig. 4-69 extrapolated)

b. $C_E P_{soe} = C_E P_{sc5} = 0.940\ (2.55) = 2.40$ psi

$D = 0.930\ (12) = 11.16$ ft

c. $t_b = t_{A4} - t_{A1} = 231 - 181 = 50$ ms

$t_e = t_{A5} - t_{A1} = 245 - 181 = 64$ ms

d. $t_d = \frac{D}{U_4}$

$$t_d = \frac{11.16}{1.21} = 9.22 \text{ ms}$$

e. $t_{of} = \frac{2\, i_{s5}}{P_{so5}}$ (eq. 4-3)

$$t_{of} = \frac{2(77)}{2.55} = 60.4 \text{ ms}$$

--66)

si (eq. 4-8)

ure 4-68.

ated)

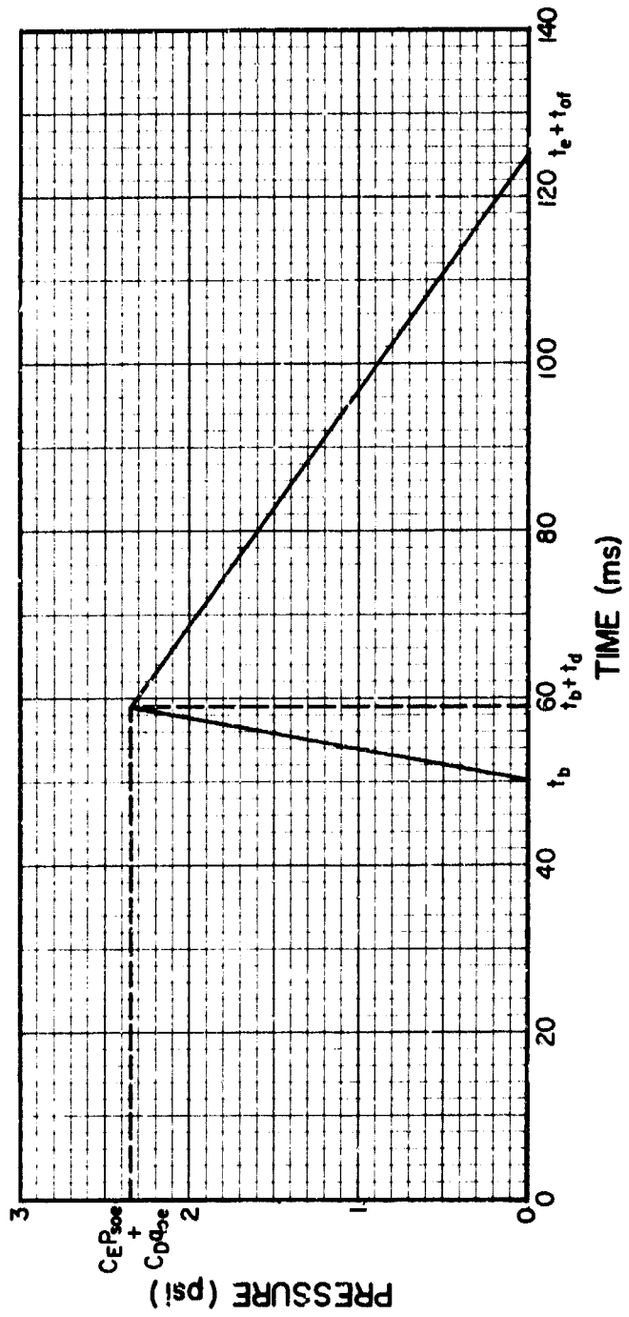


Figure 4A-15. Center roof span loading.

2

f. $q_{oe} = 0.15$ psi for $C_E P_{soe} = 2.40$ psi (fig. 4-66)

g. $C_E P_{soe} + C_D\, q_{oe} = 2.40 - 0.40\ (0.15) = 2.34$ psi

h. Construct the pressure-time curve shown in figure 4-70. The construction is shown in figure 4A-16.

PROBLEM 4A-8. PRESSURE INCREASE WITHIN A STRUCTURE

Problem: Determine the interior pressure-time curve for a structure with an opening in one of its walls and subjected to an applied blast pressure.

Procedure:

Step 1. Determine the pressure-time history of the applied blast pressure P acting on the wall surrounding the opening in the structure as presented in problem 4A-7. Also the area of the opening A_o and the volume of the structure V_o must be known.

Step 2. Divide the duration t_o of the applied pressure into n equal intervals Δt, each interval being approximately $t_o/10$ to $t_o/20$, and determine the pressures at the end of each interval.

Step 3. For each time interval compute the pressure differential $P-P_i$ where P_i is the interior pressure. Obtain the leakage pressure coefficient C_L for each $P-P_i$ from figure 4-72.

Step 4. Calculate ΔP_i from

$$\Delta P_i = C_L\left(\frac{A_o}{V_o}\right)\Delta t \quad \text{(eq. 4-9)}$$

using the proper values for C_L and Δt. Add ΔP_i to P_i for the interval being considered to obtain the new value of P_i for the next interval.

$C_E P_{so}$ + $C_D q_{o}$

PRESSURE (psi)

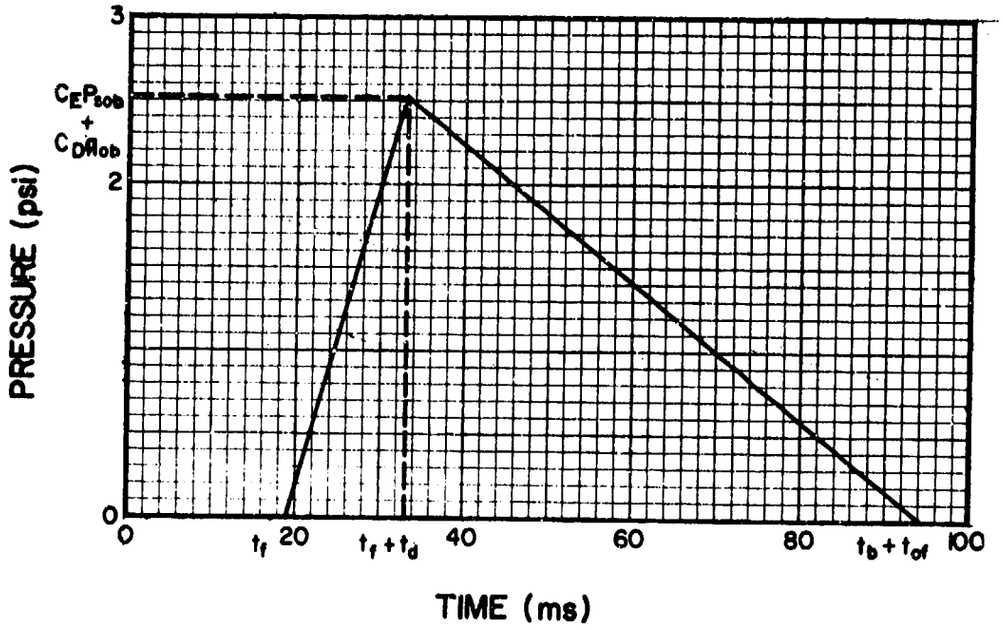


Figure 4A-16. Rear wall loading.

Step 5. Repeat steps 3 and 4 for each interval using the proper values of P and P_i. Plot curve of pressure buildup.

Note:

When $P-P_i$ becomes negative, the value of C_L must be taken as negative also.

EXAMPLE 4A-8. PRESSURE INCREASE WITHIN A STRUCTURE

Required: Interior pressure-time curve for a structure with an opening in one of its walls and subjected to an applied blast pressure.

Solution:

Step 1. The curve of the applied blast pressure P for the wall in question is shown in figure 4A-17. (Only the positive phase of the blast wave is considered in this example.)

Area of opening - A_o = 3 ft by 3 ft = 9.0 sq ft.

Volume of structure - V_o = 10 ft by 10 ft by 10 ft

V_o = 1,000 cu ft

Step 2. t_o = 55 ms

Use $n = 10$ $\Delta t = 5.5$ ms

For the first interval, $P = 3.5$ psi at $t = o$

Step 3. $P_i = o$ for the first interval

$$\therefore P-P_i = 3.50 - 0 = 3.50 \text{ psi}$$

$$C_L = 8.75 \quad \text{(fig. 4-72)}$$

Step 4. $\Delta P_i = C_L \frac{A_o}{V_o} \Delta t$ (eq. 4-9)

$$\Delta P_i = 8.75 \left(\frac{9.0}{1000}\right) (5.5) = 0.433 \text{ psi}$$

$$\therefore \text{new } P_i = 0 + 0.433 = 0.433 \text{ psi}$$

per values

be taken

an opening
ure.

wall in
ve phase

Step 5. The remainder of the analysis is presented in tabular form below and the pressure buildup within the structure is plotted in figure 4A-17.

$t^{(1)}$ (ms)	P (psi)	P_i (psi)	$P-P_i$ (psi)	C_L (psi-ft/ms)	ΔP_i (psi)
0	3.50	0	3.50	8.75	0.433
5.5	3.15	0.433	2.72	7.00	0.347
11.0	2.80	0.780	2.02	5.45	0.270
16.5	2.45	1.05	1.40	3.78	0.187
22.0	2.10	1.24	0.86	2,32	0.115
27.5	1.75	1.36	0.39	1.05	0.052
33.0	1.40	1.41	-0.01	-0.027	-0.0013
38.5	1.05	1.41	-0.36	-0.972	-0.048
44.0	0.70	1.36	-0.66	-1.78	-0.088
49.5	0.35	1.27	-0.92	-2.48	-0.123
55.0	0	1.14	—	—	

(1) Maximum P_i occurs between t = 27.5 and t = 33.0 ms

PROBLEM 4A-9. PRIMARY FRAGMENTS FROM CASED CYLINDRICAL CHARGES

Problem: Determine the striking velocity of primary fragments, the weight of the largest fragment, and the number of fragments having a weight greater than a specified amount.

Procedure:

Step 1. Determine the physical properties of the explosive charge including the type and density of the explosive and the dimensions of the explosive charge.

Step 2. Calculate the total weight of the explosive W and the total weight of the cylindrical portion of the metal casing W_c.

Also calculate the ratio of the explosive weight to the casing weight W/W_c.

Step 3. Determine the Gurney Energy Constant $(2E')^{\frac{1}{2}}$ for the explosive charge from table 4-2. With this value and the value of W/W_c from step 2, calculate the initial velocity v_o of the primary fragments from

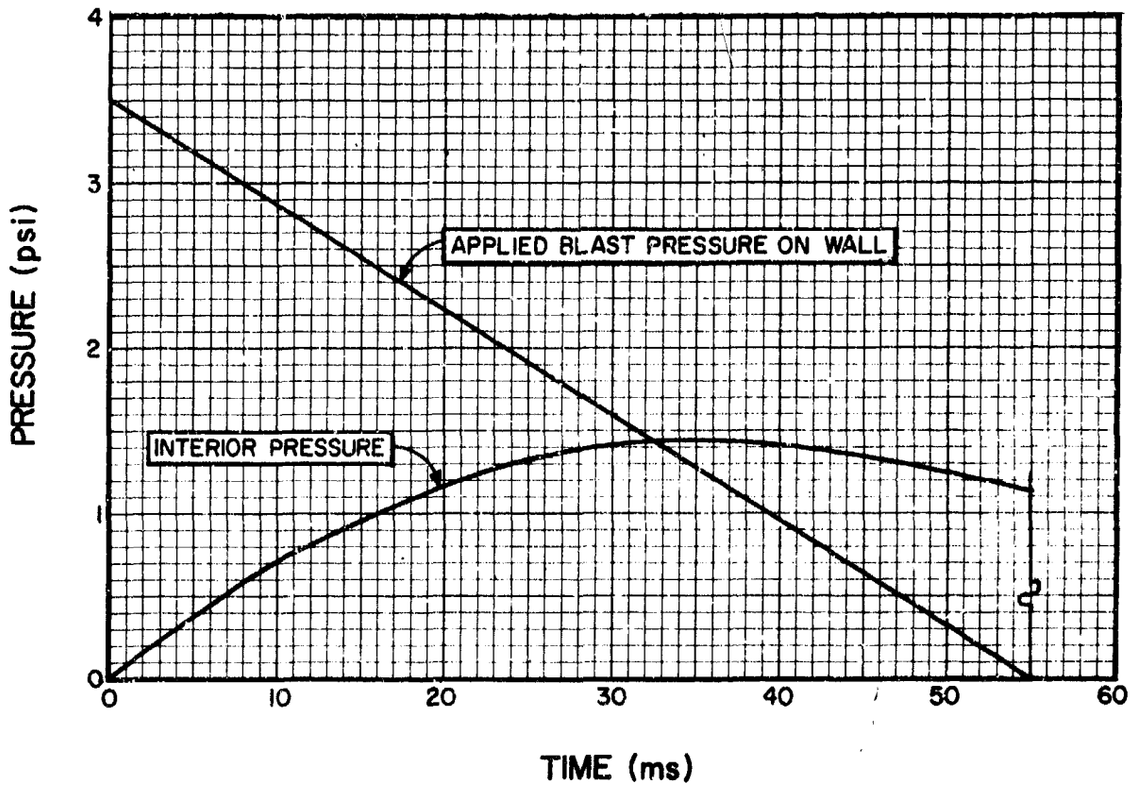


Figure 4A-17. Pressure-time curves.

$$v_o = (2E')^{1/2}\left[\frac{W/W_c}{1 + W/2W_c}\right]^{1/2} \quad \text{(eq. 4-10)}$$

or from figure 4-73.

tep 4

Step 4. Determine the value of the constant B for the explosive charge from table 4-2. With this value and the values of t_c and d_i from step 1, calculate the fragment distribution parameter M_A from

$$M_A = B\, t_c^{5/6}\, d_i^{1/3}\left[1 + \frac{t_c}{d_i}\right] \quad \text{(eq. 4-13)}$$

tep 5

Step 5. With the value of W_c from step 2 and M_A from step 4 calculate the weight of the largest fragment from

$$W_f = \left[M_A \quad \ln\left(\frac{8W_c}{M_A^{\,2}}\right)\right]^{1/2} \quad \text{(eq. 4-14)}$$

tep 6

Step 6. For the distance traveled by the fragments R_f, calculate the striking velocity v_s of the largest fragment from

$$v_s = v_o\, e^{\left(-0.004\, R_f/W_f^{1/3}\right)} \quad \text{(eq. 4-15)}$$

or from figure 4-74. In some cases it may be necessary to determine the striking velocity of the smaller fragments since the change in velocity is less. However, if the distance traveled is less than 20 feet, the striking velocity is taken as equal to the initial velocity for all size fragments.

60

tep 7

Step 7. Calculate the number of fragments having a weight greater than a critical weight which may cause detonation of an acceptor charge (ch. 3) and/or perforate or cause spalling of a structural element (ch. 8) from

$$\ln N_f = \ln\left[\frac{8W_c}{M_A^{\,2}}\right] - \frac{W_f^{1/2}}{M_A} \quad \text{(eq. 4-12)}$$

2

EXAMPLE 4A-9. PRIMARY FRAGMENTS FROM CASED CYLINDRICAL CHARGES

Required: Striking velocity of a primary fragment for close-in effects the weight of the largest fragment and the number of fragments having a weight greater than 1-1/2 ounces.

Solution:

Step 1. Given:
Type of explosive - TNT
Density of explosive - 0.0558 lb/in^3
Mild steel casing
Density of casing - 0.281 lb/in^3
Thickness of casing - t_c = 0.5 inch
Inside diameter of casing - d_i = 12 inches
Length of charge - 40 inches

Step 2.

$$W = \frac{\pi (12)^2 (40)(0.0558)}{4} = 252 \text{ lbs}$$

$$W_c = \frac{\pi \left[(13)^2 - (12)^2\right](40)(0.281)}{4} = 221 \text{ lbs}$$

$$\frac{W}{W_c} = \frac{252}{221} = 1.14$$

Step 3. For TNT in mild steel casing, $(2E')^{\frac{1}{2}} = 6{,}940$ (table 4-2).

$$v_o = (2E')^{\frac{1}{2}} \left[\frac{\frac{W}{W_c}}{1 + \frac{W}{2W_c}}\right]^{\frac{1}{2}} \quad \text{(eq. 4-10)}$$

$$v_o = 6{,}940 \left[\frac{1.14}{1 + \frac{1.14}{2}}\right]^{\frac{1}{2}} = 5{,}910 \text{ ft/sec}$$

CHARGES

e-in effects
ments having

Step 4. For TNT in mild steel casing B = 0.30 (table 4-2).

$$M_A = B\, t_c^{5/6}\, d_i^{1/3} \left(1 + \frac{t_c}{d_i}\right) \quad \text{(eq. 4-13)}$$

$$= 0.30\,(0.5)^{5/6}\,(12)^{1/3}\left(1 + \frac{0.5}{12}\right) = 0.402$$

Step 5. Weight of largest fragment.

$$W_f = \left[M_A \ln\left(\frac{8\,W_c}{M_A^2}\right)\right]^{1/2} \quad \text{(eq. 4-14)}$$

$$\ln\left(\frac{8\,W_c}{M_A^2}\right) = \ln\left(\frac{8(221)}{(0.402)^2}\right) = 9.29$$

$$W_f = \left[0.402\,(9.29)\right]^{1/2} = 1.93 \text{ oz.}$$

s

Step 6. For R_f less than 20 feet, $v_s \simeq v_o$

$$v_s = v_o = 5910 \text{ ft/sec}$$

Step 7. Number of fragments having a weight greater than 1-1/2 ounces.

ble 4-2).

$$\ln N_f = \ln\left[\frac{8\,W_c}{M_A^2}\right] - \frac{W_f^{1/2}}{M_A} \quad \text{(eq. 4-12)}$$

$$\ln N_f = \ln\left[\frac{8(221)}{(0.402)^2}\right] - \frac{(1.5)^{1/2}}{0.402} = 6.25$$

$$N_f = 520 \text{ fragments}$$

CHAPTER 5

STRUCTURAL BEHAVIOR OF REINFORCED CONCRETE

Section I. ULTIMATE STRENGTH

5–1. General

a. Depending upon the magnitudes of the blast output and deflections permitted, one of three types of reinforced concrete cross sections can be utilized in the design: (1) Type I where the concrete cover over the reinforcement on both surfaces of the element remains intact, (2) Type II where the concrete cover over the compression reinforcement is crushed but still connected to the element, and (3) Type III where the concrete cover on both surfaces of the element is disengaged. All three cross sections are illustrated in figure 5–1.

b. Elements which are designed using the full cross section (Type I) usually are encountered in those structures or portions of structures designed to resist the blast output at the intermediate- and/or low-pressure design ranges. This type of cross section is utilized in elements with maximum deflections corresponding to support rotations less than 2 degrees. Maximum strength of an element is obtained with a full cross section. Type I elements may be reinforced on either one or both faces.

c. Elements which undergo support rotations greater than 2 degrees exhibit crushing of the concrete cover over the compression reinforcement (Type II). This failure results in a transfer of the compression stresses from the concrete to the compression reinforcement which, in turn, results in a loss in strength.

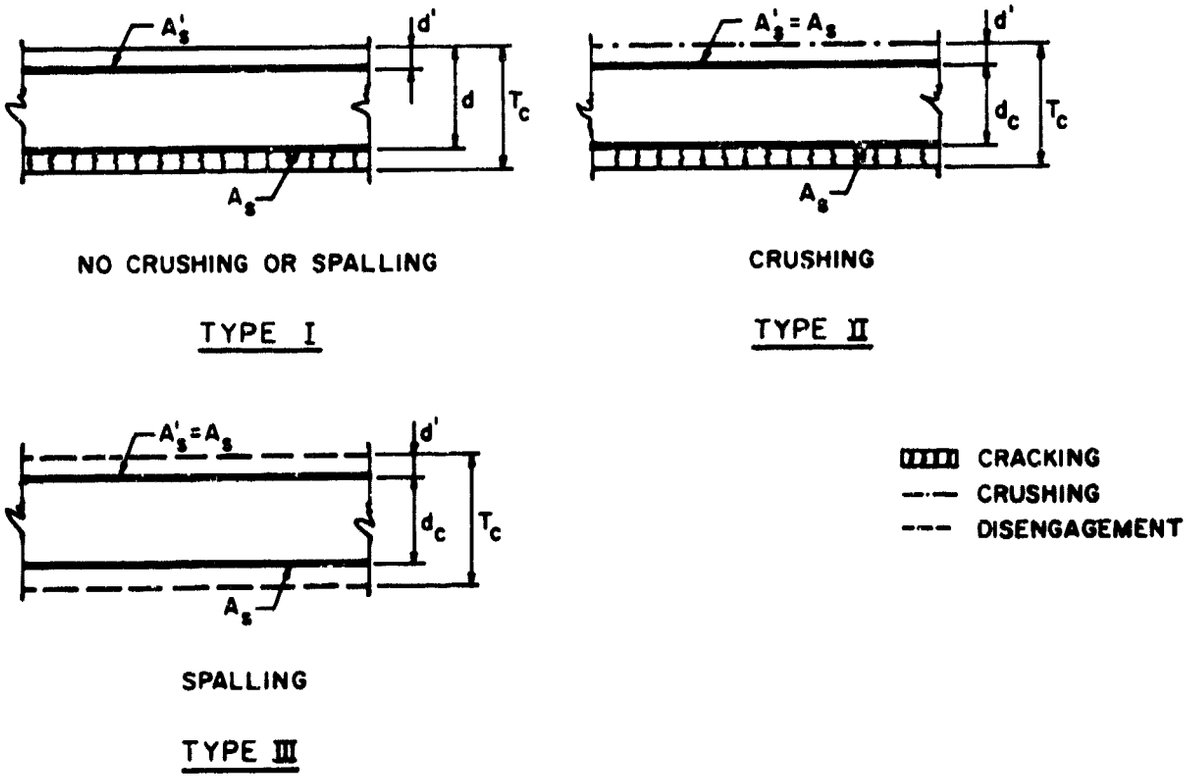


Figure 5–1. Typical reinforced concrete cross sections.

d. Sufficient compression reinforcement must be available to fully develop the tension steel (tension and compression reinforcement must be equal), and lacing reinforcement must be present to prevent buckling of the compression steel and disengagement of the concrete between the layers of reinforcement. Elements which sustain crushing of the concrete without any additional disengagement of the concrete cover are encountered in structures at the intermediate- and low-pressure design ranges when the maximum deflections conform to support rotations greater than 2 degrees but less than 5 degrees.

e. Although the ultimate strength of elements with Type III cross sections is no less than that of elements with Type II, the overall capacity to resist the blast output is reduced. The spalling of the concrete cover over both layers of reinforcement, caused by either the direct transmission of the high pressures through the element at the high-pressure range or large deflections at the intermediate- and low-pressure ranges, produces a loss of capacity due to the reduction in the concrete mass.

f. A more detailed treatment of the phenomena of crushing and spalling is presented in chapter 7.

g. The ultimate strength of reinforced concrete sections may be calculated in accordance with the ultimate strength design methods of the American Concrete Institute Standard Building Code Requirements for Reinforced Concrete (hereafter referred to as the ACI Building Code). The capacity reduction factor ϕ which has been established for conventional static load conditions was omitted from the equations for ultimate resisting moment. However, in the equations involving shear stress, the ϕ factor was maintained to insure against a premature failure due to shear which would substantially reduce the overall blast-resistant capacity of the element. Safety or reliability of the protective structure is inherent in the establishment of the magnitude of the blast output for the donor charge, and in the criteria specified for deflection, support rotation, or fragment velocity. Other permissible departures from the criteria for static or quasi-static loadings are described below.

h. Although certain formulae for elements constructed with conventional weight concrete are given in the following paragraphs of this chapter, more detailed information and design aids are given in the bibliography. Because tests have not yet been conducted to determine the response of lightweight concrete elements designed for the high- and intermediate-pressure ranges, the pertinent formulae for this type of concrete are not included in the manual. However, lightweight concrete may be utilized for structures designed for the low-pressure range, but the reduction in mass from conventional weight concrete must be accounted for in the design to maintain the blast-resistant capacity of the structure.

5–2. Ultimate Static Moment Capacity

a. Cross Section Type I.

(1) The ultimate unit resisting moment M_u of a rectangular section of width b with tension reinforcement only is given by

$$M_u = \frac{A_s f_s}{b}\left(d - \frac{a}{2}\right) \qquad \text{Equation 5–1}$$

where A_s = area of tension reinforcement within the width b
f_s = static design stress for reinforcement (para 5–6)
d = distance from extreme compression fiber to centroid of tension reinforcement
a = depth of equivalent rectangular stress block = $\dfrac{A_s f_s}{0.85 b f_c'}$
b = width of compression face
f_c' = static ultimate compressive strength of concrete

The reinforcement ratio p is defined as

$$p = \frac{A_s}{bd} \qquad \text{Equation 5–2}$$

(2) To insure against sudden compression failures, the reinforcement ratio p must not exceed 0.75 of the ratio p_b which produces balanced conditions at ultimate strength and is given by

$$p_b = \frac{0.85 K_1 f_c'}{f_s}\left(\frac{87{,}000}{87{,}000 + f_s}\right) \qquad \text{Equation 5–3}$$

where $K_1 = 0.85$ for f_c' up to 4,000 psi and is reduced 0.05 for each 1,000 psi in excess of 4,000 psi.

(3) Figure 5–2 is a universal design chart giving the ultimate moment capacities of rectangular sections with tension reinforcement only for all values of p, f_c', and f_s.

(4) For a rectangular section of width b with compression reinforcement, the ultimate unit resisting moment is

$$M_u = \frac{(A_s - A_s')f_s}{b}\left(d - \frac{a}{2}\right) + \frac{A_s' f_s}{b}(d - d') \qquad \text{Equation 5–4}$$

where A_s' = area of compression reinforcement within the width b
d' = distance from extreme compression fiber centroid of compression reinforcement
a = depth of equivalent rectangular stress block = $\dfrac{(A_s - A_s')f_s}{0.85 b f_c'}$

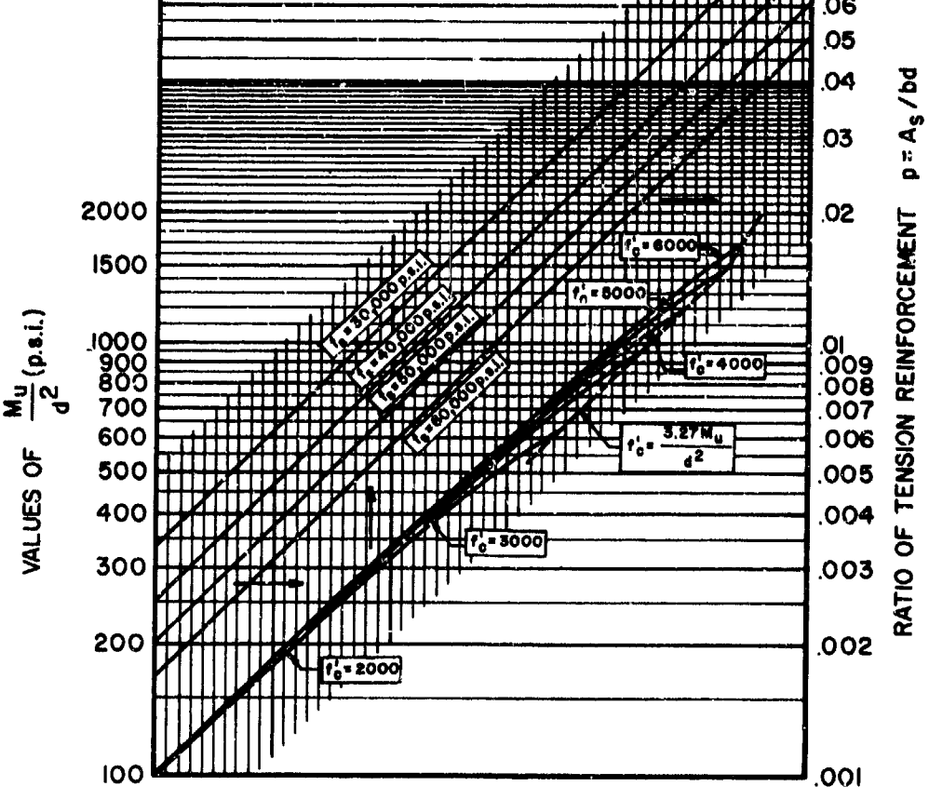


Figure 5–2. Moment capacity of rectangular sections without compression reinforcement.

The reinforcement ratio p' is

$$p' = \frac{A_s'}{bd} \qquad \textbf{Equation 5–5}$$

(5) Equation 5–4 is valid only when the compression steel reaches the value f_s at ultimate strength, and this condition is satisfied when

$$p - p' \geq 0.85 K_1 \frac{f_c' d'}{f_s d} \left(\frac{87{,}000}{87{,}000 - f_s} \right) \qquad \textbf{Equation 5–6}$$

(6) If $p - p'$ is less than the value given by equation 5–6 or when compression steel is neglected, the calculated ultimate unit resisting moment should not exceed that given by equation 5–1. The quantity $p - p'$ must not exceed 0.75 of the value of p_b given in equation 5–3.

b. Cross Section Types II and III.

(1) The ultimate unit resisting moment of Type II and Type III rectangular sections of width b is

$$M_u = \frac{A_s f_s d_c}{b} \qquad \textbf{Equation 5–7}$$

where A_s = area of tension or compression reinforcement within the width b

d_c = distance between the centroids of the compression and the tension reinforcement

The reinforcement ratios p and p' are equal to

$$p = p' = \frac{A_s}{bd_c} \qquad \textbf{Equation 5–8}$$

(2) The above moment capacity can be obtained only when lacing reinforcement is provided to maintain the integrity of the element when larger deflections are encountered.

c. Minimum Flexural Reinforcement. To insure the proper structural behavior and also to prevent excessive cracking and deformations under conventional loadings,

the minimum areas of flexural reinforcement listed in table 5–1 are recommended.

Table 5–1. Minimum Area of Flexural Reinforcement

Pressure design range	Reinforcement	Two-way elements	One-way elements
Intermediate and low	Main	$A_s=0.0025bd$	$A_s=0.0025bd$
	Other	$A_s=0.0018bd$	$A_s+A_s'=0.0020bT_s$
High	Main	$A_s=A_s'=0.0025bd_c$	$A_s=A_s'=0.0025bd_c$
	Other	$A_s=A_s'=0.0018bd_c$*	$A_s=A_s'=0.0018bd_c$*

* but not less than $A_s/4$ used in main direction

5–3. Ultimate Static Shear Capacity

a. Diagonal Tension

(1) The ultimate shear stress v_u, as a measure of diagonal tension, is computed for Type I sections from

$$v_u=\frac{V_u}{bd} \qquad \textbf{Equation 5–9a}$$

and for Type II and III sections from

$$v_u=\frac{V_u}{bd_c} \qquad \textbf{Equation 5–9b}$$

where V_u is the total shear on a width b at the section a distance d (Type I) or d_c (Types II and III) from the face of the support. The shear at sections between the face of the support and the section d or d_c therefrom need not be considered critical.

(2) The shear stress permitted on an unreinforced web is limited to

$$v_c=\phi[1.9\sqrt{f_c'}+2500p]\leq 2.28\phi\sqrt{f_c'} \qquad \textbf{Equation 5–10}$$

where ϕ is the capacity reduction factor and is equal to 0.85 for all cross sections. The above expression for the maximum value of v_c corresponds to a 20 percent increase in the 1.9 factor. This value of 2.28 is less than the 3.5 factor of the ACI Building Code and is recommended, in addition to the ϕ factor, to further insure against a premature failure of an element due to excessive shear stresses.

(3) Wherever the ultimate shear stress v_u exceeds the shear capacity v_c of the concrete, shear reinforcement must be provided to carry the excess. For elements with a Type I cross section, stirrups or lacing may be used to resist the excess, while only lacing is used to provide the additional shear capacity in elements whose cross section conforms to Type II or Type III. When stirrups are used, they should be provided for a distance d beyond the point theoretically required, and, between the face of the support and the section at a distance d from the support, must be the same as required at that section. When lacing is used, it should be made continuous in at least one direction and carried past the face of the support in all cases.

(4) The required area of stirrups for Type I cross sections is calculated using

$$A_s=\frac{(v_u-v_c)b_s s_s}{\phi f_s(\sin\alpha+\cos\alpha)} \qquad \textbf{Equation 5–11a}$$

while for cross sections conforming to Types I, II, and III, the required area of lacing reinforcement is

$$A_s=\frac{(v_u-v_c)b_l s_l}{\phi f_s(\sin\alpha+\cos\alpha)} \qquad \textbf{Equation 5–11b}$$

where A_s = total area of stirrups or lacing reinforcement in tension within a width b_s or b_l and a distance s_s or s_l

v_u-v_c = excess shear stress except as noted below. The ultimate shear stress v_u is determined from either equation 5–9a or 5–9b depending upon the type of cross section.

b_s = width of concrete strip in which the diagonal tension stresses are resisted by stirrups of area A_s

b_l = width of concrete strip in which the diagonal tension stresses are resisted by lacing of area A_s

s_s = spacing of stirrups in the direction parallel to the longitudinal reinforcement

s_l = spacing of lacing in the direction parallel to the longitudinal reinforcement

α = angle formed by the plane of the stirrups or lacing and the plane of the longitudinal reinforcement

(5) In order to insure the full development of the flexural reinforcement by preventing shear failure, the following limitations should be considered in the design of either stirrups or lacing:

(*a*) The excess shear stress v_u-v_c used in equations 5–11a and 5–11b should conform to the following limitations:

Limits	*Excess Shear Stress v_u-v_c*	
	Stirrups	*Lacing*
$v_u\leq v_c$	0	v_c
$v_c<v_u\leq 2v_c$	v_u-v_c	v_c
$v_u>2v_c$	v_u-v_c	v_u-v_c

(*b*) The ultimate shear stress v_u must not exceed $10\phi\sqrt{f_c'}$ in sections using stirrups. In sections using lacing there is no restriction on v_u because of the continuity provided by this type of shear reinforcement.

(*c*) Wherever stirrups are required ($v_u>v_c$), the area A_s should not be less than $0.0015bs_s$, and for

lacing reinforcement, the area A_v should be at least equal to $0.0015bs_l$.

(*d*) Where stirrups are required, they should be spaced so that every 45-degree line, representing a potential diagonal crack and extending from mid-depth $\frac{d}{2}$ to the longitudinal tension bars, is crossed by at least one line of reinforcement. When the shear stress v_u exceeds $6\phi\sqrt{f_c'}$, every such line should be crossed by at least two lines of reinforcement.

(6) The maximum spacing of lacing is limited to d_c or 24 inches, whichever is smaller, for all cases.

b. Direct Shear.

(1) Even though an element is reinforced for diagonal tension, failure due to direct shear is theoretically possible. Failure of this type is characterized by the rapid propagation of a vertical crack through the depth of the member and is usually of concern at the supports where the maximum stress occurs.

(2) In those elements whose cross section conforms to Type I and with support rotations less than 2 degrees, the magnitude of the ultimate direct shear force V_d which can be resisted by the concrete is given by

$$V_d = 0.18 f_c' bd \qquad \textbf{Equation 5–12}$$

(3) When the support rotation of an element exceeds 2 degrees, the concrete between the reinforcement is severely cracked and thereby incapable of transferring the direct shear stresses produced by the applied load. In these laced elements, direct shear stresses at the supports are resisted by diagonal bars which extend from the element into the supports. The required area of the diagonal bars is determined from

$$A_d = \frac{V_s b}{f_s \sin\alpha} \qquad \textbf{Equation 5–13}$$

where A_d = total area of diagonal bars at the support within a width b
V_s = shear at the support on a unit width b
α = angle formed by the plane of the diagonal reinforcement and the plane of the longitudinal reinforcement

(4) Equation 5–13 assumes that the diagonal bar is resisting the shear either in tension or compression. In some elements it may be desirable to use both tension and compression bars at any one section thereby reducing the required area of each bar to one half that specified in equation 5–13. The minimum size of the diagonal bars should conform to that shear force which will produce a concrete stress equal to the ultimate shear capacity v_c of the element.

5–4. Ultimate Static Bond Capacity and Anchorage

a. In flexural elements without lacing and where the tension reinforcement is parallel to the compression face, the ultimate flexural bond stress u_u at any cross section is determined from

$$u_u = \frac{V_u}{\phi \Sigma o j d} \qquad \textbf{Equation 5–14}$$

where j = ratio of distance between centroids of compression and tension forces to the depth d
Σo = sum of the perimeters of the effective bars crossing the section on the tension side when size is uniform; for mixed sizes, substitute $4A_s$ (where A_s is the total steel area) divided by the largest bar diameter

b. Critical sections occur at the face of the support, where tension bars terminate within the span and at the points of inflection.

c. To prevent bond failure or splitting, the calculated tension or compression in any bar at any section must be developed on each side of that section by proper embedment length, end anchorage, or, for tension only, hooks. Anchorage or development bond stress u_u is computed as

$$u_u = \frac{F_0}{\Sigma o L_0} \qquad \textbf{Equation 5–15}$$

where F_0 = bar force determined from M
M = bending moment at the section
L_0 = embedment length of reinforcing bars

d. Neither the flexural nor the anchorage bond stresses should exceed the limits prescribed in table 5-2, where D_0 is the nominal diameter of the reinforcing bars, except that flexural bond stress need not be considered in compression nor in those cases of tension where the anchorage bond stress is less than 0.8 of the permissible value.

e. Recent tests of laced elements have indicated that if continuity of the lacing and flexural reinforcement is maintained throughout the element, and all flexural and lacing bars are anchored and/or lapped 40-bar diameters, flexural and anchorage bond stresses need not be evaluated. Details indicating the proper anchorage of laced elements are given in chapter 9.

5–5. Dynamic Strengths

a. Under the rapid rates of strain that occur in structural elements subjected to blast loads, both the reinforcement and the concrete exhibit higher strengths than in the case of statically loaded elements. These increased stresses or dynamic strengths are used to calculate the element's dynamic resistance to the applied blast loads.

b. Pictorial representations of typical stress-strain curves for concrete and reinforcing bars are shown in figure 5–3. The solid curves show the stress-strain relationship for the material when tested at the standard ASTM rate of strain. At higher strain rates, the ma-

o the compression
ess u_u at any cross

Equation 5–14

n centroids of com-
orces to the depth d
f the effective bars
n the tension side
; for mixed sizes,
A_s is the total steel
argest bar diameter
face of the support,
in the span and at

tting, the calculated
t any section must
section by proper
or, for tension only,
bond stress u_u is

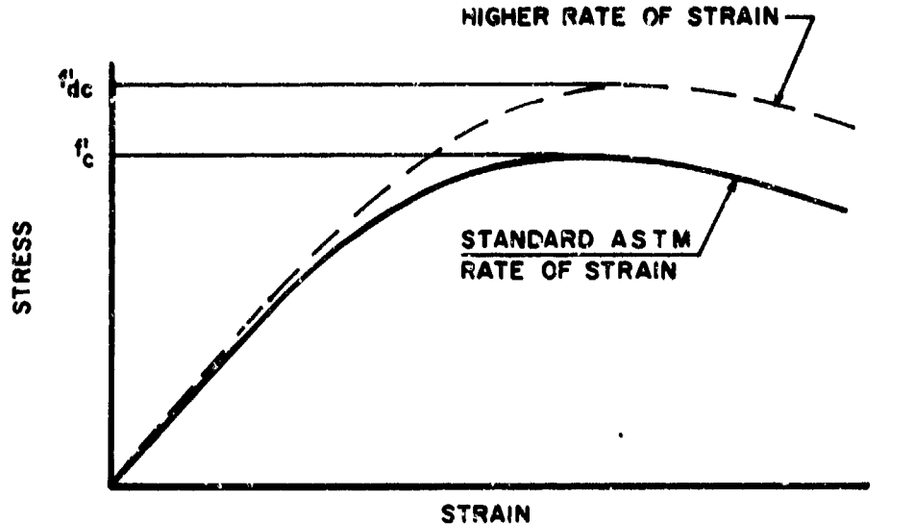
Equation 5–15

om M
section
einforcing bars
e anchorage bond
prescribed in table
er of the reinforcing
tress need not be
ose cases of tension
is less than 0.8 of

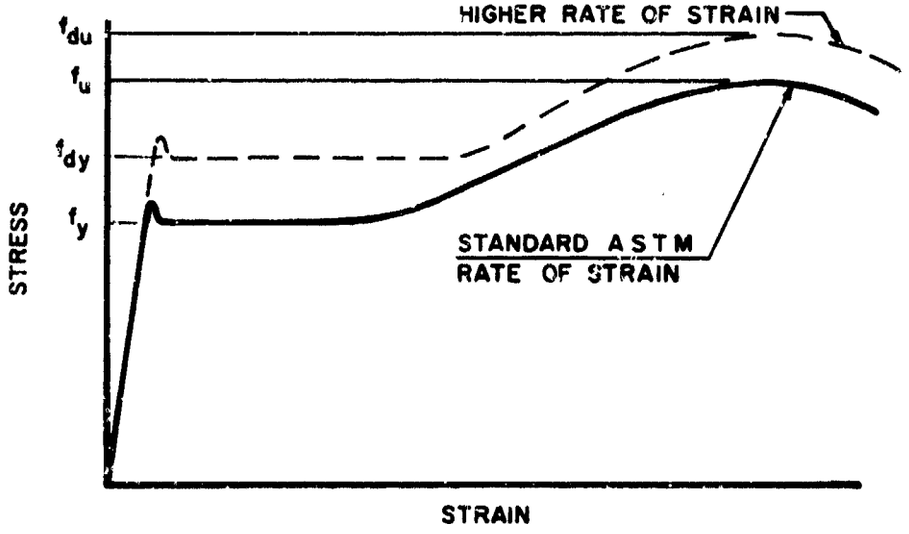
have indicated that
ral reinforcement is
t, and all flexural
l/or lapped 40-bar
bond stresses need
the proper anchor-
hapter 9.

rain that occur in
last loads, both the
bit higher strengths
od elements. These
engths are used to
esistance to the ap-

ypical stress-strain
bars are shown in
w the stress-strain
sted at the standard
rain rates, the ma-



a) CONCRETE



b) REINFORCING BARS

Figure 5–9. Stress-strain curves for concrete and reinforcing bars.

terial
curves
f_c'
f_{dc}'
f_y
f_{dy}
f_u
f_{du}

terial strengths increase as indicated by the dotted curves. Definitions of the symbols are as follows:

f_c' = static ultimate compressive strength of concrete
f_{dc}' = dynamic ultimate compressive strength of concrete
f_y = static yield stress of reinforcement
f_{dy} = dynamic yield stress of reinforcement
f_u = static ultimate stress of reinforcement
f_{du} = dynamic ultimate stress of reinforcement

c. The dynamic increase factor, denoted as DIF and equal to the ratio of the dynamic to static stresses, depends upon the rate of strain of the element, increasing as the strain rate increases. In flexural elements this increase in capacity is primarily a function of the rate of strain of the reinforcement as shown in figure 5–4 and, in particular, the time-to-reach yield of the reinforcing steel. Because of the increased magnitude of the blast loads and subsequent increase in strain rate, the dynamic increase factors for elements sub-

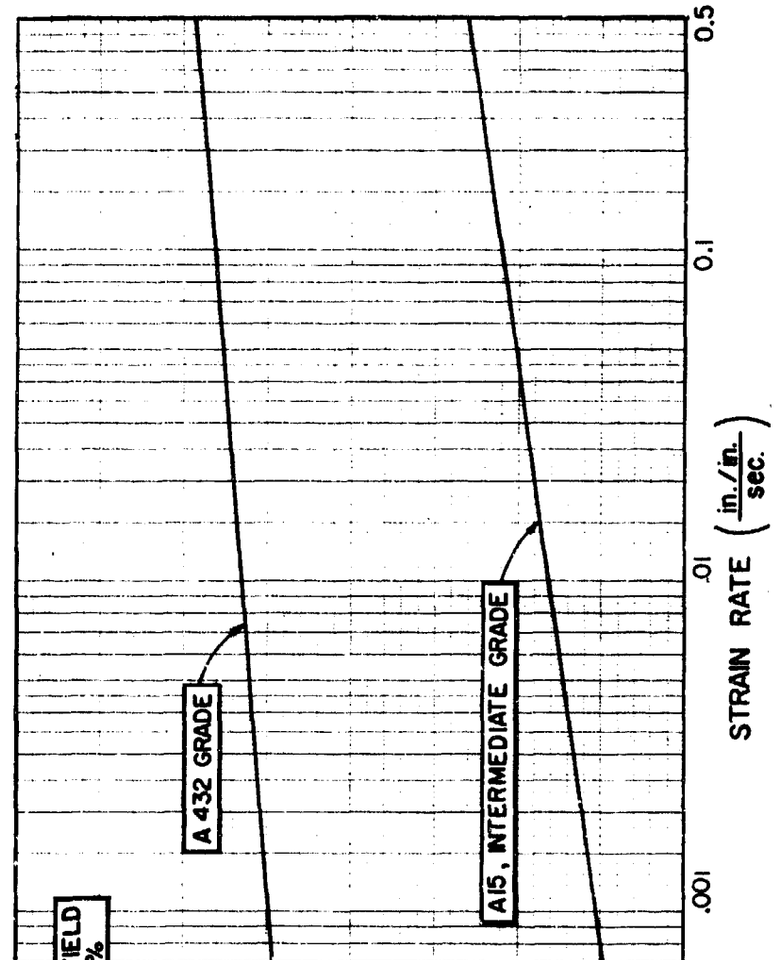


Figure 5–4. Recommended dynamic yield stresses for reinforcing steels.

jected to the high-pressure effects of a detonation are higher than those for elements subjected to the intermediate- or low-pressure range effects.

d. Dynamic increase factors for concrete and reinforcing steel are listed in table 5–3 as a function of the structure location and type of stress being considered. It is recommended that no dynamic stress increase be considered when determining shear or bond capacities nor when calculating quantities of lacing, stirrups, or diagonal bars.

e. The dynamic moment capacities of concrete sections are determined from the equations listed in paragraph 5–2 by substituting the dynamic design stress for the reinforcement f_{ds} for f_s and the dynamic

Table 5–8. Al

Reinforcing bar location
Tension:
Top bars*
Bars other than top bars
Compression

* Horisontal bars so the member below th
D_p (in.)
f_c' (psi)

Table 5–

Stresses
Reinforcing steel:
Bending
Shear
Concrete:
Compression
Diagonal tensi
Direct shear
Bond

ultimate compre
as applicable, wh

$f_{dc}' = (DIF)f$

$f_{ds} = (DIF)f$

5–6. Allowab

a. The behavi
blast loading dep
ductility of its
ductile elements,
peak strengths t
less than that ne
abruptly with li
range. Reinforced
ductile reinforcen
terial.

b. Reinforcing
Society for Testi
may usually be c
in sizes up to N
(No's. 14S and 1
available. Bends,

Table 5–2. Allowable Bond Stresses (Nonlaced Sections)

Reinforcing bar location	Bar Deformations	
	ASTM A305	ASTM A408
Tension:		
Top bars*	$\frac{6.7\sqrt{f_c'}}{D_0}$ nor 560 psi	$4.2\sqrt{f_c'}$
Bars other than top bars	$\frac{9.5\sqrt{f_c'}}{D_0}$ nor 800 psi	$6\sqrt{f_c'}$
Compression	$13\sqrt{f_c'}$ nor 800 psi	$13\sqrt{f_c'}$ nor 800 psi

* Horizontal bars so placed that more than 12 inches of concrete is cast in the member below the bar.
D_0 (in.)
f_c' (psi)

Table 5–3. Dynamic Increase Factors (DIF)

Stresses	Pressure design range	
	High	Intermediate and low
Reinforcing steel:		
Bending	1.20	1.10
Shear	1.00	1.00
Concrete:		
Compression	1.25	1.25
Diagonal tension	1.00	1.00
Direct shear		1.10
Bond		1.00

ultimate compressive strength of concrete f_{dc}' for f_c', as applicable, where

$$f_{dc}' = (DIF) f_c' \qquad \textbf{Equation 5–16a}$$

$$f_{ds} = (DIF) f_s \qquad \textbf{Equation 5–16b}$$

5–6. Allowable Stresses

a. The behavior of structural elements subjected to blast loading depends upon the ultimate strength and ductility of its materials. The required strength of ductile elements, which can maintain their peak or near-peak strengths through large strains, is considerably less than that necessary for brittle elements which fail abruptly with little energy absorbed in the plastic range. Reinforced concrete with well tied and anchored ductile reinforcement can be classified as ductile material.

b. Reinforcing steel, designated by the American Society for Testing and Materials as A15 and A432, may usually be considered to have adequate ductility in sizes up to No. 11 bars. For the larger size bars (No's. 14S and 18S), the desired ductility is often not available. Bends, lapped or welded splices, etc., near points of maximum stress are also undesirable because of the reduced ductility.

c. It is desirable to know the reinforcement stress-strain relationship in order to calculate the ultimate resistance of an element. This information is not usually available; however, a set of minimum values which will assure a safe design has been determined. Table 5–4 lists these recommended static design stresses for both concrete and reinforcing steel.

d. The magnitude of the stresses produced in the reinforcement of an element responding in the plastic range cannot be related directly to the strains, but an estimate of the average stress over portions of the plastic range can be made by relating this average stress to the deflection of the element. The deflection is defined in terms of the angular rotation at the supports, whereas the average static stress is expressed as a function of the yield stress f_y and the ultimate stress f_u.

Maximum support rotation angle θ_m	*Static design stress* f_s
$0° < \theta_m \leq 2°$	f_y
$2° < \theta_m < 5°$	$f_y + \frac{1}{6}(f_u - f_y)$
$5° \leq \theta_m \leq 12°$	$\frac{1}{2}(f_y + f_u)$

e. Even though the magnitude of the concrete strength is only significant in the calculation of the strength of elements with support rotations less than 2 degrees, its effects on the behavior of elements with both small and large support rotations is of equal importance. For elements with small support rotations (less than 2 degrees), the shear capacity of the element is usually dependent upon the magnitude of the concrete strength. For elements with larger support rotations, the cracking and crushing of the concrete between the layers of reinforcement associated with the larger rotations is less severe when higher strength concrete is employed.

Table 5–4. Minimum Static Design Stresses

Material	Support rotation angle θ	Stresses (psi)*		
		f_y	f_u	f_c'
Reinforcing steel, A15 and A432.	—	40,000 60,000	70,000 90,000	— —
Concrete	$0° < \theta \leq 2°$ $2° < \theta \leq 12°$	— —	— —	$\geq$2,500 $\geq$3,000**

* Minimum stresses may be substituted for stresses obtained from tests.
** Recommended value of f_c' equals 4,000 psi.

f. Once the static stresses have been determined, then the dynamic stresses can be calculated by multiplying the static stresses by the dynamic increase factors of the previous section.

Section II. STATIC PROPERTIES

5–7. Modulus of Elasticity

a. Concrete. The modulus of elasticity of concrete E_c is equal to

$$E_c = w^{1.5} 33 \sqrt{f_c'} \text{ psi} \qquad \textbf{Equation 5–17}$$

for values of w between 90 and 155 lbs/ft^3 where w is the unit weight of concrete and normally equal to 145 lbs/ft^3.

b. Reinforcing Steel. The modulus of elasticity of reinforcing steel E_s is

$$E_s = 29(10^6) \text{ psi} \qquad \textbf{Equation 5–18}$$

c. Modular Ratio. The modular ratio n is

$$n = \frac{E_s}{E_c} \qquad \textbf{Equation 5–19}$$

and may be taken as the nearest whole number.

5–8. Moment of Inertia

a. The determination of the deflection of a reinforced concrete member in the elastic and elasto-plastic ranges is complicated by the fact that the effective moment of inertia of the cross section along the element changes continually as cracking progresses, and further by the fact that the modulus of elasticity changes as the stress increases. It is recommended that the computation of deflections in this and subsequent chapters of this manual be based upon empirical relations determined from test data.

b. The average moment of inertia I_a to be used in calculating deflections is

$$I_a = \frac{I_g + I_c}{2} \qquad \textbf{Equation 5–20}$$

where I_g = moment of inertia of the gross concrete cross section of width b about its centroid (neglecting steel areas) and is equal to

$$I_g = \frac{bT_c^3}{12} \qquad \textbf{Equation 5–21}$$

and I_c = moment of inertia of the cracked concrete section of width b considering the compression concrete area and steel areas transformed into equivalent concrete areas and computed about the centroid of the transformed section. I_c is calculated from

$$I_c = Fbd^3 \qquad \textbf{Equation 5–22}$$

The coefficient F varies as the modular ratio n and the amount of reinforcement used. For sections with tension reinforcement, only F is given in figure 5–5. For other elements which are reinforced both in the compression and tension regions, the value of F cannot be obtained from any available design aids and, therefore, I_c must be calculated using the transformed section method as described above.

l relations determined

ertia I_e to be used in

Equation 5–20

of the gross concrete
ts centroid (neglecting

Equation 5–21

f the cracked concrete
e compression concrete
d into equivalent con-
ut the centroid of the
ated from

Equation 5–22

modular ratio n and the
or sections with tension
in figure 5–5. For other
both in the compression
f F cannot be obtained
and, therefore, I_c must
rmed section method as

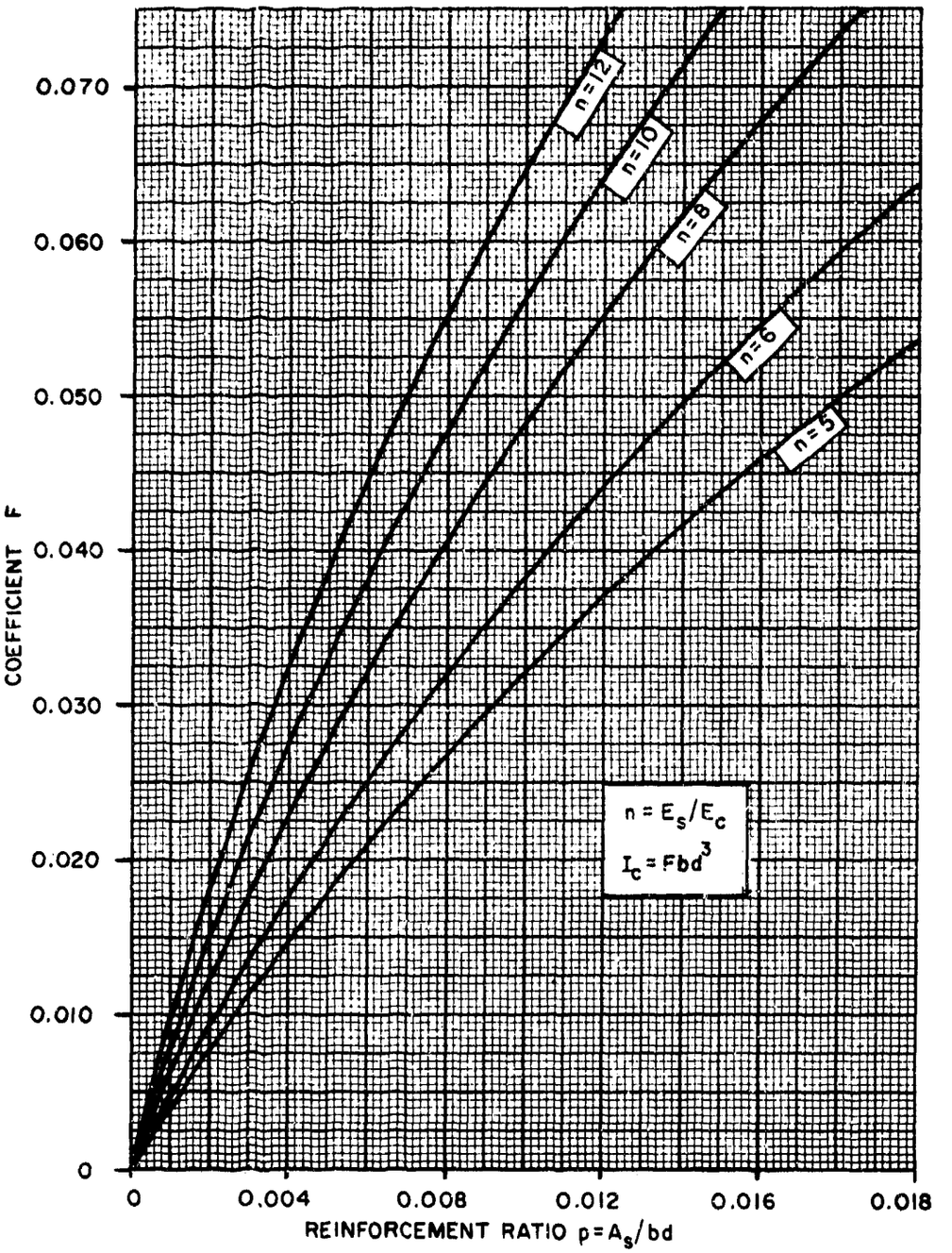


Figure 5–5. Coefficients for moment of inertia of cracked sections with tension reinforcement only.

2

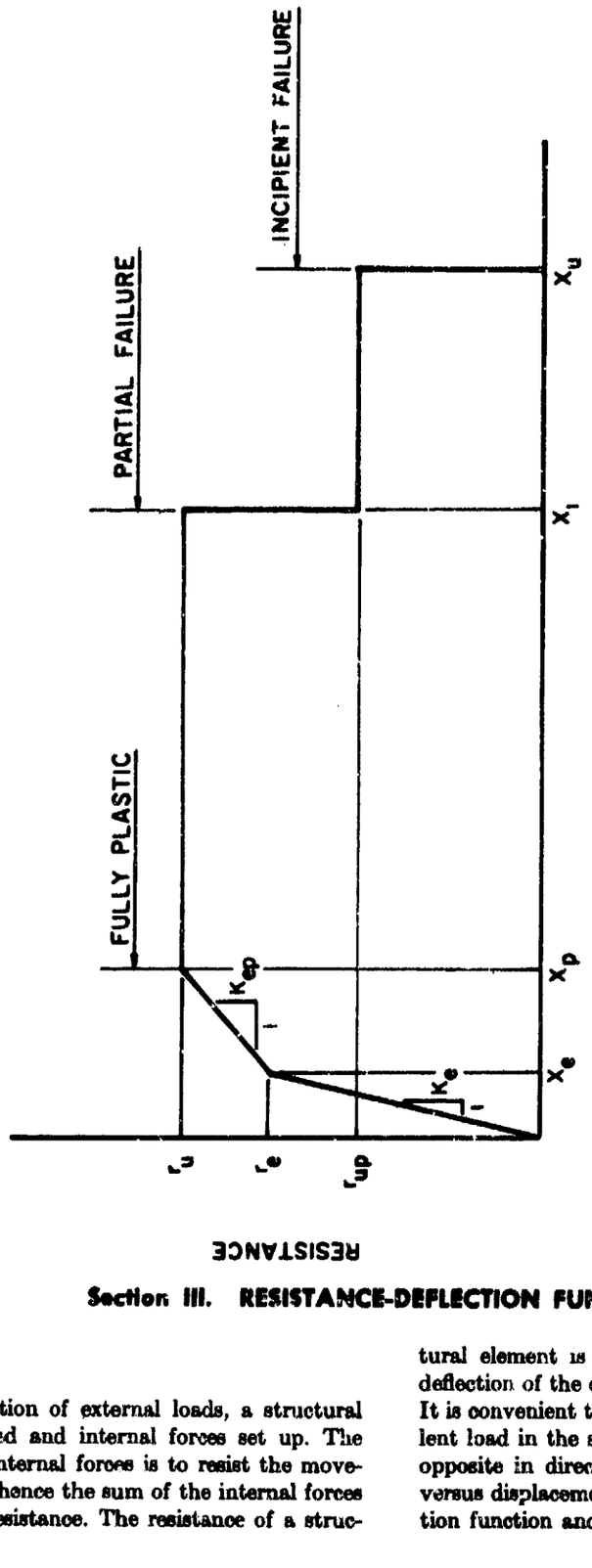


Figure 5–6. Typical resistance-deflection function for two-way element.

Section III. RESISTANCE-DEFLECTION FUNCTIONS

5–9. General

a. Under the action of external loads, a structural element is deformed and internal forces set up. The function of these internal forces is to resist the movement of the mass; hence the sum of the internal forces is defined as the resistance. The resistance of a structural element is a reactive force associated with the deflection of the element produced by the applied load. It is convenient to consider the resistance as an equivalent load in the same manner as the applied load, but opposite in direction. The variation of the resistance versus displacement is expressed by a resistance-deflection function and may be represented graphically. An

idealized resistance-deflection function for an element spanning in two directions and covering the complete flexural range to incipient failure is shown in figure 5–6.

b. Initially, as load is applied to the element, the element deflects and at any instant exerts a resistance to further deformation, which is a function of its unit stiffness K, until the ultimate unit resistance r_u (total resistance is r_uA where A is the element area) of the element is reached at deflection X_p. This initial portion of the resistance-deflection diagram is composed of the elastic and elasto-plastic ranges, each with its corresponding stiffness, the transition from one range to another occurring as plastic hinges are formed at points of maximum stress (yield lines). The number of elasto-plastic ranges required before the ultimate resistance of a particular element is reached depends upon the type and number of supports and the placement of the reinforcing steel.

c. Once the ultimate unit resistance r_u is attained, its magnitude remains essentially constant until deflection X_1 where failure of one or more of the supports occurs resulting in a loss of strength and a drop in the resistance. This point is referred to as partial failure and denotes the deflection after which all further flexural action conforms to that of a one-way element. The element, spanning one way with the reduced post-ultimate resistance r_{up}, continues to deflect until the ultimate deflection X_u is reached which is the point of incipient failure. Any further increase in deflection beyond this point results in total collapse.

d. When the element in question is initially spanning in one direction, the deflection X_1 at partial failure is numerically equal to the deflection X_u at incipient failure, and therefore a partial failure of the element results in total collapse without the latter range of deflection described for the two-way element.

e. In subsequent paragraphs of this chapter, various procedures, equations, and illustrations are presented to enable the designer to determine the resistances, deflections, and other quantities necessary for the design of both one-way and two-way elements. The procedures outlined are general as are the equations appearing in the text, unless the equations are given as part of an illustrative example. These general procedures and equations are applicable to all situations; however, certain illustrations (figs. 5–9 through 5–11 and figs. 5–14 through 5–19), and also the equations appearing in certain tables (tables 5–5 through 5–15), have been derived for specific cases most often encountered in practice and are necessarily restricted in application. The following requirements must be fulfilled before they can be used.

(1) The reinforcing steel across any yield line (para 5–10c) must have a uniform distribution in both the vertical and horizontal directions.

(2) Opposite supports of two-way elements must provide the same degree of restraint so that a symmetrical yield line pattern results. To achieve this, the reinforcing steel must be symmetrical about the centerline of the element; however, the reinforcement across the positive yield lines can be different from that across the negative yield lines, and the reinforcing pattern in the vertical direction different from that in the horizontal direction.

(3) All edges with the exception of free edges must be fully or partially fixed, or simply-supported.

(4) Elements must be of constant thickness.

(5) Any openings must be compact in shape and small in area compared to the total area of the panel element (para 5–10*d*).

5–10. Ultimate Resistance

a. General.

(1) The ultimate resistance of an element varies as (*a*) the distribution of the applied loads, (*b*) the geometry of the element (length and width), (*c*) the amount and distribution of the reinforcement, and (*d*) the number and type of supports.

(2) The distribution of the loads depends upon the design range of the element, i.e., high, intermediate, or low pressure. At the latter two ranges, the blast loads acting on an element are usually fairly uniform even though they vary with time. On the other hand, at the high-pressure range, the blast loads are variable across the surface of the element. However, results of tests have indicated that for elements which utilize laced reinforcement, a good estimate of the resulting deflections can be made using the resistance functions conforming to those of uniformly loaded elements.

(3) The remaining three parameters, which affect the magnitude of the ultimate resistance, are predetermined by the requirements of the protective structure (where the element is used) and the magnitude of the blast output.

b. One-Way Elements.

(1) For one-way elements (such as beams or slabs) with nonelastic distribution of reinforcing, the ultimate resistance is a function of the moment capacity at the first yield plus the added moment capacity due to subsequent yielding at other critical sections. The ultimate resistance of an element with an elastic distribution of its reinforcing steel, and also for cantilever and simply-supported elements, is based on the moment capacity at first yield since all critical sections yield simultaneously.

(2) Values of the ultimate unit resistance r_u for several one-way elements are shown in table 5–5 where the following symbols are used:

M_N = ultimate unit negative moment capacity at the support

M_P = ultimate unit positive moment capacity at midspan

L = span length

The procedure for determining these resistances is simi-

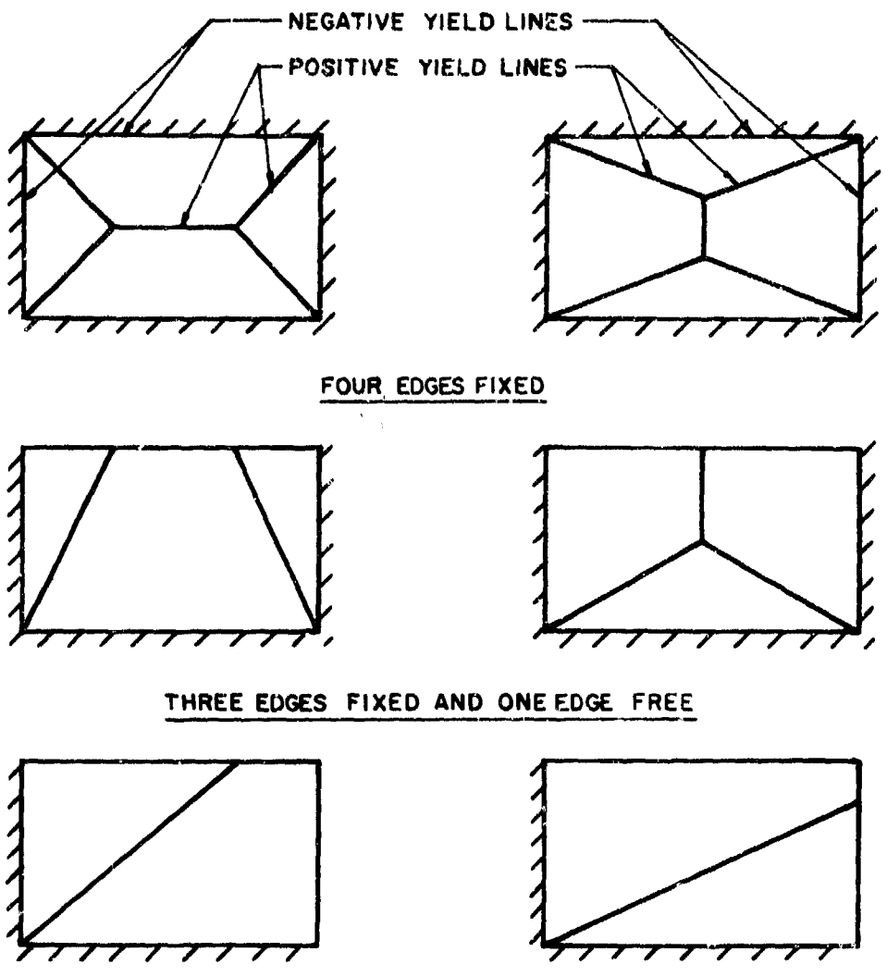


Figure 5–7. Idealized yield-line locations for several two-way elements.

lar to that outlined for two-way elements in *c* below, except that no moment variation is used.

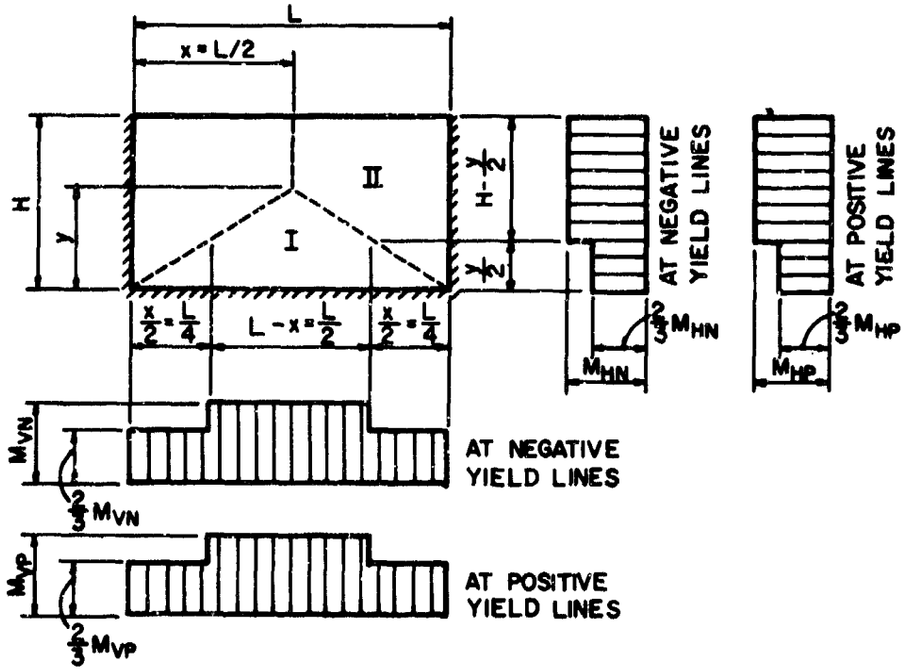
c. Two-Way Elements.

(1) In the design of two-way elements, it is not necessary to define accurately the stress distribution during the initial and intermediate stages of loading since the ultimate load capacity can be readily determined by use of "yield-line procedures". The yield-line method assumes that after initial cracking of the concrete at points of maximum moment, yielding spreads until the full moment capacity is developed along the length of the cracks on which failure will take place. Several illustrative examples of the simplified yield or crack lines for two-way elements are illustrated in figure 5–7.

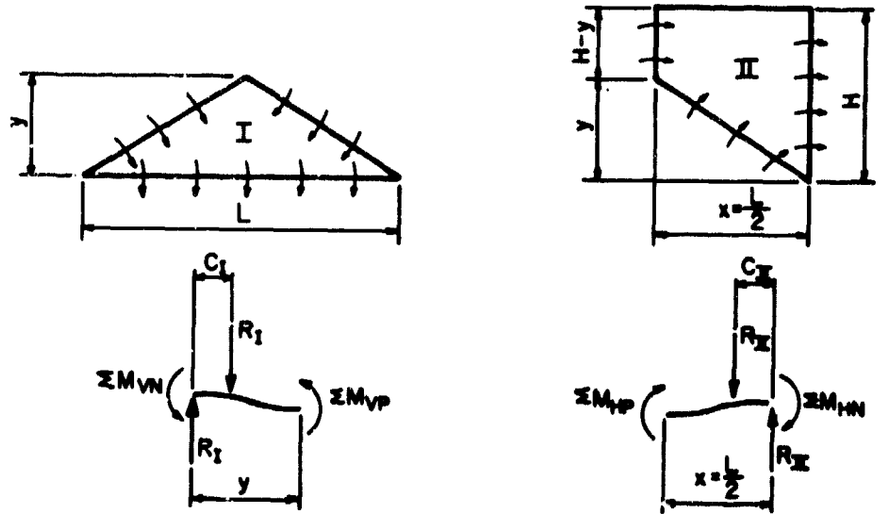
(2) Tests indicate that the actual location and extent of these lines differ only slightly at failure from the theoretical ones. Use of the idealized yield lines results in little error in the determination of the ultimate resistance, and that error is on the side of safety.

(3) Generally, the yield lines are determined from the condition that the unit resistance must be the same for all of the sectors formed. The corner sections of two-way elements are stiff in comparison to the remainder of the member; therefore straining of the reinforcement which is associated with the reduced rotations at these sections will be less. To account for the corner effects, the design of any one particular sector of a two-way element should consider a variation

actual location and
ghtly at failure from
idealized yield lines
nation of the ultimate
e side of safety.
are determined from
nce must be the same
ne corner sections of
mparison to the re-
ore straining of the
ed with the reduced
e less. To account for
f any one particular
d consider a variation



a) YIELD LINES AND DISTRIBUTION OF MOMENTS



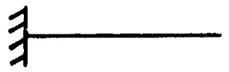
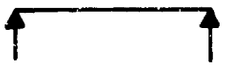
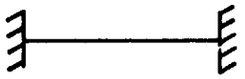
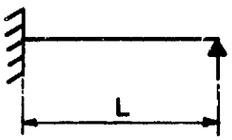
b) FREE-BODY DIAGRAMS FOR INDIVIDUAL SECTORS

Figure 5-8. Determination of ultimate unit resistance.

2

of the moment capacity across the yield lines rather than a uniform distribution.

Table 5-5. Ultimate Unit Resistance for One-Way Elements

Edge conditions	Ultimate unit resistance r_u
Cantilever 	$\frac{2M_N}{L^2}$
Simple supports 	$\frac{8M_P}{L^2}$
Fixed supports 	$\frac{8}{L^2}(M_N+M_P)$
Fixed-simple supports 	$\frac{4}{L^2}(M_N+2M_P)$

r_u (psi)
M_N, M_P (in.-lb/in.)
L (in.)

This variation is approximated by taking the full moment capacity along the yield lines, except in the corners where two thirds of the moment capacity over the lengths described in figure 5-8 is used. The variation applies to both the negative moments along the supports and the positive moments at the interior.

(4) In order to calculate the ultimate unit resistance r_u of a two-way element, the equation of equilibrium of each sector formed by the yield lines is expressed in terms of the moments produced by the internal and external forces. The sum of the resisting moments acting along the yield lines (both positive and negative) of each sector is equated to the moment produced by the applied load about the axis of rotation (support of the sector), assuming that the shear forces are zero along the positive yield lines.

$$\Sigma M_N + \Sigma M_P = Rc = r_u A c \qquad \textbf{Equation 5-23}$$

where ΣM_N = sum of the ultimate unit resisting moments acting along the support (negative yield lines)
ΣM_P = sum of ultimate unit resisting moments acting along the interior failure lines (positive yield lines)
R = total ultimate resistance of the sector
c = distance from the centroid of the load to the line of rotation of the sector
r_u = ultimate unit resistance of the sector
A = area of the sector

(5) Once the equations of equilibrium are known for all sectors, the ultimate resistance is obtained either by solving the equations simultaneously or by a trial and error procedure noting that the unit resistance of all sectors must be equal.

(6) To illustrate the above procedure (equation 5-23), consider the two-way element shown in figure 5-8 which is fixed on three edges and free on the fourth, and where the nomenclature is as follows:

L = length of the element
H = height of the element
x = yield line location in horizontal direction
y = yield line location in vertical direction
M_{VN} = ultimate unit negative moment capacity in the vertical direction
M_{VP} = ultimate unit positive moment capacity in the vertical direction
M_{HN} = ultimate unit negative moment capacity in the horizontal direction
M_{HP} = ultimate unit positive moment capacity in the horizontal direction

(7) The nomenclature as stated in (6) above is strictly applicable to two-way elements which are used as walls. However, when roof slabs or other horizontal elements are under consideration, the preceding nomenclature will also be applicable if the element is treated as being rotated into a vertical position.

(8) The first step in the solution is to assume the location of the yield lines as defined by the coordinates x and y. It should be noted that in some cases, because of geometry, the value of x or y will be known and therefore need not be evaluated. In this example, the negative reinforcement in the horizontal direction at opposite supports is assumed to be equal, and therefore the vertical yield line is located at the center of the span, and the value of x is numerically equal to $L/2$ (a, fig. 5-8). However, in other cases neither the location of x nor y will be known, and the solution will require the determination of both coordinates.

(9) Once the yield lines have been assumed, the distribution of the resisting moments along the yield lines is determined. In the case at hand, the reduced moments, as a result of the increased stiffness at the corners, act over lengths equal to $x/2$ and $y/2$ in the horizontal and vertical directions, respectively (a, fig. 5-8). The equations of equilibrium are then written for each sector with the use of the free body diagrams (b, fig. 5-8). For the triangular sector I

$$\Sigma M_{VN} = \tfrac{2}{3}M_{VN}\left(\frac{L}{4}+\frac{L}{4}\right)+M_{VN}\left(\frac{L}{2}\right)=\tfrac{5}{6}M_{VN}L$$

Equation 5-24

$$\Sigma M_{VP} = \tfrac{2}{3}M_{VP}\left(\frac{L}{4}+\frac{L}{4}\right)+M_{VP}\left(\frac{L}{2}\right)=\tfrac{5}{6}M_{VP}L$$

Equation 5-25

$$C_I = \frac{y}{3} \qquad \textbf{Equation 5-26}$$

$$R_I = \frac{\Sigma M_{VN}+$$
$$C_I$$

$$A_I = \frac{Ly}{2}$$

r_u(Sector I) =

For the trape

$$\Sigma M_{HN} = \tfrac{2}{3}M_H$$

$$\Sigma M_{HP} = \tfrac{2}{3}M_H$$

$$C_{II} = \frac{1}{3}\left(\frac{L}{2}\right)^2$$

$$R_{II} = \frac{\Sigma M_{HN}+}{C_I}$$

$$A_{II} = \frac{1}{2}\left(\frac{L}{2}\right)($$

r_u(Sector II)

(10) Eq
of equilibriu
zoidal (II)
viously, thes
or by a trial
values of y a
(Sector I) is
If a numeric
(equation 5-
or r_u, then
In this exa
pattern ($x \leq$
(three sides

(11) Th
applicable fo
reinforcemen
equal at the
would have
had to be co

(12) Sin
5-35 reveals
function of

$$R_I = \frac{\Sigma M_{VN} + \Sigma M_{VP}}{C_I} = \frac{5L(M_{VN}+M_{VP})}{2y}$$ **Equation 5-27**

$$A_I = \frac{Ly}{2}$$ **Equation 5-28**

$$r_u(\text{Sector } I) = \frac{R_I}{A_I} = \frac{5(M_{VN}+M_{VP})}{y^2}$$ **Equation 5-29**

For the trapezoidal sector II, a similar procedure gives

$$\Sigma M_{HN} = \tfrac{1}{3}M_{HN}\left(\frac{y}{2}\right) + M_{HN}\left(H-\frac{y}{2}\right) = M_{HN}\left(H-\frac{y}{6}\right)$$ **Equation 5-30**

$$\Sigma M_{HP} = \tfrac{1}{3}M_{HP}\left(\frac{y}{2}\right) + M_{HP}\left(H-\frac{y}{2}\right) = M_{HP}\left(H-\frac{y}{6}\right)$$ **Equation 5-31**

$$C_{II} = \frac{1}{3}\left(\frac{L}{2}\right)\frac{2(H-y)+H}{(H+H-y)} = \frac{L(3H-2y)}{6(2H-y)}$$ **Equation 5-32**

$$R_{II} = \frac{\Sigma M_{HN} + \Sigma M_{HP}}{C_{II}} = \frac{(6H-y)(2H-y)(M_{HN}+M_{HP})}{L(3H-2y)}$$ **Equation 5-33**

$$A_{II} = \frac{1}{2}\left(\frac{L}{2}\right)(H+H-y) = \frac{L(2H-y)}{4}$$ **Equation 5-34**

$$r_u(\text{Sector II}) = \frac{R_{II}}{A_{II}} = \frac{4(M_{HN}+M_{HP})(6H-y)}{L^2(3H-2y)}$$ **Equation 5-35**

(10) Equations 5–29 and 5–35 are the equations of equilibrium for the triangular (I) and the trapezoidal (II) sectors, respectively. As mentioned previously, these equations can be solved simultaneously or by a trial and error procedure. In the latter method, values of y are substituted into both equations until r_u (Sector I) is equal to r_u (Sector II).

If a numerical solution based on the above procedure (equation 5–23) yields negative values for either x, y, or r_u, then the assumed yield line location is wrong. In this example, the only other possible yield line pattern ($x \leq L/2$) would be as shown in figure 5–7 (three sides fixed, one side free).

(11) The solution of equation 5–23 is universally applicable for any two-way element. If the negative reinforcement in the horizontal direction had been unequal at the opposing supports, the value of $x = L/2$ would have changed, and all three sectors would have had to be considered to determine x, y, and hence r_u.

(12) Simultaneous solution of equations 5–29 and 5–35 reveals that the locations of the yield lines are a function of the ratio of the spans L/H and the ratio of the sum of the unit vertical to horizontal moment capacities as follows:

$$r_u(\text{Sector I}) = r_u(\text{Sector II})$$ **Equation 5-36**

$$\frac{5(M_{VN}+M_{VP})}{y^2} = \frac{4(M_{HN}+M_{HP})(6H-y)}{L^2(3H-2y)}$$ **Equation 5-37a**

$$\frac{L^2(M_{VN}+M_{VP})}{H^2(M_{HN}+M_{HP})} = \frac{4y^2\left(6-\frac{y}{H}\right)}{5H^2\left(3-\frac{2y}{H}\right)}$$ **Equation 5-37b**

$$\frac{L}{H}\left(\frac{M_{VN}+M_{VP}}{M_{HN}+M_{HP}}\right)^{1/2} = \frac{y}{H}\left[\frac{4\left(6-\frac{y}{H}\right)}{5\left(3-\frac{2y}{H}\right)}\right]^{1/2}$$ **Equation 5-37c**

(13) Values of the ultimate unit resistance for several two-way elements with various support conditions are given in table 5–6, the nomenclature conforming to that previously listed. Yield line location ratios x/L and y/H for the same elements are depicted in figures 5–9 through 5–11. It should be noted that the nonfree edges are designated as being simply-supported or fully or partially fixed. However, the number of instances when simply-supported edges are encountered will be limited.

d. Openings in Two-Way Elements.

(1) The use of openings in two-way elements, whether for access as a door opening or for visual communication as in the case of observation ports, is permissible with certain reservations. It is difficult to state exact rules concerning openings, but their effect on the design is generally a function of location, size, and shape.

(2) Small compact openings with approximate areas of less than 5 percent of the panel area and located away from regions of high stress can usually be ignored in the design. However, as in the case of conventional design, reinforcement at least equal to the amount interrupted should be placed adjacent to the opening. For example, in figure 5–12 the openings shown in (a) and (b) can be disregarded. If the opening in (b) were made more rectangular as in (c), then the design must be modified to account for the change in the yield lines and hence the change in the resistance.

(3) Door openings invariably require special analysis because of their size. As depicted in (d), (e), and (f), figure 5–12, the presence of door openings causes gross relocations of the yield lines which generally propagate from the corners of the openings. Since

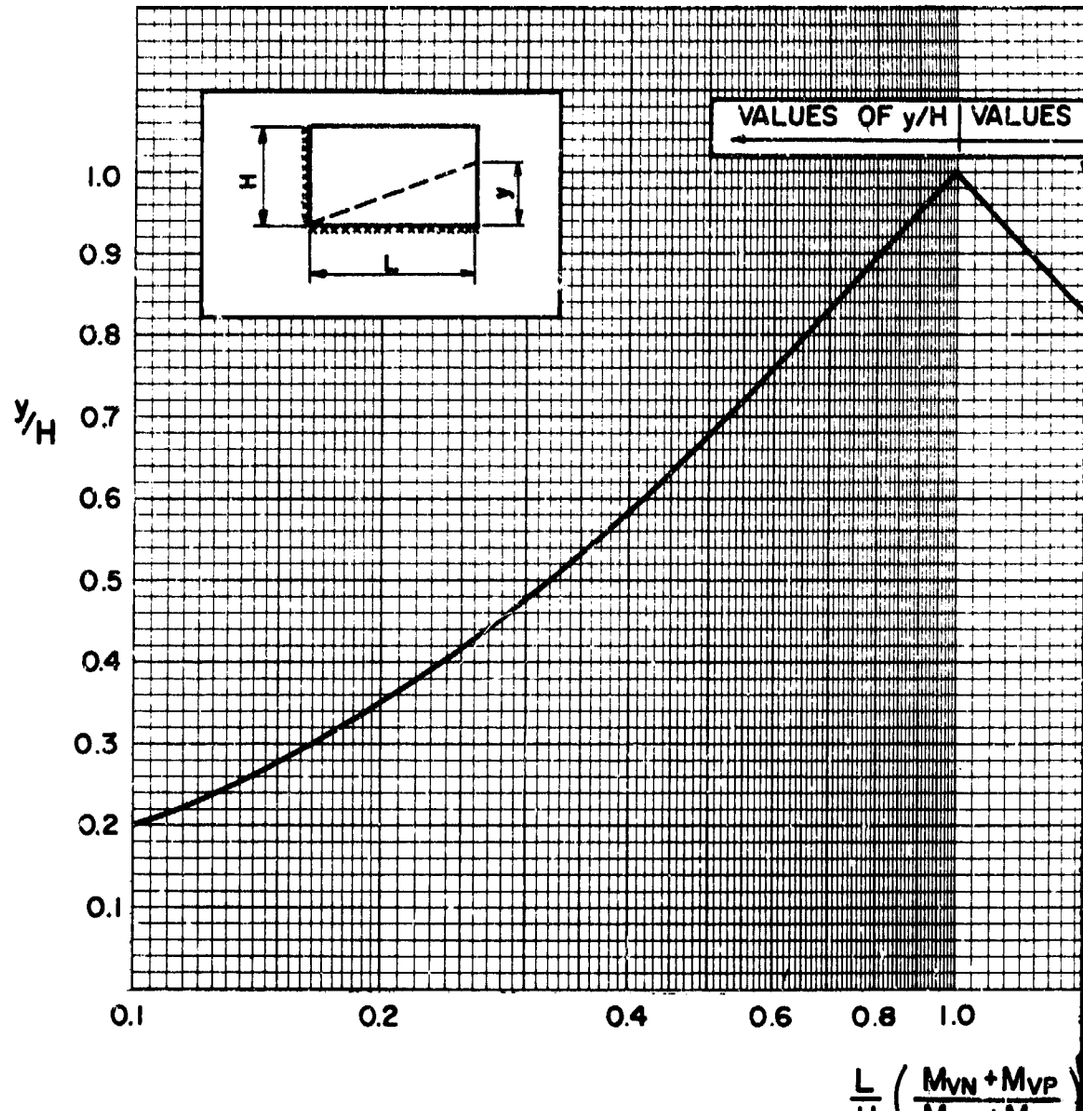
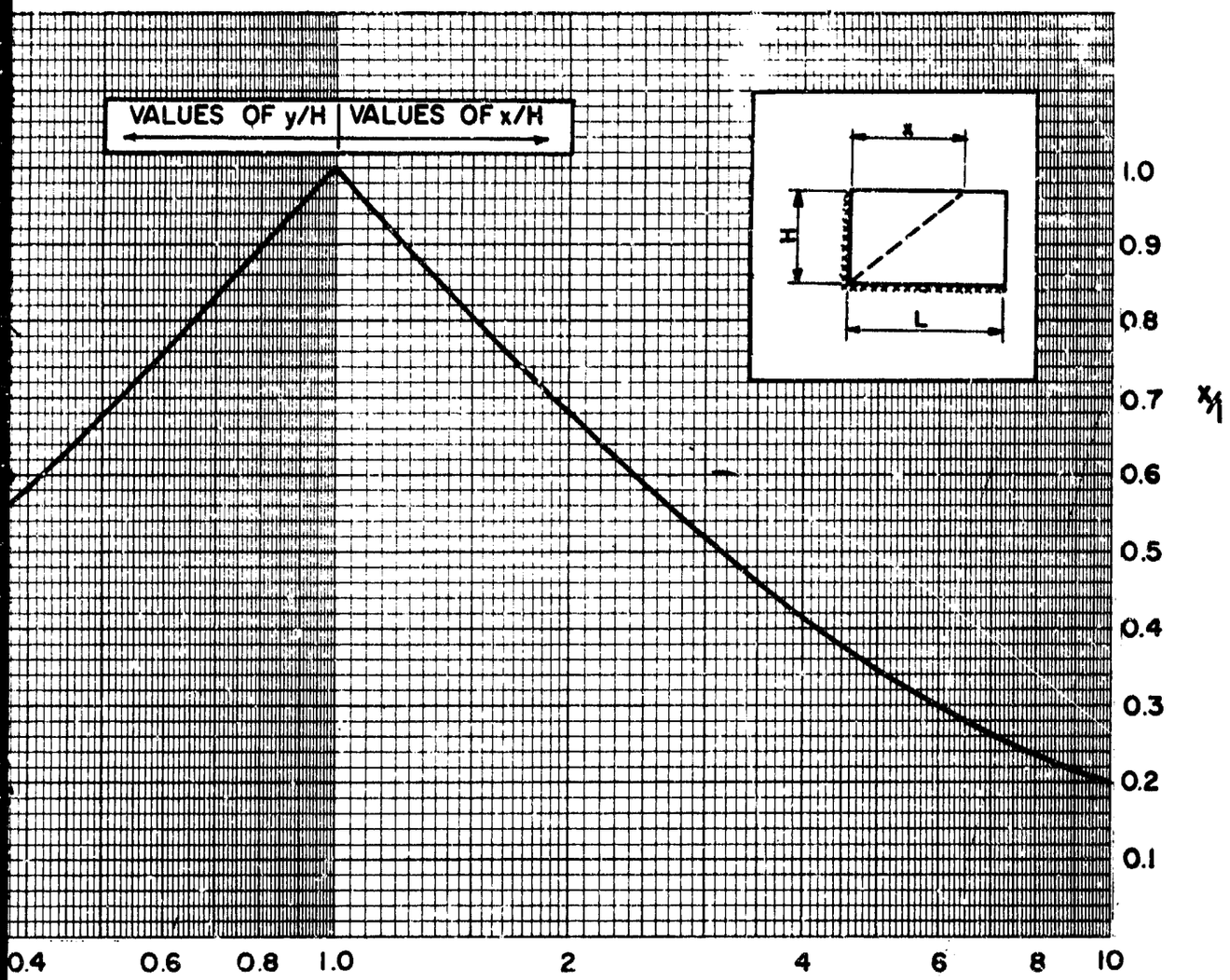


Figure 5-9. Yield line location for two-way element with two adjace



9. Yield line location for two-way element with two adjacent edges supported and two edges free.

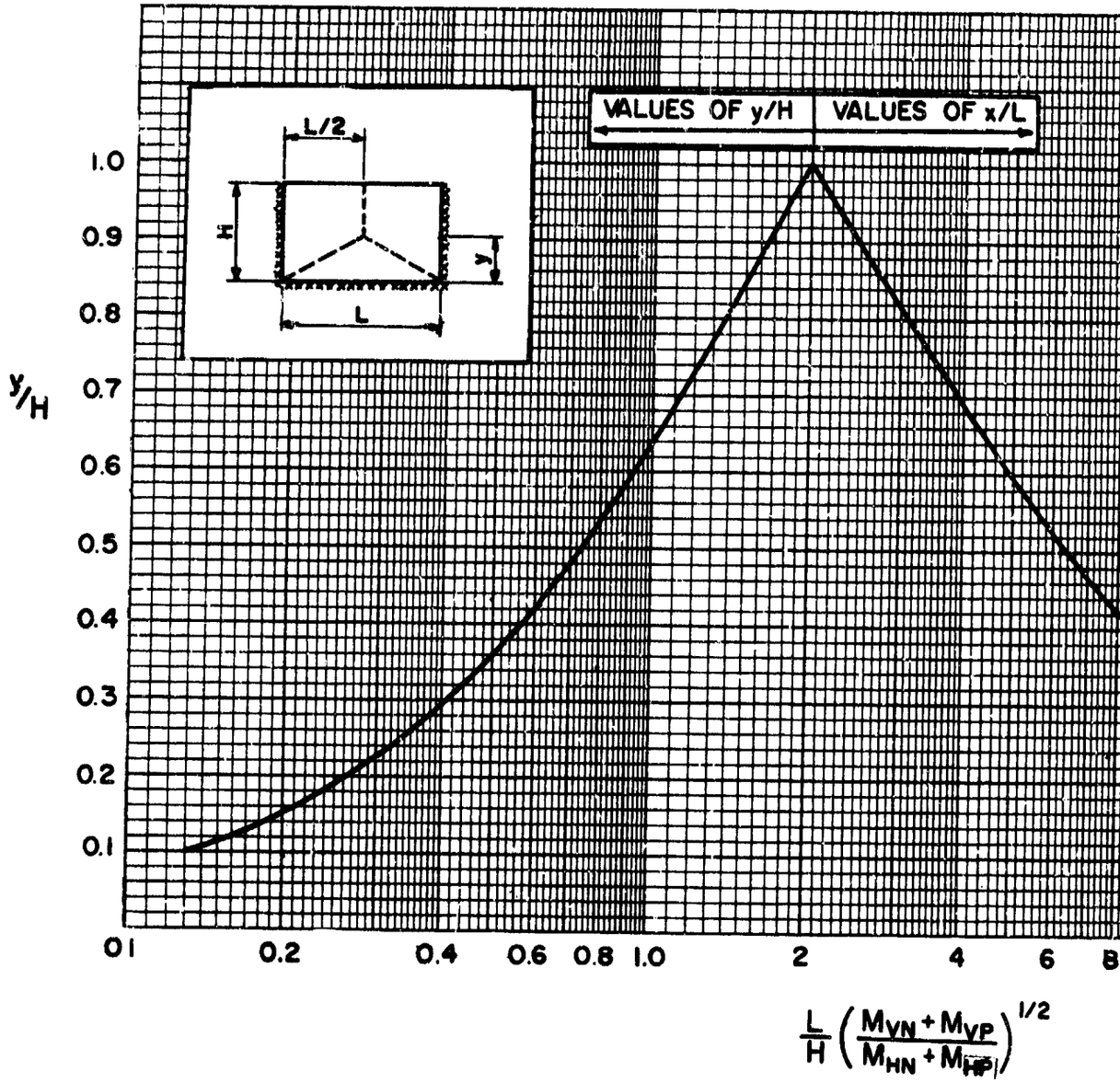
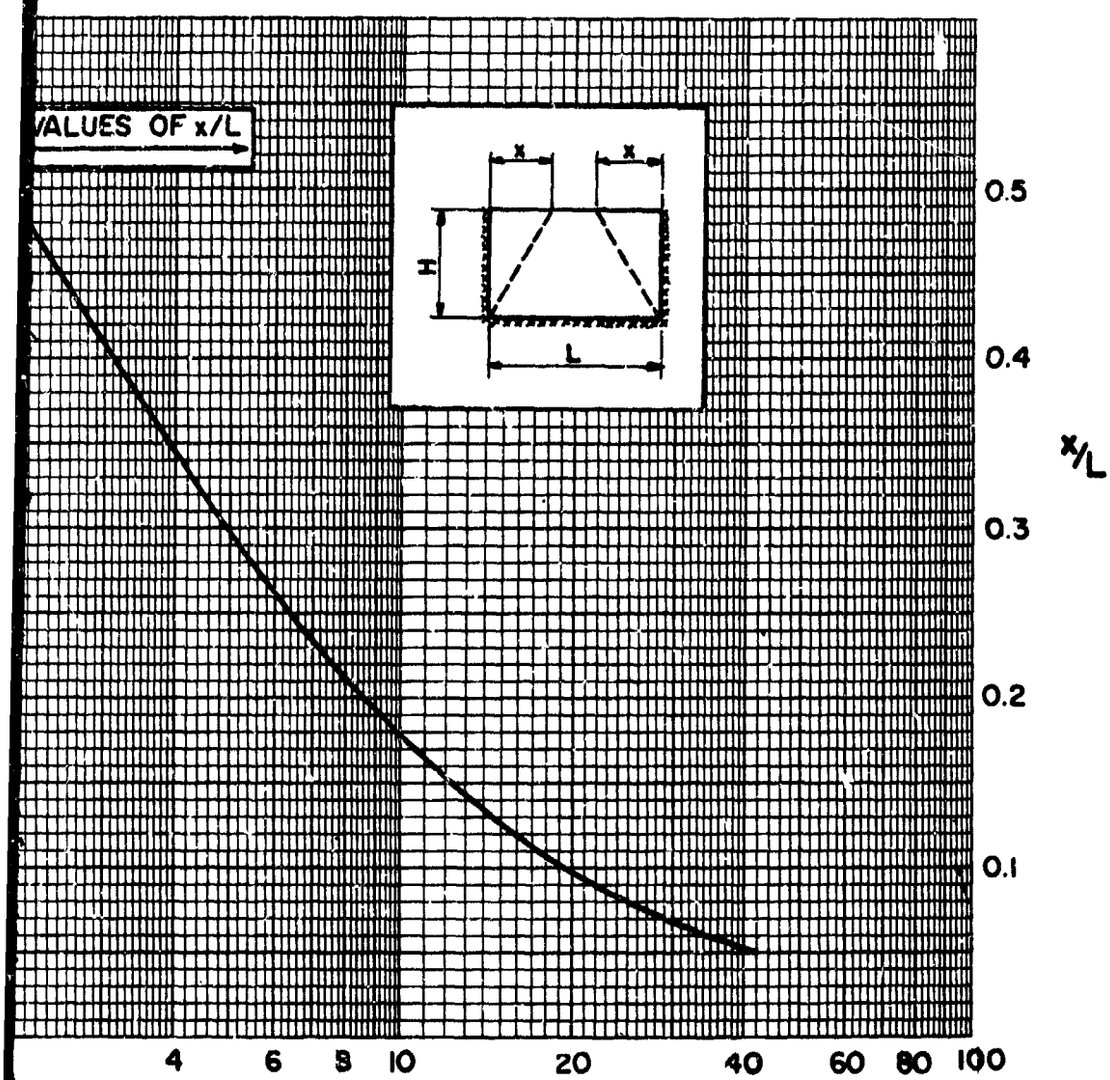


Figure 5-10. Yield line location for two-way element with three edges supporte



$$\frac{}{H}\left(\frac{M_{VN}+M_{VP}}{M_{HN}+M_{HP}}\right)^{1/2}$$

wo-way element with three edges supported and one edge free.

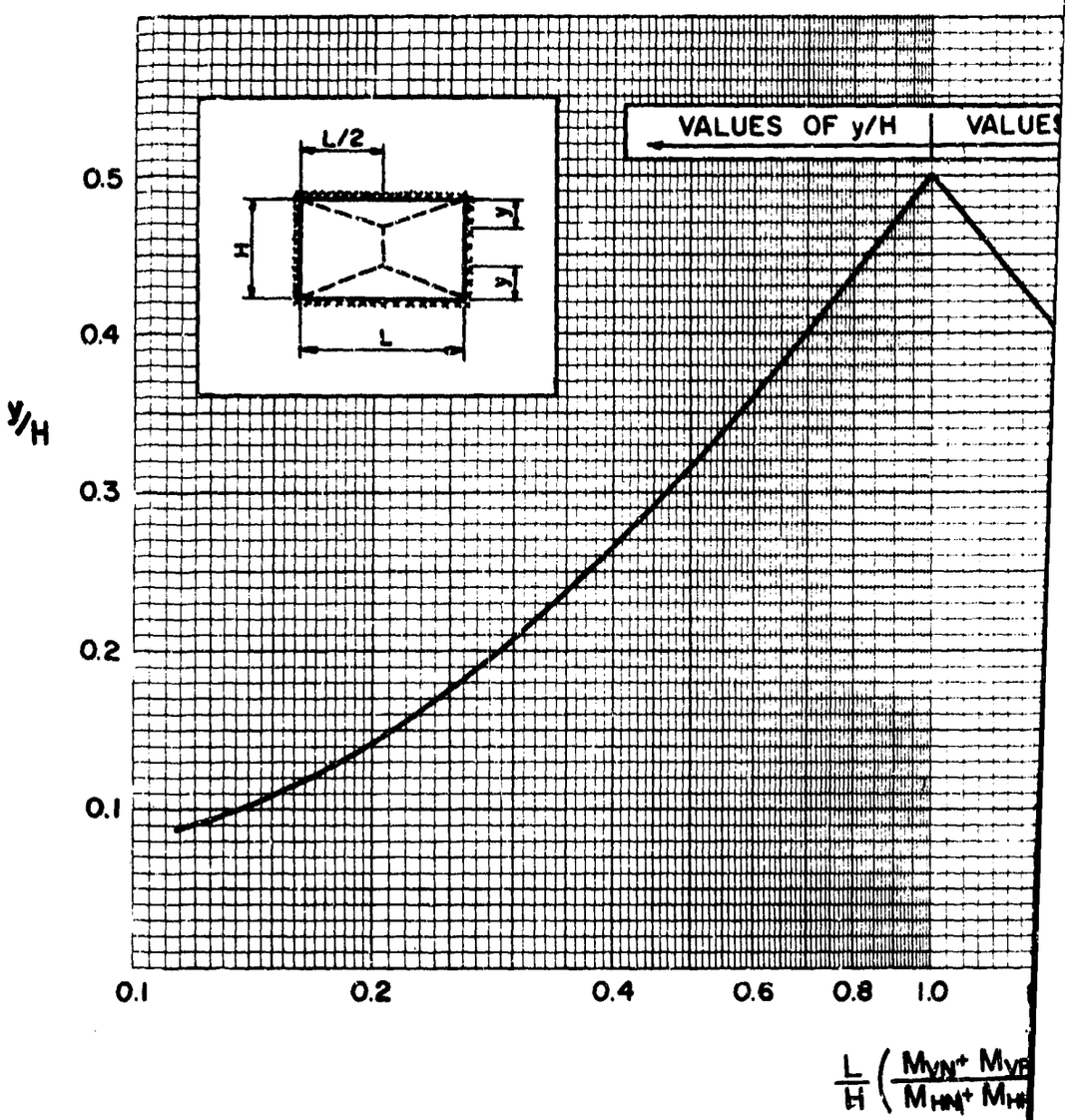
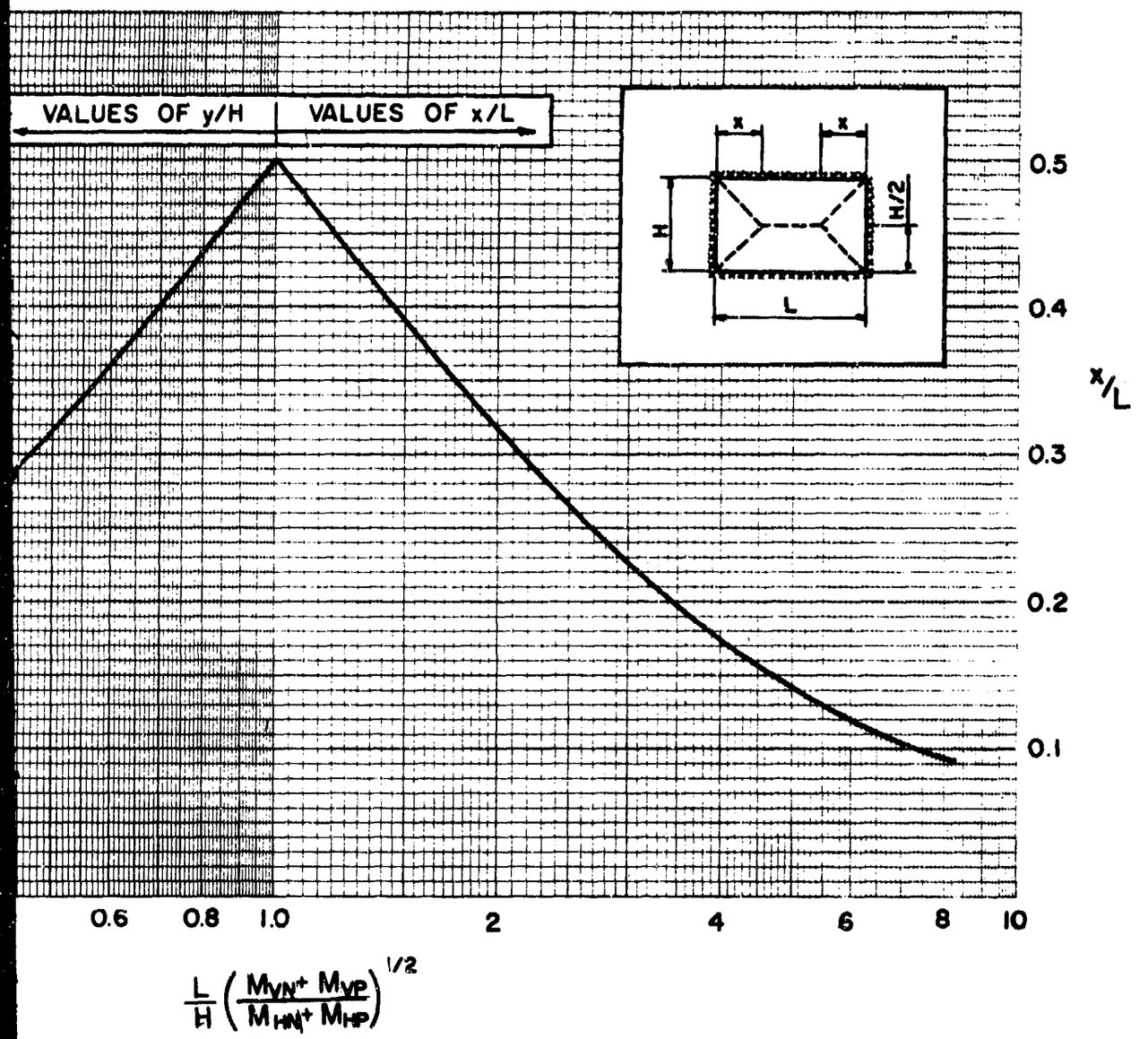


Figure 5–11. Yield line location for two-way elemen



e 5-11. Yield line location for two-way element with four edges supported.

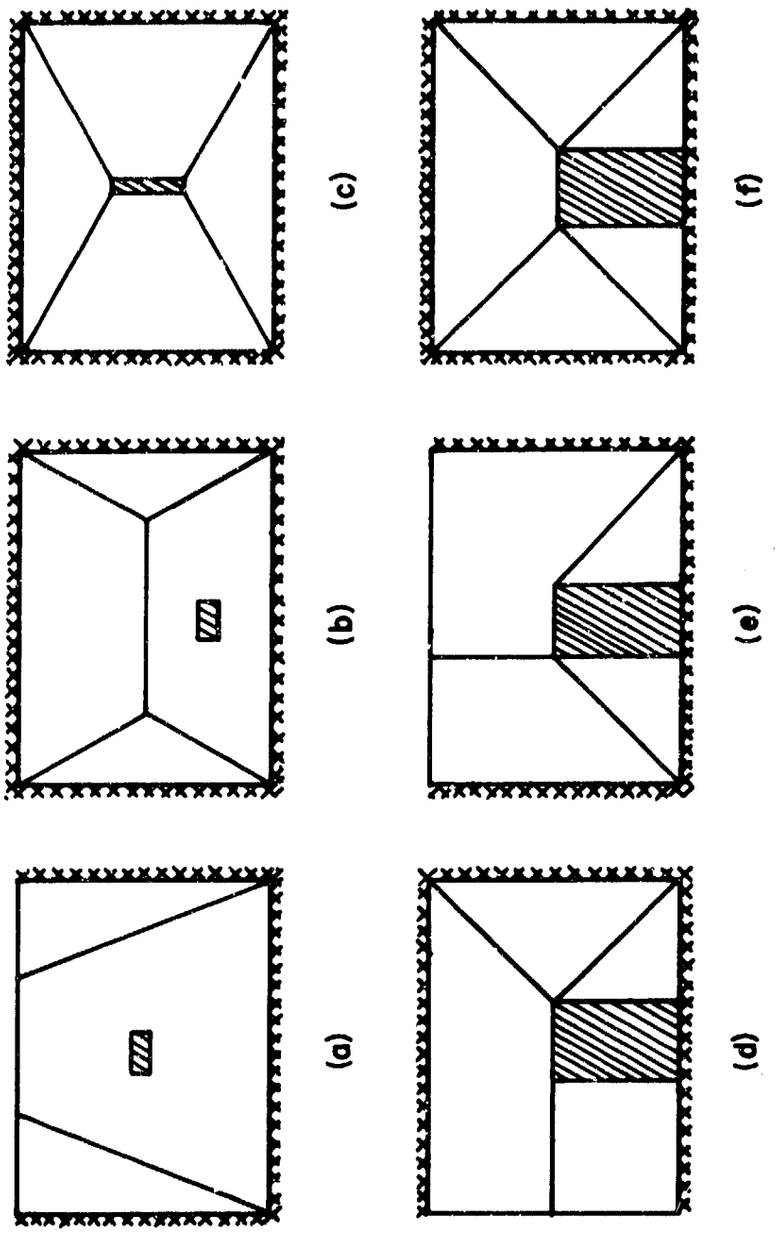


Figure 5–12. Effects of openings on yield line locations.

the door also sustains the blast loading, concentrated line loads are present around the periphery of such openings. These concentrated loads must be included in the analysis since they change the resistance. As previously outlined for solid elements and for this case also, the yield line locations are assumed and each sector is individually analyzed. The presence of line loads modifies equation 5–23 to

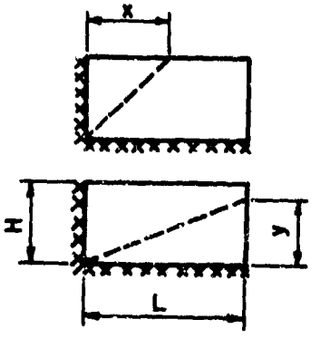
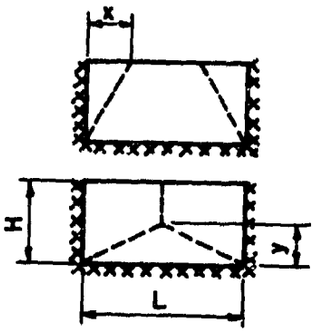
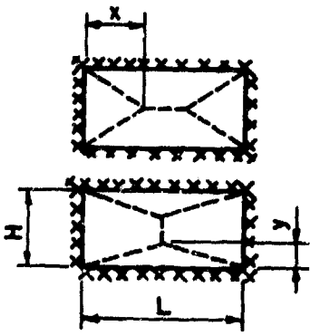
$$\Sigma M_N + \Sigma M_P = r_u Ac + M_c \qquad \textbf{Equation 5–38}$$

where M_c is the moment of the concentrated loads about the line of rotation of the sector being considered. Solution of elements with openings is most easily accomplished through a trial and error procedure by setting up the simultaneous equations for each sector and assuming various values of x and y until the several values of r_u agree to within a few percent.

5–11. Post-Ultimate Resistance

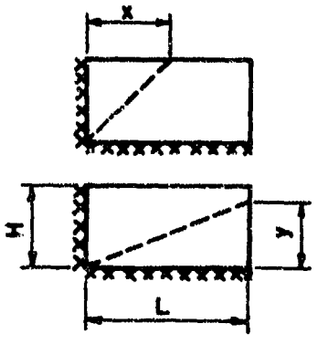
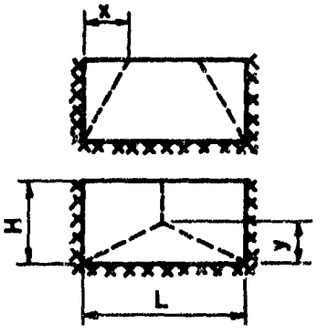
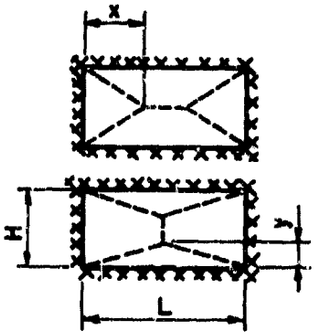
a. In general, the two-way elements described in this manual exhibit a post-ultimate resistance after initial failure occurs as indicated in figure 5–6. Prior

Table 5–6. Ultimate Unit Resistances for Two-Way Elements

Edge conditions	Yield line location	Limits	Ultimate unit resistance r_u
Two adjacent edges supported and two edges free.		$x \le L$	$\frac{5(M_{HN}+M_{HP})}{x^2}$ or $\frac{(M_{VN}+M_{VP})(3L+2x)}{H^2(3L-2x)}$
		$y \le H$	$\frac{5(M_{VN}+M_{VP})}{y^2}$ or $\frac{(M_{HN}+M_{HP})(3H+2y)}{L^2(3H-2y)}$
Three edges supported and one edge free		$x \le \frac{L}{2}$	$\frac{5(M_{HN}+M_{HP})}{x^2}$ or $\frac{(M_{VN}+M_{VP})(3L+4x)}{H^2(3L-4x)}$
		$y \le H$	$\frac{5(M_{VN}+M_{VP})}{y^2}$ or $\frac{4(M_{HN}+M_{HP})(6H-y)}{L^2(3H-2y)}$
Four edges supported		$x \le \frac{L}{2}$	$\frac{5(M_{HN}+M_{HP})}{x^2}$ or $\frac{8(M_{VN}+M_{VP})(3L-x)}{H^2(3L-4x)}$
		$y \le \frac{H}{2}$	$\frac{5(M_{VN}+M_{VP})}{y^2}$ or $\frac{8(M_{HN}+M_{HP})(3H-y)}{L^2(3H-4y)}$

r_u (psi)
M_V, M_H (in.-lb/in.)
x, y, L, H (in.)

Table 6-7. Post-Ultimate Unit Resistances for Two-Way Elements

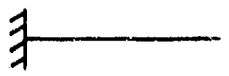
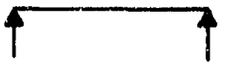
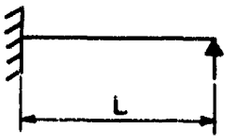
Edge conditions	Yield line location	Limits	Post-ultimate unit resistance r_{up}
Two adjacent edges supported and two edges free*.		$x<H$	$(M_{VN}+M_{VP})/H^2$
		$x>H$	$(M_{HN}+M_{HP})/L^2$
		$y<L$	$(M_{HN}+M_{HP})/L^2$
		$y>L$	$(M_{VN}+M_{VP})/H^2$
Three edges supported and one edge free**.		$x<H$	$(M_{VN}+M_{VP})/H^2$
		$x>H$	$8(M_{HN}+M_{HP})/L^2$
		$y<\frac{L}{2}$	$8(M_{HN}+M_{HP})/L^2$
		$y>\frac{L}{2}$	
Four edges supported.		$x<\frac{H}{2}$	$8(M_{VN}+M_{VP})/H^2$
		$x>\frac{H}{2}$	$8(M_{HN}+M_{HP})/L^2$
		$y<\frac{L}{2}$	$8(M_{HN}+M_{HP})/L^2$
		$y>\frac{L}{2}$	$8(M_{VN}+M_{VP})/H^2$

r_{up} (psi)
M_V, M_H (in.-lb/in.)
x, y, L, H (in.)

* $r_{up}=0$ if the element has:
(1) a simple horisontal support and $x<H$
(2) a simple vertical support and $x>H$
(3) a simple vertical support and $y<L$
(4) a simple horisontal support and $y>L$

** $r_{up}=0$ if the edge opposite to the free edge is simply supported and $x<H$

Table 5–8. General and Ultimate Deflections for One-Way Elements

Edge conditions	Maximum deflection X_m	Ultimate deflection X_u
Cantilever 	$L \tan \theta$	$L \tan 12°$
Simple supports 	$\frac{L \tan \theta}{2}$	$\frac{L \tan 12°}{2}$
Fixed supports 	$\frac{L \tan \theta}{2}$	$\frac{L \tan 12°}{2}$
Fixed-simple supports 	$\frac{L \tan \theta}{2}$	$\frac{L \tan 12°}{2}$

X_m, X_u, L (in.)
θ (deg)

to this partial failure, the element is spanning in two directions with a resistance equal to the ultimate unit resistance r_u. At a particular deflection, denoted as X_1, failure occurs along one side or two opposite sides, and the element then spans in one direction with the reduced post-ultimate unit resistance r_{up} until complete failure occurs at deflection X_u. One-way elements do not exhibit this behavior.

b. The location of the yield lines determines the presence or absence of this range. If the yield lines emanating from the corners of the element bisect the 90-degree corner angle, then all supports fail simultaneously and there is no post-ultimate range. As previously shown, the location of the yield lines for a particular element is a function of L/H and the ratio of the unit vertical to horizontal moment capacities.

c. Post-ultimate resistances for two-way elements are shown in table 5–7.

5–12. Partial Failure and Ultimate Deflections

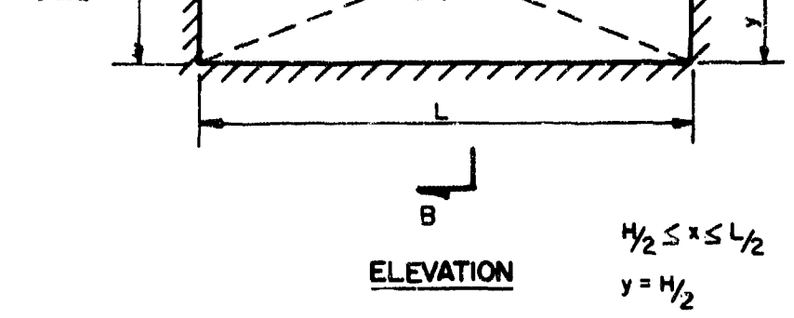
a. Partial failure deflections X_1 for two-way elements and ultimate deflections X_u for both one-way and two-way elements are a function of the angle of rotation of the element at its supports and the geometry of the sectors formed by the positive yield lines.

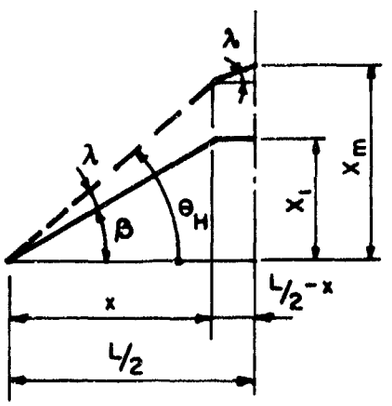
b. Once the ultimate resistance r_u is reached (full moment capacity developed along the yield lines), the structural element becomes a mechanism which rotates with no further increase in either the moment or curvature between the hinges. For one-way elements, the rotation continues and the deflection increases until either the maximum deflection X_m is reached or failure occurs at a 12-degree rotation. The equations for the maximum deflection X_m in the range $0 \leq X_m \leq X_u$ for several one-way elements as a function of the rotation angle θ and the ultimate deflection X_u are given in table 5–8, where the values for X_u are based on the development of a maximum support rotation of 12 degrees prior to failure.

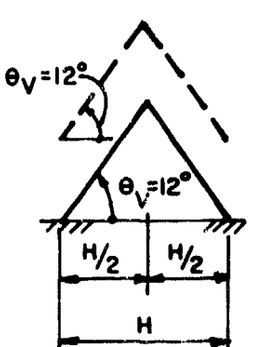
c. Actually, the maximum support rotation will vary with the geometry of the element. Tests are currently being conducted to determine this variation. In the interim, and based on present data, it appears that a 12-degree rotation can be used as the criteria to define incipient failure of flexural elements.

d. For two-way elements, the rotations of all the sectors must be considered in order to define the deflections at partial and incipient failure. Prior to partial failure ($0 \leq X_m \leq X_1$), the maximum deflection is a function of the larger angle of rotation formed along either the vertical or horizontal supports. At deflection X_1, this larger angle equals 12 degrees and failure occurs along this support. Beyond this point, the element spans in one direction until the angle of rotation at the adjacent supports (in the direction opposite to that at which failure has already occurred) reaches 12 degrees at which time total collapse occurs ($X_m = X_u$).

e. To illustrate the above, consider a two-way ele-







— PARTIAL FAILURE
--- INCIPIENT FAILURE

Figure 5–13. Deflection of two-way element.

ment (fig. 5–13) wh
and whose positive
$x \leq L/2$ and $y = H/$
tation in the horiz
ports) and θ_V as t
horizontal support
the center of the
flection X_1 is

$$X_m = \frac{H \tan\theta_V}{2}$$

and at the partial
12 degrees

$$X_1 = \frac{H \tan 12°}{2}$$

f. Referring to
deflection X_1 is in
the value β which

$$\beta = \tan^{-1}\frac{X_1}{x} =$$

g. As the eleme
rotation θ_H increa

$$\theta_H = \lambda + \beta$$

where λ is the an
two-way element
does reach incipie
in the range $X_1 \leq$

$$X_m = x \tan\theta_H + \left($$

When θ_H equals 1
at incipient failure

$$X_u = x \tan 12° + \left($$

Equations 5–39 t
way element desc
other two-way ele

h. The maximu
elements in the ra
a function of the
table 5–9 along
(X_1) and ultimat
fails at partial de

5–13. Elasto-

a. The initial
5–6) generally is

ment (fig. 5–13) which is fully restrained on four edges and whose positive yield lines are defined by $H/2 \leq x \leq L/2$ and $y = H/2$. Denoting θ_H as the angle of rotation in the horizontal direction (along vertical supports) and θ_V as the vertical angle of rotation (along horizontal supports), the maximum deflection X_m at the center of the element prior to reaching the deflection X_1 is

$$X_m = \frac{H \tan\theta_V}{2} \qquad \textbf{Equation 5–39}$$

and at the partial failure deflection X_1 where θ_V equals 12 degrees

$$X_1 = \frac{H \tan 12°}{2} \qquad \textbf{Equation 5–40}$$

f. Referring to figure 5–13, the deflected shape at deflection X_1 is indicated by the solid line and θ_H has the value β which is defined as

$$\beta = \tan^{-1}\frac{X_1}{x} = \tan^{-1}\left(\frac{\tan 12°}{\frac{2x}{H}}\right) \qquad \textbf{Equation 5–41}$$

g. As the element continues to deflect, the angle of rotation θ_H increases, its magnitude becoming equal to

$$\theta_H = \lambda + \beta \qquad \textbf{Equation 5–42}$$

where λ is the angular rotation in excess of β. For a two-way element which undergoes partial failure but does reach incipient failure, the maximum deflection in the range $X_1 \leq X_m \leq X_u$ becomes

$$X_m = x \tan\theta_H + \left(\frac{L}{2} - x\right)\tan(\theta_H - \beta) \qquad \textbf{Equation 5–43}$$

When θ_H equals 12 degrees, the ultimate deflection X_u at incipient failure is

$$X_u = x \tan 12° + \left(\frac{L}{2} - x\right)\tan\left[12° - \tan^{-1}\left(\frac{\tan 12°}{\frac{2x}{H}}\right)\right] \qquad \textbf{Equation 5–44}$$

Equations 5–39 through 5–44 are specific for the two-way element described in figure 5–13 and will vary for other two-way elements with different geometry.

h. The maximum deflections X_m for several two-way elements in the ranges $0 \leq X_m \leq X_1$ and $X_1 \leq X_m \leq X_u$ as a function of the rotation angles θ_H and θ_V are given in table 5–9 along with the values of the partial failure (X_1) and ultimate (X_u) deflections. The support which fails at partial deflection X_1 is also indicated.

5–13. Elasto-Plastic Resistance

a. The initial portion of the resistance function (fig. 5–6) generally is composed of an elastic and one or more elasto-plastic ranges. The elastic unit resistance r_e is defined as the resistance at which first yield occurs; similarly, the elasto-plastic unit resistance r_{ep} is the resistance at which second yield occurs. Where all hinges form in a member at one time, r_e will be equal to the ultimate unit resistance r_u; where two or more hinges are formed at separate times, the maximum value of r_{ep} will be equal to r_u (depending upon the hinges formed, one or more values of r_{ep} may exist).

b. The above resistances for one-way elements are listed in table 5–10. In those cases where the elasto-plastic resistance is equal to the ultimate resistance, the value can be determined from table 5–5.

c. The determination of the elasto-plastic resistances of two-way elements is more complicated than that for one-way elements, since the resistance varies with the span ratio and the placement of the reinforcement. Data for calculating the resistances of two-way elements during the elasto-plastic ranges are presented in figures 5–14 through 5–19.

d. Figures 5–14 through 5–16 are for a two-way element initially fixed on three sides and free on the fourth, while figures 5–17 through 5–19 are for elements initially fixed on four sides. The resistances in each range can readily be determined using the coefficients β, the subscripts referring to the points listed in the accompanying illustration. For example, in figure 5–14, for an element fixed on three sides and free on the fourth, if the ultimate unit resisting moments M_u are known for points 1, 2, and 3, a resistance r for each point can be calculated from

$$M = \beta r H^2 \qquad \textbf{Equation 5–45}$$

by finding the corresponding values of β. The smallest of the three values (say at point 2) corresponds to the first yield and is equal to r_e. Next, the moments at the remaining two points are computed for this value of r_e, and the differences between these and the ultimate values are determined. These differences represent the remaining moment capacities available for additional load. At r_e, the element supports become free, fixed, and simply-supported on opposite sides. Using the moment differences and entering figure 5–15, two values of the change in resistance can be calculated as above, the smallest being Δr and then

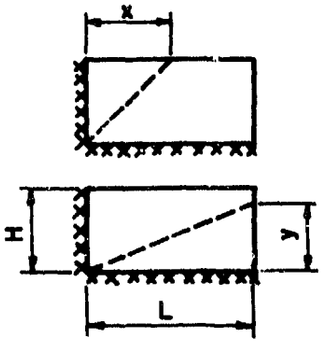
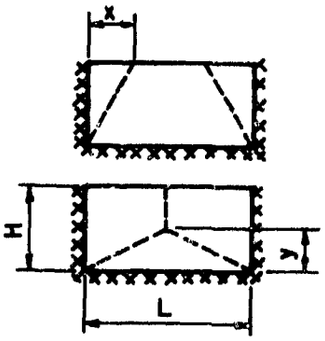
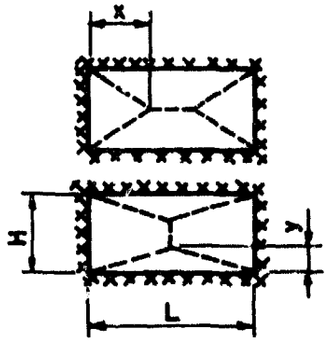
$$r_{ep} = r_e + \Delta r \qquad \textbf{Equation 5–46}$$

In similar fashion, the resistance at the end of each range can be determined until the ultimate unit resistance r_u is reached. A numerical example illustrating the use of these charts is presented in appendix 5A.

5–14. Elasto-Plastic Stiffnesses and Deflections

a. The slopes of the elastic and elasto-plastic ranges of the resistance function are defined by the unit stiff-

Table 5–9. General, Partial Failure, and Ultimate Dej

Edge conditions	Yield line location	Limits	Maximum deflection Δ	
			$(0 \leq X_m < X_1)$	$(X_1 <$
Two adjacent edges supported and two edges free*.		$x \leq H$	$x \tan \theta_H$	H t
		$x \geq H$	$H \tan \theta_V$	$x \tan \theta_H + (L-x) \tan$
		$y \leq L$	$y \tan \theta_V$	L t
		$y \geq L$	$L \tan \theta_H$	$y \tan \theta_V + (H-y) \tan$
Three edges supported and one edge free**.		$x \leq H$	$x \tan \theta_V$	H
		$x \geq H$	$H \tan \theta_V$	$x \tan \theta_H + \left(\frac{L}{2} - x\right) \tan$
		$y \leq \frac{L}{2}$	$y \tan \theta_V$	$\frac{L}{}$
		$y \geq \frac{L}{2}$	$\frac{L \tan \theta_H}{2}$	$y \tan \theta_V + (H-y) \tan$
Four edges supported.		$x \leq \frac{H}{2}$	$x \tan \theta_H$	$\frac{H}{}$
		$x \geq \frac{H}{2}$	$\frac{H \tan \theta_V}{2}$	$x \tan \theta_H + \left(\frac{L}{2} - x\right)$ ta
		$y \leq \frac{L}{2}$	$y \tan \theta_V$	$\frac{L}{}$
		$y \geq \frac{L}{2}$	$\frac{L \tan \theta_H}{2}$	$y \tan \theta_V + \left(\frac{H}{2} - y\right)$ ta

X_m, X, X_u, x, y, L, H (in.)
θ_H, θ_V (deg)

* $X_u = X_1$ if the element has:
(1) a simple horizontal support and $x < H$
(2) a simple vertical support and $x > H$
(3) a simple vertical support and $y < L$
(4) a simple horizontal support and $y > L$

** $X_u = X_1$ if the edge opposite to the free edge is simply supported and $x < H$

5-9. *General, Partial Failure, and Ultimate Deflections for Two-Way Elements*

Maximum deflection X_m		Partial failure deflection X_1	Ultimate deflection X_u	Support failing at deflection X_1
$(0 \le X_m < X_1)$	$(X_1 < X_m < X_u)$			
$x \tan \theta_H$	$H \tan \theta_V$	$x \tan 12°$	$H \tan 12°$	H
$H \tan \theta_V$	$x \tan \theta_H + (L-x) \tan \left[\theta_H - \tan^{-1} \left(\frac{\tan \theta_V}{x/H} \right) \right]$	$H \tan 12°$	$x \tan 12° + (L-x) \tan \left[12° - \tan^{-1} \left(\frac{\tan 12°}{x/H} \right) \right]$	L
$y \tan \theta_V$	$L \tan \theta_H$	$y \tan 12°$	$L \tan 12°$	L
$L \tan \theta_H$	$y \tan \theta_V + (H-y) \tan \left[\theta_V - \tan^{-1} \left(\frac{\tan \theta_H}{y/L} \right) \right]$	$L \tan 12°$	$y \tan 12° + (H-y) \tan \left[12° - \tan^{-1} \left(\frac{\tan 12°}{y/L} \right) \right]$	H
$x \tan \theta_V$	$H \tan \theta_V$	$x \tan 12°$	$H \tan 12°$	H
$H \tan \theta_V$	$x \tan \theta_H + \left(\frac{L}{2} - x \right) \tan \left[\theta_H - \tan^{-1} \left(\frac{\tan \theta_V}{x/H} \right) \right]$	$H \tan 12°$	$x \tan 12° + \left(\frac{L}{2} - x \right) \tan \left[12° - \tan^{-1} \left(\frac{\tan 12°}{x/H} \right) \right]$	L
$y \tan \theta_V$	$\frac{L \tan \theta_H}{2}$	$y \tan 12°$	$\frac{L \tan 12°}{2}$	L
$\frac{L \tan \theta_H}{2}$	$y \tan \theta_V + (H-y) \tan \left[\theta_V - \tan^{-1} \left(\frac{\tan \theta_H}{2y/L} \right) \right]$	$\frac{L \tan 12°}{2}$	$y \tan 12° + (H-y) \tan \left[12° - \tan^{-1} \left(\frac{\tan 12°}{2y/L} \right) \right]$	H
$x \tan \theta_H$	$\frac{H \tan \theta_V}{2}$	$x \tan 12°$	$\frac{H \tan 12°}{2}$	H
$\frac{H \tan \theta_V}{2}$	$x \tan \theta_H + \left(\frac{L}{2} - x \right) \tan \left[\theta_H - \tan^{-1} \left(\frac{\tan \theta_V}{2x/H} \right) \right]$	$\frac{H \tan 12°}{2}$	$x \tan 12° + \left(\frac{L}{2} - x \right) \tan \left[12° - \tan^{-1} \left(\frac{\tan 12°}{2x/H} \right) \right]$	L
$y \tan \theta_V$	$\frac{L \tan \theta_H}{2}$	$y \tan 12°$	$\frac{L \tan 12°}{2}$	L
$\frac{L \tan \theta_H}{2}$	$y \tan \theta_V + \left(\frac{H}{2} - y \right) \tan \left[\theta_V - \tan^{-1} \left(\frac{\tan \theta_H}{2y/L} \right) \right]$	$\frac{L \tan 12°}{2}$	$y \tan 12° + \left(\frac{H}{2} - y \right) \tan \left[12° - \tan^{-1} \left(\frac{\tan 12°}{2y/L} \right) \right]$	H

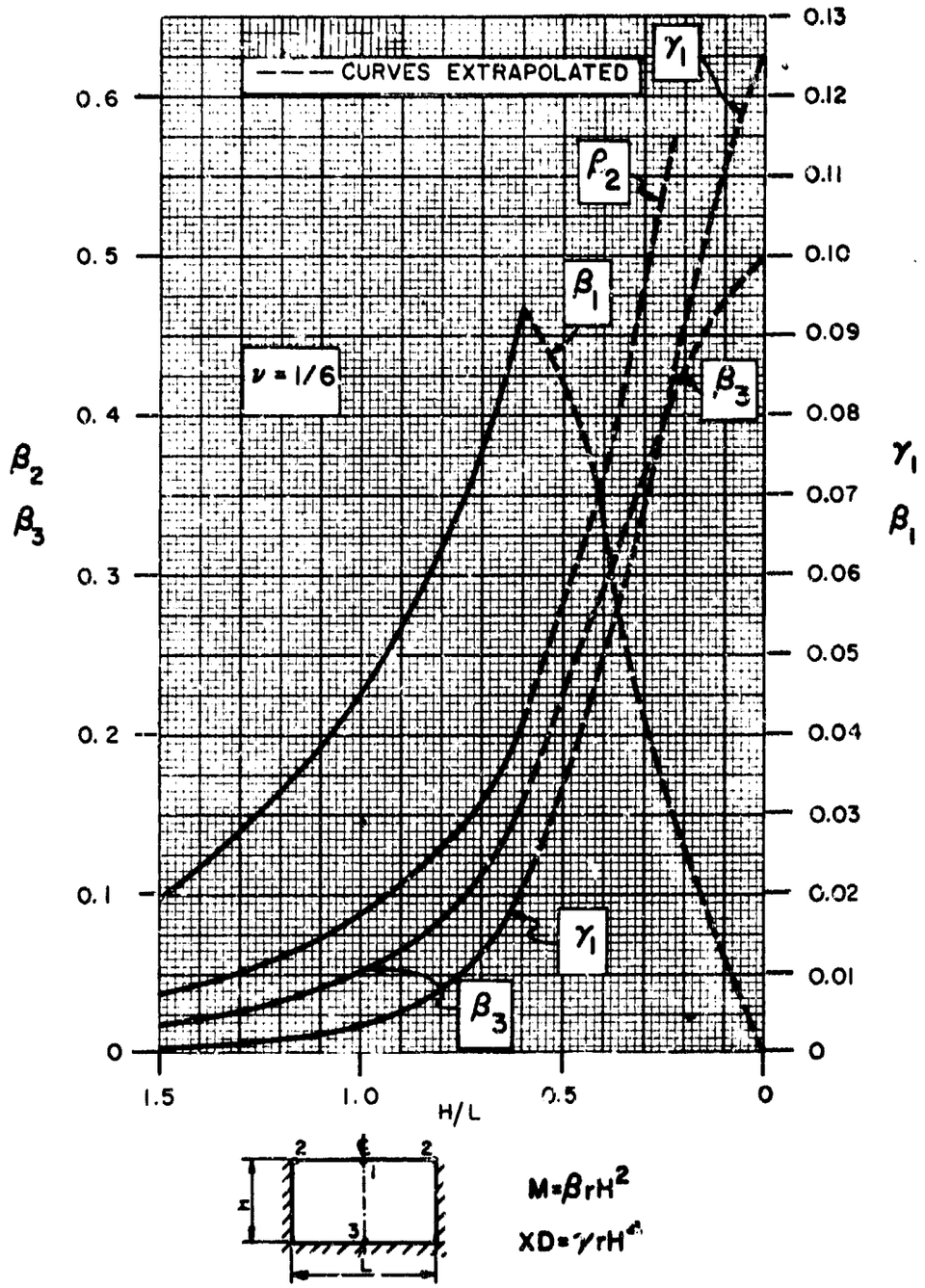


Figure 5-14. Deflection and moments for uniformly loaded two-way element with three edges fixed and one edge free.

Cantilever

Simple supports.

Fixed supports.

Fixed-simple supports.

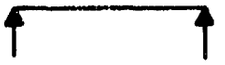
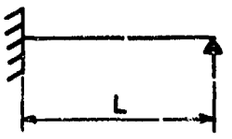
r_e, r_{ep}, r_u (psi)
M_N (in.-lb/in.)
L (in.)

ness K of the element

$$K = \frac{r}{X}$$

where r is the unit re
corresponding to the
stiffness is denoted a
K_{ep}, while in the pla
b. Elasto-plastic uni
are listed in table 5-
modulus of elasticity
I_e, and span length
corresponding elasti
be computed from eq

Table 5–10. Elasto-Plastic Unit Resistances for One-Way Elements

Edge conditions	Elastic unit resistance r_e	Elasto-plastic unit resistance r_{ep}
Cantilever 	r_u	--
Simple supports. 	r_u	--
Fixed supports. 	$\frac{12M_N}{L^2}$	r_u
Fixed-simple supports. 	$\frac{8M_N}{L^2}$	r_u

r_e, r_{ep}, r_u (psi)
M_N (in.-lb/in.)
L (in.)

ness K of the element:

$$K = \frac{r}{X} \qquad \textbf{Equation 5–47}$$

where r is the unit resistance and X is the deflection corresponding to the value of r. The elastic range unit stiffness is denoted as K_e, the elasto-plastic range as K_{ep}, while in the plastic range the stiffness is zero.

b. Elasto-plastic unit stiffnesses for one-way elements are listed in table 5–11 as a function of the concrete modulus of elasticity E_c, average moment of inertia I_a, and span length L. Knowing the stiffnesses, the corresponding elastic and elasto-plastic deflections can be computed from equation 5–47.

c. For two-way elements, the γ coefficients presented in figures 5–14 through 5–19 are used to determine the deflections at the end of each range of behavior from

$$XD = \gamma r H^4 \qquad \textbf{Equation 5–48}$$

where D, the flexural rigidity of the member, is defined as

$$D = \frac{E_c I_a}{b(1-\upsilon^2)} \qquad \textbf{Equation 5–49}$$

and υ is Poisson's ratio. An illustrative example in which the deflections and unit stiffnesses of a two-way element are computed is given in appendix 5A.

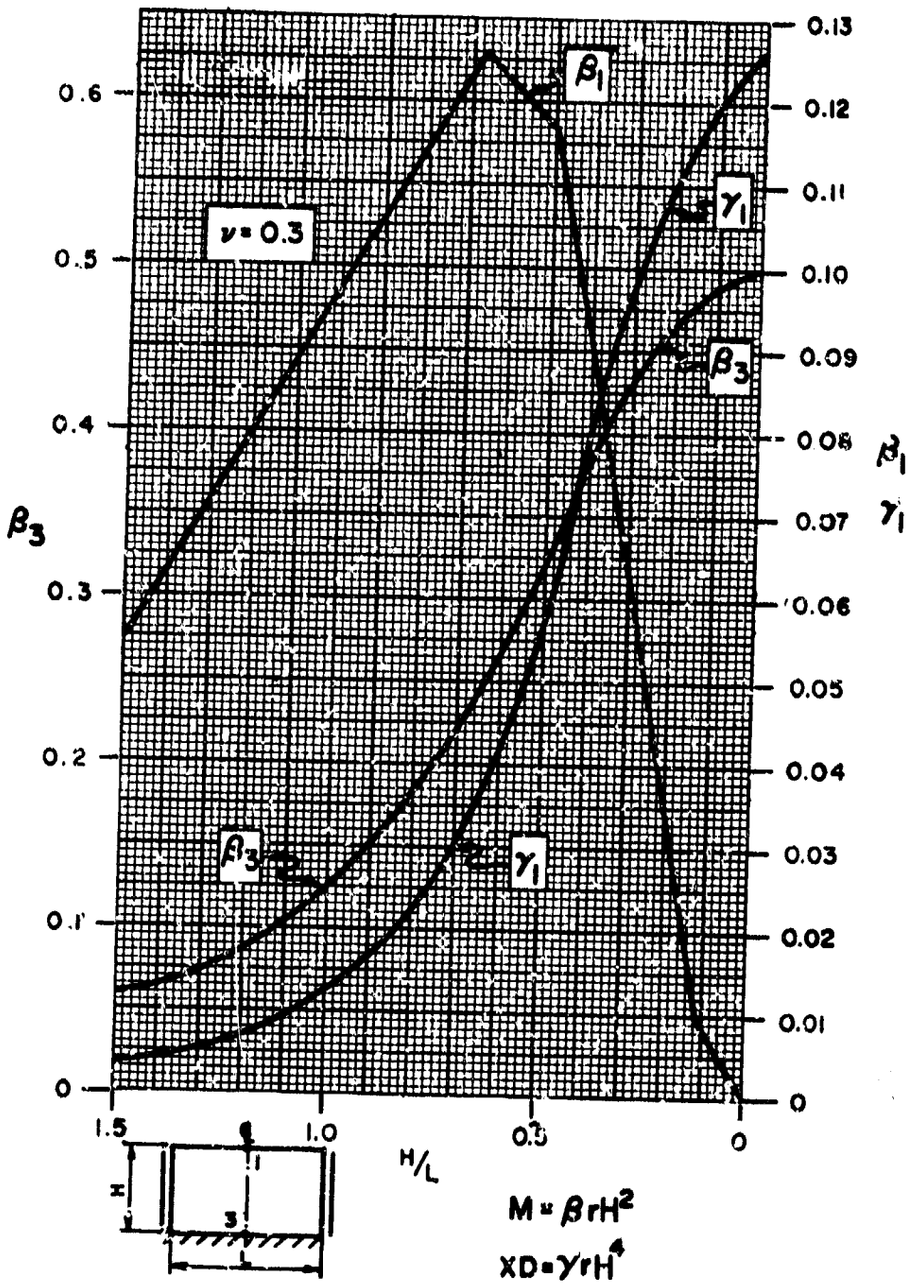


Figure 5–15. Deflection and moments for uniformly loaded two-way element with two opposite edges simply-supported, one edge free, and one edge fixed.

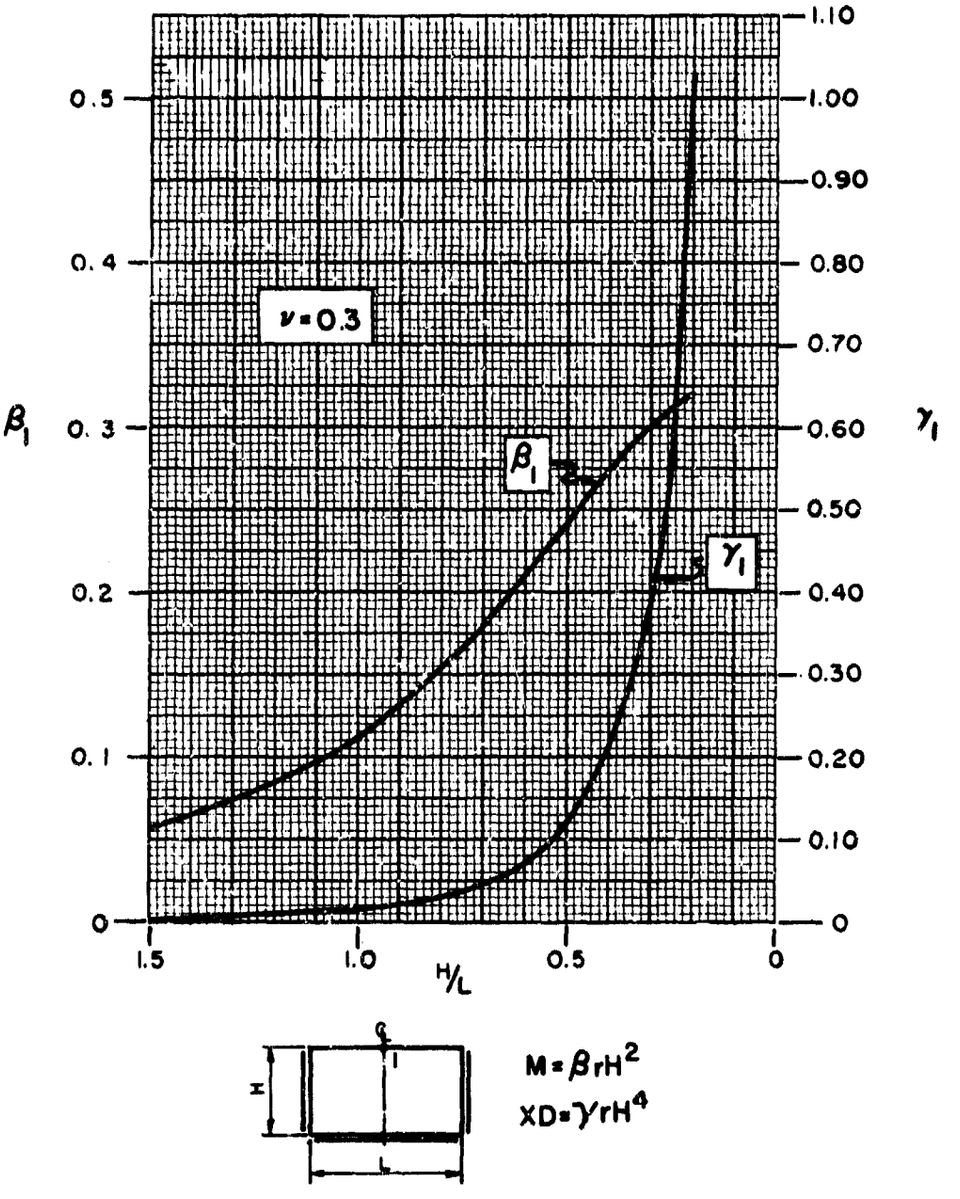


Figure 5-16. Deflection and moments for uniformly loaded two-way element with three edges simply-supported and one edge free.

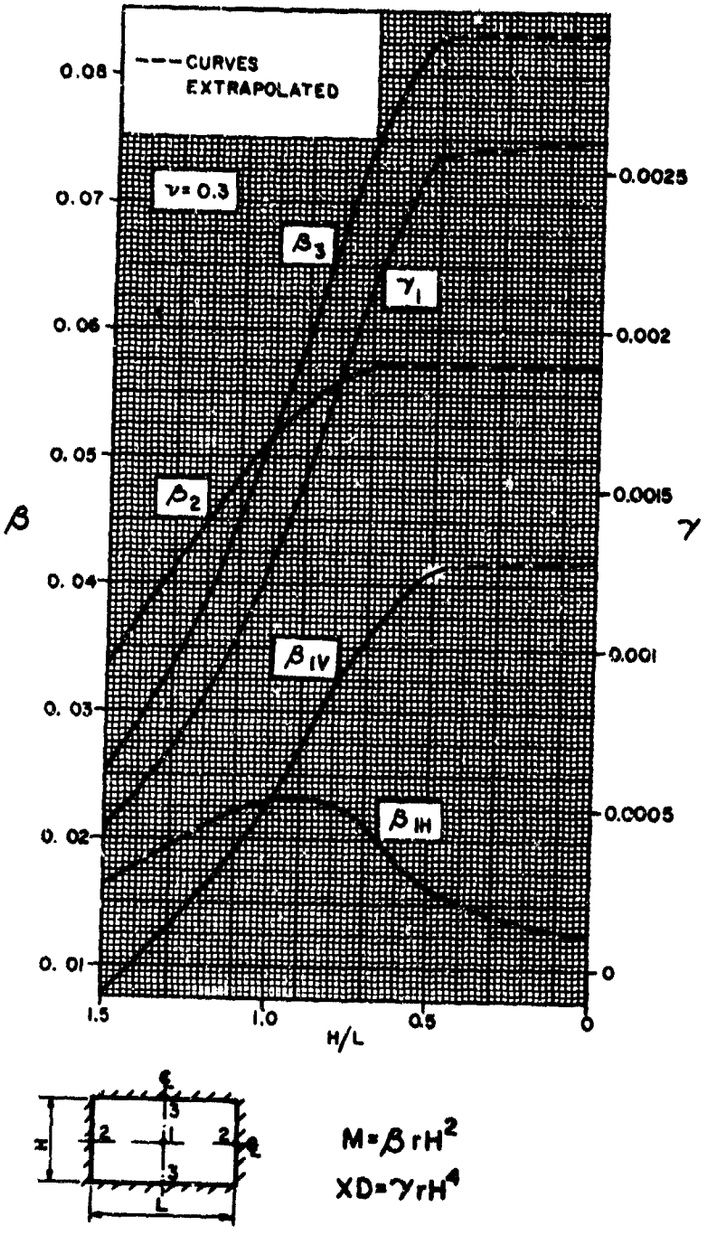


Figure 5–17. Deflection and moments for uniformly loaded two-way element with all edges fixed.

Figure 5–18. Deflection a

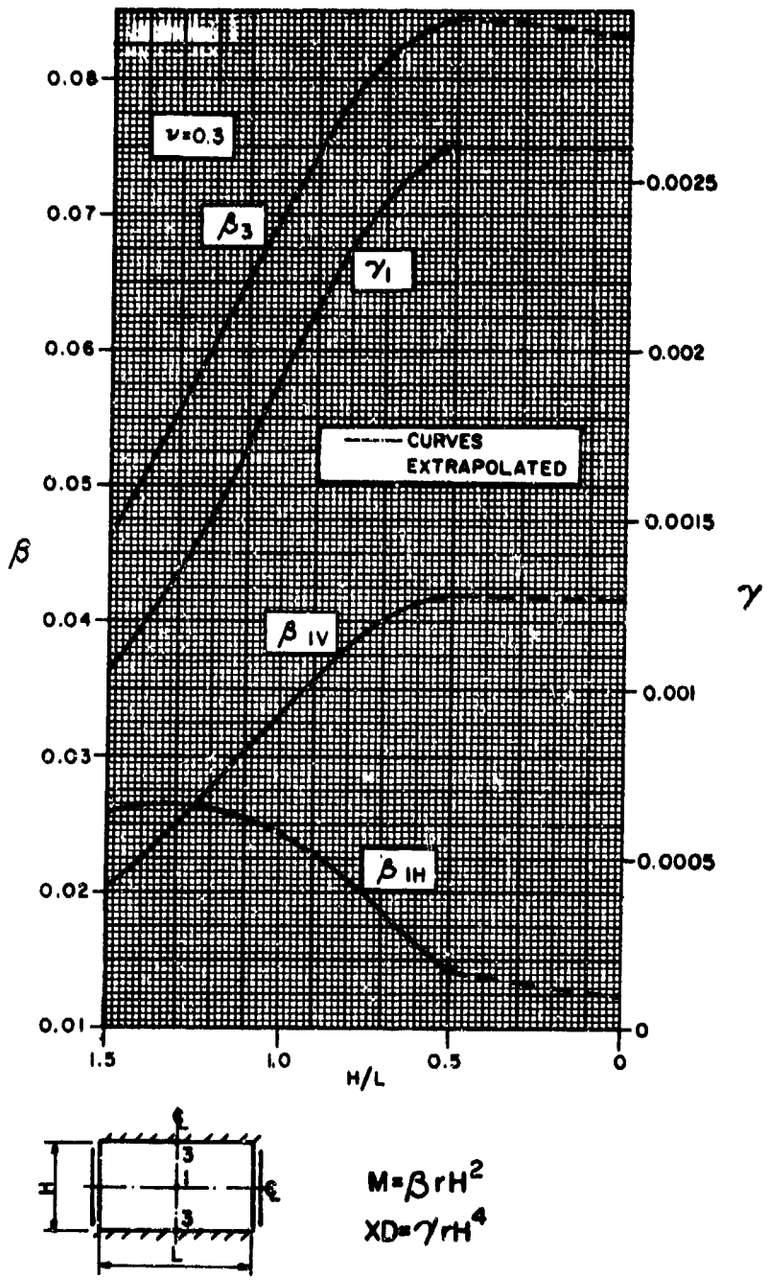
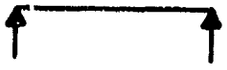
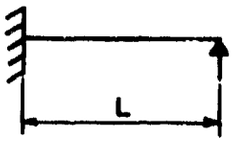


Figure 5–18. Deflection and moments for uniformly loaded two-way element with two opposite edges fixed and two edges simply-supported.

Table 5–11. Elasto-Plastic Stiffness for One-Way Elements

Edge conditions	Elastic unit stiffness K_e	Elasto-plastic unit stiffness K_{ep}
Cantilever 	$\frac{8E_cI_a}{bL^4}$	—
Simple supports. 	$\frac{384E_cI_a}{5bL^4}$	—
Fixed supports. 	$\frac{384E_cI_a}{bL^4}$	$\frac{384E_cI_a}{5bL^4}$
Fixed-simple supports. 	$\frac{185E_cI_a}{bL^4}$	$\frac{384E_cI_a}{5bL^4}$

K_e, K_{ep} (psi/in.)
E_c (psi)
I_a (in.^{4})
b, L (in.)

Section IV. RESISTANCE-DEFLECTION FUNCTIONS FOR DESIGN

5–15. General

The resistance-deflection function used for design depends upon the maximum deflection X_m of the element being considered. This maximum deflection can be categorized as either limited or large. When the maximum deflection falls within the limited deflection range, then the variation of the resistance with deflection in the elastic and elasto-plastic ranges must be considered. If the maximum deflection is within the large deflection range, the elastic and elasto-plastic ranges need not be considered. The demarcation between the two ranges differs for each element, but tests have shown that for the design of elements with maximum support rotations greater than 5 degrees, the error resulting from the omission of the elasto-plastic portions in an analysis will be negligible.

5–16. Limited Deflections

When designing for limited deflections ($\theta_m \leq 5°$), the maximum deflection X_m of the element will be smaller than the partial failure deflection X_1, and the resistance function for design takes the form shown in a, figure 5–20 for a two-step system or b, figure 5–20 for a three-step system. The method of analysis presented in chapter 6 may be simplified further by replacing these functions with an equivalent elastic resistance-deflection function defined by K_E and X_E as indicated by the dotted lines in figure 5–20. The equivalent elastic unit stiffness K_E and the equivalent maximum elastic deflection X_E are calculated such that the area under the dotted curve is equal to the area under the solid curve, thereby producing the same potential energy in each system. The equivalent maximum elastic deflection X_E for the two-step and three-step systems shown is expressed by equations 5–50 and 5–51, respectively.

$$X_E = X_e + X_p\left(1 - \frac{r_e}{r_u}\right) \qquad \text{Equation 5–50}$$

$$X_E = X_e\left(\frac{r_{ep}}{r_u}\right) + X_{ep}\left(1 - \frac{r_e}{r_u}\right) + X_p\left(1 - \frac{r_{ep}}{r_u}\right) \qquad \text{Equation 5–51}$$

The equivalent elastic unit stiffness K_E in each case is equal to

$$K_E = \frac{r_u}{X_E} \qquad \text{Equation 5–52}$$

...stic-plastic unit stiffness K_{ep}
—
—
$\frac{384E_cI_c}{5bL^4}$
$\frac{384E_cI_c}{5bL^4}$

...GN

...ther by replacing these ...tic resistance-deflection ...$_E$ as indicated by the ... equivalent elastic unit ...t maximum elastic de... ...hat the area under the ... under the solid curve, ...tential energy in each ...m elastic deflection X_E ... systems shown in ex... ...5–51, respectively.

Equation 5–50

$$\left(1-\frac{r_{ep}}{r_u}\right)$$

Equation 5–51

...ness K_E in each case is

Equation 5–52

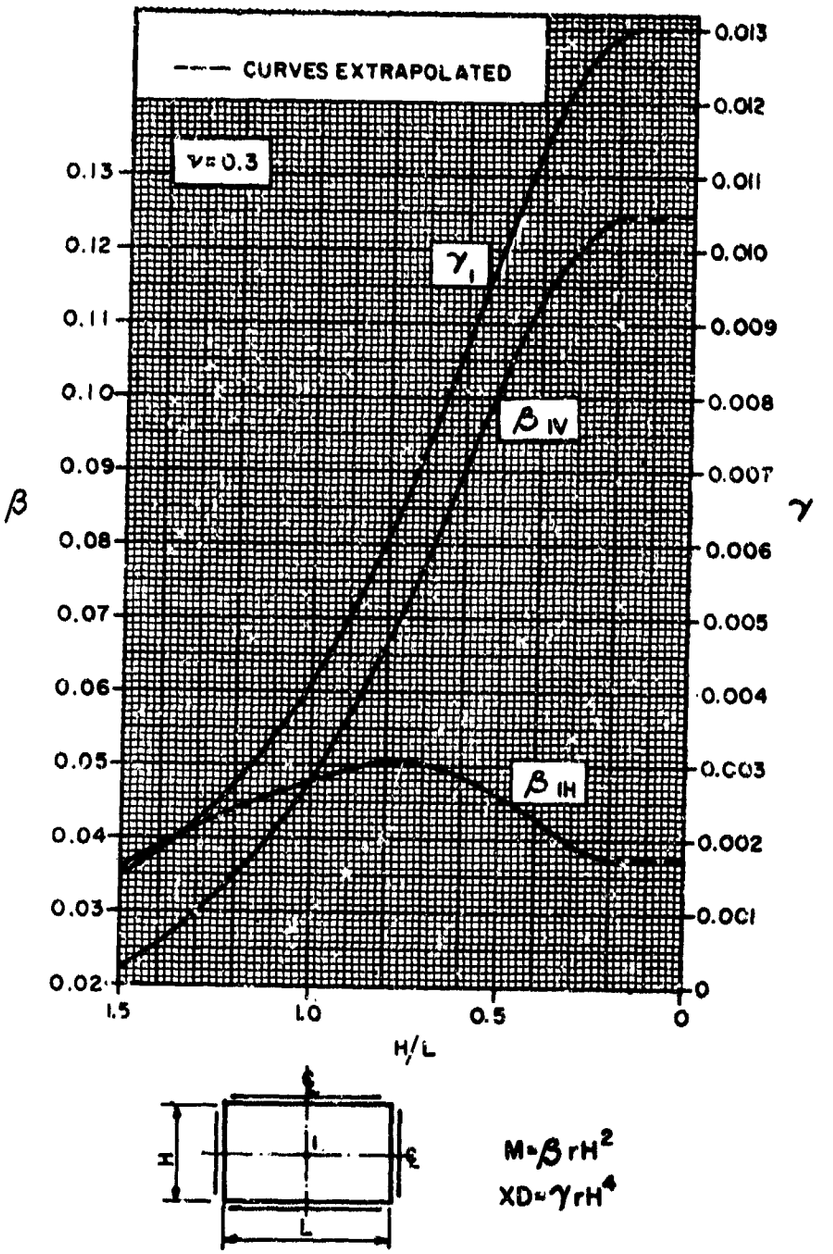
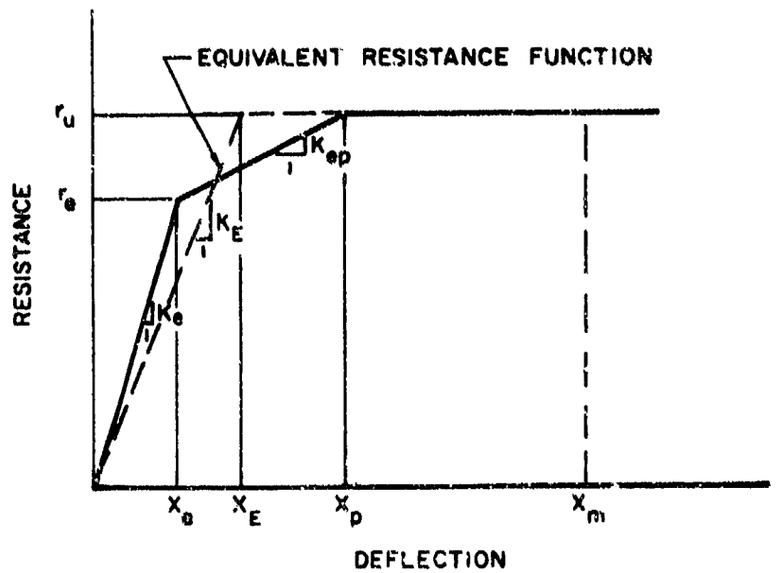


Figure 5–19. Deflection and moments for uniformly loaded two-way element with all edges simply-supported.

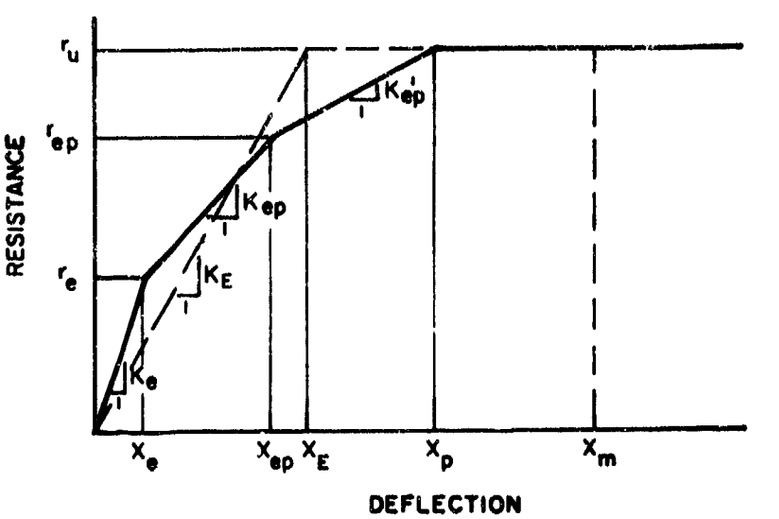
2

5–17. Large Deflections

When designing for large deflections ($\theta_m > 5°$), assume that the resistance rises instantaneously from zero to its ultimate value r_u at the onset of the blast loading. For one-way elements, the design resistance function is approximated by a constant plastic range resistance as shown in a, figure 5–21, while for two-way elements the resistance function becomes that shown in *b*, figure 5–21 where the maximum deflection X_m can be either smaller or larger than the partial failure deflection X_1.

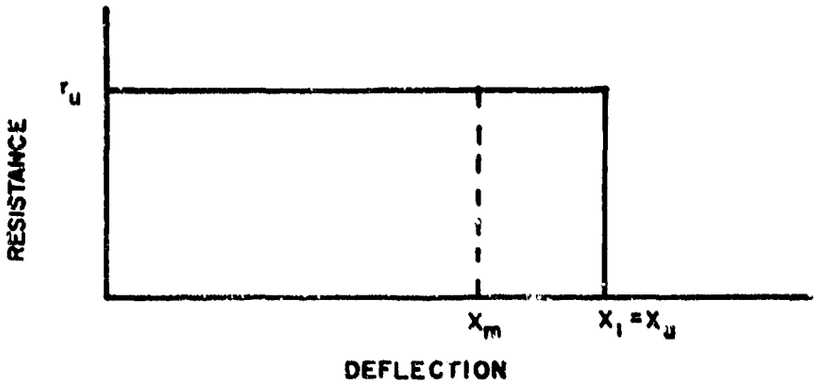


a) TWO STEP ELASTO-PLASTIC SYSTEM

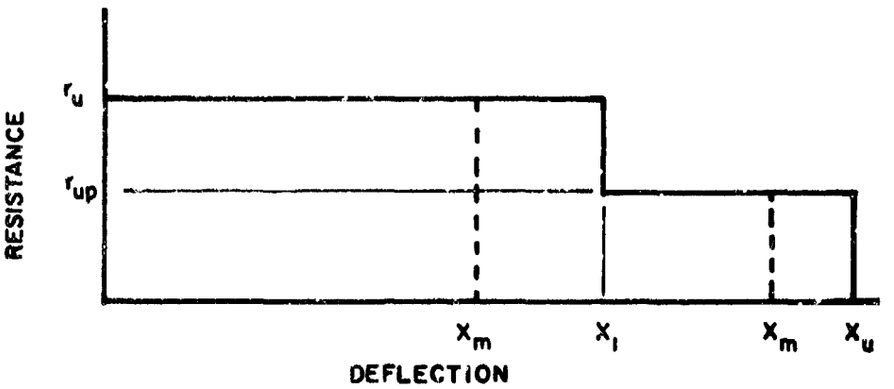


b) THREE STEP ELASTO-PLASTIC SYSTEM

Figure 5-20. Resistance-deflection functions for limited deflections ($\theta_m \leq 5°$).



a) ONE-WAY ELEMENT



b) TWO-WAY ELEMENT

Figure 5-21. Resistance-deflection functions for large deflections ($\theta_m > 5°$).

Section V. ULTIMATE SHEARS AND SHEAR STRESSES

5-18. General

a. The ultimate shear V_u at any section of a flexural element is a function of its geometry, yield line locations, and unit resistance r. For one-way elements, the ultimate shear is developed when the resistance reaches the ultimate value r_u; for two-way elements the ultimate shear may occur when the resistance is r_u or, if the maximum deflection X_m exceeds the partial failure deflection X_1, r_{up}. In the latter case, the shear forces are redistributed as the spanning changes from two-way elements to one-way elements after partial failure.

b. Generally, there are two critical locations where shear must be considered: (1) at distance d or d_c from the supports for checking the diagonal tension stresses and providing shear reinforcement (stirrups or lacing) if necessary, and (2) at the supports where the direct shear forces must be determined. For location (1)

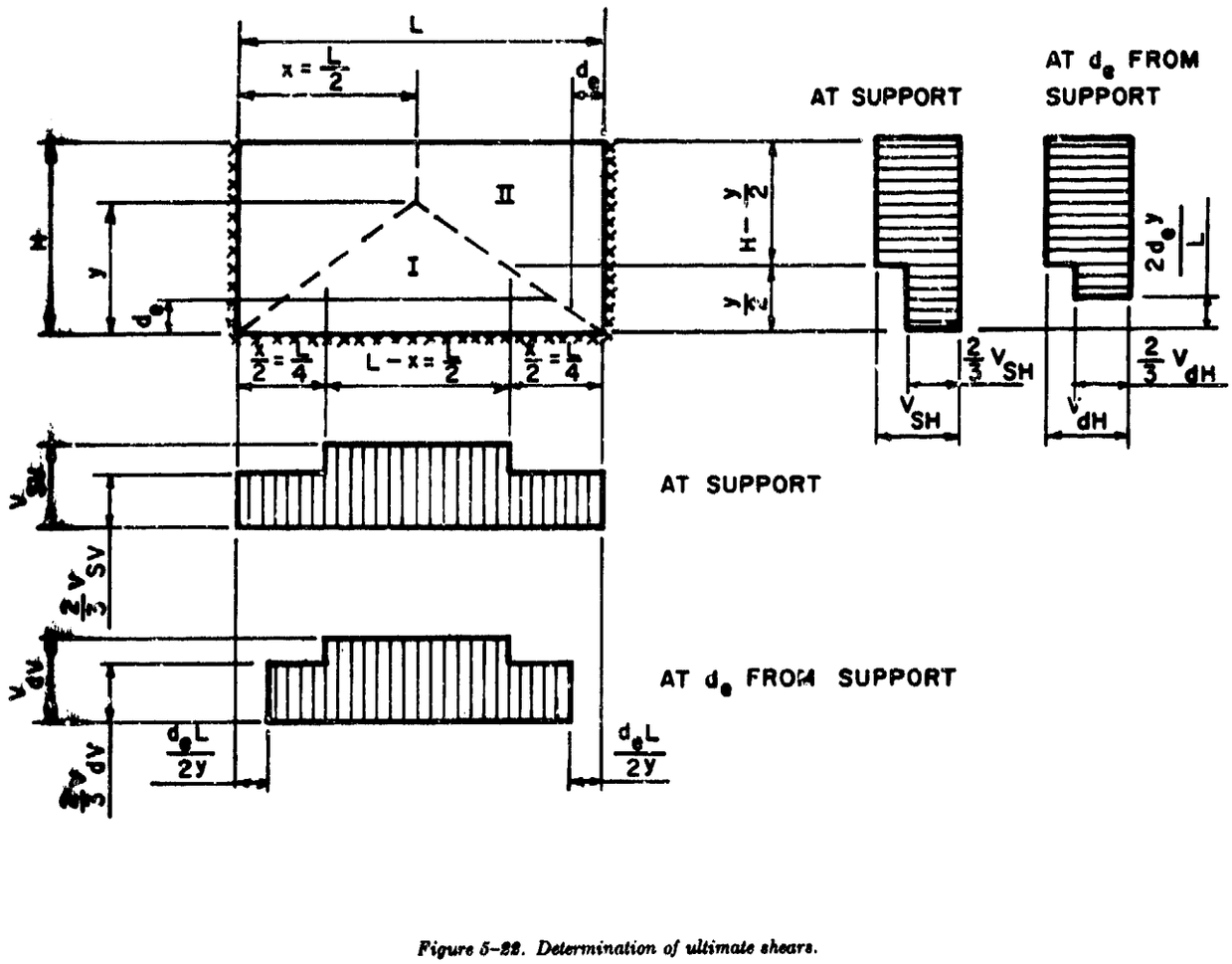
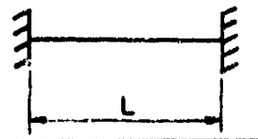


Figure 5–22. Determination of ultimate shears.

Table 5-12. Ultimate Support Shears for One-Way Elements

Edge conditions	Support shear V_s
Cantilever 	$r_u L$
Fixed supports 	$\frac{r_u L}{2}$

V_s (lbs/in.)
r_u (psi)
L (in.)

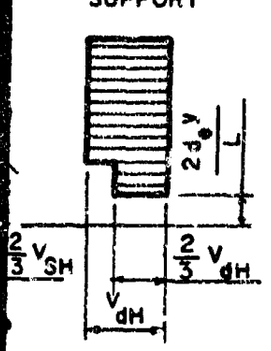
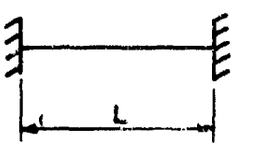


Table 5-13. Ultimate Shear Stress at Distance d_s From Face of Support for One-Way Elements

Edge conditions	Ultimate shear stress v_u
Cantilever 	$\frac{r_u(L-d_s)}{d_s}$
Fixed supports 	$\frac{r_u(L/2-d_s)}{d_s}$

v_u, r_u (psi)
L, d_s (in.)

above, the ultimate shear stress v_u is required, while at location (2) above, the ultimate support shear V_s is needed.

5-19. One-Way Elements

Equations for the ultimate support shears V_s for one-way elements are given in table 5-12, and the ultimate shear stresses v_u at a distance d_s from the support are given in table 5-13 where d_s represents either d or d_c, depending upon the section type being considered.

5-20. Two-Way Elements

a. For two-way elements, the critical sections for shear must be checked at each support. The shears acting at each section are calculated by use of the "yield-line procedure" previously outlined for the determination of the ultimate resistance r_u. The shear along any section parallel to the support is assumed to vary in the same manner as the moment varies ($\frac{3}{4}V$ at the corners and V elsewhere) to account for the higher stiffness of the corners (fig. 5-22). Since the shear is assumed zero along the yield lines, the total shear at any section of a sector is equal to the resistance r_u times the area between the section being considered and the positive yield lines. Referring to figure 5-22, the support shear V_{sV} for the triangular sector I is

$$\tfrac{3}{4}V_{sV}\left(\frac{L}{4}+\frac{L}{4}\right)+V_{sV}\left(\frac{L}{2}\right)=r_u\left(\frac{Ly}{2}\right) \qquad \textbf{Equation 5-53a}$$

$$V_{sV}=\frac{3r_u y}{5} \qquad \textbf{Equation 5-53b}$$

and for the trapezoidal sector II

$$\tfrac{3}{4}V_{sH}\left(\frac{y}{2}\right)+V_{sH}\left(H-\frac{y}{2}\right)=r_u\left(\frac{L}{2}\right)\left(\frac{H-y+H}{2}\right) \qquad \textbf{Equation 5-54a}$$

$$V_{sH}=\frac{3r_u L\left(2-\frac{y}{H}\right)}{2\left(6-\frac{y}{H}\right)} \qquad \textbf{Equation 5-54b}$$

b. Utilizing the same procedure as that used to determine the shear at the supports, the shear V_{dV} and shear stress v_{uV} at distance d_s from the support for the triangular sector I is

$$\tfrac{3}{4}V_{dV}\left(\frac{L}{4}-\frac{d_s L}{2y}+\frac{L}{4}-\frac{d_s L}{2y}\right)+V_{dV}\left(\frac{L}{2}\right)=r_u\left(\frac{y-d_s}{2}\right)\left(L-\frac{d_s L}{y}\right) \qquad \textbf{Equation 5-55a}$$

$$V_{dV}=\frac{3r_u y\left(1-\frac{d_s}{y}\right)^2}{\left(5-4\frac{d_s}{y}\right)} \qquad \textbf{Equation 5-55b}$$

and, since the shear stress v_u is equal to $\frac{V}{bd_s}$ and b equals one inch

$$v_{uV}=\frac{3r_u\left(1-\frac{d_s}{y}\right)^2}{\frac{d_s}{y}\left(5-4\frac{d_s}{y}\right)} \qquad \textbf{Equation 5-56}$$

For the trapezoidal sector II

$$\tfrac{1}{2}V_{dH}\left(\frac{y}{2}-\frac{2d_e y}{L}\right)+V_{dH}\left(H-\frac{y}{2}\right) \qquad \text{Equation 5-57a}$$

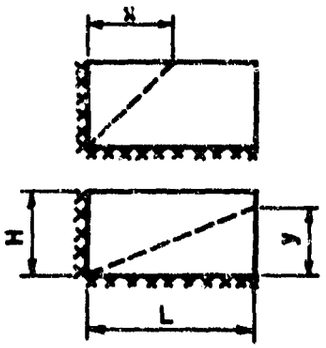
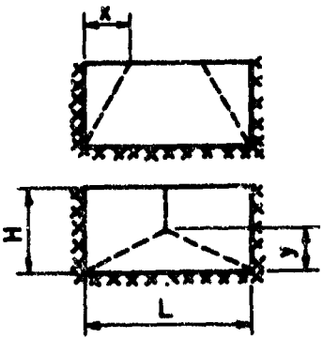
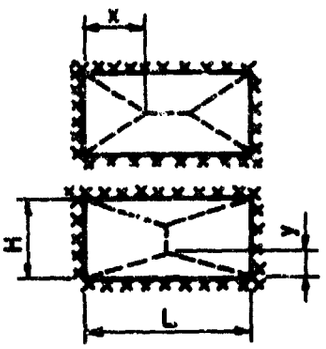
$$=r_u\left(\frac{L}{2}-d_e\right)\frac{1}{2}\left(H-y+H-\frac{2d_e y}{L}\right)$$

$$V_{dH}=\frac{3r_u(L-2d_e)\left(2H-y-\frac{2d_e y}{L}\right)}{2\left(6H-y-\frac{8d_e y}{L}\right)} \qquad \text{Equation 5-57b}$$

$$v_{uy}=\frac{3r_u\left(1-\frac{2d_e}{L}\right)\left(2-\frac{y}{H}-\frac{2d_e y}{LH}\right)}{2\frac{d_e}{L}\left(6-\frac{y}{H}-\frac{8d_e y}{LH}\right)} \qquad \text{Equation 5-58}$$

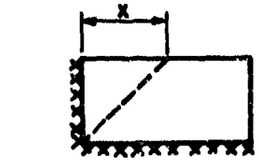
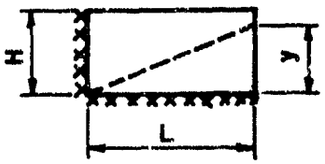
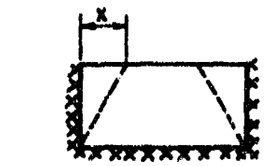
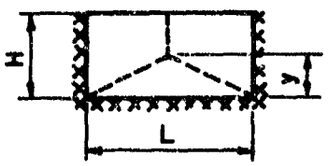
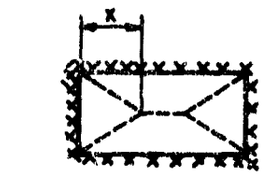
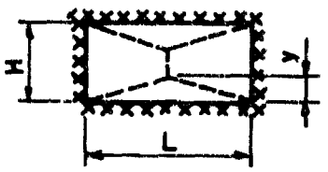
c. Values of the ultimate support shears V_{eH} and V_{eV} for several two-way elements derived as above are presented in table 5–14, and for the ultimate shear stresses v_{uH} and v_{uV} at distance d_e from the support are presented in table 5–15 where again d_e is either d or d_c. As previously mentioned, when the partial failure deflection X_1 is exceeded, these elements must be checked as one-way elements with the post-ultimate resistance r_{up}. The equations presented in tables 5–12 and 5–13 are used replacing r_u by r_{up} and using either L or H for the L given, as required.

Table 5-14. Ultimate Support Shears for Two-Way Elements

Edge conditions	Yield line locations	Limits	Horizontal shear V_{uH}	Vertical shear V_{uV}
Two adjacent edges supported and two edges free.		$x \le L$	$\frac{3r_u x}{5}$	$\frac{3r_u H\left(2-\frac{x}{L}\right)}{\left(6-\frac{x}{L}\right)}$
		$y \le H$	$\frac{3r_u L\left(2-\frac{y}{H}\right)}{\left(6-\frac{y}{H}\right)}$	$\frac{3r_u y}{8}$
Three edges supported and one edge free.		$x \le \frac{L}{2}$	$\frac{3r_u x}{5}$	$\frac{3r_u H\left(1-\frac{x}{L}\right)}{\left(3-\frac{x}{L}\right)}$
		$y \le H$	$\frac{3r_u L\left(2-\frac{y}{H}\right)}{2\left(6-\frac{y}{H}\right)}$	$\frac{3r_u y}{5}$
Four edges supported.		$x \le \frac{L}{2}$	$\frac{3r_u x}{5}$	$\frac{3r_u H\left(1-\frac{x}{L}\right)}{2\left(3-\frac{x}{L}\right)}$
		$y \le \frac{H}{2}$	$\frac{3r_u L\left(1-\frac{y}{H}\right)}{2\left(3-\frac{y}{H}\right)}$	$\frac{3r_u y}{5}$

V_{uH}, V_{uV} (lbs/in.)
x, y, L, H (in.)
r_u (psi)

Table 5–15. Ultimate Shear Stresses at Distance d_s From the Supports for

Edge conditions	Yield location	Limits	Ultimate horizontal shear stress v_{uH}
Two adjacent edges supported and two edges free.		$0 \le d_s/x \le \frac{1}{2}$	$\frac{3r_u(1-d_s/x)^2}{d_s/x(5-4d_s/x)}$
		$\frac{1}{2} \le d_s/x \le 1$	$\frac{r_u(1-d_s/x)}{2(d_s/x)}$
		$0 \le d_s/L \le \frac{1}{2}$	$\frac{3r_u(1-d_s/L)(2-y/H-d_sy/LH}{d_s/L(6-y/H-4d_sy/LH)}$
		$\frac{1}{2} \le d_s/L \le 1$	$\frac{r_u(1-d_s/L)(2-y/H-d_sy/LH}{2d_s/L(1-d_sy/LH)}$
Three edges supported and one free edge.		$0 \le d_s/x \le \frac{1}{2}$	$\frac{3r_u(1-d_s/x)^2}{d_s/x(5-4d_s/x)}$
		$\frac{1}{2} \le d_s/x \le 1$	$\frac{r_u(1-d_s/x)}{2(d_s/x)}$
		$0 \le d_s/L \le \frac{1}{2}$	$\frac{3r_u(1-2d_s/L)(2-y/H-2d_sy/LH}{2d_s/L(6-y/H-8d_sy/LH)}$
		$\frac{1}{2} \le d_s/L \le \frac{1}{2}$	$\frac{r_u(1-2d_s/L)(2-y/H-2d_sy/LH}{4d_s/L(1-2d_sy/LH)}$
Four edges supported.		$0 \le d_s/x \le \frac{1}{2}$	$\frac{3r_u(1-d_s/x)^2}{d_s/x(5-4d_s/x)}$
		$\frac{1}{2} \le d_s/x \le 1$	$\frac{r_u(1-d_s/x)}{2d_s/x}$
		$0 \le d_s/L \le \frac{1}{2}$	$\frac{3r_u(\frac{1}{2}-d_s/L)(1-y/H-2d_sy/LH)}{d_s/L(3-y/H-8d_sy/LH)}$
		$\frac{1}{2} \le d_s/L \le \frac{1}{2}$	$\frac{r_u(\frac{1}{2}-d_s/L)(1-y/H-2d_sy/LH)}{d_s/L(1-4d_sy/LH)}$

d_s, H, L, x, y (in.)
v_{uH}, v_{uV}, r_u (psi)

...es at Distance d_s From the Supports for Two-Way Elements

Ultimate horisontal shear stress v_{uH}	Limits	Ultimate vertical shear stress v_{uV}
$\dfrac{3r_u(1-d_s/x)^2}{d_s/x(5-4d_s/x)}$	$0 \le d_s/H \le \frac{1}{2}$	$\dfrac{3r_u(1-d_s/H)(2-x/L-d_sx/HL)}{d_s/H(6-x/L-4d_sx/HL)}$
$\dfrac{r_u(1-d_s/x)}{2(d_s/x)}$	$\frac{1}{2} \le d_s/H \le 1$	$\dfrac{r_u(1-d_s/H)(2-x/L-d_sx/HL)}{2d_s/H(1-d_sx/HL)}$
$\dfrac{3r_u(1-d_s/L)(2-y/H-d_sy/LH)}{d_s/L(6-y/H-4d_sy/LH)}$	$0 \le d_s/y \le \frac{1}{2}$	$\dfrac{3r_u(1-d_s/y)^2}{d_s/y(5-4d_s/y)}$
$\dfrac{r_u(1-d_s/L)(2-y/H-d_sy/LH)}{2d_s/L(1-d_sy/LH)}$	$\frac{1}{2} \le d_s/y \le 1$	$\dfrac{r_u(1-d_s/y)}{2d_s/y}$
$\dfrac{3r_u(1-d_s/x)^2}{d_s/x(5-4d_s/x)}$	$0 \le d_s/H \le \frac{1}{2}$	$\dfrac{3r_u(1-d_s/H)(1-x/L-d_sx/HL)}{d_s/H(3-x/L-4d_sx/HL)}$
$\dfrac{r_u(1-d_s/x)}{2(d_s/x)}$	$\frac{1}{2} \le d_s/H \le 1$	$\dfrac{r_u(1-d_s/H)(1-x/L-d_sx/HL)}{d_s/H(1-2d_sx/HL)}$
$\dfrac{3r_u(1-2d_s/L)(2-y/H-2d_sy/LH)}{2d_s/L(6-y/H-8d_sy/LH)}$	$0 \le d_s/y \le \frac{1}{2}$	$\dfrac{3r_u(1-d_s/y)^2}{d_s/y(5-4d_s/y)}$
$\dfrac{r_u(1-2d_s/L)(2-y/H-2d_sy/LH)}{4d_s/L(1-2d_sy/LH)}$	$\frac{1}{2} \le d_s/y \le 1$	$\dfrac{r_u(1-d_s/y)}{2d_s/y}$
$\dfrac{3r_u(1-d_s/x)^2}{d_s/x(5-4d_s/x)}$	$0 \le d_s/H \le \frac{1}{4}$	$\dfrac{3r_u(\frac{1}{2}-d_s/H)(1-x/L-2d_sx/HL)}{d_s/H(3-x/L-8d_sx/HL)}$
$\dfrac{r_u(1-d_s/x)}{2d_s/x}$	$\frac{1}{4} \le d_s/H \le \frac{1}{2}$	$\dfrac{r_u(\frac{1}{2}-d_s/H)(1-x/L-2d_sx/HL)}{d_s/H(1-4d_sx/HL)}$
$\dfrac{3r_u(\frac{1}{2}-d_s/L)(1-y/H-2d_sy/LH)}{d_s/L(3-y/H-8d_sy/LH)}$	$0 \le d_s/y \le \frac{1}{2}$	$\dfrac{3r_u(1-d_s/y)^2}{d_s/y(5-4d_s/y)}$
$\dfrac{r_u(\frac{1}{2}-d_s/L)(1-y/H-2d_sy/LH)}{d_s/L(1-4d_sy/LH)}$	$\frac{1}{2} \le d_s/y \le 1$	$\dfrac{r_u(1-d_s/y)}{2d_s/y}$

APPENDIX 5A. STRUCTURAL BEHAVIOR OF REINFORCED CONCRETE ILLUSTRATIVE EXAMPLES

PROBLEM 5A-1. ULTIMATE UNIT RESISTANCE

Problem: Determine the ultimate unit resistance of a two-way element using (1) general solution and (2) charts (chart solution can only be used if the element conforms to the requirements listed in paragraph 5-9).

Procedure (Part a - General Solution):

Step 1. Establish design parameters:

a. Geometry of element.

b. Amount and distribution of reinforcement.

c. Support conditions.

d. Type of section available for moment capacity (sec. I, ch. 5).

e. Static design strengths (table 5-4).

f. Dynamic increase factors (table 5-3).

Step 2. Calculate dynamic design strengths for concrete and reinforcement.

Step 3. Assume yield line location in terms of x and/or y considering support conditions and distribution of reinforcement (fig. 5-7) and the presence of openings and reactions from blast closure systems (fig. 5-12). Also denote sectors formed.

Step 4. Determine negative and positive ultimate moment capacities of sections crossed by assumed yield lines (sec. I, ch. 5).

Step 5. Establish distribution of moments across negative and assumed positive yield lines considering corner effects (fig. 5-8) and the effects of openings.

Step 6. Determine the ultimate unit resistance for each sector in terms of x and/or y considering the free-body diagram of the sectors (fig. 5-8). Summation of the moments about the axis of rotation (support) of the sector yields equation 5-23.

$$\Sigma M_N + \Sigma M_P = Rc = r_u Ac$$

Step 7. Equate the ultimate unit resistance of the sectors and solve for the yield line location x and/or y.

Step 8. With known yield line location, solve for ultimate unit resistance of the element, using equations obtained in step 6.

Note:

For complex problems (three or more different sectors), the solution for the ultimate unit resistance is most easily accomplished through a trial-and-error procedure by determining r_u for each sector for a given (assumed) yield line location and adjusting the yield lines until the several values of r_u agree to within a few percent.

Procedure (Part b - Chart Solution):

Step 1. Same as step 1 of part a.

Step 2. Same as step 2 of part a.

Step 3. Calculate negative and positive ultimate moment capacities in vertical and horizontal directions.

Step 4. Calculate the value of the quantity

$$\frac{L}{H}\left[\frac{M_{VN} + M_{VP}}{M_{HN} + M_{HP}}\right]^{\frac{1}{2}}$$

Step 5. For given support conditions use appropriate chart (figs. 5-9 through 5-11) to obtain yield line location ratios x/L or y/H for value of quantity obtained in step 4. Then calculate x or y.

Step 6. Using appropriate equation from table 5-6, determine the ultimate unit resistance of the element.

EXAMPLE 5A-1 (A) - ULTIMATE UNIT RESISTANCE

Required: Ultimate unit resistance of two-way element shown below using (1) general solution and (2) charts.

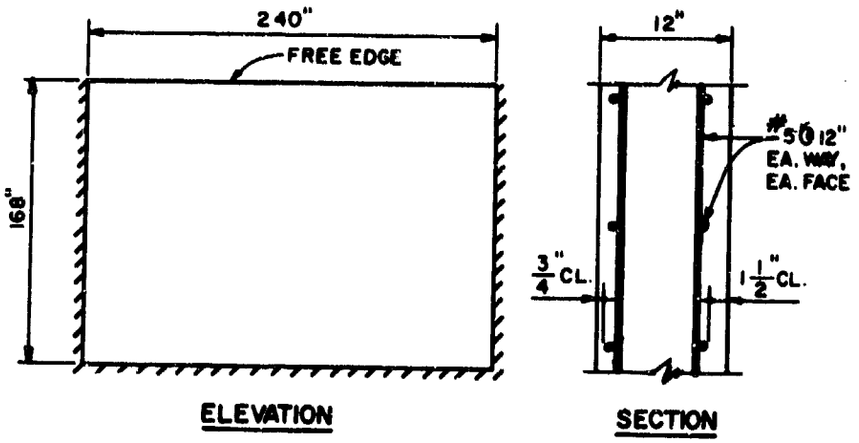


Figure 5A-1

Solution (Part a - General Solution):

Step 1. Given:

a. L = 240 in, H = 168 in, T_c = 12 in

b. Reinf. - #5 @ 12 in. each way, each face (for placement, see fig. 5A-1).

c. Three fixed supports capable of developing moment capacity of element, and one free edge.

d. Type I section (concrete resists load).

e. f'_c = 3,000 psi and f_s = 60,000 psi.

f. DIF - concrete = 1.25 and reinf. = 1.10.

Step 2. Dynamic design strengths

f'_{dc} = DIF f'_c = 1.25 (3,000) = 3,750 psi

f_{ds} = DIF f_s = 1.10 (60,000) = 66,000 psi

Step 3. Assumed yield line location (fig. 5A-2).

Step 4. For Type I sections, the ultimate moment capacity, neglecting the small effect of the compression reinforcement, is given by:

$$M_u = \frac{A_s}{b} f_{ds}\left(d - \frac{a}{2}\right) \quad \text{where } a = \frac{A_s f_{ds}}{0.85 f_{dc} b}$$

For all sections $A_s = 0.31$ sq in/ft. For b = 12 in

$$a = \frac{0.31(66{,}000)}{0.85(3{,}750)(12)} = 0.535 \text{ in}$$

a. Horizontal Direction

(1) Negative moment

$$d = 12 - \left(0.75 + \frac{0.625}{2}\right) = 10.9375 \text{ in}$$

$$M_{HN} = \frac{0.31}{12}(66{,}000)\left(10.9375 - \frac{0.535}{2}\right) = 18{,}190 \text{ in-lbs/in}$$

(2) Positive moment

$$d = 12 - \left(1.50 + \frac{0.625}{2}\right) = 10.1875 \text{ in}$$

$$M_{HP} = \frac{0.31}{12}(66{,}000)\left(10.1875 - \frac{0.535}{2}\right) = 16{,}910 \text{ in-lbs/in}$$

b. Vertical Direction

(1) Negative moment

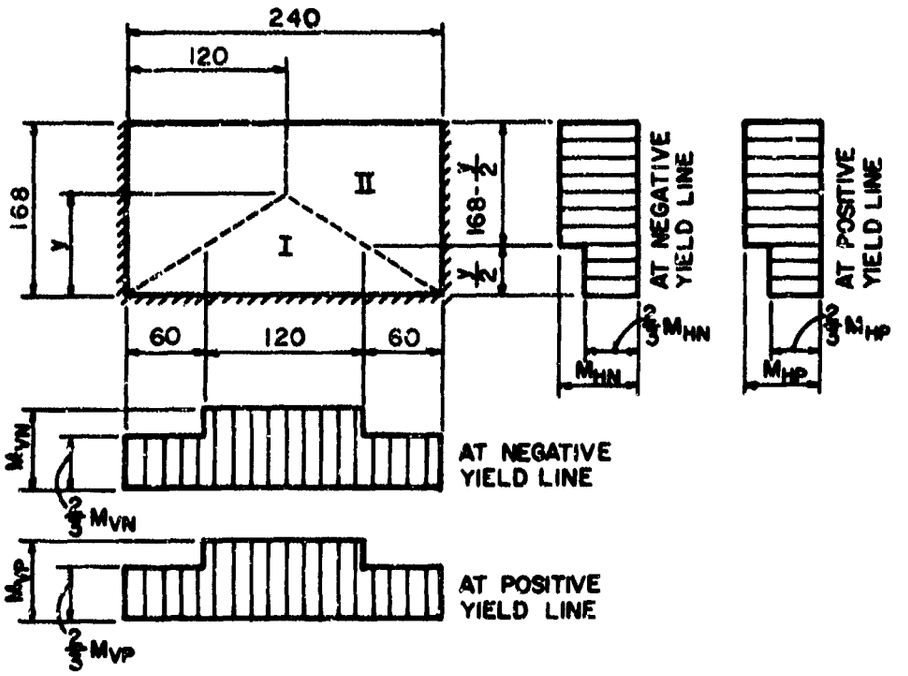
$$d = 12 - \left(0.75 + 0.625 + \frac{0.625}{2}\right) = 10.3125 \text{ in}$$

$$M_{VN} = \frac{0.31}{12}(66{,}000)\left(10.3125 - \frac{0.535}{2}\right) = 17{,}130 \text{ in-lbs/in}$$

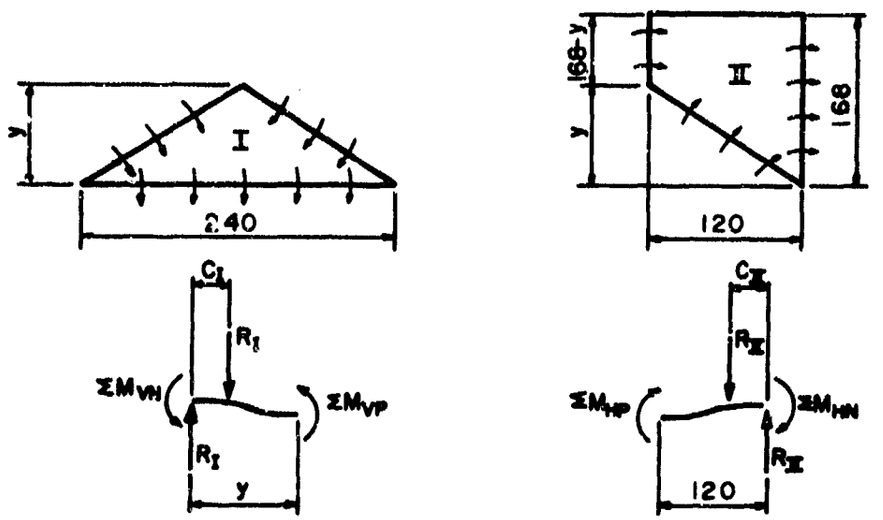
(2) Positive moment

$$d = 12 - \left(1.50 + 0.625 + \frac{0.625}{2}\right) = 9.5625 \text{ in}$$

$$M_{VP} = \frac{0.31}{12}(66{,}000)\left(9.5625 - \frac{0.535}{2}\right) = 15{,}850 \text{ in-lbs/in}$$



a) ASSUMED YIELD LINES AND DISTRIBUTION OF MOMENTS

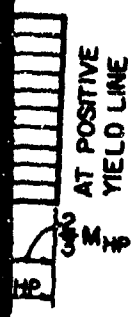


b) FREE-BODY DIAGRAMS FOR INDIVIDUAL SECTORS

Figure 5A-2. Determination of ultimate unit resistance.

Step

Step



Step 5. For distribution of moments across negative and assumed positive lines, see figure 5A-2(a).

Step 6. The ultimate unit resistance of each sector is obtained by taking the summation of the moments about its axis of rotation (support) so that

$$\Sigma M_N + \Sigma M_P = Rc = r_u Ac$$

a. Sector I (fig. 5A-2).

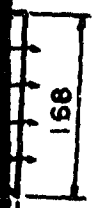
$$\Sigma M_{VN} + \Sigma M_{VP} = 17{,}130\ (120) + 2\left(\frac{2}{3}\right)(17{,}130)(60) + 15{,}850\ (120) + 2\left(\frac{2}{3}\right)(15{,}850)(60) = 6.6 \times 10^6 \text{ in-lbs}$$

$$r_u Ac = r_u \left[\frac{240(y)}{2}\right]\left[\frac{y}{3}\right] = 40\, r_u y^2$$

therefore,

$$r_u = \frac{6.6 \times 10^6}{40y^2} = \frac{164{,}300}{y^2}$$

b. Sector II (fig. 5A-2).



$$\Sigma M_{HN} + \Sigma M_{HP} = 18{,}190\left(168 - \frac{y}{2}\right) + \frac{2}{3}(18{,}190)\left(\frac{y}{2}\right) + 16{,}910\left(168 - \frac{y}{2}\right) + \frac{2}{3}(16{,}910)\left(\frac{y}{2}\right) = 5{,}850\ (1008 - y)$$

$$r_u Ac = r_u \left[\frac{120(168 + 168 - y)}{2}\right]\left[\frac{120\,[168 + 2\,(168 - y)]}{3\,(168 - 168 - y)}\right] = 4800\, r_u\ (252 - y)$$

therefore,

$$r_u = \frac{5{,}850\ (1008 - y)}{4800\ (252 - y)} = \frac{1.219\ (1008 - y)}{(252 - y)}$$

Step 7. Equate the ultimate unit resistance of the sectors.

$$\frac{164,900}{y^2} = \frac{1.219\ (1008 - y)}{(252 - y)}$$

simplifying:

$$y^3 - 1008y^2 - 135,300\ y + 34,100,000 = 0$$

and the desired root is:

$$y = 134.8 \text{ in}$$

Step 8. The ultimate unit resistance is obtained by substituting the value of y into either equation obtained in step 6, both of which yield:

$$r_u = 9.08 \text{ psi}$$

Solution (Part b - Chart Solution):

Note:

Element conforms to requirements of paragraph 5-9 since it is fixed on three sides and free on the remaining side (vertical axis of symmetry) and has a uniform steel distribution in both the vertical and horizontal directions. Also, the reinforcing steel and hence the yield line pattern (whether x or y) are symmetrical about the vertical axis of symmetry. (Equal positive and negative steel is not required nor is equal steel in the vertical and horizontal directions.)

Step 1. Same as step 1 of part a.

Step 2. Sam as step 2 of part a.

Step 3. For ultimate moment capacities see step 4 of part a.

Step 4. Calculate parameter

$$\frac{L}{H}\left[\frac{M_{VN} + M_{VP}}{M_{HN} + M_{HP}}\right]^{\frac{1}{2}} = \frac{240}{168}\left[\frac{17,130 + 15,850}{18,190 + 16,910}\right]^{\frac{1}{2}} = 1.386$$

p 5.

Step 5. From figure 5-10, read yield line location.

$$y/H = 0.803 \; ; \; y = 0.803 \; (168) = 134.9 \text{ in}$$

p 6.

Step 6. From table 5-6,

$$r_u = \frac{5\left(M_{VN} + M_{VP}\right)}{y^2} = \frac{5\ (17{,}130 + 15{,}850)}{(134.9)^2} = 9.06 \text{ psi}$$

EXAMPLE 5A-1.(B). ULTIMATE UNIT RESISTANCE

ired:
A-1(A)
losur
losur

Required: Ultimate unit resistance of the element considered in example 5A-1(A) except there is an opening as shown below. There is no blast closure system over the opening, therefore, no loads (reaction from closure system) are applied to edge of opening.

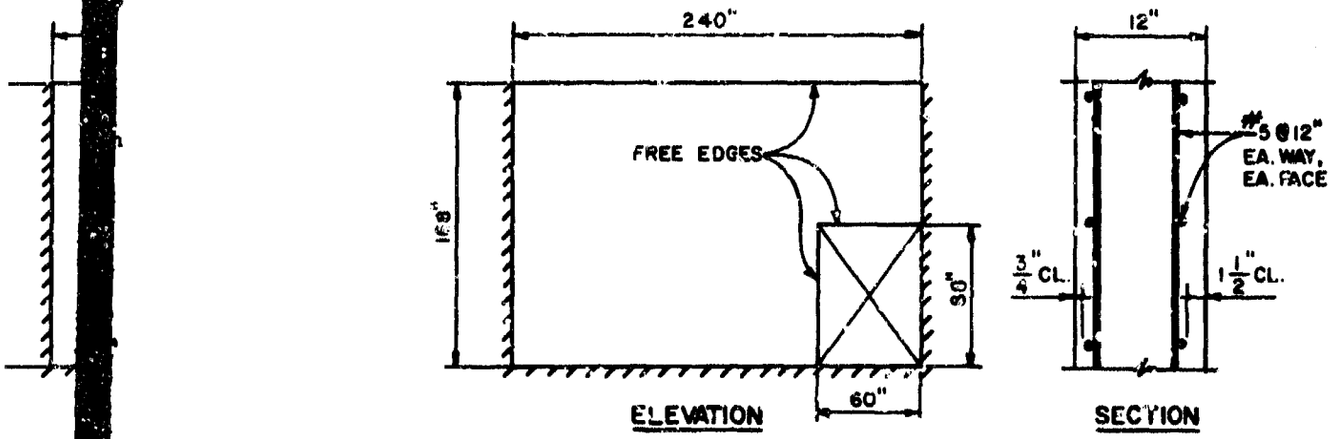


Figure 5A-3

Solution:

Step 1. Given: Same as step 1 of example 5A-1(A), part a. Also, two additional free edges are formed due to the presence of the opening.

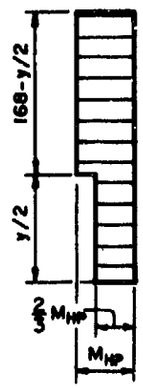
Step 2. Same as step 2 of example 5A-1(A), part a.

Step 3. Assumed yield line location is shown in figure 5A-4. (three different sectors are formed.)

Step 4. Same as step 4 of example 5A-1(A), part a,

where: $M_{HN} = 18{,}190$ in-lbs/in $\quad M_{HP} = 16{,}910$ in-lbs/in

$M_{VN} = 17{,}130$ in-lbs/in $\quad M_{VP} = 15{,}850$ in-lbs/in



Step 5. For distribution of moments across negative and assumed positive yield lines see figure 5A-4. (Since opening is located at lower right corner, do not have reduced moment capacity.)

Step 6. The ultimate unit resistance is obtained from

$$\Sigma M_N + \Sigma M_P = Rc = r_u Ac$$

a. Sector I (fig. 5A-4).

$$\Sigma M_{HN} + \Sigma M_{HP} = 18{,}190\left(168 - \frac{y}{2}\right) + \frac{2}{3}(18{,}190)\left(\frac{y}{2}\right) + 16{,}910\left(168 - \frac{y}{2}\right) + \frac{2}{3}(16{,}910)\left(\frac{y}{2}\right)$$

$$= 5{,}850\,(1{,}008 - y)$$

$$r_u Ac = r_u \left[\frac{x\,(168 + 168 - y)}{2}\right]\left[\frac{x\,[168 + 2\,(168 - y)]}{3\,(168 + 168 - y)}\right]$$

$$= \frac{r_u x^2}{3}\,(252 - y)$$

Therefore,

$$r_u = \frac{17{,}550\,(1008 - y)}{x^2\,(252 - y)}$$

Also, two
e of the

s/in

s/in

med posi-
located
pacity.)

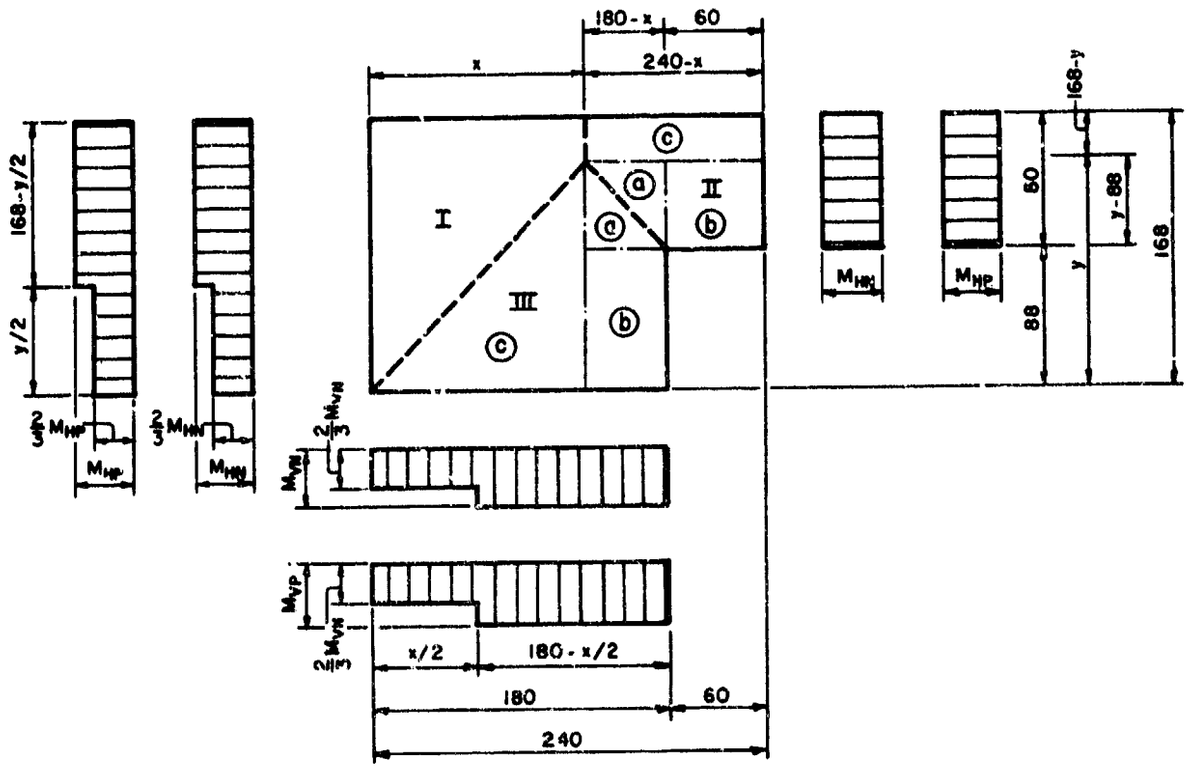


Figure 5A-4. Assumed yield lines and distribution of moments.

b. Sector II (fig. 5A-4).

$$\Sigma M_{HN} + \Sigma M_{HP} = 18{,}190\ (80) + 16{,}190\ (80) = 2{,}810{,}000\ \text{in-lbs}$$

Note:

The sector is divided into parts a, b, and c so that the centroid may be obtained (see table below).

Portion of Sector	Area (A')	Distance from centroid to axis of rotation (c')	A'c'
a	$\frac{(y-88)(180-x)}{2}$	$\frac{(180-x)}{3} + 60 = \frac{360-x}{3}$	$\frac{(y-88)(180-x)(360-x)}{6}$
b	$(y-88)(60)$	$\frac{60}{2}$	$\frac{(y-88)(60)^2}{2}$
c	$(168-y)(240-x)$	$\frac{240-x}{2}$	$\frac{(168-y)(240-x)^2}{2}$

$$Ac = \Sigma A'c' = \frac{(y-88)(180-x)(360-x)}{6} + \frac{(y-88)(60)^2}{2}$$

$$+ \frac{(168-y)(240-x)^2}{2}$$

$$= \frac{1}{2}\left\{\frac{(y-88)}{3}\left[(180-x)(360-x) + 10{,}800\right] + (168-y)(240-x)^2\right\}$$

$$r_u = \frac{\Sigma M_{HN} + \Sigma M_{HP}}{Ac}$$

$$= \frac{5{,}620{,}000}{\frac{y-88}{3}\left[(180-x)(360-x) + 10{,}800\right] + (168-y)(240-x)^2}$$

c. Sector III (fig. 5A-4).

$$\Sigma M_{VN} + \Sigma M_{VP} = 17,130\left(180 - \frac{x}{2}\right) + \frac{2}{3}\ (17,130)\left(\frac{x}{2}\right)$$

$$+ 15,850\left(180 - \frac{x}{2}\right) + \frac{2}{3}\ (15,850)\left(\frac{x}{2}\right) = 5,500\ (1080-x)$$

Portion of Sector	Area (A')	Distance from centroid to axis of rotation (c')	A'c'
a	$\frac{(180-x)(y-88)}{2}$	$\frac{y-88}{3} + 88 = \frac{y+176}{3}$	$\frac{(180-x)(y-88)(y+176)}{6}$
b	$(180-x)(88)$	$\frac{88}{2}$	$\frac{(180-x)(88)^2}{2}$
c	$\frac{xy}{2}$	$\frac{y}{3}$	$\frac{xy^2}{6}$

$$Ac = \Sigma A'c' = \frac{(180-x)(y-88)(y+176)}{6} + \frac{(180-x)(88)^2}{2} + \frac{xy^2}{6}$$

$$= \frac{1}{6}\left\{(180-x)\left[(y-88)(y+176) + 23,200\right] + xy^2\right\}$$

$$r_u = \frac{\Sigma M_{VN} + \Sigma M_{VP}}{Ac}$$

$$= \frac{33,000\ (1080-x)}{(180-x)\ \left[(y-88)(y+176) + 23,200\right] + xy^2}$$

Step 7. Due to the complexity of obtaining a direct solution for the ultimate unit resistance, a trial-and-error solution will be used (see table below).

x	y	r_I	r_{II}	r_{III}
125	130	8.08	6.73	9.59
125	140	8.70	7.19	8.69
130	140	8.05	7.74	8.66
130	145	8.38	8.00	8.23
132	146	8.19	8.30	8.13
131	145	8.25	8.12	8.22
131.5	145.3	8.21	8.20	8.19

Therefore: $x = 131.5$ in

$y = 145.3$ in

$r_u = 8.20$ psi

PROBLEM 5A-2. RESISTANCE-DEFLECTION FUNCTION

Problem: Determine the actual and equivalent resistance-deflection function in the elasto-plastic region for a two-way element.

Note:

Charts for two-way elements which fulfill the requirements of paragraph 5-9 are presently available for only two support conditions: (1) an element fixed on three sides with the remaining side free and (2) an element fixed on all four sides. Therefore, the following procedure will apply specifically to the above-mentioned elements.

Procedure:

Step 1. Establish design parameters:

a. Geometry of element.

b. Amount and distribution of reinforcement.

c. Support conditions.

d. Type of section available for moment capacity (sec. I, ch. 5).

e. Static design strengths (table 5-4).

f. Dynamic increase factors (table 5-3).

Step 2. Calculate dynamic design strengths for concrete and reinforcement.

Step 3. Determine ultimate positive and negative moment capacities in vertical and horizontal directions.

Step 4. Determine static properties:

a. Modulus of elasticity for concrete and reinforcing steel and the modular ratio (para. 5-7).

b. Moment of inertia of the element (para. 5-8).

Step 5. Establish points of interest and their ultimate moment capacities (fig. 5A-5).

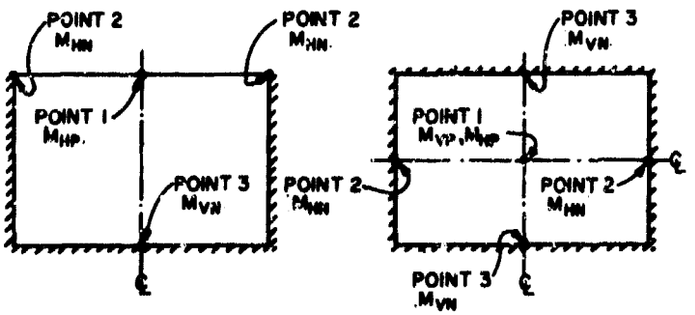


Figure 5A-5

Step 6. Compute properties at first yield (fig. 5-14 or fig. 5-17):

a. Location of first yield (usually point 2) (eq. 5-45).

b. Resistance at first yield r_e.

c. Moments at remaining points consistent with r_e.

d. Deflection at point 1, X_e (eqs. 5-48 and 5-49).

Step 7. Compute properties at second yield (fig. 5-15 or fig. 5-18).

a. Remaining moment capacity at points 1 and 3.

b. Location of second yield (usually point 3).

c. Change in unit resistance Δr between first and second yield.

d. Unit resistance at second yield r_{ep}.

e. Moment at remaining point consistent with r_{ep}.

f. Change in deflection at point 1.

g. Total deflection at point 1, X_{ep}.

Note:

An element fixed on four sides exhibits a third yield (point 1 either in the horizontal or vertical direction). Therefore, repeat step 7 using figure 5-19 to obtain the properties at this yield.

Step 8. Compute properties at final yield (ultimate unit resistance):

a. Ultimate unit resistance (part b of problem 5A-1).

b. Change in resistance between ultimate unit resistance and resistance at prior yield.

c. Change in deflection at point 1 (for element fixed on three sides, use stiffness obtained from figure 5-16 and for an element fixed on four sides, use stiffness of a simply supported one-way element given in table 5-11).

d. Total deflection at point 1, X_p.

Step 9

Step 1

Requir
(cur
ered

Soluti

Step 1

Step 2

Step 3

Step 4

Step 9. Draw the actual resistance-deflection curve (fig. 5-20).

Step 10. Calculate equivalent maximum elastic deflection of the element (para. 5-16).

EXAMPLE 5A-2. RESISTANCE-DEFLECTION FUNCTION

Required: The actual and equivalent resistance-deflection function (curve) in the elasto-plastic region for the two-way element considered in example 5A-1(A).

Solution:

Step 1. Same as step 1 of example 5A-1(A), part a.

Step 2. Same as step 2 of example 5A-1(A), part a.

Step 3. Same as step 4 of example 5A-1(A), part a.

where: M_{HN} = 18,190 in-lbs/in M_{HP} = 16,910 in-lbs/in

M_{VN} = 17,130 in-lbs/in M_{VP} = 15,850 in-lbs/in

Step 4. Static properties.

a. $E_c = w^{1.5}\, 33\sqrt{f'_c} = (145)^{1.5}\,(33)(3{,}000)^{\frac{1}{2}} = 3.16 \times 10^6$ psi

$E_s = 29 \times 10^6$ psi

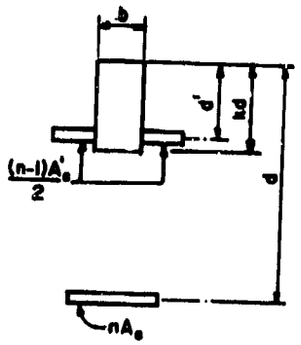
$$n = \frac{E_s}{E_c} = \frac{29 \times 10^6}{3.16 \times 10^6} = 9.18$$

b. Considering a 1-inch strip (b = 1 in)

$$I_g = \frac{1\,(12)^3}{12} = 144 \text{ in}^4$$

$$d \text{ (avg.)} = \frac{10.9375 + 10.1875 + 10.3125 + 9.5625}{4} = 10.25 \text{ in}$$

$$A_s = A'_s = \frac{0.31}{12} = 0.0258 \text{ sq in/in}$$



where

b = 1 in

d = 10.25 in (avg.)

d' = T-d = 1.75 in

Figure 5A-6

$$kd = \frac{\frac{b(kd)^2}{2} + (n-1)\,A_s'd' + nA_sd}{b(kd) + (n-1)\,A_s' + nA_s}$$

$$kd = \frac{\frac{1(kd)^2}{2} + 8.18(0.0258)(1.75) + 9.18(0.0258)(10.25)}{1(kd) + 8.18(0.0258) + 9.18(0.0258)}$$

Solving, $kd = 1.96$ in

$$I_c = \frac{1(1.96)^3}{3} + 8.18(0.0258)(1.96-1.75)^2 + 9.18(0.0258)(10.25 - 1.96)^2$$

$I_c = 18.8\ in^4$ (using fig. 5-5, $I_c = 17.3\ in^4$)

$$I_a = \frac{I_g + I_c}{2} = \frac{144 + 18.8}{2} = 81.4\ in^4$$

Step 5. For point of interest, see figure 5A-7.

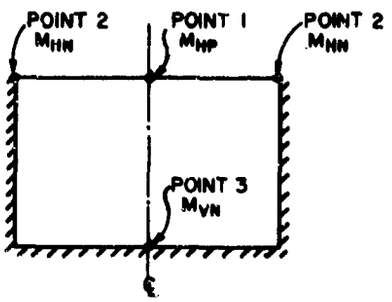


Figure 5A-7

Step 6. Properties at first yield

From figure 5-14 for H/L = 0.7:

$$\beta_1 = 0.075, \quad \beta_2 = 0.158, \quad \beta_3 = 0.110,$$

$$\gamma_1 = 0.0123, \quad \nu = \frac{1}{6}$$

a. $M_{HP} = 16,910 = \beta_1 rH^2 = 0.075 rH^2$

$$r = \frac{225,000}{H^2}$$

$M_{HN} = 18,190 = \beta_2 rH^2 = 0.158 rH^2$

$$r = \frac{115,000}{H^2}$$

$M_{VN} = 17,130 = \beta_3 rH^2 = 0.110 rH^2$

$$r = \frac{155,700}{H^2}$$

First yield at point 2 (smallest r).

b. $r_e = \frac{115,000}{(168)^2} = 4.07$ psi

a. M_P (Point 1) = 0.075 (4.07)(168)^2 = 8,620 in-lbs/in

M_N (Point 3) = 0.110 (4.07)(168)^2 = 12,640 in-lbs/in

d. $$D = \frac{E_c I_a}{b(1-\nu^2)} = \frac{3.16 \times 10^6 (81.4)}{1\left[1 - (0.1667)^2\right]} = 2.65 \times 10^8 \text{ in-lbs}$$

$$X_e = \frac{\gamma_1 r_e H^4}{D} = \frac{0.0123 (4.07)(168)^4}{2.65 \times 10^8} = 0.1505 \text{ in}$$

Step 7. Properties at second yield
After first yield element assumes a simple-simple-fixed-free stiffness, therefore, from figure 5-15 for H/L = 0.7,

Step 8.

β_1 = 0.123, β_3 = 0.220,

γ_1 = 0.0305, ν = 0.3

a. M_P (Point 1) = M_{HP} - M_P (at r_e)

= 16,910 - 8,620 = 8,290 in-lbs/in

M_N (Point 3) = M_{VN} - M_N (at r_e)

= 17,130 - 12,640 = 4,490 in-lbs/in

b. M_P (Point 1) = 8,290 = $\beta_1 \Delta r H^2$ = 0.123 $\Delta r H^2$

$$\Delta r = \frac{67,400}{H^2}$$

M_N (Point 3) = 4,490 = $\beta_3 \Delta r H^2$ = 0.220 $\Delta r H^2$

$$\Delta r = \frac{20,400}{H^2}$$

Step 9.

Second yield at Point 3 (smaller Δr)

a. $$\Delta r = \frac{20,400}{H^2} = \frac{20,400}{(168)^2} = 0.72 \text{ psi}$$

d. $r_{ep} = r_e + \Delta r = 4.07 + 0.72 = 4.79$ psi

e. M_p (Point 1) $= 0.123\ (0.72)(168)^2 = 2{,}500$ in-lbs/in

f. $$D = \frac{E_c\ f_a}{b(1-\nu^2)} = \frac{3.16 \times 10^6\ \ (81.4)}{\left[1-(0.3)^2\right]} = 2.83 \times 10^8 \text{ in-lbs}$$

$$\Delta X = \frac{\gamma_1\ \Delta r H^4}{D} = \frac{0.0305\ (0.72)(168)^4}{2.83 \times 10^8} = 0.0618 \text{ in}$$

g. $X_{ep} = X_e + \Delta X = 0.1505 + 0.0618 = 0.212$ in

Step 8. Properties at final yield (ultimate unit resistance). After second yield element assumes a simple-simple-simple-free stiffness, therefore, from figure 5-16 for H/L = 0.7,

$\gamma = 0.045, \quad \nu = 0.3$

a. $r_u = 9.08$ psi (part b of example 5A-1(A))

b. $\Delta r = r_u - r_{ep} = 9.08 - 4.79 = 4.29$ psi

c. $$D = \frac{E_c\ I_a}{b(1-\nu^2)} = \frac{3.16 \times 10^6\ \ (81.4)}{1\ \left[1-(0.3)^2\right]} = 2.83 \times 10^8 \text{ in-lbs}$$

$$\Delta X = \frac{\gamma_1\ \Delta r H^4}{D} = \frac{0.045\ (4.29)(168)^4}{2.83 \times 10^8} = 0.543 \text{in}$$

d. $X_p = X_{ep} + \Delta X = 0.212 + 0.543 = 0.755$ in

Step 9. For actual resistance-deflection curve, see figure 5A-8.

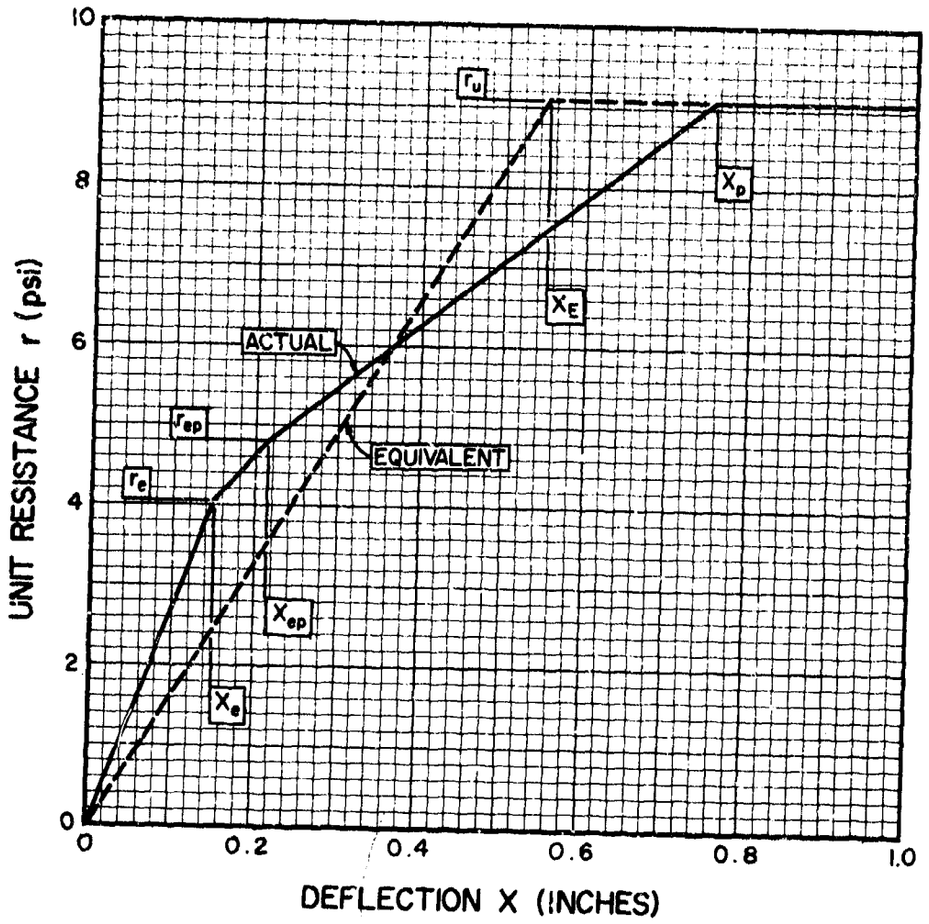


Figure 5A-8. Actual and equivalent resistance-deflection curves.

Step 10. $X_E = X_e\left(\frac{r_{ep}}{r_u}\right) + X_{ep}\left(1 - \frac{r_e}{r_u}\right) + X_p\left(1 - \frac{r_{ep}}{r_u}\right)$ (eq. 5-51)

$$X_E = 0.1505\left(\frac{4.79}{9.08}\right) + 0.212\left(1 - \frac{4.07}{9.08}\right) + 0.755\left(1 - \frac{4.07}{9.08}\right)$$

$$X_E = 0.553 \text{ in}$$

The equivalent resistance-deflection curve is shown in Figure 5A-8.



1.0

curves.

CHAPTER 6

STRUCTURAL ANALYSIS AND DESIGN FOR DUCTILE MODE RESPONSE

Section I. DESIGN PARAMETERS AND GENERAL PROCEDURE

6–1. General

Structural design of a protective structure consists of the determination of the dynamic response of the protecting structural elements to the blast environment produced by the donor system so that certain critical parameters (deflection, support rotation, and fragment velocities) specified by the protection requirements of the receiver system are met. The three components of the explosion protective system namely, the donor system, receiver system, and protective structure, are related as shown in figure 6–1. In the typical design, consideration of the first two components defines all of the parameters necessary for the structural design of the last.

6–2. Interrelationship of Design Parameter

a. The interrelationship between the several design parameters may be readily described with the use of a resistance-deflection diagram (fig. 6–2) which defines both the ductile and brittle modes of behavior of the individual structural elements and also of the protective structure as a whole. The following describes these relations and presents the general outline of the procedure to be followed.

b. The first step in the design of any protective structure is the analysis of the donor system to determine its output in terms of blast pressures (or impulse loads) and primary fragments. The methods and procedures for this analysis are covered in chapter 4. Next, the sensitivity of the receiver system is determined as outlined in chapter 3.

c. The contents of the receiver system define both the type of protective structure (shelter or barrier) and the protection category to be used. When personnel or equipment are to be protected, then shelter-type structures are used; when other explosives are to be protected, then barriers are used. Shelters are generally fully inclosed or partially open structures, and are designed to respond within the initial portion of the ductile mode with limited brittle mode behavior. Barriers are generally open (isolated walls or open cubicles) and are designed for a combination of ductile and brittle behavior.

d. Each structure type has two protection categories associated with it. Protection categories 1 and 2 apply to shelters, while protection categories 3 and 4 apply to barriers.

(1) *Protection category 1.*

(*a*) Protection category 1 is applicable to personnel and is the most stringent of the four. Personnel must be protected against fragments, blast pressures, and excessive structural motions. This category limits the response of the structural element to the initial portion of the ductile mode thereby preventing the formation of post-failure fragments. A design in this category must prevent the penetration of primary fragments formed by the donor explosive. If the formation of spalled fragments (brittle mode behavior) from the structural members is possible, shielding must be employed. Pressure increases within the structure and excessive structural motions must also be attenuated to safe levels.

(*b*) The full integrity of a shelter in protection category 1 must be maintained. Maximum deflections slightly less than those specified by partial failure of two-way elements or incipient failure of one-way elements could conceivably be used here. However, the reliability for fully achieving the desired protection cannot be guaranteed with these deflections. Therefore, the recommended maximum permissible deflections used in the design of elements protecting personnel should be limited to those corresponding to support rotations equal to, or less than, 5 degrees. This response criteria is termed limited deflections.

(2) *Protection category 2.*

(*a*) Protection category 2 applies to shelters used for the protection of equipment and stores from the same hazards listed above for protection category 1. The formation of post-failure fragments due to collapse of the shelter is also prohibited here. Penetration of primary fragments and the formation of spalled fragments are allowed, but shielding is required if their velocities exceed those which can result in damage to the receiver system. When hazardous materials are present, they must either be confined within the structure or allowed to spread by controlled means to safe

SPONSE

protection categories
gories 1 and 2 apply
ories 3 and 4 apply

is applicable to per-
the four. Personnel
nts, blast pressures,
This category limits
ement to the initial
eby preventing the
ts. A design in this
tion of primary frag-
ve. If the formation
behavior) from the
ielding must be em-
the structure and
also be attenuated

shelter in protection
Maximum deflections
by partial failure of
lure of one-way ele-
here. However, the
desired protection
eflections. Therefore,
sible deflections used
ng personnel should
to support rotations
This response criteria

applies to shelters
ent and stores from
rotection category 1.
nents due to collapse
here. Penetration of
tion of spalled frag-
is required if their
result in damage to
rdous materials are
ed within the struc-
rolled means to safe

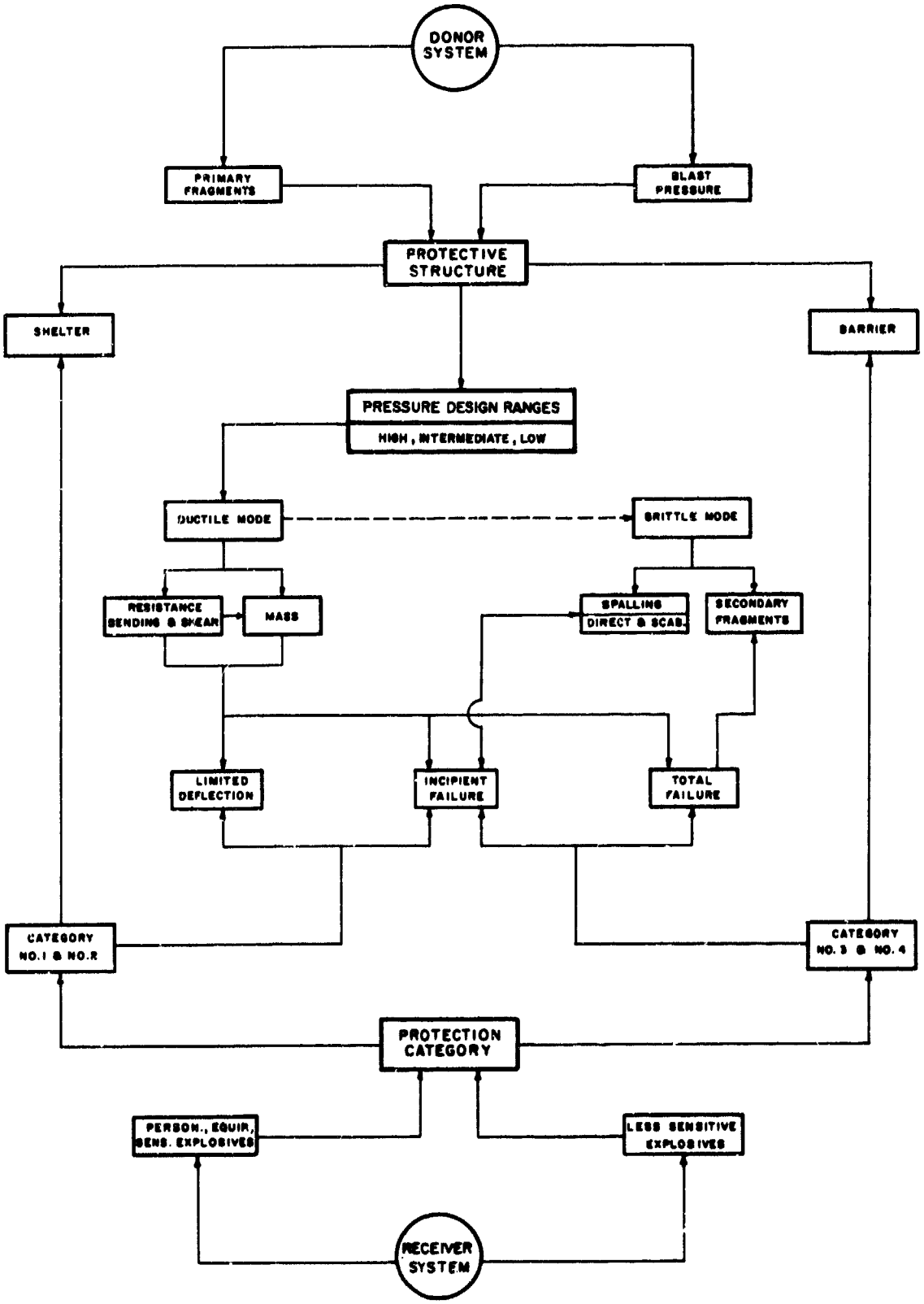


Figure 6-1. Design procedure for explosion protective structures.

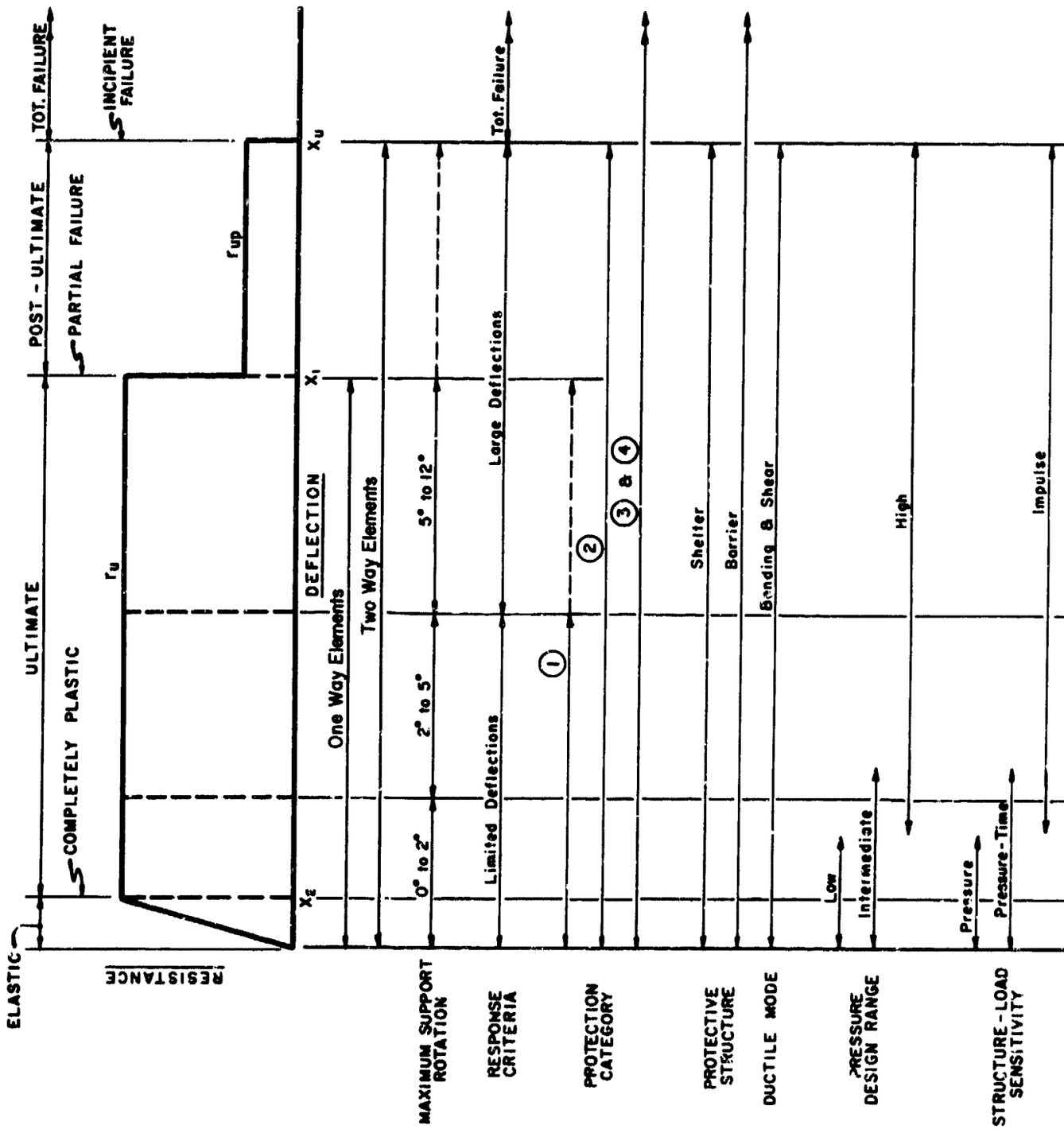


Figure 6-2. Relationships between design parameters.

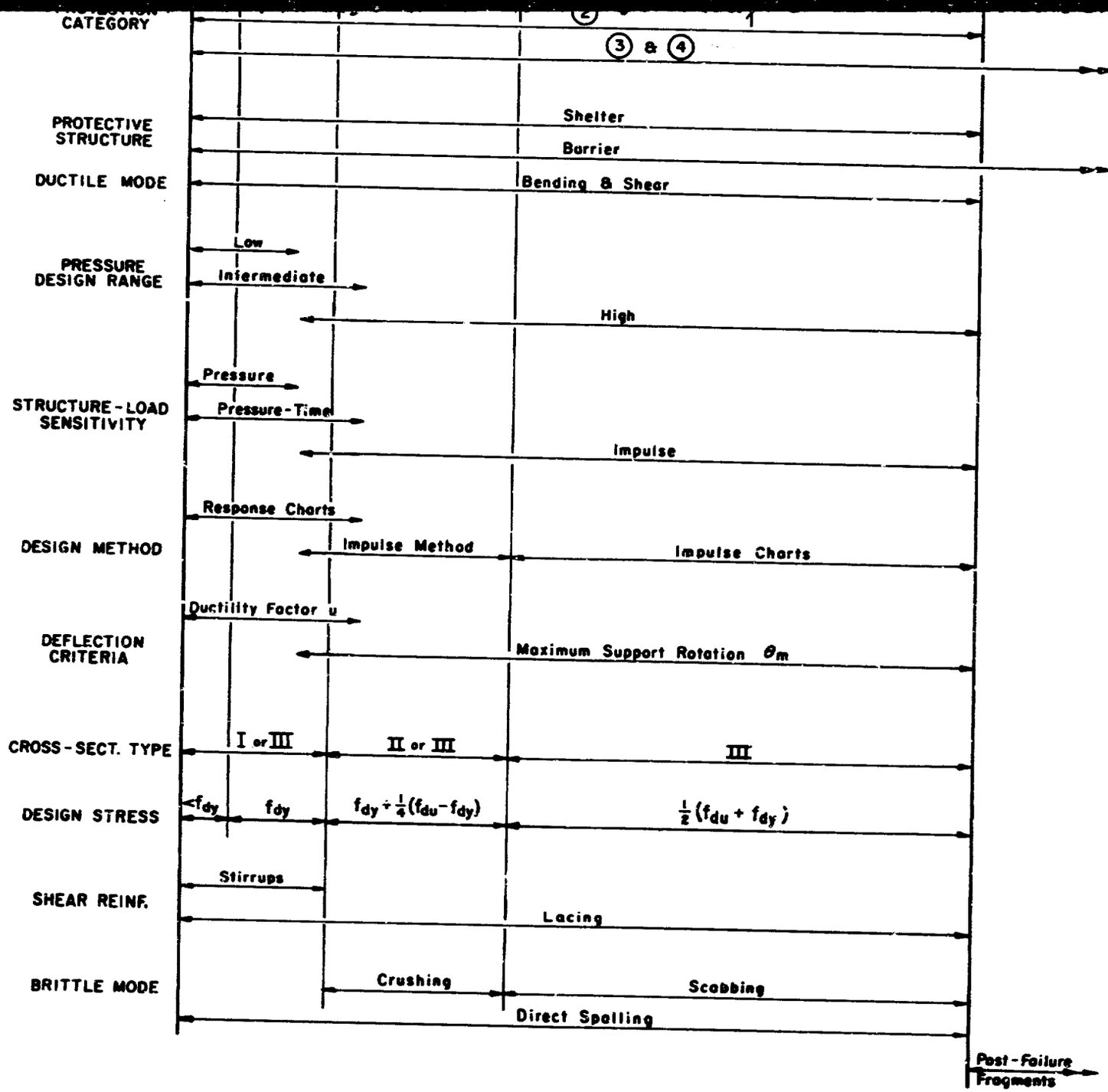


Figure 6-8. Relationships between design parameters.

areas. Attenuation of pressures and structural motions to tolerable levels is also governed by the sensitivity of the receiver system.

(*b*) Because of the nature of the contents of the protective structure, the degree of damage sustained by equipment shelters can be greater than that permitted for the design of shelters to protect personnel. Larger deflections than are allowed for the design of personnel shelters may be utilized in the design of equipment and storage shelters. Although it is theoretically possible to allow deflections which approach incipient failure conditions, the damage to the structure would be severe and, in some cases, might result in partial collapse. To avoid this situation, it is recommended that a maximum deflection less than that which produces partial failure of two-way elements or incipient failure of one-way elements be used as the criteria for the design of equipment and storage shelters. If extremely sensitive explosives or expensive equipment are contained within the shelter, then it is reasonable to consider using deflections somewhat less than defined above.

(3) *Protection category 3.*

(*a*) Protection category 3 pertains to barriers used for the partial containment of explosives to protect other structures and explosives from the impact effects of both high-velocity fragments and from high pressures. Controlled failure (deflections exceeding the incipient failure deflection) of the structural elements is allowed thereby permitting post-failure fragment formation. The pressure increase and the velocities of primary, spalled, and post-failure fragments must be limited to values so that communication of the detonation from the donor charge to the acceptor charge is prevented.

(*b*) Unlike shelters, barriers providing the protection required of protection category 3 can be designed for both ductile and brittle behavior. Where communication of a detonation by fragments and high-blast pressures must be prevented, the response criteria used for donor barrier design will vary from limited deflections for protection of sensitive acceptor explosives whose barricades are designed to withstand the additive effects of more than one explosion to total failure (deflections greater than incipient failure deflection) for protection of less sensitive explosives. Where single explosions are involved, barriers to provide protection for sensitive explosives can usually be designed for incipient failure conditions.

(4) *Protection category 4.* Protection category 4 is similar to category 3 except that a limited communication of detonation is permitted, but mass detonation is not. In a facility consisting of several cells containing explosives, the propagation of the explosion is allowed to one or more adjacent cells, but not to all cells. When the facility is composed of several separated groups of cells, propagation is allowed to one or more adjacent cells of a group, or from one group of cells to an adjacent group, but not to all groups. Total failure criteria is used for the design of barriers under protection category 4.

e. The degree of protection required within any protection category is a function of the sensitivity of the receiver system and increases as the sensitivity increases. The degree of protection defines the maximum permissible deflection, in terms of the support rotation angle, within the various deflection zones: (1) limited deflections (maximum support rotation angle $\theta_m \leq 5°$), (2) large deflections ($\theta_m > 5°$ but less than the incipient failure rotation), and (3) total destruction (exceeding the incipient failure rotation where $\theta_m = 12°$). The maximum deflection permitted in a particular design is derived from consideration of the sensitivity of the material to be protected (ch. 3). It should be noted here that spalled fragments are generally found in all three deflection zones, but may not occur in the initial portion ($\theta_m \leq 2°$) of the limited deflection zone in certain cases. Post-failure fragments are present only in the total destruction case.

f. Designs for limited deflection response must take into account the elasto-plastic resistance variation to avoid overestimating the structural capacity. In the other two deflection ranges, this variation is safely ignored with little error.

g. Design for limited deflections encompasses all three of the specified design ranges, high pressure, intermediate pressure, and low pressure, while large deflection and total failure designs are used only for the high-pressure design range. As pointed out in chapter 3, the term "design range" implies an interrelationship between several parameters (location of structure relative to the detonation, pressure magnitude and duration, member resistance, and response time) and defines the element as responding to the pressure only, pressure-time relationship, or impulse. Although it is theoretically possible to design a structure all three ways for any donor output, limitations on sizes, materials, strength, etc., obviate this, and in the practical situations usually encountered, the above response sensitivity designations are true. Structures falling in the high-pressure design range will respond to the impulse; in the intermediate range will respond to the pressure-time relationship; and in the low-pressure range, will respond to the pressure only. Although the structural integrity of shelters must be maintained, the range of design for a given element may differ from that of another element of the same structure. This variation will depend upon the location or orientation of the individual elements relative to the detonation and to the magnitude of the explosion. For example, a shelter located adjacent to an explosion may have its front wall (wall facing the explosion) designed utilizing the high-pressure range design procedures whereas the use of the intermediate pressure

or, in the case of small explosives, low-pressure range design procedures may be used for the design of the roof and side and back walls.

h. Even though the design ranges for the various elements of a protective shelter vary, the response (deflection) criteria should be consistent for all elements in order that a uniform level of protection is achieved throughout the structure. The degree of this protection and the deflection criteria is governed by the contents (personnel or equipment) of the structure.

i. The design method varies depending upon the design range and the response criteria. Response charts are used for the low-pressure and intermediate-pressure ranges with limited deflections, impulse charts are used for the high-pressure range with large deflections or total failure, and an impulse method is used for the high-pressure range with limited deflections. It should be noted, however, that the design range designations are not completely rigid, and some overlapping can occur since strict rules cannot be set to govern all of the variables involved.

j. Deflection criteria for the response chart solution is based on the ductility factor u which is the ratio of the maximum deflection X_m to the equivalent elastic deflection X_E. For the impulse chart and impulse method solutions, the deflection criteria is based on the maximum support rotation angle θ_m.

k. The type of cross section used in the design is governed by the brittle mode behavior which can be briefly summarized, as follows, for the typical case. Crushing of the concrete on the compression face of an element starts at a support rotation of 2 degrees and scabbing (disengagement of crushed concrete) at 5 degrees. Direct spalling is generally associated with the high-pressure design range where spalling can be virtually instantaneous. Thus the low-pressure design range always uses type I cross sections, the intermediate-pressure design range uses either type I or II depending on the magnitude of the rotations, and the high-pressure design range usually uses type III, unless methods are employed to minimize spalling effects as discussed in chapter 7, in which case, type II is used.

l. The maximum allowable deflection also defines the allowable stresses to be employed in the design. As shown in figure 6–2, the allowable design stress increases as the maximum support rotation angle increases.

m. Shear reinforcement used at the low-pressure and intermediate-pressure design ranges is usually stirrups, but for the high-pressure design range, lacing must always be used to insure the proper structural behavior. Lacing is required in the first two design ranges when deflections corresponding to support rotation greater than 2 degrees are allowed.

n. Subsequent sections of this chapter present the principles and methods of dynamic analysis and equations, charts, and procedures for the flexural and shear design of elements in the ductile mode. Other analyses (ch 7) must be performed to determine the velocities of spalled and post-failure fragments.

Section II. PRINCIPLES OF DYNAMIC ANALYSIS

6–3. Basic Principles

a. Before discussing the fundamental principles of dynamic analysis, the principles used in the analysis of structures under static load will be reviewed briefly. Two different methods are used either separately or concurrently in static analysis: one is based on the principle of equilibrium and the other on work done and internal energy considerations.

b. Under the application of external loads, a given structure is deformed and internal forces developed in its members. In order to satisfy static equilibrium, the vector sum of all the external and internal forces acting on any free body portion of the structure must be equal to zero. For the equilibrium of the structure as a whole, the vector sum of the external forces and the reactions of the foundation must also be equal to zero.

c. The method based on work done and energy considerations is sometimes used when it is necessary to determine the deformation of a structure. In this method, use is made of the fact that the deformation of the structure causes the point of application of the external load to be displaced. The force then does work on the structure. Meanwhile, because of the structural deformations, potential energy is stored in the structure in the form of strain energy. By the principle of conservation of energy, the work done by the external force and the energy stored in the members must be equal. In static analysis, simplified methods such as the method of virtual work and the method of the unit load are derived from the general principle of energy conservation.

d. In the analysis of statically indeterminate structures, in addition to satisfying the equations of equilibrium, it is necessary to include a calculation of the deformation of the structure in order to arrive at a complete solution of the internal forces in the structure. The methods based on energy considerations, such as the method of least work and the method based on Castigliano's theorems, are generally used.

e. For the analysis of structures under dynamic loading, the same two methods are basically used, but the load changes rapidly with time, and the acceleration, velocity, and hence the inertial force and kinetic energy are of magnitudes requiring consideration. Thus, in addition to the internal and external forces, the equation of equilibrium includes the inertial force, and the equation of dynamic equilibrium takes the form of Newton's

equation of motion:

$$F - R = Ma \qquad \text{Equation 6-1}$$

where F = total external force as a function of time
R = total internal force as a function of time
M = total mass
a = acceleration of the mass

f. As for the principle of conservation of energy, the work done must be equal to the sum of the kinetic energy and the strain energy:

$$WD = KE + SE \qquad \text{Equation 6-2}$$

where WD = work done
KE = kinetic energy
SE = strain energy

and the strain energy includes both the reversible elastic strain energy and the irreversible plastic strain energy. Thus the difference between structures under static and dynamic loads is the presence of inertial force (Ma) in the equation of dynamic equilibrium, and of kinetic energy in the equation of energy conservation. Both terms are related to the mass of the structure. Hence, the mass of the structure becomes an important consideration in dynamic analysis.

g. In the above discussion, the two methods of analysis are described as if they were independent of each other. This is not the case. The force and energy equations are interdependent and are derived from each other. Although these two methods are not independent, the conveniences of applying them to a given problem varies depending on the particular problem under consideration. Generally, the force equation is convenient for analysis of structures, and the energy equation is convenient for design.

6–4. Dynamically Equivalent Systems

a. In dynamic analysis there are only three quantities to be considered: (1) the work done, (2) the strain energy, and (3) the kinetic energy. To evaluate the work done, the displacement at any point on the structure under external distributed or concentrated loads must be known. The strain energy is equal to the summation of the strain energies in all the structural elements, which may be in bending, compression, shear, or torsion. The kinetic energy involves the energy of translation and rotation of all the masses of the structure. The actual evaluation of these quantities for a given structure under dynamic load would be complicated. However, for practical problems this can be avoided by using appropriate assumptions.

b. In order to simplify the problem, a given structure is replaced by a dynamically equivalent system. The distributed masses of the given structure are lumped together into a number of concentrated masses. The strain energy is assumed to be stored in several weightless springs which do not have to behave elastically. Similarly, the distributed load is replaced by a number of concentrated loads acting on the concentrated masses. Therefore, the equivalent system consists merely of a number of concentrated masses joined together by weightless springs and subjected to concentrated loads which vary with time. This concentrated mass-spring-load system is defined as an equivalent dynamic system.

c. The reduction of a given structure to an equivalent dynamic system involves the principle of dynamic similarity which is the requirement that the work done, strain energy, and kinetic energy of the equivalent system must be identical, respectively, with those of the given structure. Any given structure, a multi-story building or an individual structural element such as a beam or column, can be approximated by an equivalent dynamic system for the purpose of dynamic analysis.

6–5. Dynamic Analysis and Design

a. The analysis of a structural member under applied dynamic loads consists of the determination of the deflection of the member using Newton's equation of motion. Analysis is a direct procedure while design is a verification by analysis. The acceleration, velocity, and displacement versus time relationships are obtainable from the mathematical solution of the equation of motion of the structural system. But the solution also requires expression of the load and structural parameters.

b. In the typical design problem, the load-time relationship is known while the structural parameters are not and, therefore, must be assumed. The displacement of the structural element at certain critical points can be related to moments or stresses at these same points. Solution of the equation of motion will give the maximum deflection of the system which can be compared to acceptable or limit values, and, if adequate, the structural properties originally assumed are satisfactory for the loading parameters. If not, the assumption of a new set of structural properties will give a new equation of motion which, in turn, can be solved. The process of structural design is a trial-and-error procedure—a series of analyses to verify assumed designs.

c. It can be seen that the writing and solution of the equation of motion for a structure are essential, but usually mechanical, steps in the design process. They are not always readily apparent in the equations and charts presented here, but they are nevertheless there.

d. The simplest dynamic system consists of a concentrated mass supported by a weightless spring and subjected to a concentrated load as shown in figure 6–3. A single displacement variable X is sufficient to describe its motion; hence this system is called a single-degree-of-freedom system. The degree of freedom of a dynamic system is defined as the number of independent displacement variables needed to specify completely the configuration of the system. This manual is restricted to consideration of single-degree-of-freedom systems only.

e. Two fund
ing simple sys
first of these
differential equ
numerical, or
analysis, a cha
have been det
is an approxim
procedures use
but may be fou

6–6. Effecti

a. The valu
motion is equ
only if all ele
which case th
concentrated a
the assumptio
cannot be mad
is true for me
which bend or
the motion of
length of the
distributed ma
degrees of free
of motion for a
mass is replace
equivalent sing

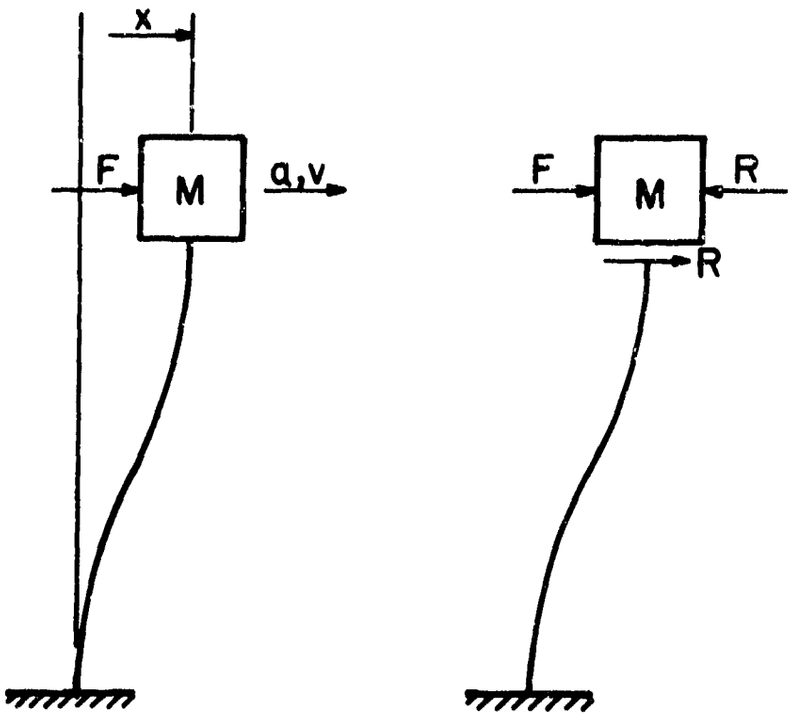


Figure 6–3. Typical single-degree-of-freedom system.

e. Two fundamental methods are available for treating simple systems subjected to dynamic forces. The first of these methods is concerned with solving the differential equations of the system by either classical, numerical, or graphical means. The second method of analysis, a chart solution, depends on solutions which have been determined by use of the first method and is an approximate solution to the problem. The various procedures used in these methods are not derived here but may be found in the bibliography.

6–6. Effective Mass

a. The value of the mass used in the equation of motion is equal to the actual mass of the structure only if all elements of the mass move as a unit, in which case the entire mass may be assumed to be concentrated at its center of gravity. In other cases, the assumption of uniform motion of the entire mass cannot be made without introducing serious error. This is true for members with uniformly distributed mass which bend or rotate under load. In each of these cases, the motion of the particles of mass varies along the length of the member. Beams, slabs, etc., with such distributed mass actually have an infinite number of degrees of freedom. Even in these cases, the equation of motion for a single particle may be used if the actual mass is replaced by an effective mass, the mass of an equivalent single-degree-of-freedom system.

b. The value of the effective mass M_e is dependent upon the deflected shape of the structural member, varying with the type of spanning, end conditions, etc., and therefore is different in the elastic, elastoplastic, and plastic ranges of behavior.

c. The effective total mass of the equivalent system is related to the total mass of the actual system by

$$M_e = K_{LM} M \qquad \textbf{Equation 6–3}$$

where M_e is the effective total mass

M is the total mass

K_{LM} is the load-mass factor determined from consideration of the load, resistance, and mass factors necessary to transform the actual dynamic system to the equivalent single-degree-of-freedom system.

d. The load factor K_L is defined as

$$K_L = \frac{F_E}{F} \qquad \textbf{Equation 6–4}$$

where F is the actual total load and F_E the equivalent concentrated load acting on the equivalent system. This factor is derived from the equality of the external work done by the equivalent load on the equivalent system and the external work done by the actual load on the actual system, the primary requirement being that the deflection of the equivalent system at any time be equal to the maximum deflection of the actual element.

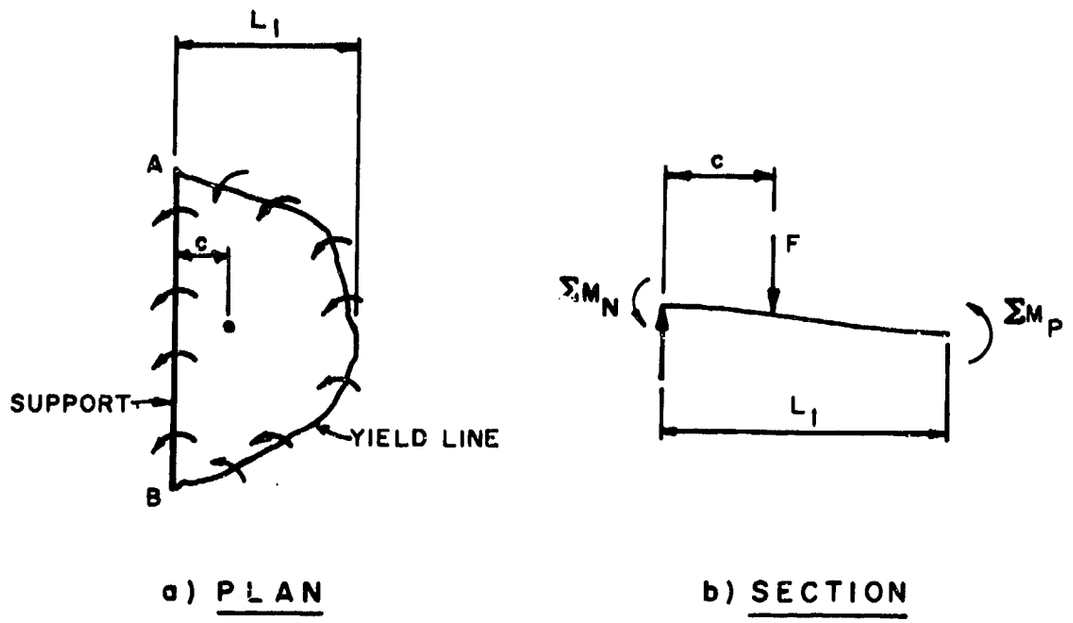


Figure 6–4. Determination of load-mass factor in the plastic range.

e. The resistance factor K_R is

$$K_R = \frac{R_E}{R} \qquad \textbf{Equation 6–5}$$

R being the actual total resistance and R_E the equivalent total resistance of the equivalent system. This resistance factor, obtained by equating the strain energies of the actual and equivalent systems, is found to be equal to K_L.

f. The mass factor K_M is

$$K_M = \frac{M_E}{M} \qquad \textbf{Equation 6–6}$$

where M is the actual total mass and M_E the equivalent total mass of the equivalent system. This factor is calculated by equating the kinetic energy of the actual system at any time to that of the equivalent system.

g. Summarizing, for the actual system the equation of motion is

$$F - R = Ma \qquad \textbf{Equation 6–7}$$

and for the equivalent system

$$K_L F - K_L R = K_M M a \qquad \textbf{Equation 6–8a}$$

$$F - R = \frac{K_M}{K_L} Ma \qquad \textbf{Equation 6–8b}$$

$$F - R = K_{LM} Ma = M_e a \qquad \textbf{Equation 6–8c}$$

where M_e is the effective total mass of the equivalent system. When expressed in terms of the unit area of the element, this equation is rewritten as

$$f - r = K_{LM} ma = m_e a \qquad \textbf{Equation 6–9}$$

h. Instead of computing the several factors above, the load-mass factors in the elastic and elasto-plastic ranges can be determined by relating the primary mode of vibration of the member to that of an equivalent single-degree-of-freedom system. In the plastic range it can be assumed that neither the moment nor curvature changes between the plastic hinges under increasing deflection. This behavior results in a linkage action, consideration of which can be used to evaluate the effective plastic mass as follows.

i. In figure 6–4, a portion of a two-way element bounded by the support and the yield line is shown. The equation of angular motion for this section is

$$\Sigma M = I_m \ddot{\theta} \qquad \textbf{Equation 6–10}$$

where ΣM = summation of the moments
I_m = mass moment of inertia about the axis of rotation AB
$\ddot{\theta}$ = angular acceleration

Substituting

$$Fc - (\Sigma M_N + \Sigma M_P) = \frac{I_m}{L_1} a \qquad \textbf{Equation 6–11a}$$

where a is the acceleration and, dividing through by c,

$$F - \left(\frac{\Sigma M_N + \Sigma M_P}{c}\right) = \frac{I_m}{cL_1} a \qquad \textbf{Equation 6–11b}$$

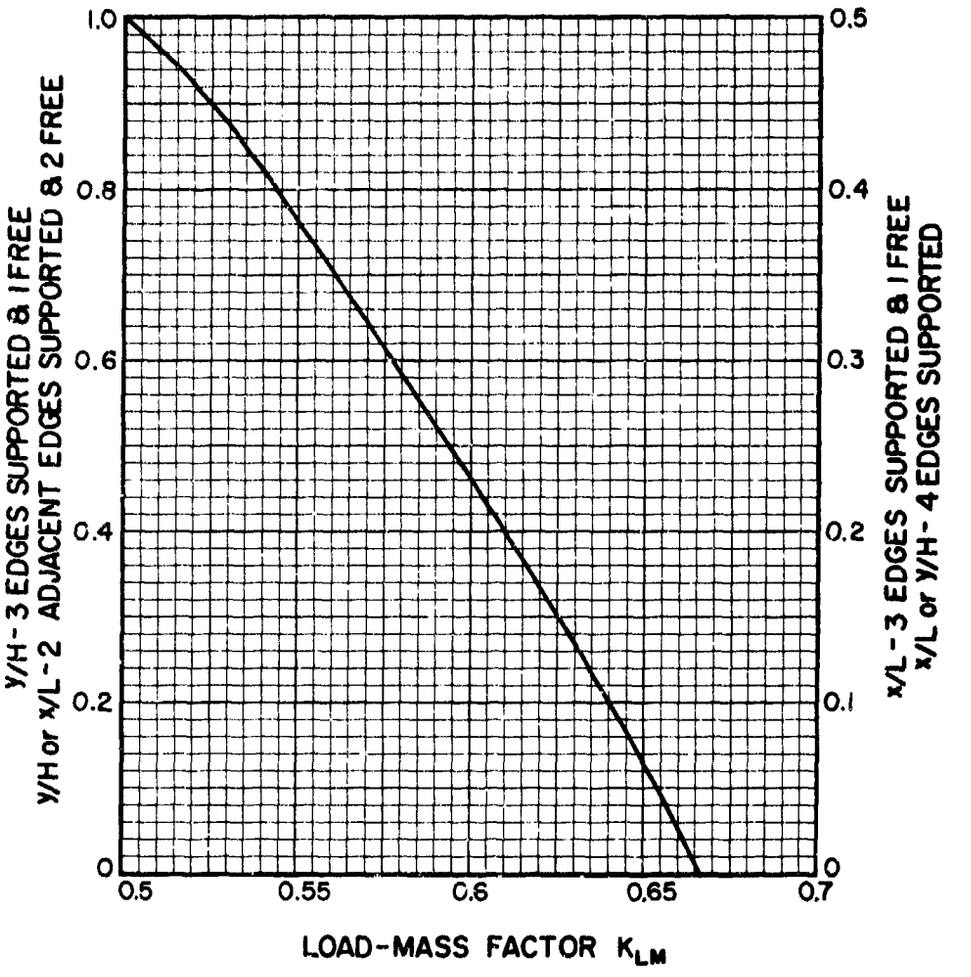


Figure 6–5. Load-mass factors in plastic range for two-way elements.

Since the second term is the resistance R

$$F - R = \frac{I_m}{cL_1} a = M_e a \qquad \textbf{Equation 6–11c}$$

and the load-mass factor K_{LM} for the sector shown is

$$K_{LM} = \frac{I_m}{cL_1 M} \qquad \textbf{Equation 6–12}$$

where c is the distance from the resultant applied load to the axis of rotation, L_1 is the total length of the sector normal to line AB and M is the total mass of the sector.

j. When the element is composed of several sectors, each sector must be considered separately and the contributions then summed to determine the load-mass factor for the entire element.

$$K_{LM} = \frac{\Sigma \frac{I_m}{cL_1}}{\Sigma M} \qquad \textbf{Equation 6–13}$$

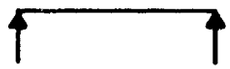
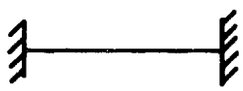
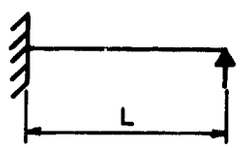
k. For elements of constant depth and therefore of constant unit mass, the above equation can be written in terms of the area moment of inertia I and the areas A of the individual sectors.

$$K_{LM} = \frac{\Sigma \frac{I}{cL_1}}{\Sigma A} \qquad \textbf{Equation 6–14}$$

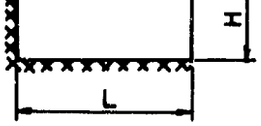
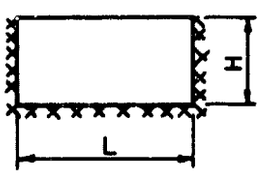
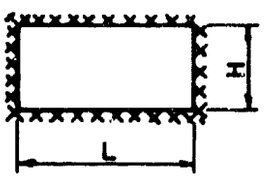
l. Values of the load-mass factors K_{LM} for the various ranges of behavior are shown in table 6–1 for one-way elements and in both table 6–1 and figure 6–5 for two-way elements. It should be noted that the load-mass factors given in figure 6–5 are only for those two-

Table 6-1 Load-Mass Factors K_{LM} for One- and Two-Way Elements with

One-Way Elements

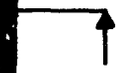
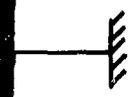
Edge conditions	
Cantilever	
Simple supports	
Fixed supports	
Fixed-simple supports	

Two-Way Elements

Edge conditions		Values of L/H	All supports fixed	One an other s
Two adjacent edges supported and two edges free		All	0.65	
Three edges supported and one edge free		$L/H<0.5$	0.77	
		$0.5\leq L/H\leq 2$	$0.65-0.16\left(\frac{L}{2H}-1\right)$	0.66−0.
		$L/H\geq 2$	0.65	
Four edges supported		$L/H=1$	0.61	
		$1\leq L/H\leq 2$	$0.61+0.16\left(\frac{L}{H}-1\right)$	0.61+0
		$L/H\geq 2$	0.77	

for One- and Two-Way Elements with Uniform Loading

One-Way Elements

	Range of behavior		
	Elastic	Elasto-Plastic	Plastic
	0.65	—	0.66
	0.79	—	0.66
	0.77	0.79	0.66
	0.78	0.78	0.66

Two-Way Elements

L/H	Elastic and elasto-plastic ranges (support conditions)					Plastic range	
	All supports fixed	One support simple, other supports fixed	Two supports simple, other supports fixed	Three supports simple, other supports fixed	All supports simple	Before partial failure	After partial failure
	0.65	0.66	—	—	0.66		0.66
.5	0.77	0.77	0.79	—	0.79		
$H \leq 2$	$0.65-0.16\left(\frac{L}{2H}-1\right)$	$0.66-0.144\left(\frac{L}{2H}-1\right)$	$0.65-0.186\left(\frac{L}{2H}-1\right)$	—	$0.66-0.175\left(\frac{L}{H}-1\right)$	See figure 6–5	0.66
2	0.65	0.66	0.65	—	0.66		
1	0.61	0.61	0.62	0.63	0.63		
≤ 2	$0.61+0.16\left(\frac{L}{H}-1\right)$	$0.61+0.16\left(\frac{L}{H}-1\right)$	$0.62+0.16\left(\frac{L}{N}-1\right)$	$0.63+0.16\left(\frac{L}{H}-1\right)$	$0.63+0.16\left(\frac{L}{H}-1\right)$		0.66
2	0.77	0.77	0.78	0.79	0.79		

way elements which conform to the limitations given in paragraph 5–9. For those elements which do not conform to the limitations, the load-mass factors must be calculated using the above procedures. An illustrative example of the determination of K_{LM} in the plastic range is given in appendix 5A.

m. Mass calculations should include the reduced thickness of the structural element when spalling is anticipated.

Section III. DESIGN FOR FLEXURE

6–7. General

a. Structural elements must develop an internal resistance sufficient to stop all motion within the limits of deflection prescribed for the particular design; flexural design is the determination of this required resistance. The load capacity of the member depends on the peak strength developed by the member and on the ability of the member to sustain its resistance for a specific though relatively short period of time. This section describes the methods used for flexural design of structural elements and is divided into two parts: (1) elements which respond to the pressure only and pressure-time relationship which correspond to the low-pressure and intermediate-pressure design ranges, respectively, and (2) elements which respond to the impulse which fall into the high-pressure design range.

b. Both the method of analysis and the maximum deflection criteria are different. Elements which respond to the pressure only and pressure-time relationship are designed using a response chart, while elements which respond to the impulse are designed using either impulse charts for large deflection designs or an impulse method for designs with limited deflections. Maximum allowable deflections for the first case are based on the ductility ratio, and in the second case, on the angle of rotation at the supports.

c. Design methods for determining the shear reinforcement necessary to fully develop the bending resistance are presented in section IV of this chapter.

6–8. Elements Which Respond to Pressure Only and Pressure-Time Relationship

a. These elements were previously shown to be those where the true magnitudes of the pressure and duration of the applied blast loads must be known. The determination of the dynamic response of these systems is accomplished using a response chart which relates the dynamic properties of the blast loads (pressure and duration) to those of the element (natural period of vibration, resistance, and deflection).

b. The maximum allowable deflection is expressed in terms of the ductility ratio or the ratio of the maximum deflection X_m to the equivalent maximum elastic deflection X_E of the element. Maximum deflections associated with the analysis of elements which respond to pressure only and elements which respond to pressure-time relationship usually conform to those designated as limited deflections.

c. In order to utilize these response charts, both the blast load (pressure-time history) and the resistance-deflection curve are idealized to linear or bilinear functions. The idealization of these functions consists of replacing the true functions by one or a series of straight lines.

(1) *Idealization of load and resistance functions.*

(*a*) The most commonly used idealized pressure-time function is an initially peaked triangle defined by a peak pressure B and a duration T. This simplified loading function has been studied extensively. The basic consideration in replacing the given loading by an idealized loading shape is that the maximum displacement produced by each must be equal. No general rules can be given for the idealization; however, the following will serve as a guide. Since t_m is the time at which the maximum deflection X_m occurs, the idealized load and the given load should be very close to each other in the time interval from zero to t_m and have the same area under the respective curves in the same time interval.

(*b*) For example, consider the solid loading curve shown in figure 6–6. For a time t_{m1} to reach maximum deflection, the idealized loading curve is best defined by B_1 and T_1, while for a time t_{m2} the loading would be defined by B_2 and T_2.

(*c*) The typical resistance function for limited deflection design consists of elastic, elasto-plastic, and plastic ranges, and for the large majority of problems, can be adequately idealized to a bilinear form as outlined in paragraph 5–16. For the particular case where the structural element exhibits only elastic and plastic behavior, idealization of the resistance function is not necessary.

(2) *Natural period of vibration.*

(*a*) When designing for limited deflections using the response chart, the effective natural period of vibration is required. This effective period of vibration, when related to the duration of a blast loading of given intensity and a given structural resistance, determines the maximum transient deflection X_m of the structural element.

(*b*) The effective natural period of vibration is

$$T_N = 2\pi \sqrt{\frac{m_e}{K_E}} = 2\pi \sqrt{\frac{K_{LM} m}{K_E}} \qquad \text{Equation 6–15}$$

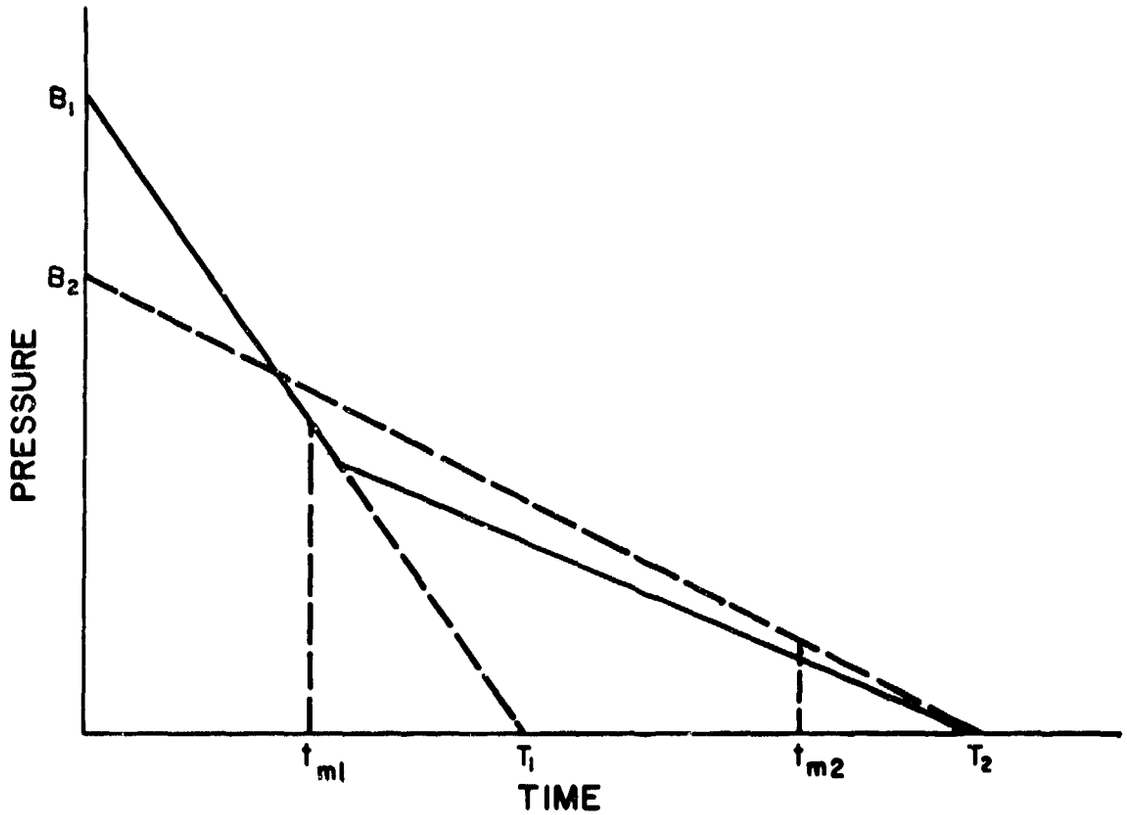


Figure 6–6. Idealization of pressure-time functions.

where m_e is the effective unit mass and K_E is the equivalent unit stiffness of the system.

(*c*) The values used for m_e and K_E for a particular element depend upon the allowable maximum deflections permitted. For example, when designing for completely elastic behavior, the elastic values of the effective unit mass and unit stiffness would be used; for elasto-plastic action, the effective unit mass is the average of the elastic and elasto-plastic values and the stiffness is the equivalent unit stiffness K_E. For design in the plastic range, a weighted value of the effective unit mass is used with the equivalent unit stiffness K_E. When plastic deformations less than those specified by the limited deflection criteria are used, the use of the average value of the average elastic and elasto-plastic effective unit masses and the plastic effective unit mass will suffice for most structural elements considered in this manual.

(3) *Determination of maximum response.*

(*a*) The maximum response of a pressure or pressure-time sensitive system with an elasto-plastic resistance function subjected to a triangular loading pulse is shown in figure 6–7. This nondimensional chart is a convenient plot of solutions made by numerical integration of the equation of motion using a digital computer. If any two of the four parameters are known, the remaining two can be found. It should be noted that since the blast load is expressed in terms of pressure (force/unit area), unit values are used for the resistance and stiffness of an element.

(*b*) In the typical design example, the pressure-time loading is calculated, and this curve is then idealized to the triangular form defined by B and T. If a structural member is assumed, the idealized resistance function defined by r_u, X_E, and K_E can be determined along with the natural period T_N. Then, knowing the ratios B/r_u and T/T_N, X_m and t_m can be readily obtained from figure 6–7 by reading the ratios X_m/X_E and t_m/T_N.

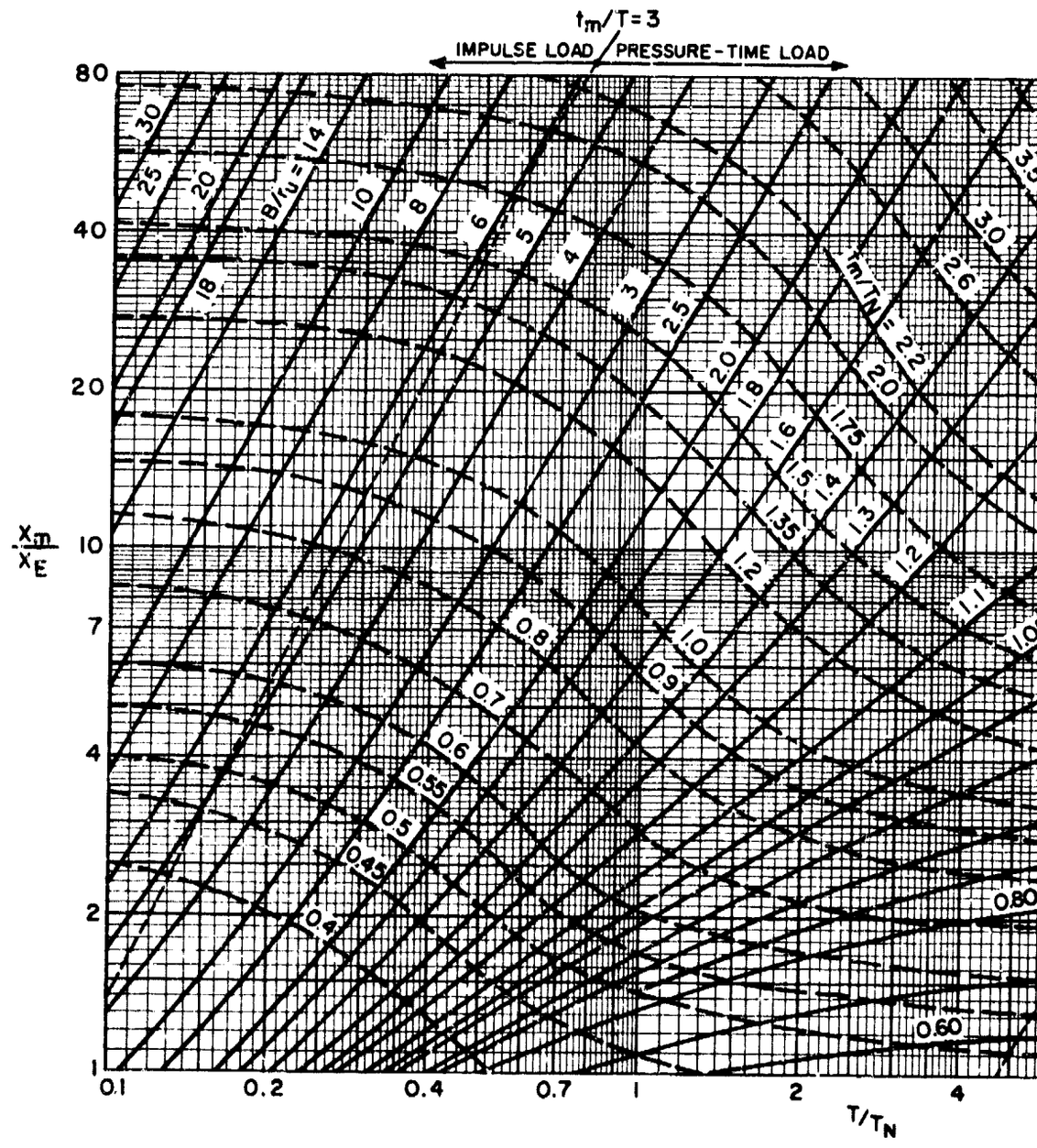
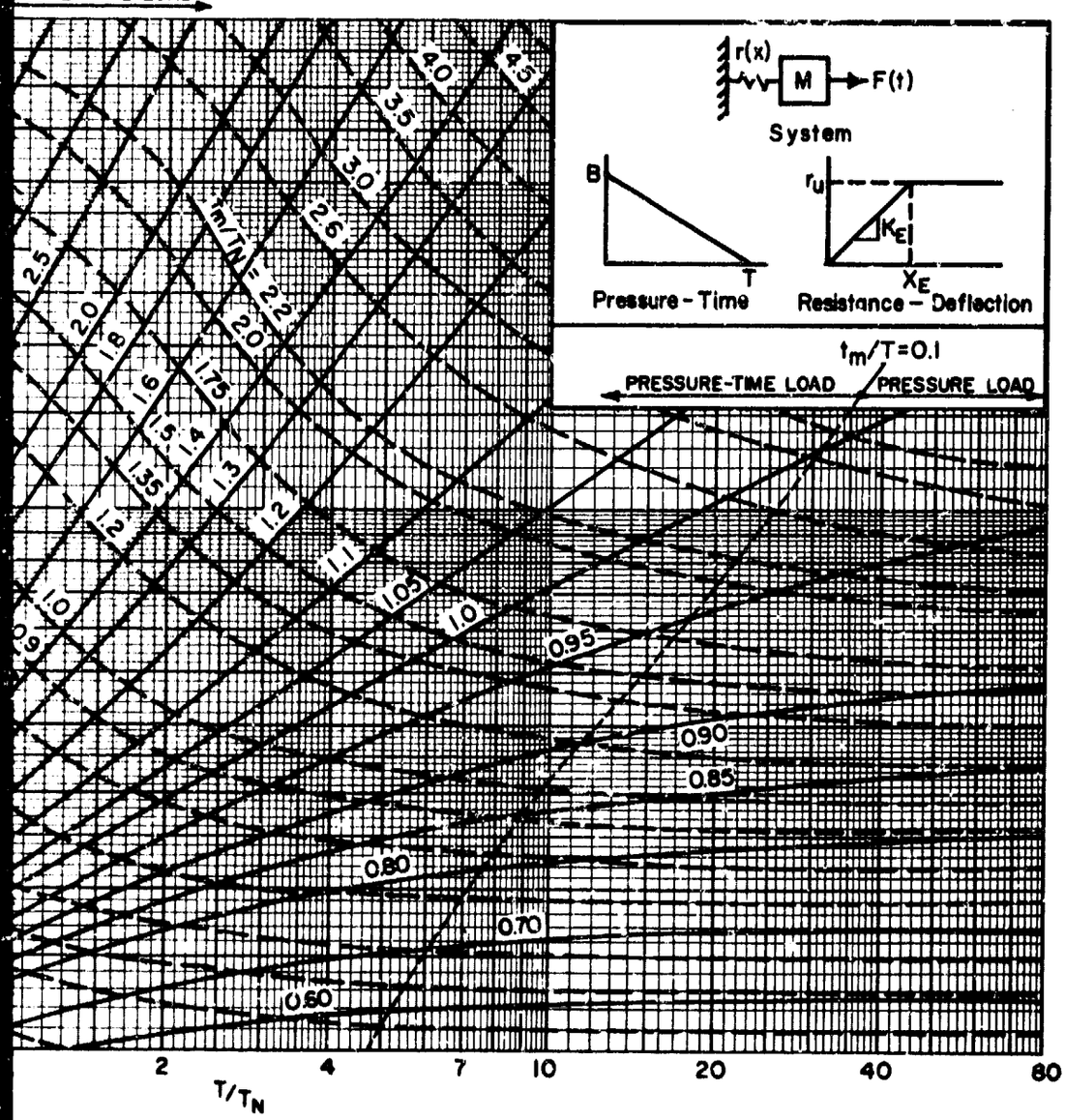


Figure 6-7. Maximum response of simple spring-mass system to initially peake

SSURE - TIME LOAD



e of simple spring-mass system to initially peaked triangular pressure pulse.

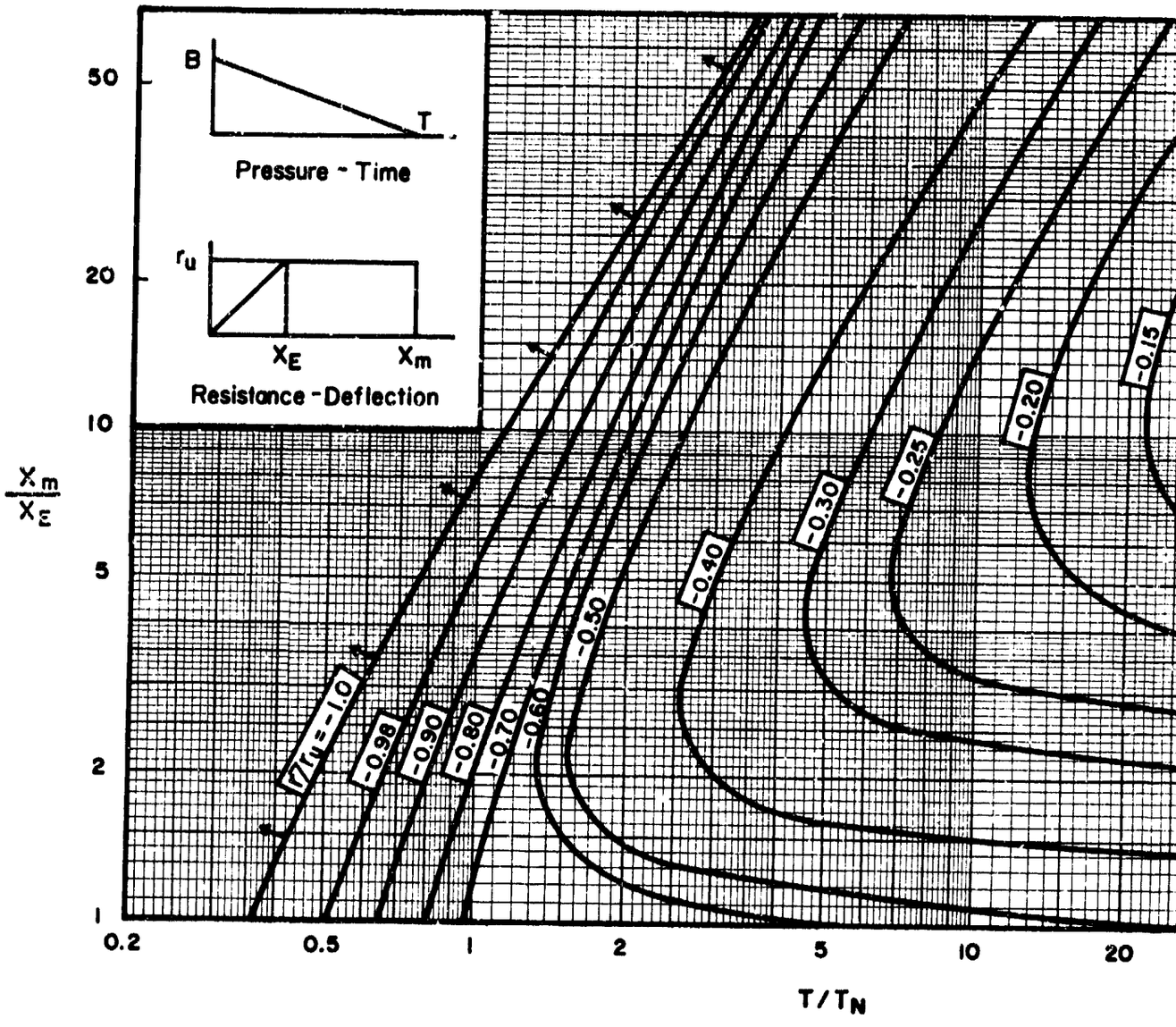


Figure 6-8. Elastic rebound of simple spring-mass system.

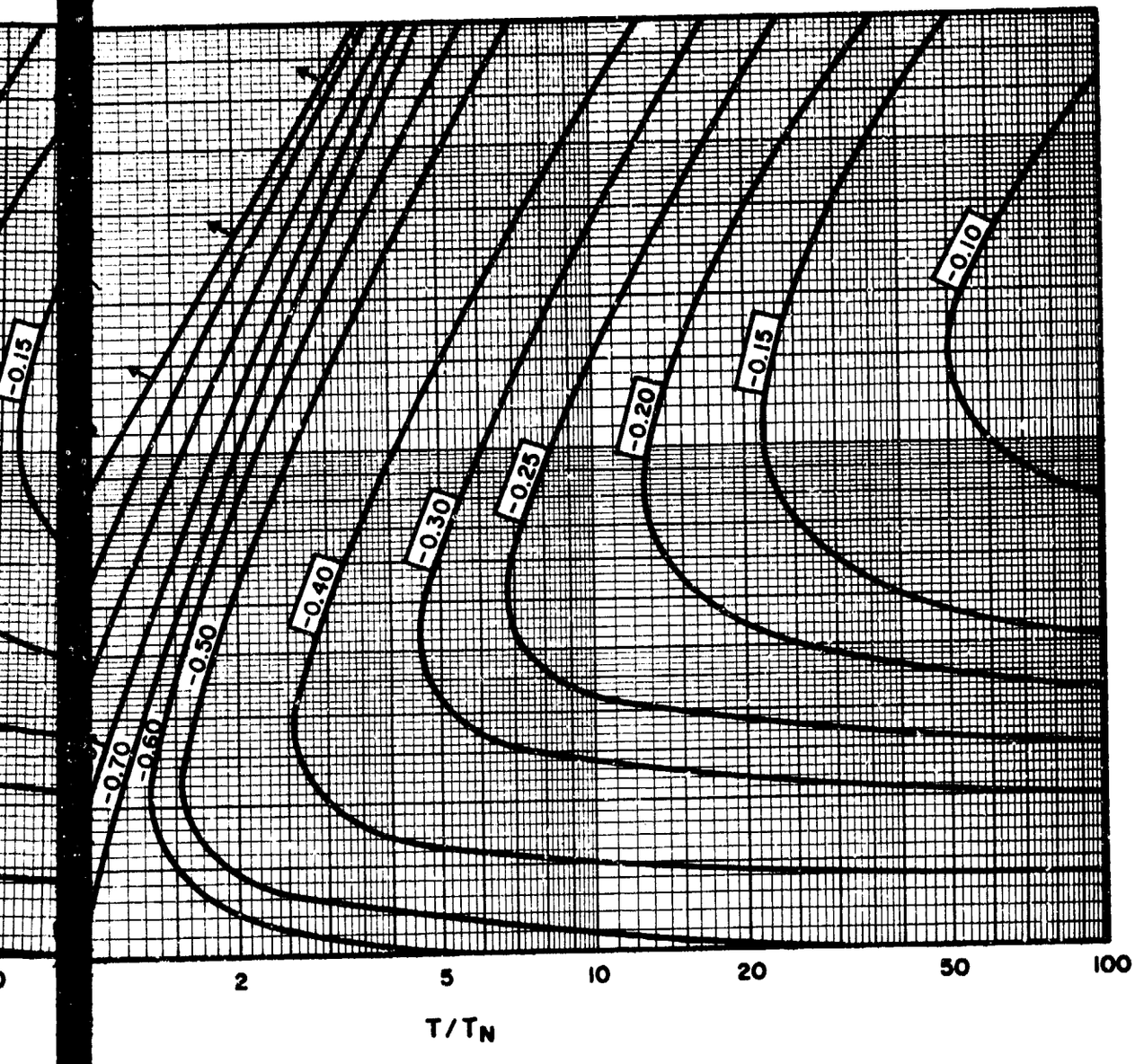


Figure 6-8. Elastic rebound of simple spring-mass system.

(*c*) The deflection X_m is the maximum deflection corresponding to the assumed parameters. The value of t_m is the time at which the maximum deflection occurs and is used to check the adequacy of the idealization of the loading curve. If either t_m or X_m are unsatisfactory, the procedure is repeated.

(*d*) Procedures for determining the pressure-time loading are given in chapter 4, and for the resistance function and deflection criteria, in chapter 5.

(4) *Determination of rebound.*

(*a*) In the design of elements which respond to the pressure only and pressure-time relationship, the element must be designed to resist the negative deflection or rebound which can occur after the maximum positive deflection has been reached. The ratio of the required unit rebound resistance to the ultimate unit resistance r/r_u, such that the element will remain elastic during rebound, is obtained from figure 6–8. Entering with the ratios X_m/X_E and T/T_N previously determined for the design, the required unit rebound resistance $r-$ can be read in terms of the originally designed ultimate unit resistance r_u.

(*b*) It may be noted that if the loading is applied in a relatively short time compared to the natural period of vibration, the required rebound resistance can be equal to the resistance in the initial design direction. When the loading is applied for a relatively long time, the maximum deflection is reached when the positive forces are still large, and the rebound resistance is reduced.

6–9. Elements Which Respond to Impulse

a. General Equations for Maximum Response.

(1) When an element responds to the impulse, the maximum response depends upon the area under the pressure-time curve (impulse of the blast loading). The magnitude and time variation of the pressure are not important. Response charts based on pressure-time relationships are therefore not applicable to these problems. Instead, the element resistance required to limit the maximum deflection to a specified value is obtained through the use of a semigraphical method of analysis.

(2) Consider the pressure-time and resistance-time curves shown in figure 6–9. The resistance curve depicted is for a two-way element with a resistance-deflection function having a post-ultimate range. From Newton's equation of motion it can be shown that the summation of the areas (considering area A as positive and area B as negative) under the time curves up to any time t_a divided by the corresponding effective masses is equal to the instantaneous velocity at that time:

$$v_a = \int_0^{t_a} \frac{(f-r)}{m_e}\,dt \qquad \textbf{Equation 6–16}$$

The displacement at time t_a is found by multiplying

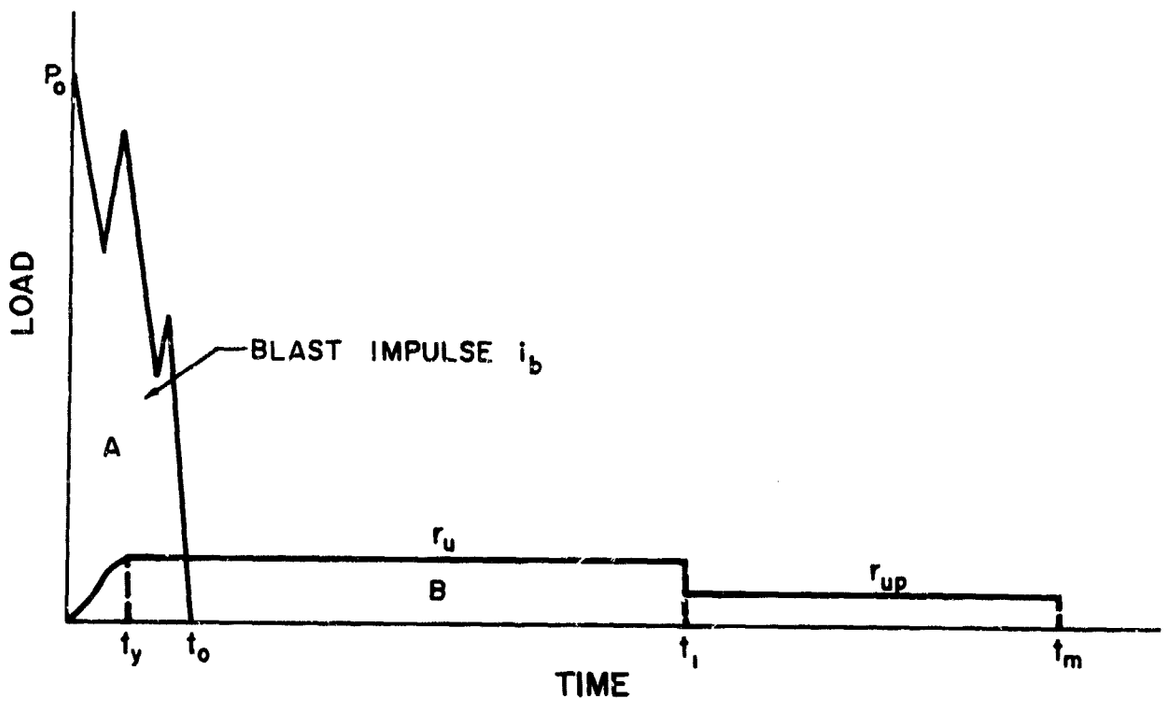


Figure 6–9. Pressure time and resistance-time curves for elements which respond to impulse.

each differential area divided by the appropriate effective mass by its distance to t_a and summing the values algebraically:

$$X_a = \int_0^{t_a} \frac{(f-r)}{m_e} (t_a - t)\, dt \qquad \textbf{Equation 6–17}$$

In each range the mass m_e is the effective plastic mass:

Time interval	*Resistance*	*Effective mass*
$0 \le t \le t_1$	r_u	$m_u = (K_{LM})_u m$
$t_1 \le t \le tm$	r_{up}	$m_{up} = (K_{LM})_{up} m$

Time t_1 is the time at which the partial failure deflection X_1 occurs, and time t_m is the time at which the maximum deflection X_m is reached ($X_m < X_u$).

(3) For an element to be in equilibrium at its maximum deflection, its impulse capacity must be numerically equal to the impulse of the applied blast load. With the use of the foregoing equations, the expressions, which define the motion and capacity of elements subjected to impulse type loads, can be defined. These expressions are presented for both large and limited deflection criteria.

(4) Case 1—large deflections.

(*a*) Utilizing equation 6–17 and by taking moments of the areas under the pressure-time and resistance-time curves (fig. 6–9) about time t_m, assuming that the unit blast impulse i_b is applied instantaneously at $t = 0$, and that the time to reach yield t_y is also close to zero, the expression for the maximum deflection X_m is

$$X_m = \frac{i_b t_m}{m_u} - \frac{r_u t_1 \left(t_m - \frac{t_1}{2}\right)}{m_u} - \frac{r_{up}(t_m - t_1)(t_m - t_1)}{2m_{up}}$$

Equation 6–18

If moments of the areas are taken about t_1, then the deflection at partial failure X_1, is

$$X_1 = \frac{i_b t_1}{m_u} - \frac{r_u t_1^2}{2m_u} \qquad \textbf{Equation 6–19}$$

Using equation 6–16 and summing the areas to t_m and recognizing that the instantaneous velocity at t_m equals zero

$$\frac{i_b}{m_u} - \frac{r_u t_1}{m_u} - \frac{r_{up}(t_m - t_1)}{m_{up}} = 0 \qquad \textbf{Equation 6–20}$$

(*b*) Solution of the above three simultaneous equations is accomplished by solving equation 6–20 for t_m and substituting this expression into equation 6–18, and solving equation 6–19 for t_1 and substituting this expression into the modified equation 6–18. After combining and rearranging terms, the general response equation becomes

$$\frac{i_b^2}{2m_u} = r_u X_1 + \frac{m_u}{m_{up}} r_{up}(X_m - X_1) \qquad \textbf{Equation 6–21}$$

The left side of this equation is simply the initial kinetic energy resulting from the applied blast impulse and the right side is the modified potential energy of the element. The modification is required since the above analysis requires the use of two equivalent dynamic systems (before and after time t_1). The modification factor m_u/m_{up} equates the two dynamic systems. If the effective mass in each range was the same, m_u/m_{up} would equal one and the right side of the expression would be ΣrX which is the potential energy.

(*c*) For one-way elements which do not exhibit the post-ultimate resistance range, or for two-way panels where the maximum deflection X_m is less than X_1, equation 6–21 becomes

$$\frac{i_b^2}{2m_u} = r_u X_m \qquad \textbf{Equation 6–22}$$

(*d*) The above solutions are valid only for large deflection design (support rotations > 5 degrees) since the variation of resistance with deflection in the elasto-plastic range has been ignored. This limitation is based on the assumption that the time to reach yield t_y and the duration of the impulse t_0 are small in comparison to t_m.

(5) Case 2—limited deflections.

(*a*) For elements which respond to the impulse with limited deflections where the time to reach maximum deflection t_m is greater than three times the duration t_0 of the load, but where the support rotations are equal to, or less than, 5 degrees, the elasto-plastic range behavior of the element must be accounted for in determining the overall response of the element to the applied blast load. For this case, equation 6–21 becomes

$$\frac{i_b^2}{2m_a} = \frac{r_u X_E}{2} + \frac{m_a}{m_u} r_u (X_m - X_E) \qquad \textbf{Equation 6–23}$$

where m_a is the average of the effective elastic and plastic masses and X_E the equivalent deflection.

(*b*) When the response time t_m of an element is less than three times the load duration t_0, the element will respond to the pressure pulse rather than to the impulse alone. In this case the response of the element may be obtained through the use of a response chart (fig. 6–7) considering a fictitious pressure pulse as explained in paragraph 4–10*a*. However, if the element's maximum deflection is greater than that given in the response chart (ductility ratio X_m/X_E greater than 80), the response of the element may be obtained through the use of the semigraphical method of analysis as outlined in this paragraph considering the fictitious pressure pulse. It should be noted that the resistance-time relationship used in the analysis to express the element's response should include the elasto-plastic region.

b. Determination of Time to Reach Maximum Deflection. The time t_m for each of the cases covered previously can be determined by applying equations 6–16

and 6–17 to the particular problem. The resulting equations are as follows:

(1) *Case 1—large deflections.*

A. $X_1 \leq X_m \leq X_u$

$$t_m = \frac{i_b}{r_u} + \left(\frac{m_{up}}{m_u r_{up}} - \frac{1}{r_u}\right)\sqrt{i_b^2 - 2m_u r_u X_1}$$

Equation 6–24

B. $X_m \leq X_1$

$$t_m = \frac{i_b}{r_u}$$

Equation 6–25

(2) *Case 2—limited deflections.* Since the variation of resistance with time is not known in the elasto-plastic range, t_m can only be determined *approximately* by assuming a linear variation of resistance with time.

t_m(approx.)

$$= \frac{i_b}{r_u}\left(3 - \frac{m_u}{2m_a}\right) + \frac{1}{r_u}\left(\frac{m_u}{2m_a} - 1\right)\sqrt{9i_b^2 - 6m_a r_u X_E}$$

Equation 6–26

c. Design For Large Deflections.

(1) *Impulse coefficients.*

(*a*) The basic equation for the analysis of elements which respond to the impulse where large deflections are permitted was previously derived as

$$\frac{i_b^2}{2m_u} = r_u X_1 + \frac{m_u}{m_{up}} r_{up}(X_m - X_1)$$

Equation 6–27

where i_b = applied unit blast impulse
m_u, m_{up} = unit effective masses
r_u, r_{up} = unit resistances
X_m, X_1 = deflections

(*b*) The expressions presented in chapter 5 for m_a, r, and X can now be substituted into this equation. The resulting design equation will be in terms of the geometry, reinforcement, allowable design stress, and applied blast impulse.

(*c*) For example, consider a two-way element (slab or wall) fixed on two adjacent edges and free on the other two where the crack line location is defined by y and $L \leq y \leq H$. The solution desired is for incipient failure of a spalled section (cross section Type III) at deflection X_u.

(*d*) From chapter 5 the equations for the resistances, deflections, and effective masses of this example are as follows:

1. Ultimate unit resistance

$$r_u = \frac{5(M_{VN} + M_{VP})}{y^2} \quad \text{(table 5–6)}$$

where

$$M_{VN} = M_{VP} = \frac{A_s f_{ds} d_c}{b} = P_V f_{ds} d_c^2 \text{ (Eqs 5–7 and 5–8)}$$

and p_V is defined as the vertical reinforcement ratio on each face.

2. Post-ultimate unit resistance

$$r_{up} = \frac{(M_{VN} + M_{VP})}{H^2} \text{ (table 5–7)}$$

3. Partial failure deflection

$$X_1 = L \tan 12° \text{ (table 5–9)}$$

4. Ultimate deflection

$$X_u = y \tan 12° + (H - y)\tan\lambda \text{ (table 5–9)}$$

where

$$\lambda = 12° - \tan^{-1}\left(\frac{\tan 12°}{y/L}\right).$$

5. Effective mass $m_u = (K_{LM})_u m$ for r_u range (table 6–5)

6. Effective mass

$$m_{up} = (K_{LM})_{up} m = \tfrac{2}{3} m \text{ for } r_{up} \text{ range (table 6–1)}$$

and

$$m = \frac{d_c}{1728}\left[\frac{150}{386(10^{-6})}\right] = 225 d_c.$$

The units used are

$y, L, H, d_c, b, X_1, X_u$	inches
i_b	psi-ms
M_{VN}, M_{VP}	in.-lbs/in.
f_{ds}, r_u, r_{up}	psi
A_s	in.^{2}
m, m_u, m_{up}	psi-ms^2/in.

Substituting into equation 6–21

$$i_b^2 = 2\left[225 d_c (K_{LM})_u \left(\frac{10 p_V d_c^2 f_{ds}}{y^2}\right) L \tan 12°\right.$$

$$+ 225 d_c \left(\tfrac{2}{3}\right)(K_{LM})_u^2 \left(\frac{2 p_V d_c^2 f_{ds}}{H^2}\right) y \tan 12°$$

$$\left. + (H - y)\tan\lambda - L \tan 12°)\right]$$

Equation 6–28a

Factoring

$$i_b^2 = 2(225 d_c) p_V d_c^2 f_{ds} \tan 12° \left[\frac{10(K_{LM})_u L}{y^2}\right.$$

$$\left. + \frac{3(K_{LM})_u^2}{H^2}\left\{y - L + \frac{(H - y)\tan\lambda}{\tan 12°}\right\}\right]$$

Equation 6–28b

Dividir
ratio, a

$\frac{i_b^2 H}{p_H d_c^2 f_{ds}}$

$+3(K_L$

$\frac{i_b^2 H}{p_H d_c^2 f_{ds}} =$

$+(K_{LM}$

where

Similarly
6–22, the

$\frac{i_b^2 H}{p_H d_c^2 f_{ds}} =$

(e

Dividing each side by p_H, the horizontal reinforcement ratio, and rearranging

$$\frac{i_b^2 H}{p_H d_c^3 f_{da}} = 450\left(\frac{p_V}{p_H}\right)\tan 12^\circ\left[\frac{10(K_{LM})_u(L/H)}{(y/H)^2}\right.$$

$$\left.+3(K_{LM})_u^2\left\{\left(\frac{y}{H}-\frac{L}{H}\right)+\left(1-\frac{y}{H}\right)\frac{\tan\lambda}{\tan 12^\circ}\right\}\right]$$

Equation 6-28c

$$\frac{i_b^2 H}{p_H d_c^3 f_{da}} = 287\left(\frac{p_V}{p_H}\right)(K_{LM})_u\left[\frac{10(L/H)}{3(y/H)^2}\right.$$

$$\left.+(K_{LM})_u\left\{\left(\frac{y}{H}-\frac{L}{H}\right)+4.70\left(1-\frac{y}{H}\right)\tan\lambda\right\}\right]$$

Equation 6-28d

where

$$\lambda = 12^\circ - \tan^{-1}\left(\frac{0.2126}{\frac{y}{L}}\right)$$

Similarly, for the same example and using equation 6-22, the solution for partial failure at deflection X_1 is

$$\frac{i_b^2 H}{p_H d_c^3 f_{da}} = 957\left(\frac{p_V}{p_H}\right)(K_{LM})_u\frac{\left(\frac{L}{H}\right)}{\left(\frac{y}{H}\right)^2}$$

Equation 6-29

(*e*) Expressions have been derived as above for other crack line locations and support conditions and also for unspalled sections. In all cases the right-hand side of the equation has been designated as the impulse coefficient, using C_1 for the case at deflection X_1 and C_u for that at deflection X_u. These impulse coefficients are a proportional measure of the impulse capacity under the resistance-deflection curve up to the given deflection. For one-way elements which do not exhibit the secondary resistance range ($X_u = X_1$), the coefficient C_1 is equal to C_u. Values of C_u for one-way elements are given in table 6-2, and equations for C_1 and C_u for two-way elements are given in table 6-3.

(*f*) The left side of the impulse equations, though derived in a similar manner, is different for unspalled sections to account for the change in physical properties of the cross section. Generally, all of the expressions for impulse capacity take the form:

Table 6-2. Impulse Coefficients C_u for One-Way Elements

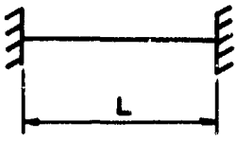
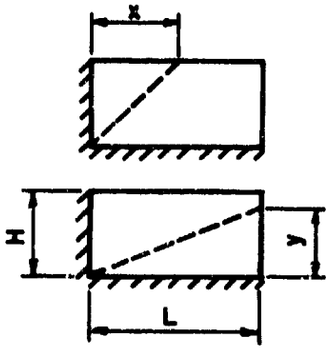
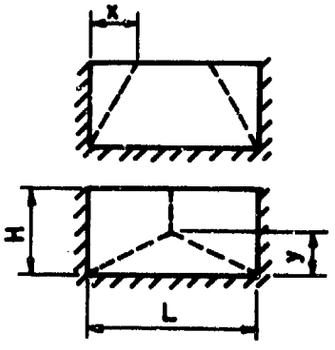
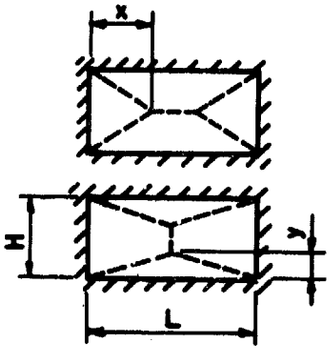
Edge conditions		Impulse coefficient C_u
Cantilever		127
Fixed supports		510

Table 6-3. Impulse Coefficients C_1 and C_u for Two-Way El

Edge conditions	Yield line location	Limits	Impulse coefficient $C_1 \times 144$ (10^{-4})	
Two adjacent edges fixed and two edges free.		$0 \le x/H \le 1$	$13.77 \frac{(K_{LM})_u}{(x/H)}$	$4.132\left[\frac{3.333(K_{LM})_u}{x/H}+($
		$H \le x \le L$	$13.77 \frac{(K_{LM})_u}{(x/H)^2}$	$4.132\left[\frac{3.333(K_{LM})_u}{(x/H)^2}+($
		$0 \le y/L \le 1$	$13.77 \frac{(K_{LM})_u (p_V/p_H)}{(y/H)}$	$4.132\left[\frac{3.333(K_{LM})_u (p_V$
		$L \le y \le H$	$13.77 \frac{(K_{LM})_u (p_V/p_H)(L/H)}{(y/H)^2}$	$4.132(p_V/p_H)\left[\frac{3.333(K_$
Three edges fixed and one edge free.		$0 \le x/H \le 1$	$13.77 \frac{(K_{LM})_u}{(x/H)}$	$4.132\left[\frac{3.333(K_{LM})_u}{x/H}+($
		$H \le x \le L/2$	$13.77 \frac{(K_{LM})_u}{(x/H)^2}$	$16.528\left[\frac{0.833(K_{LM})_u}{(x/H)^2}+2$
		$0 \le y/L \le \frac{1}{2}$	$13.77 \frac{(K_{LM})_u (p_V/p_H)}{(y/H)}$	$10.330\left[\frac{1.333(K_{LM})_u (p_V$
		$L/2 \le y \le H$	$6.89 \frac{(K_{LM})_u (p_V/p_H)(L/H)}{(y/H)^2}$	$4.132(p_V/p_H)\left[\frac{1.667(K_L$
Four edges fixed.		$0 \le x/H \le \frac{1}{2}$	$13.77 \frac{(K_{LM})_u}{(x/H)}$	$16.528\left[\frac{0.833(K_{LM})_u}{x/H}+($
		$H/2 \le x \le L/2$	$6.89 \frac{(K_{LM})_u}{(x/H)^2}$	$16.528\left[\frac{0.417(K_{LM})_u}{(x/H)^2}+2$
		$0 \le y/L \le \frac{1}{2}$	$13.77 \frac{(K_{LM})_u (p_V/p_H)}{(y/H)^2}$	$16.528\left[\frac{0.833(K_{LM})_u (p_V$
		$L/2 \le y \le H/2$	$6.89 \frac{(K_{LM})_u (p_V/p_H)(L/H)}{(y/H)^2}$	$16.528(p_V/p_H)\left[\frac{0.417(K_L$

x, y, L, H (in.)

...y Elemen... ...se Coefficients C_1 and C_u for Two-Way Elements

...C_1×144 (10^{-6})	Impulse coefficient C_u×144 (10^{-6})
...$)_u + (K_L$	$4.132\left[\frac{3.333\,(K_{LM})_u}{x/H} + (K_{LM})_u{}^3(p_V/p_H)\,(1-x/H)\right]$
...$)_u + (K_L$	$4.132\left[\frac{3.333\,(K_{LM})_u}{(x/H)^2} + (K_{LM})_u{}^3\left(\frac{x/H-1}{(L/H)^2} + \frac{4.705\,(L/H-x/H)\,\tan\lambda}{(L/H)^2}\right)\right]$ Where, $\lambda = 12° - \tan^{-1}\left(\frac{0.2126}{x/H}\right)$
...$)_u (p_V/p_H$ ... $H)$	$4.132\left[\frac{3.333\,(K_{LM})_u\,(p_V/p_H)}{y/H} + \frac{(K_{LM})_u{}^3(L/H-y/H)}{(L/H)^2}\right]$
...$33\,(K_{LM})_u$ ... $H)\,(L/H)$	$4.132\,(p_V/p_H)\left[\frac{3.333\,(K_{LM})_u\,(L/H)}{(y/H)^2} + (K_{LM})_u{}^3(y/H-L/H+4.705\,(1-y/H)\,\tan\lambda)\right]$ Where, $\lambda = 12° - \tan^{-1}\left(\frac{0.2126}{y/L}\right)$
...$)_u + (K_{LM}$	$4.132\left[\frac{3.333\,(K_{LM})_u}{x/H} + (K_{LM})_u{}^3(p_V/p_H)\,(1-x/H)\right]$
...$)_u + 2(K$	$16.528\left[\frac{0.833\,(K_{LM})_u}{(x/H)^2} + 2\,(K_{LM})_u{}^3\left(\frac{x/H-1}{(L/H)^2} + \frac{4.705\,(L/2H-x/H)\,\tan\lambda}{(L/H)^2}\right)\right]$ Where, $\lambda = 12° - \tan^{-1}\left(\frac{0.2126}{x/H}\right)$
...$)_u (p_V/p_H$ ... $H)$	$10.330\left[\frac{1.333\,(K_{LM})_u\,(p_V/p_H)}{y/H} + 3.2\,(K_{LM})_u{}^3\,\frac{(L/2H-y/H)}{(L/H)^2}\right]$
...$7\,(K_{LM})_u$ ... $H)\,(L/H)$	$4.132\,(p_V/p_H)\left[\frac{1.667\,(K_{LM})_u\,(L/H)}{(y/H)^2} + (K_{LM})_u{}^3(y/H-L/2H+4.705\,(1-y/H)\,\tan\lambda)\right]$ Where, $\lambda = 12° - \tan^{-1}\left(\frac{0.2126}{2y/L}\right)$
...$)_u + (K_{LM}$	$16.528\left[\frac{0.833\,(K_{LM})_u}{x/H} + (K_{LM})_u{}^3(p_V/p_H)\left(1-2\,\frac{x}{H}\right)\right]$
...$)_u + 2(K_L$	$16.528\left[\frac{0.417\,(K_{LM})_u}{(x/H)^2} + 2\,(K_{LM})_u{}^3\left(\frac{x/H-\frac{1}{2}}{(L/H)^2} + \frac{4.705\,(L/2H-x/H)\,\tan\lambda}{(L/H)^2}\right)\right]$ Where, $\lambda = 12° - \tan^{-1}\left(\frac{0.2126}{2x/H}\right)$
...$)_u (p_V/p_H$ ... $H)$	$16.528\left[\frac{0.833\,(K_{LM})_u\,(p_V/p_H)}{y/H} + (K_{LM})_u{}^3\,\frac{(L/H-2y/H)}{(L/H)^2}\right]$
...$7\,(K_{LM})_u$ ... $H)\,(L/H)$	$16.528\,(p_V/p_H)\left[\frac{0.417\,(K_{LM})_u\,(L/H)}{(y/H)^2} + (K_{LM})_u{}^3(2y/H-L/H+4.705\,(1-2y/H)\,\tan\lambda)\right]$ Where, $\lambda = 12° - \tan^{-1}\left(\frac{0.2126}{2y/L}\right)$

2

Spalled Section (Type III)

$$\frac{i_b^2 H}{p_H d_c^2 f_{de}} = C_1 \text{ or } C_u \qquad \textbf{Equation 6–30}$$

Unspalled Section (Type II)

$$\frac{i_b^2 H}{p_H T_c d_c^2 f_{de}} = C_1 \text{ or } C_u \qquad \textbf{Equation 6–31}$$

(2) *Reduced rotations and reduced deflections.*

(*a*) For certain conditions, it is sometimes desired to design a structural element for maximum deflections other than the partial failure deflection X_1 or the ultimate deflection X_u. For those cases, the impulse coefficients can be scaled relative to the deflections. For a maximum deflection X_m in the deflection range $0 \leq X_m \leq X_1$, the impulse coefficient becomes

$$C_1' = \left(\frac{X_m}{X_1}\right) C_1 \qquad \textbf{Equation 6–32}$$

and for the range $X_1 \leq X_m \leq X_u$, since $(C_u - C_1)$ is a measure of the impulse capacity between X_1 and X_u, the impulse coefficient is

$$C_u' = C_1 + \frac{X_m - X_1}{X_u - X_1}(C_u - C_1) \qquad \textbf{Equation 6–33}$$

(*b*) The final design equations for spalled and unspalled sections and for any maximum deflection X_m are shown in table 6–4.

(*c*) To facilitate the design procedure, charts have been constructed for the impulse coefficients C_1 and C_u for two-way elements (the coefficient C_u for one-way elements is a constant). It was shown at the beginning of this chapter that the effective mass factor $(K_{LM})_u$ for a two-way element varies as the yield line location ratio y/H or x/L. Furthermore, in chapter 5 it was shown that the yield line location ratio is a function of the span ratio L/H and the moment ratio $[(M_{VN}+M_{VP})/(M_{HN}+M_{HP})]$. Since the cross sections used for large deflection design are equally reinforced on each face, the moment ratio is, in effect, the ratio of the reinforcement ratios p_V/p_H. Thus it can be seen that the impulse coefficients are solely functions of L/H and p_V/p_H and they have been plotted against p_V/p_H for varying values of L/H. These curves for various support conditions are given in figures 6–10 through 6–12 for C_1 and in figures 6–13 through 6–15 for C_u.

(3) *Optimum distribution of flexural reinforcement.*

(*a*) A prime factor in the design of any facility is construction economy. Proper selection of section sizes and reinforcing steel will result in a design having optimum capacity and minimum cost. To determine the optimum design of any particular two-way structural element, consideration must be given to the following:

1. There is an ideal distribution of flexural reinforcing, defined by the reinforcement ratio p_V/p_H, which will yield the maximum blast impulse capacity for a given total amount of flexural reinforcing p_T. This ratio is independent of the section depth.

2. There is an ideal section depth which, in combination with the flexural reinforcing distribution defined above and the lacing reinforcement, will give minimum cost for the element.

(*b*) In this chapter, the first item is presented. Later, in chapter 10, procedures are outlined to enable the designer to choose the proper section depth which will result in minimum cost.

(*c*) Equations for the determination of the impulse capacity for two-way panels with large deflections were previously presented in tables 6–3 and 6–4. If a generalized equation is written for the case of a spalled section, it can be seen that

$$\frac{i_b^2 H}{d_c^2 f_{de}} = f\left[\frac{p_V}{p_H}, p_H, \frac{L}{H}\right] \qquad \textbf{Equation 6–34}$$

(*d*) As an illustration of the determination of the optimum reinforcing distribution ratio p_V/p_H, consider a two-way panel fixed on three sides having a span ratio L/H equal to 3 and a total percentage of reinforcing p_T $(p_T = p_H + p_V)$ equal to 1 percent. The impulse capacity can be determined for varying values of p_V/p_H for the deflection X_1 and also X_u from figures 6–11 and 6–14.

(*e*) If $i_b^2 H/d_c^2 f_{de}$ is plotted versus p_V/p_H, the

Table 6–4 Design Equations for Elements Which Respond to Impulse

Section	Deflection range $(0 \leq X_m \leq X_1)$	Deflection range $(X_1 \leq X_m \leq X_u)$
Spalled section	$\frac{i_b^2 H}{p_H d_c^2 f_{de}} = C_1 (X_m/X_1)$	$\frac{i_b^2 H}{p_H d_c^2 f_{de}} = C_1 + (C_u - C_1)\frac{X_m - X_1}{X_u - X_1}$
Unspalled section (crushing of concrete)	$\frac{i_b^2 H}{p_H T_c d_c^2 f_{de}} = C_1 (X_m/X_1)$	$\frac{i_b^2 H}{p_H T_c d_c^2 f_{de}} = C_1 + (C_u - C_1)\frac{X_m - X_1}{X_u - X_1}$

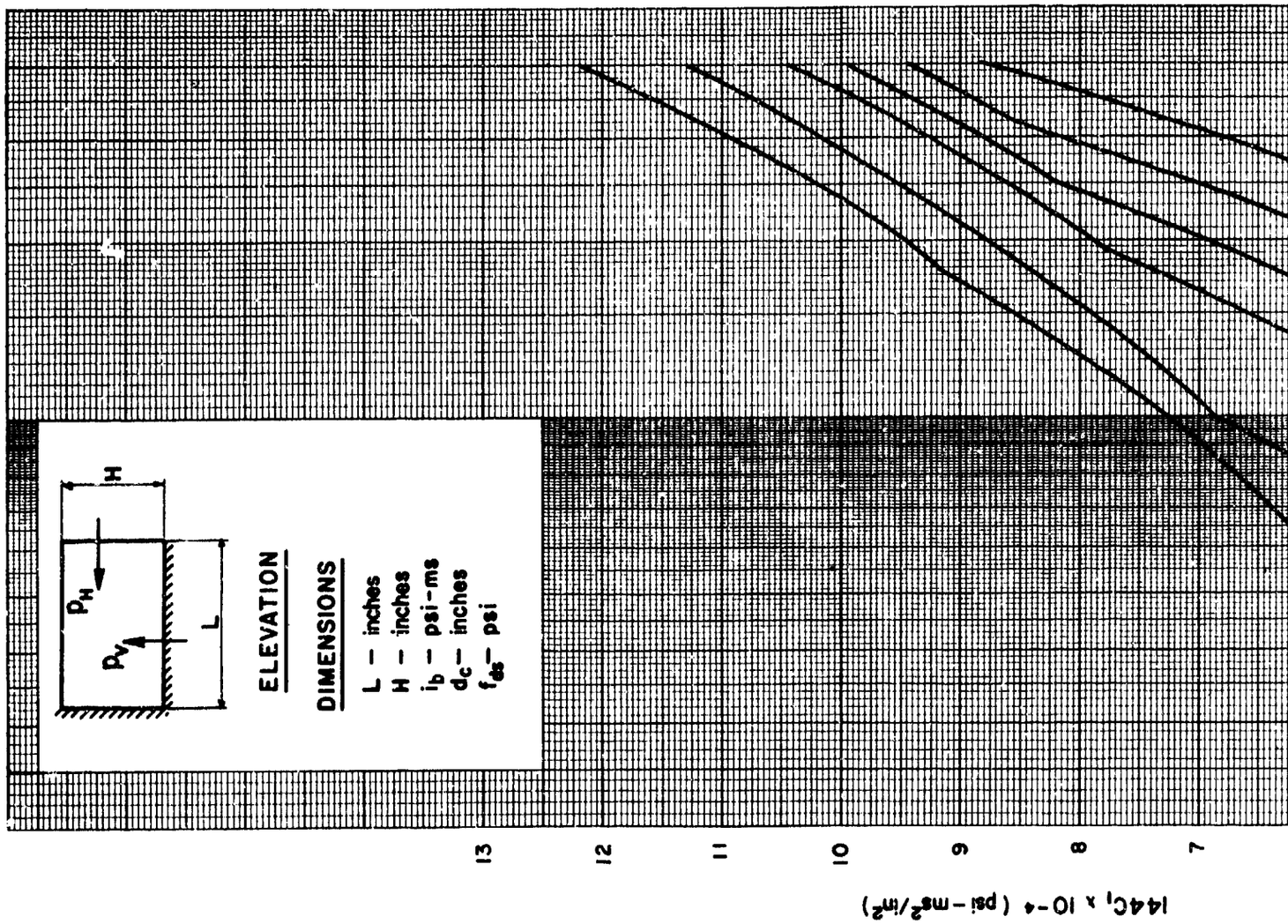
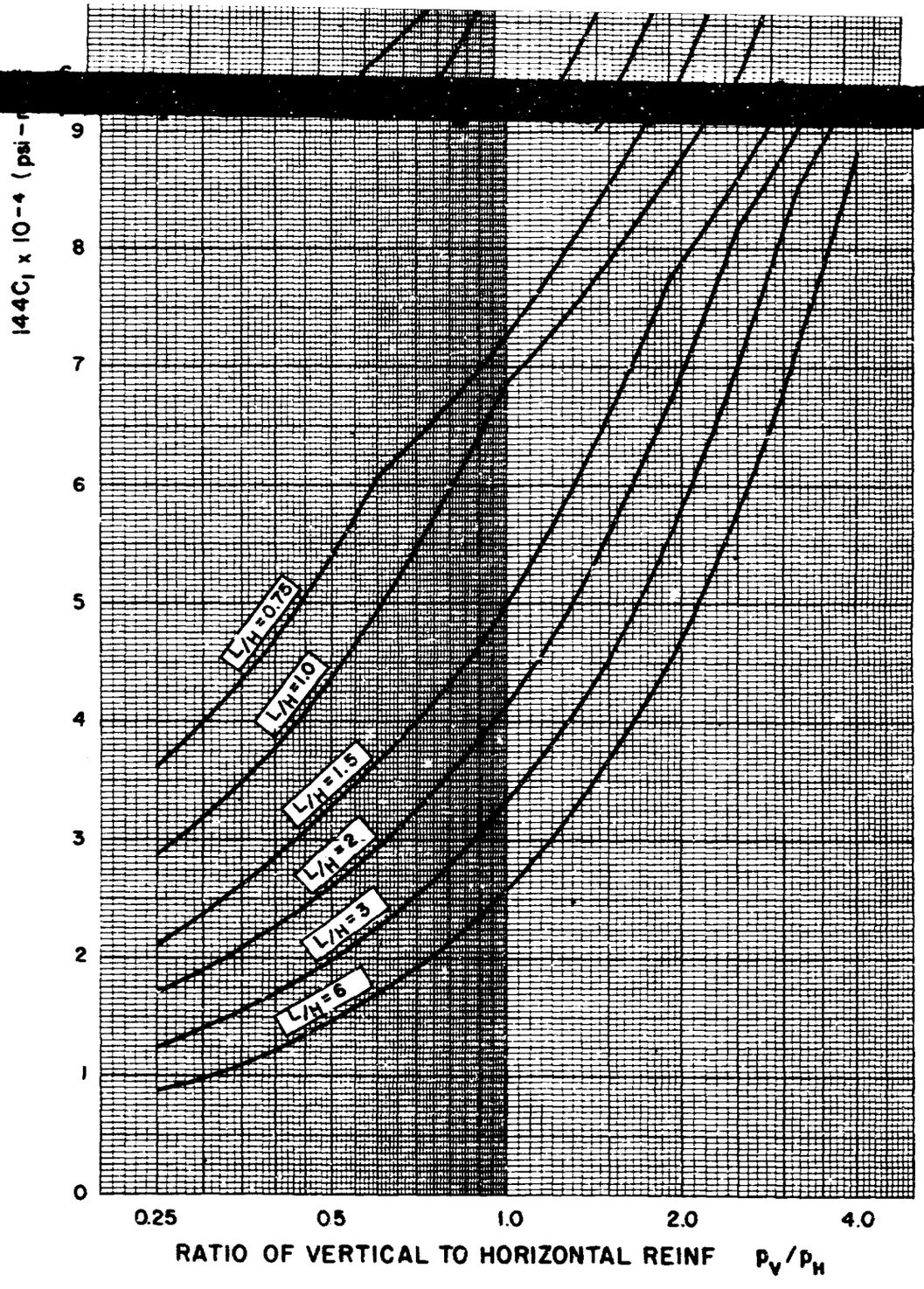


Figure 6–10. Impulse coefficient C_1 for an element with two adjacent edges fixed

fixed and

C_1 for an element with two adjacent edges fixed and two edges free.



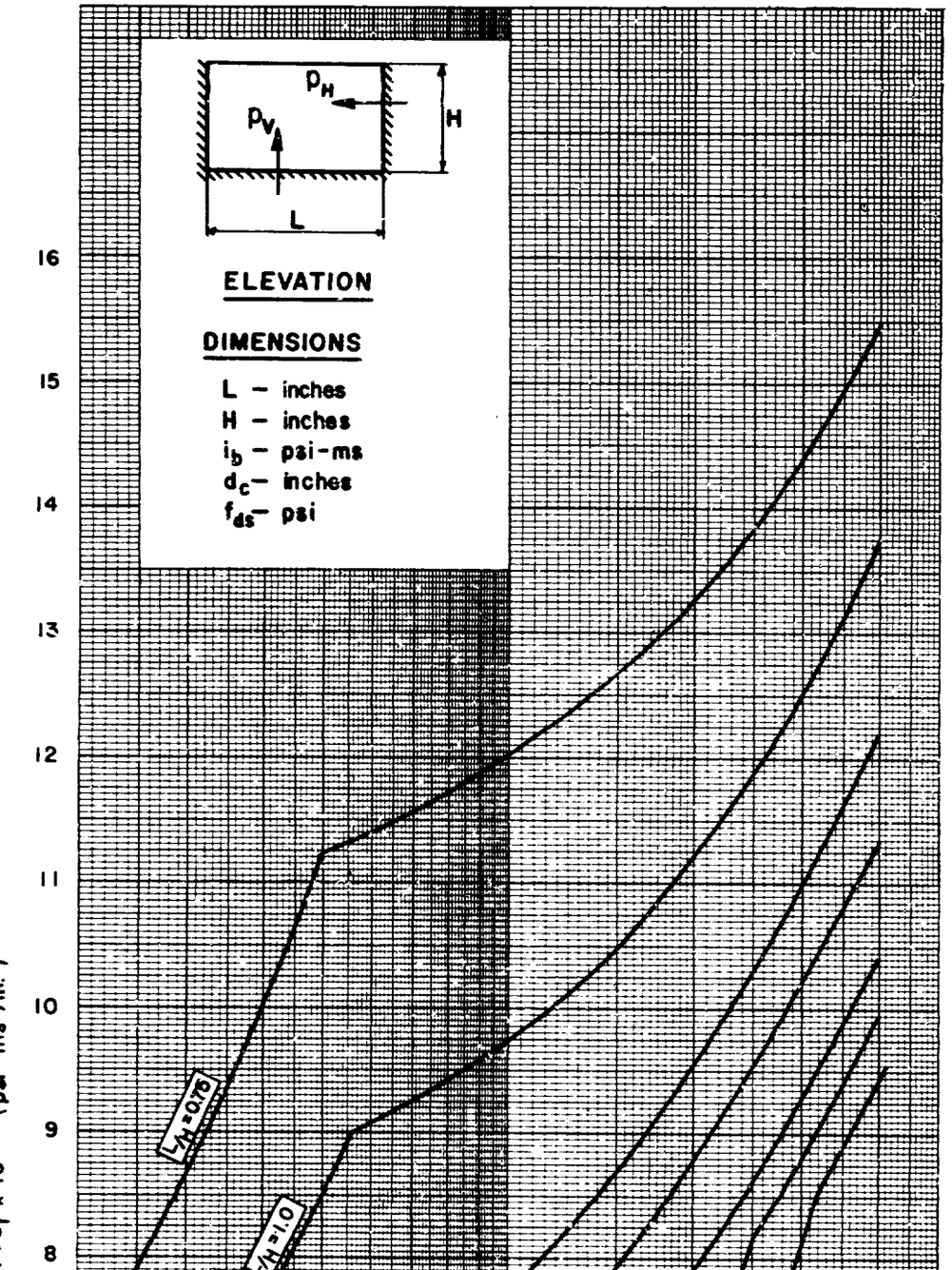
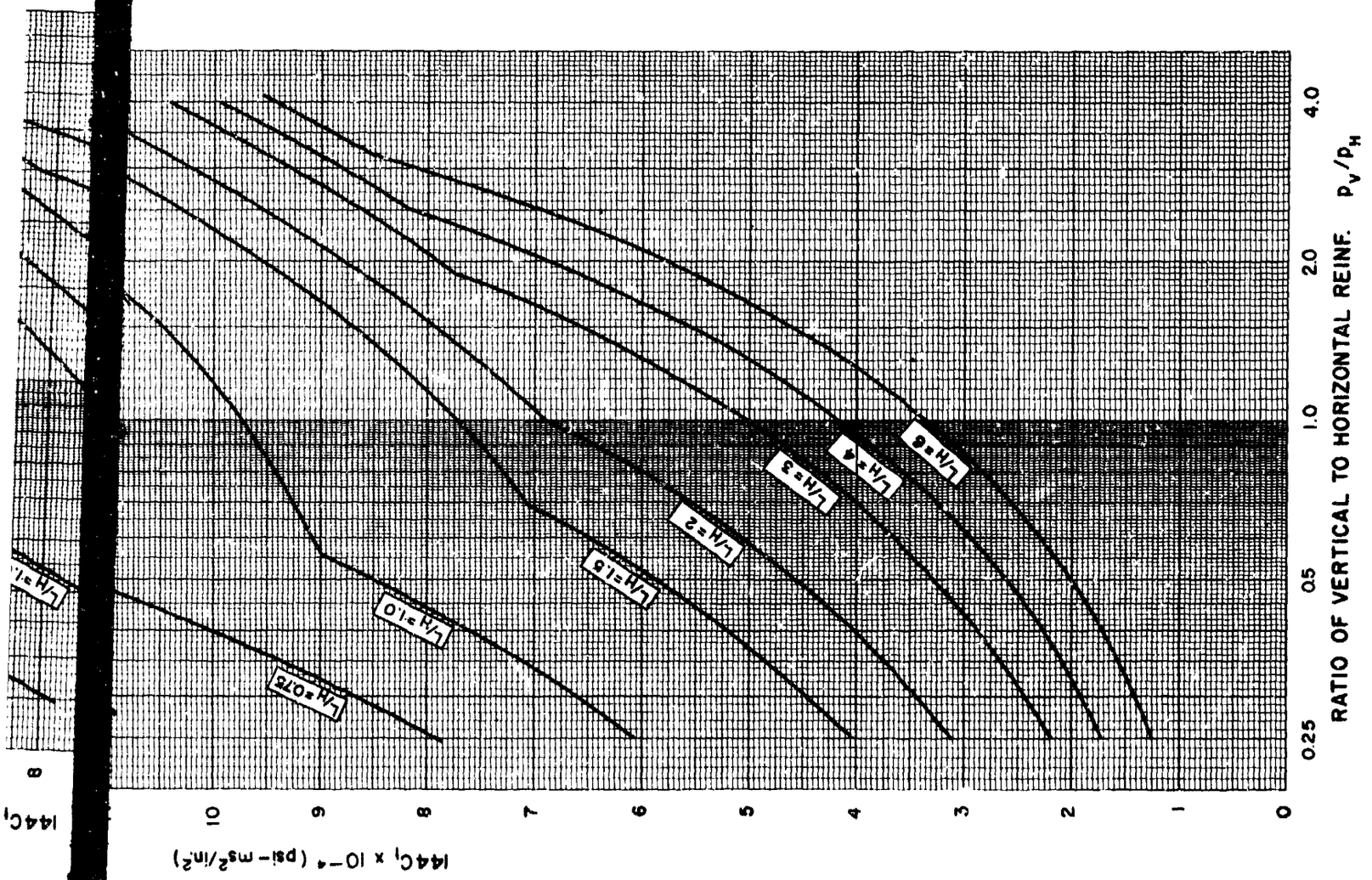


Figure 6-11. Impulse coefficient C_1 for an element with



with three

11. Impulse coefficient C_1 for an element with three edges fixed and one edge free.

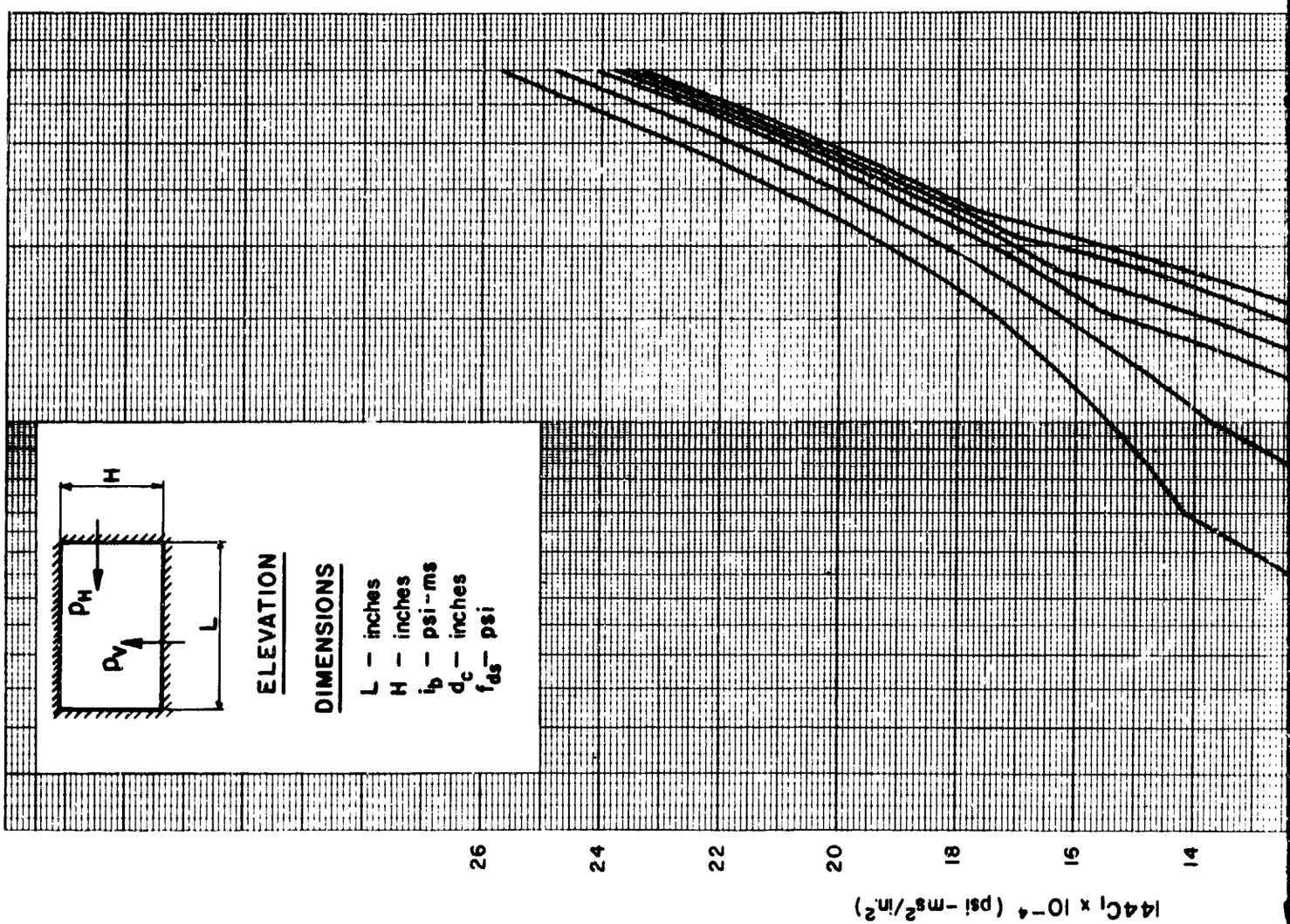
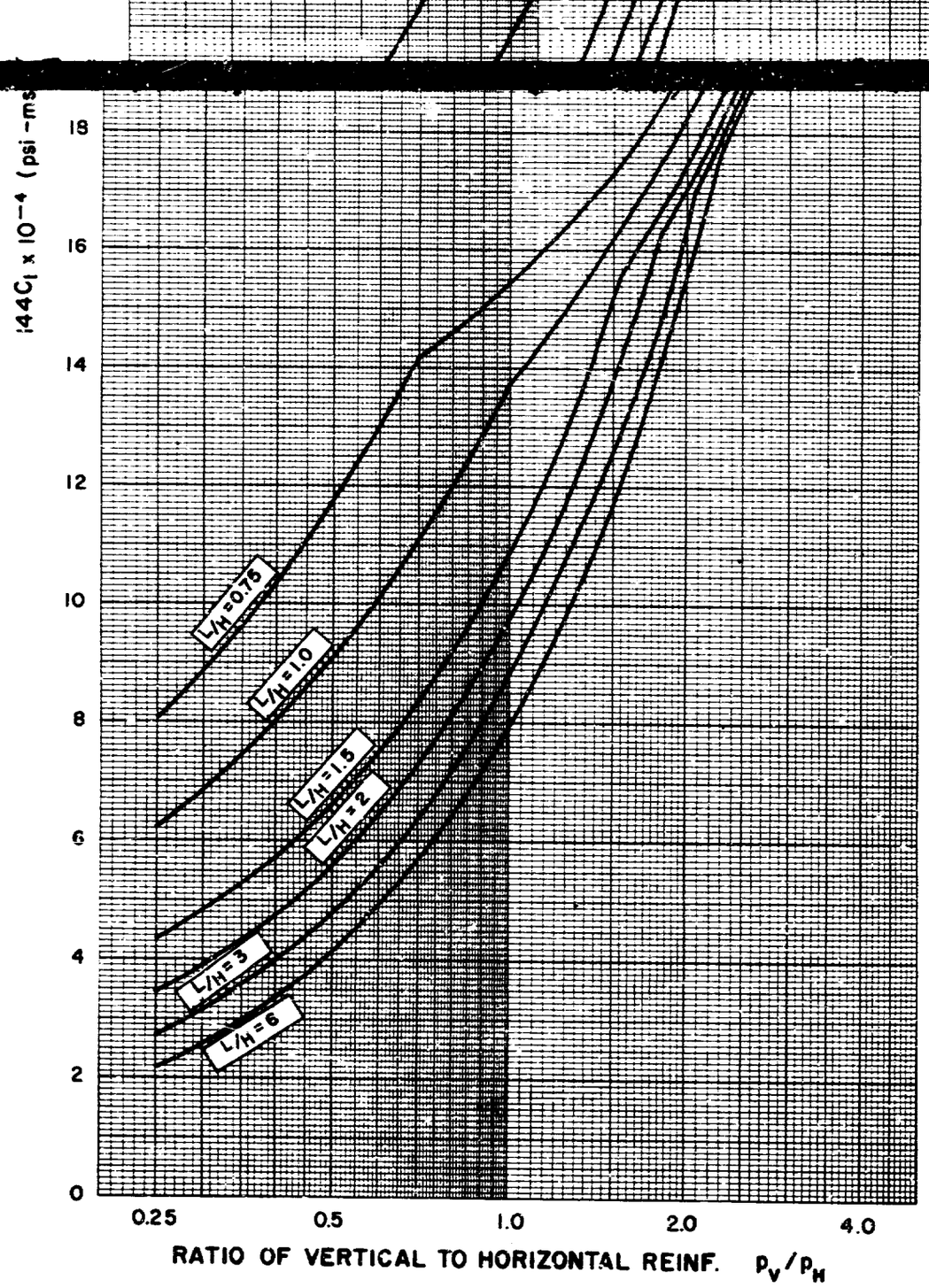


Figure 6-12. Impulse coefficient C_1 for an element with four edges



pulse coefficient C_1 for an element with four edges fixed.

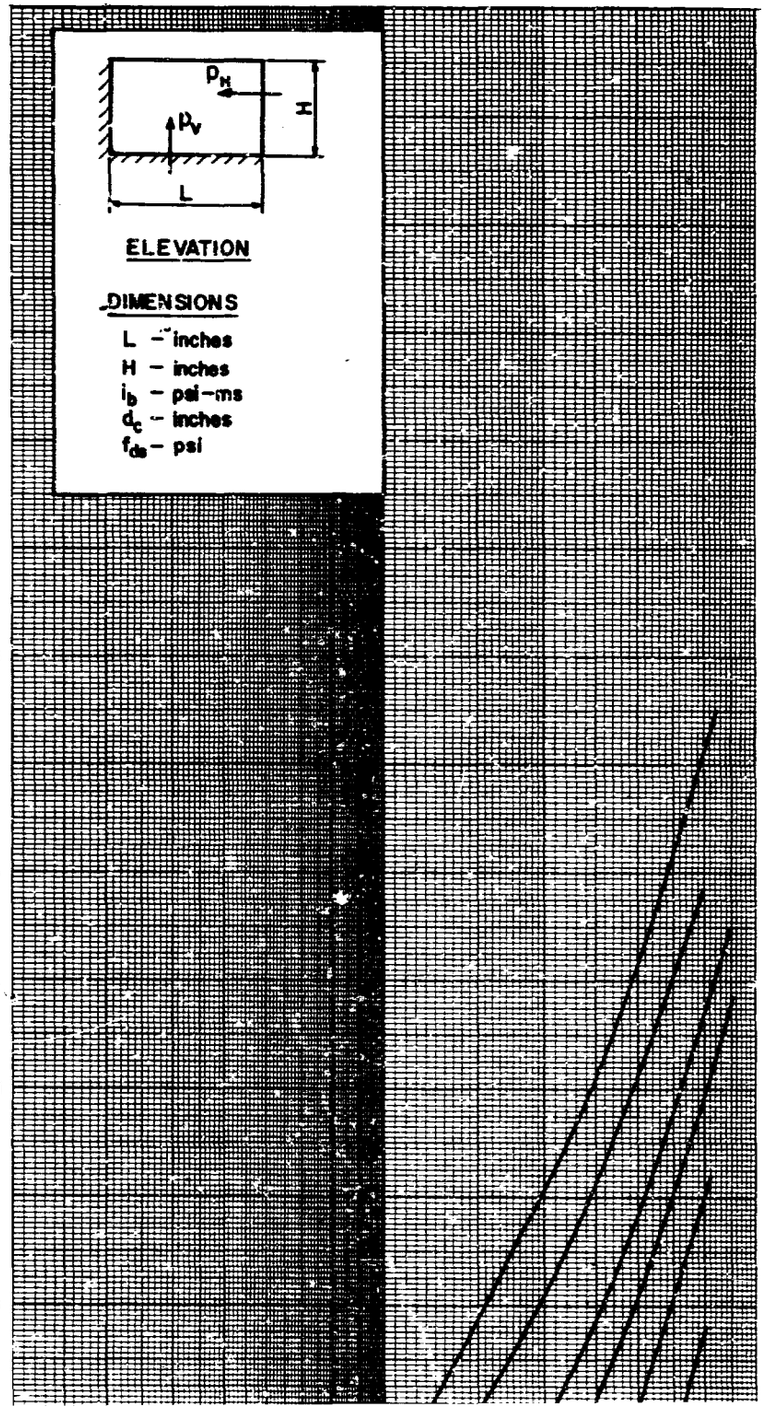
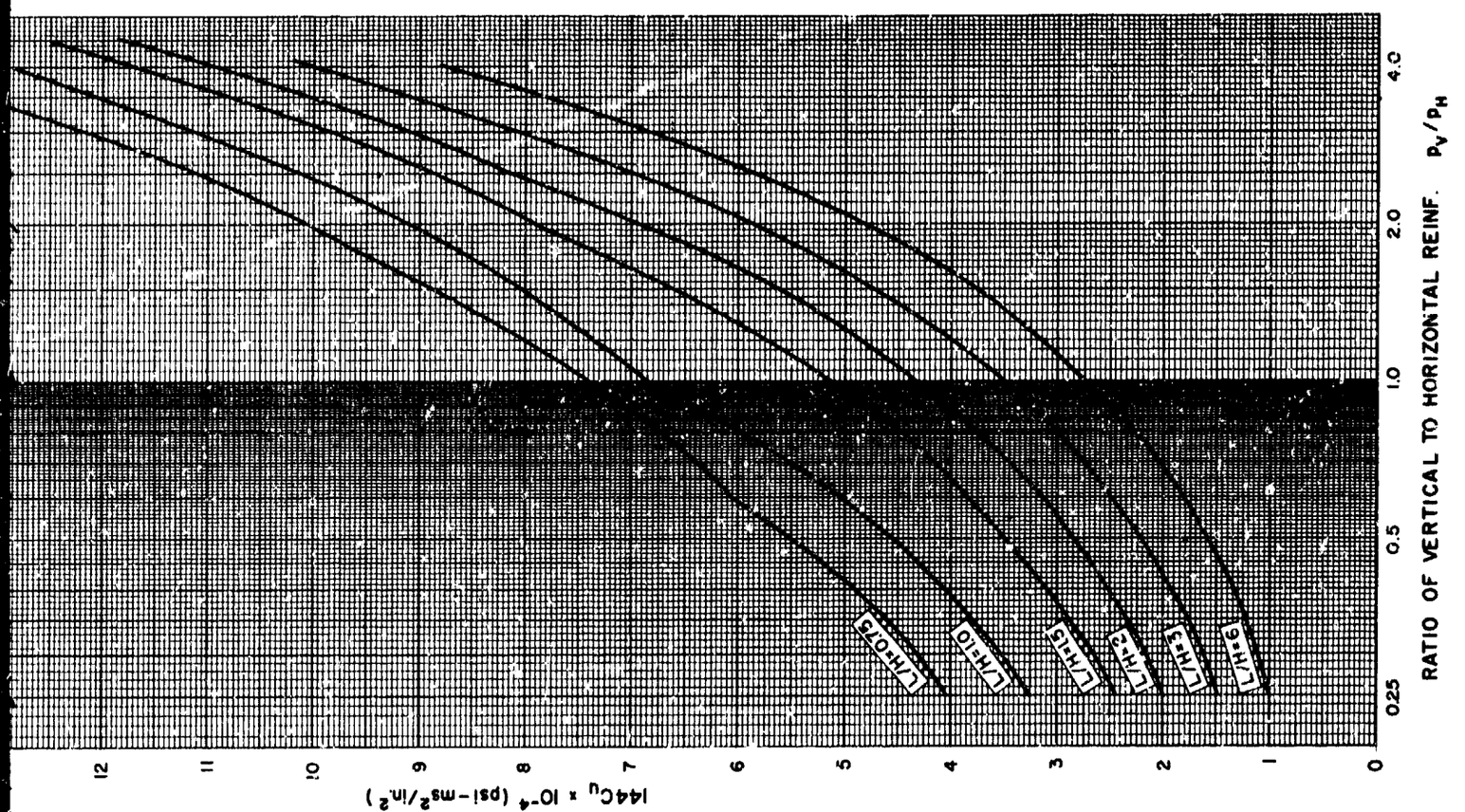


Figure 6-13. Impulse coefficient C_u for an element with two adjacent edges fixed



mpulse coefficient C_u for an element with two adjacent edges fixed and two edges free.

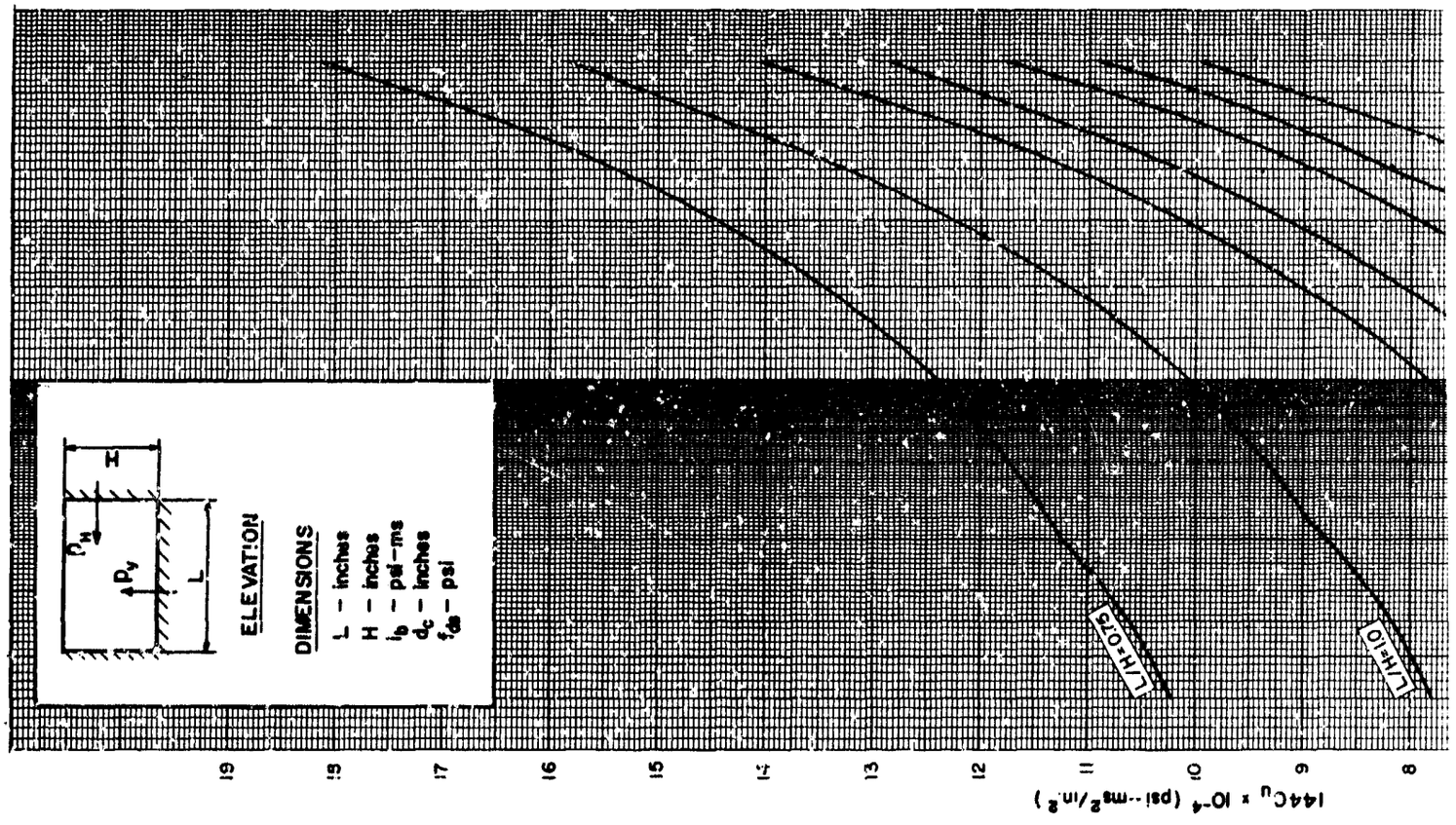
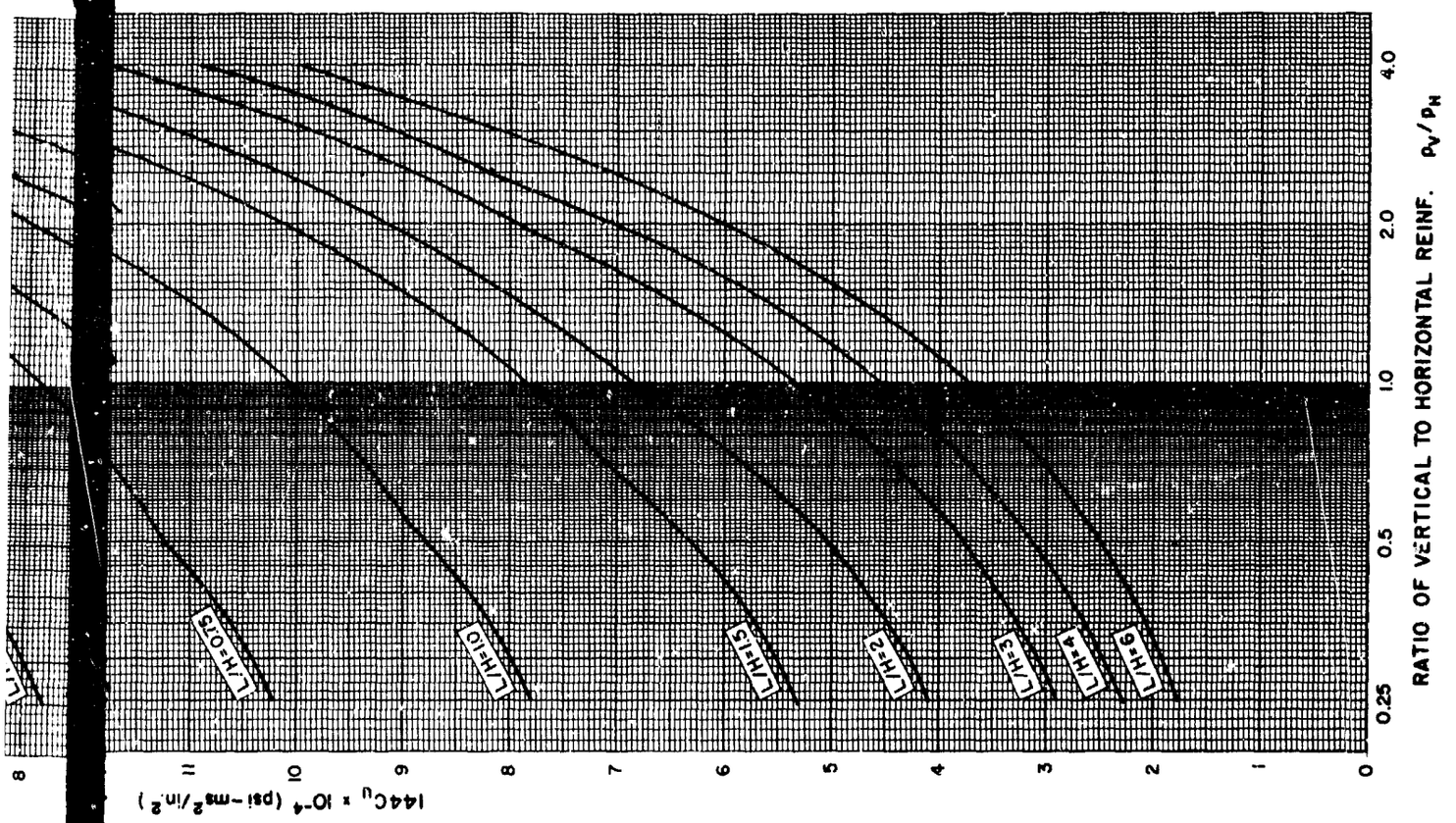
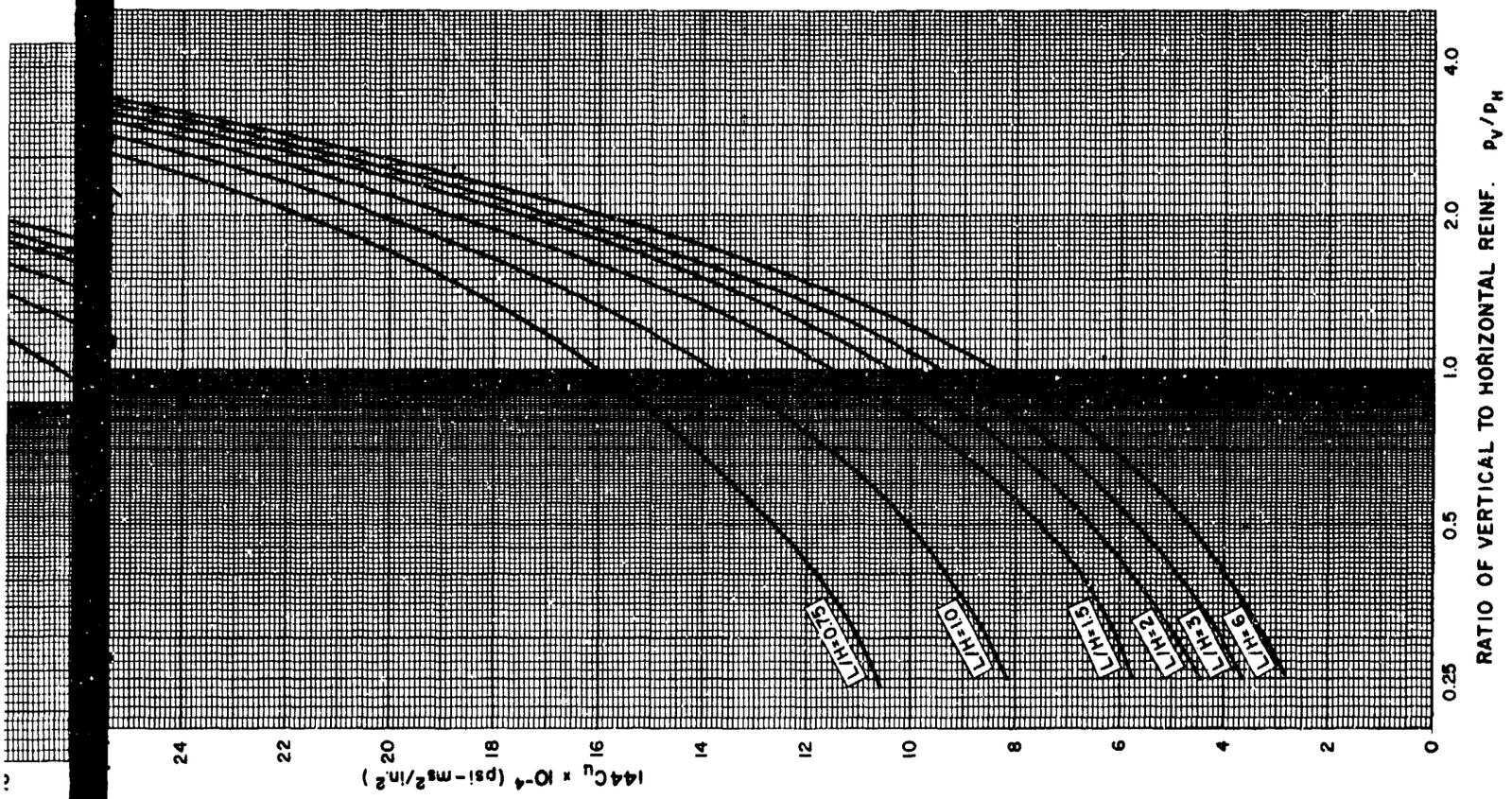


Figure 6-14. Impulse coefficient C_u for an element with three edges fixed and on



and one ... coefficient C_u for an element with three edges fixed and one edge free.

Figure 6-15. Impulse coefficient C_u for an element with fc



ure 6–15. Impulse coefficient C_u for an element with four edges fixed.

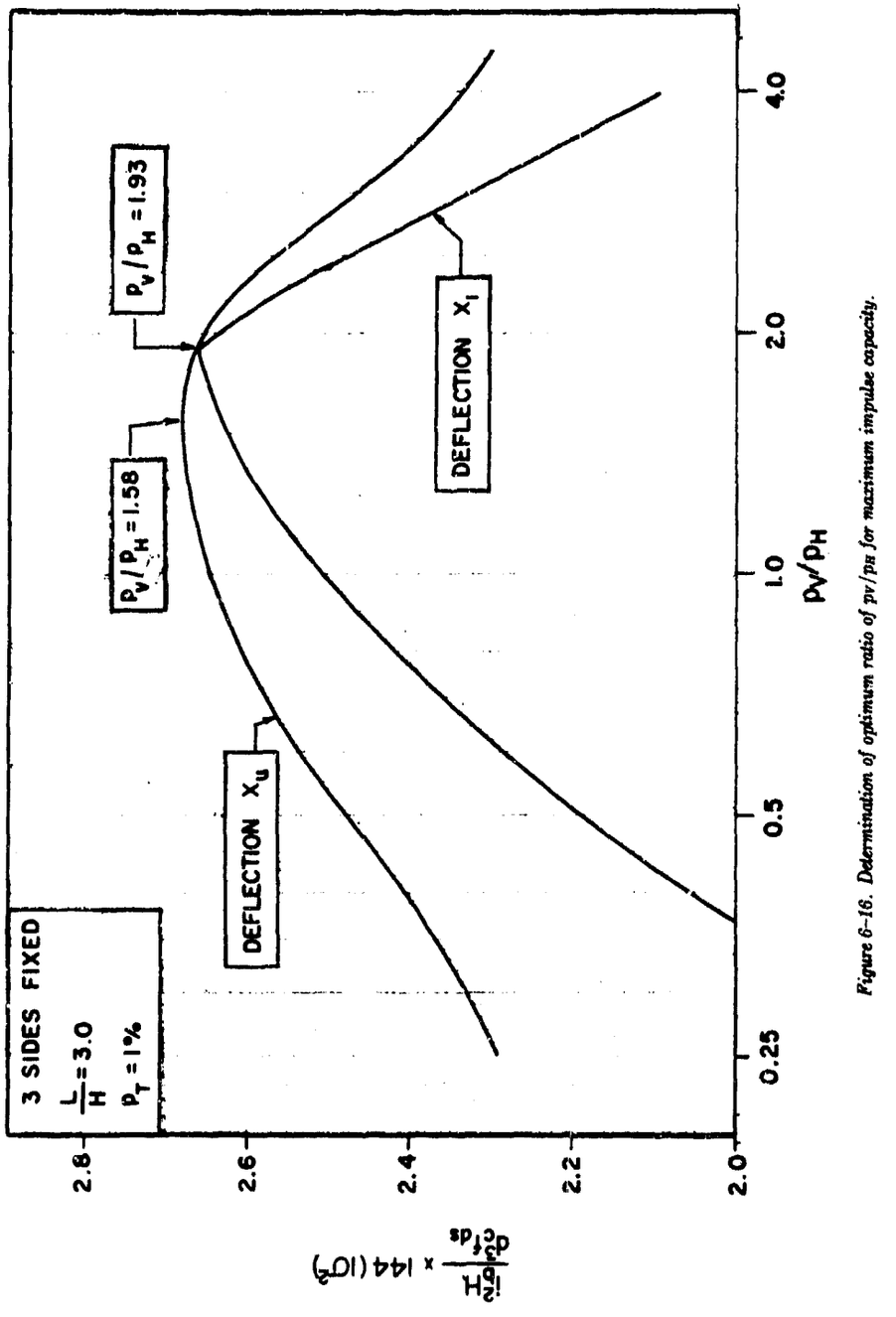
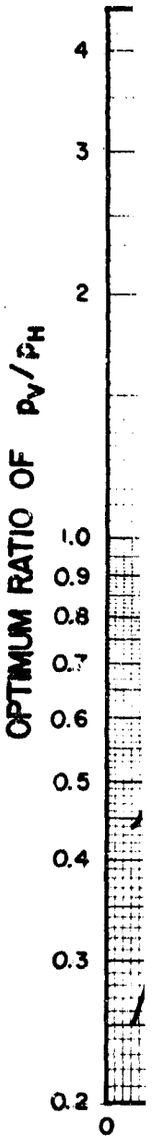
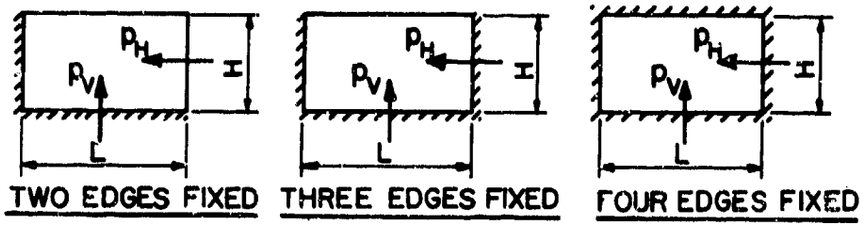


Figure 6–16. Determination of optimum ratio of p_V/p_H for maximum impulse capacity.



resulting curves are as shown in figure 6–16. The ideal p_V/p_H occurs at the maximum value of $i_n^2H/d_c^2f_{ds}$ and is indicated on the illustration as 1.58 for deflection X_u and 1.93 for deflection X_1. Note that the two curves have a common point which coincides with the maximum impulse capacity for the partial failure case. This is true for all L/H values and also for the various support cases.

(*f*) Similar curves can be constructed for other L/H ratios and support conditions, and the ideal p_V/p_H values corresponding to the maximum values of $i_n^2H/d_c^2f_{ds}$ can be plotted against L/H as shown in



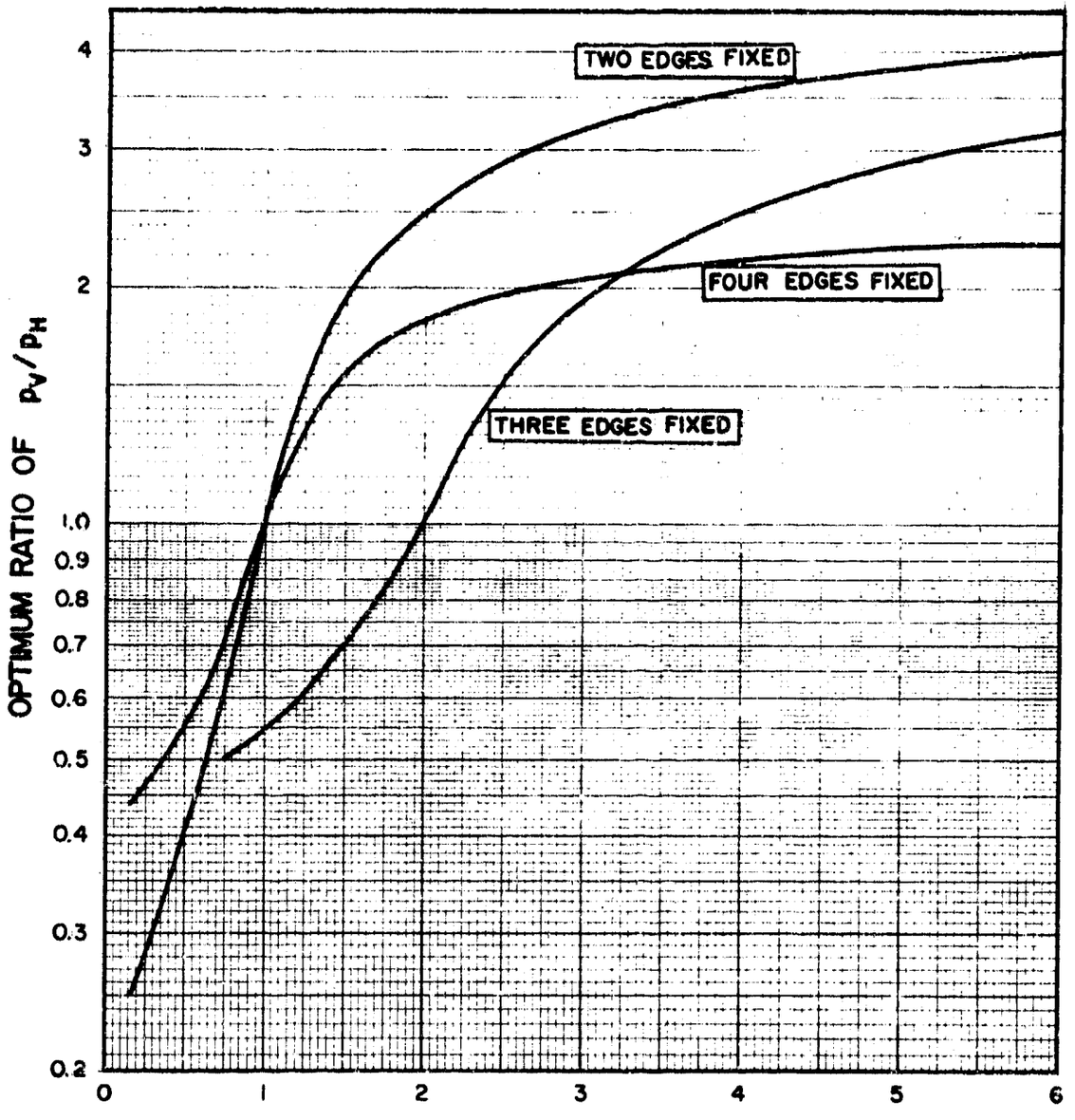


Figure 6-17. Optimum ratio of p_V/p_H for maximum impulse capacity at partial failure deflection X_1.

Figure 6-16. Determination of optimum ratio of p_V/p_H for maximum impulse capacity.

also for the various

constructed for other
ns, and the ideal p_V/p_H
maximum values of
nst L/H as shown in

2

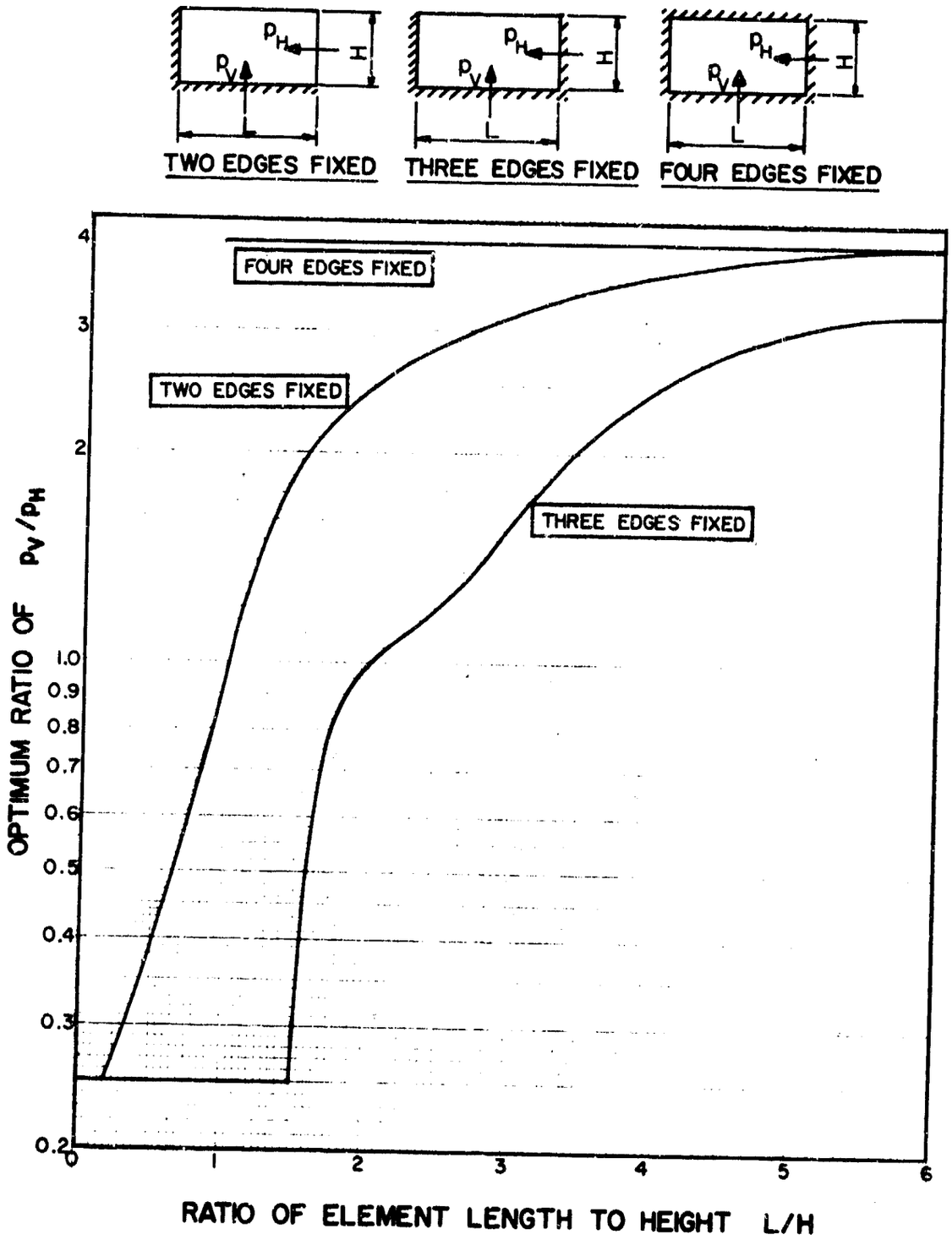


Figure 6–18. Optimum ratio of pv/pu for maximum impulse capacity at incipient failure deflection X_u.

figure 6–17 for deflection X_1 and figure 6–18 for deflection X_u. For the three support conditions presented, the crack line location for the optimum p_V/p_H is always at 45 degrees for deflection X_1. For deflection X_u the angle is 45 degrees for panels with two sides fixed and varies for the others. Thus the optimum p_V/p_H ratio is different for the two cases of structural behavior except when two sides are fixed.

(*g*) The optimum p_V/p_H ratio for a given element is a constant for any maximum deflection X_m in the range $0 \leq X_m \leq X_1$ and is determined from figure 6–17. In the deflection range $X_1 \leq X_m \leq X_u$ the optimum p_V/p_H ratio varies with the maximum deflection but can be determined by linear scaling relative to the deflection using the values obtained from figures 6–17 and 6–18.

(*h*) If the above procedure is followed for unspalled sections, the ideal p_V/p_H versus L/H curves will be the same as shown in figures 6–17 and 6–18.

d. Design for Limited Deflections. The design of elements which respond to the impulse with limited deflections is accomplished through the use of equation 6–23. Impulse coefficients have not been determined for this case even though the theory and procedures are similar. However, rapid but nonconservative preliminary designs can be performed using the impulse coefficients in the previous subparagraphs. Optimum p_V/p_H ratios are the same as for the large deflection design.

Section IV. DESIGN FOR SHEAR

6–10. General

a. After the flexural design of the element has been completed, the required quantity of shear reinforcement must be determined. This shear reinforcement insures that the desired flexural behavior in the ductile mode will be attained. When the proper shear reinforcement is not provided, brittle shear failure will occur before the element can absorb the required energy through flexural action. The shear reinforcement is a function of the resistance of the element and not the applied load.

b. The design for shear consists of the determination of the type and quantity of shear reinforcement at certain critical locations as specified in paragraph 5–18. It should be noted again, as stated in paragraph 5–5*d*, that no dynamic stress increase is allowed when determining the quantity of shear reinforcement to be used.

6–11. Elements Which Respond to Pressure Only and Pressure-Time Relationship

a. These elements employ stirrups for shear reinforcement, although isolated cases can arise where lacing would be used (for example, in certain elements which respond to the pressure-time relationship with Type II cross sections). For elements with Type I cross sections, the equations presented in section V, chapter 5, are used to calculate the ultimate support shears (table 5–12 for one-way elements and table 5–14 for two-way elements) and the ultimate shear stresses at distance d from the support (table 5–13 for one-way elements and table 5–15 for two-way elements). These values are substituted into the equations of paragraph 5–3 to determine the amounts of shear reinforcing to be provided. For the design of elements with Type II cross sections, refer to paragraph 6–12.

b. Rapid though unconservative preliminary designs of type I cross sections can also be accomplished using the method outlined in paragraph 6–12. The maximum possible error is approximately 15 percent. For the final analysis, however, the procedures in chapter 5 should be employed.

6–12. Elements Which Respond to Impulse

a. For elements which respond to impulse, the element cross section is either Type II or III, and lacing reinforcement is always used. The parameters involved enable the construction of additional charts to facilitate the design procedure. As before, the values of the shear forces or stresses are used with the equations of paragraph 5–3 to calculate the shear reinforcing needed.

b. When computing the quantity of lacing reinforcement, the angle of inclination α of the lacing bars is determined from figure 6–19

where S_l = spacing of lacing in the direction parallel to the longitudinal reinforcement
d_l = distance between center lines of lacing bends measured normal to flexural reinforcement
R_l = radius of lacing bend
D_0 = nominal diameter of reinforcing bar

(1) *Shear coefficients.*

(*a*) The equations presented in section V, chapter 5, show that the shear forces and stresses vary as the ultimate unit resistance, the geometry and yield line locations of the element, and the section depth. If r_u is evaluated and substituted into these expressions, it can be shown that the ultimate support shear V_s can be represented as an equation in the general form

$$V_s = C\frac{pd_c^2 f_{dc}}{L} \qquad \text{Equation 6–35}$$

and the ultimate shear stress at distance d_c from the support as

$$v_u = Cpf_{dc} \qquad \text{Equation 6–36}$$

where C is defined as the shear coefficient, p is the

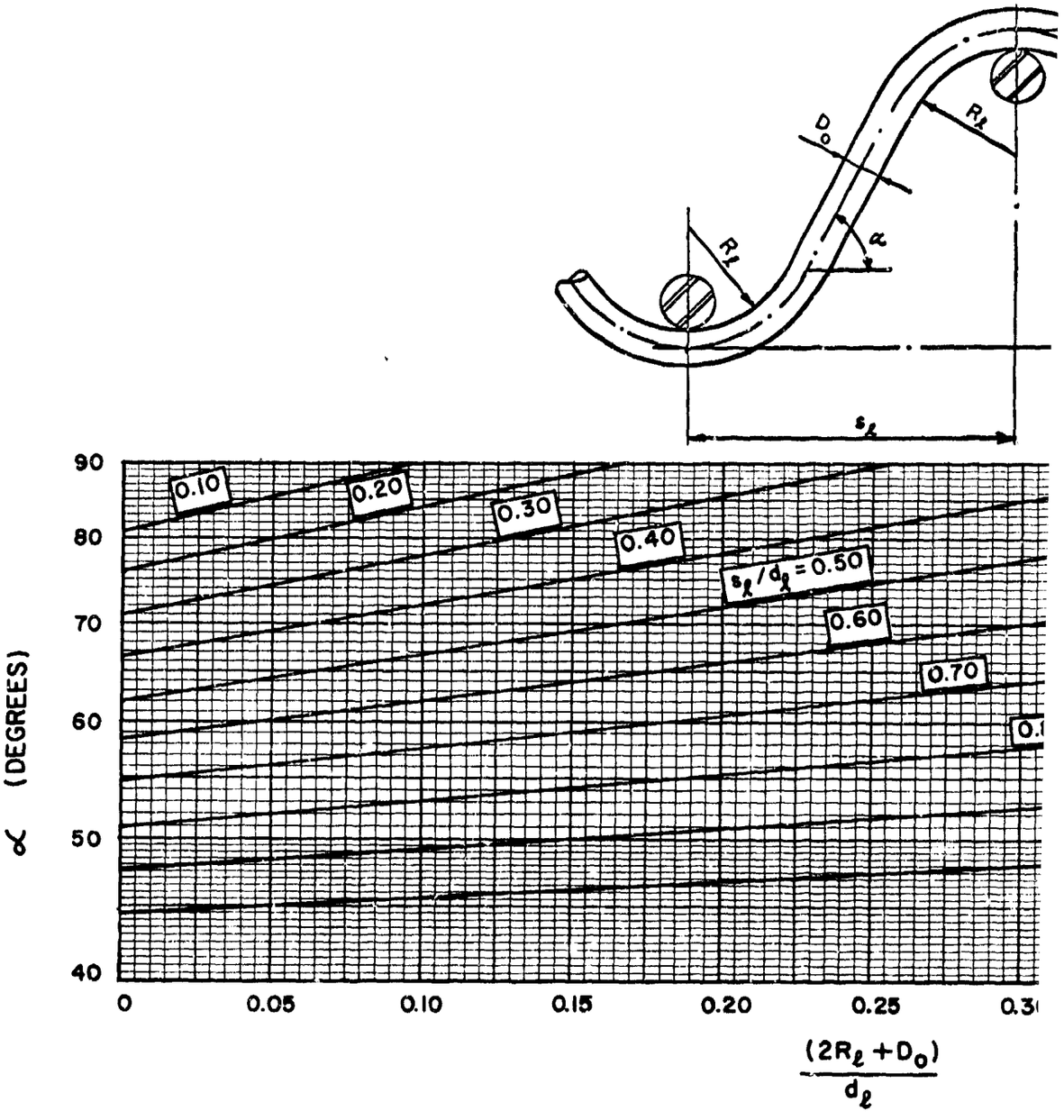
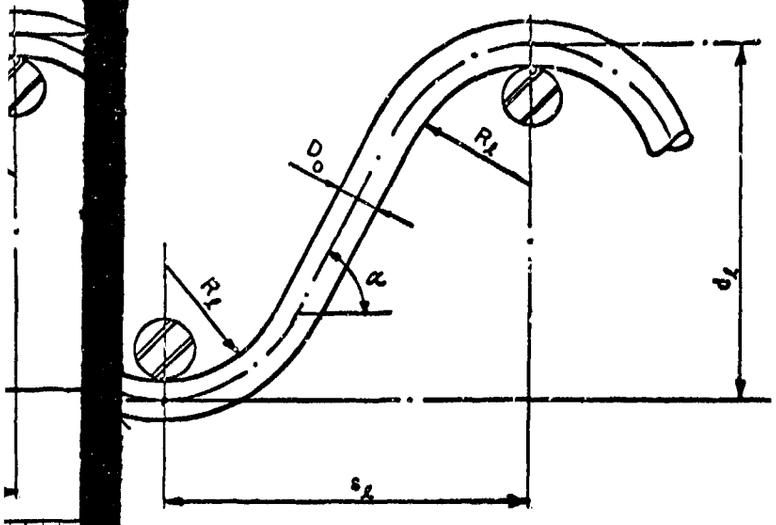


Figure 6-19. Angle of inclination of lacing bars.



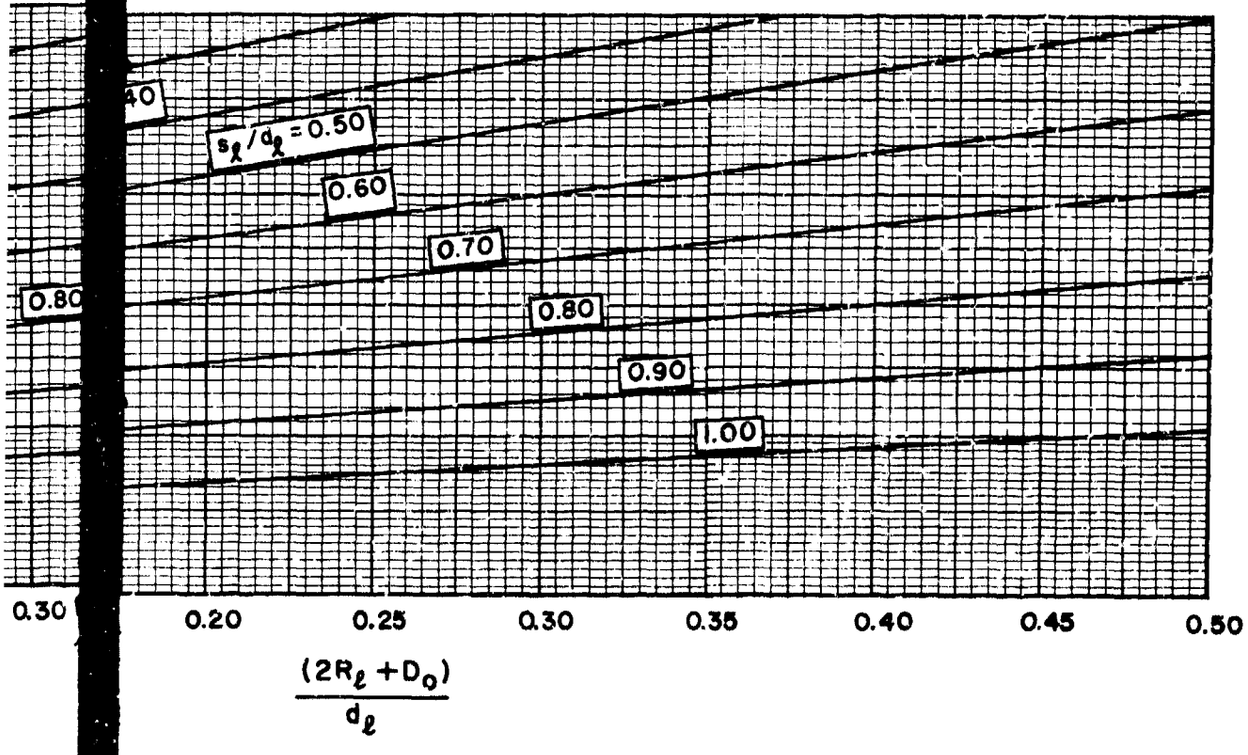
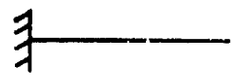
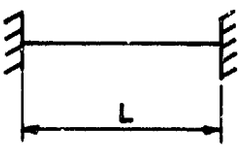


Figure 6–19. Angle of inclination of lacing bars.

Table 6–5. Shear Coefficients for Ultimate Support Shear for One-Way Elements (Cross Sections Type II and III)

Edge conditions	Ultimate support shear coefficient C_s
Cantilever 	2
Fixed supports 	8

flexural reinforcement ratio, and f_{ds} is the dynamic design stress for the flexural reinforcement.

(*b*) The shear coefficient C is different for each case and also different for one-way and two-way elements. Specific values are indicated in the following paragraphs of this section.

(2) *One-way elements.*

(*a*) *Ultimate support shear.* The ultimate support shear V_s for a one-way element (such as a beam or slab) is

$$V_s = C_s \frac{p d_c^2 f_{ds}}{L} \qquad \textbf{Equation 6–37}$$

where C_s is the shear coefficient and equal to a constant. Values of C_s for several one-way elements are given in table 6–5.

(*b*) *Ultimate shear stress.* The ultimate shear stress v_u at distance d_c from the support for a one-way element is

$$v_u = C_d p f_{ds} \qquad \textbf{Equation 6–38}$$

where C_d is the shear coefficient and a function of the ratio d_c/L. Values of C_d are shown in table 6–6.

(3) *Two-way elements.*

(*a*) *Ultimate support shear.* For a two-way element, the ultimate support shear V_{sH} in the horizontal direction (along side H) is represented as

$$V_{sH} = C_{sH} \frac{p_H d_c^2 f_{ds}}{L} \qquad \textbf{Equation 6–39}$$

and in the vertical direction (along side L), V_{sV}, as

$$V_{sV} = C_{sV} \frac{p_V d_c^2 f_{ds}}{H} \qquad \textbf{Equation 6–40}$$

where C_{sH} and C_{sV} are the horizontal and vertical shear coefficients, respectively, which vary as the yield line location ratios x/L or y/H, and p_V and p_H are the flexural reinforcement ratios in the vertical and horizontal directions, respectively. The shear coefficients are listed in table 6–7, and, for the trapezoidal sectors only, are plotted in figures 6–20 through 6–23.

(*b*) *Ultimate shear stress.* The ultimate shear stress v_{uH} in the horizontal direction (alongside H) at distance d_c from the support for a two-way element

$$v_{uH} = C_H p_H f_{ds} \qquad \textbf{Equation 6–41}$$

and in the vertical direction (alongside L) as

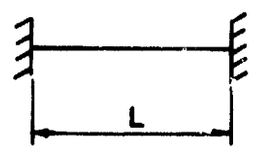
$$v_{uV} = C_V p_V f_{ds} \qquad \textbf{Equation 6–42}$$

where C_H and C_V are the horizontal and vertical shear coefficients, respectively. The shear coefficients, given in table 6–8, vary as d_c/x or d_c/y in the simpler cases and as x/L or y/H and d/H or d/L in the more complicated cases. The simpler case with only one variable is associated with the triangular sector or sectors of the element considered. The second case is associated with the trapezoidal sector or sectors.

c. The shear coefficients for the triangular sectors can be read directly from either figure 6–24 or 6–25, depending on the yield line location, since only one variable is involved. For the trapezoidal sectors, two figures are required. Plotting the shear coefficients for the trapezoidal sectors versus d_c/L for values of y/H or against d_c/H for x/L leads to a family of curves for each equation. Each curve has a different maximum value C_M which occurs at varying values of d_c/L or d_c/H, and accurate interpolation with these curves is not possible.

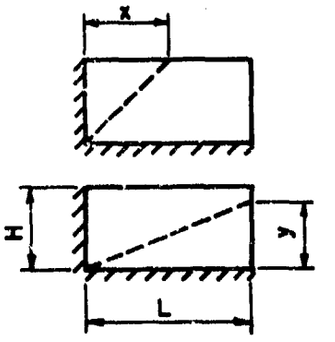
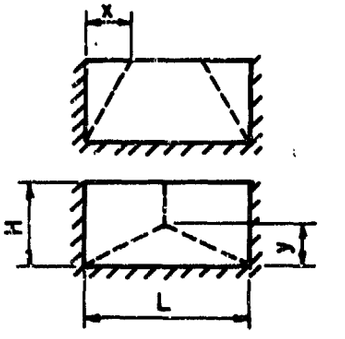
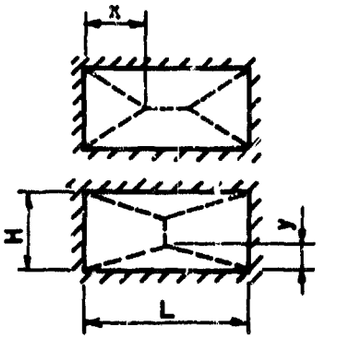
d. Using a method of coordinate transformation, the family of curves has been reduced to a set of curves with a common maximum point defined, using the horizontal shear coefficient as an example, by $C_H/C_M = 1$ and $(d_c/L)/(d_c/L)_M = 1$. By coincidence, the left-hand portions of the curves become identical, and accurate interpolation in the right-hand portion is now possible. The quantities C_M and $(d_c/L)_M$ represent the coordinates of the maximum point on the original curve.

Table 6–6. Shear Coefficients for Ultimate Shear Stress at Distance d_c From the Support for One-Way Elements (Cross Sections Type II and III)

Edge conditions	Ultimate shear stress coefficient C_d
Cantilever 	$2(d_c/L) \times (1 - d_c/L)$
Fixed supports 	$16(d_c/L) \times (\frac{1}{4} - d_c/L)$

d_c, L (in.)

Table 6–7. Shear Coefficients for Ultimate Support Shear for Two-Way Elements (Cross Sections Type II and III)

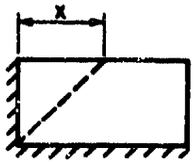
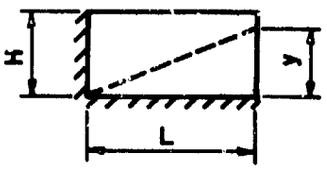
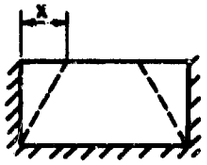
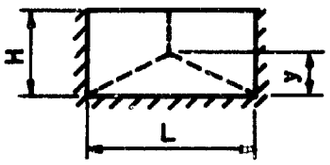
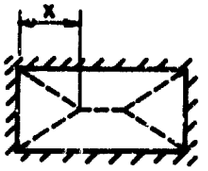
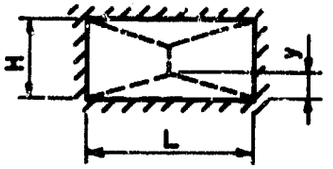
Edge conditions	Yield line location	Horizontal ultimate support shear coefficient C_{uH}	Vertical ultimate support shear coefficient C_{uV}
Two adjacent edges fixed and two edges free		$\frac{6}{x/L}$ $\frac{6(2-y/H)(3+2y/H)}{(6-y/H)(3-2y/H)}$	$\frac{6(2-x/L)(3+2x/L)}{(6-x/L)(3-2x/L)}$ $\frac{6}{y/H}$
Three edges fixed and one edge free		$\frac{6}{x/L}$ $\frac{12(2-y/H)}{(3-y/H)}$	$\frac{6(1-x/L)(3+4x/L)}{(3-x/L)(3-4x/L)}$ $\frac{6}{y/H}$
Four edges fixed		$\frac{6}{x/L}$ $\frac{24(1-y/H)}{(3-4y/H)}$	$\frac{24(1-x/L)}{(3-4x/L)}$ $\frac{6}{y/H}$

x, y, L, H (in.)

e. The above sets of curves are presented in figures 6–26 through 6–37. When using these curves, the shear parameter curve is entered first with the value of x/L or y/H to determine C_M and either $(d_c/H)_M$ or $(d_c/L)_M$. The second curve is then used to determine C_V or C_H.

f. It should be noted that when designing two-way panels, the shear forces and stresses must also be checked in the post-ultimate range using the equations for one-way elements as previously discussed in section V, chapter 5.

Table 6-8. Shear Coefficients for Ultimate Shear Stress at Distance d_e From the Support for Two-Way

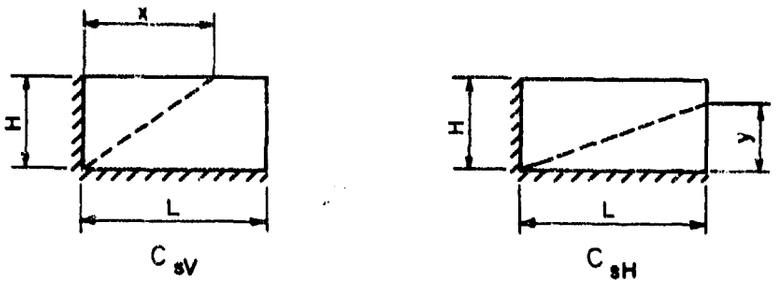
Edge conditions	Yield line location	Limits	Horizontal ultimate shear stress coefficient
Two adjacent edges fixed and two edges free		$0 \le d_e/x \le \frac{1}{2}$	$\frac{30(d_e/x)(1-d_e/x)^3}{(5-4d_e/x)}$
		$\frac{1}{2} \le d_e/x \le 1$	$5(d_e/x)(1-d_e/x)$
		$0 \le d_e/L \le \frac{1}{2}$	$\frac{6(d_e/L)(3+2y/H)(1-d_e/L)(2-y/H-d_e}{(3-2y/H)(6-y/H-d_ey/LH)}$
		$\frac{1}{2} \le d_e/L \le 1$	$\frac{(d_e/L)(3+2y/H)(1-d_e/L)(2-y/H-d_e}{(3-2y/H)(1-d_ey/LH)}$
Three edges fixed and one edge free		$0 \le d_e/x \le \frac{1}{2}$	$\frac{30(d_e/x)(1-d_e/x)^3}{(5-4d_e/x)}$
		$\frac{1}{2} \le d_e/x \le 1$	$5(d_e/x)(1-d_e/x)$
		$0 \le d_e/L \le \frac{1}{2}$	$\frac{12(d_e/L)(6-y/H)(1-2d_e/L)(2-y/H-2}{(3-2y/H)(6-y/H-8d_ey/LH)}$
		$\frac{1}{2} \le d_e/L \le \frac{1}{2}$	$\frac{2(d_e/L)(6-y/H)(1-2d_e/L)(2-y/H-2}{(3-2y/H)(1-2d_ey/LH)}$
Four edges fixed		$0 \le d_e/x \le \frac{1}{2}$	$\frac{30(d_e/x)(1-d_e/x)^3}{(5-4d_e/x)}$
		$\frac{1}{2} \le d_e/x \le 1$	$5(d_e/x)(1-d_e/x)$
		$0 \le d_e/L \le \frac{1}{2}$	$\frac{24(d_e/L)(3-y/H)(1-2d_e/L)(1-y/H-2d}{(3-4y/H)(3-y/H-8d_ey/LH)}$
		$\frac{1}{2} \le d_e/L \le \frac{1}{2}$	$\frac{8(d_e/L)(3-y/H)(1-2d_e/L)(1-y/H-2d}{(3-4y/H)(1-4d_ey/LH)}$

d_e, x, y, L, H (in.)

Distance d_c From the Support for Two-Way Elements (Cross Sections Type II and III)

Horizontal ultimate shear stress coefficient C_H	Limits	Vertical ultimate shear stress coefficient C_V
$\frac{30(d_c/x)(1-d_c/x)^3}{(5-4d_c/x)}$	$0 \le d_c/H \le \frac{1}{2}$	$\frac{6(d_c/H)(3+2x/L)(1-d_c/H)(2-x/L-d_cx/HL)}{(3-2x/L)(6-x/L-4d_cx/HL)}$
$5(d_c/x)(1-d_c/x)$	$\frac{1}{2} \le d_c/H \le 1$	$\frac{(d_c/H)(3+2x/L)(1-d_c/H)(2-x/L-d_cx/HL)}{(3-2x/L)(1-d_cx/HL)}$
$\frac{6(d_c/L)(3+2y/H)(1-d_c/L)(2-y/H-d_cy/LH)}{(3-2y/H)(6-y/H-d_cy/LH)}$	$0 \le d_c/y \le \frac{1}{2}$	$\frac{30(d_c/y)(1-d_c/y)^3}{(5-4d_c/y)}$
$\frac{(d_c/L)(3+2y/H)(1-d_c/L)(2-y/H-d_cy/LH)}{(3-2y/H)(1-d_cy/LH)}$	$\frac{1}{2} \le d_c/y \le 1$	$5(d_c/y)(1-d_c/y)$
$\frac{30(d_c/x)(1-d_c/x)^3}{(5-4d_c/x)}$	$0 \le d_c/H \le \frac{1}{2}$	$\frac{6(d_c/H)(3+4x/L)(1-d_c/H)(1-x/L-d_cx/HL)}{(3-4x/L)(3-x/L-4d_cx/HL)}$
$5(d_c/x)(1-d_c/x)$	$\frac{1}{2} \le d_c/H \le 1$	$\frac{2(d_c/H)(3+4x/L)(1-d_c/H)(1-x/L-d_cx/HL)}{(3-4x/L)(1-2d_cx/HL)}$
$\frac{12(d_c/L)(6-y/H)(1-2d_c/L)(2-y/H-2d_cy/LH)}{(3-2y/H)(6-y/H-8d_cy/LH)}$	$0 \le d_c/y \le \frac{1}{2}$	$\frac{30(d_c/y)(1-d_c/y)^3}{(5-4d_c/y)}$
$\frac{2(d_c/L)(6-y/H)(1-2d_c/L)(2-y/H-2d_cy/LH)}{(3-2y/H)(1-2d_cy/LH)}$	$\frac{1}{2} \le d_c/y \le 1$	$5(d_c/y)(1-d_c/y)$
$\frac{30(d_c/x)(1-d_c/x)^3}{(5-4d_c/x)}$	$0 \le d_c/H \le \frac{1}{2}$	$\frac{24(d_c/H)(3-x/L)(1-2d_c/H)(1-x/L-2d_cx/HL)}{(3-4x/L)(3-x/L-8d_cx/HL)}$
$5(d_c/x)(1-d_c/x)$	$\frac{1}{2} \le d_c/H \le 1$	$\frac{8(d_c/H)(3-x/L)(1-2d_c/H)(1-x/L-2d_cx/HL)}{(3-4x/L)(1-4d_cx/HL)}$
$\frac{24(d_c/L)(3-y/H)(1-2d_c/L)(1-y/H-2d_cy/LH)}{(3-4y/H)(3-y/H-8d_cy/LH)}$	$0 \le d_c/y \le \frac{1}{2}$	$\frac{30(d_c/y)(1-d_c/y)^3}{(5-4d_c/y)}$
$\frac{8(d_c/L)(3-y/H)(1-2d_c/L)(1-y/H-2d_cy/LH)}{(3-4y/H)(1-4d_cy/LH)}$	$\frac{1}{2} \le d_c/y \le 1$	$5(d_c/y)(1-d_c/y)$

2



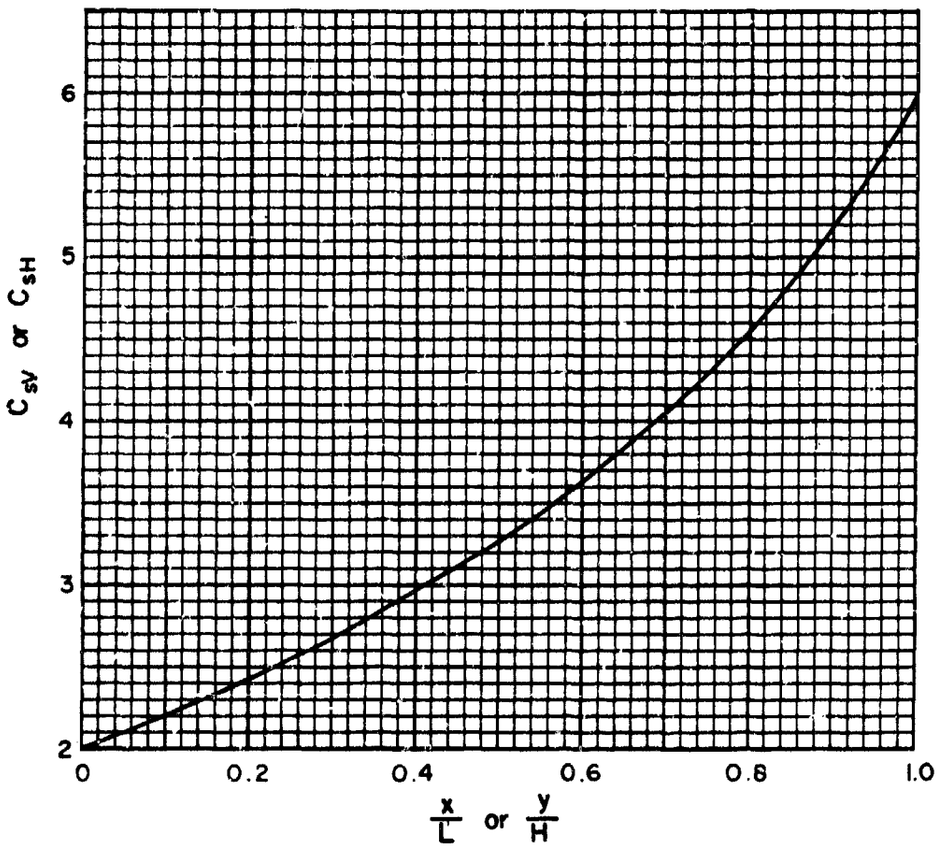
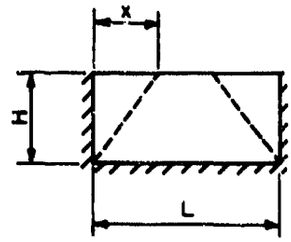
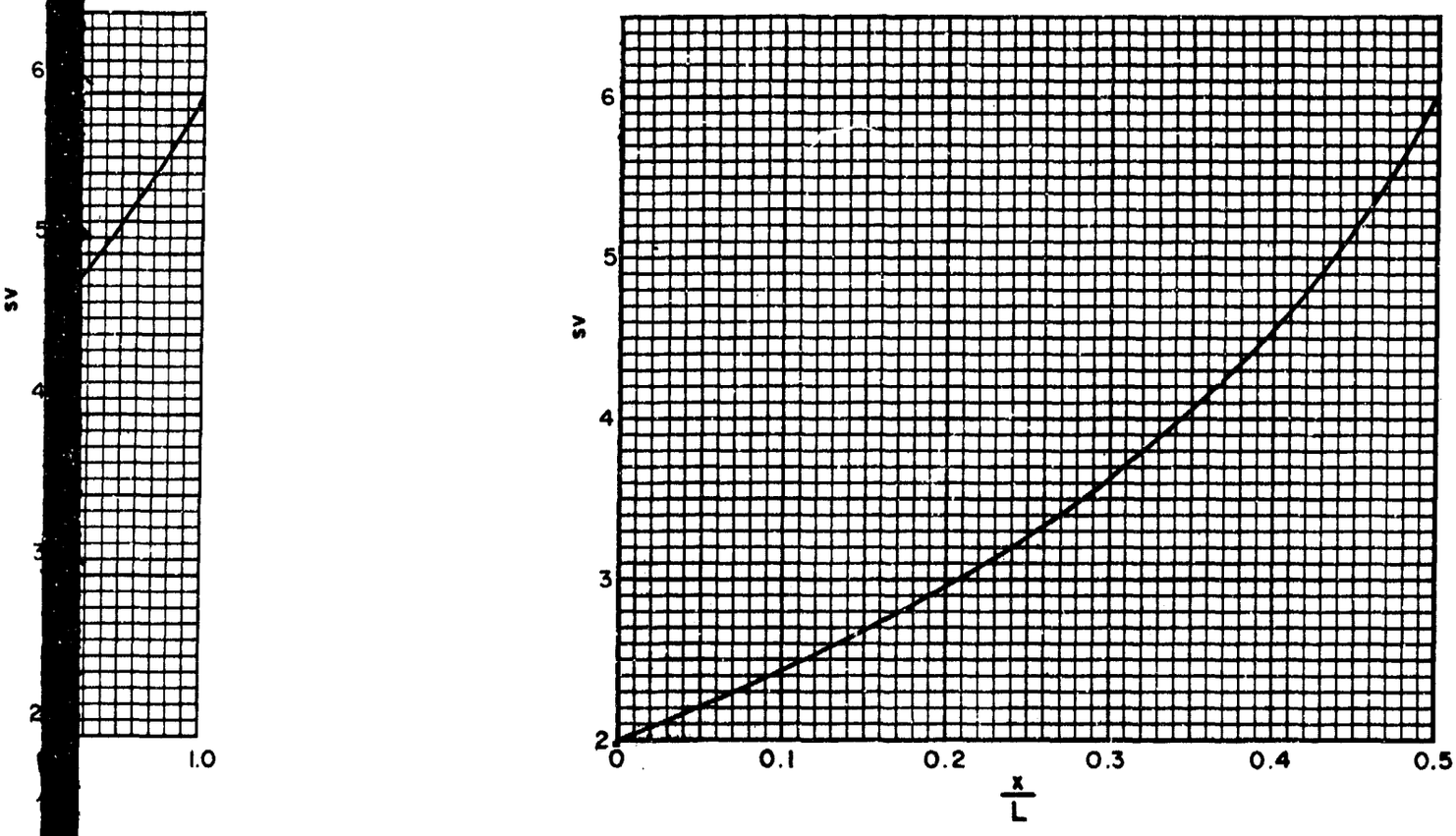


Figure 6-20. Shear coefficients for ultimate support shear (cross section type II and III).

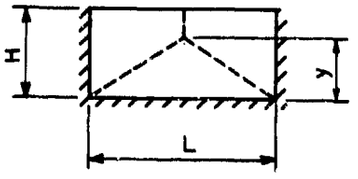


y



III).

Figure 6-21. Shear coefficients for ultimate support shear (cross section type II and III).



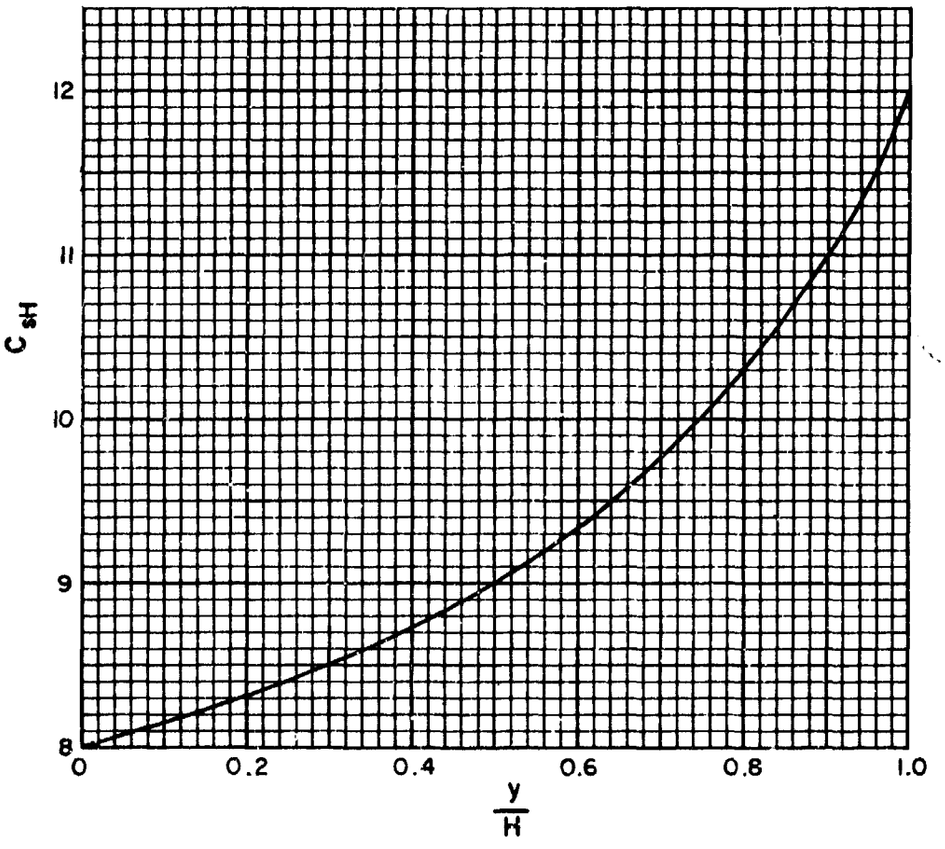
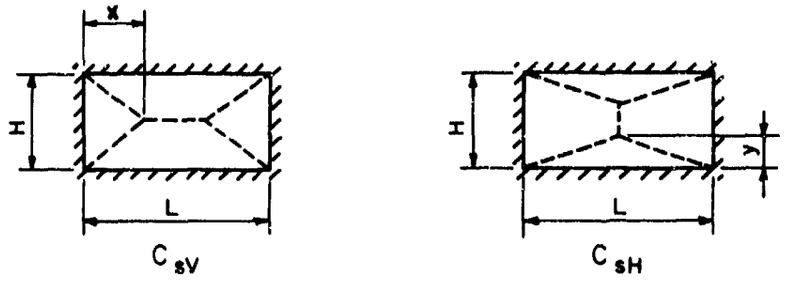
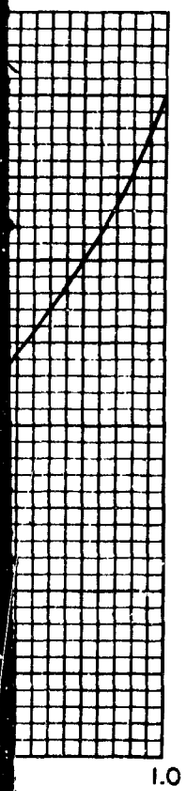
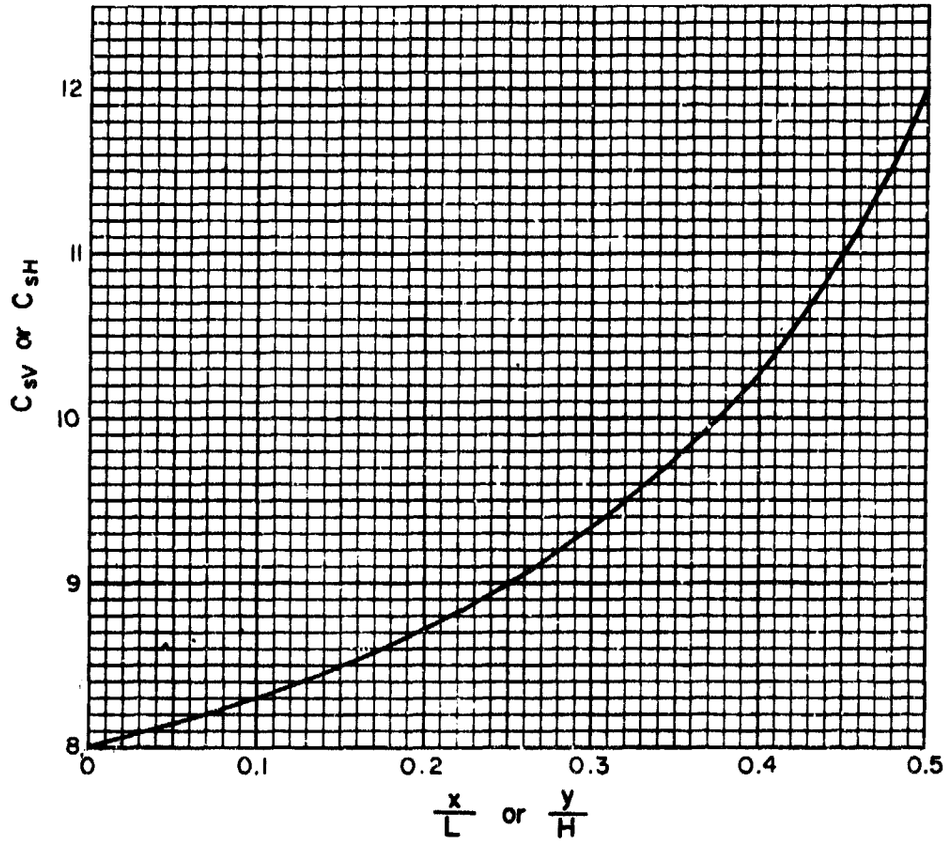


Figure 6-22. Shear coefficients for ultimate support shear (cross section type II and III).







and III).

Figure 6-23. Shear coefficients for ultimate support shear (cross section type II and III).

2

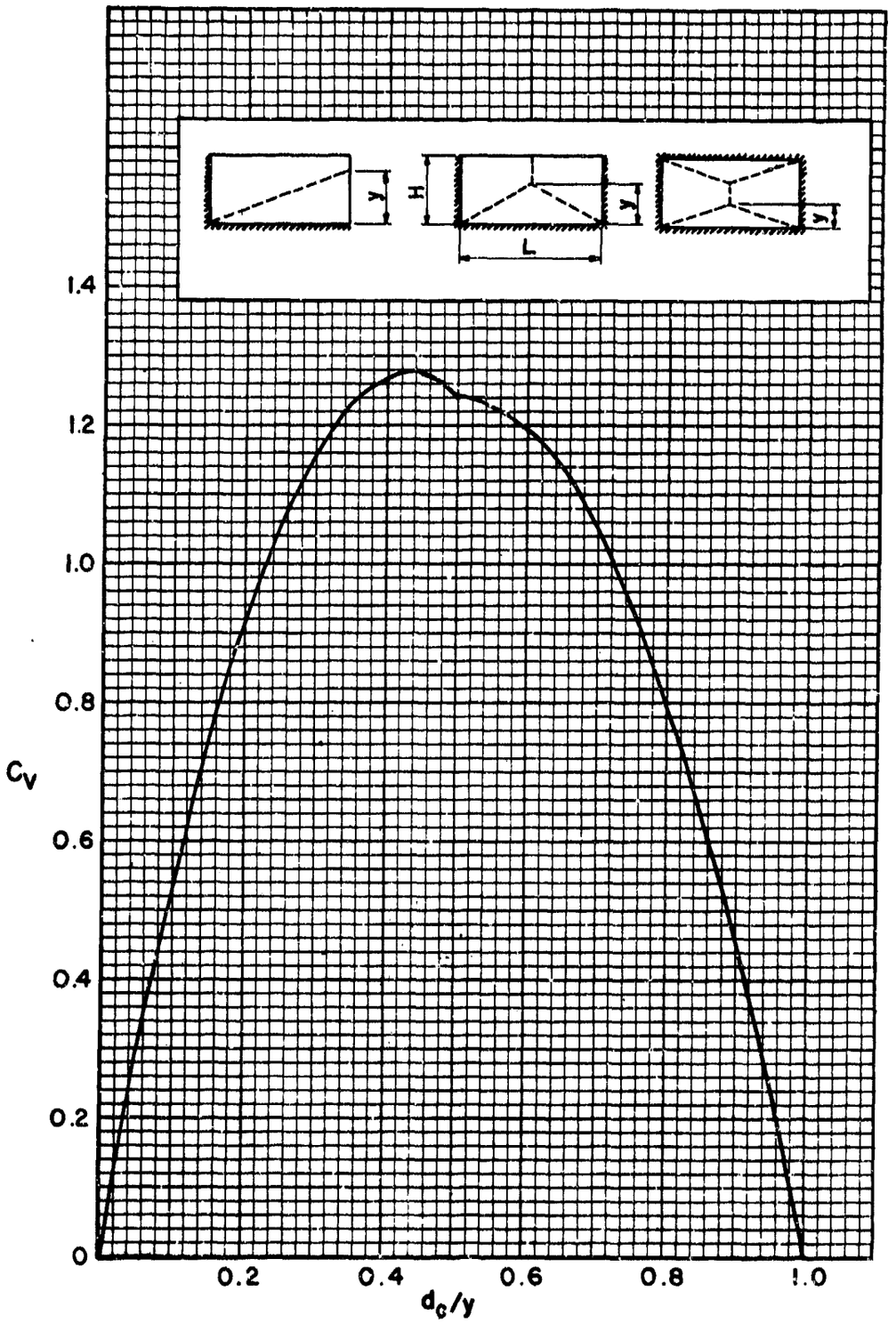
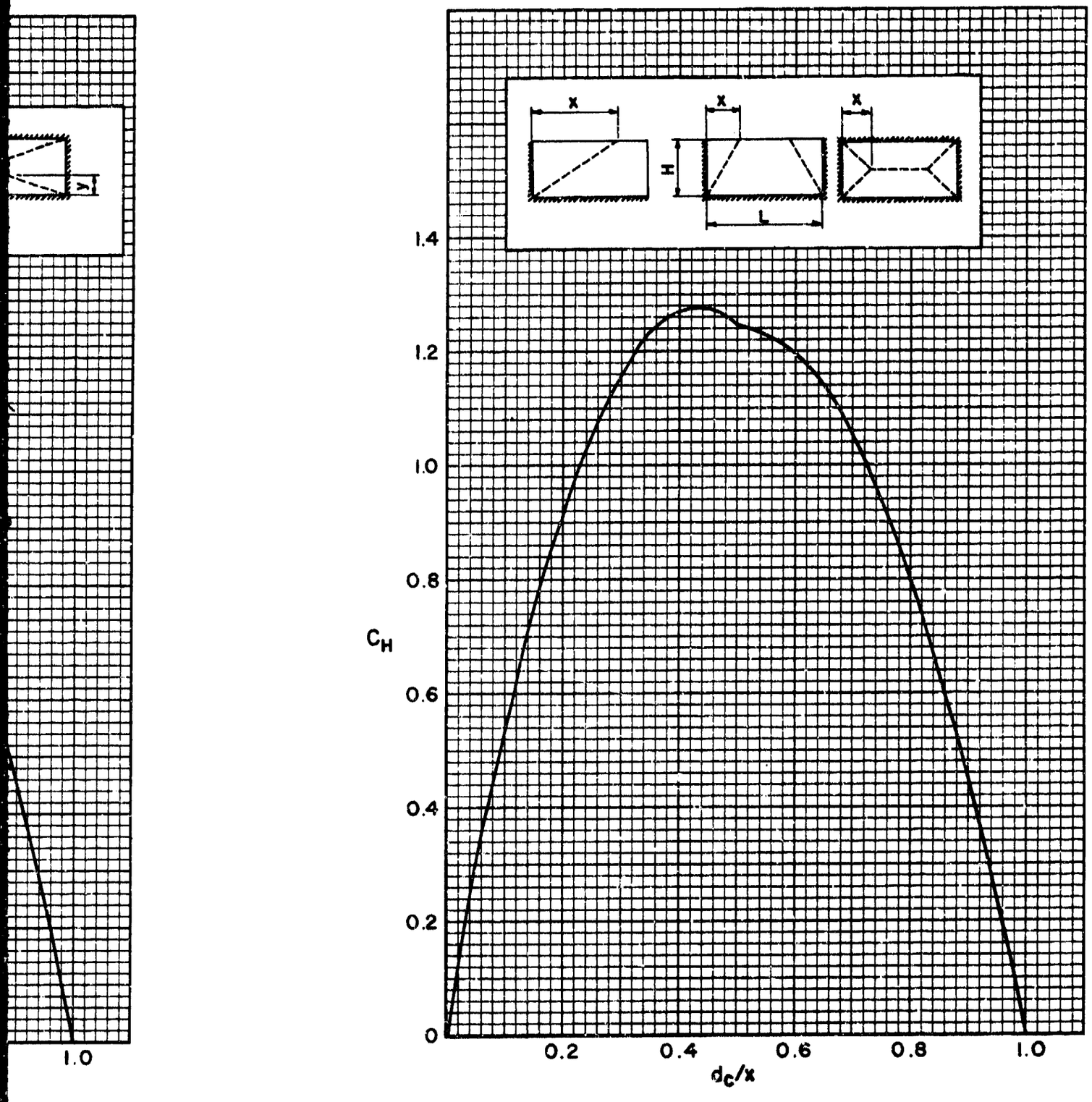


Figure 6–24. Vertical shear coefficients for ultimate shear stress at distance d_c from the support (cross section type II and III).

Figure 6–25. H



section type II and III).

Figure 6-25. Horizontal shear coefficients for ultimate shear stress at distance d_c from the support (cross section type II and III).

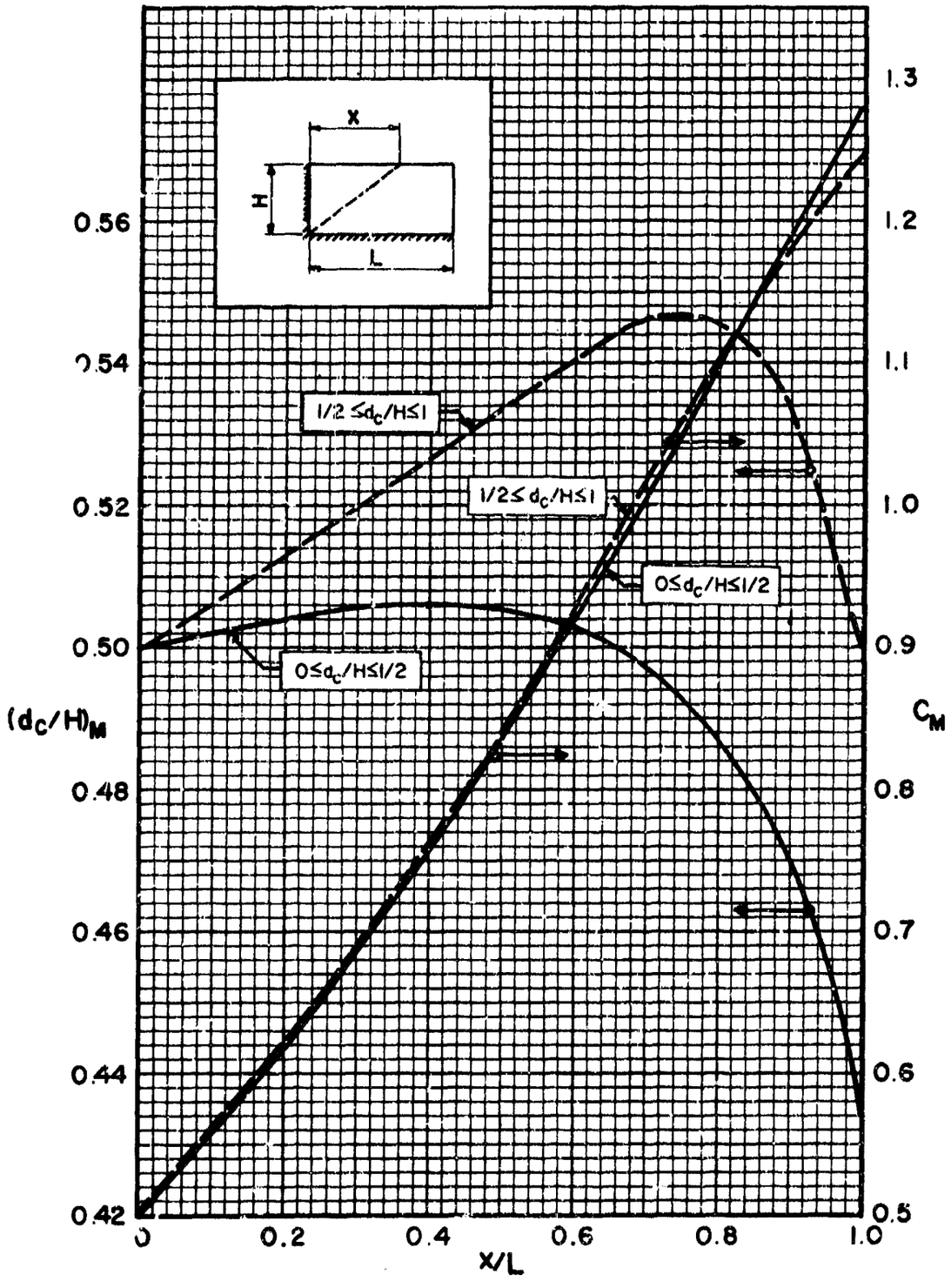


Figure 6-86. Vertical shear parameters for ultimate shear stress at distance d_c from the support (cross section type II and III).

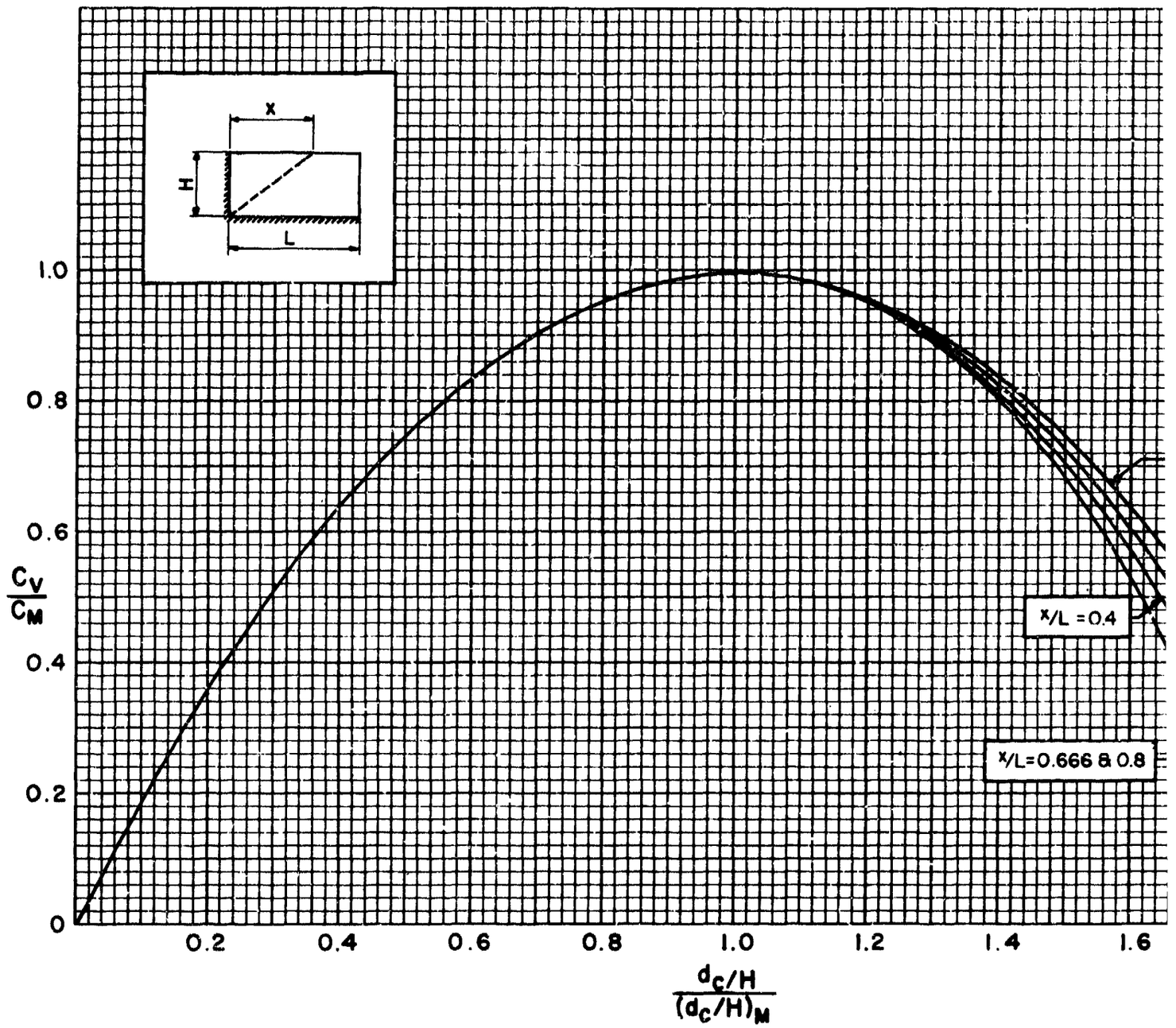
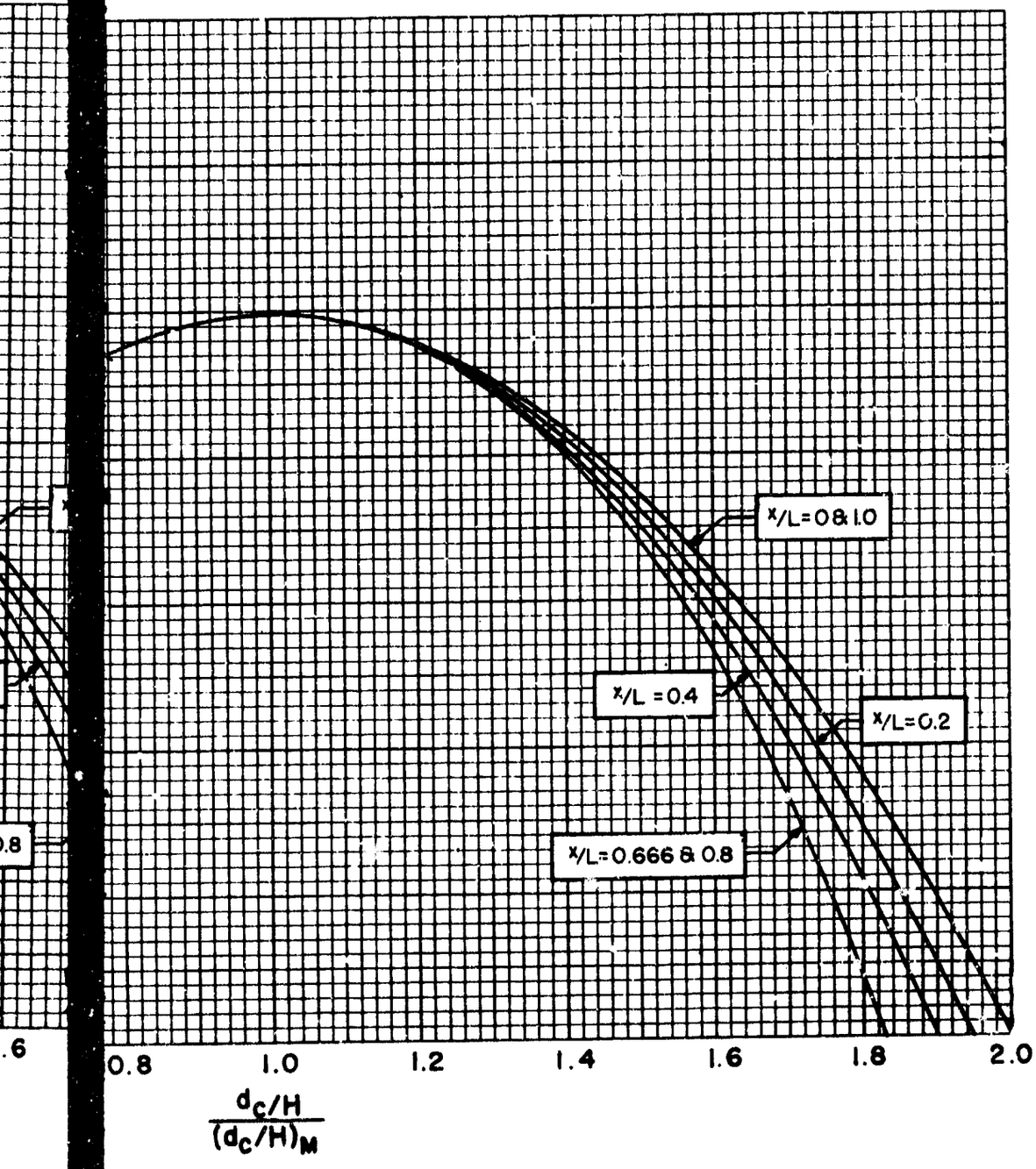


Figure 6-87. Vertical shear coefficient ratios for ultimate shear stress at distance d_c from the support (cross section type II and III).



ir ultimate shear stress at distance d_c from the support (cross section type II and III).

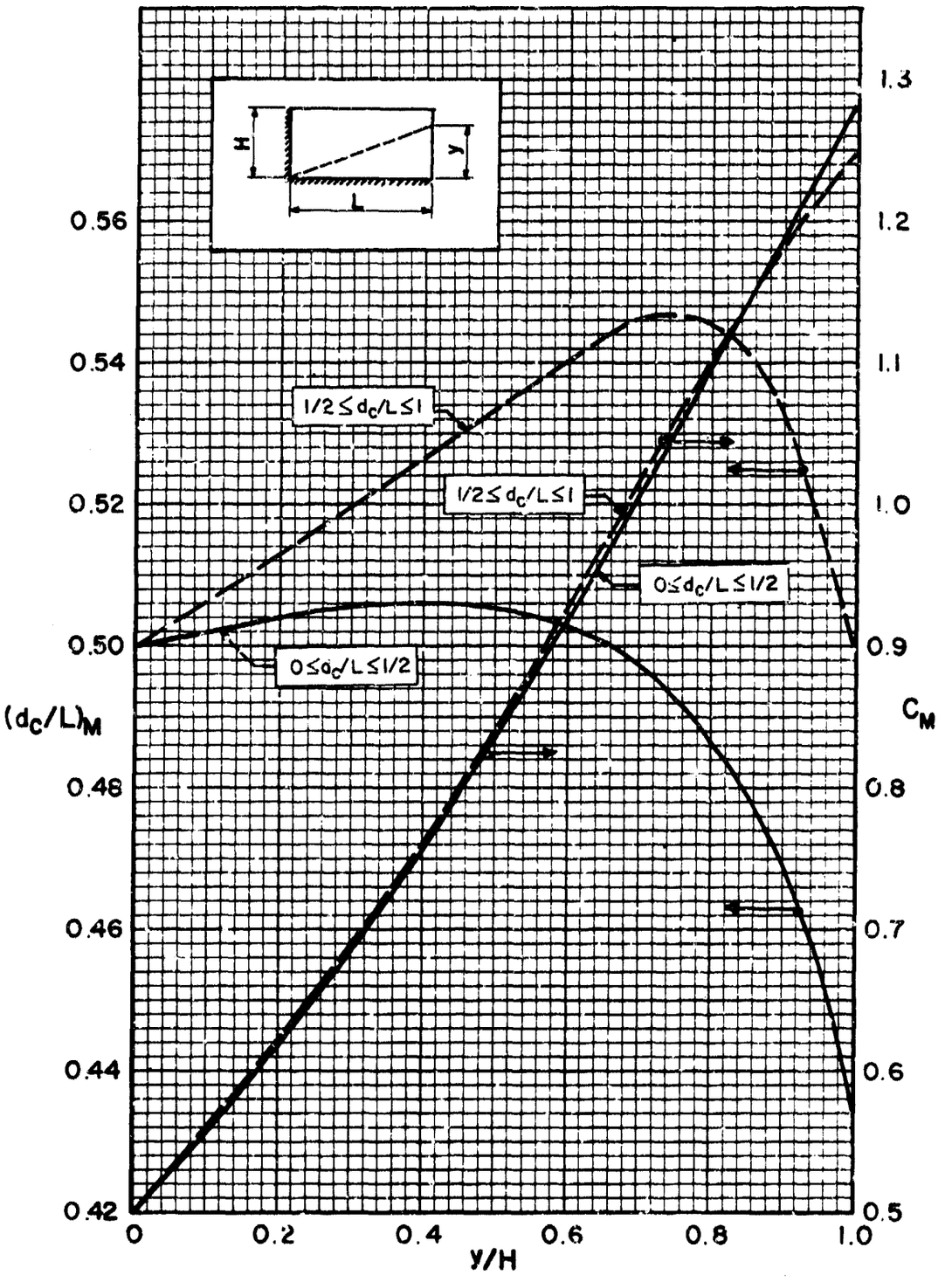


Figure 6–88. Horisontal shear parameters for ultimate shear stress at distance d_c from the support (cross section type II and III).

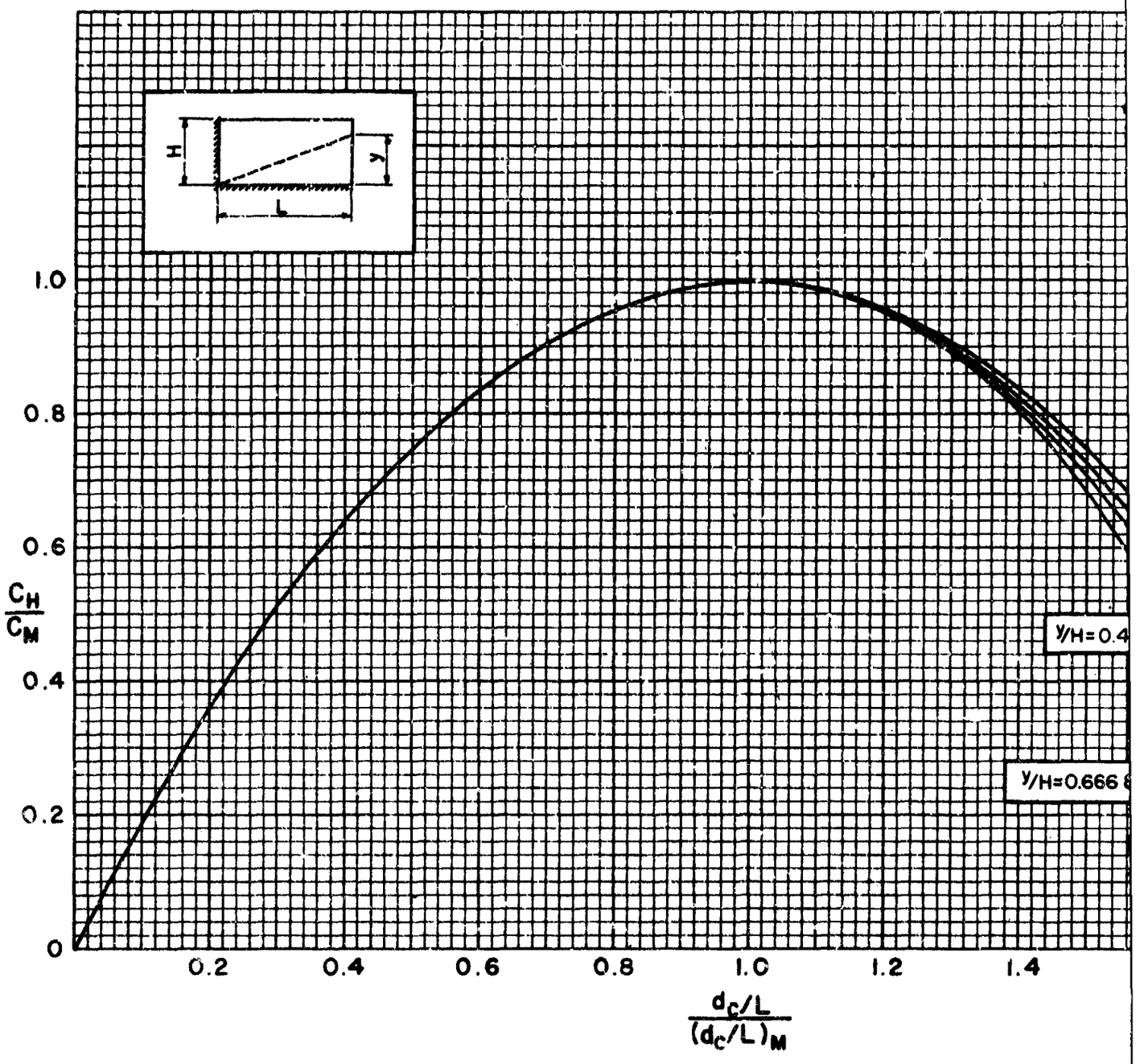
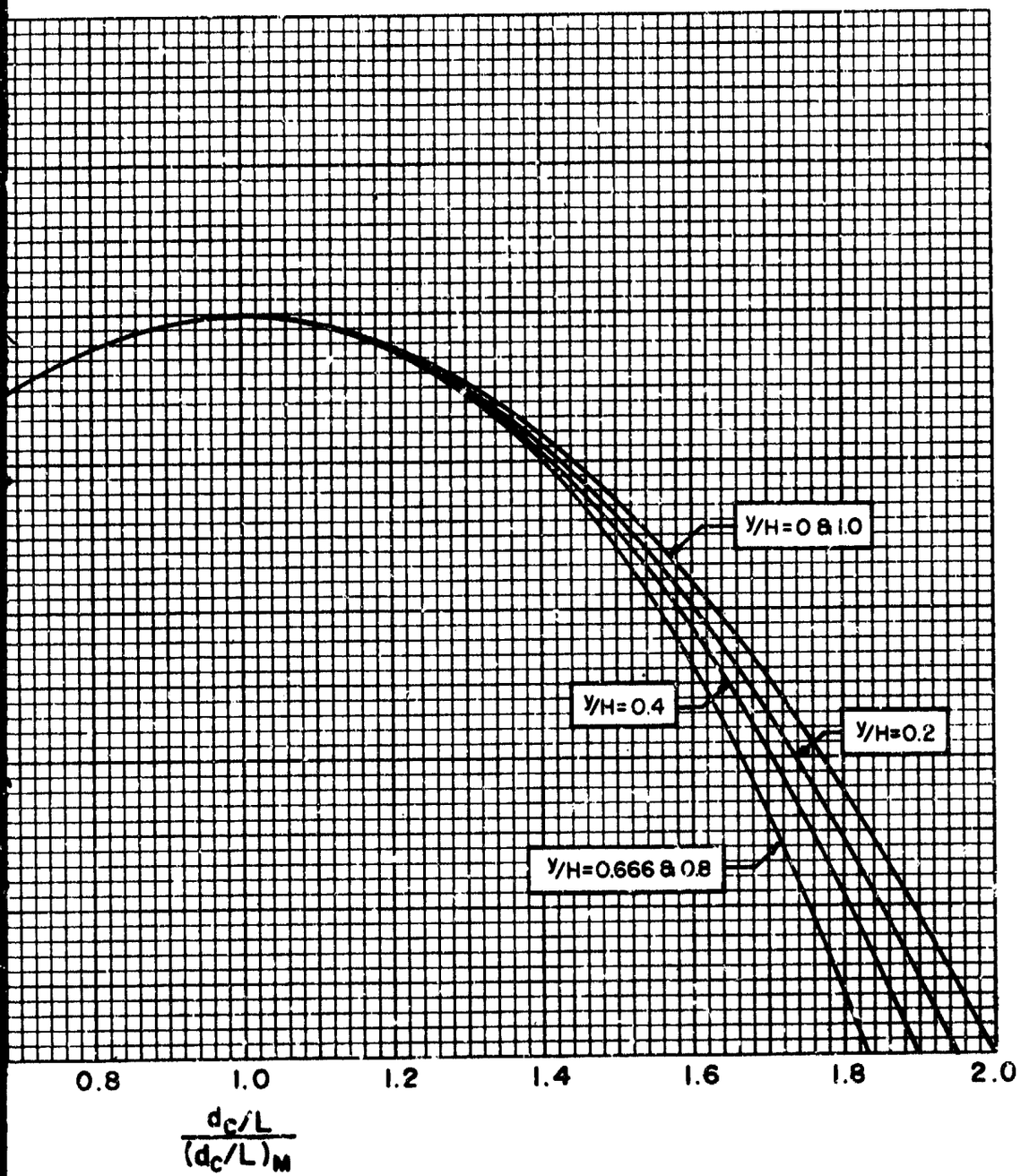


Figure 6-29. Horizontal shear coefficient ratios for ultimate shear stress at distance d_c from the support (cross section type II a



ent ration for ultimate shear stress at distance d_c from the support (cross section type II and III).

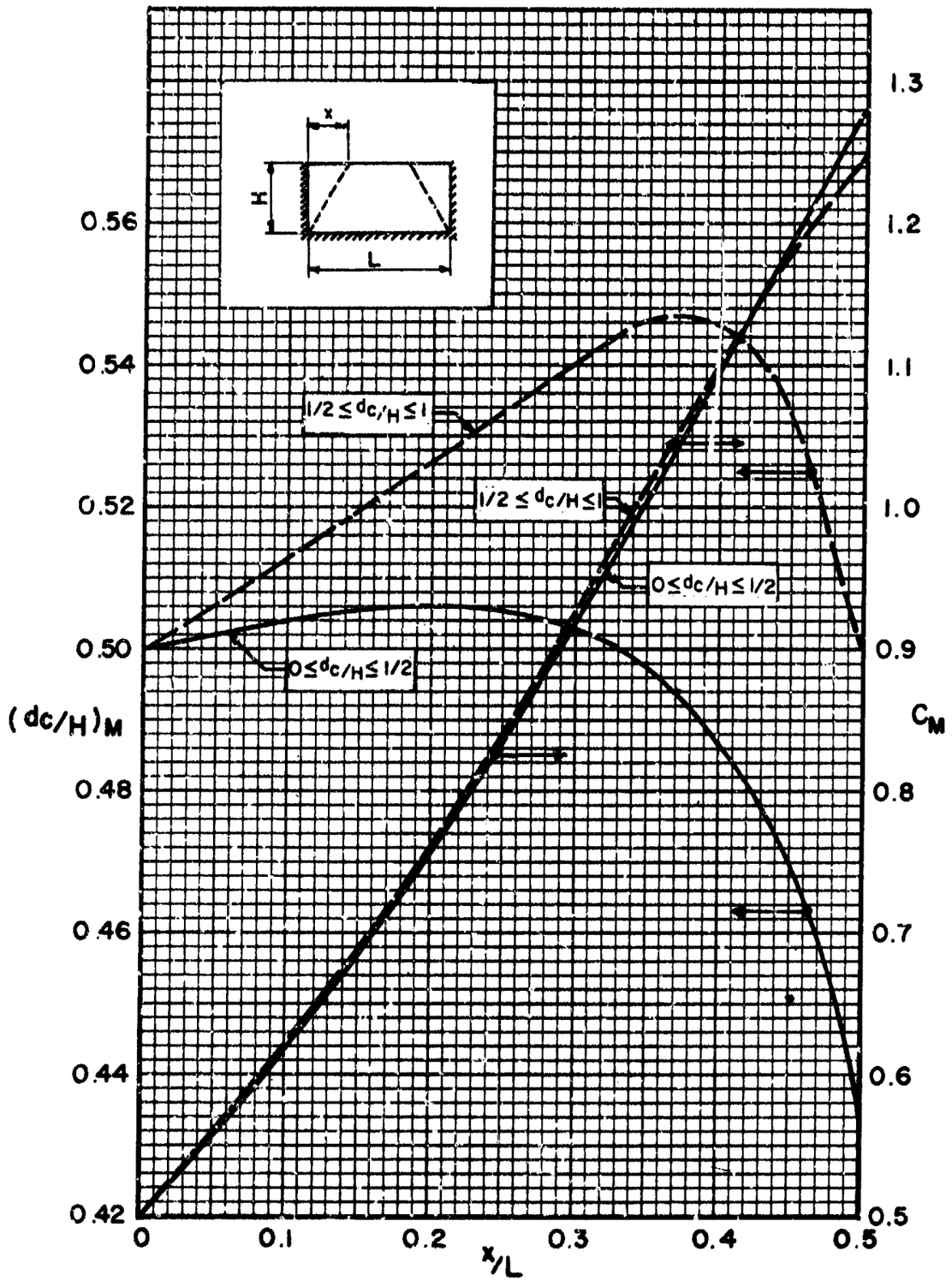


Figure 6–30. Vertical shear parameters for ultimate shear stress at distance d_c from the support (cross section type II and III).

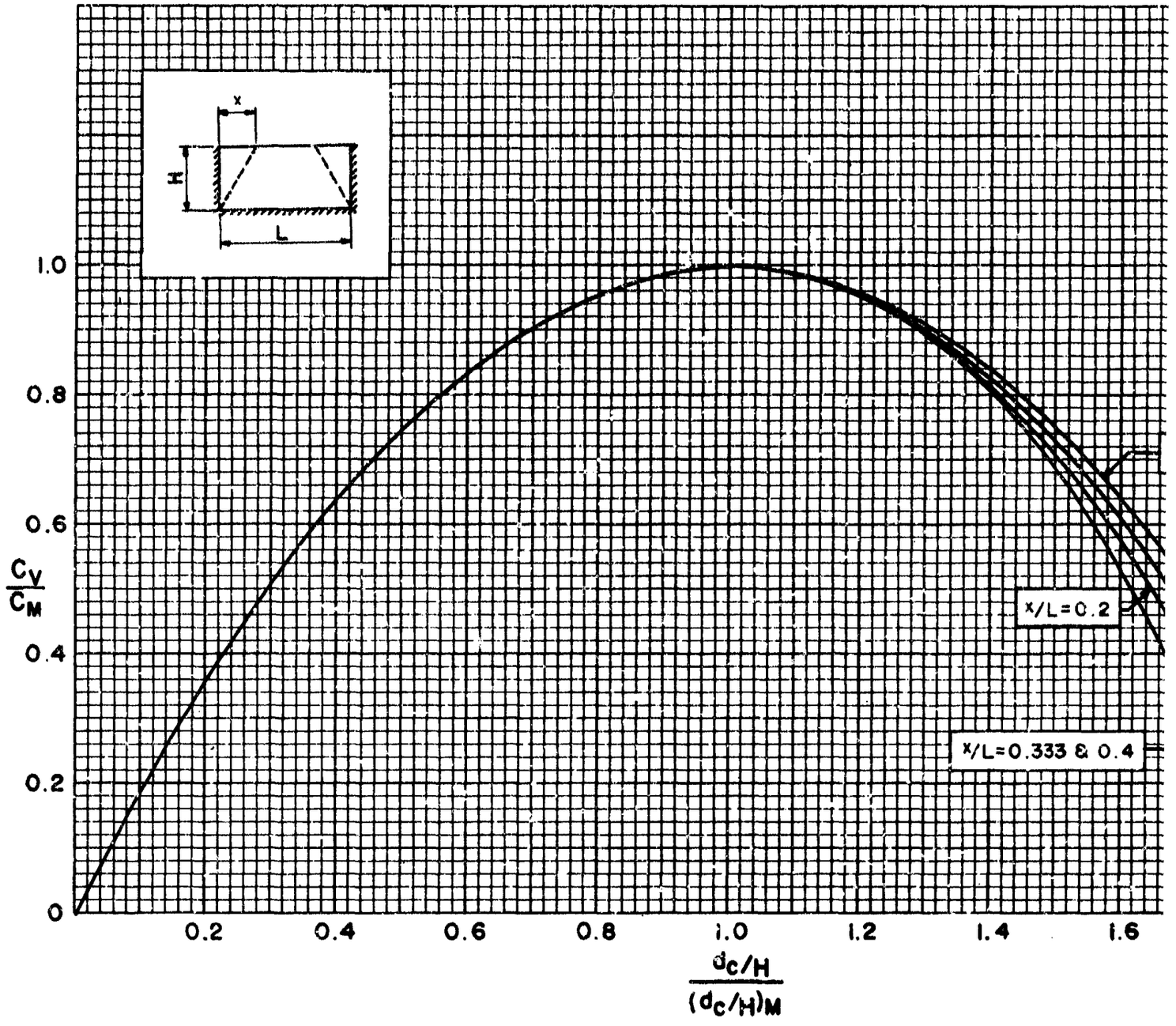
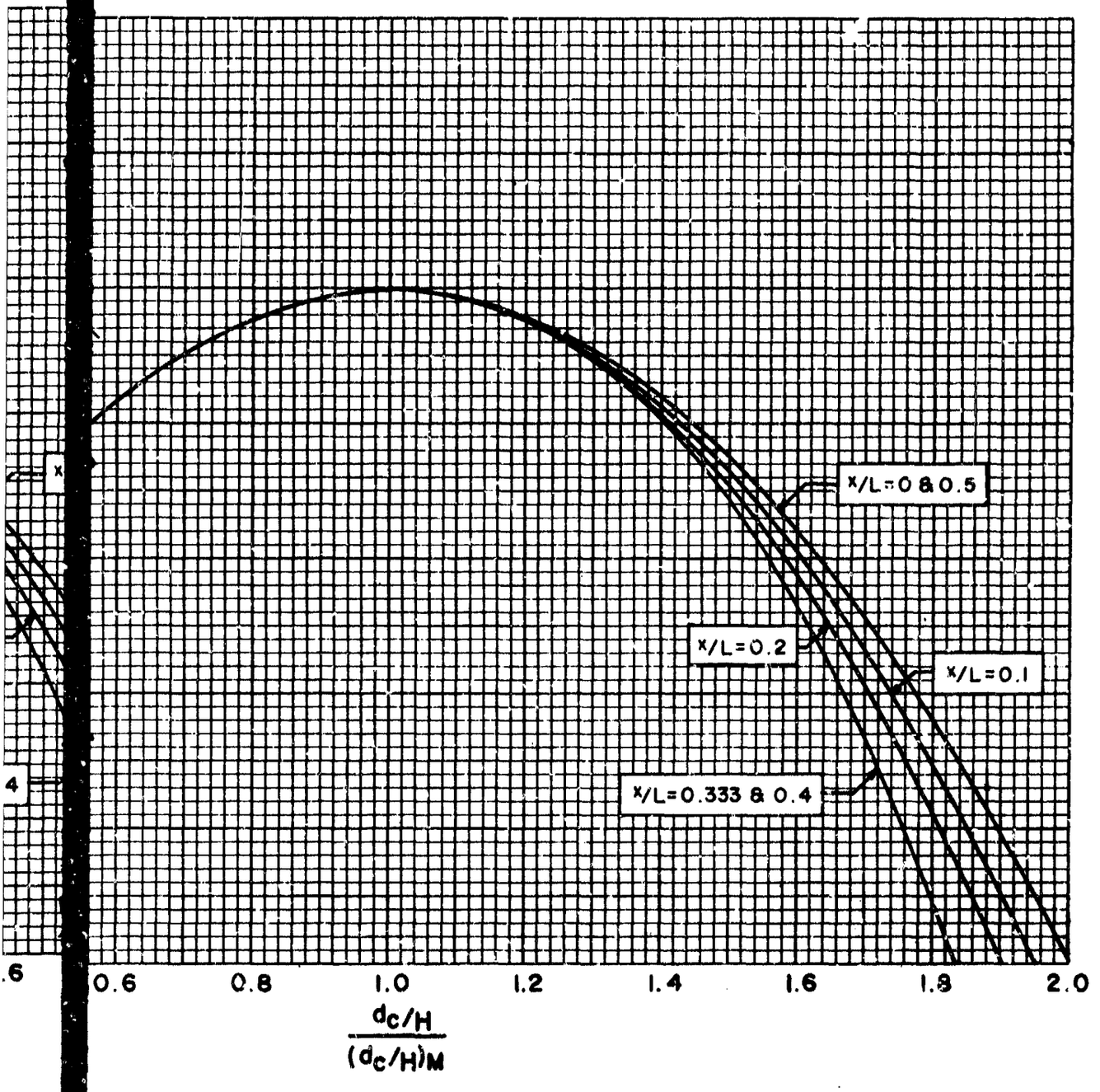


Figure 6-31. Vertical shear coefficient ratios for ultimate shear stress at distance d_c from the support (cross section type II and III).



coefficient ratios for ultimate shear stress at distance d_c from the support (cross section type II and III).

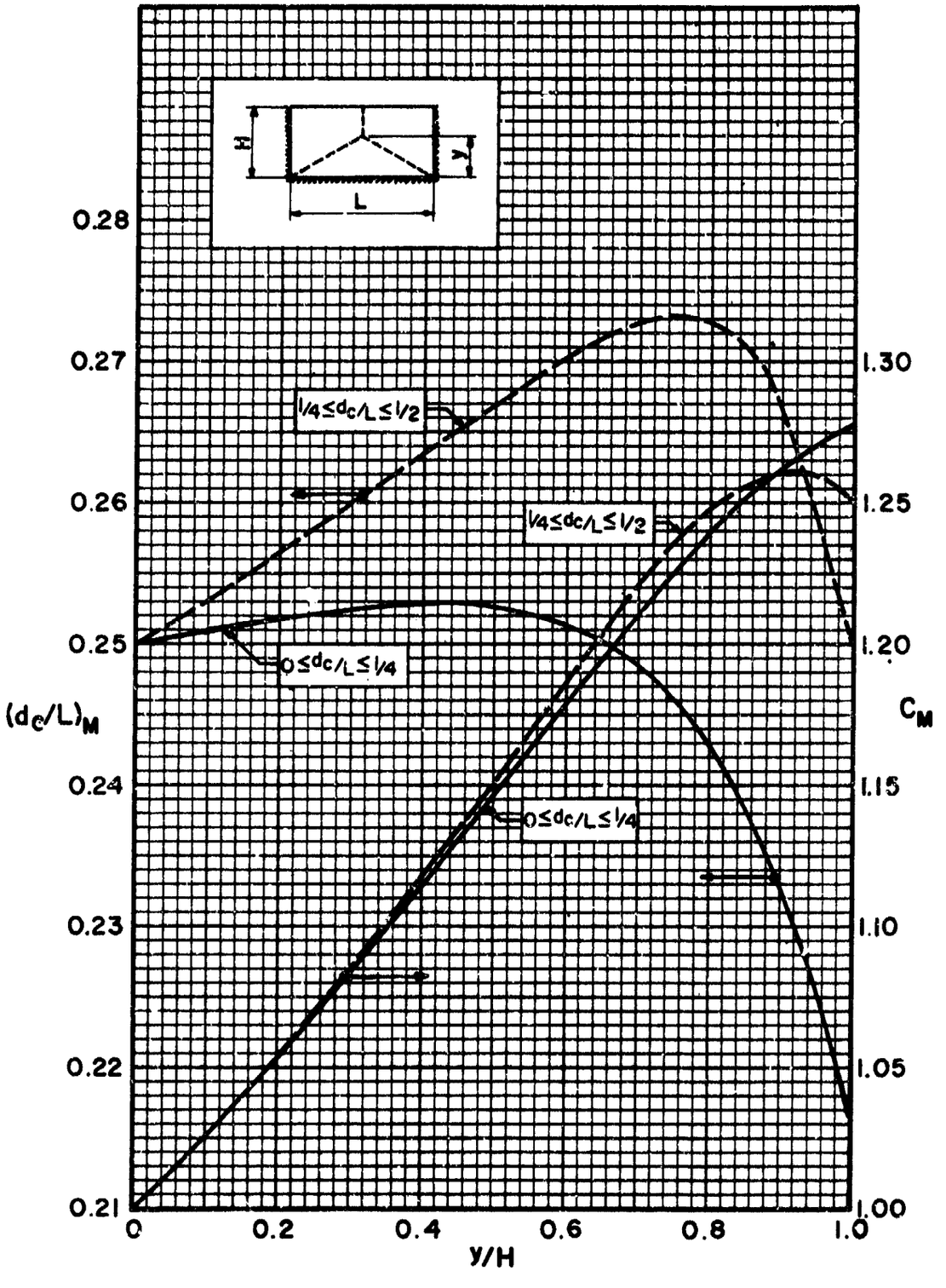


Figure 8-38. Horizontal shear parameters for ultimate shear stress at distance d_c from the support (cross section type II and III).

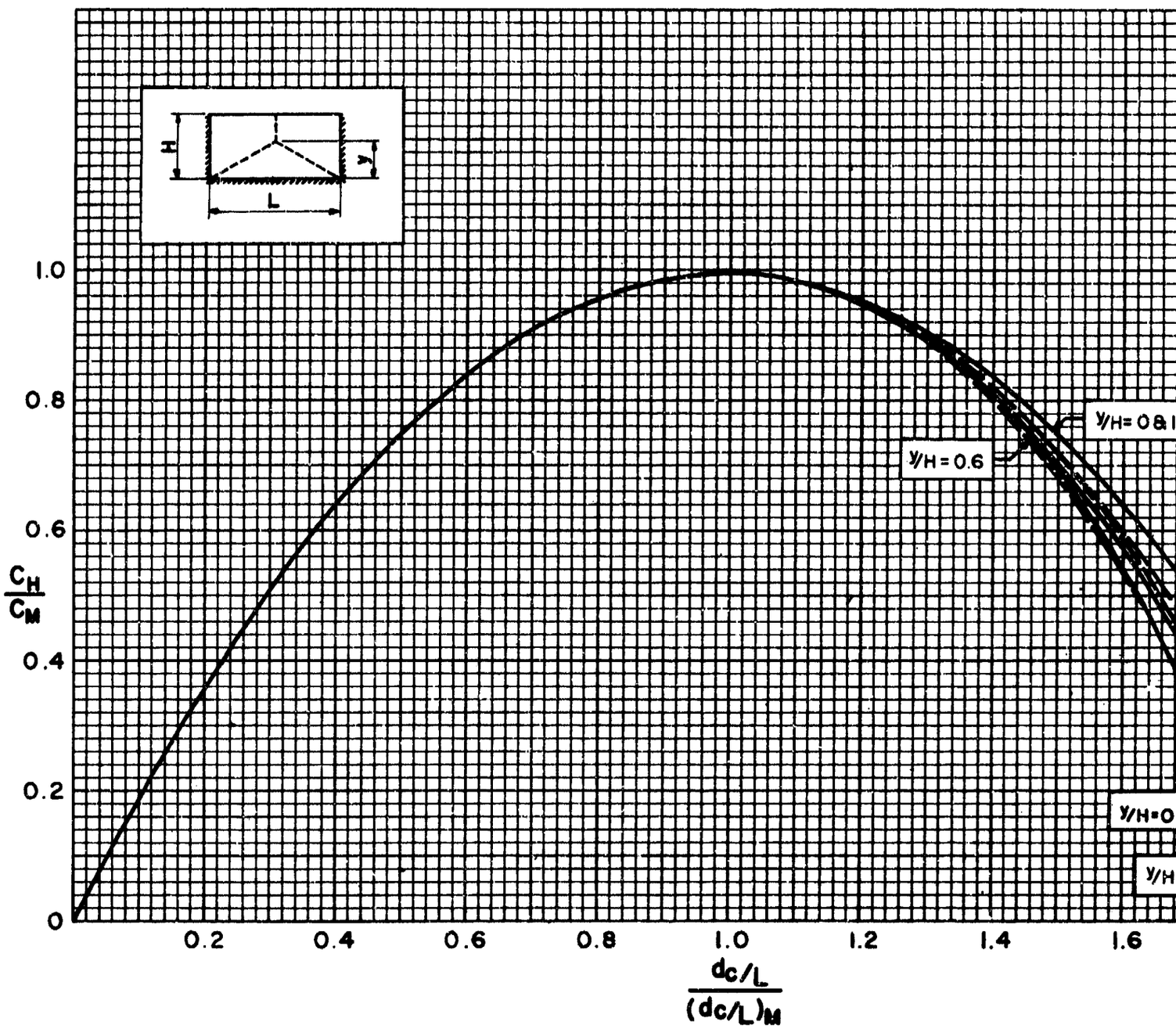
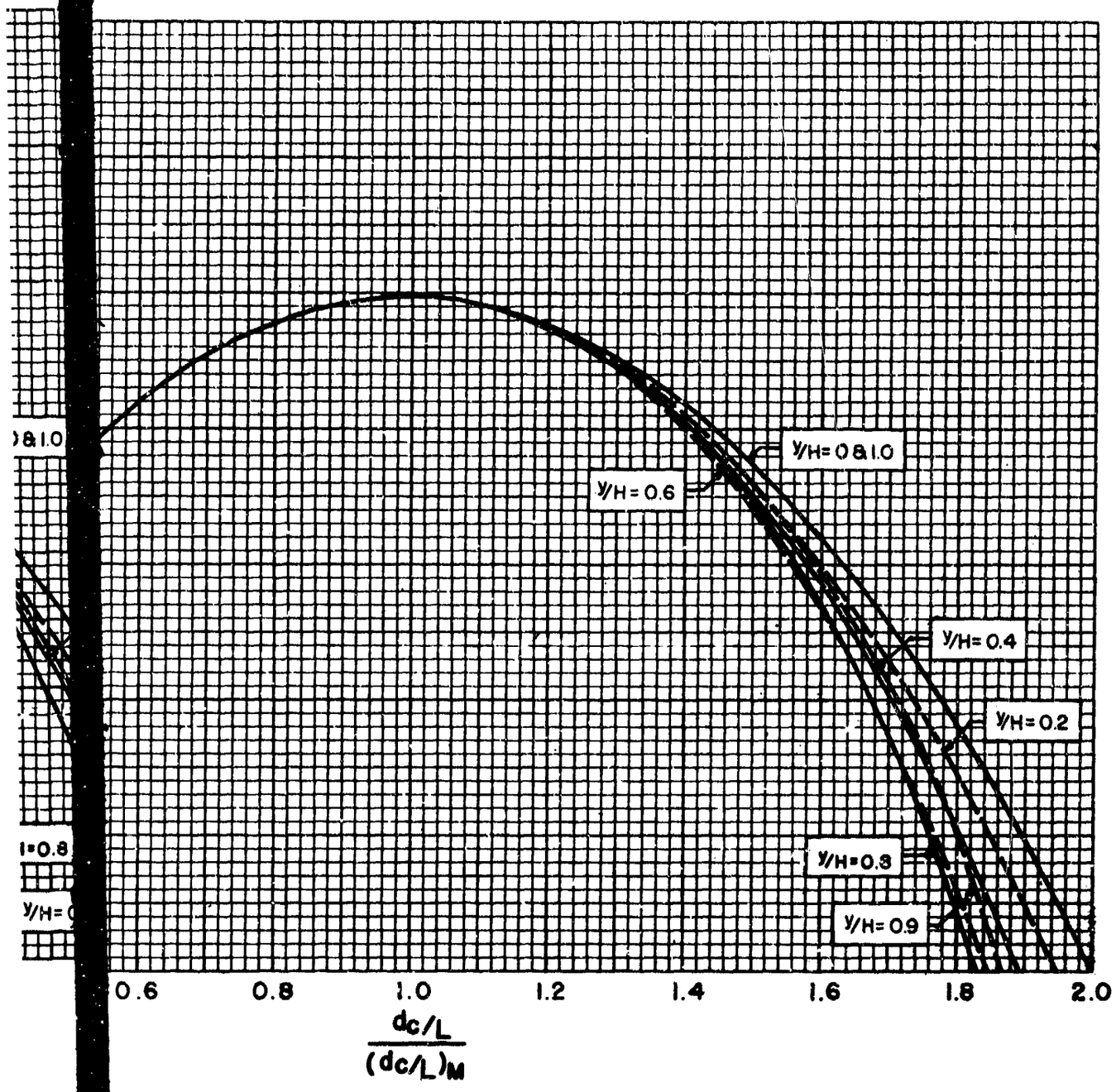


Figure 6–33. Horizontal shear coefficient ratios for ultimate shear stress at distance d_c from the support (cross section type II and III).



ar coefficient ratios for ultimate shear stress at distance d_c from the support (cross section type II and III).

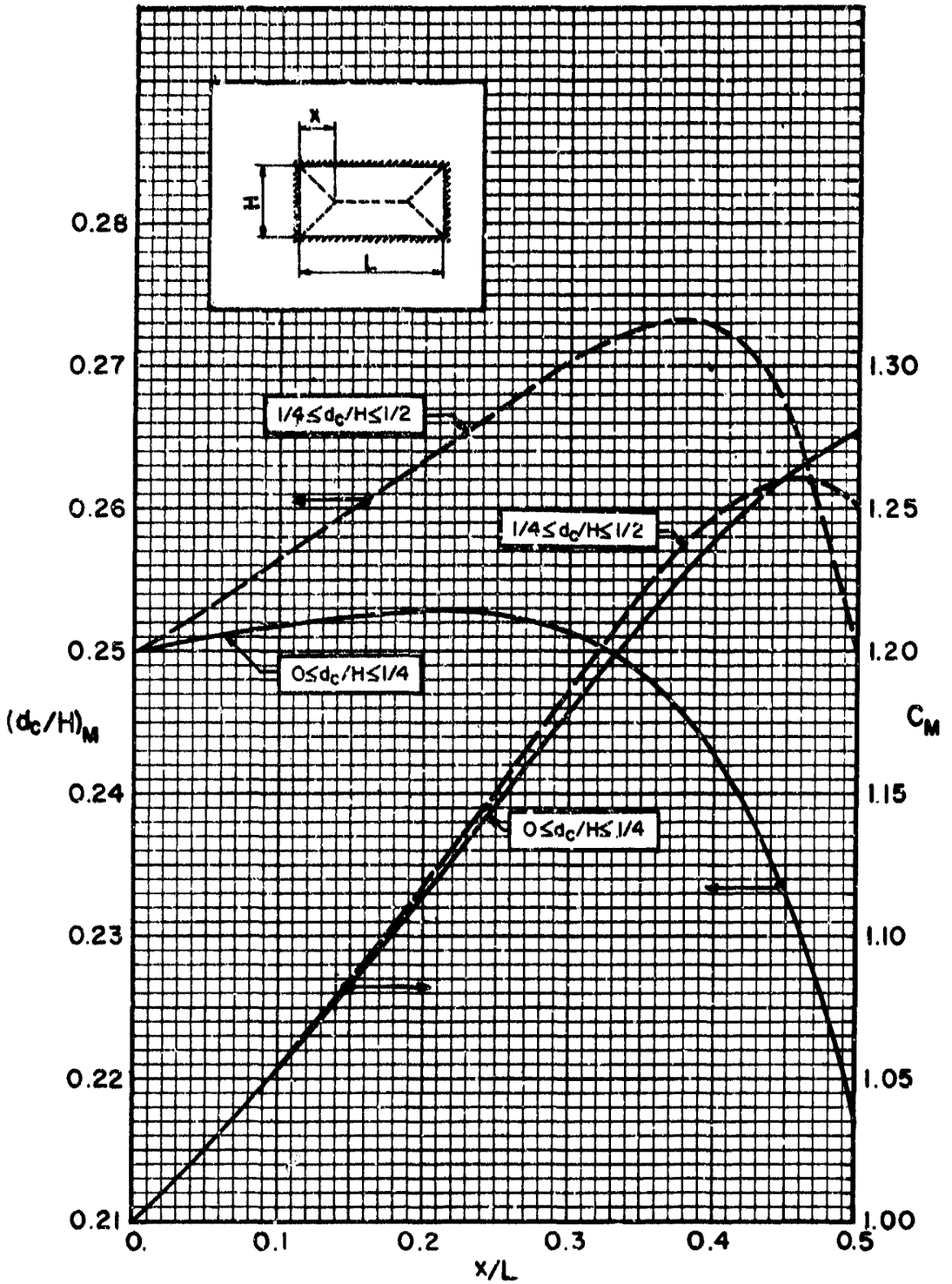


Figure 6-34. Vertical shear parameters for ultimate shear stress at distance d_c from the support (cross section type II and III).

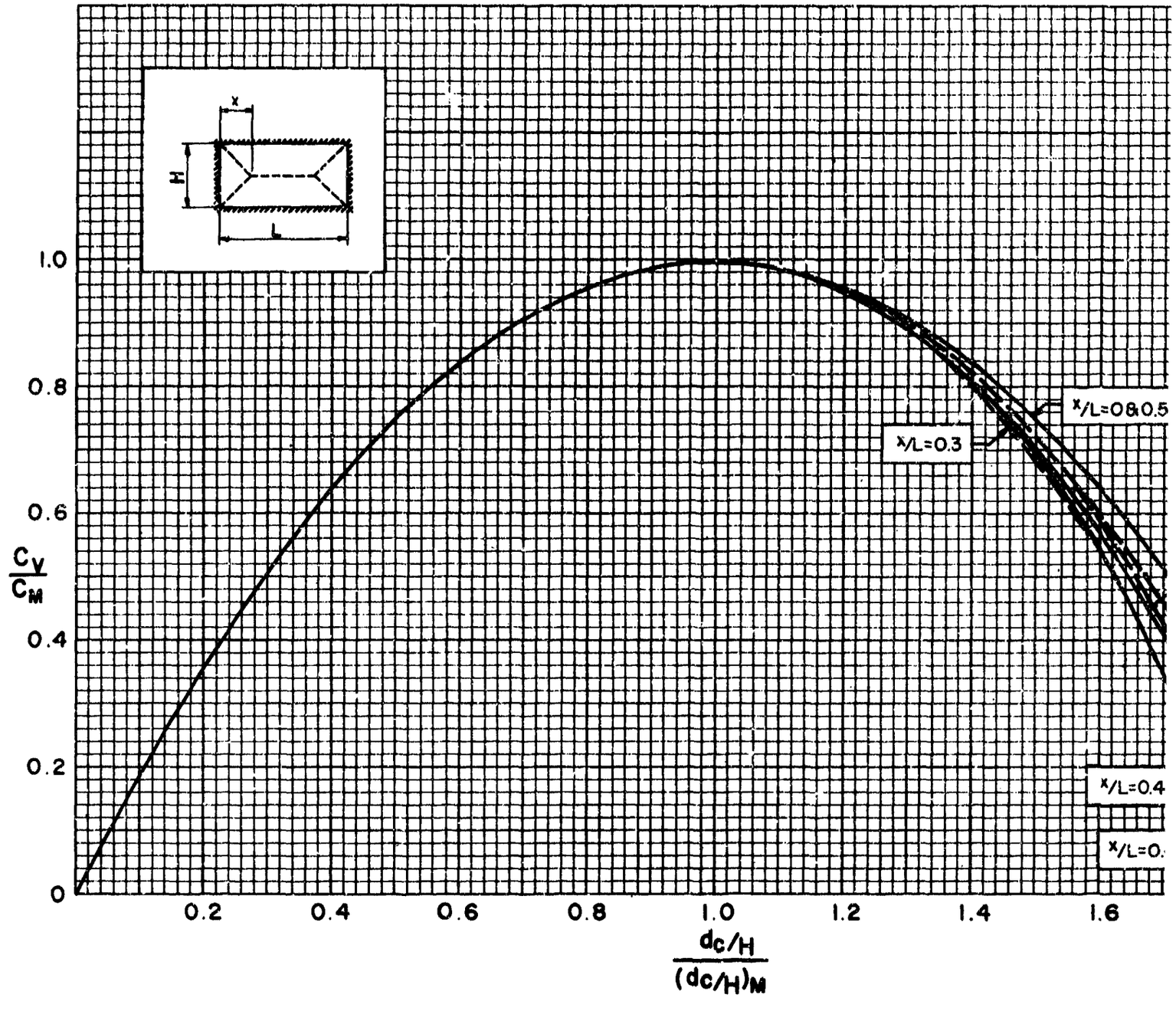
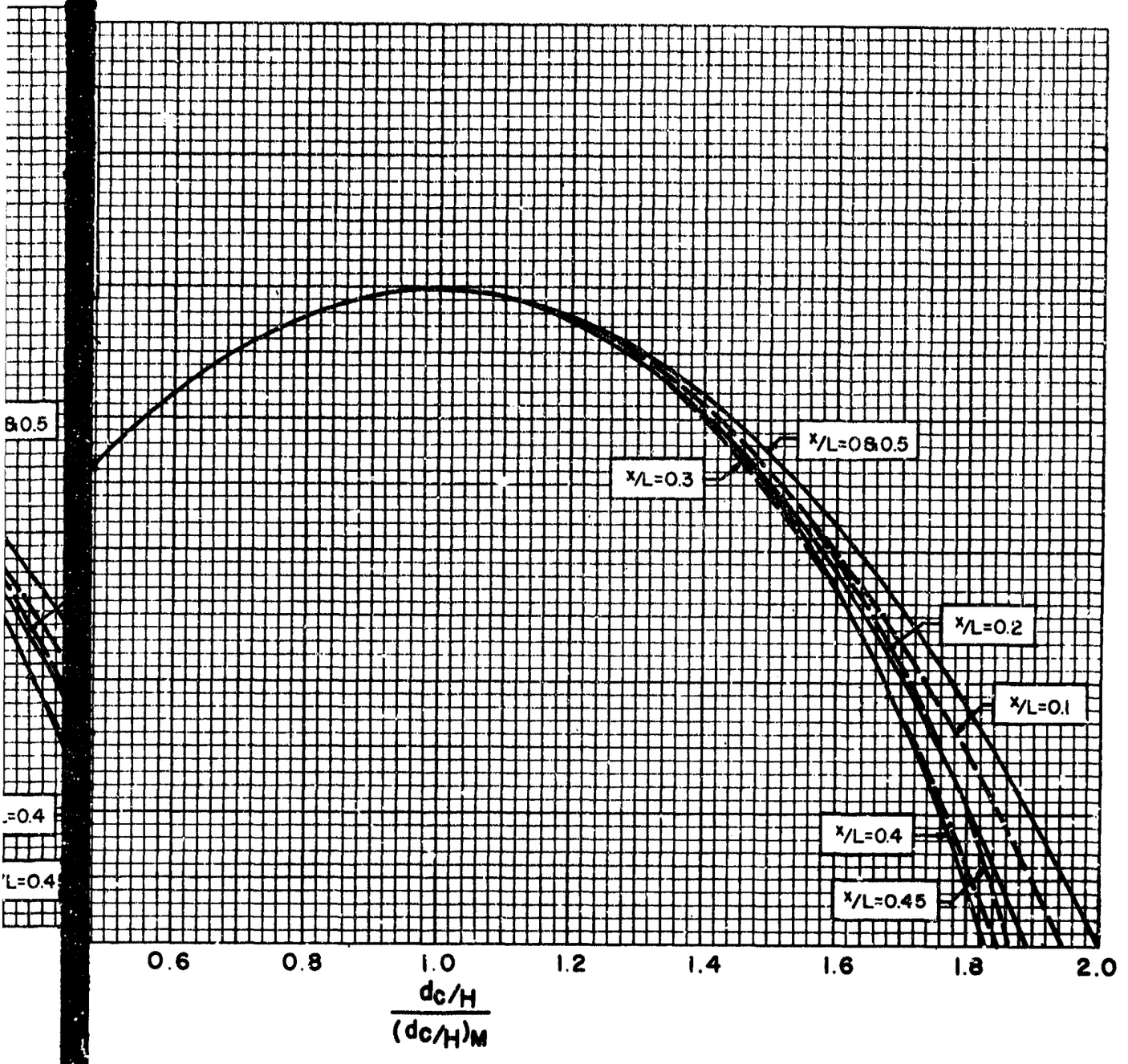


Figure 6–35. Vertical shear coefficient ratios for ultimate shear stress at distance d_c from the support (cross section type II and III).



ical shear coefficient ratios for ultimate shear stress at distance d_c from the support (cross section type II and III).

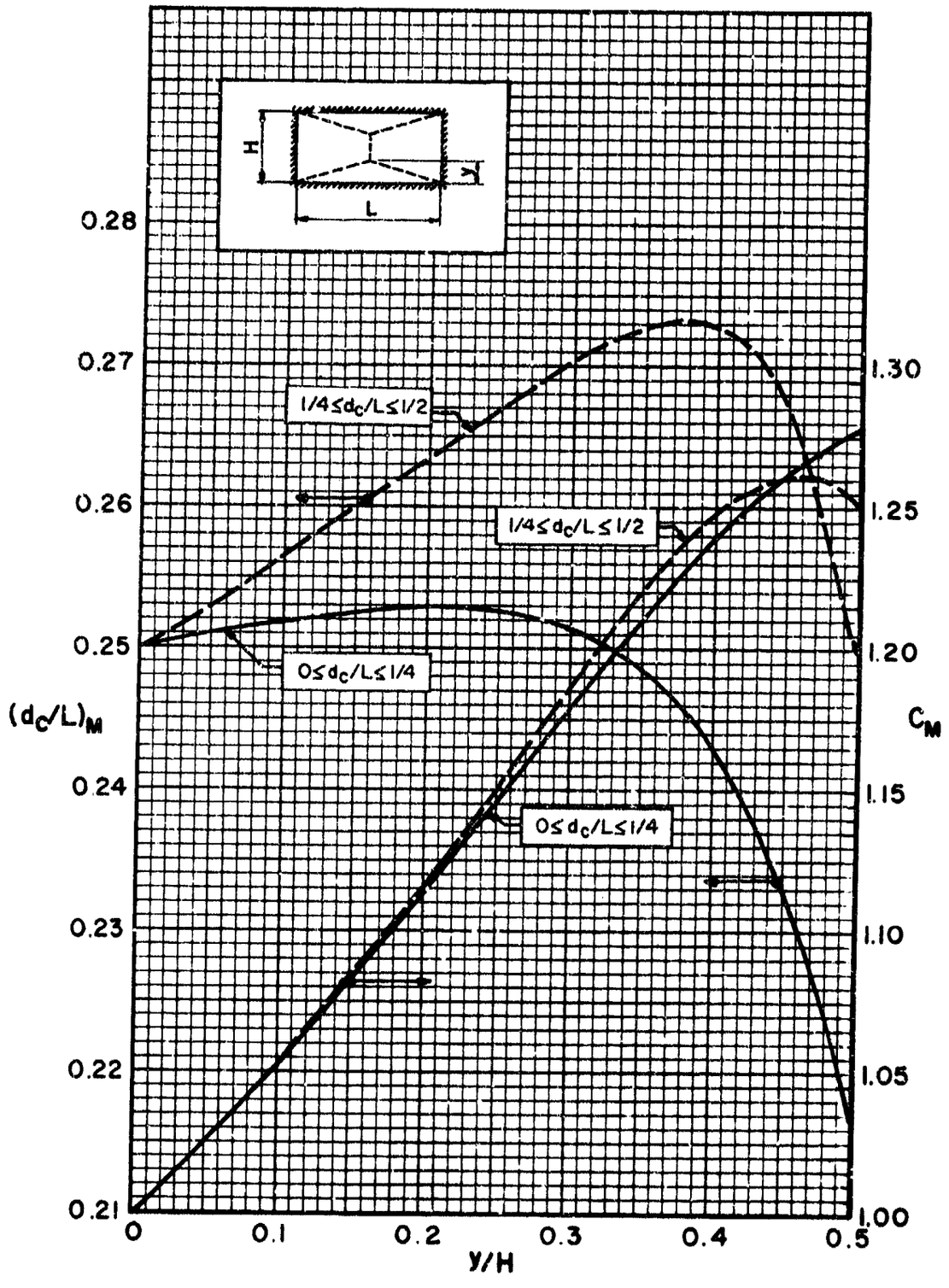


Figure 6-36. Horizontal shear parameters for ultimate shear stress at distance d_c from the support (cross section type II and III).

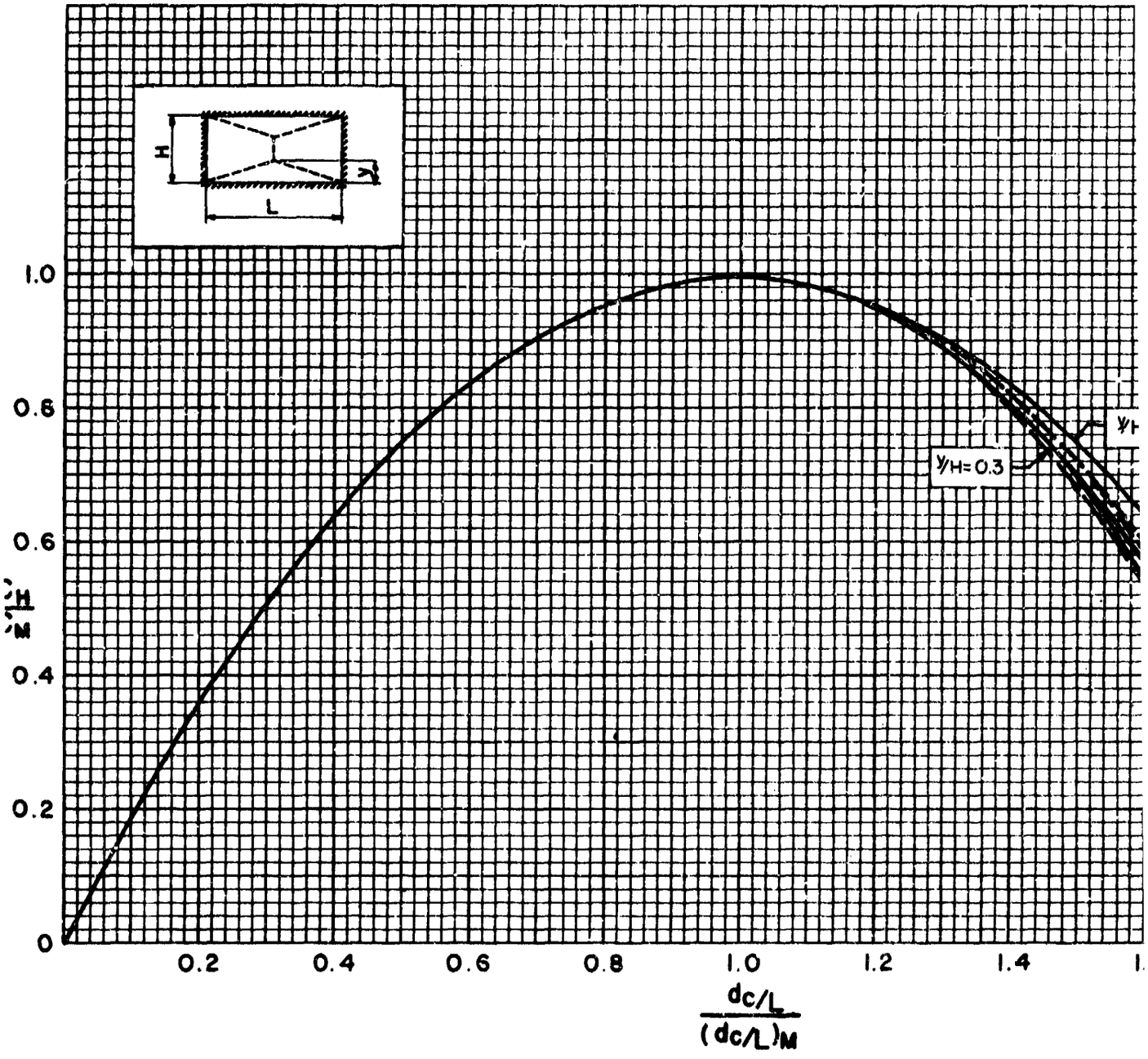
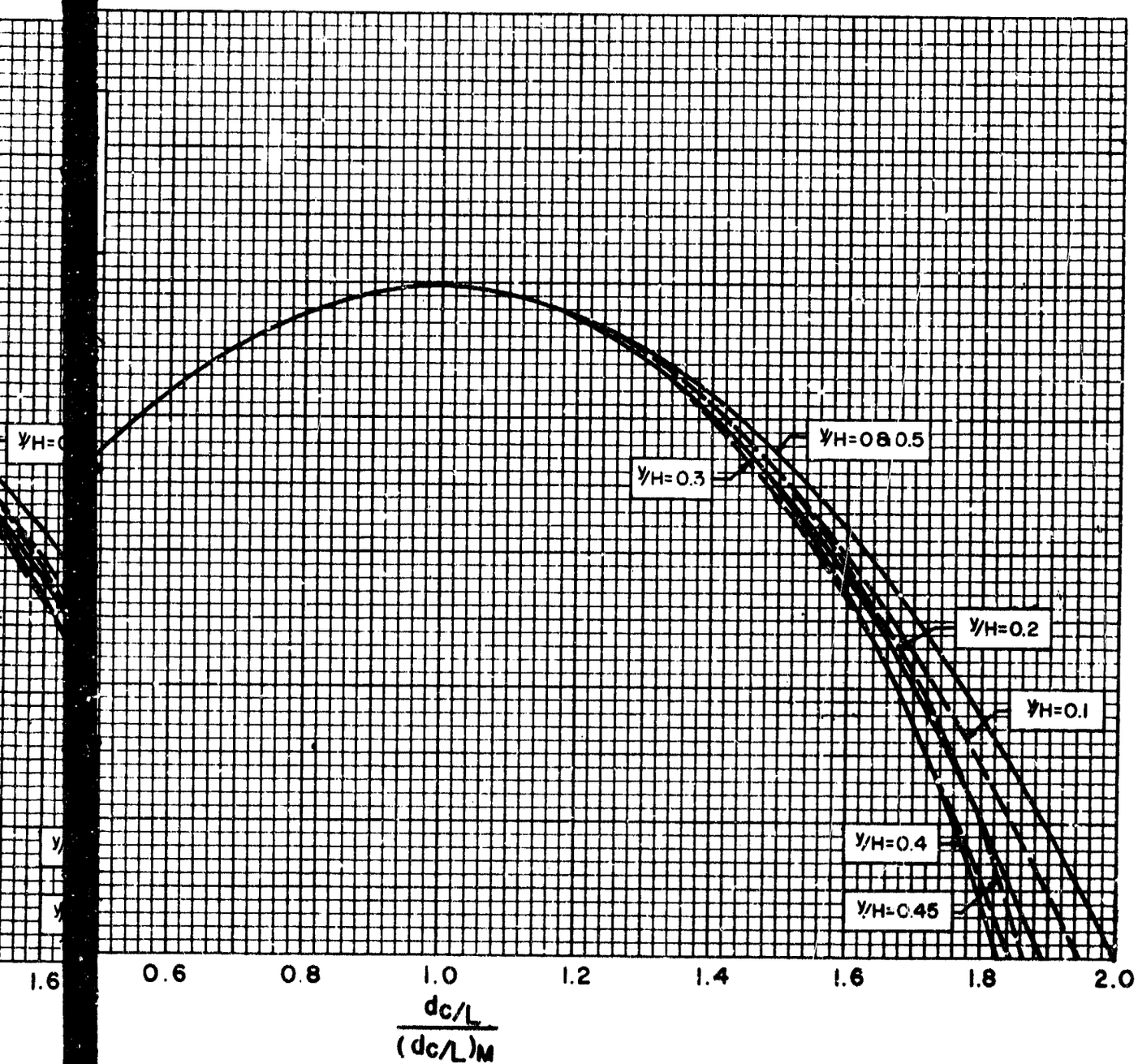


Figure 6-37. Horizontal shear coefficient ratios for ultimate shear stress at distance d_c from the support (cross section type II and III



...l shear coefficient ratios for ultimate shear stress at distance d_c from the support (cross section type II and III).

...ad III).

Section V. COMPOSITE CONSTRUCTION

6–13. General

The use of composite construction, elements composed of two concrete panels (donor and receiver) separated by a sand-filled cavity, has certain characteristics useful in the blast resistant design of structures located close-in to a detonation. The mechanisms by which composite elements resist the blast pressures are (1) the strength and ductility of the concrete panels and (2) the blast attenuating ability of the sand fill. The attenuation of the blast by the sand is accomplished by (1) the increased mass it affords to the concrete portions of the wall, (2) the increased distance the blast wave must travel due to the increased wall thickness produced by the sand (dispersion of blast wave), and (3) the blast energy absorbed by the displacement and compression of the sand particles.

6–14. Analysis of Composite Elements

a. The method of calculating the impulse capacity of composite elements is similar to that for single concrete elements except that the blast attenuating ability of the sand (para 6–13) must be included in the calculation. The following empirical procedure illustrates the method used for the analysis of composite elements. The attenuating ability of the sand for blast wave dispersion and energy absorption is obtained from either figure 6–38 or 6–39:

(1) Assume charge weight W.

(2) Calculate $\bar{T}_c$ and $\bar{T}_s$ (where $\bar{T}_c$ equals scaled thickness of the concrete panel and $\bar{T}_s$ equals scaled thickness of the sand).

(3) Calculate $\bar{i}_b$ (scaled unit blast impulse) which can be resisted by each concrete panel.

(4) Using either figure 6–38 or 6–39,

(*a*) Enter ordinate at value of $\bar{i}_{ba}$ (scaled blast impulse which can be resisted by the receiver panel).

(*b*) Proceed horizontally from $\bar{i}_{ba}$ to $\bar{T}_s$.

(*c*) Proceed vertically from $\bar{T}_s$ to $\bar{T}_c$.

(*d*) Proceed horizontally from $\bar{T}_c$ to $\bar{i}_a$ (sum of scaled unit blast impulse resisted by the receiver panel and the scaled unit blast impulse absorbed by the sand).

(5) Calculate the summation of $\bar{i}_{bd}$ (scaled unit impulse which can be resisted by the donor panel) and $\bar{i}_a$ to give $\bar{i}_{bt}$ be resisted by the

(6) Determin acting on the com

(7) Compare cipient failure con

(8) If the b by the composite produced by the must be repeated

b. In the above the mass of the sa concrete. Therefo pacity of each pa as the mass of t one-half the sand (para 6–6). Becau pression (equation impulse resisted by

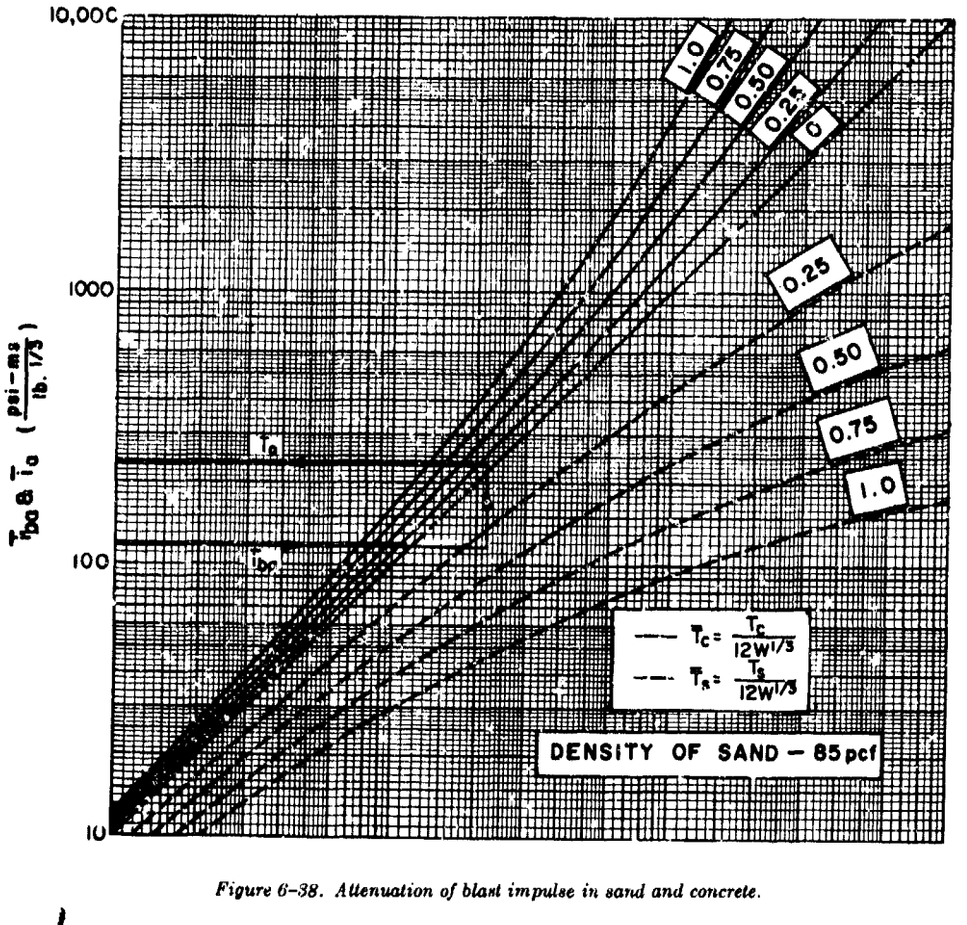


Figure 6–38. Attenuation of blast impulse in sand and concrete.

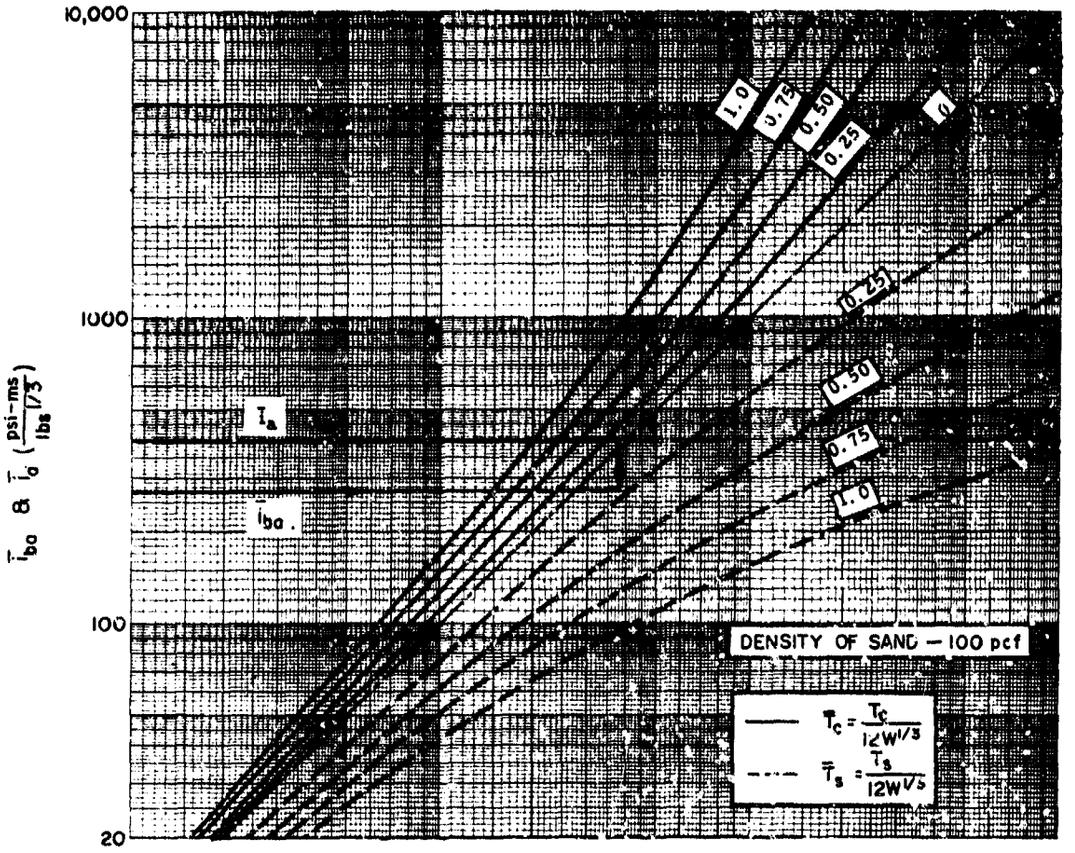


Figure 6–39. Attenuation of blast impulse in sand and concrete.

and $\bar{i}_a$ to give $\bar{i}_{bt}$ (total unit blast impulse which can be resisted by the wall).

(6) Determine the scaled unit blast impulse $\bar{i}_b$ acting on the composite element (ch. 4).

(7) Compare $\bar{i}_{bt}$ and $\bar{i}_b$ ($\bar{i}_{bt}$ is equal to $\bar{i}_b$ for incipient failure conditions or less).

(8) If the blast impulse which can be resisted by the composite element is not equal to the impulse produced by the blast, then (1) through (7) above must be repeated for another assumed charge weight.

b. In the above procedure (*a*(1) through (7) above), the mass of the sand is assumed to act with that of the concrete. Therefore, for computing the impulse capacity of each panel, the total effective mass is taken as the mass of the concrete which is effective plus one-half the sand mass times the load-mass factor (para 6–6). Because of this increase in mass, the expression (equation 6–30) which defines the unit blast impulse resisted by either the donor or receiver panels must be modified by multiplying the values of C_1 and C_u by $\left[d+\frac{w_s}{W}\left(\frac{T_s}{2}\right)\right]\Big/ d$ where w_s is the weight density of the sand. If neither scabbing nor spalling of the receiver panel occurs, then the above correction is modified by replacing the value of d by T_c. This correction factor is applied to equation 6–31.

c. Explosion response slab tests have indicated that the density of the sand fill affects the amount of blast energy absorbed by the sand displacement, i.e., the higher the initial sand density, the smaller the amount of blast energy absorbed. Also, it was observed in the above response tests that for a unit weight of sand equal to 100 pcf, the deflection of the donor panel is approximately equal in magnitude to the deflection of the receiver panel. On the other hand, with a unit weight of sand fill equal to 85 pcf, it was observed that the deflection of the donor panel usually was signifi-

cantly larger than that of the receiver panel. This latter phenomenon was caused by the fact that, with the lower density, the sand had more voids and therefore more room for movement of the sand particles. This sand movement in turn permitted larger displacements of the donor panel before the near solid state of the sand occurred.

d. Based on the above information, it can be seen that if near equal displacement of the donor and receiver panels are desired, then a unit weight of sand fill equal to 100 pcf should be used, whereas a variation of the displacement of donor and receiver panels can be achieved using a unit weight of sand equal to 85 pcf.

APPENDIX 6A. STRUCTURAL DESIGN IN THE DUCTILE MODE ILLUSTRATIVE EXAMPLES

PROBLEM 6A-1. PLASTIC LOAD-MASS FACTOR

Problem: Determine the plastic load-mass factor K_{LM} for a two-way element using (1) general solution and (2) chart solution.

Note:

The determination of the plastic load-mass factor follows the calculations for the ultimate resistance, hence the structural configuration and the location of the plastic yield lines will be known.

Procedure (Part a - General Solution):

Step 1. See part a, problem 5A-1 of appendix 5A for the structural configuration and location of plastic yield lines. Denote sectors formed by yield lines.

Step 2. Determine the load-mass factor properties I, c, and L' for all sectors.

Step 3. Determine the factor I/cL' for all sectors.

Step 4. Calculate the total area of the element.

Step 5. With values obtained above, calculate the plastic load-mass factor for the element using equation 6-14.

$$K_{LM} = \frac{\Sigma \frac{I}{cL'}}{A} \qquad \text{(eq. 6-14)}$$

Note:

In the above problem an element of uniform thickness was considered. For non-uniform elements, the load-mass factor is calculated using equation 6-13 where the mass of the individual sectors must be considered.

Procedure (Part b - Chart Solution):

Step 1. See part b, problem 5A-1 of appendix 5A for structural configuration and location of plastic yield lines in terms of x/L or y/H.

Step 2. For known value of x/L or y/H and support condition, determine the load-mass factor for the element from figure 6-5.

Note:

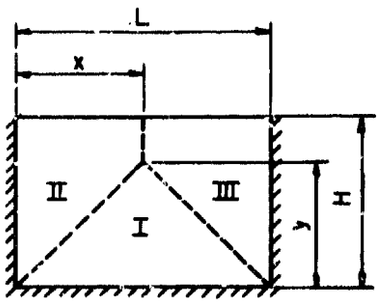
Chart solution may be used only if the element conforms to the requirements listed in paragraph 5-9.

EXAMPLE 6A-1. PLASTIC LOAD-MASS FACTOR

Required: Plastic load-mass factor for the element considered in example 5A-1(A) of appendix 5A using (1) general solution and (2) chart solution.

Solution (Part a - General Solution):

Step 1. Given structural configuration and location of yield lines shown below (see part a, example 5A-1(A) of appendix 5A).



L = 240 in

H = 168 in

x = 120 in

y = 134.8 in

T_c = const. thick.

Figure 6A-1

Step 2. Load-mass factor properties.

a. Sector I

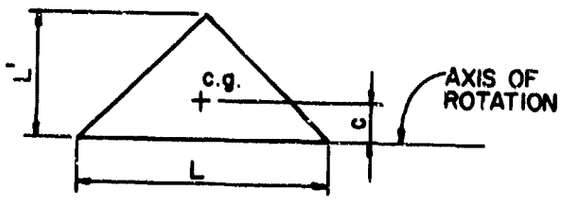


Figure 6A-2

$L' = y = 134.8$ in

$c = y/3 = 134.8/3$

$$I = \frac{L\,(L')^3}{12} = \frac{240(134.8)^3}{12}$$

b. Sector II

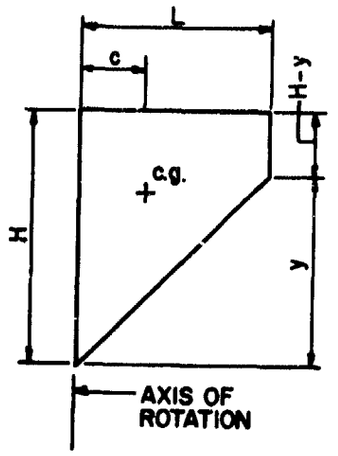


Figure 6A-3

$L' = x = 120$ in

$H - y = 168 - 134.8 = 33.2$ in

$$c = \frac{L'\left[H + 2\,(H-y)\right]}{3\,\left[H + (H-y)\right]} = \frac{120\left[168 + 2\,(33.2)\right]}{3\,(168 + 33.2)}$$

AXIS OF ROTATION

$c = 120\,(0.388)$

$$I = \frac{(H-y)(L')^3}{3} + \frac{y(L')^3}{12}$$

$$= \frac{33.2\,(120)^3}{3} + \frac{134.8\,(120)^3}{12} = 22.3\,(120)^3$$

Step 3. Calculate factor I/cL' for each sector:

Sector I. $$\frac{I}{cL'} = \frac{\frac{240(134.8)^3}{12}}{\left(\frac{134.8}{3}\right)(134.8)} = 8{,}090 \text{ in}^2$$

Sector II. $$\frac{I}{cL'} = \frac{22.3(120)^3}{(0.388 \times 120)(120)} = 6{,}900 \text{ in}^2$$

Sector III. $$\frac{I}{cL'} = 6{,}900 \text{ in}^2$$

Step 4. Area of panel

$$A = LH = 240\,(168) = 40{,}320 \text{ in}^2$$

Step 5. Load-mass factor

$$K_{LM} = \frac{\Sigma \frac{I}{cL'}}{A} \quad \text{(eq. 6-14)}$$

$$K_{LM} = \frac{8{,}090 + 2(6{,}900)}{40{,}320} = 0.543$$

Solution (Part b - Chart Solution):

Step 1. Given: Panel fixed on 3 edges, 1 free and y/H = 0.803 (see part b, example 5A-1(A) of appendix 5A).

Step 2. From figure 6-5, read load-mass factor

$$K_{LM} = 0.543$$

PROBLEM 6A-2. ELEMENTS DESIGNED FOR THE PRESSURE-TIME RELATIONSHIP

Problem: Design an element which responds to the pressure-time relationship.

Note:

Steps 1 through 5, 12, and 13 are general for both one- and two-way elements. Steps 6 through 11, 15, and 16 are specific for one-way elements, however, references are given defining similar procedures for two-way elements.

Procedure:

Step 1. Establish design parameters:

a. Blast loads including pressure-time relationship (ch. 4).

b. Deflection criteria.

c. Structural configuration including geometry and support condition.

d. Type of section available to resist blast, Type I, II or III depending upon the occurrence of spalling and/or crushing of the concrete cover.

Step 2. Select cross section of element including thickness and concrete cover over reinforcement. Also determine static stresses of concrete and reinforcing steel (table 5-4).

Step 3. Determine dynamic increase factors for both concrete and reinforcement from table 5-3. Using the above DIF and the static stresses of step 2, calculate dynamic stresses.

Step 4. Assume percent reinforcement and bar size. Also, calculate d_e (d or d_c depending upon type of cross section available to resist blast) for both the positive and negative moments.

Step 5. Using the area of reinforcement and the value of d_e from step 4, and the dynamic stresses of step 3, calculate the moment capacity (para. 5-2) of both the positive and negative reinforcement.

Step 6.

Step 7.

Step 8.

Step 9.

Step 10.

Step 11.

Step 12

Note:

Steps 6 through 11 are required to determine the actual and equivalent resistance-deflection curves for one-way elements. To obtain these curves for two-way elements see problem 5A-2.

Step 6. Using the equations of tables 5-5 and 5-10 and the moment capacities of step 5, calculate the peak resistance in the elastic range and the ultimate resistance in the plastic range.

Step 7. Using equation 5-17, the static concrete stress of step 2, and the unit weight for concrete equal to 150 pcf, calculate the modulus of elasticity for concrete. With the above modulus for concrete and that for steel (equation 5-18) and equation 5-19, calculate the modular ratio.

Step 8. With the use of equation 5-21 and the assumed concrete thickness of step 2, calculate the gross moment of inertia of the concrete. Using the values of d_e for the negative and positive reinforcement of step 4, calculate an average value of d_e. Also calculate an average percent of positive and negative reinforcement using the above d_e and the area of reinforcement of step 4. With the value of p (avg) and figure 5-5, determine the value of the constant F and calculate the moment of inertia of a cracked section with equation 5-22. Also calculate the average moment of inertia for the element by averaging the gross and cracked moments of inertia.

Step 9. Using the equations of table 5-11, and the modulus of elasticity of step 7 and the moment of inertia of step 8, calculate the stiffness of the element in the elastic and elasto-plastic ranges.

Step 10. Using the resistances and the stiffnesses calculated in steps 6 and 9, respectively, calculate the deflection in the elastic and elasto-plastic ranges.

Step 11. With the use of the deflections of step 10 and equation 5-50 or 5-51, calculate the equivalent maximum elastic deflection X_E. Also calculate the equivalent elastic unit stiffness K_E from equation 5-52.

Step 12. Determine the load-mass factor K_{LM} for the elastic, elasto-plastic and plastic ranges from table 6-1. The average load-mass factor for the element is obtained by taking the average K_{LM} for the elastic and elasto-plastic ranges and averaging this value with the K_{LM} of the plastic range. In addition, calculate the unit mass of the element (account for reduced concrete thickness if spalling is anticipated) and multiply this unit mass by K_{LM} for the element to obtain the effective unit mass of the element.

Step 13. Using the effective mass of step 12 and the equivalent stiffness of step 11, calculate the natural period of vibration T_N using equation 6-15.

Step 14. Determine the response chart parameters:

a. Peak pressure B (step 1).

b. Peak resistance r_u (step 6).

c. Duration of load T (step 1).

d. Natural period of vibration T_N (step 13).

Also calculate the ratios of peak pressure B to peak resistance r_u and duration T to period T_N. Using the ratios and figure 6-7, determine the value of X_m/X_E and t_m/T_N. Compute the value of X_m and compare it to the maximum permissible deflection of step 1, and if found satisfactory proceed to step 15. If comparison is unsatisfactory, repeat step 2 to step 14. In addition, compute the value of t_m/t_o from t_m/T_N and T/T_N and assuming that $T = t_o$. Determine whether or not correct procedure has been used; for elements to respond to the pressure-time relationship, $3 < t_m/t_o < 0.1$.

Step 15. Using the ultimate resistance of step 6, the value of d_e of step 4 and equation of table 5-13, calculate the ultimate diagonal tension shear stress at distance d_e from the support. Also calculate the shear capacity of the element from equation 5-10. If the capacity is greater than that produced by the load, shear reinforcement is not required. However, if the shear produced by the load is greater than the capacity, then shear reinforcement must be added to resist the excess. (For two-way elements use equations of table 5-15).

Step 16. Using the equations of table 5-12 and the ultimate resistance of step 6, calculate the shear at the support. Also calculate the direct shear capacity of the element using equation 5-12. If the capacity is greater than that produced by the load, the member is safe. But, if the reverse is true, then the thickness of the element must be increased. However, if lacing is used then diagonal bars must be provided to resist the direct shear. (For two-way elements use equations of table 5-14).

Required:
strained

Step 1. G

a

b

c

d

Step 2. S
m

EXAMPLE 6A-2 ELEMENTS DESIGNED FOR THE PRESSURE-TIME RELATIONSHIP

Required: Design a wall which spans in one direction and is fully restrained at both supports for a given blast load.

Step 1. Given:

a. Pressure-time loading (fig. 6A-4).

b. Maximum deflection equal to 3 times elastic.

c. Structural configuration (fig. 6A-4).

d. Type I cross section.

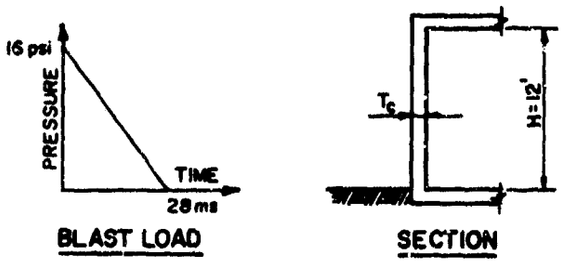


Figure 6A-4

Step 2. Select cross section of element and static stress of reinforcement (A432) and concrete.

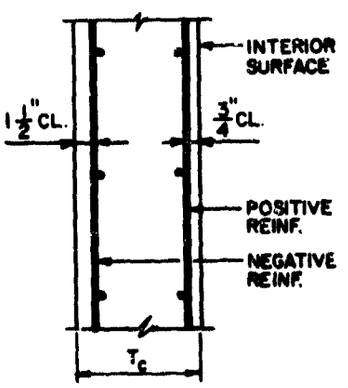


Figure 6A-5

f'_c = 3,000 psi (assumed)

f_y = 60,000 psi (table 5-4)

Assume T_c = 12 in. and concrete cover as shown.

Step 3. Determine dynamic stresses.

a. Dynamic increase factors - DIF (table 5-3).

Concrete:

Compression - 1.25
Diag. tension - 1.00
Direct shear - 1.10

Reinforcement:

Bending - 1.10
Shear - 1.00

b. Dynamic stresses.

Concrete:

Compression - 1.25 (3,000) = 3,750 psi
Diag. tension - 1.00 (3,000) = 3,000 psi
Direct shear - 1.10 (0.18)(3,000) = 600 psi*

Reinforcement:

Bending - 1.10 (60,000) = 66,000 psi
Shear - 1.00 (60,000) = 60,000 psi

*See equation 5-12.

Step 4. Assume reinforcement and calculate d.

Note:

Assume minimum reinforcement and No. 5 bars.

p (min) = 0.25% (table 5-1)

Negative moment. d = 12 - 1.5 - 0.3125 = 10.1875 in

Positive moment. d = 12 - 0.75 - 0.3125 = 10.9375 in

$$A_s = 0.0025(12)(10.9375) = 0.328 \text{ in}^2/\text{ft} \quad \text{(eq. 5-2)}$$

Use No. 5 bars at 11 in. o.c.

$$A_s = 0.34 > 0.328 \text{ in}^2/\text{ft}$$

Step 5. Calculate moment capacity of both positive and negative reinf.

a. Depth of equivalent rectangular stress block.

$$a = \frac{A_s f_{dy}}{0.85\ b\ f'_{dc}} = \frac{0.34\ (66,000)}{0.85\ (12)(3750)} = 0.586 \text{ in}$$

b. Moment capacity (eq. 5-1).

$$M_u = \frac{A_s f_{dy}}{b}\left(d - \frac{a}{2}\right)$$

$$M_N = \frac{0.34\ (66,000)(10.1875 - 0.586/2)}{12}$$

$$= 18,500 \text{ in-lbs/in}$$

$$M_p = \frac{0.34\ (66,000)(10.9375 - 0.586/2)}{12}$$

$$= 19,900 \text{ in-lbs/in}$$

Step 6. Determine elastic and ultimate resistances.

a. Elastic resistance (table 5-10).

$$r_u = \frac{12\ M_N}{L^2} = \frac{12\ (18,500)}{(144)^2} = 10.71 \text{ psi}$$

b. Ultimate resistance (table 5-5).

$$r_u = \frac{8\left(M_N + M_p\right)}{L^2} = \frac{8\ (18,500 + 19,900)}{(144)^2} = 14.81 \text{ psi}$$

Step 7. Determine modulus of elasticity and modular ratio.

a. Concrete (eq. 5-17)

$$E_c = w^{1.5}\, 33\sqrt{f'_c} = (150)^{1.5}\,(33)(3000)^{\frac{1}{2}} = 3.32 \times 10^6 \text{ psi}$$

b. Steel (eq. 5-18)

$$E_s = 29 \times 10^6 \text{ psi}$$

c. $$n = \frac{E_s}{E_c} = \frac{29 \times 10^6}{3.32 \times 10^6} = 8.73$$

Step 8. Determine average moment of inertia for a one inch strip.

a. Gross moment of inertia (eq. 5-21).

$$I_g = \frac{b\, T_c^{\,3}}{12} = \frac{1\,(12)^3}{12} = 144 \text{ in}^4$$

b. Moment of inertia of cracked section (eq. 5-22).

$$d(\text{avg}) = \frac{10.1875 + 10.9375}{2} = 10.5625 \text{ in}$$

$$p(\text{avg}) = \frac{A_s}{bd(\text{avg})} = \frac{0.34}{12(10.56)} = 0.00268$$

$\therefore F = 0.0175$ (fig. 5-5)

$$I_c = F\, b\, d^3(\text{avg}) = 0.0175\,(1)(10.56)^3 = 20.6 \text{ in}^4$$

c. Average moment of inertia (eq. 5-20).

$$I_a = \frac{I_g + I_c}{2} = \frac{144 + 20.6}{2} = 82.3 \text{ in}^4$$

Step 9. Calculate unit stiffnesses.

a. Elastic range unit stiffness (table 5-11).

10^6 psi

$$K_e = \frac{384\ E_c\ I_a}{b\ L^4} = \frac{384\ (3.32 \times 10^6)\ (82.3)}{1\ (144)^4} = 244\ \text{lbs/in}^3$$

b. Elasto-plastic range unit stiffness (table 5-11).

$$K_{ep} = \frac{384\ E_c\ I_a}{5b\ L^4} = \frac{K_e}{5} = \frac{244}{5} = 48.8\ \text{lbs/in}^3$$

Step 10. Calculate elastic and elasto-plastic deflections.

a. Elastic deflections.

$$X_e = \frac{r_e}{K_e} = \frac{10.71}{244} = 0.0439\ \text{in}$$

b. Elasto-plastic deflection.

$$X_p - X_e = \frac{r_u - r_e}{K_{ep}} = \frac{14.81 - 10.71}{48.8} = 0.0840\ \text{in}$$

$$X_p = 0.0439 + 0.0840 = 0.1279\ \text{in}$$

Step 11. Calculate equivalent elastic deflection and stiffness.

$$X_E = X_e + X_p\ (1 - r_e/r_u) \quad \text{(fig. 5-50)}$$

$$= 0.0439 + 0.1279\left(1 - \frac{10.71}{14.81}\right) = 0.0793\ \text{in}$$

$$K_E = \frac{r_u}{X_E} = \frac{14.81}{0.0793} = 186.8\ \text{lbs/in}^3$$

Step 12. Calculate effective mass of element.

a. Load mass factors (table 6-1).

Elastic range - $K_{LM} = 0.77$

Elasto-plastic range - $K_{LM} = 0.78$

Plastic range - $K_{LM} = 0.66$

K_{LM} (avg. elastic and elasto-plastic) = 0.78

$$K_{LM} \text{ (avg. elastic and plastic)} = \frac{0.78 + 0.66}{2} = 0.72$$

b. Unit mass of element.

$$m = \frac{w\, T_c}{g} = \frac{150\ (1)\ 10^6}{32.2\ (1728)} = 2{,}700\ \text{lb-ms}^2/\text{in}^3$$

c. Effective unit mass of element.

$$m_e = K_{LM}\, m = 0.72\ (2{,}700) = 1{,}944\ \text{lb-ms}^2/\text{in}^3$$

Step 13. Calculate natural period of vibration.

$$T_N = 2\pi \sqrt{\frac{m_e}{K_E}} \quad \text{(eq. 6-15)}$$

$$= 2(3.14)\sqrt{\frac{1944}{186.8}} = 20.3\ \text{ms}$$

Step 14. Determine response chart parameters (fig. 6-7).

Peak pressure, $B = 16$ psi (step 1)

Peak resistance, $r_u = 14.81$ psi (step 6)

Duration, $T = 28$ ms (step 1)

Period of vibration, $T_N = 20.3$ ms (step 13)

$B/r_u = 16/14.81 = 1.08$ and $T/T_N = 28/20.3 = 1.38$

From figure 6-7:

$X_m/X_E = 2.80 < 3$ (step 1)

∴use assumed section.

$$\frac{t_m}{T_N} = 0.75 \rightarrow \frac{t_m}{t_o} = \frac{t_m}{T} = \frac{t_m/T_N}{T/T_N} = \frac{0.75}{1.38} = 0.543$$

The correct procedure has been used since $t_m/t_o = 0.543$ is within the range, $3 > t_m/t_o > 0.1$.

Step 15. Check of diagonal tension at d distance from support.

a. Ultimate shear stress (table 5-13).

$$v_u = \frac{r_u\left(\frac{L}{2} - d_e\right)}{d_e} \quad \text{where } d_e = d \text{ (of negative moment)}$$

$$= \frac{14.81\ (72 - 10.1875)}{10.1875} = 89.9 \text{ psi}$$

b. Allowable shear stress (eq. 5-10).

$$v_c = \phi\left[1.9\sqrt{f'_c} + 2{,}500\ p\right] \leq 2.28\ \phi\sqrt{f'_c}$$

$$= 0.85\left[1.9\ (3{,}000)^{\frac{1}{2}} + \frac{2{,}500\ (0.34)}{12\ (10.1875)}\right]$$

$$= 94.4 \text{ psi} > 89.9 \text{ psi}$$

Note:

No stirrups required.

Step 16. Check of shear at supports.

a. Ultimate shear (table 5-12).

$$V_s = \frac{r_u L}{2} = \frac{14.81\ (144)}{2} = 1{,}066\ \text{lb/in}$$

b. Allowable shear (eq. 5-12).

$$V_d = 0.18\ f'_{dc}\ bd = 0.18\ (3300)(1)(10.1875)$$

$$= 6{,}050\ \text{lb/in} > 1{,}066\ \text{lb/in}$$

PROBLEM 6A-3. ELEMENTS DESIGNED FOR IMPULSE-LARGE DEFLECTIONS

Problem: Design an element subjected to an impulse load for a large deflection.

Procedure:

Step 1. Establish design parameters:

a. Impulse load and duration (ch. 4).

b. Deflection criteria.

c. Geometry of element.

d. Support conditions.

e. Type of section available to resist blast, Type II or III depending upon the occurrence of spalling (ch. 7).

f. Materials to be used and corresponding static design strengths (table 5-4).

g. Dynamic increase factors (table 5-3).

Step 2. Determine static design stress for the reinforcement according to the deflection range (support rotation) required by the desired protection level (para. 5-6).

Step 3. Determine dynamic design stress for the reinforcement.

Step 4. Determine optimum distribution of the reinforcement according to the deflection range considered (para. 6-9*c* and figs. 6-17 and 6-18). Step not necessary for one-way elements.

Step 5. Establish design equation for deflection range considered and type of section (type II or III) available (table 6-4).

Step 6. Determine impulse coefficient C_1 and/or C_u for optimum p_V/p_H ratio and L/H ratio.

Note:

If the desired deflection X_m is not equal to X_1 or X_u, determine yield line location (figs. 5-9 through 5-11) for optimum p_V/p_H ratio and L/H ratio and calculate X_m, X_1, and, if necessary, X_u (table 5-9).

Step 7. Substitute known parameters into equation of step 5 to obtain relationship between p_H and d_c.

Step 8. Assume value of d_c and calculate p_H and from optimum p_V/p_H calculate p_V. Select bar sizes and spacings necessary to furnish required reinforcement (see ch. 9 for limitations).

Step 9. For actual distribution of flexural reinforcement, establish yield line location (figs. 5-9 through 5-11).

Note:

$$\frac{L}{H}\left[\frac{M_{VN}+M_{VP}}{M_{HN}+M_{HP}}\right]^{\frac{1}{2}} = \frac{L}{H}\left[\frac{p_V}{p_H}\right]^{\frac{1}{2}} = \frac{L}{H}\left[\frac{A_{sV}}{A_{sH}}\right]^{\frac{1}{2}}$$

since $M_N = M_P = p\, d_c^{\,2} f_{ds} = \frac{A_s}{b}\, d_c\, f_{ds}$

Step 10. Determine the ultimate shear stress at distance d_c from the support in both the vertical (v_{uV} from eq. 6-42) and horizontal (v_{uH} from eq. 6-41) directions where the coefficients C_V and C_H are determined from figures 6-24 through 6-37 (see para. 6-12*b*(1) for an explanation of the figures and parameters involved).

Step 11. Determine the shear capacity v_c of the concrete in both the vertical and horizontal directions (shear stress permitted on an unreinforced web (eq. 5-10)).

Step 12. Select lacing method to be used (fig. 9-4). (Note. Lacing making an angle of 45° with the longitudinal reinforcement is most efficient.)

Step 13. Determine the required lacing bar sizes for both the vertical and horizontal directions from equation 5-11b where the parameters b_ℓ and s_ℓ are determined from the lacing method used (fig. 9-4), and the angle of inclination of the lacing bars α is obtained from figure 6-19. The lacing bar size D_o must be assumed in order to compute d_ℓ and R_ℓ. (Note. See paragraph 5-3*a* for limitations imposed upon the design of the lacing.)

Step 14. Determine required thickness T_c for assumed d_c, selected flexural and lacing bar sizes, and required concrete cover. Adjust T_c to the nearest whole inch and calculate the actual d_c.

Step 15. Check flexural capacity based on either impulse or deflection. Generally, lacing bar sizes do not have to be checked since they are not usually affected by a small change in d_c.

a. Check of impulse. Compute actual impulse capacity of the element using the equation determined in step 5 and compare with anticipated blast load. Repeat design (from step 8 on) if capacity is less than required.

b. Check of deflection. Compute actual maximum deflection of the element using equation determined in step 5 and compare with deflection permitted by design criteria. Repeat design (from step 8 on) if actual deflection is greater than that permitted.

Step 16. Determine whether correct procedure has been used by first computing the response time of the element t_m (time to reach maximum deflection) from equation 6-24 or 6-25, depending on the deflection range considered in the design, and then compare response time t_m with duration of load t_o. For elements to be designed for impulse, $t_m > 3\ t_o$.

Step 17. Determine the ultimate support shear in both the vertical (V_{sV} from eq. 6-40) and horizontal (V_{sH} from eq. 6-39) directions. The coefficients C_{sV} and C_{sH} are determined from table 6-7 and figures 6-20 through 6-23 (see para. 6-12*b*(3) for an explanation of the figures and parameters involved).

Step 18. Determine the required diagonal bar sizes for the vertical and horizontal (intersecting elements may control) directions from equation 5-13. Diagonal bars should have the same spacing as the flexural reinforcement (fig. 9-8).

Note:

To obtain the most economical design repeat the above steps for several wall thicknesses and compare costs. Percentages of reinforcement may be used to reduce the amount of calculations. In determining the required quantities of reinforcement, lapping of the bars should be considered.

EXAMPLE 6A-3. ELEMENTS DESIGNED FOR IMPULSE-LARGE DEFLECTIONS

Required: Design the back wall of the interior cell (fig. 6A-6) of a multicubicle structure for incipient failure.

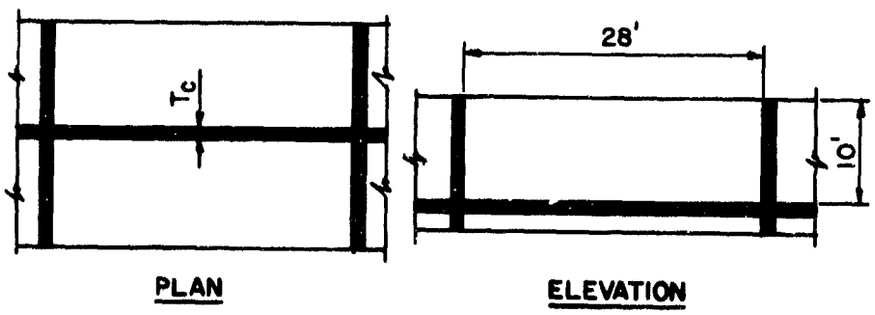


Figure 6A-6

Solution:

Step 1. Given:

a. $i_b = 3{,}200$ psi-ms and $t_o = 5$ ms

b. Incipient failure

c. L = 336 in, H = 120 in

d. Fixed on three edges and one edge free

e. Type III cross section

f. A432 reinf. $f_y = 60{,}000$ psi and $f_u = 90{,}000$ psi
concrete $f'_c = 4{,}000$ psi

g. For reinf. DIF = 1.20

Step 2. Static design stress.

$$f_s = \frac{f_y + f_u}{2} = \frac{60{,}000 + 90{,}000}{2} = 75{,}000 \text{ psi}$$

Step 3. Dynamic design stress.

$$f_{ds} = (\text{DIF})\, f_s = 1.20\ (75{,}000) = 90{,}000 \text{ psi}$$

Step 4. From figure 6-18 for $\frac{L}{H} = \frac{336}{120} = 2.8$

Optimum $P_V/P_H = 1.41$

Step 5. From table 6-4 for type III cross section

$$\frac{i_b^{\,2} H}{p_H d_c^{\,3} f_{ds}} = C_1 + (C_u - C_1)\, \frac{X_m - X_1}{X_u - X_1}$$

But since $X_m = X_u$ (incipient failure)

$$\frac{i_b^{\,2} H}{p_H d_c^{\,3} f_{ds}} = C_u$$

Step 6.

Step 7.

Step 8.

Step 6. L/H = 2.8 is not plotted on figure 6-14, therefore must interpolate for optimum p_V/p_H.

For $p_V/p_H = 1.41$

L/H	144 $C_u \times 10^{-4}$
1.5	8.82
2.0	7.87
3.0	6.44
4.0	5.57

From figure 6A-7, $144\ C_u \times 10^{-4} = 6.70$

so that

$$C_u = \frac{6.70 \times 10^4}{144}$$

Step 7.

$$p_H d_c^3 = \frac{i_b^2 H}{C_u f_{ds}}$$

$$p_H d_c^3 = \frac{(3,200)^2 (120)(144)}{(6.7 \times 10^4)(9 \times 10^4)} = 29.3$$

Step 8. Assume $d_c = 21$ in

$$p_H = \frac{29.3}{d_c^3} = \frac{29.3}{(21)^3} = 0.00317$$

$$p_V = \frac{p_V}{p_H}(p_H) = 1.41\ (0.00317) = 0.00447$$

$A_{sH} = 0.00317\ (12)(21) = 0.80$ in^2/ft - Use #8 @ 11 ($\Lambda_s = 0.86$)

$A_{sV} = 0.00447\ (12)(21) = 1.13$ in^2/ft - Use #9 @ 10 ($\Lambda_s = 1.20$)

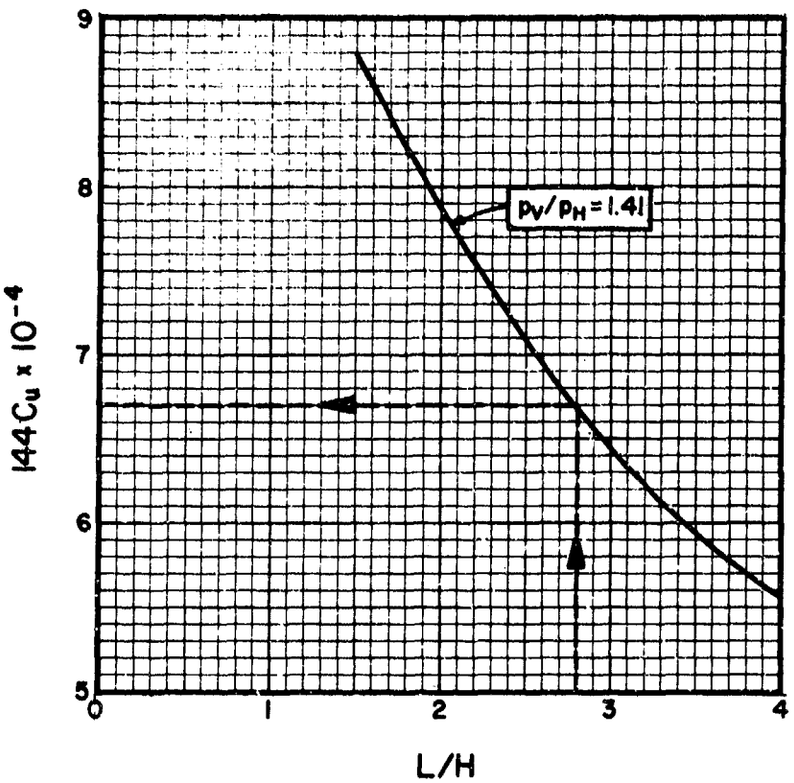


Figure 6A-7. Interpolation for L/H = 2.8.

Step 9. Yield line location.

$$\text{Actual } \frac{p_V}{p_H} = \frac{A_{sV}}{A_{sH}} = \frac{1.20}{0.86} = 1.40$$

$$\text{From figure 5-10 for } \frac{L}{H}\left[\frac{A_{sV}}{A_{sH}}\right]^{\frac{1}{2}} = 2.8\ (1.40)^{\frac{1}{2}} = 3.31$$

$$x/L = 0.385,\ x = 0.385\ (336) = 129 \text{ in}$$

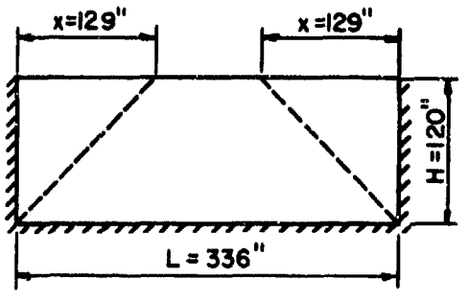


Figure 6A-8

Step 10. Ultimate shear stress at distance d_c from support.

a. Vertical Direction (along L)

$$\text{For } \frac{d_c}{H} = \frac{21}{120} = 0.175 \text{ and } x/L = 0.385$$

$$\text{From figure 6-30, } \left(\frac{d_c}{H}\right)_M = 0.49 \text{ and } C_M = 1.07$$

$$\text{For } \frac{d_c/H}{(d_c/H)_M} = \frac{0.175}{0.49} = 0.357$$

From figure 6-31, $\frac{C_V}{C_M} = 0.58$

therefore:

$$C_V = 1.07\ (0.58) = 0.62$$

$$p_V = \frac{A_{sV}}{b\ d_c} = \frac{1.20}{12(21)} = 0.00476$$

so that

$$v_{uV} = C_V\ p_V\ f_{ds} = 0.62\ (0.00476)(90{,}000) = 266\ \text{psi}$$

b. Horizontal Direction (along H)

For $\frac{d_c}{x} = \frac{21}{129} = 0.163$

From figure 6-25, $C_H = 0.81$

$$p_H = \frac{A_{sH}}{b\ d_c} = \frac{0.86}{12(21)} = 0.00341$$

so that

$$v_{uH} = C_H\ p_H\ f_{ds} = 0.81\ (0.00341)(90{,}000) = 248\ \text{psi}$$

Step 11. Shear capacity of concrete.

a. Vertical Direction

$$v_c = \phi\ \left(1.9\sqrt{f'_c} + 2{,}500\ p_V\right)$$

$$= 0.85\left[1.9\sqrt{4{,}000} + 2{,}500\ (0.00476)\right] = 112\ \text{psi}$$

b. Horizontal Direction

$$v_c = \phi\left(1.9\sqrt{f'_c} + 2{,}500\ p_H\right)$$

$$= 0.85\left[1.9\sqrt{4{,}000} + 2{,}500\ (0.00341)\right] = 110\ \text{psi}$$

Step 12. Use lacing method No. 3 (see figure 9-4).

Step 13. L

a.

Step 13. Lacing bar sizes.

a. Vertical Lacing Bars

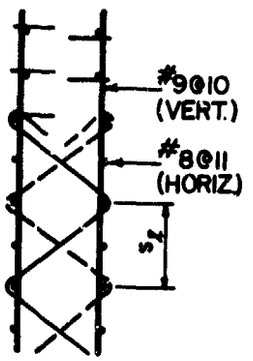


Figure 6A-9

$b_\ell = 10$ in $\quad s_\ell = 22$ in

Assume no.6 bars, $D_o = 0.75$ in

$d_\ell = 21 + 1.13 + 2.00 + 0.75$

$= 24.88$ in

Min. $R_\ell = 3D_o$

For $\frac{s_\ell}{d_\ell} = \frac{22}{24.88} = 0.884$

$$\frac{2R_\ell + D_o}{d_\ell} = \frac{7D_o}{d_\ell} = \frac{7(0.75)}{24.88} = 0.211$$

From figure 6-19, $\alpha = 51.5^o$

$$A_v = \frac{(v_{uV} - v_c)\, b_\ell\, s_\ell}{\phi\, f_s\, (\sin\alpha + \cos\alpha)}$$

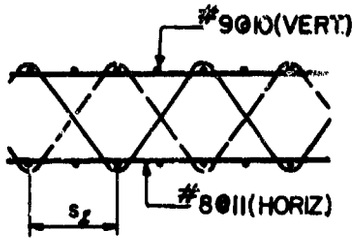
$$= \frac{(266 - 112)(10)(22)}{0.85\,(75{,}000)(0.782 + 0.622)} = 0.378 \text{ in}^2$$

Min $A_v = 0.0015\ b_\ell\, s_\ell = 0.0015\,(10)(22) = 0.330$ in^2

use no. 6 bars ($A = 0.44$ in^2)

b. Horizontal Lacing

Step 14.



d_ℓ = 11 in s_ℓ = 20 in

Step 15.

Figure 6A-10

Assume no. 6 bars, D_o = 0.75 in

d_ℓ = 21.0 + 1.13 + 0.75 = 22.88 in

Min. $R_\ell = 3\ D_o$

For $\frac{s_\ell}{d_\ell} = \frac{20}{22.88} = 0.874$

$$\frac{2\ R_\ell + D_o}{d_\ell} = \frac{7\ D_o}{d_\ell} = \frac{7\ (0.75)}{22.88} = 0.229$$

From figure 6-19, $\alpha = 52.5^o$

$$A_V = \frac{(v_{uH} - v_c)\ b_\ell\ s_\ell}{\phi\ f_s\ (\sin\alpha + \cos\alpha)}$$

$$= \frac{(248 - 110)(11)(20)}{0.85\ (75{,}000)(0.795 + 0.609)} = 0.339\ in^2$$

Min. $A_v = 0.0015\ b_\ell\ s_\ell = 0.0015\ (11)(20) = 0.330\ in^2$

use no. 6 bars ($A = 0.44\ in^2$)

Step 14. Actual d_c depends upon vertical lacing.

Cover - 2 x 0.75 = 1.50
Lacing - 2 x 0.75 = 1.50
Horizontal - 2 x 1.00 = 2.00
Vertical - 1.13 = 1.13
6.13 in

$T_c = d_c + 6.13 = 21 + 6.13 = 27.13$ in $\therefore$ Use 27 in

Actual $d_c = 27 - 6.13 = 20.87$ in

Step 15. Check capacity.

a. Actual impulse capacity.

For $\frac{P_V}{P_H} = 1.40 \approx 1.41$, $C_u = \frac{6.70 \times 10^4}{144}$

For $d_c = 20.87$ in $P_H = \frac{0.86}{12(20.87)} = 0.00343$

$$i_c^2 = \frac{P_H d_c^3 f_{ds} C_u}{H}$$

$$= \frac{0.00343(20.87)^3 (9 \times 10^4)(6.7 \times 10^4)}{144 (120)}$$

$i_c = 3310$ psi-ms $> i_b = 3200$ psi-ms

b. Actual maximum deflection.

For $\frac{P_V}{P_H} = 1.40$, $C_1 = \frac{6.5 \times 10^4}{144}$ (fig. 6-11)

$C_u = \frac{6.7 \times 10^4}{144}$

From table 5-9 for x > H.

$X_1 = H \tan 12^\circ = 120\ (0.2125) = 25.5$ in

$X_u = \frac{L}{2} \tan 12^\circ = 168\ (0.2125) = 35.7$ in

From step 5

$$\frac{i_b^2 H}{P_H d_c^3 f_{ds}} = C_1 + (C_u - C_1)\left[\frac{X_m - X_1}{X_u - X_1}\right]$$

$$\frac{(3200)^2 (120)}{0.00343(20.87)^3 (90 \times 10^3)} = \frac{10^4}{144}\left[6.5 + (6.7-6.5)\right]\left[\frac{X_m - 25.5}{35.7 - 25.5}\right]$$

From which $X_m = 15.82$ in $< X_1$

Note:

Since the deflection X_m is less than X_1, the above solution ($X_m = 15.82$) is incorrect because the equation used is for the deflection range $X_1 \leq X_m \leq X_u$. Therefore, an equation for the deflection range $0 \leq X_m \leq X_1$ must be used to obtain the correct solution

From table 6-4 for Type III cross sections and valid for deflection range $0 \leq X_m \leq X_1$.

$$\frac{i_b^2 H}{p_H d_c^3 f_{ds}} = C_1 \left(\frac{X_m}{X_1} \right)$$

$$X_m = \frac{i_b^2 H X_1}{p_H d_c^3 f_{ds} C_1} = \frac{(3200)^2 (120) (25.5)}{(0.00343)(20.87)^3 (90 \times 10^3)\left(\frac{6.5 \times 10^4}{144}\right)}$$

$$X_m = 24.7 \text{ in}$$

Note:

The element is slightly over-designed. To obtain a more economical design, the amount of flexural reinforcement may be reduced.

Step 16. The response time of the element is obtained from

$$t_m = \frac{i_b}{r_u} \quad \text{(eq. 6-25)}$$

where $r_u = \frac{5 \left(M_{HN} + M_{HP} \right)}{x^2}$ (table 5-6)

But $M_{HN} = M_{HP} = \frac{A_{sH} f_{ds} d_c}{b} = \frac{0.86 (90 \times 10^3) (20.87)}{12}$

$= 134{,}600$ in-lbs/in

e above solution
used is for the
equation for
o obtain the

valid for de-

(25.5)
$0 \times 10^3)\left(\frac{6.5 \times 10^4}{144}\right)$

in a more econ-
ement may be re-

om

(20.87)

therefore,

$$r_u = \frac{5\ (2)(134,600)}{(129)^2} = 80.9 \text{ psi}$$

so that

$$t_m = \frac{i_b}{r_u} = \frac{3,200}{80.9} = 39.6 \text{ ms}$$

$$\frac{t_m}{t_o} = \frac{39.6}{5} = 7.92$$

The correct procedure has been used since $\frac{t_m}{t_o} > 3$

Step 17. Ultimate support shear.

a. Vertical Direction (along L).

From figure 6-21, for x/L = 0.385

$$C_{sV} = 4.40$$

$$V_{sV} = \frac{C_{sV}\ p_V\ d_c^2\ f_{ds}}{H}$$

$$= \frac{4.40\ (1.20)(20.87)^2\ (90,000)}{12\ (20.87)(120)} = 6,885 \text{ lbs/in}$$

b. Horizontal Direction (along H).

From table 6-7,

$$C_{sH} = \frac{6}{x/L} = \frac{6}{0.385} = 15.6$$

$$V_{sH} = \frac{C_{sH}\ p_H\ d_c^2\ f_{ds}}{L}$$

$$= \frac{15.6\ (0.00343)(20.87)^2\ (90,000)}{336} = 6,250 \text{ lbs/in}$$

2

Step 18. Diagonal bar sizes.

Note:

Place bars on a 45° angle.
$\therefore \sin \alpha = 0.707$

a. Vertical Direction (at floor slab).

$$A_d = \frac{V_{sV}\, b}{f_s \sin \alpha} = \frac{6{,}885\ (10)}{75{,}000\ (0.707)} = 1.30\ \text{in}^2$$

$$\text{Req'd area of bar} = \frac{A_d}{2} = 0.65\ \text{in}^2$$

Use No. 8 @ 10

b. Horizontal Direction (at wall intersections).

$$A_d = \frac{V_{sH}\, b}{f_s \sin \alpha} = \frac{6{,}250\ (11)}{75{,}000\ (0.707)} = 1.30\ \text{in}^2$$

$$\text{Req'd area of bar} = \frac{A_d}{2} = 0.65\ \text{in}^2$$

Use No. 8 @ 11

PROBLEM 6A-4. ELEMENTS DESIGNED FOR IMPULSE-COMPOSITE CONSTRUCTION

Problem: Design a composite (concrete-sand-concrete) wall to resist a given blast output for incipient failure.

Procedure:

Step 1. Establish design parameters:

a. Structure configuration.

b. Charge weight.

c. Blast impulse load (ch. 4).

d. Thicknesses of concrete and sand portions of wall.

e. Blast impulse resisted by concrete panels.

Step 2. Determine scaled thicknesses of concrete and sand using:

$$\overline{T}_c = T_c/W^{1/3} \text{ and } \overline{T}_s = T_s/W^{1/3}$$

Step 3. Dertamine scaled blast impulse resisted by each concrete panel using:

$$\overline{i}_{bd} = i_{bd}/W^{1/3} \text{ (donor panel)}$$

$$\overline{i}_{ba} = i_{ba}/W^{1/3} \text{ (receiver panel)}$$

Step 4. Correct scaled blast impulse resisted by concrete (step 3) to account for the increased mass produced by the sand and the reduction of the concrete mass produced by spalling and scabbing of the concrete panels using:

$$\overline{i}_{bd} \text{ (corr.)} = \overline{i}_{bd} \left[\frac{d + \left(\frac{w_s}{w}\right)\left(\frac{T_s}{2}\right)}{d}\right]^{1/2}$$

$$\overline{i}_{ba} \text{ (corr.)} = \overline{i}_{ba} \left[\frac{d + \left(\frac{w_s}{w}\right)\left(\frac{T_s}{2}\right)}{d}\right]^{1/2}$$

Note:

The value of $w_s = 100$ pcf is predetermined by incipient failure criteria while $w_s = 85$ pcf is used when limited deflections of the receiver panel are required.

esist a

Step 5. Determine scaled blast impulse attenuated by receiver panel and the sand $\overline{i}_a$ from figure 6-38 or 6-39. Figures 6-38 and 6-39 are used for w_s equal to 85 and 100 pcf, respectively.

Step 6. Calculate total impulse resisted by the wall using:

$$\overline{i}_{bt} = \overline{i}_a + \overline{i}_{bd}$$

Step 7. Compare blast impulse which is resisted by wall to that of the applied blast loads.

EXAMPLE 6A-4. ELEMENTS DESIGNED FOR IMPULSE- COMPOSITE CONSTRUCTION

Required: Design the composite wall shown below for incipient failure conditions.

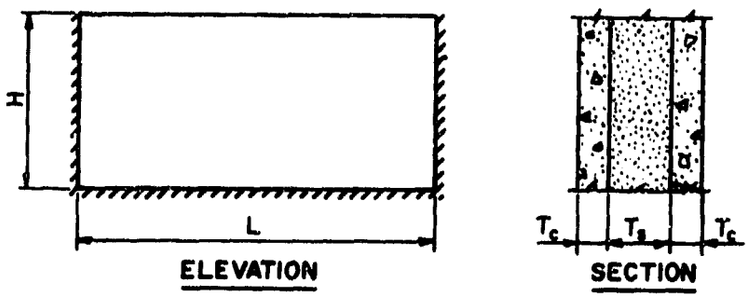


Figure 6A-11

Step 1. Given:

a. W = 1,000 lbs.

b. i_b = 4,800 psi-ms (ch. 4).

c. $i_{bd} = i_{ba}$ = 1,500 psi-ms (ch. 6).

d. T_c = 1 ft, T_s = 2 ft, and d = 0.833 ft.

e. w = 150 pcf and w_s = 100 pcf.

Step 2. Scaled thicknesses of concrete and sand.

$$\overline{T}_c = T_c/W^{1/3} = 1/(1000)^{1/3} = 0.1 \text{ ft/lb}^{1/3}$$

$$\overline{T}_s = T_s/W^{1/3} = 2/(1000)^{1/3} = 0.2 \text{ ft/lb}^{1/3}$$

Step 3. Scaled blast impulse resisted by individual concrete panels.

$$\overline{i}_{bd} = \overline{i}_{ba} = \frac{1500}{(1000)^{1/3}} = 150 \text{ psi-ms/lb}^{1/3}$$

Step 4. Correction of scaled impulse resisted by concrete panel used in composite walls.

$$i_{bd}(\text{corr.}) = i_{bd}\left[\frac{d + \frac{w_s}{w}\left(\frac{T_s}{2}\right)}{d}\right]^{1/2}$$

$$= 150\left[\frac{0.833 + \frac{100}{150}\left(\frac{2}{2}\right)}{0.833}\right]^{1/2}$$

$$= 202 \text{ psi-ms/lb}^{1/3} = i_{ba}(\text{corr.})$$

Step 5. Scaled blast impulse attenuated by receiver panel and sand.

$$\bar{i}_a = 280 \text{ psi-ms/lb}^{1/3} \text{ (fig. 6-39)}$$

Step 6. Total scaled blast impulse resisted by wall.

$$\bar{i}_{bt} = \bar{i}_a + \bar{i}_{bd} = 280 + 202 = 482 \text{ psi-ms/lb}^{1/3}$$

Step 7. Comparison of wall capacity and applied blast load.

$$\bar{i}_{bt} = 482 \approx \bar{i}_b = 480 \text{ psi-ms/lb}^{1/3}$$

CHAPTER 7

STRUCTURAL ANALYSIS AND DESIGN FOR BRITTLE MODE RESPONSE

Section I. INTRODUCTION

7–1. Types of Fragmentation

The response of a structural element in the brittle mode consists of that structural behavior which is associated with either partial or total failure of the element and is characterized by two types of concrete fragmentation: (1) spalling (either direct spalling or scabbing) which is the dynamic disengagement of the surface of the element, and (2) post-failure fragmentation which is associated with structural collapse.

7–2. Design Considerations

Spalling is usually of concern only for those receiver systems where personnel, valuable equipment, and/or extremely sensitive explosives require protection. Where the receiver system consists of relatively insensitive explosives so that fragment impact will not result in propagation of explosion or mass detonation, then post-failure fragmentation can be considered in the design. For this latter case, even though the velocity of the spalls can be greater than the velocity of the post-failure fragments, the effects of spalling can be neglected because of the smaller masses involved. Post-failure fragmentation cannot be permitted when personnel are being protected.

Section II. SPALLING OF CONCRETE

7–3. Direct Spalling

a. Direct spalling of a concrete element (fig. 7–1) is the result of a tension failure in the concrete normal to its free surface and is caused by the shock pressures of an impinging blast wave being transmitted through the element.

b. When a shock front strikes the donor surface of a concrete element, compression stresses are transmitted from the air to the element. This stress disturbance propagates through the element in the form of a compression wave, and upon reaching the rear (receiver) free surface, is reflected as a tension wave identical in shape and magnitude to the compression wave. During the return passage, if the tension stresses in the reflected wave exceed the stresses in the compression wave plus the tensile capacity of the concrete, the material will fracture with that part of the element between the rear free surface and the plane of failure being displaced from the remainder of the element. A portion of the stress wave is trapped in the failed section and contributes to its velocity. The part of the stress wave which remains within the main section continues to propagate with additional reflections and concrete fractures until its magnitude is reduced to that level below which spalling does not occur.

c. Direct spalling generally results in the formation of small concrete fragments, the size being attributed to the nonuniformity of the shock wave (close-in effects) and the further distortions of the wave during its propagation through the element (nonhomogeneous material, nonelastic effects, etc.). Localized failures occur under the action of both flexural and shear stresses resulting in the rupture of the mortar binding the stone aggregate together. The failure zone propagates across the concrete surface forming a large number of comparatively small concrete fragments. The thickness of concrete between the rear (receiver) surface of the element and the centroid of the rear face reinforcement is the usual depth of concrete dynamically disengaged from the element. Although the concrete between the layers of reinforcement may be cracked to some extent, it is confined by the flexural and lacing reinforcement, thus preventing its disengagement.

d. The size of the surface area which spalls depends upon the magnitude and duration of the applied blast loads striking and subsequently being transmitted through the element, in addition to the size and shape of the element itself. For long cantilever-type barricades, only a portion of the wall will usually spall since the magnitudes of the applied blast pressures decrease rapidly along its length, while for cubicle-type structures, the entire wall surface will usually spall because of the amplification of the blast pressures due to their multiple reflections within the structures.

e. A wide range of velocities exists for spalled frag-

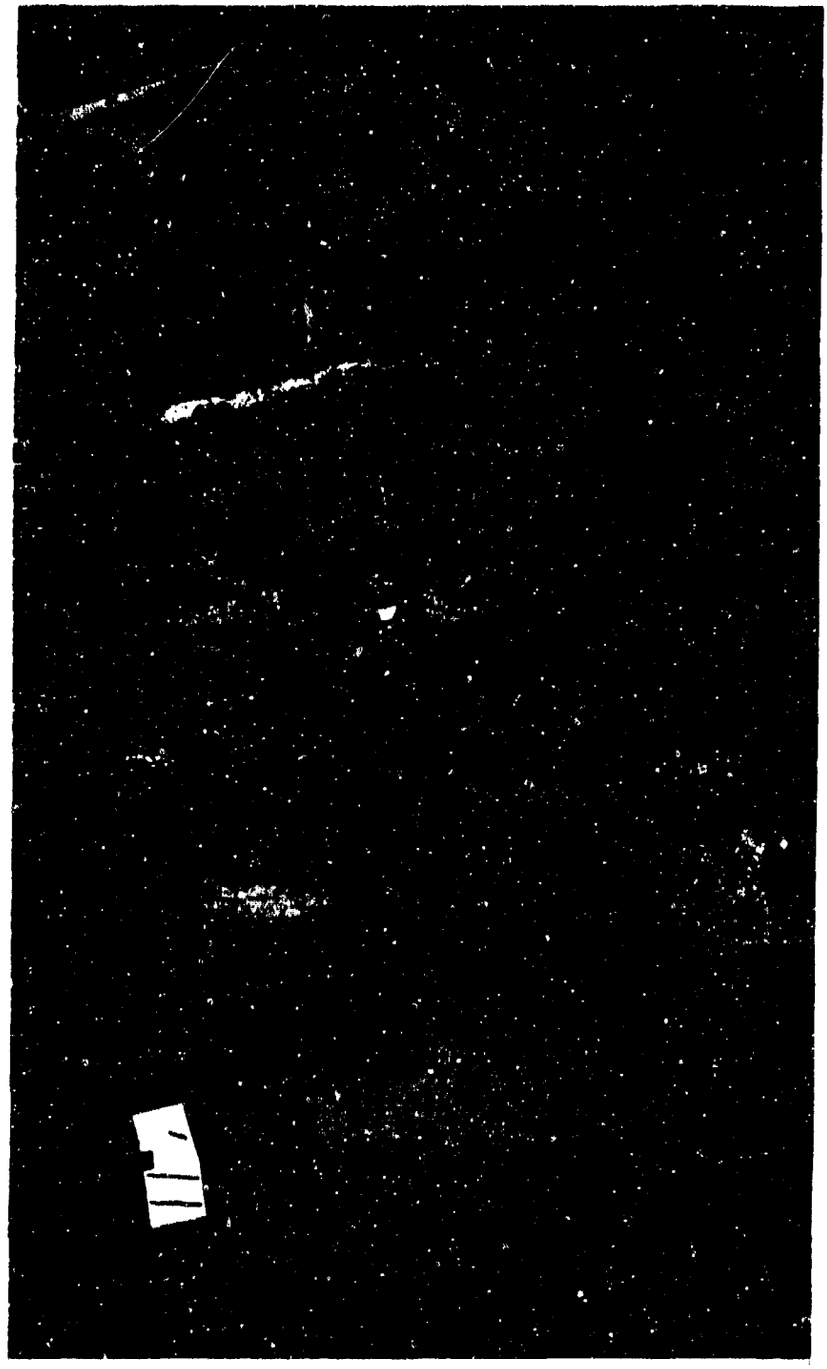


Figure 7-1. Direct spalled element.

ments. The initial velocity at which spalled fragments leave a structural element has been found to be low (50 feet per second or less). However, concrete elements subjected to the close-in effects of a detonation are generally accelerating before or soon after spalling takes place. This accelerated motion of the element in turn accelerates the spalled fragments. The fragment velocities produced by these acceleration effects may be as high as several hundred feet per second. For analytical purposes, an upper limit for the velocities of direct spalled fragments from elements sensitive to impulse may be taken as the initial velocity of the

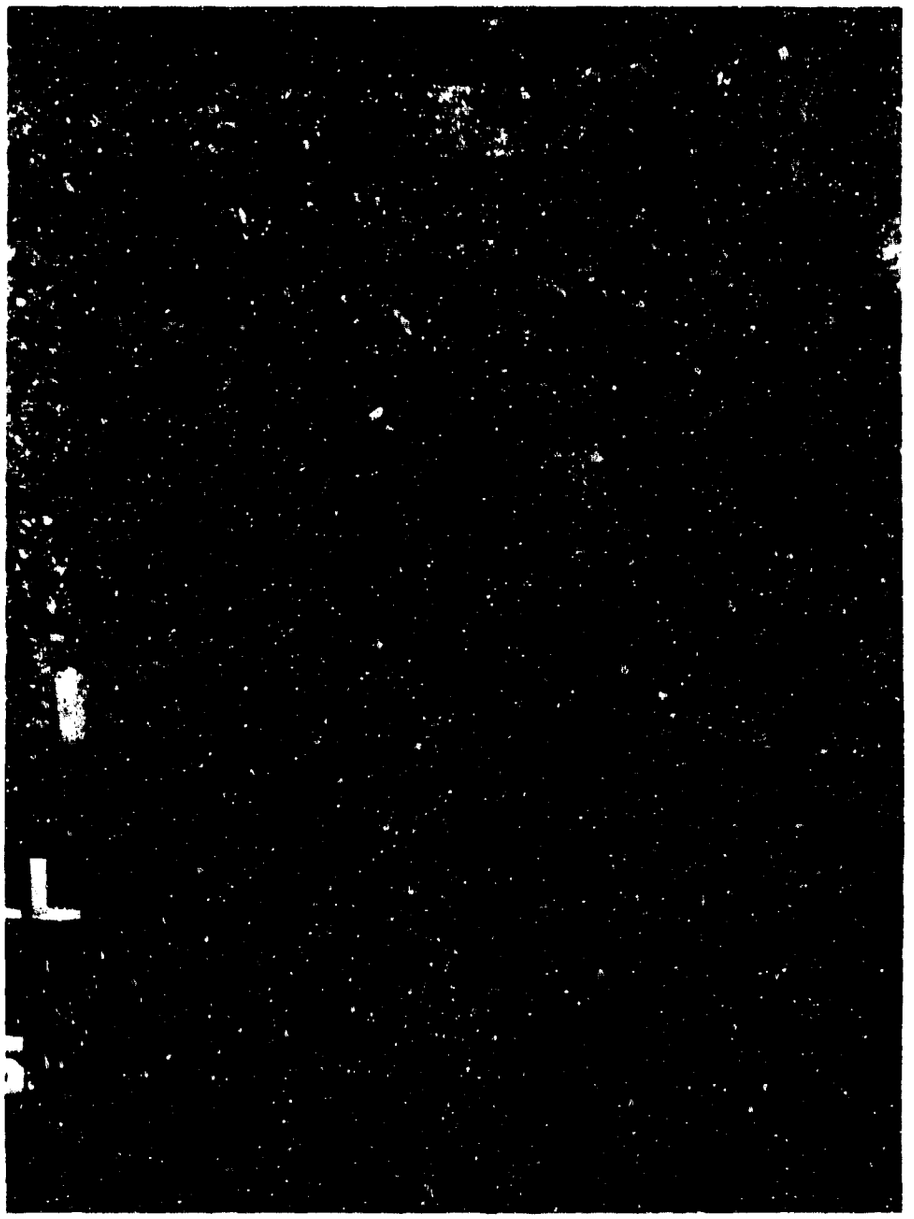


Figure 7-2. Scabbed element.

element which is also assumed to be the maximum velocity. However, for elements which respond to the pressure only or pressure-time relationship, an evaluation of the resistance-time and pressure-time curves must be performed to obtain the maximum fragment velocity. The procedures and equations that are necessary to determine the above velocities are contained in paragraph 7-8.

7-4. Scabbing

Scabbing of reinforced concrete elements (fig. 7-2) is the end result of a tension failure in the concrete normal to its free surface and is associated with large deflections. In the later stages of the ductile response mode of a reinforced concrete element, extremely large deflections are developed producing large strains in the

flexural reinforcement and, consequently, severe cracking and/or crushing of the concrete perpendicular to the free surfaces. Because the tension and compression strains are highest at the surface and since the lacing reinforcement in the later stages of deflection confines the concrete between the layers of flexural reinforcement, damage to the concrete is more severe exterior of the reinforcement than between the layers. The applied loads having long since passed, the element is in a stage of deceleration at these large deflections. Therefore, the velocities of scabbed fragments, which are equal to the velocity of the element at $\theta = 5^0$ (start of scabbing), are lower than the velocities of accelerated direct spalled fragments. However, the velocities of scabbed fragments also may be in the order of several hundred feet per second. Refer to paragraph 7–8 to determine the velocity of the element at a support rotation of 5 degrees.

7–5. Minimization of Effects of Spalling

a. General. Although the factors which effect the spalling of concrete elements are qualitatively known, analytical procedures for predicting the onset of spalling and the mass-velocity characteristics of the resulting fragments are not presently available. There are certain procedures, however, which permit minimization of the effects of spalling in facility design.

b. Design Parameters.

(1) The occurrence of direct spalling can be eliminated by an adjustment of the charge location, *i.e.*, if an explosive charge is placed at a sufficient distance away from the surface of an element, the magnitude of the blast pressures striking the element will be less than those which will cause tension failure of the concrete. Scaled tests have indicated that for charge weights as large as 270 pounds of high explosive, direct spalling will not occur at scaled distances greater than approximately four. Future tests are contemplated to determine whether spalling will occur with larger charge weights.

(2) Large adjustments of the donor charge location in a design for the sole purpose of preventing direct spalling is usually not economically feasible.

(3) Although sufficient separation distance between a detonation and an element prevents direct spalling, its effect in reducing scabbing is negligible. A reduction of scabbing is accomplished by limiting the magnitude of the maximum deflection of the element. By reducing this deflection, the strains in the concrete and reinforcement are lowered to a level where tensile failure of the concrete and subsequent scabbed fragment formation is prevented. Scaled tests have indicated that scabbing does not occur when deflections are limited to values less than those corresponding to support rotations of no larger than 5 degrees. To maintain the same response of the element, the resistance-mass product of the element must be increased proportionally to the decrease in deflection, and this capacity (resistance and/or mass) increase results in an increased construction cost.

c. Admixtures.

(1) The use of either chopped steel wire or nylon fibers at least 3 inches in length reduces both direct spalling and scabbing. Additionally, if their use is combined with a separation distance between the concrete element and the donor charge equal to or greater than a scaled distance of 1.5, then direct spalling and scabbing are eliminated.

(2) The admixtures resist spalling by increasing the inherently low tensile capacity of the concrete and reduce scabbing by increasing the strains at which concrete crushing occurs, thereby maintaining the compression restraint over a larger deflection range. The use of these materials in concrete construction is relatively expensive, but new concrete mixing procedures and manufacturing methods of wire and nylon are being developed which will hopefully allow their economical use in the future.

d. Composite Construction.

(1) Direct spalling and scabbing can be eliminated through the use of composite elements composed of two concrete panels (donor and receiver) separated by a sand filled cavity. Spalling of the donor panel is not generally of concern since resulting fragments enter and are trapped in the sand fill. On the other hand, spalling of the receiver panel will endanger the receiver system. By maintaining certain design parameters, both direct spalling and scabbing of the receiver panel can be prevented.

(2) To prevent the occurrence of direct spalling, the high peak blast pressures applied to the donor panel of a composite element must be attenuated by the sand fill. This attenuating capability of the sand is attained by providing: (1) a thickness of the sand fill at least equal to twice the thickness of the donor panel where the panel thickness is predicated upon the required strength to resist the applied loads, (2) for one-way elements a ratio of the cavity thickness to span length not less than 0.25 for cantilevers and 0.05 for elements fixed on two opposite sides shall be used, and for two-way elements each direction (span) shall be considered separately as shown above and the larger cavity thickness used, and (3) the sand density shall not be greater than 85 pounds per cubic foot. Since scabbing is eliminated by limiting the element's deflection, scabbing of composite elements is prevented by limiting the deflection of the receiver panel to the support rotation previously cited.

(3) Figure 7–3 illustrates the use of composite construction to prevent spalling. The magnitude of the donor panel deflection was such that the panel was near incipient failure, the panel experiencing the effects of both direct spalling and scabbing. On the other hand, the deflection of the receiver panel has been limited

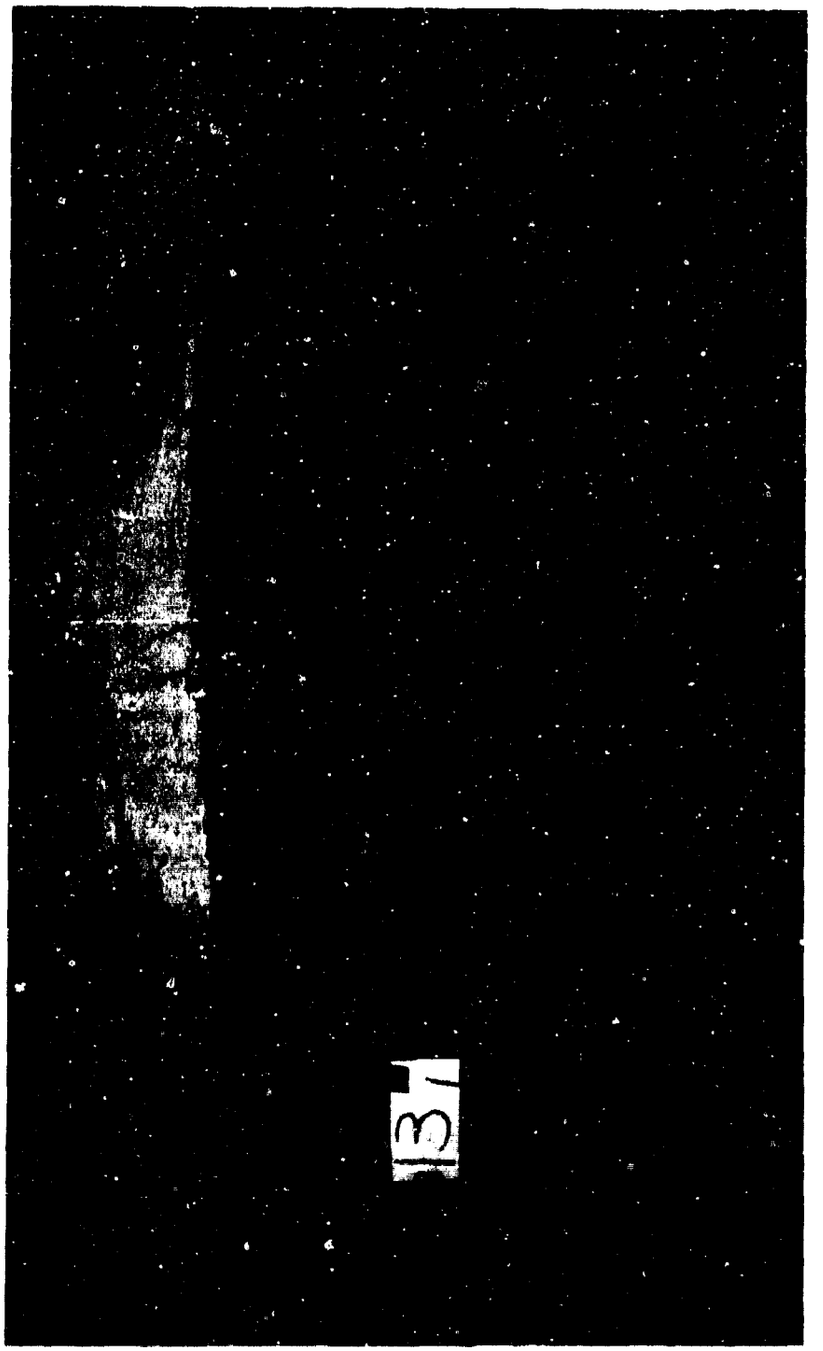


Figure 7–3. Unspalled receiver panel of composite panel.

and therefore had only minor cracking. Direct spalled or scabbed fragments were not formed on the exterior surface of the receiver panel.

(4) The use of composite barriers for the sole purpose of eliminating spalling is not usually economically feasible (chap. 10). However, if the magnitude of the applied blast loads warrant the use of composite construction, then the elimination of spalling can be achieved at a slight increase in cost by conforming to the previously stated element configurations and response.

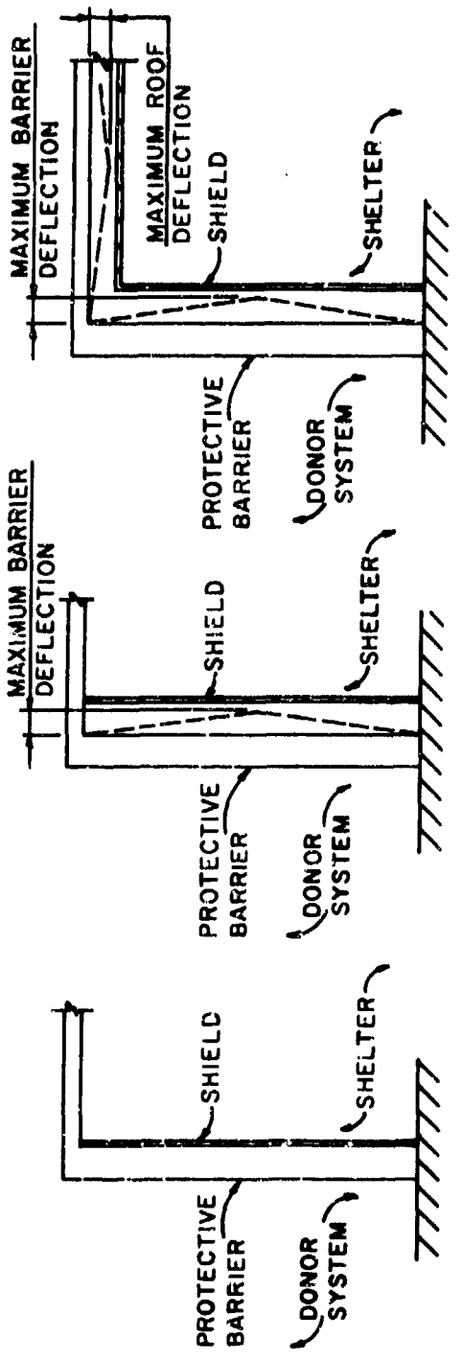


Figure 7-4. Shielding systems for protection against concrete fragments.

e. Fragment Shields.

(1) Fragment shields are composed of steel plates or other structural material which can be attached to, or placed a short distance from, a protective barrier (fig. 7–4). Unlike the other methods, the use of shields does not reduce or deter the formation of spalled fragments but rather confines and prevents them from striking the receiver system.

(2) If the permissible maximum deflection of a barrier is relatively small, then steel plates, blast mats, or other similar material attached rigidly to the barrier may be used to confine the concrete fragments, thus preventing their ejection from the barrier (a, fig. 7–4). It is recommended that for rigidly attached shields the deflection be limited to a value corresponding to an approximate 5-degree support rotation to prevent fail-

se of composite
spalling can be
conforming to
rations and re-

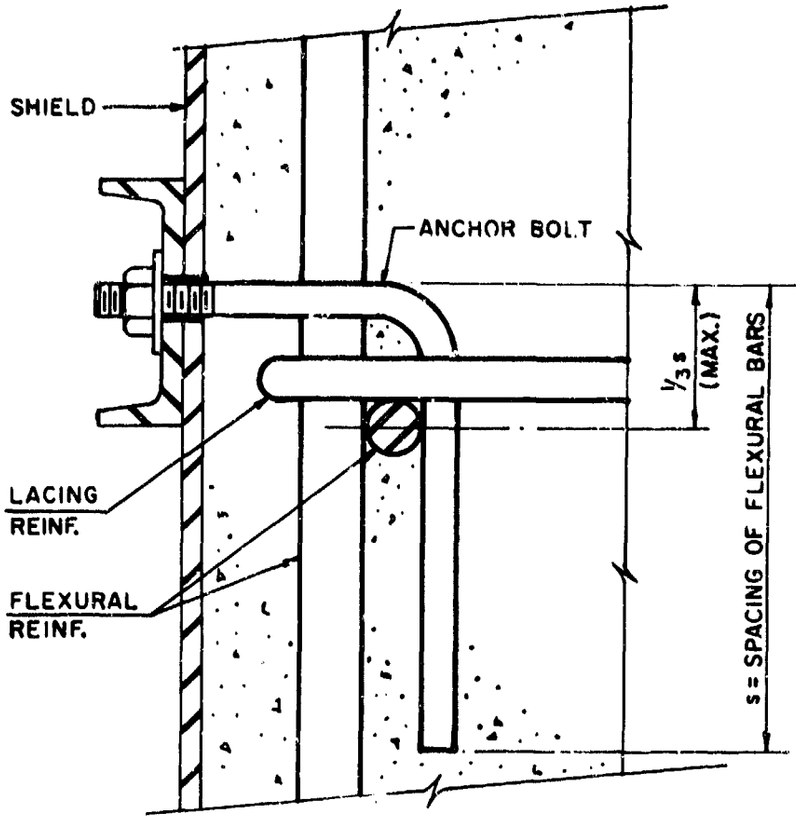


Figure 7–5. Rigid attachment of fragment shield to barrier.

ure of the shield and its connections as a result of excessive straining. The shield and its connections must be designed to resist the overall motion of the barrier. Figure 7–5 illustrates the connection of the shield to the barrier, the shield being anchored by a channel beam and anchor bolt arrangement. The bolts must be hooked around the flexural reinforcement closest to the shield, to prevent disengagement of the bolts from either the spalling of the concrete cover or the direct shock transmission through the bolts from the donor side of the structure.

(3) If the barrier is permitted to attain large deflections (greater than the maximum deflection permitted for personnel protection), then the shields should be separated from the barrier. This distance should be sufficient to eliminate the possibility of impact between the deflecting barrier and shield. Fragment shields separated from the main protective elements and affording protection against spalled fragments from the walls and/or roof are shown in *b*, figure 7–4. The shield may consist of structural steel, reinforced concrete, wood, etc., and must be designed to resist the impact and penetration of the spalled fragments as well as the overall motion of the main protective structure and any leakage pressures which may occur. To design a separated shield, the mass and velocity of the spalled fragments must be determined. As an approximation, an average velocity for all the fragments can be utilized in conjunction with a concrete mass conforming to the depth of the cover over the reinforcement. A parabolic variation of the velocities of the spalled fragments over the element can be assumed. The cost of separated shields may be somewhat more expensive than shields attached directly to the barrier. However, the cost reduction achieved by permitting the larger barrier deflections may offset the increased cost of the separated shield.

Section III. POST-FAILURE CONCRETE FRAGMENTS

7–6. General

a. When a reinforced concrete element is substantially overloaded by the blast output, the element fails and concrete fragments (post-failure) are formed and displaced at high velocities. The type of failure as well as the size and number of the fragments depends upon whether the element has laced or unlaced reinforcement.

b. Failure of an unlaced element (fig. 7–6) is characterized by the disporsal of concrete fragments formed by the cracking and displacement of the concrete between the donor and receiver layers of the reinforcement. As an element deflects and the concrete begins to crush, the compression stresses normally resisted by the concrete are transferred to the reinforcement. With increased deflections, these compression forces tend to buckle the reinforcement outward thereby initiating the rapid disintegration of the element.

c. Laced concrete elements exhibit a different type of failure from unlaced elements, the failure being characterized by reinforcement failures occurring at points of maximum flexural stress (plastic hinges) with the sections of the element between the points of failure remaining essentially intact. When fracture due to excessive straining of the tension reinforcement occurs at the positive yield lines, some small concrete fragments will be formed at the receiver side of the barrier. Quite often if the overload is not too severe, the compression reinforcement at the hinge points does not fail and thereby prevents total disengagement of the sections between the hinges (fig. 7–7). In cubicle type structures where continuous laced and flexural reinforcement is used throughout, failure is sometimes initiated at the positive yield lines where the flexural and lacing reinforcement fail, while at the supports only, the tension reinforcement fails. The intact sections between the failure points rotate with the compression reinforcement at the supports, acting as the mechanical hinges of an analogous swinging door (fig. 7–8). The compression reinforcement at the supports, serving as hinges, produces rotational rather than translational motion of the failed sections, and energy which would ordinarily result in translational velocities is transferred to sections of the structure adjacent to the failed element. In other situations, where there is a larger overloading of the element, the failed sections of the laced element are completely disengaged and displaced from the structure. The translational velocities of these sections are usually less than the maximum velocity of the element at incipient failure.

7–7. Fragment Velocities

a. The velocity of individual fragments of unlaced elements varies and depends upon: (1) the magnitude of the excess impulse defined as the blast impulse minus the flexural impulse capacity of the element (area under the resistance-time curve (a, fig. 7–9)), (2) the mass of the fragment, (3) the location of the fragment prior

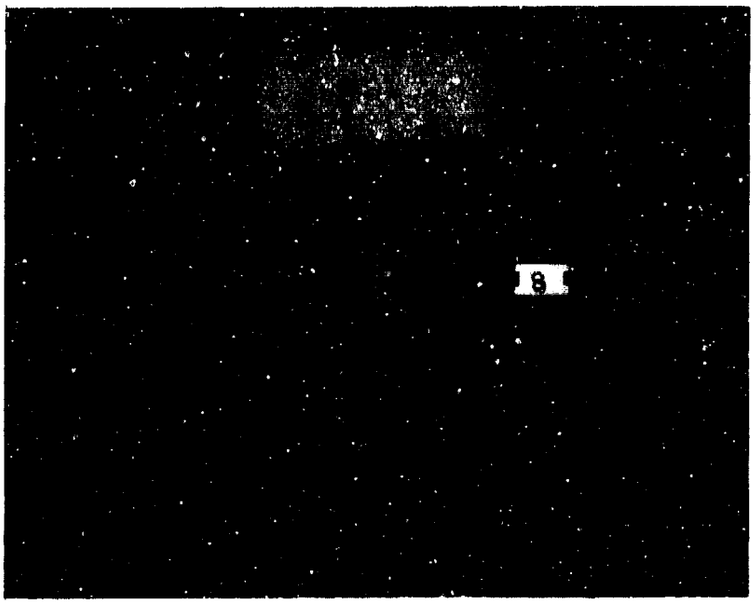


Figure 7–6. Failure of an unlaced element.



Figure 7–7. Failure at plastic hinges of laced element.

to collapse, and (4) the interaction between the fragments during their flight. Although the velocities of individual fragments differ, the average translational velocity v_f (avg) of the debris after complete failure can be approximated from the excess impulse i_e and the unit mass m of the barrier, i.e., the momentum of the wall after collapse is numerically equal to the excess impulse:

$$i_e = mv_f \text{ (avg)} \qquad \textbf{Equation 7–1}$$

b. The maximum fragment velocities obtained from cubicle tests in which concrete rubble was formed from

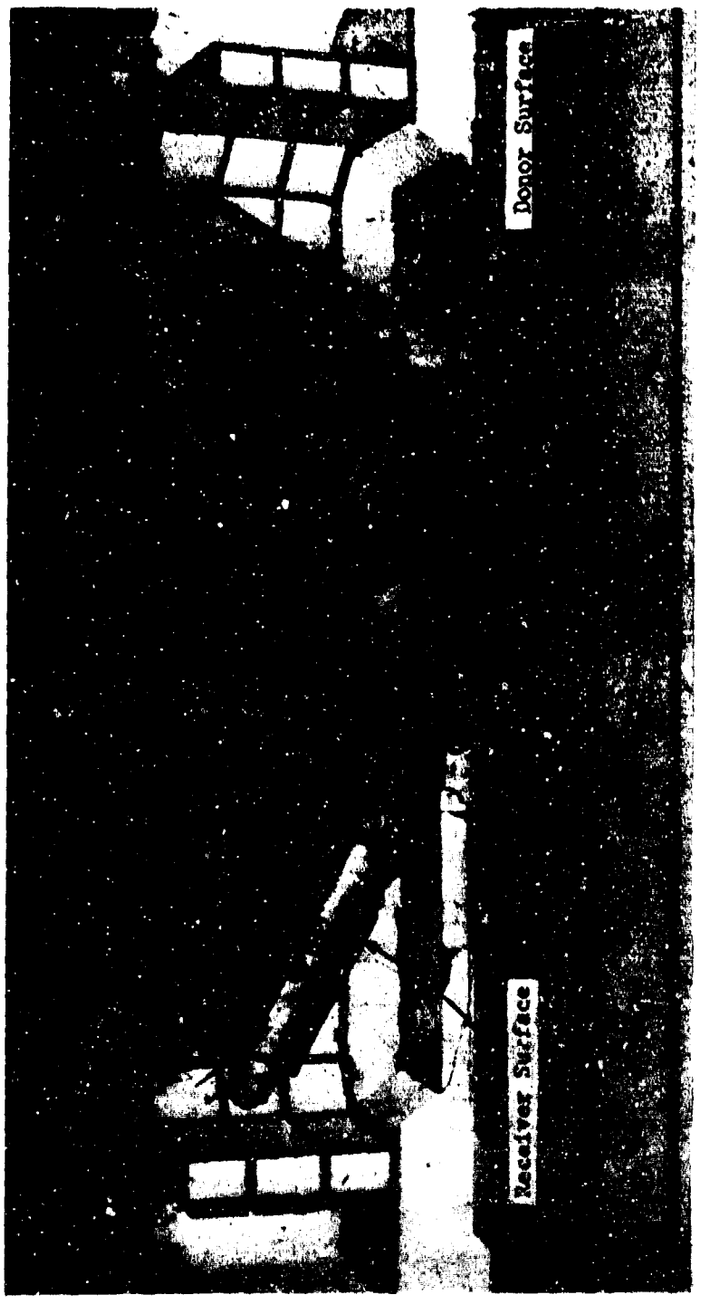


Figure 7-8. Backwall failure of cubicle with laced reinforcement.

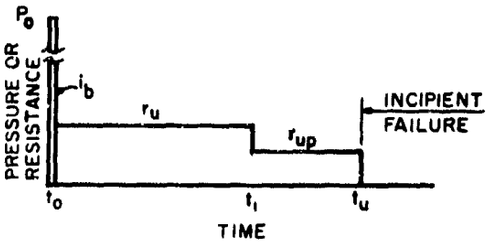
...l to the excess

Equation 7-1

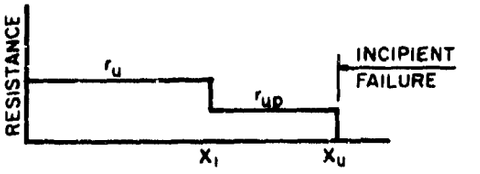
...obtained from

...s formed from

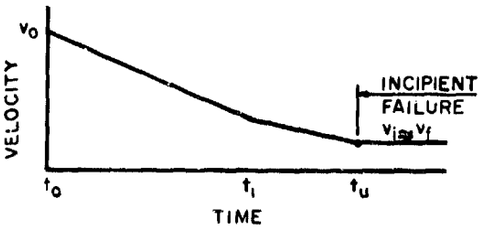
unlaced elements have been compared to the average velocities calculated by the above method. This comparison indicated that the ratio of the calculated velocity v_f (avg), using the impulse loads from chapter 4, to the maximum fragment velocity v_f of the rubble obtained from the test results was equal to 0.206 and 0.485 for side and back walls, respectively. This variation of the ratios for the two walls is probably due to the more uniform blast loads acting on the back wall in comparison to those on the side walls which were more affected by the open surfaces of the structures. These cubicles, which afforded negligible structural resistance



a) IDEALIZED PRESSURE – TIME AND RESISTANCE – TIME CURVES



C) IDEALIZED RESISTANCE - DEFLECTION CURVE



b) IDEALIZED VELOCITY – TIME CURVE

i_b = unit blast impulse
r_u = ultimate unit resistance
r_{up} = post-ultimate unit resistance
t_o = duration of positive phase of blast pressure
t_l = time at which partial failure occurs
t_u = time at which ultimate deflection occurs
v_f = post-failure fragment velocity
v_i = velocity of element at incipient failure
v_o = initial velocity of element
X_l = partial failure deflection
X_u = ultimate deflection

Figure 7–9. Idealized curves for determination of post-failure fragment velocities.

to the blast loads, were three-wall structures with the roof and one wall open and/or frangible. The length to height ratio of the back wall of these cubicles varied from 1.0 to 1.5, while similar dimensions of the side walls were approximately the same as those of the back walls. The size of the cubicles probably had an effect on the ratios of the maximum to average velocities of the fragments. The ratios of the velocities of fragments from cubicles of different size would probably vary from those listed above.

c. As previously mentioned, when laced walls are overloaded, failure occurs at the hinge lines, and the

wall breaks into a small number of large sections. The magnitude of the velocity of each sector immediately before failure varies from a maximum at the point of maximum deflection to zero at the supports, while immediately after failure (total disengagement), the translational velocity is approximately equal to the average velocity of the sector before failure (the average momentum of the element before failure is equal to the average momentum after failure).

d. The variation of the fragment velocity across a section produces tumbling. This tumbling action may result in an acceptor charge which is located close to the barrier being struck by that portion of a failed sector traveling at the highest velocity.

e. The velocity of fragments striking an acceptor charge located some distance from the barrier may be approximated using equation 7–1. In most cases the receiver system will be situated close to the protective barrier, and the design of the structure must consider the maximum fragment velocity. This velocity can be related to the impulse capacity of the element before failure (flexural capacity) and the momentum of the fragments after failure.

7–8. Post-Fragment Impulse Capacity

a. The idealized curves of figure 7–9 illustrate the two-way element which responds to the impulse when the applied blast impulse load is larger than its flexural impulse capacity (area under the resistance-time curve (a. fig. 7–9)). The assumptions made in these curves are the same as those for impulse-sensitive systems (chap. 6) namely: (1) the element prior to being loaded is at rest, and (2) the duration of the applied blast load and the time to reach yield are small in comparison to the time to reach the ultimate deflection and, therefore, have been taken as equal to zero so that the element will respond and reach its maximum velocity (at $t_o = 0$ and $v_o = i_b/m_u$) instantaneously.

b. When the element is designed to remain intact (equal to or less than incipient failure conditions), its velocity at time t_u (deflection X_u) is equal to zero. However, if the element is overloaded, then the velocity just prior to failure is a finite value, the magnitude of which depends upon: (1) the magnitude of the overload, (2) the magnitude of the flexural capacity, and (3) the mass of the element.

c. The analytical relationship which describes the response of a laced element, both in its flexural and post-failure ranges of action, is obtained through a semigraphical solution of Newton's equation of motion similar to that described for incipient failure design in chapter 6.

d. If the areas under the pressure-time and resistance-time curves (a, fig. 7–9) are considered to be positive and negative, respectively, and the velocity of the system before the onset of the load is zero, the summation of the areas at any time divided by the appropriate effective mass for each range is equal to the instantaneous velocity at that time. The velocity v_i at the incipient failure deflection X_u (time, t_u) may be expressed as:

$$v_i = \frac{i_b}{m_u} - \frac{r_u t_1}{m_u} - \frac{r_{up}(t_u - t_1)}{m_{up}} \qquad \textbf{Equation 7–2}$$

where the values of i_b, r_u, r_{up}, t_1, and t_u are defined in figure 7–9 and m_u and m_{up} are the effective masses of the single-degree-of-freedom system in the various flexural ranges (ultimate and post-ultimate) of the two-way element.

e. The expression for the deflection at any time may be found by multiplying each differential area (between the time t_o and the time in question), divided by the appropriate effective mass, by the time which is defined by the distance between the centroid of the area and the time in question, and adding these values algebraically. Using this procedure the expression for the deflection at partial failure (initial failure of a two-way element) at time t_1 is:

$$X_1 = \frac{i_b t_1}{m_u} - \frac{r_u t_1^2}{2m_u} \qquad \textbf{Equation 7–3}$$

while the equation for the deflection at incipient failure at time t_u is given by:

$$X_u = \frac{i_b t_u}{m_u} - \frac{r_u t_1}{m_u}\left[t_u - \frac{t_1}{2}\right] - \frac{r_{up}(t_u - t_1)^2}{2m_{up}} \qquad \textbf{Equation 7–4}$$

f. By solving equations 7–2 through 7–4 simultaneously, the expression for the blast overload impulse capacity of a two-way element, including both the flexural capacity and the post-failure fragment momentum portion of the element's response, is given by:

$$\frac{i_b^2}{2m_u} = r_u X_1 + \left[\frac{m_u}{m_{up}}\right] r_{up}(X_u - X_1) + \frac{m_u v_f^2}{2} \qquad \textbf{Equation 7–5}$$

while the blast overload impulse capacity of a one-way element, or of a two-way element which does not exhibit a post-ultimate range is:

$$\frac{i_b^2}{2m_u} = r_u X_u + \frac{m_u v_f^2}{2} \qquad \textbf{Equation 7–6}$$

Similarly, by solving equations 7–2 and 7–3 simultaneously, the expression for the time at which the ultimate deflection X_u occurs (response time) for a two-way element is given by

$$t_u = \frac{i_b}{r_u} + \left(\frac{m_{up}}{m_u r_{up}} - \frac{1}{r_u}\right)\sqrt{i_b^2 - 2m_u r_u X_1} - \left(\frac{m_{up}}{r_{up}}\right) v_f \qquad \textbf{Equation 7–7}$$

while the time to reach the ultimate deflection X_u for a one-way element, or for a two-way element which

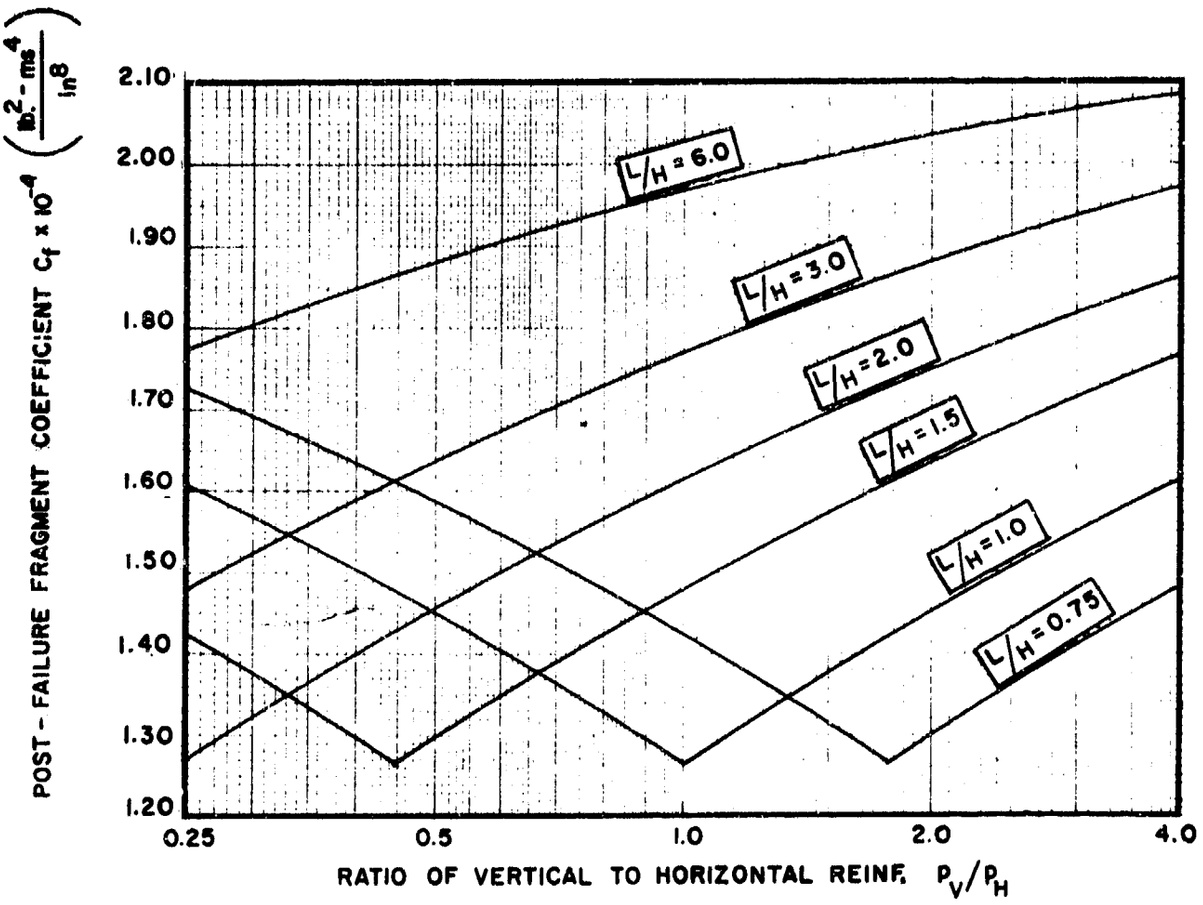


Figure 7–10. Post-failure fragment coefficient C_f for an element fixed on two adjacent sides and two sides free.

does not exhibit a post-ultimate range is:

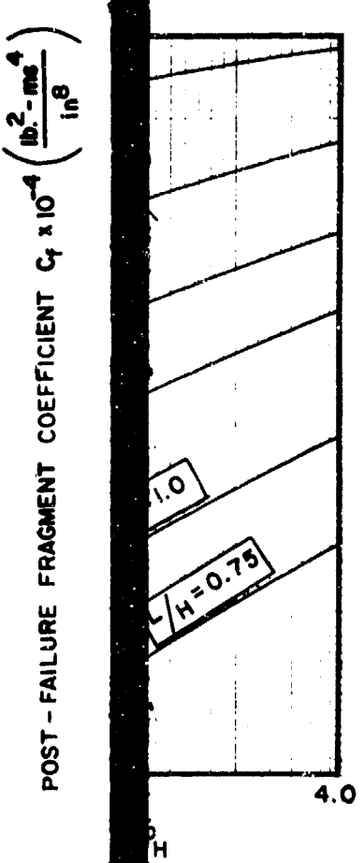
$$t_u = \frac{i_b}{r_u} - \left(\frac{m_u}{r_u}\right) v_f \qquad \textbf{Equation 7–8}$$

g. In the above equations, the maximum velocity of the fragment v_f after failure is assumed to be equal to the maximum velocity of the wall v_i immediately before failure (incipient failure).

h. If equations 7–5 and 7–6 are compared with equations 6–11 and 6–12 of chapter 6, it may be seen that except for the right-hand term in each of the above equations, the corresponding analytical expressions are the same if X_u is substituted for X_m. The additional term in the above equations is the kinetic energy of the fragments after failure. Because of this similarity, equations 7–5 and 7–6 may be expressed in a form which will be a function of the impulse coefficients of chapter 6, post-failure fragment coefficients, the geometry of the element and the applied blast load such that:

$$i_b^2 = C_u \left(\frac{p_H d_c^2 f_{du}}{H}\right) + C_f d_c^2 v_f^2 \qquad \textbf{Equation 7–9}$$

where i_b = applied unit blast impulse



des free.

X_m. The additional
inetic energy of the
is similarity, equa-
d in a form which
fficients of chapter
, the geometry of
ad such that:

Equation 7-9

p_H =
d_c =
f_{fe} =
H =
v_f =
C_u =
C_f = se

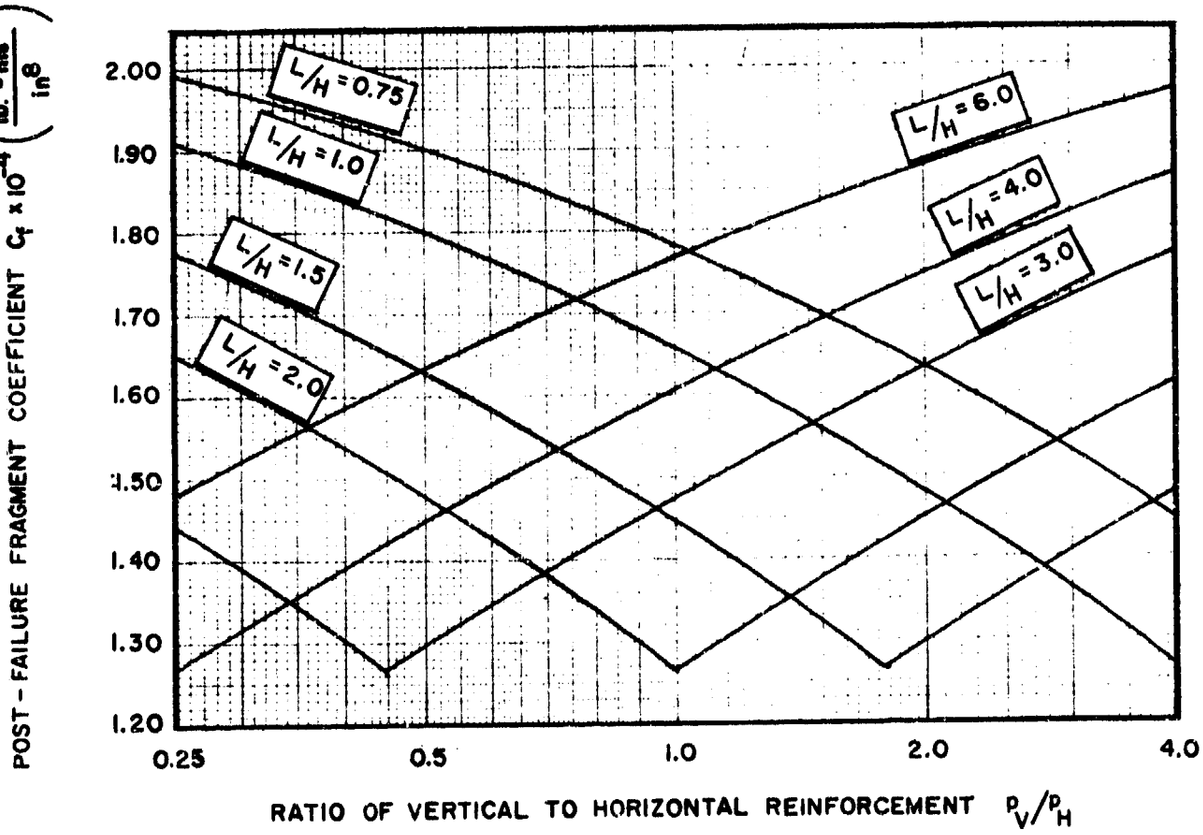


Figure 7-11. Post-failure fragment coefficient C_f for an element fixed on three sides and one side free.

p_H = reinforcement ratio in the horizontal direction
d_c = distance between the centroids of the compression and tension reinforcement
f_{fe} = dynamic design stress for the reinforcement
H = span height
v_f = maximum velocity of the post-failure fragments
C_u = impulse coefficient for ultimate deflection X_u (chap. 6)
C_f = post-failure fragment coefficient

Equation 7-9 is applicable to both one-way and two-way elements which are uniformly loaded. The value of the coefficient C_f is the same for all one-way elements ($C_f = 22{,}500$) whereas the coefficients for two-way elements are given in figures 7-10, 7-11, and 7-12 for elements supported on two adjacent edges, three edges, and four edges, respectively.

j. The optimum arrangement of the flexural reinforcement in two-way elements designed for post-failure fragments will not necessarily be the same as that for similar elements which are designed for incipient failure

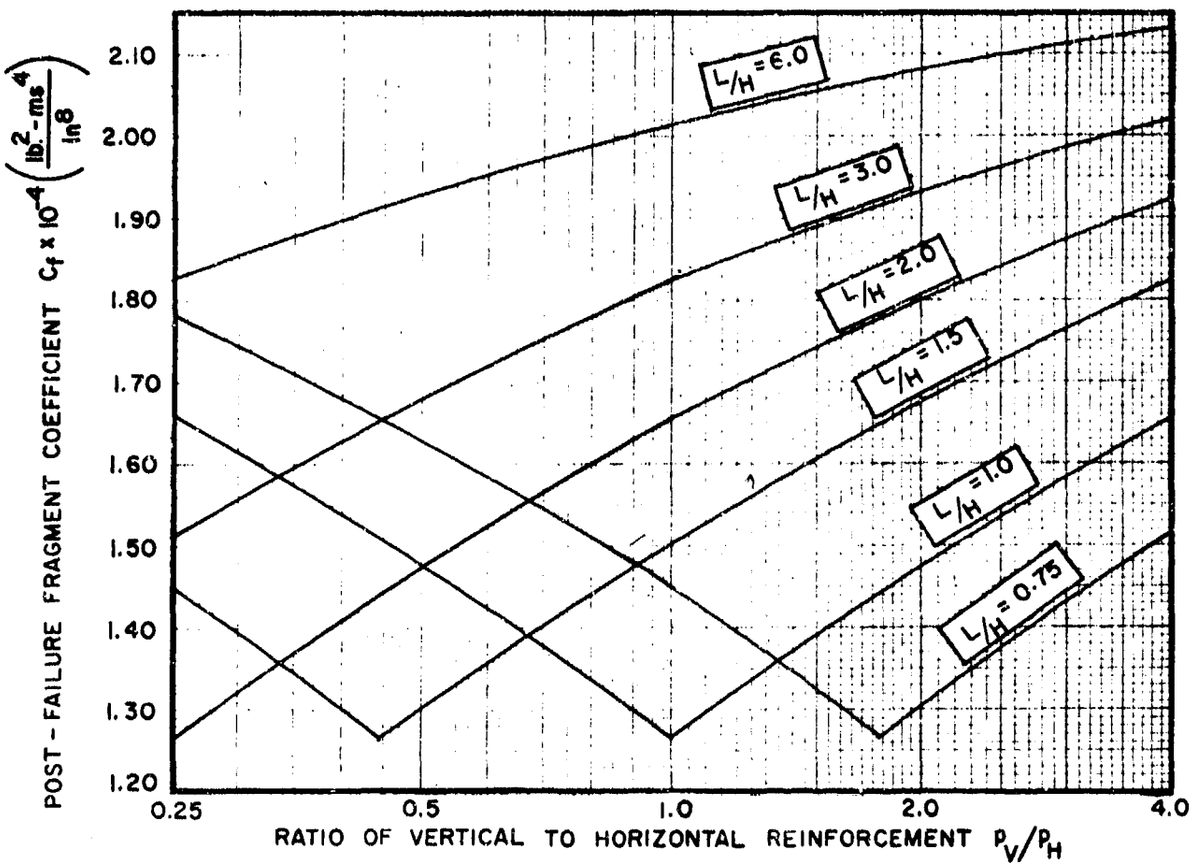


Figure 7-12. Post-failure fragment coefficient C_f for an element fixed on four sides.

damage or less. The optimum ratio of the vertical to horizontal reinforcement will be a function of the amount of the blast impulse absorbed through the flexural action of the element in comparison to that which contributes to the momentum of the post-failure fragments. In a given situation, the designer must obtain by a trial and error procedure the optimum ratio of vertical to horizontal reinforcing steel which will give the maximum impulse absorbed for the least total amount of reinforcement. Unlike the design for incipient failure damage or less, the optimum ratio will vary with a variation in the depth of the element. As explained further in chapter 10, the optimum depth of an element is a function of the individual cost of the concrete and reinforcement.

APPENDIX 7A. STRUCTURAL DESIGN IN THE BRITTLE MODE ILLUSTRATIVE EXAMPLES

PROBLEM 7A-1. BRITTLE MODE - POST-FAILURE FRAGMENTS

Problem: Design an element, which responds to the blast impulse, for controlled post-failure fragments.

Procedure:

Step 1. Establish design parameters:

a. Impulse load and duration (ch. 4).

b Maximum average velocity of post-failure fragments v_f as required by receiver sensitivity (ch. 3).

c. Geometry of element.

d. Support conditions.

e. Materials to be used and corresponding static design strengths (table 5-4).

f. Dynamic increase factors (table 5-3).

Step 2. Determine design stresses for the flexural reinforcement.

$$f_s = \frac{f_y + f_u}{2} \quad \text{and} \quad f_{ds} = (\text{DIF})\, f_s$$

Step 3. Substitute known quantities i_b, f_{ds}, H, v_f into equation 7-9.

Step 4. Obtain optimum ratio of vertical to horizontal reinforcement p_v/p_H for a given wall thickness T_c (graphical solution):

a. Assume value of d_c and substitute into equation obtained in step 3.

b. Complete table shown below by assuming various values of p_v/p_H. For each value of p_v/p_H obtain C_f (figs. 7-10 through 7-12) and C_u (figs. 6-10 through 6-15) given support conditions and calculate p_{ll} (from equation of step 4*a*), p_V (from p_V/p_H ratio) and p_T ($p_V + p_H$).

p_V/p_H	C_f	C_u	p_H	p_V	p_T

a. Plot curve of p_T versus p_V/p_H and read optimum p_V/p_H ratio (lowest p_T).

Note:

For one-way elements, the ratio of the main to secondary reinforcement is always 4 to 1 unless minimum conditions govern (table 5-1). Obtain C_u (table 6-2) for support condition considered and C_f (22,500 - ch. 7).

Step 5. For optimum p_V/p_H ratio determine C_u and C_f and calculate p_H and p_V. Select bar sizes and spacings necessary to furnish required reinforcement (see ch. 9 for limitations).

Step 6. Determine required lacing and diagonal bars. (Procedure is exactly the same as that for elements designed for incipient failure or less - ductile mode - see Appendix 6A).

Step 7. Determine required T_c for assumed d_c, selected flexural and lacing bar sizes, and required concrete cover. Adjust T_c to the nearest whole inch and calculate the actual d_c.

Step 8. Check flexural capacity of element based on either blast impulse or post-failure fragment velocity. Generally, lacing bar sizes do not have to be checked since they are not usually affected by a small change in d_c.

a. Compute actual impulse capacity of the element using equation 7-9 and check with the anticipated blast load. Repeat design (from step 4 on) if the capacity is less than that required.

b. Compute actual post-failure fragment velocity using equation 7-9 and check with value permitted by the receiver sensitivity. Repeat design (from step 4 on) if the actual velocity is greater than that permitted.

Step 9. Determine whether the correct design procedure has been utilized by first computing the response time of the element t_u (time to reach ultimate deflection) from equation 7-7 or 7-8. Then compare the response time t_u with the duration of the blast load t_o. For elements that respond to the impulse $t_m/t_o > 3$.

Note:

To obtain the most economical design, repeat steps 4 through 9 for several wall thicknesses and compare their costs. Percentages of reinforcement can be used to reduce the amount of calculations. In determining the required quantities of reinforcement, lapping of the bars should be considered.

EXAMPLE 7A-1. BRITTLE MODE - POST-FAILURE FRAGMENTS

Required: Design the back wall of the interior cell (fig. 7A-1) of a multicubicle structure for controlled post-failure fragments.

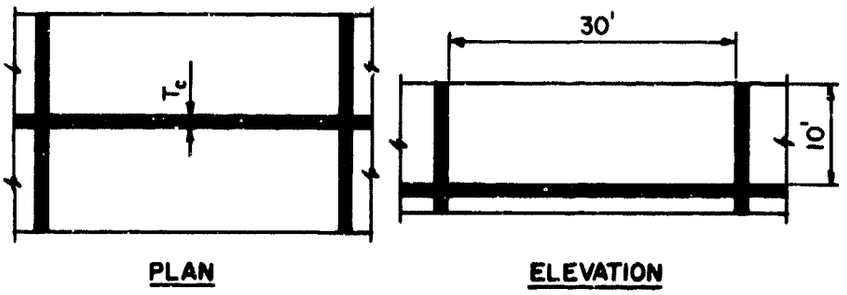


Figure 7A-1

Solution:

Step 1. Given:

a. $i_b = 4{,}800$ psi-ms and $t_o = 4$ ms.

b. $v_f = 100$ fps $= 1.2$ in/ms.

c. $L = 360$ in, $H = 120$ in

d. Fixed on three edges and one edge free.

e. A432 reinf., $f_y = 60{,}000$ psi and $f_u = 90{,}000$ psi.

Concrete, $f'_c = 4{,}000$ psi.

f. For reinf., DIF $= 1.20$ (bending).

Step 2. Design stresses.

$$f_s = \frac{f_y + f_u}{2} = \frac{60{,}000 + 90{,}000}{2} = 75{,}000 \text{ psi}$$

$$f_{ds} = (\text{DIF})\, f_s = 1.20\ (75{,}000) = 90{,}000 \text{ psi}$$

Step 3.

$$i_b^2 = C_u \left[\frac{p_H\, d_c^3\, f_{ds}}{H}\right] + C_f\, d_c^2\, v_f^2 \quad \text{(eq. 7-9)}$$

$$(4800)^2 = \frac{C_u\, p_H\, d_c^3\ (90{,}000)}{120} + C_f\, d_c^2\ (1.2)^2$$

$$23.04 \times 10^6 = 750\, C_u\, p_H\, d_c^3 + 1.44\, C_f\, d_c^2 \quad \text{(eq. 7A-1)}$$

Step 4. Assume $d_c = 21$ in. and substitute into equation 7A-1.

$$23.04 \times 10^6 = 750\, C_u\, p_H\, (21)^3 + 1.44\, C_f\, (21)^2$$

therefore:

$$p_H = \frac{23.04 \times 10^6 - 635\, C_f}{6.95 \times 10^6\, C_u} \quad \text{(eq. 7A-2)}$$

b. Determine the required percentages of reinforcement for various values of p_V/p_H (see table below).

$\frac{p_V}{p_H}$	144 $C_u \times 10^{-4}$ (1) psi-ms^2/in^2	$C_f \times 10^{-4}$ (2) lb-ms^4/in^8	p_H %	p_V %	p_T %
1.0	5.34	1.475	0.530	0.530	1.060
1.2	5.88	1.517	0.472	0.566	1.038
1.4	6.42	1.553	0.425	0.595	1.020
1.6	6.93	1.583	0.388	0.621	1.009
1.8	7.45	1.608	0.356	0.642	0.998
1.9	7.73	1.620	0.342	0.650	0.992
2.0	7.93	1.632	0.331	0.662	0.993
2.1	8.13	1.642	0.321	0.674	0.995
2.2	8.32	1.652	0.312	0.687	0.999
2.4	8.72	1.670	0.295	0.708	1.003
2.6	9.10	1.688	0.280	0.728	1.008
2.8	9.48	1.702	0.267	0.748	1.015
3.0	9.87	1.717	0.255	0.765	1.020

(1) From figure 6-14

(2) From figure 7-11

a. Plot curves of p_T versus p_V/p_H (fig. 7A-2). Read optimum $p_V/p_H = 1.92$ (lowest p_T).

p_T (%)

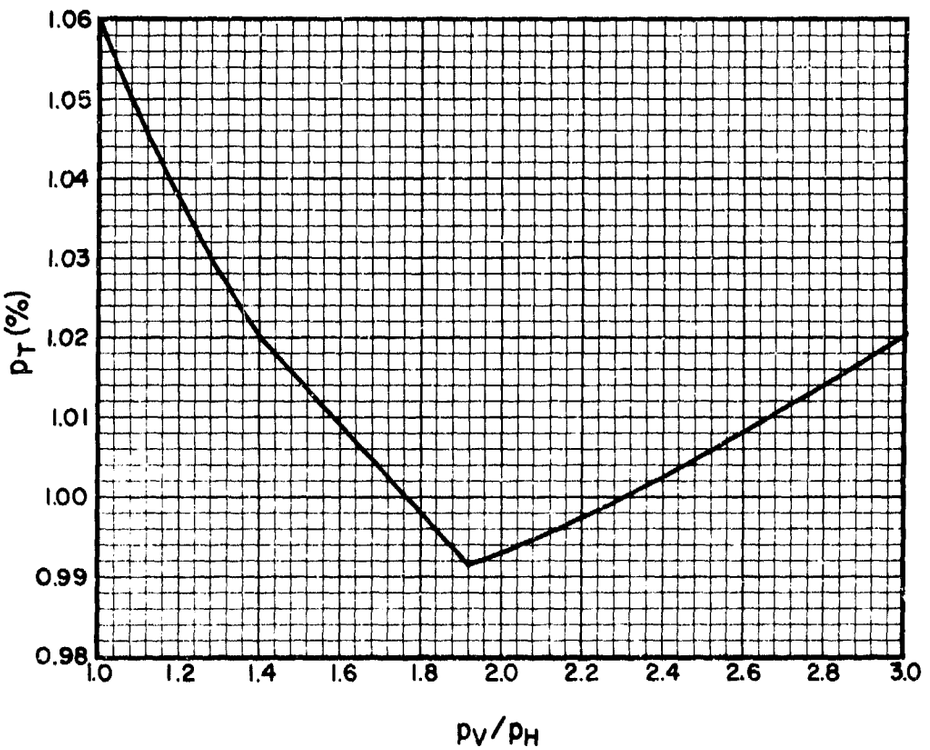


Figure 7A-2. Determination of optimum ratio of p_V/p_H

Step 5. For optimum $P_V/P_H = 1.92$ S

From figure 6-14, $C_u = \frac{7.77 \times 10^4}{144}$

From figure 7-11, $C_f = 1.623 \times 10^4$

$$P_H = \frac{\left[23.04 \times 10^6 - 635\left(1.623 \times 10^4\right)\right](144)}{(6.95 \times 10^6)(7.77 \times 10^4)}$$

$$= 0.00339$$

$$P_V = \frac{P_V}{P_H} P_H = 1.92\ (0.00339) = 0.00651$$

$A_{sH} = 0.00339\ (12)(21) = 0.854\ in^2/ft$, use #8 @ 11 ($A_s = 0.86$)

$A_{sV} = 0.00651\ (12)(21) = 1.64\ in^2/ft$, use #11 @ 11 ($A_s = 1.70$)

Actual $\frac{P_V}{P_H} = \frac{A_{sV}}{A_{sH}} = \frac{1.70}{0.86} = 1.977$

Step 6. Using lacing method No. 3, No. 7 vertical lacing bars are required. (Calculations are not shown since they are similar to those presented in appendix 6A for incipient failure design. Also, the remainder of the design for shear will not be shown).

Step 7. The actual d_c depends upon the details of the base of the wall (region of vertical lacing).

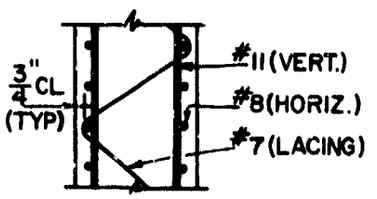


Figure 7A-3

Cover - 2 x 0.75 = 1.50

Lacing - 2 x 0.875 = 1.75

Horiz. - 2 x 1.00 = 2.00

Vert. - 1.41 = 1.41

6.66 in S

$T_c = d_c + 6.66 = 21 + 6.66 = 27.66$ in., use 28 in

...actual $d_c = 28 - 6.66 = 21.34$ in

Step 8.

a. Actual impulse capacity.

For $\frac{p_V}{p_H} = 1.977$, $C_u = \frac{7.87 \times 10^4}{144}$

$C_f = 1.63 \times 10^4$

$d_c = 21.34$ in, $p_H = \frac{0.86}{12(21.34)}$

$$i_c^2 = C_u \left[\frac{p_H d_c^3 f_{ds}}{H}\right] + C_f d_c^2 v_f^2$$

$$i_c^2 = \frac{(7.87 \times 10^4)(0.86)(21.34)^2 (9 \times 10^4)}{144 (12 \times 21.34)(120)} + (1.63 \times 10^4)(21.34)^2 (1.2)^2$$

$$i_c^2 = 24.07 \times 10^6$$

$i_c = 4{,}910$ psi-ms $> i_b = 4{,}800$ psi-ms

b. Actual post-failure fragment velocity.

$$i_b^2 = C_u \left[\frac{p_H d_c^3 f_{ds}}{H}\right] + C_f d_c^2 v_f^2$$

$$(4800)^2 \quad \frac{(7.87 \times 10^4)(0.86)(21.34)^3 (9 \times 10^4)}{(144)(12)(21.34)(120)} + (1.63 \times 10^4)(21.34)^2 v_f^2$$

$v_f =$ ... 1.2 in/ms = 100 fps

Step 9. Response time of element t_u:

$M_{VN} = M_{VP}$ and $M_{HN} = M_{HP} = A_{sH} f_{ds} d_c/b$

$$M_H = \frac{(0.86)(90{,}000)(21.34)}{12} = 137{,}640 \text{ in-lbs/in}$$

2

$$\frac{L}{H}\left[\frac{p_v}{p_H}\right]^{\frac{1}{2}} = \left(\frac{360}{120}\right)(1.977)^{\frac{1}{2}} = 4.22$$

From figure 5-10,

$x/L = 0.333$

$x = 0.333(360) = 120$ in

$r_u = \frac{5(M_{HN} + M_{HP})}{x^2}$ for $x \leq L/2$ (table 5-6)

$r_u = 5(2)(137,640)/(120)^2 = 95.8$ psi

$m = 225\ d_c = 225\ (21.34) = 4802$ psi-ms^2 / in

$K_{LM} = 0.567$ (fig. 6-5)

$m_u = 0.567\ (4802) = 2723$ psi-ms^2 / in

$x = 120 = H$ ∴All supports fail simultaneously and there is no post-ultimate range, that is, $r_{up} = 0$.

Therefore, use eq. 7-3, $t_u = \frac{i_b}{r_u} - \left(\frac{m_u}{r_u}\right) v_f$

$t_u = \frac{4800}{95.8} - \left(\frac{2723}{95.8}\right)\ (1.14) = 17.7$ ms

$\frac{t_m}{t_o} = \frac{17.7}{4.0} = 4.43 > 3$ ∴correct procedure has been used.

CHAPTER 8

STRUCTURAL BEHAVIOR TO PRIMARY FRAGMENT IMPACT

Section I. INTRODUCTION

8–1. Fragment Characteristics

Detonation of contained explosives results in the formation of primary fragments due to the shattering of the casing. These fragments are usually small in size and initially travel at velocities in the order of thousands of feet per second. Upon contact with a barrier, the fragments will either pass through (perforate), be embedded in, or be deflected by the structural element. The occurrence of any one of the three element behaviors is dependent on: (1) The magnitude of the initial velocity v_o of the fragments, (2) distance between the explosion and element, (3) the angle at which the fragment strikes the wall (angle of obliquity), and (4) the physical properties of the fragment (mass, shape, and material strength) and the element (strength, thickness, dimensions, etc.).

8–2. Velocity and Impact Limitations

This chapter deals with the situation where the fragment striking velocity may be assumed equal to its initial velocity, and the angle of obliquity between the fragment trajectory path and the surface of the element is 90 degrees (normal impact). The procedures presented, however, are applicable to other angles of obliquity and to situations where the variation between the initial and striking velocities may not be neglected. Refer to section III, chapter 4, for a discussion of primary fragment velocities.

Section II. FRAGMENT IMPACT ON CONCRETE

8–3. General

a. When a primary fragment strikes a concrete barrier, penetration resisting pressures, in the order of thousands of psi, act on the cross-sectional area of the fragment. As the striking velocity is increased, the resisting pressures also increase, while for an increase in cross-sectional area of the fragment, the resisting pressures decrease. If the fragment can withstand these pressures acting on its frontal surface, then the amount of penetration will be governed by its mass, shape, and striking velocity. On the other hand, if the fragment deforms under the applied loads, then the resisting pressures of the concrete become effective over an increased cross-sectional area, thereby reducing the possible penetration for a given available kinetic energy of the fragment. Generally, larger penetrations may be expected with less ductile metals such as fragments from armor-piercing casings.

b. As a fragment impinges on a wall surface, a section of the wall adjacent to the point of impact spalls, forming a crater around the impact area (fig. 8–1). This crater is conical in shape but irregular. As the striking velocity of the fragment increases, the size of the crater also increases. At small velocities, the increase in the crater size for a given velocity increment is more rapid than at higher velocities in the order of several thousand feet per second. At a striking velocity of approximately a thousand feet per second or less, the fragment does not usually penetrate beyond the depth of the crater, while for larger velocities, the fragment penetrates beyond the front of the crater and either lodges within or passes through the barrier.

c. A crater similar to that formed on the front face of the barrier is also produced on the back side if the kinetic energy of the fragment upon impact is sufficient to produce excessive tensile stresses in the concrete. As in the case of the front-face crater, the size of the crater on the back face increases with an increase in striking velocity of a particular fragment. The back-face crater is generally wider and shallower than the front-face crater, though again the surface of the crater is irregular. Quite often, the kinetic energy afforded by the striking fragment is only sufficient to dislodge the concrete on the exterior side of the rear face reinforcement. In this case, only spalling will occur. As the striking velocity is increased beyond the limit to cause spalling, the penetration of the fragment into the slab increases more and more until perforation is attained.

8–4.

a.

analo
accun
the el
struct
develc
into c
the p
and th

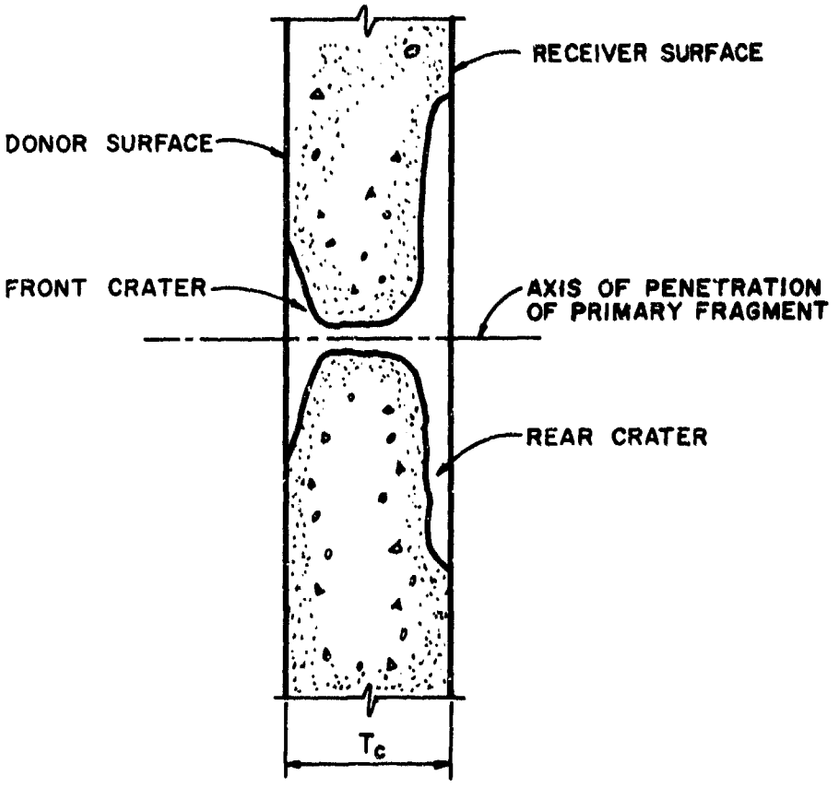


Figure 8–1. Perforation and spalling of concrete due to primary fragments.

8–4. Penetration of Armor-Piercing Fragments

a. A certain amount of experimental data, which is analogous to primary fragment penetration, has been accumulated in connection with projects to determine the effects of bomb and projectile impact on concrete structures. This data was analyzed and relationships developed where the amount of fragment penetration into concrete elements could be expressed in terms of the physical properties of both the metal fragment and the concrete. The general expression for the maximum penetration X_f of an armor-piercing fragment with a shape as indicated in figure 8–2 was derived in terms of the fragment weight W_f and striking velocity v_s:

$$X_f = 0.162(10^{-3}) W_f^{0.4} v_s^{1.8} \qquad \textbf{Equation 8–1}$$

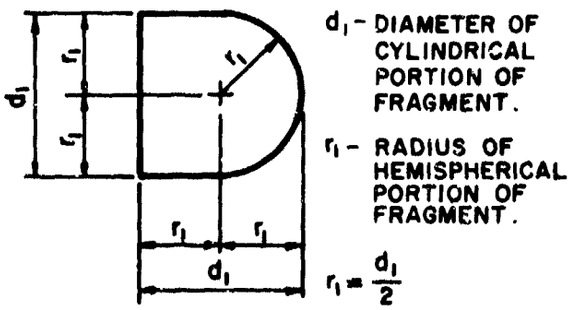


Figure 8–2. Shape of primary fragment.

b. Equation 8–1 is based on a concrete compression strength f_c' equal to 5,000 psi. Maximum penetrations of fragments in concrete of other strengths may be obtained by multiplying the value of X_f of equation 8–1 by the square root of the ratio of 5,000 psi to the compressive strength of the concrete in question. Figure 8–3 is a plot of the maximum penetration through 5,000 psi concrete for various fragment sizes and striking velocities.

c. In addition to the weight and striking velocity of a primary fragment, its shape will also affect the penetration ability. The sharper the leading edge of a fragment, the greater the distance traveled through the concrete. The shape indicated in figure 8–2 is not necessarily the most critical. When the container of an explosive shatters, it is statistically probable that some of the resulting fragments will have a shape that is sharper than the bullet shape assumed in this manual. However, the number of these sharper fragments is

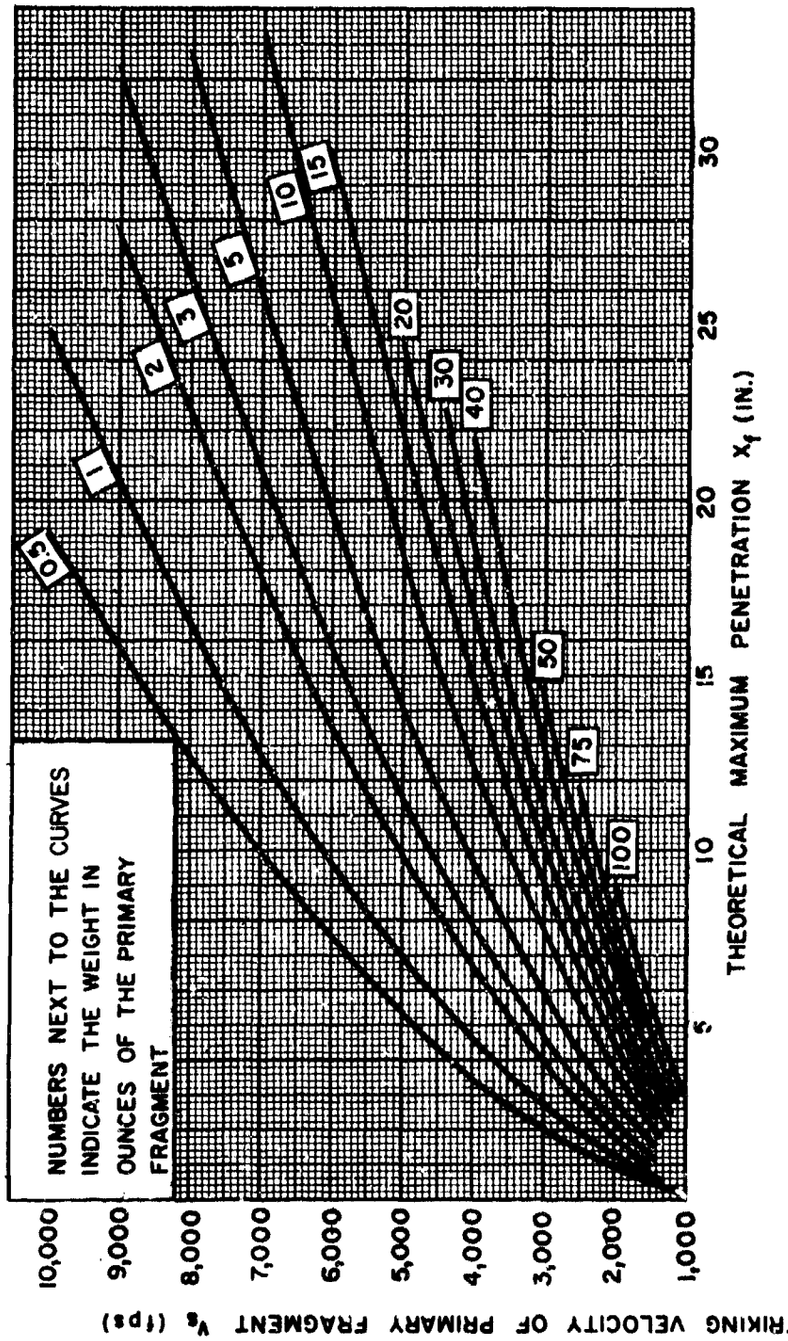


Figure 8-3. Fragment penetration through concrete.

usually very small in comparison to the total number formed, and the probability that these sharper fragments will have normal penetrations through the concrete is low. In most instances, the majority of the primary fragments will have a more ragged and blunter shape than that shown. Therefore, for design purposes, the normal penetrations defined for a bullet-shaped fragment can usually be assumed as critical.

d. Quite often the magnitude of the initial kinetic energy of primary fragments will be large enough to produce perforation of the concrete. The limiting thickness of concrete at which perforation will occur can be

obtained f
coefficient
and maxim
c_e of the el

$c_e = 5.1$

and the mo
in chapter

e. Fragn

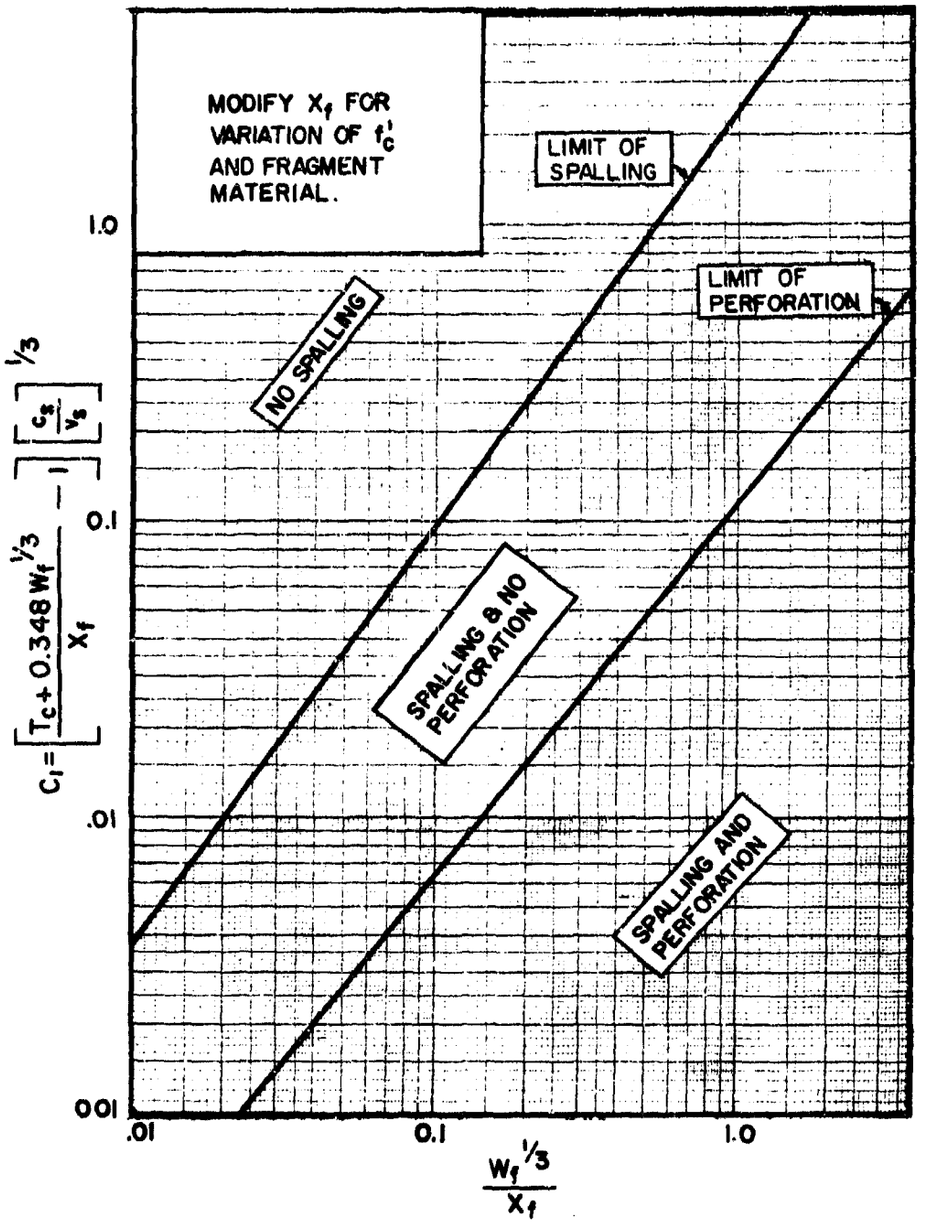


Figure 8-4. Limits of concrete spalling and perforation.

obtained from figure 8-4 and is a function of the coefficient C_1, the fragment weight, striking velocity, and maximum penetration and the dilatational velocity c_s of the elastic wave through concrete where:

$$c_s = 5.16E_c^{1/2} \qquad \textbf{Equation 8-2}$$

and the modulus of elasticity of concrete E_c is as defined in chapter 5.

e. Fragments which perforate a concrete element will have a residual velocity v_r which may endanger the receiver system. The magnitude of this velocity may be approximated from the expression which defines the velocity of the fragment at any time as it penetrates the concrete:

$$(v_r/v_s)^{1/2} = 1 - \frac{T_e}{X_f} \qquad \textbf{Equation 8-3}$$

where T_e is the finite thickness of an element, the

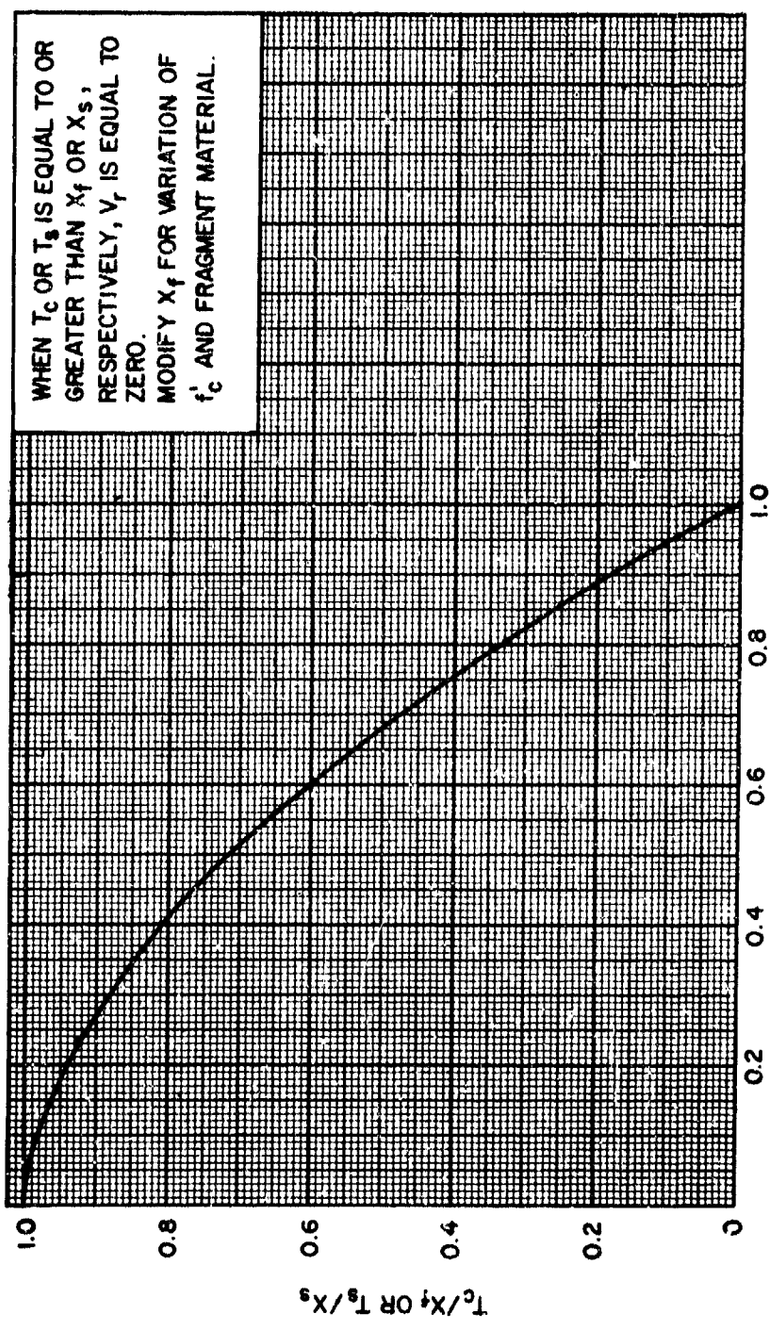


Figure 8–5. Residual velocity of primary fragment after perforation.

magnitude of which is equal to, or less than, the maximum penetration of a fragment into an infinitely thick element and v_r is the residual velocity of the fragment as it leaves the finite element. A plot of the ratio v_r/v_s against T_c/X_f or T_s/X_s is given in figure 8–5.

8–5. Penetration of Fragments Other than Armor-Piercing

To estimate the concrete penetration of metal fragments other than armor-piercing, a procedure has been devel-

oped where the concrete penetrating capabilities of armor-piercing fragments have been related to those of other metal fragments. This relationship is expressed in terms of relative metal hardness (the ability of the metal to resist deformation) and density, and is represented by the constant k in equation 8–4:

$$X_f' = kX_f \qquad \text{Equation 8–4}$$

where X_f' is the maximum penetration in concrete of metal fragments other than armor-piercing fragments. The numerical values of k for several of the more common casing metals are listed below:

Type of metal	*Constant k*
Armor-piercing steel	1.00
Mild steel	0.70
Lead	0.50
Aluminum	0.25

8–6. Spalling Due to Fragment Impact

a. When a primary fragment traveling at a high velocity strikes the donor surface of a concrete barrier, large compression stresses are produced in the vicinity of the point of impact. These stresses form a compressional wave which travels from the impact point, expanding spherically as it travels, until it reaches the receiver side of the structure. At this free surface, the compression wave is reflected (reversed in direction and magnitude). When the stresses in the resulting tension wave exceed the stresses in the incident compression wave plus the tensile capacity of the concrete, spalling of the concrete at the receiver surface occurs. The spalling forms the previously mentioned crater on the receiver surface. This crater and, therefore, the spalling do not usually penetrate beyond the reinforcement at the receiver surface.

b. The occurrence of spalling is a function of the fragment penetration, i.e., the fragment must penetrate an element of a given thickness a distance such that sufficiently large stresses are formed at the receiver surface to produce spalling. If the thickness of the element is increased above that at which spalling occurs for a particular fragment with a given penetration, then the spalling is eliminated (fig. 8–4). On the other hand, concrete spalling always occurs with fragment perforation.

c. The secondary fragment velocities associated with spalling resulting from fragment impact are usually small (less than 5 fps). However, when blast pressures are also involved, the magnitude of the resulting velocities can be quite large. The secondary concrete fragments will be accelerated by the motion of the element resulting in velocities in the order of several hundred feet per second.

d. Because of the potentially large secondary fragment velocities associated with primary fragment impact, full protection is usually required for personnel, valuable equipment, and sensitive explosives. This protection may be accomplished either by providing sufficient concrete thickness to eliminate spalling or by other mechanical means used to minimize the effects of spalling resulting from blast pressures as described in chapter 7. The required concrete thickness to eliminate spalling caused by primary fragment impact may be obtained from figure 8–4.

Section III. COMPOSITE CONSTRUCTION

8–7. General

a. To evaluate the effect of primary fragments on composite (concrete-sand-concrete) barriers, the penetration of the fragment through both the concrete and sand must be considered.

b. For damage to be sustained at the rear of a composite barrier, a fragment must first perforate both the donor concrete panel and the sand, and then penetrate or perforate the receiver panel. If the fragment penetrates only part way through the receiver panel, then spalling may or may not occur, depending on the panel thickness. Conversely, fragment perforation of the receiver panel means perforation of the entire barrier.

8–8. Penetration of Composite Barriers

a. To determine the degree of damage at the receiver side, the penetration of the fragment in each section of the barrier must be investigated in sequence. Starting with the striking velocity and the weight of the primary fragment, the donor concrete section is first analyzed to determine whether or not perforation of the section occurs. If the calculations indicate that the fragment will stop within this section, then no damage will be sustained by the remainder of the barrier. On the other hand, if perforation does occur in the forward (donor) section, then the fragment penetration through the sand must be investigated.

b. The amount of the penetration through the sand depends upon the magnitude of the residual velocity as the fragment leaves the rear of the donor panel. This residual velocity is determined from figure 8–5 utilizing the striking velocity, the thickness of the donor panel, and the theoretical maximum fragment penetration obtained from figure 8–3. The maximum penetration X_s through the sand is obtained from figure 8–6, using the residual velocity calculated above as the striking velocity of the fragment on the surface of the sand. If the penetration in the sand is found to be less than the thickness of the sand layer, no damage is sustained at the rear surface of the barrier. In case of perforation, the penetration of the fragment through the rear section (receiver) of the barrier is governed by the residual velocity as the fragment leaves the sand. This residual velocity is calculated in a manner similar

to that used for computing the residual velocity for the donor panel (fig. 8–5), except that the fragment penetration and striking velocity are those associated with movement of the fragment through the sand.

c. Similar to the fragment penetration through the donor panel and sand, penetration of the fragment through the receiver panel is a function of the magnitude of the fragment velocity as the fragment strikes the forward surface of the panel. This velocity is equal to the residual velocity as the fragment leaves the sand. Once the penetration in the receiver panel is known, then the damage sustained at the rear of the composite barrier can be defined in terms of either spalling or fragment perforation.

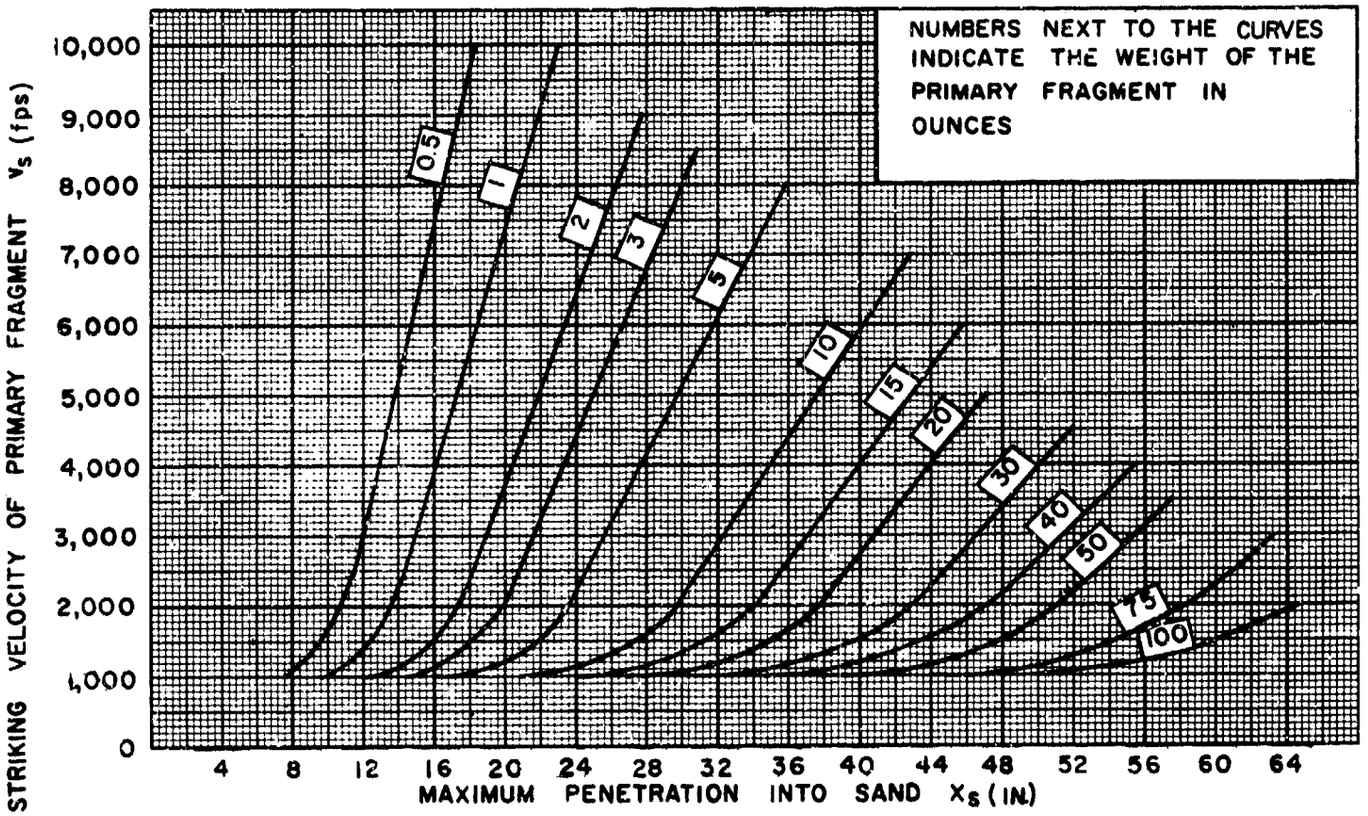


Figure 8–6. Fragment penetration through sand.

APPENDIX 8A. PRIMARY FRAGMENTS ILLUSTRATIVE EXAMPLES

PROBLEM 8A-1. MAXIMUM PENETRATION

Problem: Determine the maximum penetration (embedment or perforation) of a primary metal fragment into a concrete wall.

Procedure:

Step 1. Determine the type, weight W_f, and the striking velocity v_s of the primary fragment. Also, the thickness of the concrete wall T_c and the ultimate compressive strength of concrete f'_c must be known.

Step 2. Determine the maximum penetration X_f from figure 8-3 for the values of W_f and v_s in step 1 where X_f in figure 8-3 is for 5,000 psi concrete and armor- piercing steel fragments.

Step 3. To obtain the maximum penetration in concrete of metal fragments other than those of armor-piercing steel X'_f, use

$$X'_f = kX_f \quad \text{(eq. 8-4)}$$

Obtain k from paragraph 8-5.

Step 4. To determine penetration through concrete other than 5,000 psi ultimate strength, multiply either X_f or X'_f by

$$\sqrt{5{,}000 / f'_c \text{(in question)}}$$

Note:

If X_f (modified for fragment material and/or concrete strength) is less than T_c, embedment will occur; if X_f (modified) is greater than T_c, perforation will take place.

EXAMPLE 8A-1. MAXIMUM PENETRATION

Required: Maximum penetration (embedment or perforation) of a primary fragment into a concrete wall.

Solution:

Step 1. Type of metal: mild steel
Primary fragment weight: W_f = 30 ounces
Striking velocity: v_s = 4,200 fps
Thickness of wall: T_c = 18 in
Ultimate concrete compressive stress: f'_c = 4,000 psi

Step 2. For W_f = 30 oz and v_s = 4,200 fps:
X_f = 20.4 in (fig. 8-3)

Step 3. For mild steel fragment:
k = 0.70 (para. 8-5)
X'_f = 0.70 (20.4) = 14.3 in

Step 4. Actual maximum penetration = $14.3\sqrt{\frac{5,000}{4,000}}$ = 16.0 in

Since T_c = 18 in. is greater than 16.0 in, embedment occurs.

PROBLEM 8A-2, DETERMINATION OF THE OCCURRENCE AND EFFECTS OF PERFORATION

Problem: Determine the residual velocity of a primary fragment if it perforates a concrete wall.

Procedure:

Step 1. Determine the type, weight W_f, and striking velocity v_s of the primary fragment. Also, the thickness of the concrete wall T_c and the ultimate compressive stress f'_c of the concrete must be known.

Step 2. Proceed through steps 2, 3, and 4 of problem 8A-1. If the maximum penetration is greater than T_c, perforation will occur.

Step 3. If perforation is not indicated by the calculations in step 2, then discontinue the analysis. If perforation does result, then compute the value of T_c/X_f where X_f is modified for fragment material and/or concrete strength.

Step 4. Utilizing the value of T_c/X_f, obtain v_r/v_s from figure 8-5.

Step 5. With the use of the values for v_s and v_r/v_s of steps 1 and 4, calculate the residual velocity v_r.

EXAMPLE 8A-2. DETERMINATION OF THE OCCURRENCE AND EFFECTS OF PERFORATION

Required: Residual velocity of a primary fragment if it perforates a concrete wall.

Solution:

Step 1. Type of metal: mild steel

Primary fragment weight: W_f = 20 ounces

Striking velocity: v_s = 4,700 fps

Thickness of wall: T_c = 12 in

Ultimate concrete compressive stress: f'_c = 4,500 psi

Step 2. For given conditions:

X_f = 22.0 in (fig. 8-3)

k = 0.70 (para. 8-5)

X'_f = 0.70(22.0) = 15.4 in.

Actual maximum penetration = $15.4 \sqrt{\frac{5,000}{4,500}}$ = 16.2 in.

Since T_c = 12 in. is less than 16.2 in, perforation occurs.

Step 3.

T_c/X_f (actual) = 12/16.2 = 0.741

Step 4.

$$v_r/v_s = 0.475 \quad \text{(fig. 8-5)}$$

Step 5.

$$v_r = 0.475\ v_s$$

$$v_r = 0.475\ (4{,}700) = 2{,}230 \text{ fps}$$

PROBLEM 8A-3. DETERMINATION OF THE OCCURRENCE OF SPALLING

Problem: To determine if spalling of a concrete wall occurs if there is no perforation by the primary fragment.

Procedure:

Step 1. Determine the type, weight W_f, and striking velocity v_s of the primary fragment. Also, the thickness of the concrete wall and the ultimate compressive stress of the concrete f'_c must be known.

Step 2. Proceed through steps 2, 3, and 4 of problem 8A-1. If the maximum penetration is less than T_c, then embedment of the fragment will occur. For the values of W_f and X_f, compute $W_f^{1/3}/X_f$. The value of X_f is modified for fragment material and/or f'_c.

Step 3. Compute the dilatational velocity,

$$c_s = 5.16\ E_c^{\frac{1}{2}} \quad \text{(eq. 8-2)}$$

where the modulus of elasticity of concrete E_c is given by

$$E_c = w^{1.5}\ 33\sqrt{f'_c} \quad \text{(eq. 5-20)}$$

and w is the unit weight of concrete.

Step 4. For the values of T_c, W_f, X_f (modified), c_s, and v_s determine the value of

$$C_1 = \left(\frac{T_c + 0.348\ W_f^{1/3}}{X_f} - 1\right)\left(\frac{c_s}{v_s}\right)^{1/3}$$

Step 5. Plot C_1 versus $W_f^{1/3}/X_f$ on figure 8-4. If the point falls between the two lines, then spalling will occur. If the point falls left of the left hand line, then spalling will not occur.

EXAMPLE 8A-3. DETERMINATION OF THE OCCURRENCE OF SPALLING

Required: Determine if spalling of a concrete wall occurs due to penetration by a primary fragment.

Solution:

Step 1. Type of metal: armor-piercing steel

Primary fragment weight: $W_f = 40$ ounces

Striking velocity: $v_s = 3{,}000$ fps

Thickness of wall: $T_c = 14$ in.

Ultimate concrete compressive stress: $f'_c = 5{,}000$ psi

Step 2. For given conditions:

$X_f = 12.8$ in (fig. 8-3)

$k = 1.00$ (para. 8-5) $\therefore X'_f = X_f$

No correction for f'_c is necessary

Since $T_c = 14$ in. is greater than 12.8 in, embedment occurs.

$$\frac{W_f^{1/3}}{X_f} = \frac{(40)^{1/3}}{12.8} = 0.267$$

Step 3. Determine the dilatational velocity.

$$E_c = w^{1.5}\, 33\sqrt{f'_c}$$

$$E_c = (145)^{1.5}\,(33)\sqrt{5{,}000} = 4.08 \times 10^6 \text{ psi}$$

$$c_s = 5.16\ E_c^{\frac{1}{4}} = 5.16\sqrt{4.08 \times 10^6} = 10{,}420 \text{ fps}$$

Step 4.

$$C_1 = \left(\frac{T_c + 0.348\, W^{1/3}}{X_f} - 1\right)\left(\frac{c_s}{v_s}\right)^{1/3}$$

$$C_1 = \left(\frac{14 + (0.348)(40)^{1/3}}{12.8} - 1\right)\left(\frac{10{,}420}{3{,}000}\right)^{1/3} = 0.283$$

Step 5. The point $W_f^{1/3}/X_f = 0.267$ and $C_1 = 0.283$ on figure 8-4 falls between the two lines, therefore, spalling occurs.

PROBLEM 8A-4. DETERMINATION OF THE EFFECTS OF A PRIMARY FRAGMENT ON A COMPOSITE WALL

Problem: Determine the maximum penetration of a primary fragment into a composite wall and the resulting effects on the donor panel, sand layer, and receiver panel.

Procedure:

Step 1. Determine the type, weight W_f, and striking velocity v_s of the primary fragment. Also the thicknesses of the concrete donor panel T_c (donor), the sand layer T_s, and the concrete receiver panel T_c (receiver) and the ultimate compressive stress f'_c of the concrete must be known.

Step 2. Proceed through steps 2, 3, and 4 of problem 8A-1. If embedment of the fragment in the donor panel occurs, compute $W_f^{1/3}/X_f$ and perform steps 3, 4, and 5 of problem 8A-3 to determine if spalling takes place.

If perforation of the donor panel occurs, compute $T_c(\text{donor})/X_f$ and perform steps 4 and 5 of problem 8A-2 to find the residual velocity v_r.

Step 3. Utilizing v_r (donor) as the v_s of the sand layer and W_f, obtain X_s from figure 8-6.

If X_s is less than T_s, the fragment is embedded in the sand layer and the analysis is discontinued.

If X_s is greater than T_s, perforation of the sand occurs.

Step 4. Compute T_s/X_s if perforation results. Use this value and figure 8-5 to obtain v_r/v_s.

Step 5. With v_c and v_r/v_s of the sand layer, calculate v_r (sand).

Step 6. Utilizing v_r (sand) as the v_s of the receiver wall and W_f, obtain X_f (receiver) from figure 8-3. Proceed through steps 3 and 4 of problem 8A-1 if necessary.

If embedment of the fragment in the receiver panel occurs, compute $W_f^{1/3}/X_f$ (receiver) and perform steps 3, 4, and 5 of problem 8A-3 to determine if spalling takes place.

If penetration of the receiver wall occurs, compute T_c (receiver) and perform steps 4 and 5 of problem 8A-2 to find v_r.

If embed-
pute $W_f^{1/3}/X_f$
termine if

T_c(donor)/X_f
he residual

and W_f,

n the sand

occurs.

lue and

(sand).

l and W_f,
ugh steps

ccurs, com-
5 of

T_c
to find v_r.

EXAMPLE 8A-4. DETERMINATION OF THE EFFECTS OF A PRIMARY FRAGMENT ON A COMPOSITE WALL

Required: Maximum penetration of a primary fragment into a composite wall and the resulting effects on the donor panel, sand layer, and the receiver panel.

Solution:

Step 1. Type of metal: armor-piercing steel

Primary fragment weight: W_f = 20 ounces

Striking Velocity: v_s = 4,500 fps

Thicknesses: T_c (donor) = 12 in

T_s = 24 in

T_c (receiver) = 12 in

Ultimate concrete compressive stress: f'_c = 5,000 psi

Step 2.

X_f = 20.2 in (fig. 8-3)

k = 1.00 (para. 8-5) $X'_f = X_f$

No correction for f'_c is necessary.

Since T_c (donor) = 12 in. is less than 20.2 in, perforation of the donor wall occurs.

T_c (donor) / X_f = 12/20.2 = 0.594

v_r/v_s = 0.600 (fig. 8-5)

v_r (donor) = 0.600 (4500) = 2,700 fps

Step 3. For v_s (sand) = 2,700 fps

X_s = 39.6 in (fig. 8-6)

Since T_s = 24 in. is less than 39.5 in, perforation of the sand layer will occur.

Step 4.

$$T_s/X_s = 24/39.5 = 0.607$$

$$v_r/v_s = 0.595 \quad \text{(fig. 8-5)}$$

Step 5.

$$v_r = 0.595\ v_s$$

$$v_r \text{ (sand)} = 0.595\ (2{,}700) = 1{,}606 \text{ fps}$$

Step 6. For v_s (receiver) = 1,606 fps

$$X_f \text{ (receiver)} = 3.4 \text{ in} \quad \text{(fig. 8-3)}$$

$$k = 1.00 \quad \therefore X_f' \text{ (receiver)} = X_f \text{ (receiver)}$$

No correction for f_c' is necessary.

T_c (receiver) is greater than 3.4 in, therefore, fragment is embedded in receiver panel.

$$W_f^{1/3}/X_f \text{ (receiver)} = (20)^{1/3}/3.4 = 0.799$$

$$E_c = w^{1.5}(33)\sqrt{f_c'}$$

$$E_c = (145)^{1.5}\ (33)\ \sqrt{5{,}000} = 4.08 \times 10^6 \text{ psi}$$

$$c_s = 5.16\ E_c^{\frac{1}{2}} = 5.16\ \sqrt{4.08 \times 10^6} = 10{,}420 \text{ fps}$$

$$C_1 = \left(\frac{T_c \text{ (receiver)} + 0.348\ W_f^{1/3}}{X_f \text{ (receiver)}} - 1 \right) \left(\frac{c_s}{v_s} \right)^{1/2}$$

$$C_1 = \left(\frac{12 + 0.348\ (20)^{1/3}}{3.4} - 1\right)\ \left(\frac{10,420}{1,606}\right)^{1/3} = 5.24$$

The point $W_f^{1/3}/X_f$ (receiver) = 0.799 and C_1 = 5.24 plotted on figure 8-4 falls left of the left-hand line, therefore, spalling will not occur.

CHAPTER 9

CONSTRUCTION DETAILS AND PROCEDURES

Section I. LACED REINFORCED CONCRETE CONSTRUCTION

9–1. General

a. The major portion of the detailing and construction procedures required for structures designed to resist the blast output of high-explosive detonations is the same as required for structures designed conventionally. However, some differences do exist and neglecting them would result in an unsafe situation since the structure would not act as assumed in the design. This chapter describes these differences in construction with particular attention directed towards the construction of structures subjected to close-in blast effects.

b. Laced reinforced concrete elements are usually used in those facilities which are designed to resist the explosive output of close-in detonations (high-intensity pressures with short durations). The functional requirements of these facilities (storage and/or manufacture of explosives) normally dictate the use of one-story concrete buildings with austere architecture. Basically, these structures consist of a series of interconnecting structural elements (walls, floor slabs, and/or roofs) forming several compartments or cubicles. Because of this cubicle arrangement, the walls separating the individual areas are the predominant element used in laced construction and are the most critical component in the design. However, in some cases, the roof and/or floor slab can be of equal importance.

c. Although the construction of laced reinforced concrete structures is similar to conventional structures, some changes in the fabrication and construction procedures are required to insure full development of both the concrete and the reinforcement well into the range of plastic action of the various elements. Since these changes primarily affect the reinforcement rather than the concrete, the major portion of the following discussion pertains to reinforcing steel details.

9–2. Concrete

a. The dynamic characteristics and high magnitude of the applied blast loads require the strength of the concrete used in laced concrete construction to be higher than that required for conventional construction. Because of the flexural action of laced elements where large deflections are required and the high pressures associated with impulse loadings, it is recommended that a minimum concrete strength of 3,000 psi be used.

b. The properties and testing of the concrete materials (cement, aggregate, water) used in laced reinforced concrete construction are the same as those normally used and should conform to the standards specified in the ACI Building Code. High early-strength Portland cement (type III) may be used. To minimize the effects of spalling, it is recommended that the size of the aggregate used be not greater than 1 inch. This limitation of the aggregate size also facilitates the placement of the concrete, particularly where the cover over the reinforcement is held to a minimum. In all cases, the minimum concrete cover should conform to that specified in the ACI Building Code and, wherever possible, should also be the maximum thickness of the concrete cover.

c. Because of the presence of the lacing reinforcement in addition to the large amounts of flexural reinforcement, the concrete slump used is usually larger than that permitted for conventional construction. A concrete slump of 4 to 6 inches is recommended for laced elements to insure that concrete voids do not occur.

d. Wherever possible, both horizontal and vertical construction joints should be avoided. A wall whose height is equal to, or less than, 10 feet usually can be poured without a horizontal joint. On the other hand, good construction techniques and economy may require the use of horizontal joints for higher walls. These joints should be located at points of low stress intensity. A more detailed discussion of joint locations is given later in this chapter.

9–3. Flexural Reinforcement

a. All laced concrete elements (fig. 9–1) must be reinforced in two mutually perpendicular directions. In any one direction the reinforcement should be continuous and must be symmetrical (equal tension and compression steel). All flexural reinforcement should consist of straight bars, and bends in the reinforcing within the span of an element should be avoided. However, the reinforcement may be bent well within the element's supports when additional anchorage is required.

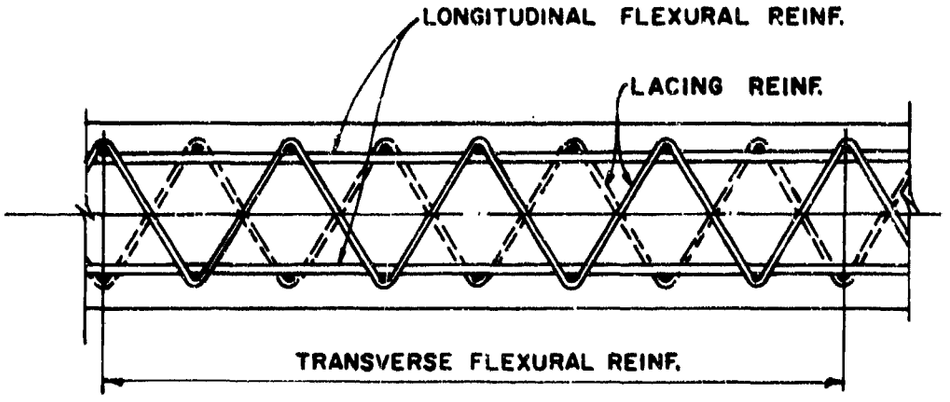


Figure 9–1. Laced reinforced element.

b. The spacing of flexural bars is governed by the required area of the reinforcing steel, the selected bar size and, as discussed later, the spacing required to achieve a working and economical arrangement of the lacing steel. In general, flexural bars should be spaced fairly close together to insure that the cracked concrete between the layers of reinforcement will not be dislodged from the wall. Tests have indicated that a maximum spacing of approximately 15 inches will insure confinement of the concrete.

c. Because of their reduced ductility, reinforcing steel larger than No. 11 bars (No. 14S and 18S) should not be used as flexural reinforcement in laced elements. Also, the size of the flexural steel should be at least equal to a No. 4 bar. Where necessary, the area of steel normally furnished by the special large bars should be provided by bundling smaller bars. However, the use of these bundled bars should be limited to one direction only for any laced element. If bundled bars are used in an element whose main span is between two opposite supports, then all bars of each bundle should be continuous across the full span. On the other hand, if the main span is between a support and a free edge, then bundled bars may be cut off at points of reduced stress. At least one bar in each bundle should be continuous across the full span. For two-way elements these cutoffs must be located beyond the positive yield line with sufficient anchorage to develop the bars.

d. Continuous reinforcement should be used in laced elements, but in many cases this is a physical impossibility. Therefore, splicing of the reinforcement is necessary. Splices should be located in regions of reduced stress and their number held to a minimum by using the longest reinforcing bars practical (bars 60 feet in length are generally available throughout the country). Tests have indicated that the preferable method of splicing flexural reinforcement in laced concrete elements is by lapping the reinforcing bars. The length of each lap should be at least equal to 40 diameters of the larger of the two bars spliced, but not less than 2 feet (usually the same size bars will be spliced). In addition, splices of adjacent parallel bars should be staggered to prevent the formation of a plane of weakness. Figure 9–2 illustrates typical splicing patterns for both single and bundled bars.

e. Mechanical splices may also be used, but they must be capable of developing the ultimate strength of the reinforcement without reducing its ductility. If the bar deformations have to be removed in the preparation of these splices, grinding rather than heat should be employed since heat can alter the chemical properties thereby changing the physical properties of the steel and possibly reducing the capacity of the element. Welding of the reinforcement should be prohibited unless it can be determined that the combination of weld and reinforcing steel will not result in a reduction of the ultimate strength and ductility. In those cases where welding is absolutely essential, it may be necessary to obtain special reinforcement manufactured with controlled chemical properties.

9–4. Lacing Reinforcement

a. All flexural reinforcing bars must be tied with continuous diagonal lacing bars (fig. 9–1). At any particular section of an element, the longitudinal or main tension and compression reinforcement is placed to the interior of the transverse or secondary flexural reinforcing steel around which the diagonal lacing bars are bent.

b. Lacing reinforcement must be fabricated without the formation of excessive stress concentrations at the bends. The bending should be performed without the use of heat, and in no case should the radius of the pin used to bend the lacing be less than three times the diameter of the bar. Figure 9–3 illustrates the typical lacing bends used with both single and bundled flexural bars.

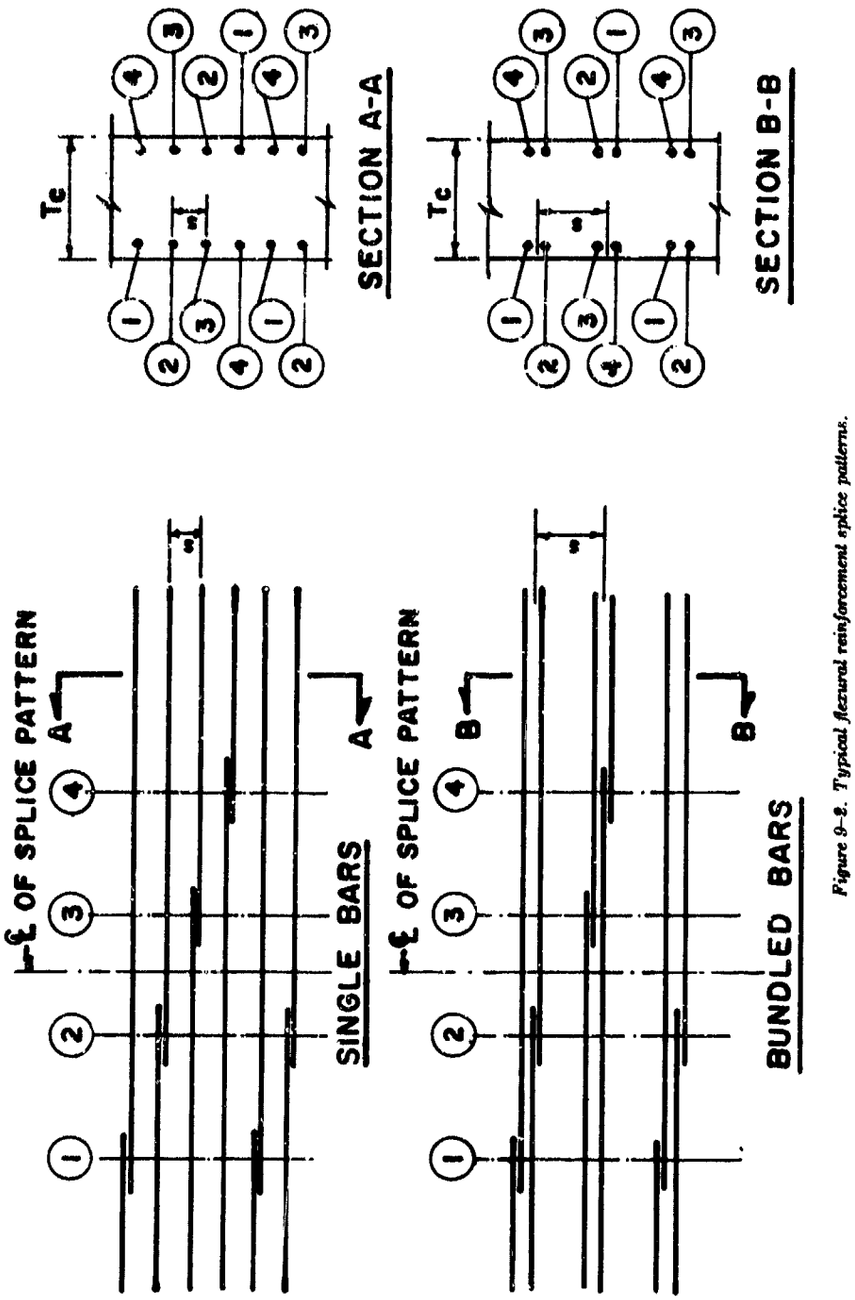


Figure 9-2. Typical flexural reinforcement splice patterns.

c. The amount of lacing reinforcement required in an element depends upon the element's capacity (quantity and distribution of flexural reinforcement, thickness of the element, and the type and number of supports) while the size of the lacing bars is a function of the required area and spacing. The maximum and minimum size of the lacing bars should be that specified by No. 8 and No. 3 bars, respectively. Several lacing schemes have been developed (fig. 9–4) which avoid excessive stress concentrations as a result of large angular bends, provide adequate restraint against buckling of the compression reinforcement, and make use of the most efficient arrangement of the lacing reinforcement (lacing making an angle of 45 degrees with the longitudinal reinforcement is most efficient). In these schemes, the transverse flexural reinforcement may or may not be tied at every intersection with a longitudinal bar. However, a grid system is established whereby bar intersec-

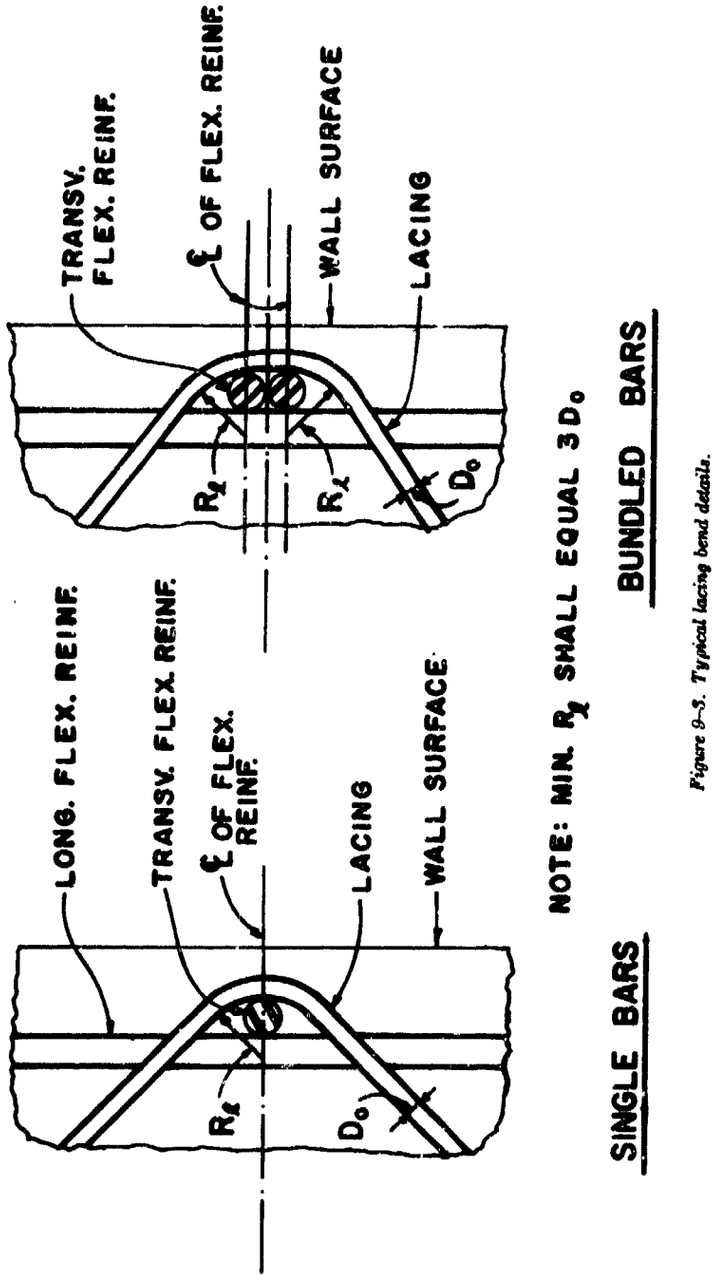
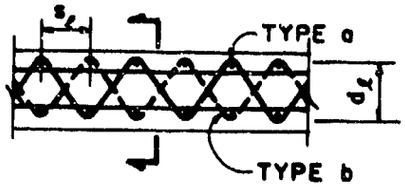


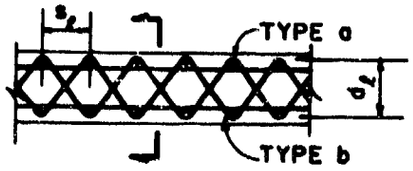
Figure 9–3. Typical lacing bend details.

tions are tied within a distance s_l or 2 feet, whichever is less. The choice of the scheme to be used depends upon the flexural bar spacing and the thickness of the element so that the angle α is approximately equal to, but never less than, 45 degrees. Although not tying every transverse flexural bar results in a larger lacing bar size, the total cost of the lacing may be reduced since the size of the lacing bend associated with an increase in the spacing s_l reduces the overall length of the bar and the number of bends required to cover a given longitudinal distance.

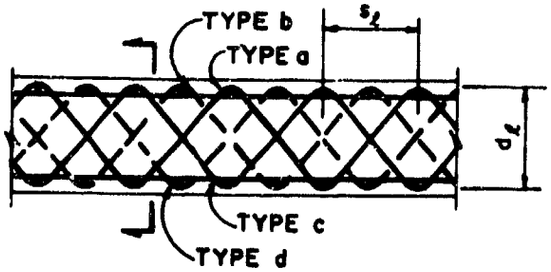
d. An additional cost saving in the fabrication of the lacing may be realized by utilizing the equipment that is used to bend the steel bars for open web steel joists. However, when detailing the flexural and lacing reinforcement and the concrete wall thickness, consideration must be given to the physical capabilities (size of bend and bar, depth of lacing, etc.) of the equipment.



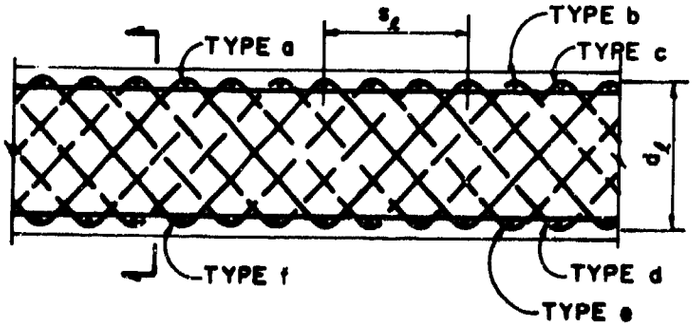
LACING METHOD NO.1



LACING METHOD NO.2



LACING METHOD NO.3



LACING METHOD NO.4

LONGITUDINAL SECTION

Figure 9-4. Typical methods of lacing.

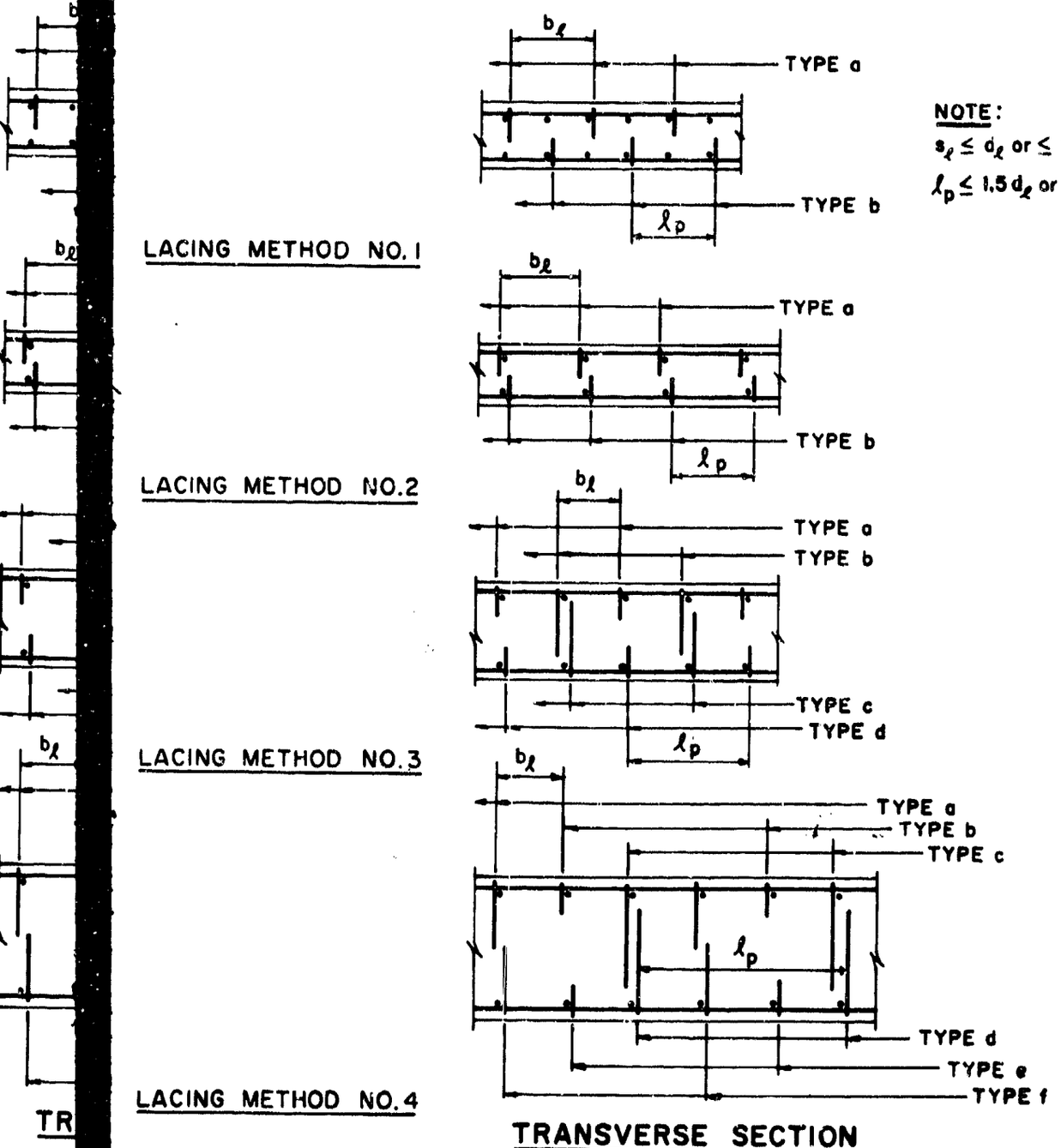
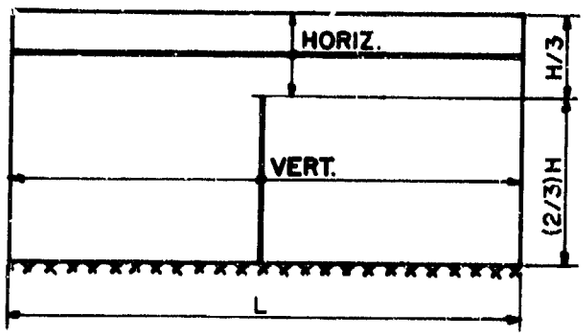
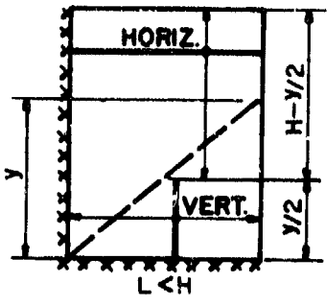


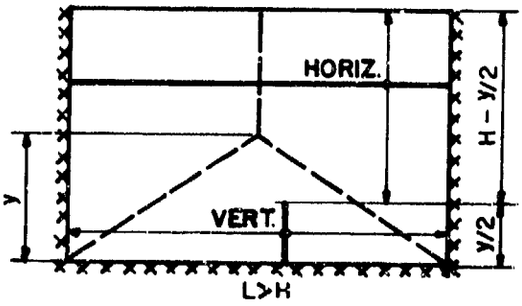
Figure 9-4. Typical methods of lacing.

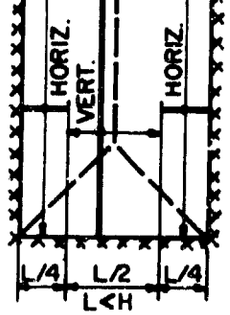


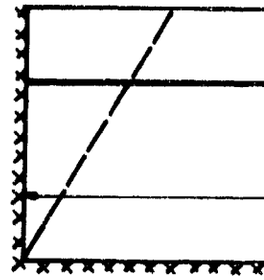
a) CANTILEVER



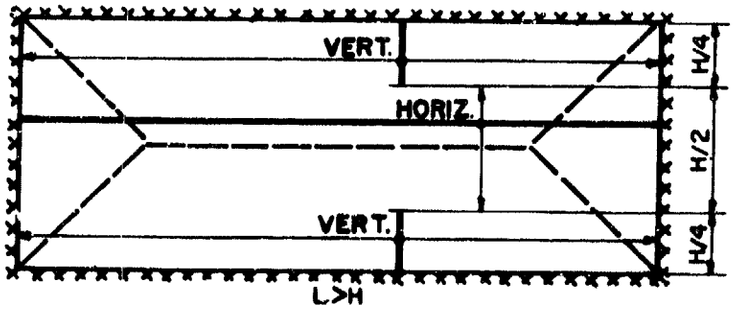
b) TWO ADJACENT SIDES SUPPOR





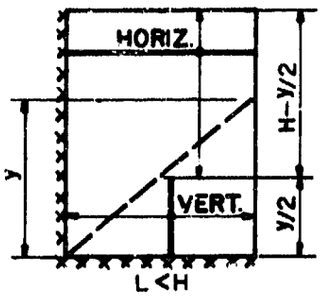


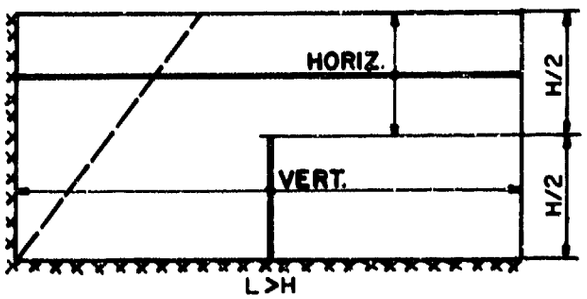
c) THREE SIDES SUPPORTED AND ONE SIDE FREE



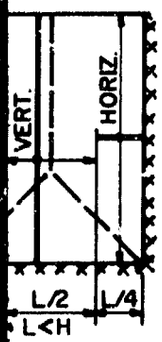
d) FOUR SIDES SUPPORTED

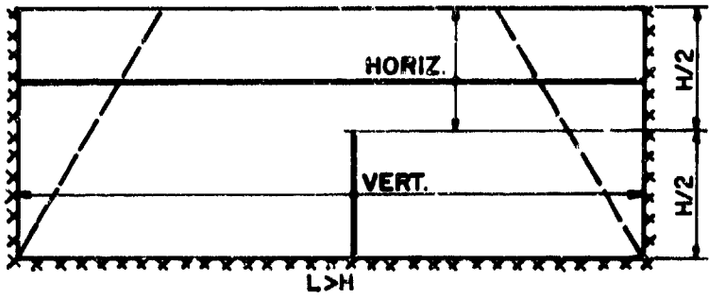
Figure 9–5. Typical location of continuous and discontinuous lacing.



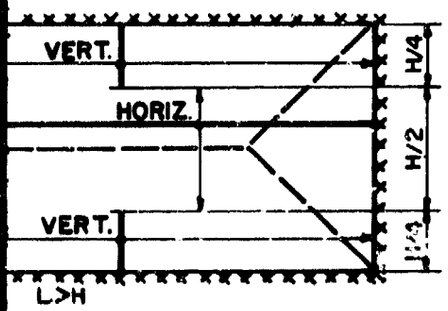


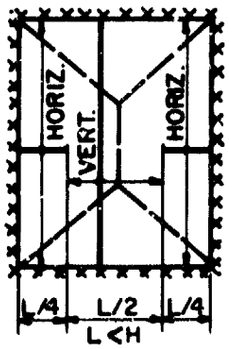
b) TWO ADJACENT SIDES SUPPORTED AND TWO SIDES FREE





SIDES SUPPORTED AND ONE SIDE FREE





d) FOUR SIDES SUPPORTED

Typical location of continuous and discontinuous lacing.

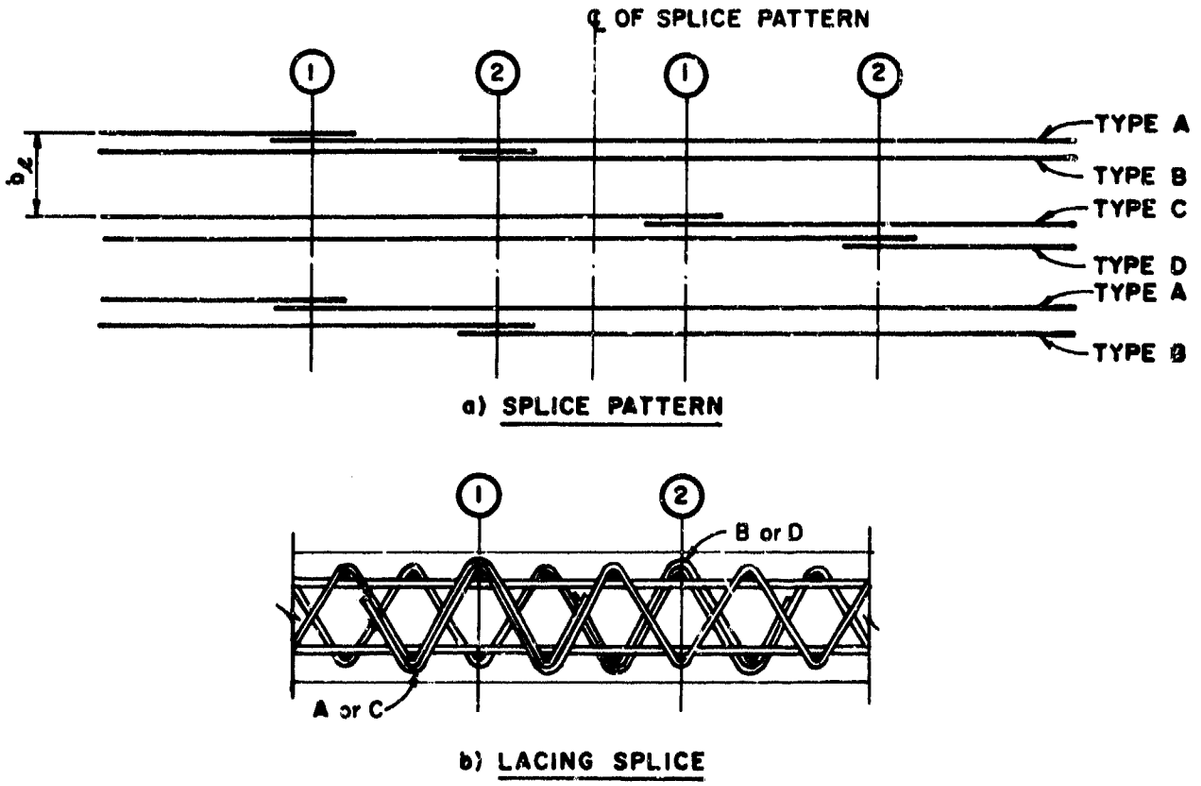


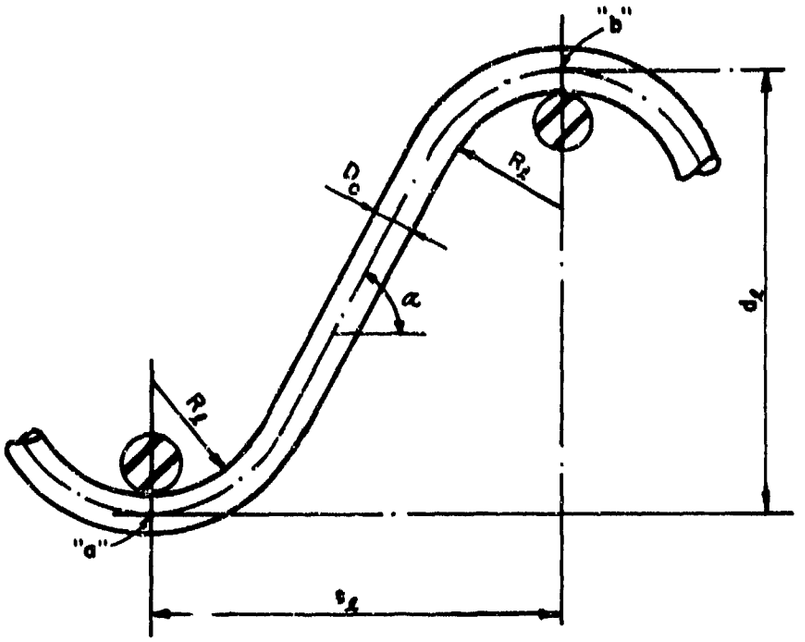
Figure 9–6. Typical details for splicing of lacing bars.

Alteration of bar joist equipment to meet the requirements of a design is not usually practical with respect to both time and cost.

e. The placement of the lacing depends upon the distribution of the flexural reinforcement and the number and type of supports. Lacing is always placed perpendicular to the element's supports to resist the diagonal tension stresses. Because of the nonuniformity of the blast loads associated with close-in detonations, continuous lacing across the span length should be used to distribute the loads. Except for cantilever elements, lacing in one-way elements is placed in the direction of and continuous across the span. Cantilever elements require lacing in two directions. Discontinuous lacing is located perpendicular and adjacent to the support while continuous lacing is placed across the full width of the element in direction parallel and adjacent to the free edge located opposite the element's support. For two-way elements, diagonal tension stresses must be resisted in two directions, and these elements require lacing in both directions. Because of interference, lacing can only be continuous in one direction, which in general is in the direction of the longest span. Figure 9–5 illustrates the location of the lacing used in a cantilever as well as in several two-way elements.

f. Similar to the flexural reinforcement, lacing will

TYPE A
TYPE B
TYPE C
TYPE D
TYPE A
TYPE B



NOTE: L_ℓ IS MEASURED ALONG CENTER LINE OF LACING BAR BETWEEN POINTS "a" AND "b".

$$L_\ell = \frac{s_\ell - (2R_\ell + D_o)\sin\alpha}{\cos\alpha} + \pi(2R_\ell + D_o)\left(\frac{\alpha}{180}\right)$$

$$\cos\alpha = \frac{-2B(1-B) \pm \sqrt{[2B(1-B)]^2 - 4[(1-B)^2 + A^2][B^2 - A^2]}}{2[(1-B)^2 + A^2]}$$

$$A = s_\ell/d_\ell \text{ AND } B = \frac{2R_\ell + D_o}{d_\ell}$$

Figure 9–7. Length of lacing bar.

requir ntinuous lacing
ble way to the support
length s the full width
ast equ adjacent to the
diame 's support. For
ound tresses must be
of adja lements require
rming erference, lacing
ces sh which in general
rom th an. Figure 9–5
cing b d in a cantilever
, weld
permi ent, lacing will usually require splices. Tests have indicated that the preferable way of splicing lacing is by lapping the bars. The lap length which is measured along the bars should be at least equal to that required for a full tension splice (40-bar diameters). However, the lacing should also be bent around a minimum of three flexural bars. The splices of adjacent lacing bars should be staggered to avoid forming a plane of weakness in the element, and the splices should be located in regions of low stress (away from the supports). Typical details for the splicing of lacing bars are presented in figure 9–6. Wherever possible, welding of lacing bars should be avoided and is only permitted where the full development of the ultimate strength can be assured without any reduction in strength or ductility.

g. The location of the splices is determined from the distance along the length of the element which can be covered by a given length of lacing bar (usually 60 feet). The expression for the actual length of lacing bar L_l required to cover the length s_l is a function of the flexural bar spacing and the geometry of the lacing and is given in figure 9–7.

9–5. Corner Details

Because of the magnitude of the blast loads associated with close-in detonations and their amplification at

2

corners, the use of concrete haunches (fig. 9–8) has been found to be a satisfactory method of maintaining the integrity of these sections of a structure. All corners should be reinforced with diagonal bars to transfer the high shear forces from the element to its support and to assist in maintaining the integrity of the intersection. Diagonal bars should be used in elements both with and without haunches.

Section II. DETAILING AND CONSTRUCTION OF LACED STRUCTURES

9–6. Laced Elements

a. Walls.

(1) Figure 9–8 illustrates the detailing procedure for a typical laced wall. The wall, which is free at the top, supported at its sides by other walls (not shown) and at its base by the floor slab, has vertical lacing which is continuous from approximately the midheight of the wall to the bottom of the wall below the floor slab. In the upper half of the wall, the horizontal lacing reinforcement is continuous over the full length of the wall and anchored in the side supports. It should be noted that the horizontal flexural steel in the lower half of the wall is located at the exterior of the vertical reinforcement, while in the upper half of the wall it is at the interior. This arrangement is necessary for the placement of the lacing so that the lacing can provide full confinement of both the flexural steel and the concrete separating the two layers of reinforcement. Reduction of the concrete cover over the reinforcement in the upper half of the wall tends to minimize the effects of spalling. The addition of U-bars at the top free edge also minimizes the formation of concrete fragments from this area.

(2) A portion of the wall should extend below the floor slab a distance not less than that required to anchor the flexural reinforcement (40-bar diameters) and in no case less than 1 foot, 6 inches. In addition to providing anchorage for the vertical reinforcement, the portion of the wall below the floor slab assists in resisting sliding of the structure by developing the passive pressure of the soil adjacent to the wall.

(3) If adequate resistance is not afforded by the soil, then additional reinforcement may have to be placed in the lower portion of the wall to resist the vertical bending moments induced by the blast loads acting on the floor slab adjacent to the wall. The horizontal reinforcement below the top of the floor slab which is normally used for tying the vertical lacing may be considered effective in resisting the vertical bending of the wall.

(4) The working pad at the base of the wall provides the support required for the erection of the wall reinforcement and also affords protection for the reinforcement after construction is completed. It should be noted that in the example illustrated in figure 9–8, the cover over the reinforcement in the portion of the wall above the floor slab is specified as ¾ inch (minimum reinforcement cover required by the ACI Building Code for concrete not exposed to the weather), while below the floor slab it is specified as 2 inches (minimum cover required by the ACI Building Code for concrete in contact with the ground after removal of the forms). The increased cover is achieved by increasing the wall thickness rather than by bending the reinforcement.

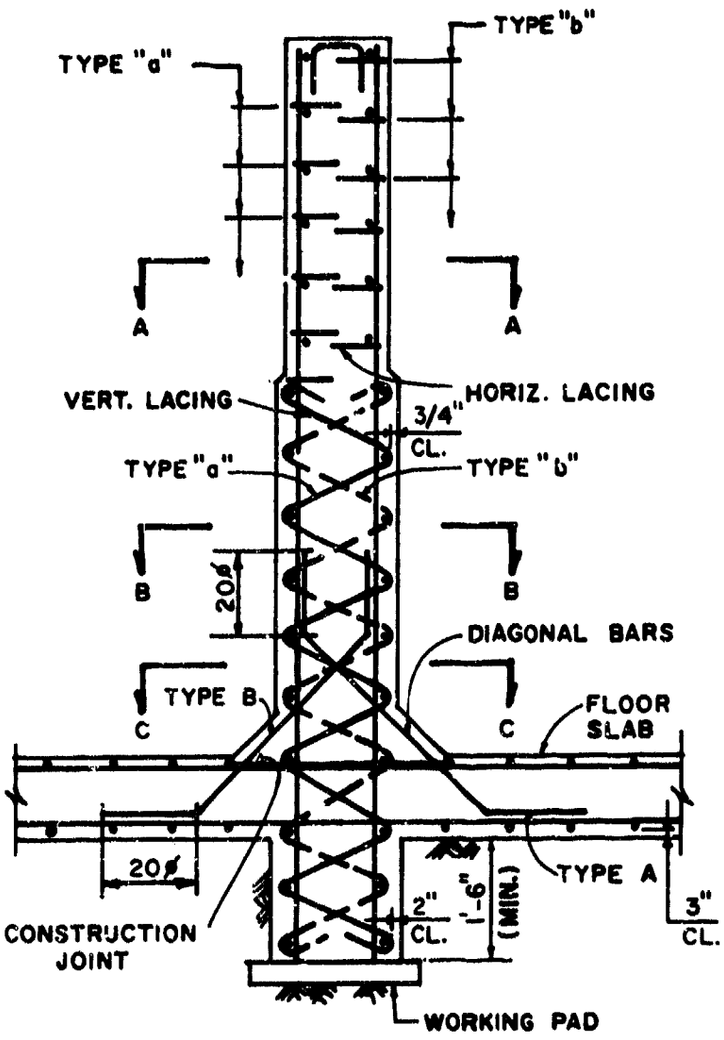
(5) Diagonal bars are provided at the intersection of the floor slab and wall. These bars transfer the high shear forces from the base of the wall through the haunch and into the floor slab. Section C–C, figure 9–8 indicates the location of the diagonal bars relative to the lacing reinforcement.

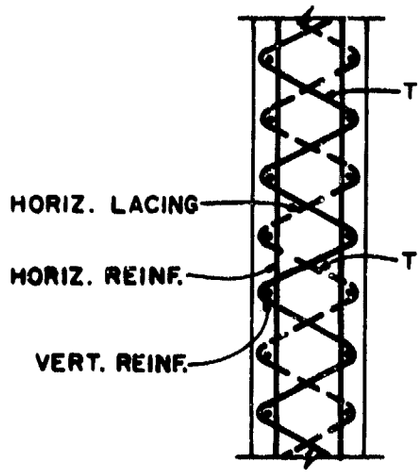
(6) Details of the reinforcement at wall intersections are similar to those at the intersection of the wall and floor slab. Figures 9–9 through 9–11 illustrate these details for the intersection of two continuous walls, one continuous and one discontinuous wall, and two discontinuous walls, respectively. In all cases both the flexural and lacing reinforcement are fully anchored either by being made continuous through the intersection or by being bent within the corner (support) to furnish the required anchorage length. Diagonal bars have been provided at all intersections to transfer the support shears and to maintain the integrity of the section. Where discontinuous walls are encountered, only one diagonal bar is effective for the continuous wall of figure 9–10 and for both discontinuous walls of figure 9–11. For these cases, bundled diagonal bars (2 bars maximum) may have to be used. If permitted by architectural criteria, discontinuous walls should be extended a distance sufficient to anchor all reinforcement, thereby enabling the details of figure 9–9 to be used. This extension (or extensions) aids in resisting both the overturning of the structure and the tension forces produced in the walls (discussed further in subsequent paragraphs).

b. Floor and Roof Slabs.

(1) Floor slabs on grade must provide sufficient capacity to develop fully the wall reinforcement. If sufficient resistance is provided by the soil, slabs poured on grade usually do not require lacing. Soil strata having a bearing capacity at least equal to 3 tons per square foot usually can be considered to provide the support required by the slab. Before placement of the slab, the top 6 inches of the subgrade should be compacted to 95 percent of maximum density in accordance with ASTM Standard D1557.

(2) Roof and floor slabs, which are not supported by some other medium such as soil, are similar to the walls since they are usually supported only at their periphery and require the addition of lacing to distribute





SECTION A-A

TYPE B

DIAGONAL BARS

VERT. REINF

Figure 9–8. Reinforcement details of laced concrete walls.

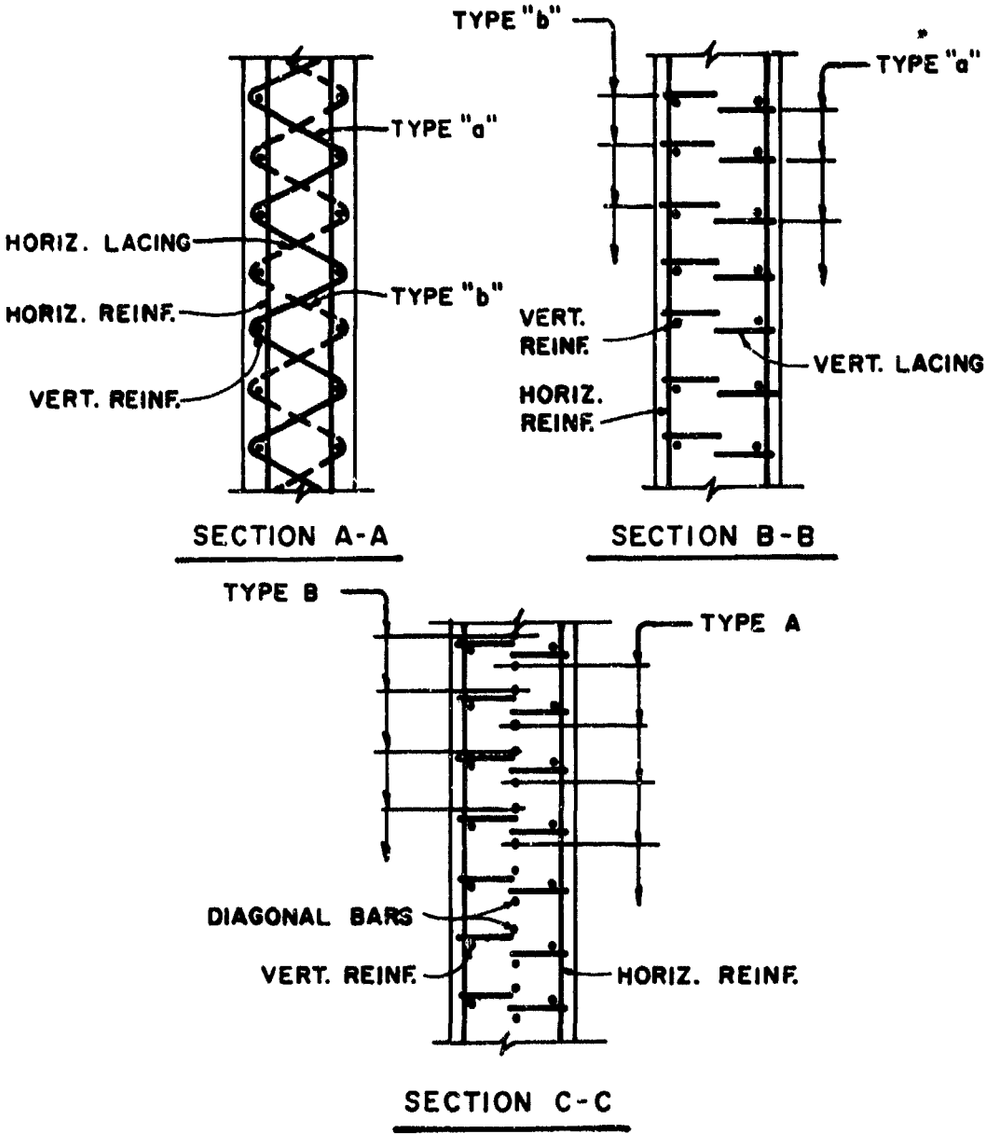


Figure 9-8. Reinforcement details of laced concrete walls.

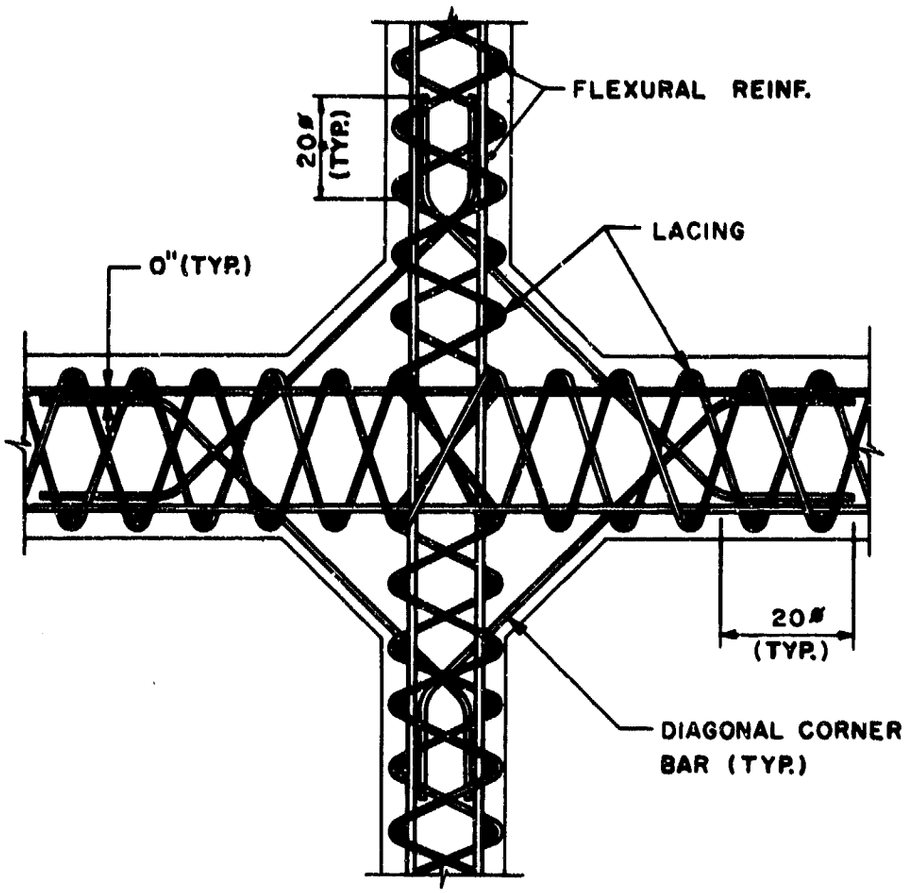


Figure 9–9. Typical detail at intersection of two continuous walls.

and resist the applied blast loads. In those facilities where the explosion occurs within a structure, the blast pressures acting on the interior surface of a nonfrangible roof cause tension stresses in the walls which require the addition of tension reinforcement above that needed for bending.

c. Beams.

(1) When beams are subjected to the high-pressure range effects of an explosion and/or are permitted to sustain support rotations exceeding 2 degrees, then lacing reinforcement is required to develop its full potential capacity.

(2) The lacing is designed in the same manner as that used in walls or slabs. In addition to lacing, a series of loop bars are used to confine the concrete between the layers of reinforcement which would otherwise be displaced along the sides of the beam. Also, the loop bars serve as upper and lower supports for the lacing similar to the transverse steel in walls. The spacing of the loops is predetermined by the spacing of the lacing while the amount of the loop bars is equal to the minimum amount of transverse reinforcement in walls, that is, the amount of the loop steel is equal to one quarter of that for the main flexural steel. Because of the continuity of the loops around the beam, they may be used to resist shear stresses produced by torsion which may require the amount of loop steel to exceed that specified by the above minimum.

9–7. Composite Construction

a. Composite construction is primarily used for wall construction and consists of two concrete panels separated by sand fill (fig. 9–12). Details of each panel are similar to those described for single laced walls.

b. The concrete panels may be supported at the base either by the floor slabs or a concrete pedestal. When the pedestal is used, reinforcement across the base of both panels terminates in the floor slab and provides a monolithic connection between the two panels. The floor reinforcement serves as the monolithic connection when pedestals are not used.

c. The upper portion of the wall may either be open

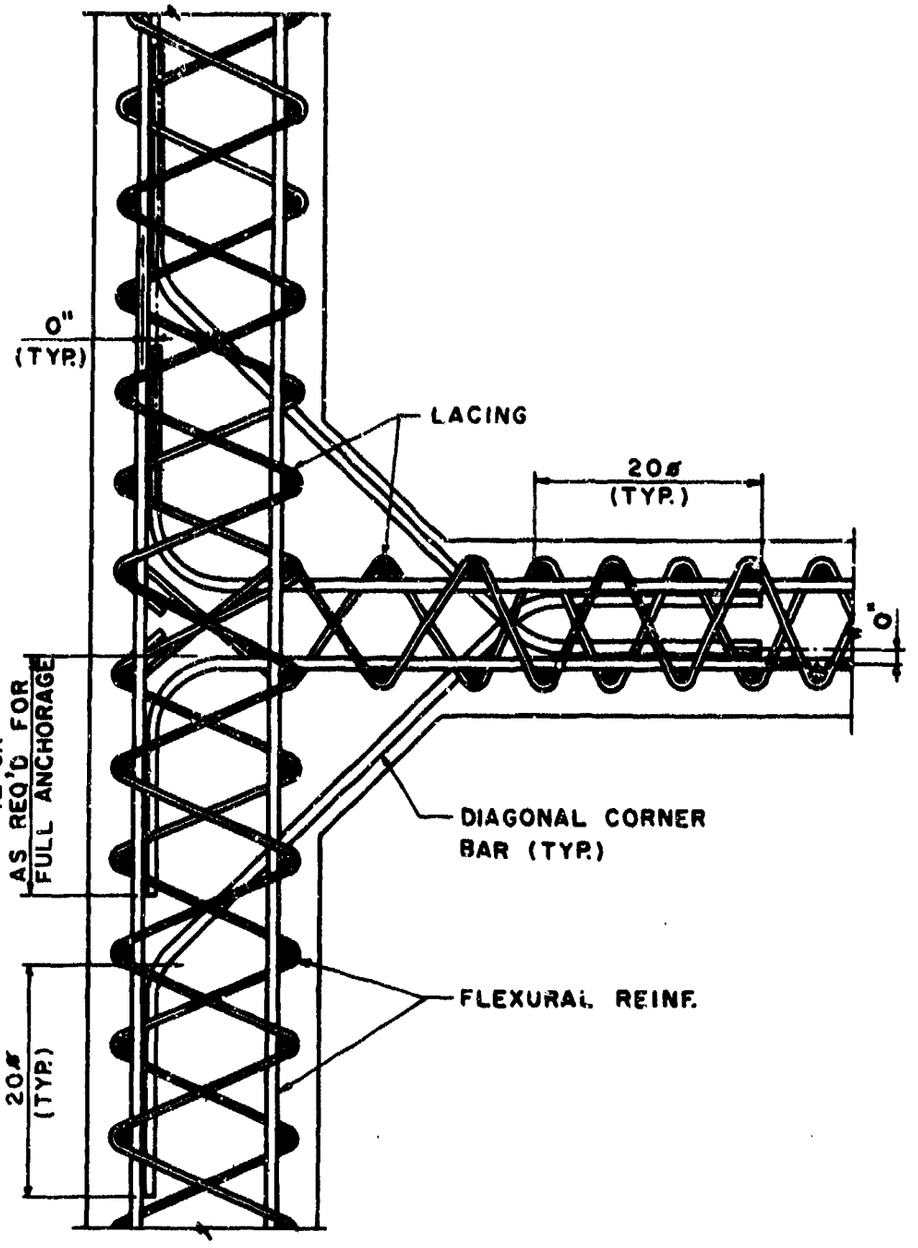
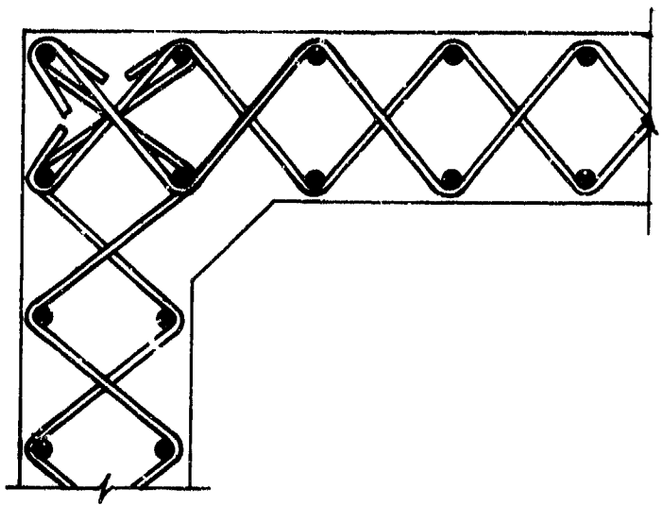


Figure 9–10. Typical detail at intersection of continuous and discontinuous walls.

or solid. Open sections are usually used when the upper edge of the wall is unsupported; the solid section is used when an external tie system is used to restrain the motion and provide support for the top of the wall. The solid section must be reinforced to resist torsion and bending induced by the ties and the panels.

d. The impulse capacity of composite walls is a function of the density of the sand fill. The sand will be compacted after construction due to its own weight and/or by water drainage when the wall is exposed to the weather. The sand fill must be continuously maintained at the level stipulated in the design by mechanical means which will allow periodic rearrangement of the sand fill. Clay pipe or other similar material may be placed in the wall cavity with the sand so that when the wall is loaded the clay pipe will be crushed



a) LACING

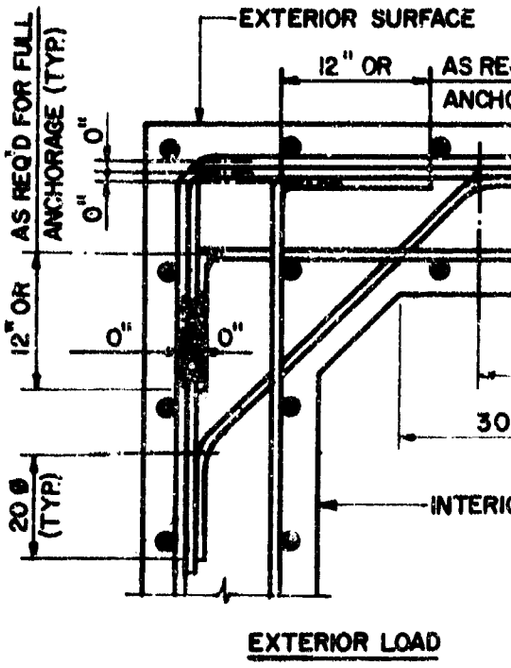
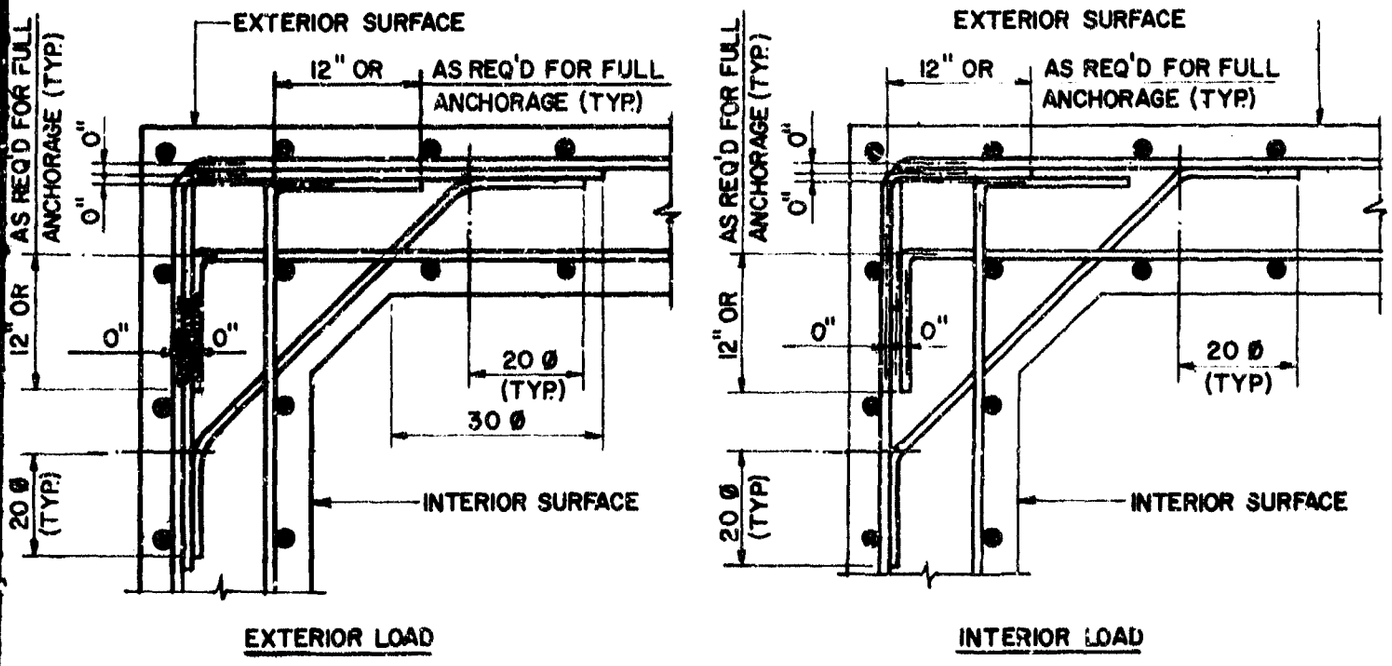


Figure 9–11. Typical detail at corner.



b) FLEXURAL REINF.

Figure 9–11. Typical detail at corner.

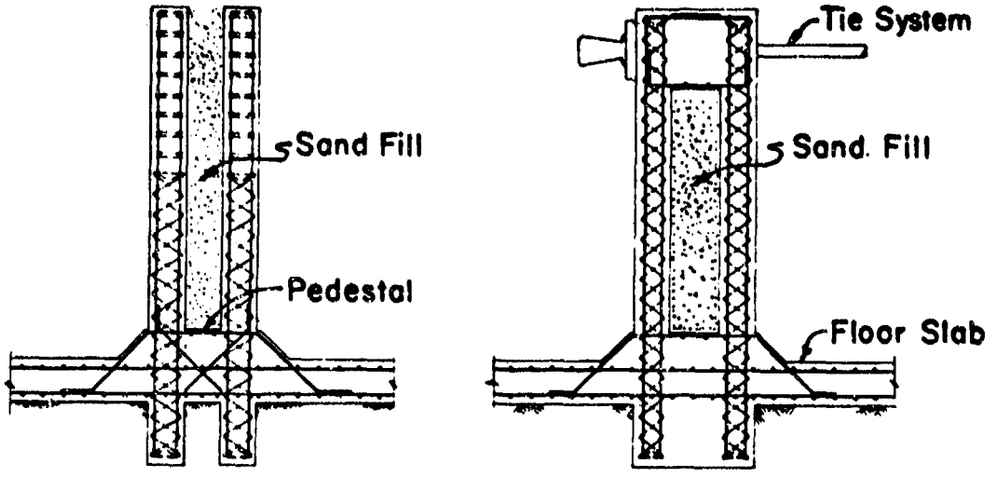


Figure 9–13. Typical composite wall details.

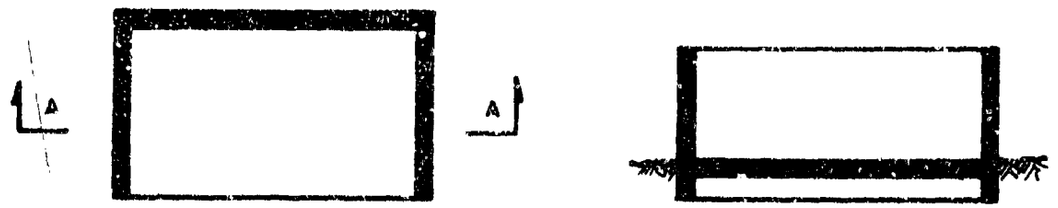
by the impact of the donor panel, thereby providing space within the wall cavity into which the compacted sand may flow, hence reducing its density. If possible, the sand should be protected from the elements by sealing the top of the cavity.

9–8. Single and Multicubicle Structures

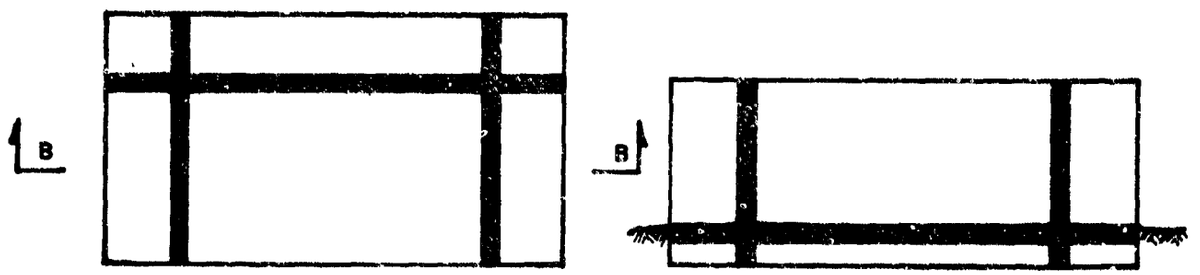
a. In single-cell structures (fig. 9–13), unbalanced forces (support reactions) exist at all element intersections (walls, and floor and wall intersections) and must be resisted by tension forces produced in the support elements. In addition to the reinforcement required to resist flexural and shear stresses, tension reinforcement distributed along the centerline of the elements is required. Horizontal tension reinforcement in the side wall and floor slab (parallel to the side walls) is required to resist the vertical and horizontal reactions of the back wall, while horizontal steel in the back wall and floor slab (parallel to the back wall) resists the tension forces produced by the side wall reactions.

b. These unbalanced forces are transmitted to the structure's foundation and, depending upon their magnitude, the size and configuration of the structure and the subgrade conditions, the structure may be subject to both translational and vertical rotational motions. Translation of the structure is resisted by the extension of the walls below the floor slab (shear key) and the friction developed between the floor slab and subgrade, whereas rotation is resisted by the mass of the structure with assistance from the blast load acting on the floor slab of the donor cell. The stability of the structure can be substantially increased by the extension of the walls and floor slab as illustrated in b, figure 9–13. This extension of the walls and floor slab (1) increases the resistance of the structure to overturning (rotation), (2) increases the rigidity of the structure, (3) reduces the effects of the unbalanced wall moments which cause twisting of the corners, (4) reduces the required thickness and/or reinforcement in the floor slab (moment capacity of the floor slab extension must be developed by bearing on the subgrade), and (5) eliminates the need to anchor the reinforcement by bending it at the corners which would ordinarily hinder the placement of the concrete.

c. End cells of multicubicle arrangments also require the addition of tension reinforcement to resist unbalanced blast loads acting on the end walls. The interior cells do not require this additional reinforcement since the mass and base friction of adjoining cells provide the restraint to resist the lateral forces. Two possible multicubicle arrangments are shown in figure 9–14. In both arrangements the back walls of the cells are continuous, whereas the side walls between the adjoining cells are either continuous or discontinuous. The type of cell arrangement (either one of those shown in figure 9–14 or a combination of both arrangements) used in a particular design depends primarily upon the functional requirements of the facility and the economy involved. However, there are certain structural features which should be considered in the final selection of either structural arrangement. The horizontal reinforcement (flexural and lacing) in the side walls may be placed continuous across the back wall of the continuous side wall sheme, whereas with the discontinuous scheme the side wall horizontal reinforcement must be bent and anchored in the back wall. This latter arrangement



a) DISCONTINUOUS WALL CONSTRUCTION



b) CONTINUOUS WALL CONSTRUCTION

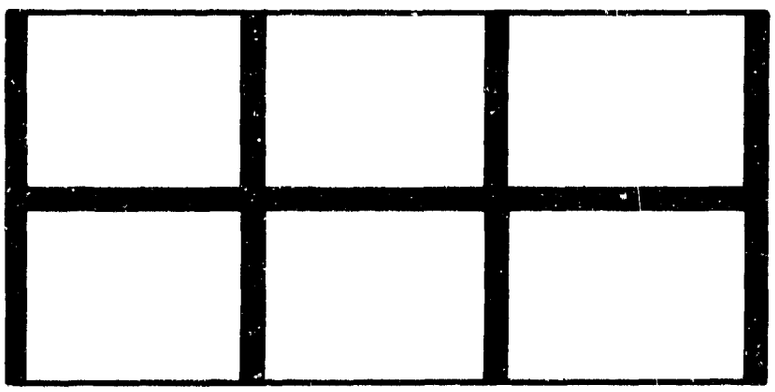
Figure 9–13. Typical single-cell structures.

can result in congestion of the horizontal reinforcement at the wall intersections. On the other hand, by offsetting the side walls at each side of the back wall, the span length of the back wall between adjacent side walls is reduced thereby reducing the required strength (concrete thickness and/or reinforcement) of the back wall.

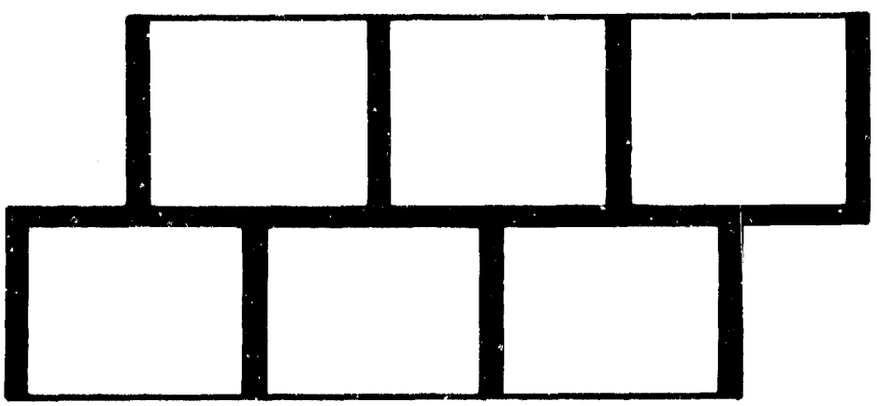
d. In general, continuous walls usually require constant concrete thickness and horizontal reinforcement. However, where economy can be achieved, it may be desirable to reduce the thickness and reinforcement of the continuous wall of one cell in comparison to those of adjoining cells. This reduction should only be made between the supports in order that a constant moment capacity can be maintained across the length of the reduced element. This capacity reduction requires the horizontal reinforcement to be spliced at the supports, and extreme caution should be exercised in the detailing of the splices.

9–9. Sequence of Construction

a. Although the construction procedure for all laced concrete elements is similar, each structure must be evaluated to determine the specific sequence of con-



a) CONTINUOUS SIDE WALL CONSTRUCTION



b) DISCONTINUOUS SIDE WALL CONSTRUCTION

Figure 9–14. Typical multicubicle structures.

struction which is most appropriate for the particular situation. This evaluation should consider: (1) the location of reinforcement splices, (2) erection sequence of the reinforcement (flexural and lacing), (3) location of vertical and horizontal construction joints, and (4) pouring sequence of the concrete.

b. To illustrate the construction of a laced concrete wall, consider the recommended construction procedure for the wall described in figure 9–8. The concrete pouring sequence is illustrated in figure 9–15 while the procedure is as follows:

Steps	*Procedures*
1.	Fabricate the reinforcement as indicated on the drawings.
2.	Pour a working pad.
3.	Erect vertical flexural reinforcement, vertical lacing, and vertical diagonal bars. Thread horisontal flexural bars between vertical lacing and flexural bars up to the top of the vertical lacing. Also place reinforcement for the floor slab.
4.	Adjust reinforcement to required positions and complete second pour.
5.	Place horisontal flexural and lacing reinforcement and diagonal bars (at wall intersections as shown in figures 9–9 through 9–11) between the top of the vertical lacing and

Steps

the top
sontal
wall.

6. Adjust r
third p
lacing i
flexural
place t
in step

7. Pour rem
8. Where tw
concret
steps 3

c. The use
horizontal)
all joints are
joints in lar

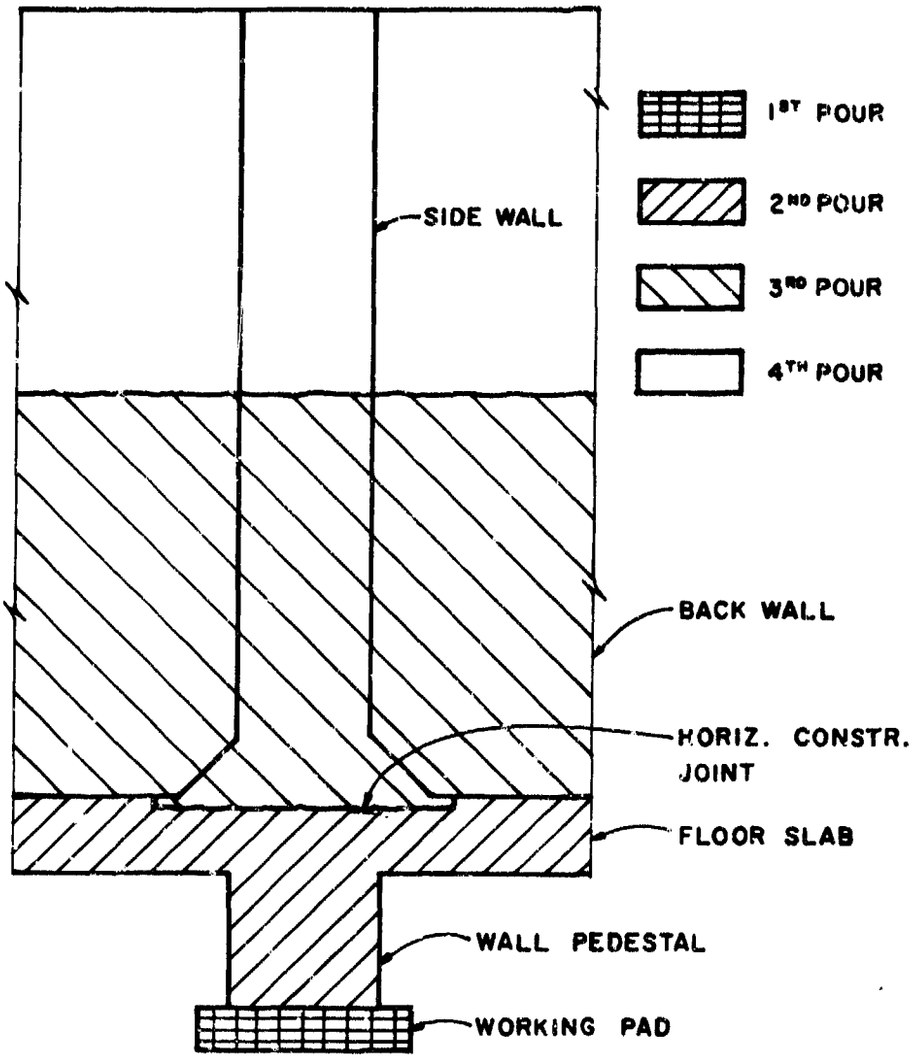


Figure 9–15. Pouring sequence.

Steps	*Procedures*
	the top of the wall. Where two walls intersect, the horizontal reinforcement must be placed alternately in each wall.
6.	Adjust reinforcement to required positions and complete third pour. (As an alternative, place sufficient horizontal lacing in step 5 to insure proper positioning of the vertical flexural reinforcement, complete third pour, and then place the remainder of the horizontal reinforcement as in step 5.)
7.	Pour remainder of wall (fourth pour).
8.	Where two walls intersect, erect reinforcement and pour concrete for both walls simultaneously as described in steps 3 and 7.

c. The use of construction joints (both vertical and horizontal) should be avoided wherever possible since all joints are a potential plane of weakness. However, joints in large structures cannot be avoided because good practice for placement of concrete and/or economy requires their use. All joints should be located in regions of low stress intensity, and, if possible, vertical joints should be situated in areas where horizontal lacing is located, and horizontal joints should be situated in areas where vertical lacing is located. In addition, concrete surfaces should be roughened at all joints.

d. The above construction procedure required the use of two horizontal construction joints. The joint located at the floor slab is generally used in all laced concrete structures while the second joint in the upper section of the wall should only be used if the height of the wall warrants it. The use of vertical construction joints is generally required for multicubicle arrangements. Walls (intersecting walls must be poured simultaneously) and corresponding floor slabs should be poured in checkerboard fashion to guard against joint

separation due to shrinkage and temperature variations. To maintain a minimum rate of pour, multiple pouring crews may have to be used, and pumping of concrete, rather than the use of tremies, may be required for high walls.

e. Expansion joints are generally not required for laced concrete elements due to the presence of relatively large amounts of reinforcement. However, their use should be considered for long buildings and/or structures subjected to extreme temperature changes.

Section III. UNLACED REINFORCED CONCRETE CONSTRUCTION

9–10. General

Unlaced reinforced concrete elements are used in those facilities designed to resist explosive output at the intermediate and low-pressure design ranges. These facilities generally consist of shelter-type structures.

9–11. Differences From Conventional Construction

Blast resistant structures utilizing unlaced reinforced concrete construction will only differ from conventional construction insofar as the increased magnitude and reversibility of the applied loads are concerned. These differences are reflected in the details of the blast resistant structure. An increase in the amount of reinforcement is required to resist the larger loads resulting from the blast. Also, the reinforcement at both surfaces of an element should be detailed to insure that failure due to elastic rebound stresses associated with short duration loads does not occur.

9–12. Details of Unlaced Elements

In general, the properties of the flexural reinforcement (anchorage, splices, etc.) specified for laced concrete elements also apply to unlaced elements. However, only a portion of the flexural reinforcement must be continuous. If increased shear capacity is required, this strength can be achieved through the use of stirrups. The detailing of the stirrups should insure full development of the plastic strength. Except for an increase in the required strength, the concrete used in the design of unlaced reinforced concrete will be the same as that used in conventional construction, that is, both standard and high early-strength concrete may be used.

CHAPTER 10

OTHER FACTORS CONSIDERED IN EXPLOSIVE FACILITY DESIGN

Section I. INTRODUCTION

10–1. Scope

In addition to the structural requirements to resist blast pressures and primary fragments, the design of protective structures to resist accidental explosions should consider: (1) site planning to achieve a safe and operationally efficient facility, (2) cost effectiveness to achieve economical design of both the protective structure and of the overall layout of the facility, (3) proper location and arrangment of entranceways and methods of closures for openings in shelters, (4) protection against structural motions, and (5) use of earth-covered steel-arch magazines.

Section II. SITE PLANNING

10–2. Guide Lines

a. Because of the wide variation in operational requirements, proper siting will usually be specific to each facility. Certain guide lines can be established which will reduce construction costs, optimize safety, and facilitate operational requirements. To achieve an economical design, the orientation of a particular building must be balanced against its operational needs and its relationships to other off- and on-site structures with particular attention to those buildings housing the maximum potential hazard.

b. Economy from siting of facilities can be achieved by minimizing distances between, and by proper orientation of, on-site structures. Required separation distances will usually be governed by the blast effects of the detonation whereas both primary fragments and blast effects will be factors in determining structure orientation.

c. New facility designs which consider both blast pressures and impulse loads for establishing safe distances will produce economy not only in land reduction from that required by the quantity-distance table, but also by cost savings realized from the reduction of the required length of roads, security fences, and other auxiliary apparatus (tramways, walkways, piping, wiring, etc.) which interconnect the various on-site buildings and off-site areas. In the case of reinforced-concrete, blast-resistant shelters for personnel, the required separation distances calculated using both parameters (pressure and impulse) and the structural response can be greatly reduced from those specified in the quantity-distance tables.

d. Another factor which can significantly affect the required separation distances is the possibility of the occurrence of simultaneous detonations. If a protective structure containing several potential explosions is designed to prevent propagation of the explosion from one area to another, then structures located adjacent to the building containing the potential hazard can be sited based on separation distances to provide safety from a single detonation. Laced reinforced concrete dividing walls can be designed to prevent propagation. On the other hand, where propagation (simultaneous detonation) occurs, safe distances between buildings must be substantially larger. The magnitude of this increased distance is dependent on the number and size of the potential explosions.

e. Structures containing explosives should be oriented to minimize damage to the remainder of the facility and to off-site areas. Barriers, cubicles, and igloos are generally oriented so that the frangible portions of the structure direct the blast and fragments away from other structures and in the direction of minimum off-site population and facilities. Cubicles and other similar storage or operating structures usually will have one or more surfaces frangible (fig. 10–1). Direction of the debris from the frangible portions of these structures can often be controlled by proper detailing.

f. To illustrate debris control, consider the two-cell cubicle structure of figure 10–1, where each cell consists of three exterior reinforced concrete walls and one common concrete interior wall. A concrete beam located midway between the exterior and interior side walls adds lateral restraint to the top of the front and back walls in addition to providing support for the roof slab.

GN

oth the protective
of the facility, (3)
entranceways and
helters, (4) protec-
(5) use of earth-

ificantly affect the
possibility of the
ons. If a protective
l explosions is de-
explosion from one
cated adjacent to
ial hazard can be
to provide safety
einforced concrete
event propagation.
ion (simultaneous
between buildings
nagnitude of this
e number and size

should be oriented
der of the facility
les, and igloos are
ble portions of the
ments away from
f minimum off-site
and other similar
ally will have one
. Direction of the
f these structures
etailing.
sider the two-cell
e each cell consists
valls and one com-
ete beam located
nterior side walls
he front and back
for the roof slab.

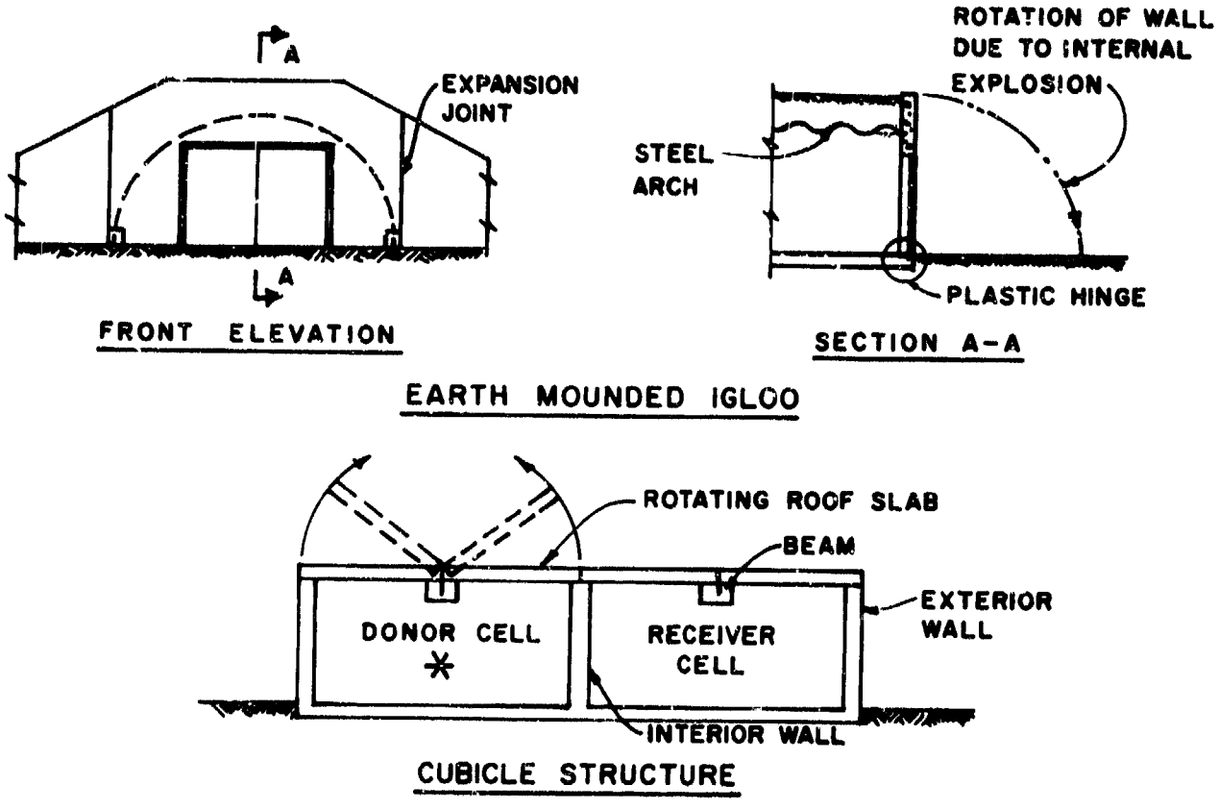


Figure 10-1. Control of debris by proper design.

All four walls and the concrete beam of each cell were designed to resist without failure the blast output of an internal explosion.

g. The roof of each cell was also constructed of reinforced concrete and was designed to blow off the donor cell, thereby relieving the pressures created by the gas buildup within the cell. This was acomplished by providing less strength in the tiedown bolts at the side walls than would be required to fully develop the ultimate capacity of the slab. As the bolts fail at both side walls, the free ends of the slab will rotate the center beam support (bolts at the center support were designed to sustain the ultimate capacity of the slab) thereby directing the concrete fragments from each free section of the slab toward one another. This slab action minimized the amount of roof slab debris directed towards the roof slab of the receiver cells. In addition to providing the mechanism required to produce rotational action of the donor cell roof, the tiedown bolts also provided the required hold-down necessary to resist the negative-phase pressures acting on the roof slab of the receiver cell produced by pressure leakage from the donor cell.

h. Another demonstration of proper debris control is with the use of earth-covered igloos, where the entranceway portion (steel doors and concrete retaining

walls) usually forms the major debris hazard to other structures. Use of laced concrete reinforcement in the retaining walls and strengthening of the door hinges reduces the travel of the debris and in many cases prevents disengagement entirely (fig. 10–1).

i. Protective structures not housing explosive hazards should be oriented to minimize the effects of the blast output on their exterior surfaces and within the structures themselves. Minimum cost is attained when the smallest exposed wall area of a building faces the hazard, thus reducing the overall blast load acting on the structure. Of particular importance in this regard is the blast load caused by the reflected pressures acting on the surface facing the detonation where amplification of the shock pressures occurs when the pressure front impinges on the structure.

j. When explosions occur in cubicle-type structures, the blast pressures propagating from the open end of the structure are higher, at a given distance, than those pressures acting on the ground surface adjacent to the cubicle walls. Economy will be achieved by siting other facility structures (containing explosives or personnel) opposite the cubicle walls with the open end of the donor cell directed towards remote off-site areas.

k. As previously mentioned, the number and size of openings in shelters should be held to a minimum, and, if possible, shelters should be windowless. When required for operational purposes, openings in shelter structures should be placed in those surfaces facing away from the potential explosion. Depending on the size of the structure, the savings by eliminating windows may offset the costs of ventilation or air conditioning when required. This and other features of orientation of openings are discussed in more detail later in this chapter.

l. Quite often windowless or almost windowless buildings can be located closer to potential explosive hazards than conventional structures with earth barricades. In these cases, cost savings achieved by the elimination of the barricades and by the land reduction offset the increased building cost. Furthermore, reduced operational costs are usually realized.

m. When barricades are required to reduce separation distances specified by the quantity-distance tables in the Army Materiel Command Safety Manual (AMCR 385-224), hereinafter referred to as Safety Manual, some economy can be achieved with the use of reinforced concrete barriers. Depending upon the distance between the explosive and the barrier, the cost of the concrete barriers has been found to be less than that for earth-mounded barricades for explosive weights as large as several thousand pounds. The maintenance of concrete walls is significantly less expensive than that for earth-mounded single and/or double revetted earth barricades. Soil erosion, dry-rot, and/or weathering of the wood supports which are continuous problems throughout most of the country, are also eliminated.

n. Although locations of site roads and walkways usually cannot conform to minimum distances required for conventional operations, they should be oriented with consideration for maximum protection and the factors involved in recovery from accidental explosions. Barricades for debris protection may be useful to achieve economy in road construction.

10–3. Typical Case Study

a. General. To illustrate the guide lines for site planning and other design features of explosive facilities discussed in this manual, consider the design of a typical ammunition maintenance facility described in figure 10–2. This facility consists of six main components interconnected with roads, walkways, and a tramway (only between two components). These components and their assigned high-explosive quantity for establishing explosive quantity-safety distances and blast parameters are as follows:

Component	*Explosive quantity*
1. Ammunition Maintenance Building (cubicle structure with 19 cells).	25,000 lb (total) 5,000 lb (per cell)
2. Earth-Covered Magazines (5 steel-arch magazines).	25,000 lb (total) 5,000 lb (per magazine)
3. Missile and Rocket Motor Hold-Down Stand (1 earth-mounded dividing wall structure).	7,000 lb
4. Vacuum Collector Building (cubicle structure with 2 cells).	400 lb (total) 200 lb (per cell)
5. Lunch Room—Change House.	None
6. Flammable Storage Building.	None

b. Safe Distances.

(1) Minimum explosive separation distances indicated on the site plan (fig. 10–2) are in accordance with the minimum requirements of the Safety Manual except that the minimum intermagazine spacing of 22 feet for the earth-mounded steel-arch magazines is based upon the formula $D = 1.25W^{1/3}$ which is now the currently accepted criteria on the basis of full scale tests. In addition, the minimum intraline separation of 150 feet between the earth-covered Steel-Arch Magazines and the Missile and Rocket Motor Hold-Down Stand is based upon the hazard of the former with respect to the latter. Because of the demonstrated hardness of the steel-arch magazines, it is not considered that an incident involving 7,000 pounds of explosive at the hold-down stand would pose a serious hazard to the contents of the magazines. These separation distances provide a level of protection consistent with protection category 3 (ch 3) where prevention of communication of detonation by fragments and high blast pressures is required.

(2) The Lunch Room—Change House, which is separated from the Maintenance Building by intraline distance, has been designed to provide full personnel protection (category 1, ch 3) against the blast impulse

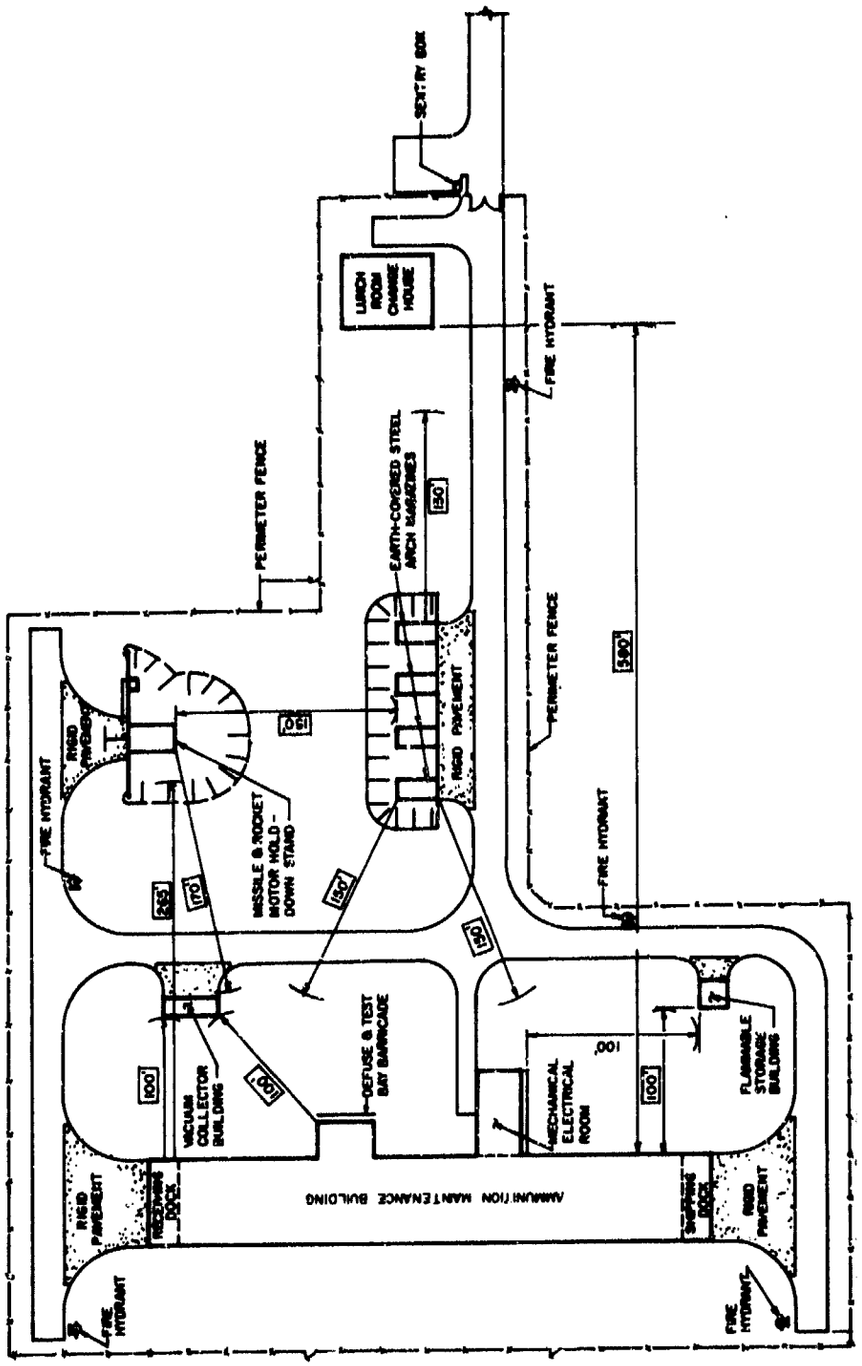


Figure 10–2. Site planning of typical ammunition maintenance facility.

loading associated with an accidental detonation of 25,000 pounds of high explosive concentrated in the Ammunition Maintenance Building or 5,000 pounds in the nearest magazine.

(3) The 100-foot intraline separation between the Vacuum Collector Building and the Ammunition Maintenance Building is based upon the 200-pound per cell explosive quantity of the former. The hazard which the Maintenance Building poses to the Vacuum Collector Building is disregarded since siting to provide this protection would not be economically warranted. This latter design technique conforms to protection category

2

TABLE OF MINIMUM SEPARATION DISTANCES (FEET) FOR SITING (1)							
BUILDING	MAX ASSOCIATE LOAD. WEIGHT W (LBS)	INTRALINE DISTANCES		INHABITED BUILDING DISTANCES (I.B.D.)		RAILROAD/PUBLIC HIGHWAY DISTANCES (RR - H WY)	
		BARR.	UNBARR.	BARR.	UNBARR.	BARR.	UNBARR.
VACUUM COLLECTOR BUILDING	200 (per CUBICLE)	80	100	235	470	140	280
EARTH-COVERED, STEEL ARCH MAGAZINES (2)	5,000 (per CUBICLE)	150	300	685	1370	410	820
MISSILE & ROCKET MOTOR HOLD-DOWN STAND	7,000	170	340	770	1800 (3)	460	1800 (3)
AMMUNITION MAINTENANCE BLDG.	25,000	266	530	1170	2110	700	1265

(1) ABOVE TABLE IS BASED UPON TM 9-1300-206 AND AMCR 385-224
(2) MINIMUM INTERMAGAZINE SPACING IS 22 FT. DERIVED FROM FORMULA $D = 1.25 W^{1/3}$
(3) ARBITRARY BECAUSE OF MISSILE HAZARD

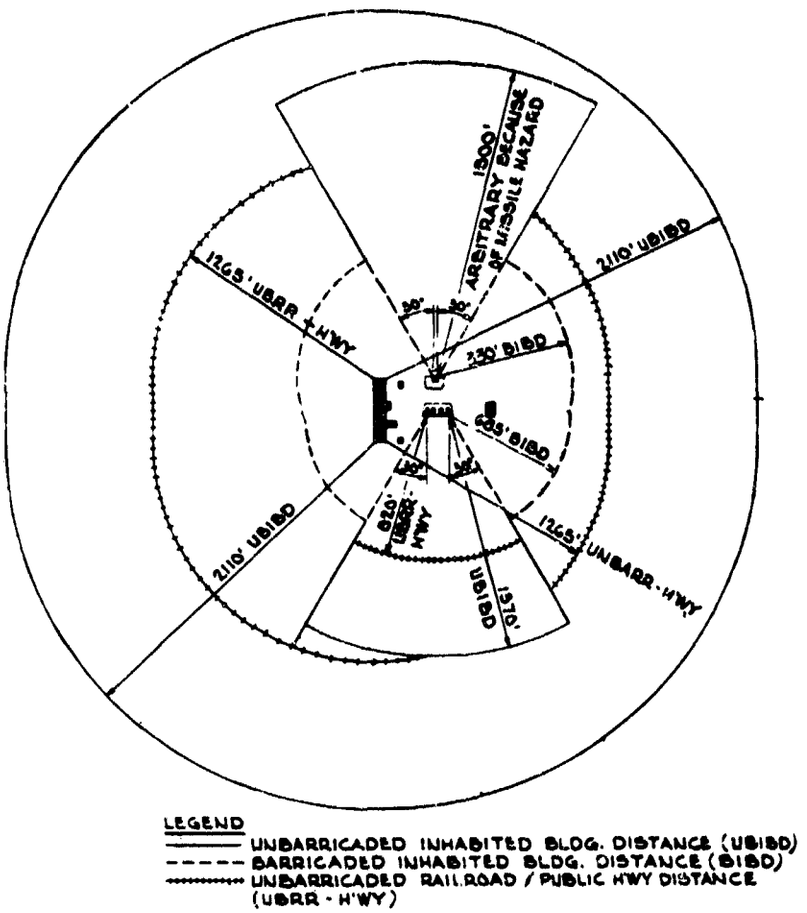


Figure 10–3. Off-site separation distances (typical ammunition maintenance facility).

4 where prevention of mass detonation as a result of subsequent detonations produced by communication of detonation between two adjoining areas is required.

(4) Off-site separation distances for inhabited buildings and public highways (fig. 10–3) conform to the Safety Manual except that the 60-degree by 1,800-foot safety sector centered on the front of the Missile and Rocket Motor Hold-Down Stand has been established as a measure of protection against the hazards of structural or motor fragments which would be thrown out in the event of an accidental explosion at the hold-down stand.

(5) For the amount of materials contained in the Flammable Storage Building, a safe fire hazard separation distance between this building and other buildings of the facility has been established by conventional fire-prevention engineering as 100 feet.

c. Relative Orientation. The relative locations of struc-

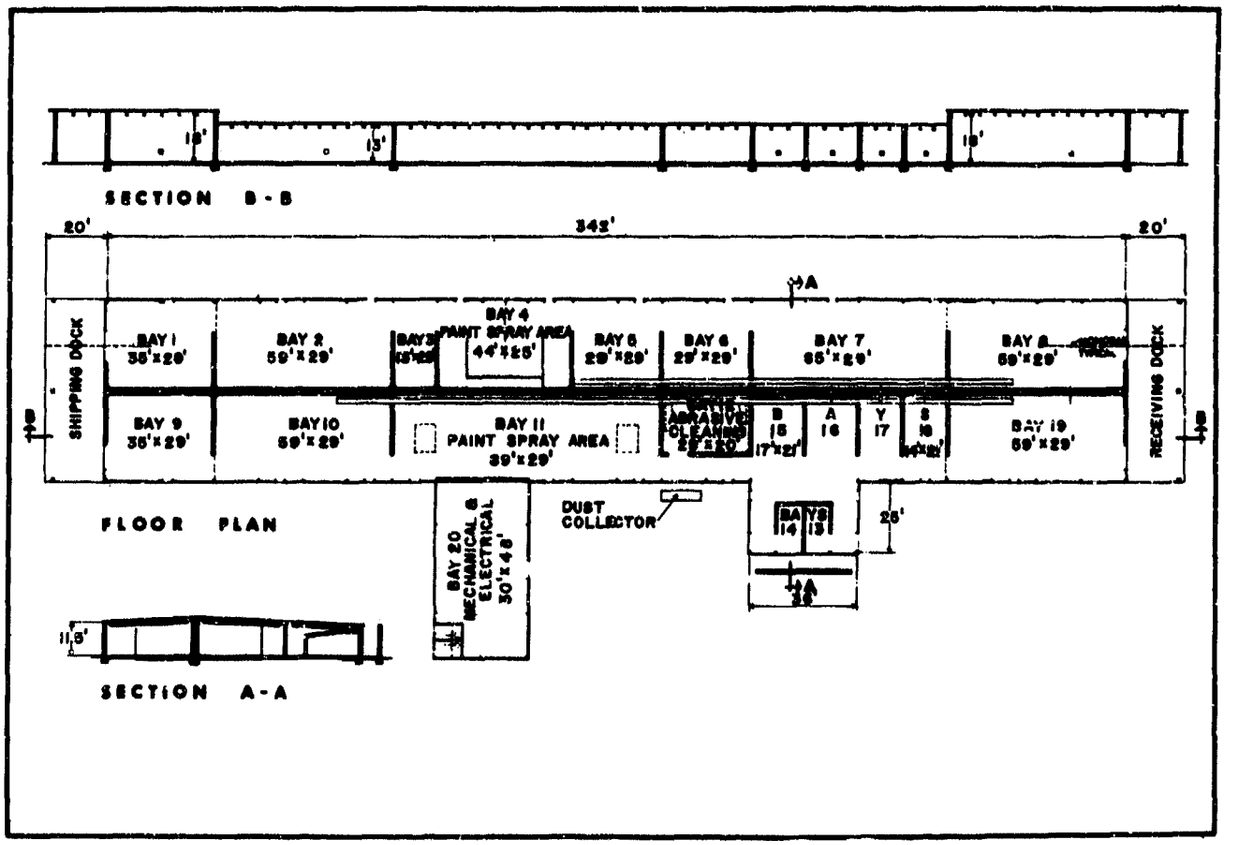


Figure 10–4. Ammunition maintenance building.

tures and roads within the facility were established to provide an efficient operational arrangement within the limitations imposed by safety requirements. The Lunch Room—Change Building is located at the entrance to the facility for convenience and maximum control. The access road is aligned as close as practical to the transverse centerline of the Ammunition Maintenance Building to minimize travel to and from the Lunch Room—Change Building and the ammunition magazines. The Ammunition Maintenance Building, which consists of two parallel operating lines (center of building separated by a continuous longitudinal dividing wall (fig. 10–4), one for equipment and small explosive charges (up to 500 pounds) and the other arranged for heavier explosives (up to 5,000 pounds)), is oriented with the smaller explosive operating line facing the facility for two reasons, i.e., (1) to minimize the road length and side area and (2) to provide the added protection afforded by the central dividing wall against accidental explosion along the operating line containing the large explosives. As was previously discussed in chapter 4, tests have shown that the magnitude of the leakage pressures from cubicle-type structures will, in addition to other factors, be dependent upon the cell dimensions in which the

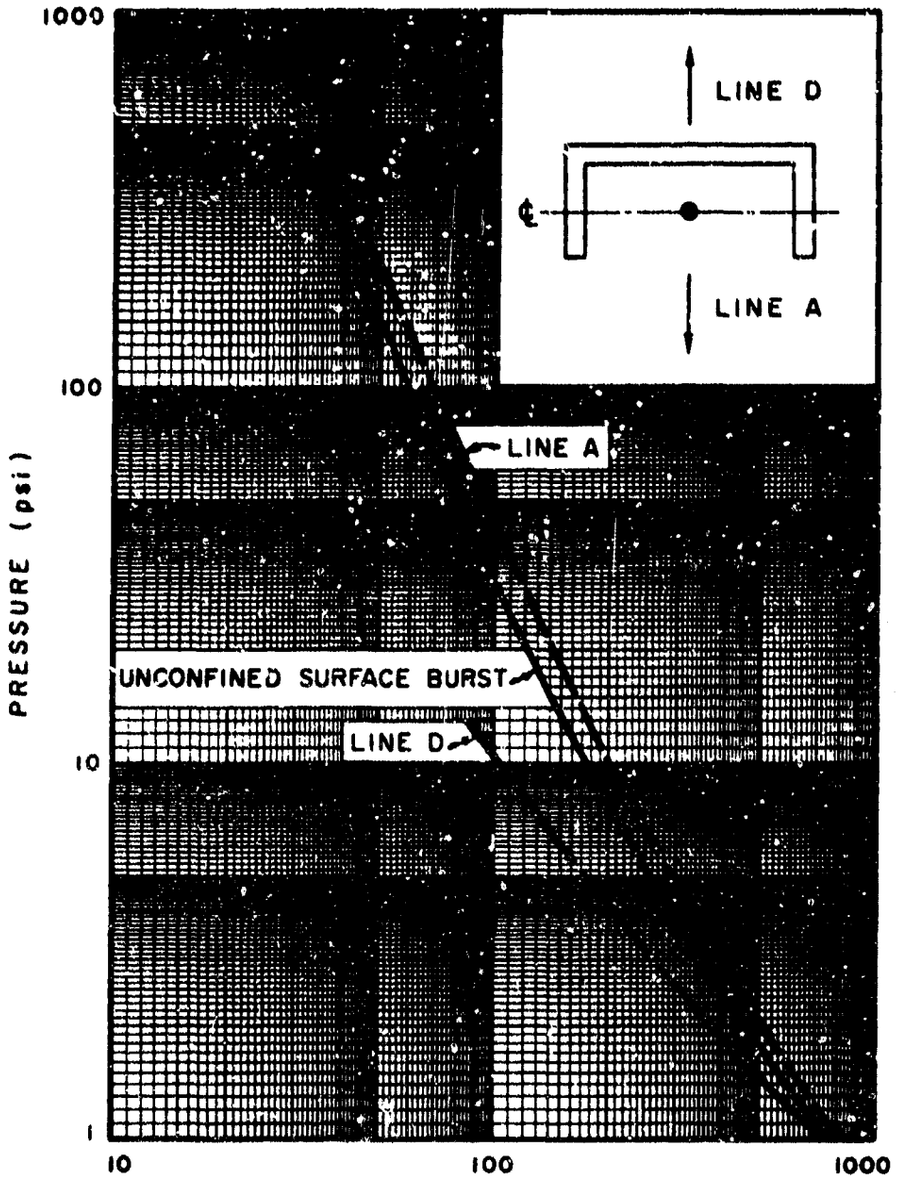


Figure 10-5. Surface pressure vs. distance for 5,000-pound charge in cubicle.

detonation occurs. As an example, for an explosion of 5,000 pounds within a cell having a length to height ratio between 0.85 to 1.6, the ground surface pressure at the 100-foot range adjacent to the back wall would be 10 psi as compared to 30 psi for an unconfined surface burst, and 45 psi if the structure is oriented with the open end facing on-site (fig. 10-5). As the L/H ratio is increased, the pressure versus distance variation approaches the unconfined case.

Section III. COST EFFECTIVENESS

10–4. General

a. Although the ultimate decision regarding the type of structure to be used in conventional construction is generally based on economy, an additional factor requiring consideration in protective design is safety. Here the relationships between the three components (donor and receiver systems and the protective structure) of an explosion protective system must be considered to insure economy and safety in both the facility layout and the protective structure design (fig. 10–6).

b. As previously mentioned, the donor system is analyzed first and the explosive output, in terms of primary fragments and blast pressures, is determined. An

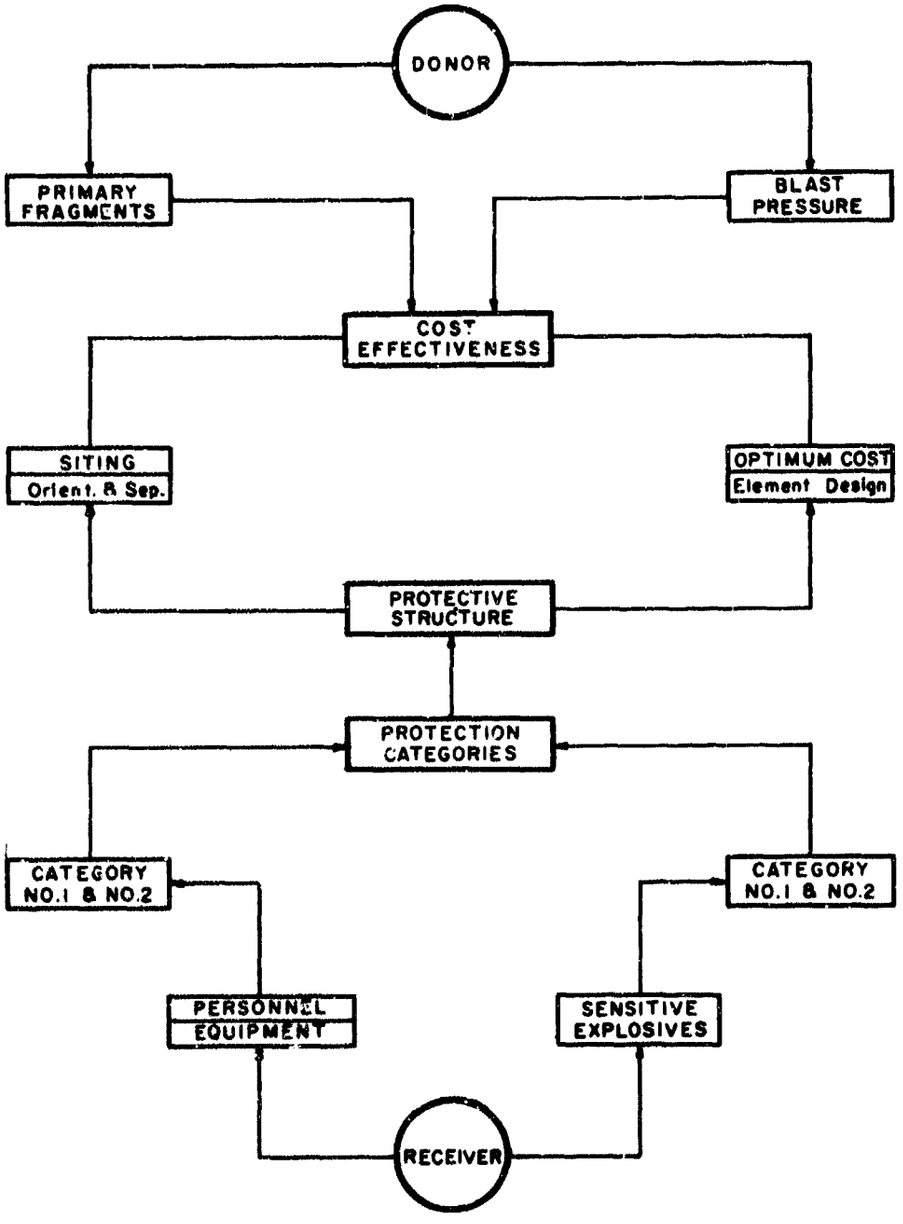


Figure 10–6. Cost effectiveness system.

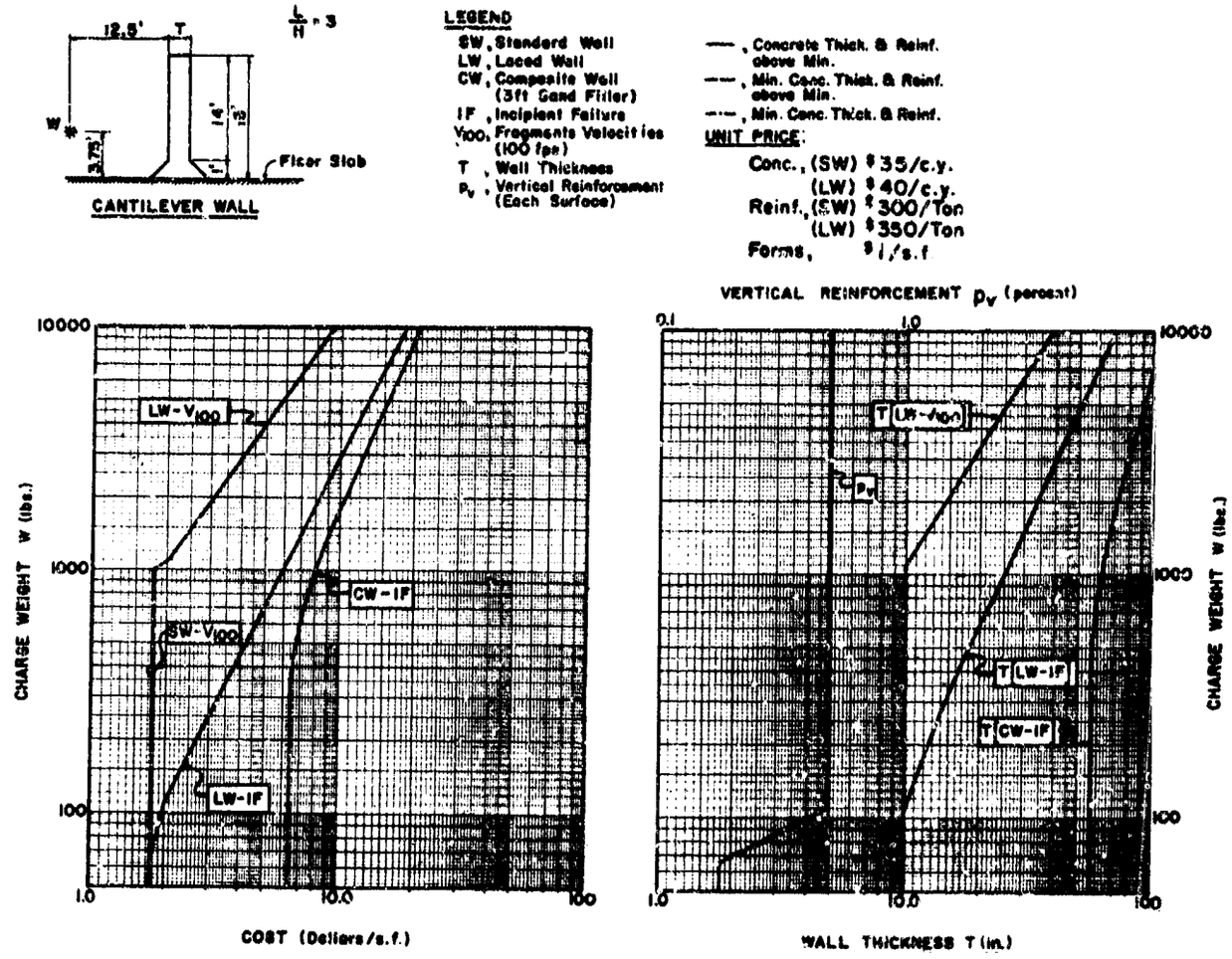


Figure 10–7. Cost analysis of laced cantilever wall.

appropriate protective structure (shelter or barrier) is then selected to afford a level of protection consistent with that required by the receiver system. This structure is then sited to achieve economy both in construction and future operation. Many factors which produce cost effectiveness by proper siting have been discussed previously in this chapter, and the remainder of the cost effectiveness discussion is devoted to that which is achieved by proper design of the individual elements, and, in particular, proper design of laced concrete walls.

10–5. Cost Comparison for Laced Concrete Elements

a. Once the arrangement of the protective structure has been selected, the individual elements (wall, floor, and roof slabs) are designed to provide the protection required. The degree of protection and the thickness required for individual elements are significant factors in determining the cost effectiveness of the structure.

b. As an example, consider a cantilever dividing wall

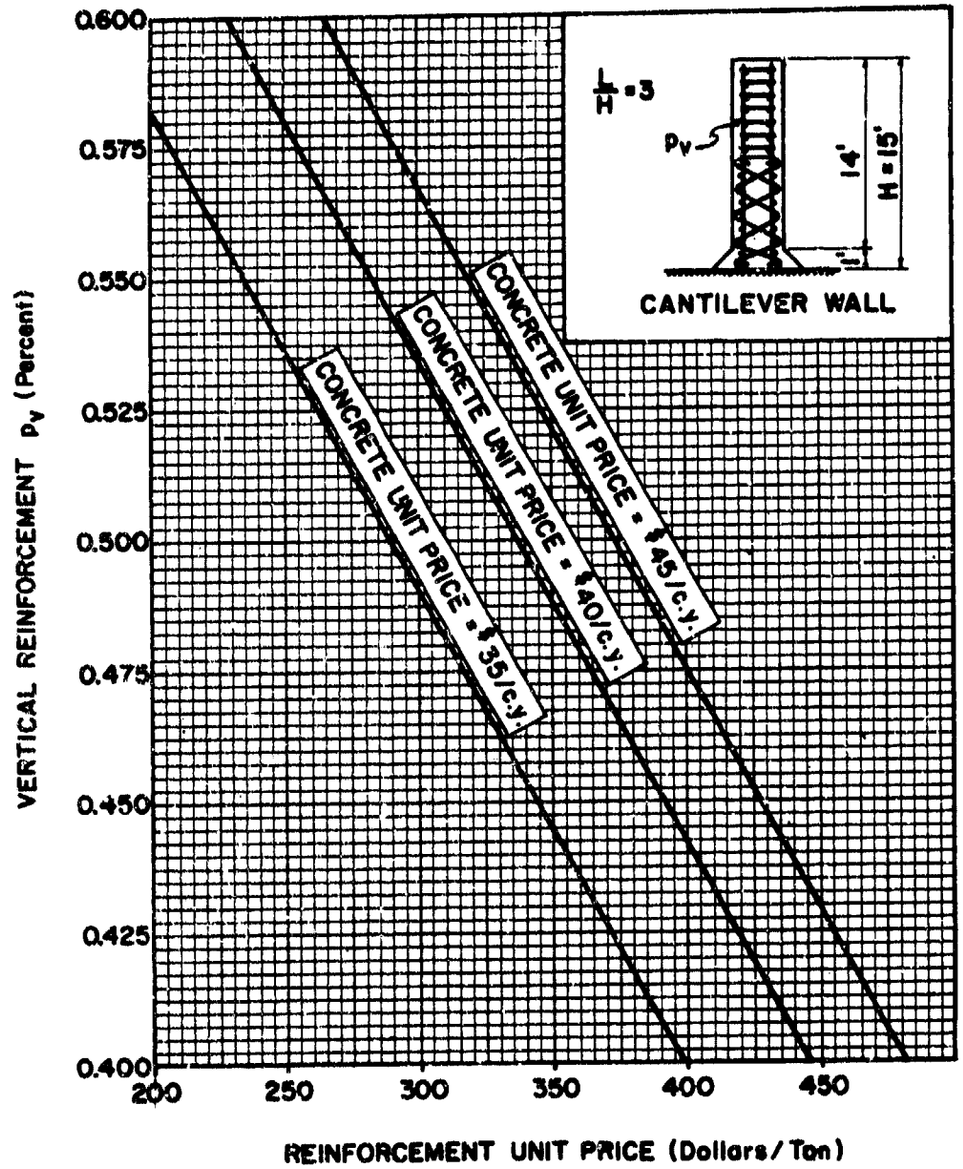
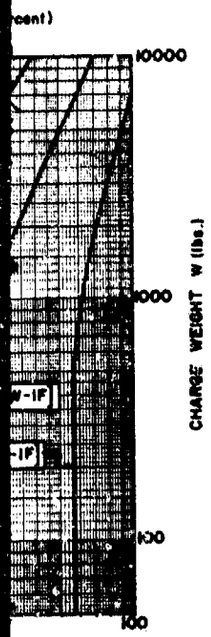


Figure 10–8. Variation of optimum reinforcement with unit price of concrete and steel.



indicat
height
the ba
height.
from a
explosi
design
sumed
c. R
laced r
teria, i
or gre

aced Concrete

otective structure
nents (wall, floor,
de the protection
and the thickness
significant factors
of the structure.
ever dividing wall

indicated on figure 10–7 where the wall has an overall height of 15 feet with a 1- by 1-foot haunch located at the base slab. The length of each wall is three times its height. The wall is designed to resist the blast output from a maximum charge weight of 7,500 pounds of high explosives located 12 feet, 6 inches from its surface. The design height of the charge above the floor slab is assumed to be equal to one-quarter of the wall height.

c. Results of cost analyses, considering the use of laced reinforcement and based on incipient failure criteria, indicated that for a potential explosion equal to, or greater than, 110 pounds, the minimum cost per square foot of wall surface excluding formwork varies as a power function of the charge weight (fig. 10–7). This power function is dependent upon the relationship between the unit prices of the reinforcement and concrete.

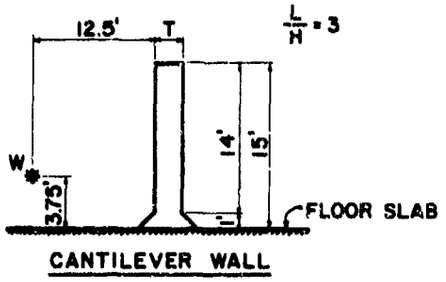
d. For the unit prices ($350 per ton for steel and $40 per cubic yard for concrete) considered, it is shown (fig. 10–7) that the cost of the wall to resist a 1,000-pound explosion would be $79 per cubic yard of concrete (including formwork) which is in the order of magnitude of conventional concrete structure costs.

e. The analysis also indicated that in order to obtain

2

minimum construction cost, the thickness of the wall should be increased as the charge weight is increased. This concrete thickness should be compatible with flexural reinforcement (vertical steel in each surface of a cantilever wall) equal to 0.49 percent (optimum reinforcing steel). Although this optimum percentage of reinforcement will vary with the cost of materials, the variation is small. For example, when the concrete price varies between $35 and $45 per cubic yard and the steel price varies from $200 to $500 per ton, the upper and lower limits of the optimum reinforcement are approximately 0.65 and 0.4 percent, respectively (fig. 10-8). This variation does not significantly affect the power function variation, charge weight versus cost, as given in figure 10-7.

f. The lower limit of the charge weight (110 pounds) in the power function relationship is dependent on the minimum thickness of concrete walls as specified in the ACI Building Code. Another power function of the charge weight versus construction cost occurs at charge



LEGEND

SW , Standard Wall
LW , Laced Wall
T , Wall Thickness

UNIT PRICE

Conc., SW - $35/c.y.
LW - $40/c.y.
Reinf., SW - $300/Ton
LW - $350/Ton

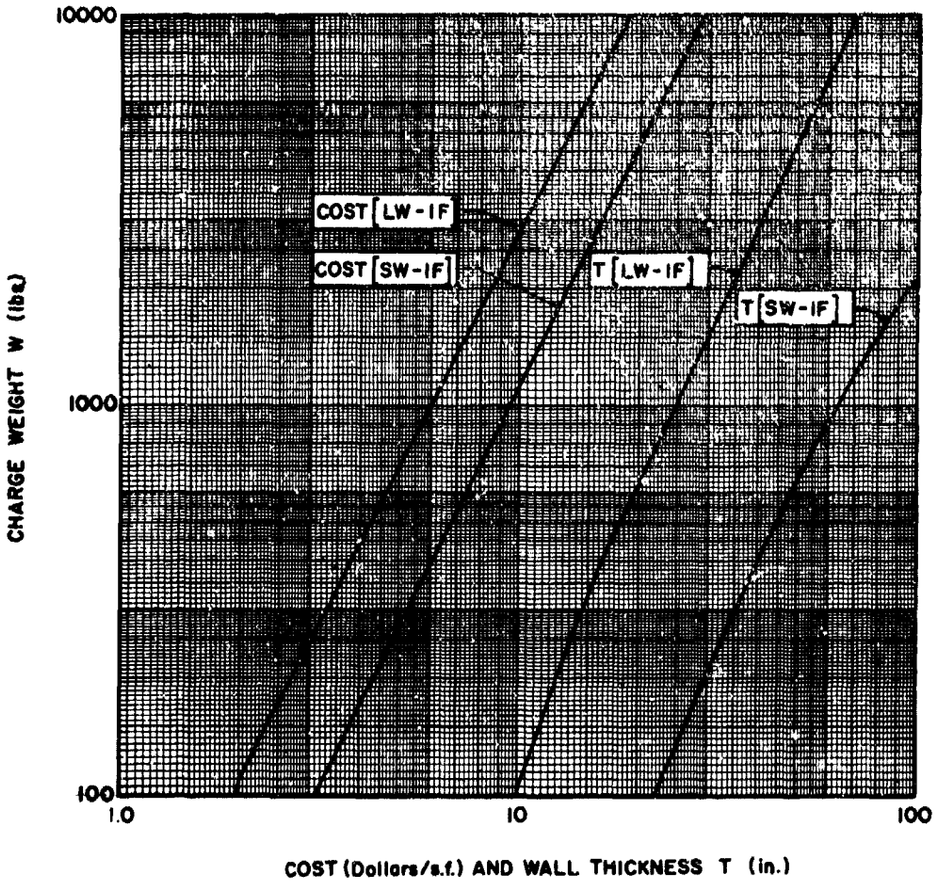


Figure 10-9. Comparison of cost and thickness of laced and standard walls.

weights less than 110 pounds. This relationship is controlled by the variation of reinforcement from the optimum to that specified for minimum steel. The cost is constant for all charge weights less than that which can be resisted by the minimum section.

g. For comparison, the costs of laced single walls designed to approach incipient failure conditions were compared with costs of composite walls (two laced concrete panels separated by 3 feet of sand) designed for the same protection, and also compared with costs of laced single walls designed to fail with controlled fragment velocities of 100 fps or less. For the range of charge weights considered, composite construction using sand as the filler material is more expensive. Furthermore, larger overall wall sections are required. However, at very large charge weights, both cost and concrete thicknesses of composite walls approach those of the laced single walls.

h. As may be expected, the post-failure fragment criteria results in a substantial cost reduction. For charge weights ranging between 1,000 and 10,000 pounds (minimum concrete and steel) (fig. 10–7), the

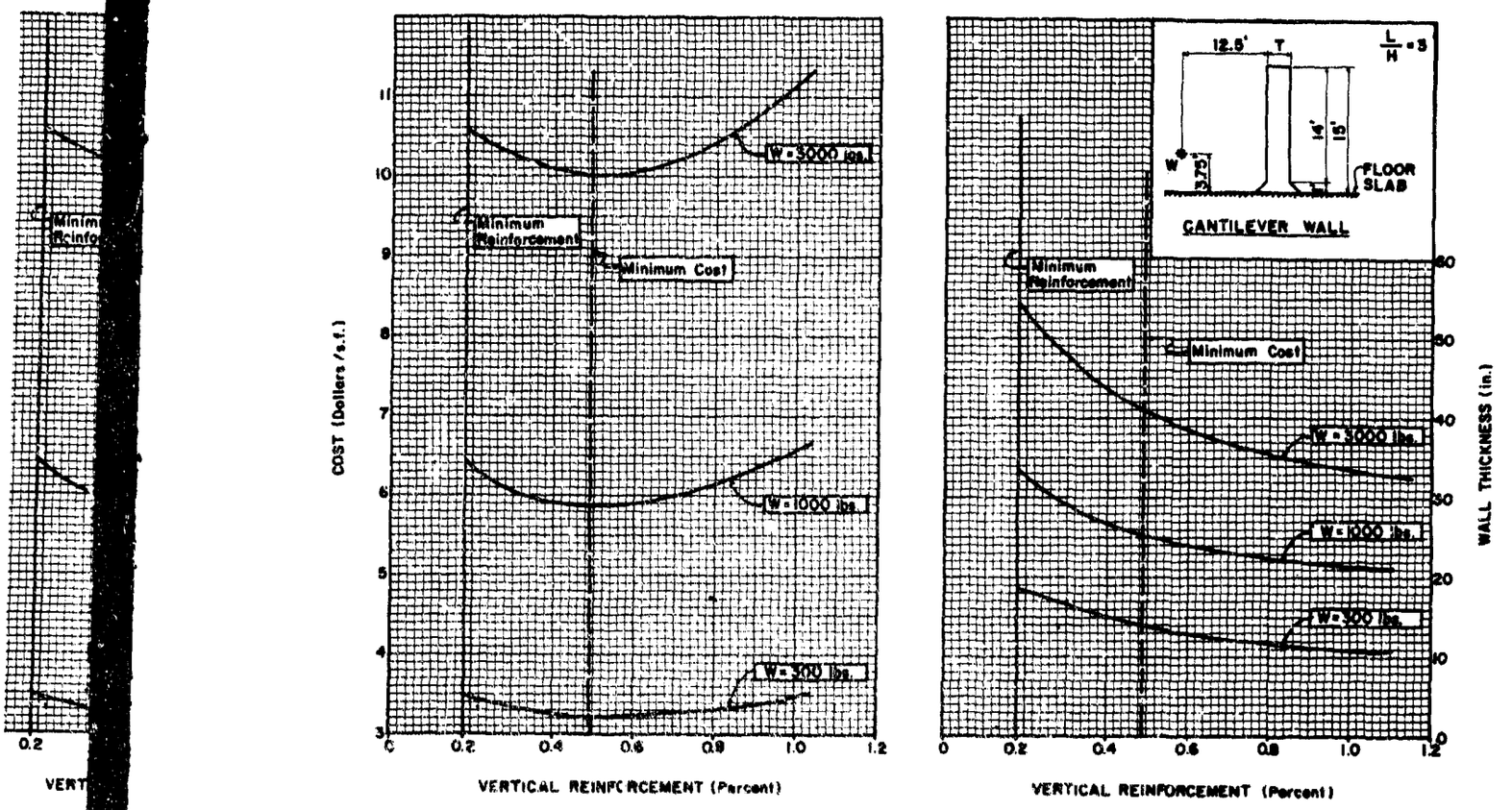


Figure 10–10. Variation of cost and thickness with percent reinforcement.

cost for walls designed for post-failure fragment criteria varies between approximately one-third and one-half the cost of walls designed for incipient failure. Therefore, the cost advantage of designing a wall for post-failure fragment criteria instead of incipient failure decreases as the charge weight increases. It may be noted that the cost of the "12-inch standard wall" is approximately the same as that of mimimum laced single walls (10-inch thick section). However, for the post-failure fragment criteria (velocity = 100 fps), the charge capacity of the "standard wall" is one-third that of a laced wall.

i. As an extension to the analysis, the costs of laced concrete walls were compared to the costs of standard concrete walls (with varying thickness) which utilize the same percent reinforcement (0.167 percent) as the "12-inch standard dividing wall" (fig. 10–9). The costs of the laced walls vary from 80 percent to 67 percent of the costs of the standard walls for charge weights of 100 and 10,000 pounds, respectively. Moreover, the thickness of the standard walls are substantially larger than those of laced walls. As a comparison, for a 100-pound charge, the required thicknesses of laced and standard walls are 10 and 22 inches, respectively.

j. In many installations, the space required for the concrete wall thicknesses corresponding to the optimum reinforcement is not available. Increased amounts of reinforcing steel must be provided to decrease the thickness of the wall. Figure 10–10 illustrates the additional cost incurred if the thickness of the previously mentioned cantilever wall is reduced. For all charge weights studied, the cost increase when 1-percent flexural steel

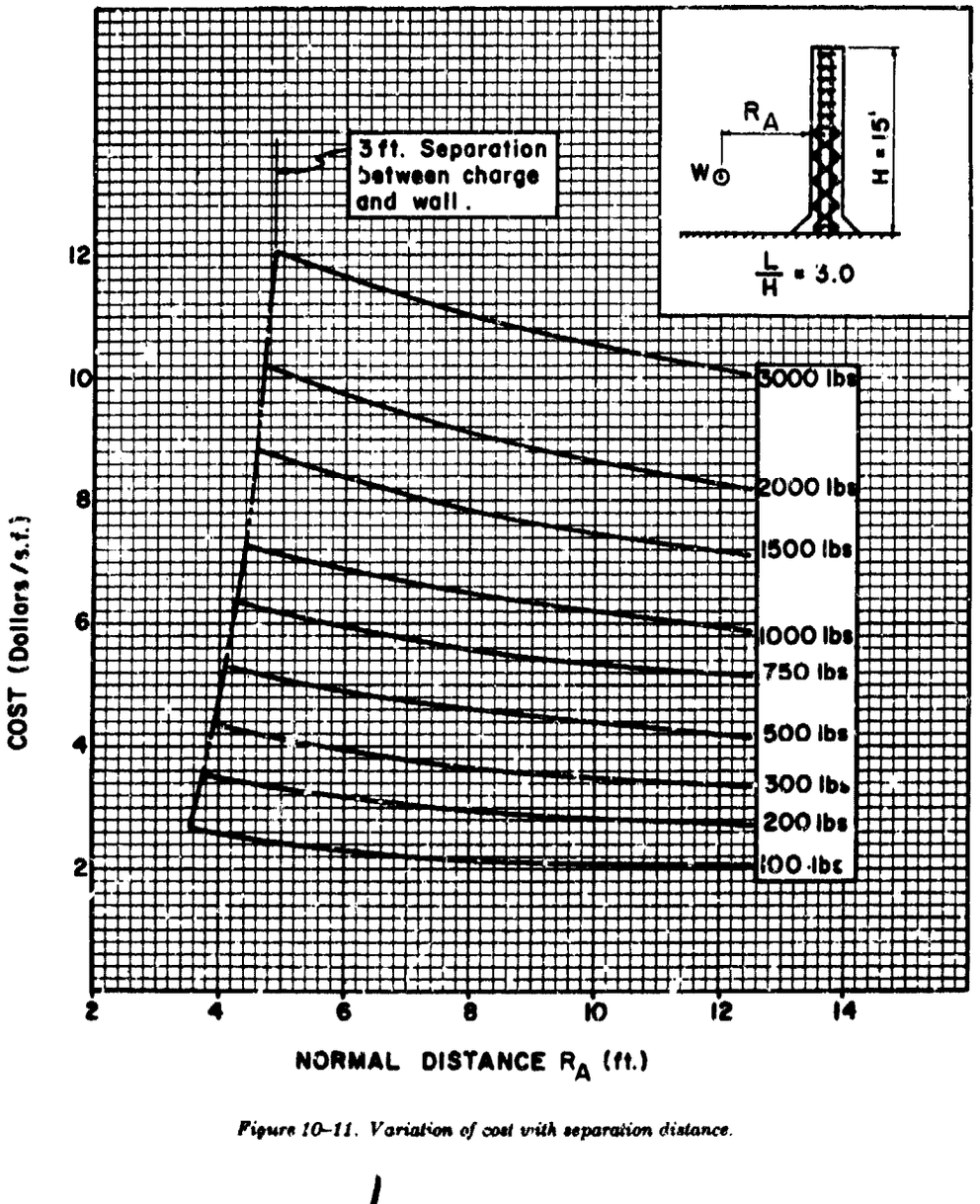
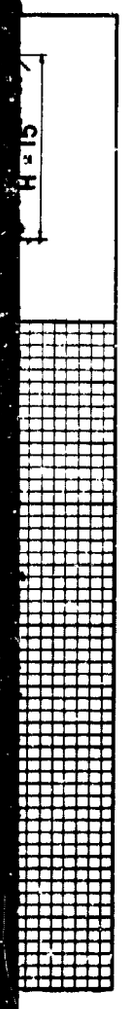


Figure 10–11. Variation of cost with separation distance.

(fig. 10–9). The costs
ercent to 67 percent
for charge weights of
ively. Moreover, the
e substantially larger
mparison, for a 100-
knesses of laced and
ches, respectively.
pace required for the
nding to the optimum
ncreased amounts of
to decrease the thick-
strates the additional
the previously men-
For all charge weights
-percent flexural steel



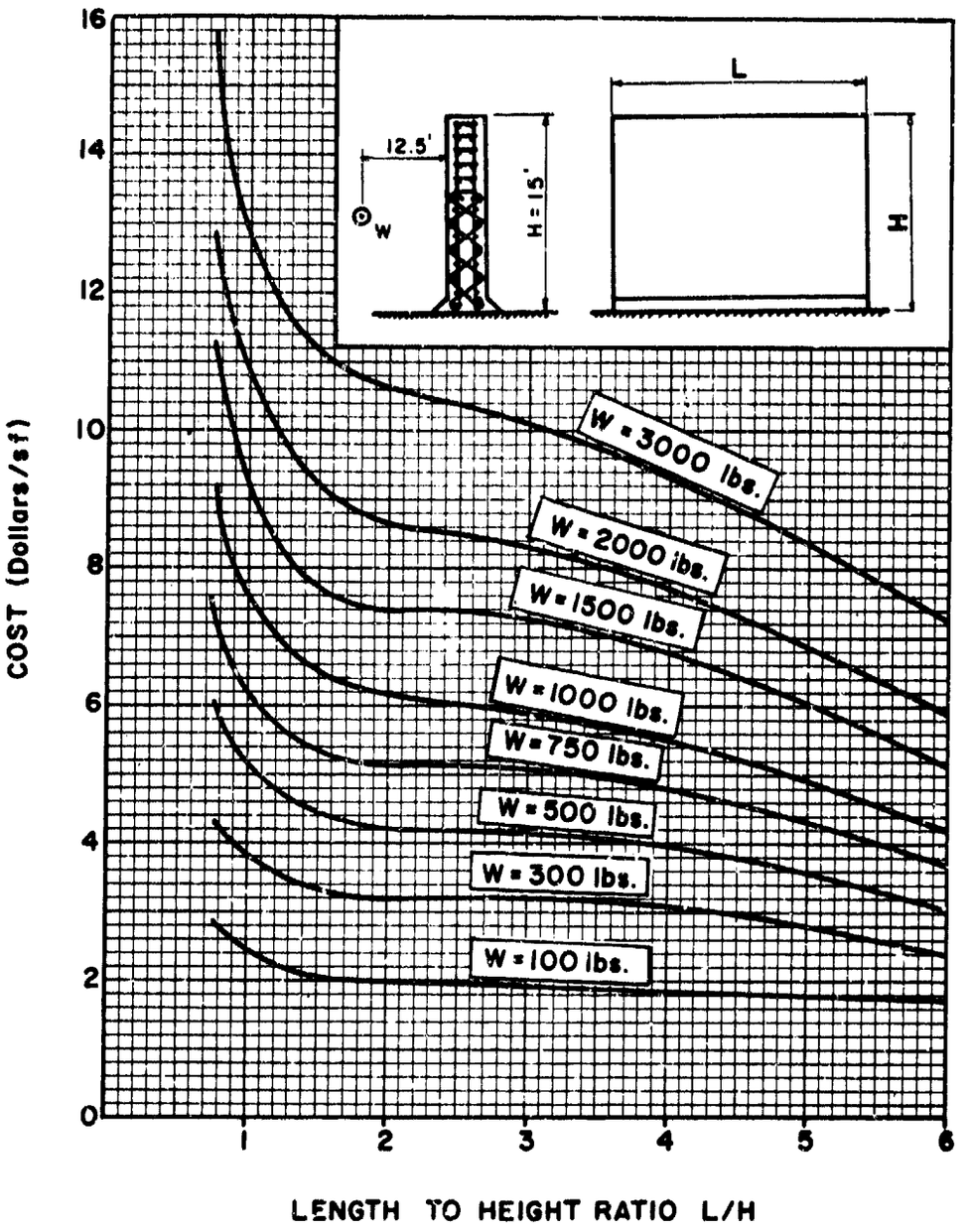


Figure 10–12. Variation of cost with wall length to height ratios.

is used in each face of the wall is approximately 10 percent (for concrete and steel) above the cost of optimum reinforcement designs. However, when the cost for formwork is included, this increase is less. Depending upon the charge weight, a wall thickness reduction of 20 to 30 percent is associated with the use of the larger percentage of steel (1 percent).

k. As an explosive charge is moved closer to a wall, higher construction costs are realized. In the case of the cantilever wall, to move the charge from its 12-foot, 6-inch separation distance to a location where the charge is 3 feet from the wall, the added cost is in the order of 15 to 20 percent (fig. 10–11).

l. Another increase in the unit cost of the wall occurs when the length to height ratio of the wall is decreased. This increase is substantial for the larger charge weights (fig. 10–12) and results from a concentration of the larger blast loads, occurring adjacent to the explosion, over a shorter length of wall.

m. The cost trends discussed for the cantilever wall also apply to walls which span in two directions. Because of the two-way action, an added factor is involved in

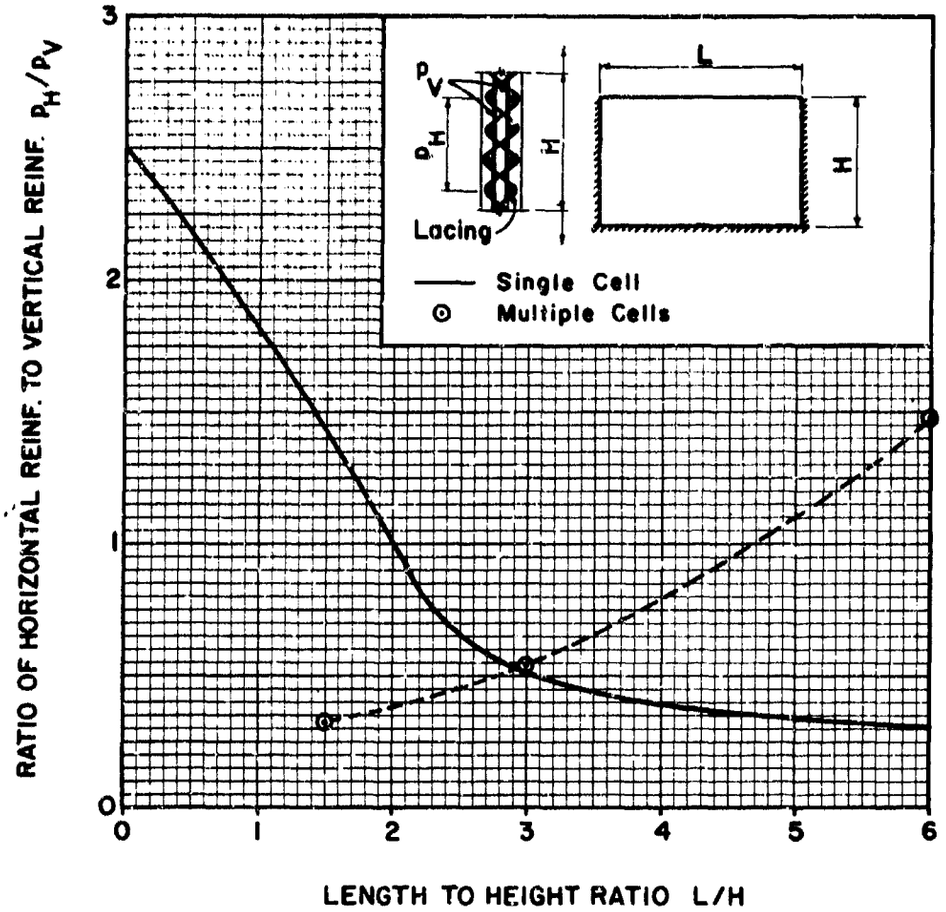


Figure 10–13. Proportioning of reinforcement in two-way elements.

determining the cost effectiveness of these walls. Before the optimum thickness and reinforcement can be established, the optimum placement of the steel in both the horizontal and vertical directions must be determined in order to obtain the maximum wall capacity for a given total amount of steel used in the wall. As shown in figure 10–13, the proper amount of reinforcing steel in each direction is a function of the length to height ratio of the wall.

n. The steel proportions indicated in figure 10–13 are optimum steel placements for single-cell arrangements and for multicubicle structures where all cells have the same dimensions and donor system (charge weight and location). For multicubicle structures with unsymmetrical cell arrangements and/or variation of the donor systems, these proportions may require adjustment to attain the optimum total amount of steel in the entire structure. As an example, consider a three-cell structure whose dimensions, of progressive cells, are defined by length to height ratios of 1.5, 3.0, and 6.0. Each cell is to contain 3,000 pounds of high explosives located 3 feet from the surface of the back wall. The results of an analysis indicated that the required ratios of percentages of the horizontal to vertical steel, to obtain minimum total steel, were approximately one-third, equal to, and four times as large as, those given in figure 10–13 for the small-, medium-, and large-size single cells, respectively.

o. Once the correct steel proportions are obtained, the optimum reinforcement and wall thickness are calculated in a manner similar to that illustrated by the cantilever wall analysis.

Section IV. PROTECTIVE CLOSURE SYSTEMS FOR SHELTERS

10–6. General

a. If it were practical to build protective shelters without openings, such structures would be considerably simplified, and the protection level of the shelters would be controlled only by the integrity of the structural shell and the ability of the interior components to withstand the effects of structure motions. Once openings are provided, the possibility of the entrance of blast pressures, heat, dust, fragments, and toxic gases through the openings into the interior must be considered and appropriate preventive measures taken.

b. Since it is necessary that protective shelters be constructed with entrances and exits for access of personnel and equipment, and provided with a source of outside fresh air for ventilation, cooling, and combustion equipment, it is evident that openings to the exterior are required. Such openings may be divided into two broad classifications: those which are open only intermittently to allow for the entrance of personnel and equipment, and those which remain open continuously for ventilation, except during the passage of the blast wave and during possible pre-shot and post-shot "button up" periods.

c. Blast closure systems consist of devices or structural elements which protect access or ventilation openings of a shelter. The general terms used in the manual are blast doors and blast valves or shields which pertain to access openings and ventilation openings, respectively.

10–7. Blast Doors

a. In protective structures, blast doors may be used to provide shielding against fragments, fire, heat, dust, gas, and smoke, in addition to blast protection. Some blast leakage past the door and buildup of pressure within the shelter may be permitted even where personnel are exposed, if the final interior pressure level does not exceed acceptable limits.

b. Entrance openings should be kept as small and few in number as possible to minimize shielding problems, but not less than that required for operational and/or emergency access and egress. The Safety Manual requires that at least one exit be provided for a small operating cubicle area whose occupancy is not more than two persons. Larger operating rooms or buildings require at least two exits, and, when more than eight persons occupy the same area, one additional exit for each five additional persons must be provided. If possible, exits should be located at opposite sides of the area, equally spaced about the perimeter of the building, and with no occupant more than 25 feet from the nearest exit. Also, each exit opening should be at least 30 inches in width.

c. The above recommendations apply to those structures which contain explosive operations. For shelters where nonhazardous operations take place, the number of openings may be reduced both in size and number. It is recommended that at least one unit (22 inches) of access and egress width be provided for every 200 shelter occupants. Each single opening should be 24 inches in width, and at least two openings should be provided in larger shelter areas.

d. If siting analysis indicates that a potential explosive hazard is more probable from one direction, the entrance should be oriented to minimize the blast loads imposed on the blast door. If the explosion is equally probable in all directions, it is possible to design a layout which will minimize the effects on the door. The preferred solution is an opening facing away from the detonation or parallel to the direction of the blast propagation. An entrance parallel to the shock front is the least desirable. Attention must also be given to the possibility of entrance blockage by blast debris. Blockage by debris is of particular interest in the design of those facilities where recovery after an explosive event may be delayed for a significant length of time by subsequent explosions, fires, blockage of roads, etc. Here, the occupants must be capable of leaving the shelter without outside assistance.

e. In addition to providing shielding for exterior openings into shelters, blast doors can also be used to separate one or more areas within a structure. A blast door may act as the closure system for openings between two adjoining cells or as the closures of entrances into one or more cells from passage ways. Also, interior blast doors serve as the inner blast shield of blast locks. Such locks consist of two blast doors (arranged so as to form a lock or chamber with the doors) interlocked either electrically and/or mechanically so that only one of the doors may be open at any one time. Blast locks are desirable for continuously-manned, explosive- handling operations or where frequent passage between two areas (one area containing a potential explosion and the other a shelter) is required. An example of this latter situation is the facility which contains both a test cell where periodic x-raying or other checking of explosive materials is accomplished, and an operational shelter containing the personnel performing the tests.

f. For low blast pressures and for those cases where primary or post-failure fragment-shielding requirements are not high, solid wood doors, metal-clad wood-core doors, and hollow-metal doors may be used. As the blast requirements increase, steel and concrete doors of various construction are required. Concrete doors or steel doors filled with concrete, sand, or other material are effective for combined blast and fragment shielding. The type of door used will be a function of the design requirements. Personnel doors have been designed and tested at peak pressures up to several hundred pounds

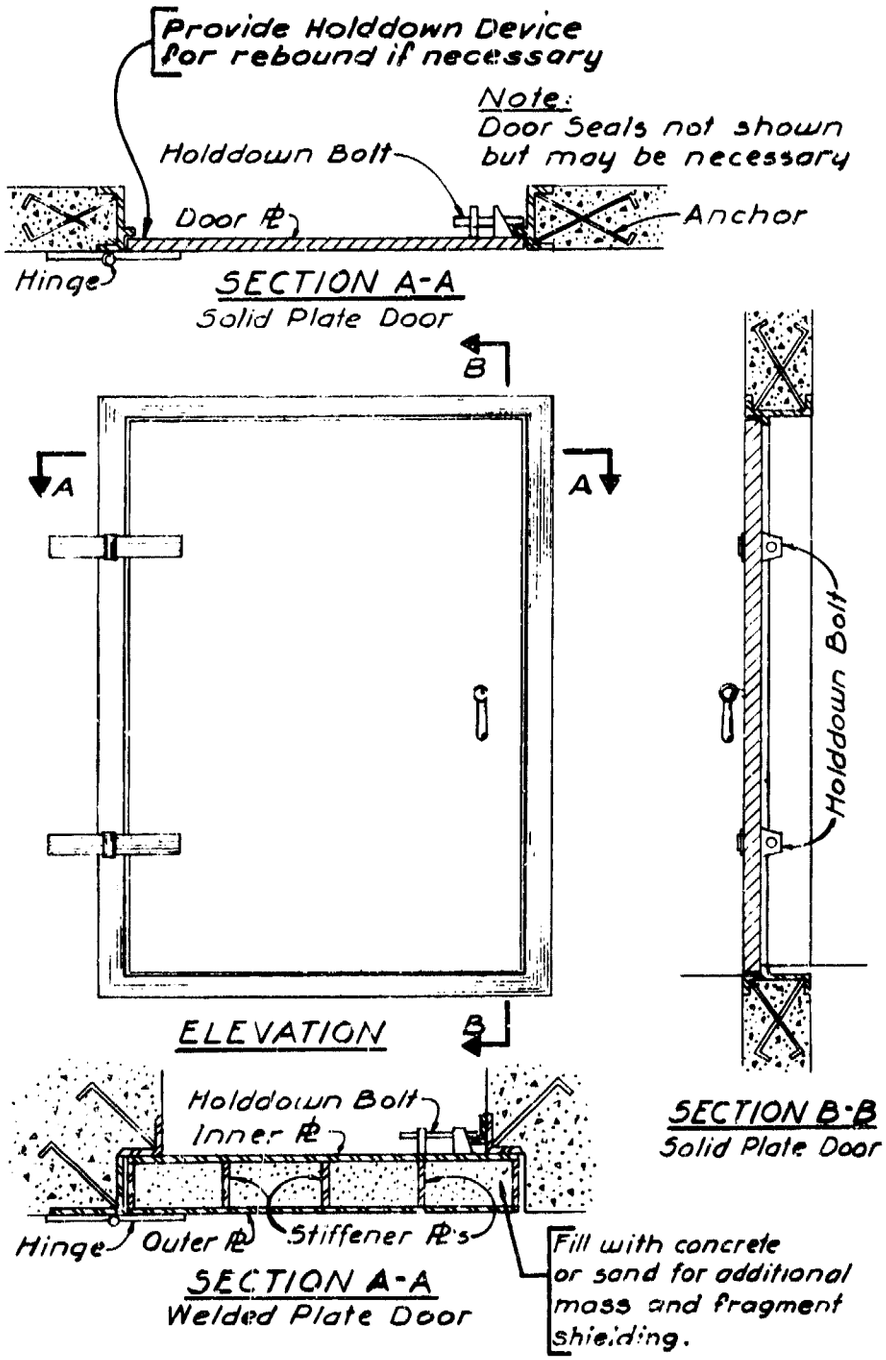


Figure 10-14. Steel-plate doors.

per square inch for long duration loads and would sustain even higher blast loads for the shorter duration loads associated with high-explosive detonations.

g. Large doors may require operating mechanisms for opening and closing the doors. The time limits set for opening and closing determine the power requirements and are reflected in the cost of the operating machinery. Operating mechanisms can be mechanical, hydraulic, or compressed-air types with an appropriate power source. Provision for manual operation should always be provided. In most cases, it is feasible for personnel doors to be manually operated.

h. Examples of steel, concrete, and composite doors are described below:

(1) Figure 10–14 illustrates typical solid and built-up steel plate doors. The solid plate door is the simplest in construction, but may result in a very heavy door. This type of door may be used to seal openings in those elements designed for the blast effects associated with the high-pressure design range. The steel plate is capable of resisting and transferring the high local shear stresses produced by the non-uniform blast loads. In addition to the steel door, laced reinforced concrete doors are also useful to resist close-in blast effects. Lacing details for these doors are similar to those for concrete walls. Because blast doors are usually not restrained from sliding at their supports and may be disengaged from their supports if large deflections are permitted, it is recommended that the design criteria for concrete doors limit support rotations to less than 5 degrees.

(2) Stiffened plates, multiple-welded beams, plates, and beams, and double-plate doors (fig. 10–14) provide doors which are lighter for the same blast pressure than a solid-plate door. Because of the need for welding and other undesirable features, the use of built-up units is not recommended for those doors designed to resist the close-in effects resulting from a detonation.

(3) Figures 10–15 through 10–18 depict flat, solid, and built-up steel-plate doors which have been tested and successfully resisted the long duration blast effects of a nuclear explosion. A heavy solid plate, bank-vault type door is shown in figure 10–15. The multiple-welded-

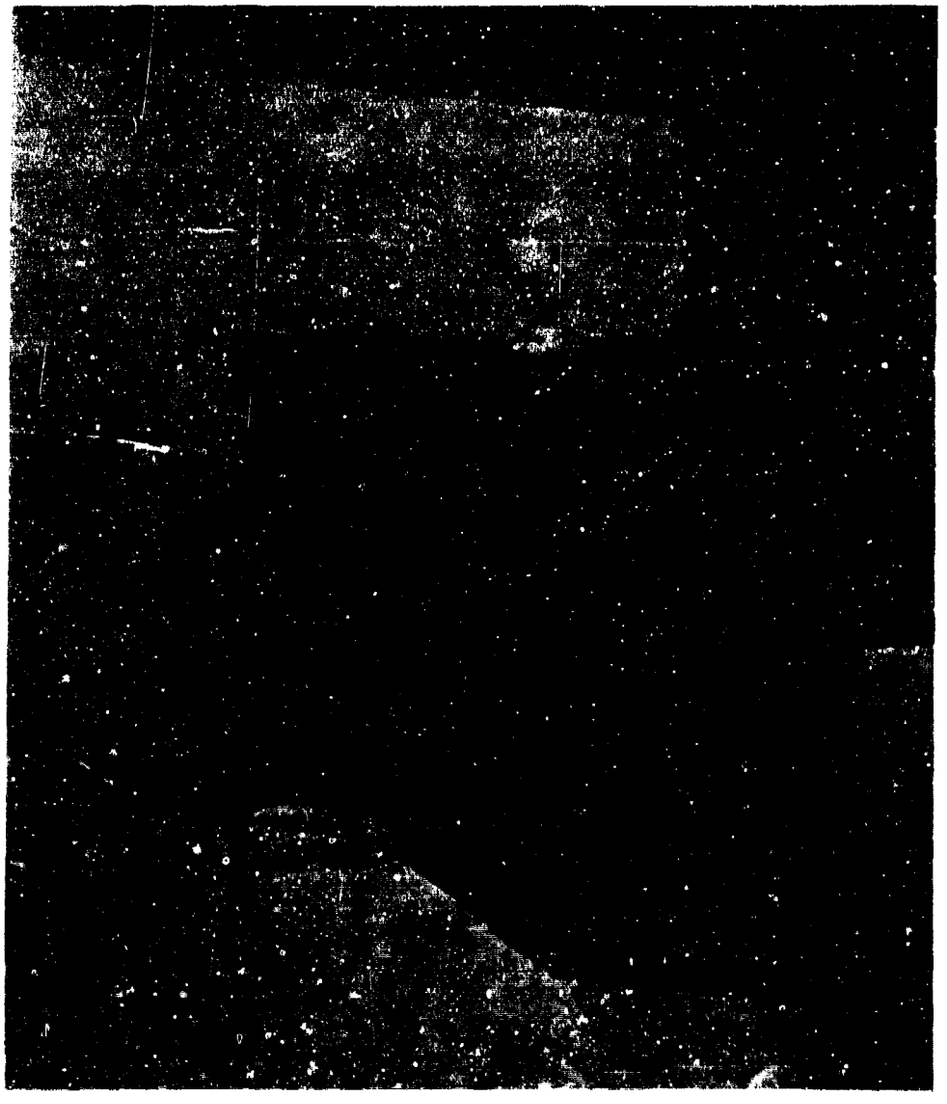


Figure 10–15. Vault-type door.

beam door in figure 10–16 is hinged at the bottom and opens in a manner similar to that of a drawbridge. Figure 10–17 illustrates a welded door composed of T-sections and channels. The reinforced airtight door shown in figure 10–18 is an adaptation of a door used to close off compartments within a ship.

(4) Arch (fig. 10–19) and dome plates provide the lightest doors for a given blast pressure. The tension arch door requires compression ties to develop the compression reactions for the arch and to prevent the door from being blown through the opening. The compression arch requires a tension tie plate to develop the reactions and to prevent large distortions in the door that may bind it in place. Similarly, the dome plate doors also require a tension ring or ties. However, these ties may be eliminated if reliable buttresses are provided. Figure 10–20 shows an example of a tension arch blast door, and figure 10–21 shows an escape-hatch, dome-plate blast door, both of which were tested with long-duration blast loads.

(5) Design of the basic portions of a blast door is not usually time consuming; however, the detailing of associated mechanisms, such as hinges, reversal mechanisms, seals, etc., may require a considerable design effort to insure proper operation of the door before, during, and after an explosion. Standard blast-door designs (table 10-1) have been prepared which will significantly reduce the amount of engineering required for blast-door design. These standard designs, which were prepared for the Department of the Army, have been developed for use in structures designed to resist the effects of nuclear events (megaton detonations) and they are directly applicable for use in structures designed for the low-pressure range where long duration blast loads are encountered. For the high- and intermediate-pressure design ranges where the load durations are relatively short, these doors may have reserve strength above that indicated in table 10–1. Therefore, these designs will require further analyses to determine the ultimate capacity of a particular blast door for its particular blast environment.

(6) The pressure levels indicated in table 10–1



Figure 10–16. Welded-beam door.

are peak incident pressures. However, the doors were designed to resist the reflected pressures associated with these incident pressures and, therefore, may be used for closures of building openings facing towards the explosion as well as for openings facing in the other directions from the pressure source.

10–8. Blast Valves and Shields

a. In most designs for protective shelters, the air requirements for personnel and equipment are provided by direct connection to the exterior. In some special instances, the air is cooled, purified, and replenished with oxygen within the shelter itself, thereby eliminating the need for ventilation openings and the associated problems. Such a solution is usually very expensive and impractical for the average shelter for extended stay times. To provide protection for a shelter's contents from the exterior blast pressure, either the sizes of air intake and exhaust openings must be restricted to those size openings which will limit pressure buildup within



Figure 10–17. Built-up steel door.

the shelter to less than that which will result in damage (or injury) to the building contents, or the openings must be sealed with blast valves or other protective closure devices. Because an internal leakage pressure of 5 psi (threshold pressure for eardrum rupture) would be produced by an external reflected blast pressure of 85 psi resulting from an explosion of 25,000 pounds of high explosives (fig. 10–22), a shelter containing personnel who are exposed to this pressure level and which has an access opening to volume ratio of 0.00444 would require blast closures.

b. For short duration blast waves, devices such as baffles, mufflers, etc., which restrict the openings and retard the passage of the blast, are partially effective when used with plenums of adequate size. For longer duration blast waves, and in shelters where normal operational air requirements are small, sand filters may be useful in the attenuation of the leakage pressures. On the other hand, if the air requirements are larger, a more automatic protection system is required and can be accomplished by using either remote-actuated valves with flash, pressure, or thermal radiation sensors,

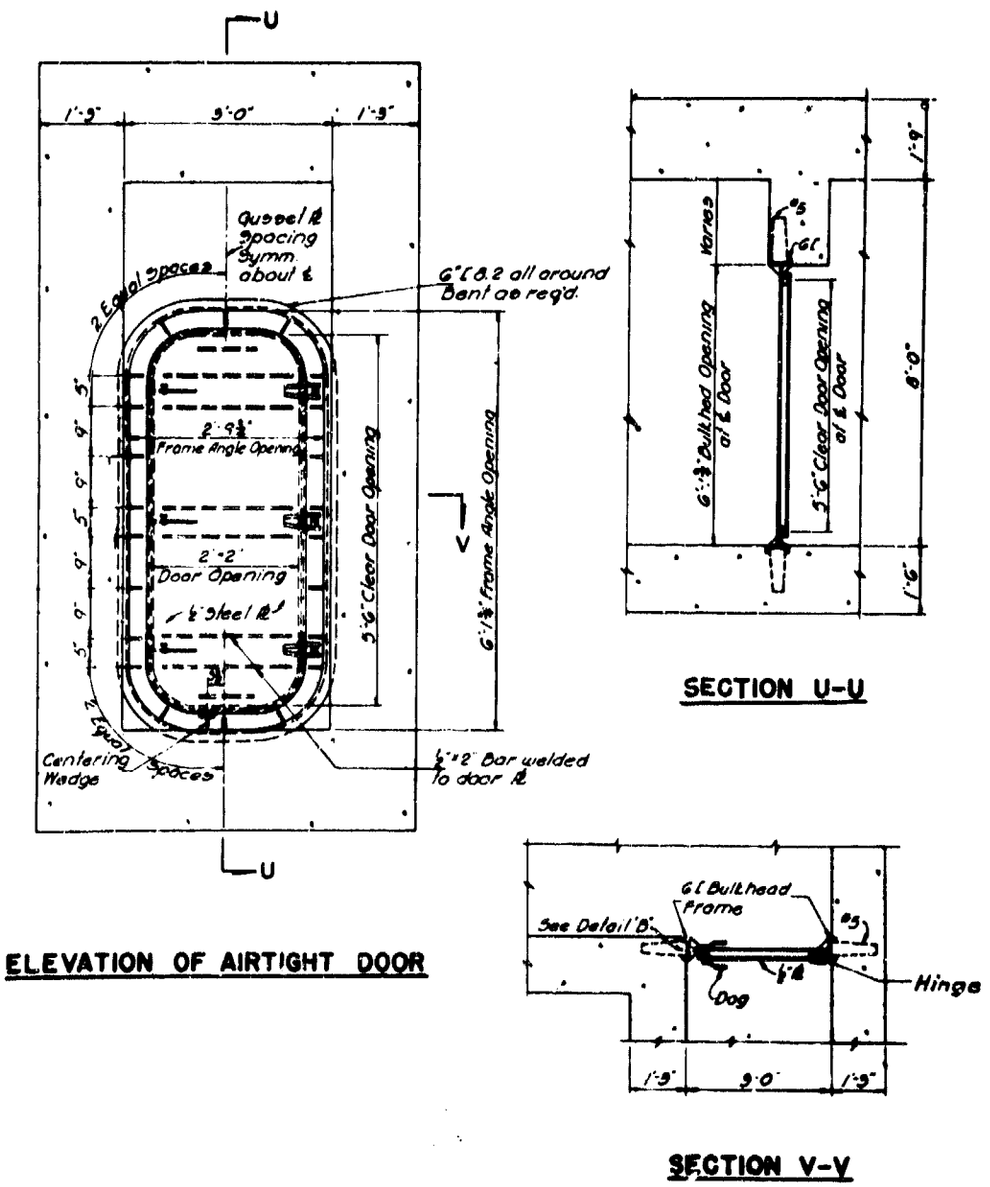
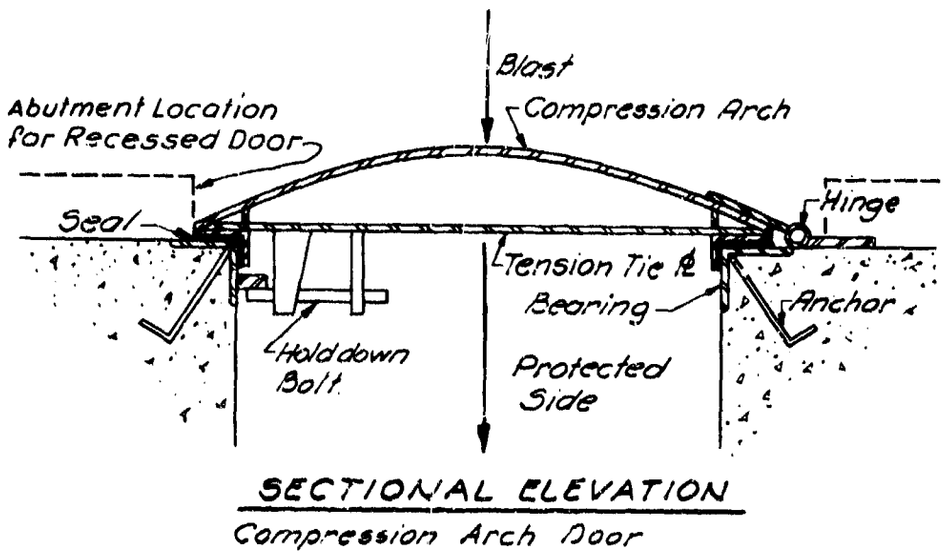


Figure 10–18. Airtight door.

waves, devices such as
trict the openings and
are partially effective
quate size. For longer
shelters where normal
small, sand filters may
the leakage pressures.
equirements are larger,
ystem is required and
either remote-actuated
rmal radiation sensors,



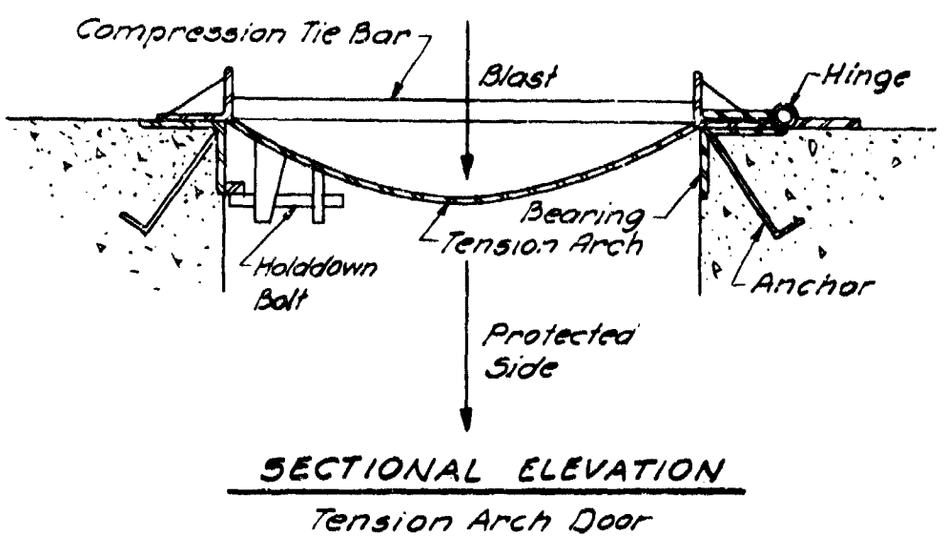


Figure 10–19. Steel-arch doors.

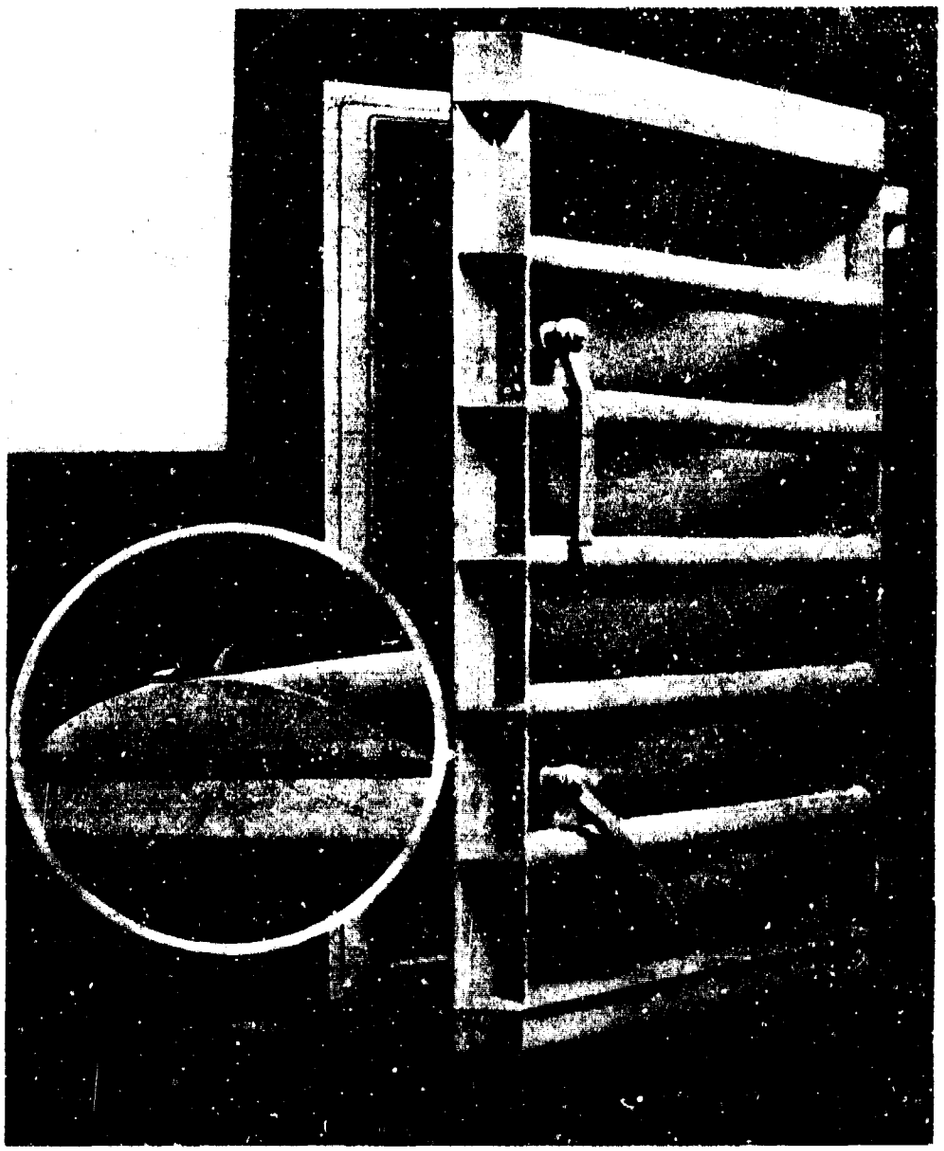


Figure 10–80. Tension-arch door.

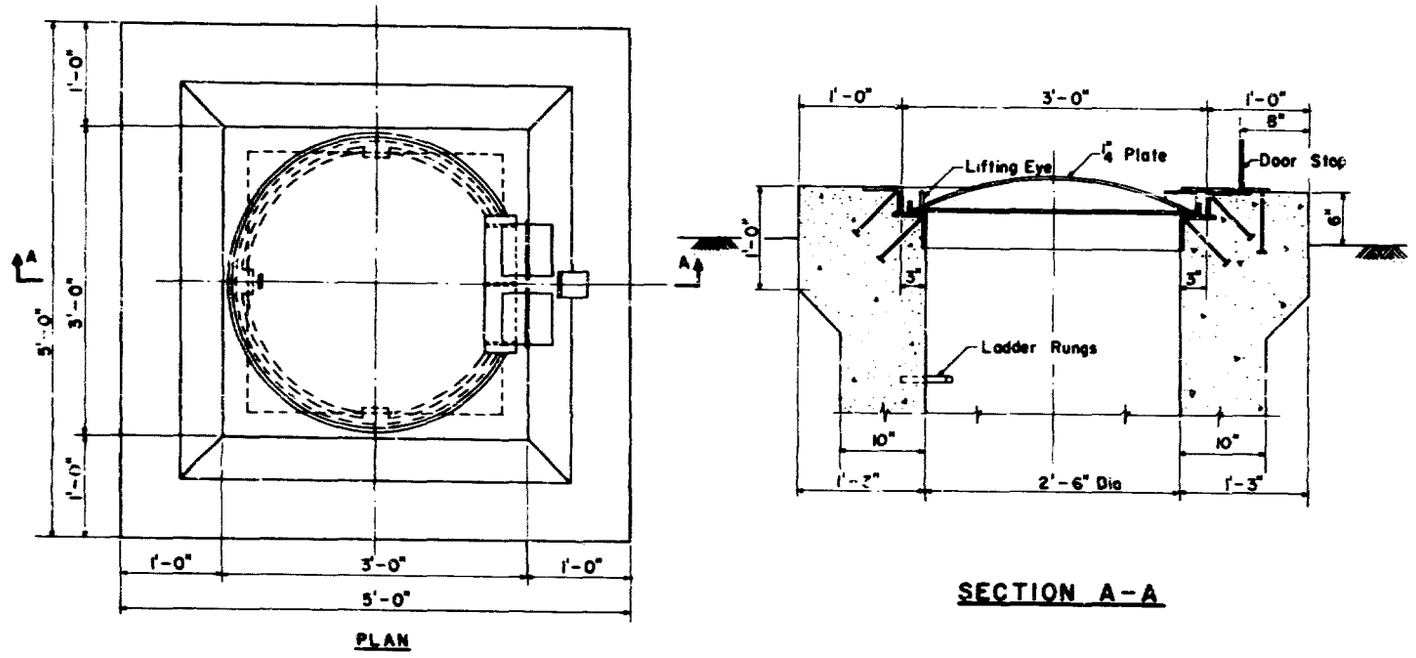


Figure 10–21. Dome-plate door.

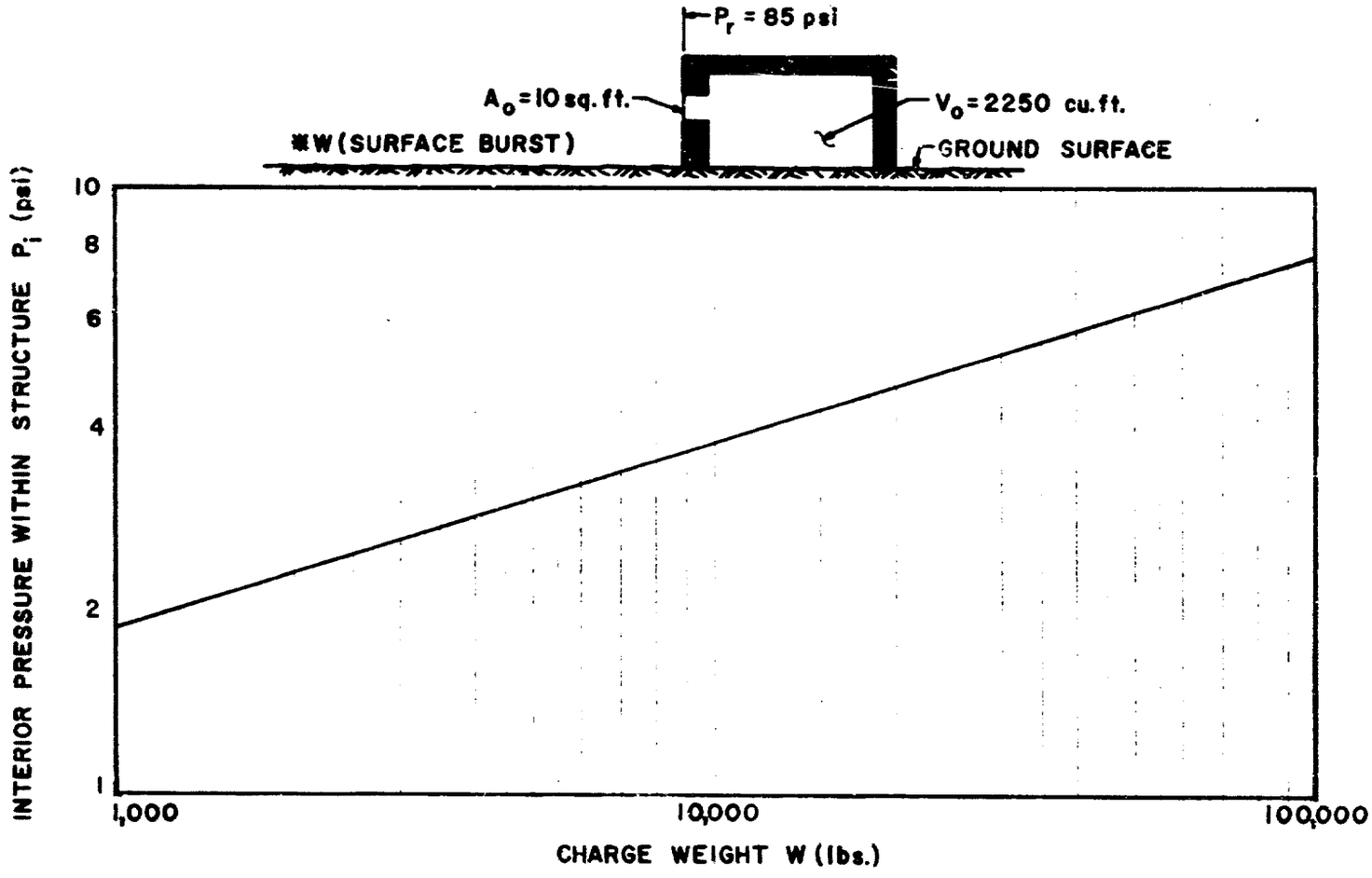


Figure 10–22. Leakage pressures into a structure.

Table 10–1. Standard Drawings for Blast Doors

Door type	Pressure level* (psi)	Size (ft.)	Standard designs**	
			Drawing No.	Spec. No.
Pedestrian	25	3-½×7	60-12-06	60-12-06-60
	50		60-12-07	
	100		60-12-08	
	25	6×7	60-12-09	60-12-09-60
	50		60-12-10	
	100		60-12-11	
Vehicular	25	8×8	60-12-12	60-12-12-60
	50		60-12-13	
	100		60-12-14	
	25	12×12	60-12-15	60-12-15-60
	50		60-12-16	
	100		60-12-17	
	25	14×18	60-12-18	60-12-18-60
	50		60-12-19	
	100		60-12-20	
Hatch	25	3×3	60-12-21	60-12-21-60
	50		60-12-22	
	100		60-12-23	
Service Access	25	2-½×4	60-12-24	60-12-24-60
	50		60-12-25	
	100		60-12-26	

* Incident pressure capacity (long duration).
** Available to authorized persons from Office of Chief of Engineers (ENGMC-EM).

Figure 10–22. Leakage pressures into a structure.

or by using blast-actuated valves (depending on the blast pressure required to close them). Where large volumes of air must be handled during normal operation, positive closures are needed which, under normal operating conditions, do not unduly obstruct the air passage. These obstructions would increase pressure losses in the system, thereby increasing the ventilation power requirements which, in turn, would result in higher operating costs.

c. If it can be assumed that the ventilation system can be closed off prior to the occurrence of an explosion and kept closed until there is no danger of further blast, a relatively simple structural closure (blast shield), such as a steel plate, can be utilized. Blast shields are particularly useful for closure of exterior openings which would be opened only periodically, such as maintenance facilities, where the release of toxic fumes from within the structure is required.

d. Remote-actuated valves are dependent on external sensing devices which trigger the closure mechanism and close the valve before arrival of the blast wave. Actuating devices have been developed that are sensitive to the blast pressure of an explosion and react electrically to trigger protective closure systems. Other actuating devices sensitive to flash and thermal radiation are also available. The pressure sensing device is placed on a circumference at a predetermined radius from the valve (closer to ground zero) in order to compensate for time delays of electrical and mechanical control equipment and to permit valve closure before the blast arrives. Thermal sensors are designed to detect the characteristic pulse emitted by an explosion to prevent actuation by other sources such as lightning, fires, etc., which may occur with flash sensors.

e. Arrival time for various peak blast pressures is given in figure 10–23 for unconfined surface bursts. It is seen that with remote-actuated valves, a closing time of less than about 20 milliseconds (approximate minimum closure time of available remote-actuated valves) is acceptable for an incident pressure level of 25 psi for an explosion of 1,000 pounds or larger. However, for smaller weight charges and/or higher pressures for the same size explosion, this closing time would be inadequate. For the latter situation, a delay in the arrival of the blast at the valve would have to be designed into the system. This may be accomplished by locating the ventilation inlet (fig. 10–24) at a sufficient distance L from the blast valve such that the combined travel time of the blast wave from the explosion to the inlet and back to the valve will be longer than the closing time for the valve after it is actuated. Figure 10–24 illustrates this method of delaying the blast arrival at the valve. After the blast wave passes the shelter and reaches the inlet, it will propagate down the air intake and return to the shelter with the blast pressure entering the plenum chamber after the valves have been actuated. The pressure in the plenum will be significantly less than that initially applied to the shelter shell. As a result of the blast effects, the air intake hood and screen may be severely damaged or demolished, but this should not affect subsequent operation. A debris pit will enable foreign matter, which may enter during the blast, to be deposited below the horizontal run of the intake duct. The plenum will enable the valves to be serviced and replaced without difficulty and may also alter the shock rise time, resulting in less severe loading condition for the valves.

f. Self-acting blast-actuated valves, which close under the action of the blast pressure, overcome some of the disadvantages described above and present other factors to be considered. Since the valves are closed by pressure, they are not dependent upon sensing devices for operation. They can be automatically reopened after passage of the positive phase or latched closed during the negative phase if this is required. Double-acting valves automatically seal the opening during the negative phase. Since blast-actuated valves are closed by the blast, there is an inherent leakage problem to be considered due to the finite closing time. Although this is in the order of milliseconds for most valves, sufficient flow to cause damage may pass the port openings for certain valve designs and pressure levels. Effectiveness

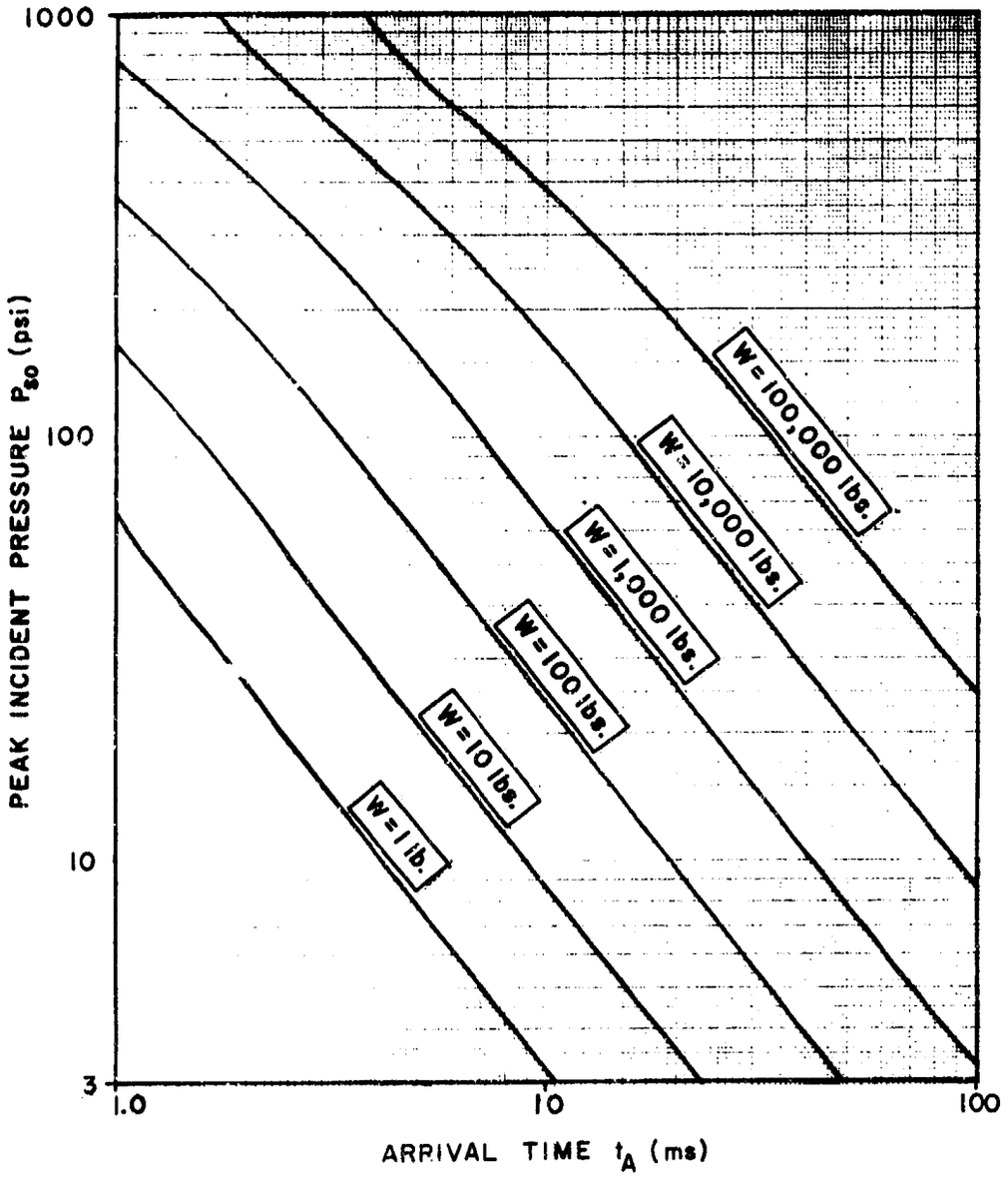


Figure 10–23. Peak incident pressure vs. time of arrival (surface burst).

of closing at both high- and low-pressure ranges must be checked. The amount of blast entering depends on the closing time of the valve which, in turn, depends on the mass of the moving parts, disk diameter, and the distribution of pressures on both faces of the disk.

g. Ideally, a blast-actuated valve should possess the following characteristics: instantaneous closure or no leakage beyond the valve during and after closure, no rebound of moving parts, equal efficiency at all pressures below the design pressure, operational and structural reliability, minimum of moving parts, low-pressure drop through the valve at normal ventilation or combustion air flows, multiple detonation capability, durability, and easy maintenance.

h. Although instantaneous closure is not physically possible, the closing time can be reduced sufficiently to reduce the leakage to insignificant values. This may be accomplished by increasing the activating pressure-force-to-moving-mass ratio, decreasing the length of travel, permitting no deceleration during closure, and other methods.

i. A blast-actuated valve can be made completely blast-tight by extending the blast travel path sufficiently to allow the valve to close before the blast

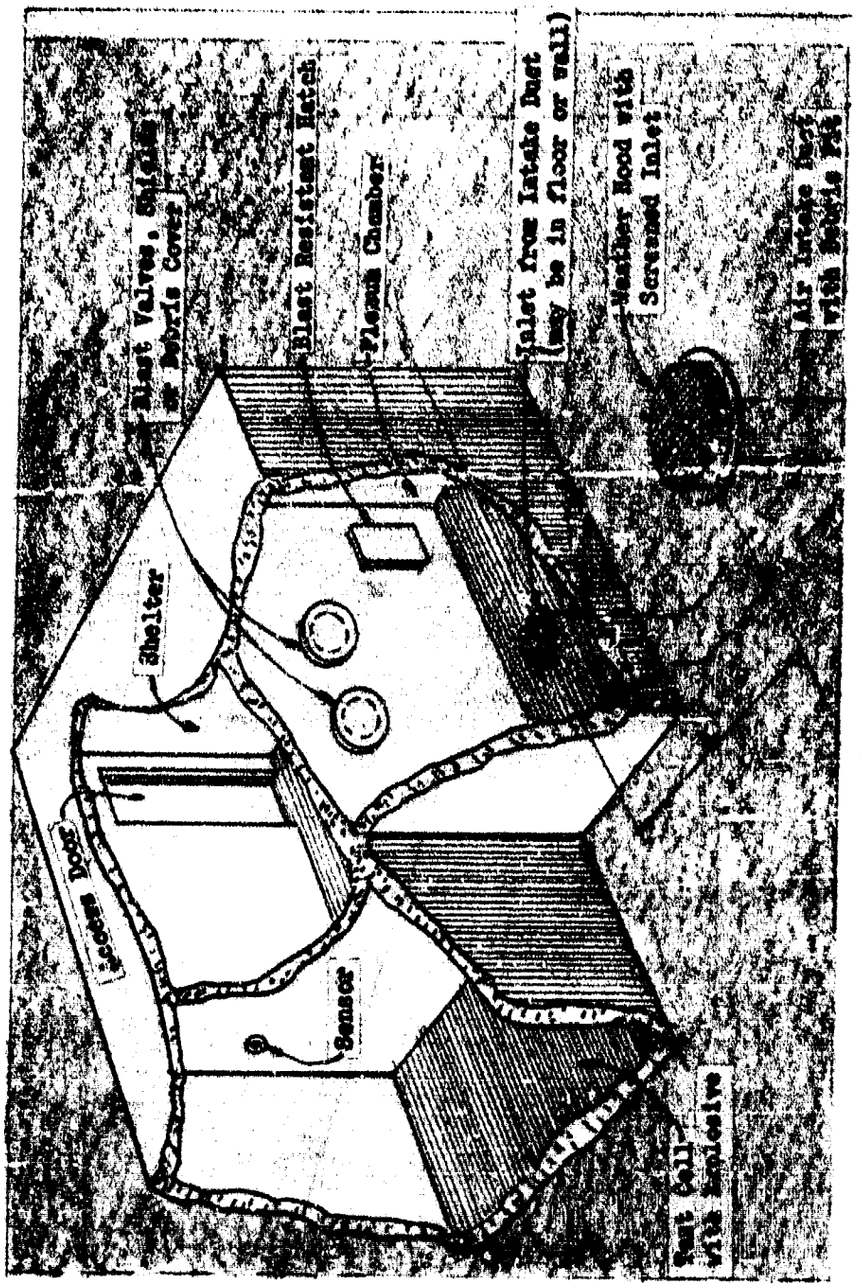


Figure 10–24. Air intake system.

reaches the interior, as illustrated schematically in figure 10–25. As shown, the blast path to the facility entrance is lengthened by increasing the duct length. The length of duct required to insure positive closure depends on the closing time of the valve and on the velocity of the shock wave. As an alternate to the long duct, an expansion chamber may be used to delay the blast. With this arrangement, normal ventilation flow will enter the facility through the blast valve after traveling through the delay path. An exhaust duct will operate in reverse manner. In addition to providing a delay path for the shock wave, the long duct and expansion chamber may be used to attenuate the shock in its passage to the facility.

j. By proper selection of the plenum chamber size, the maximum leakage pressures will be reduced to tolerable limits before the flow enters the facility proper (fig. 10–24). Plenum chambers should be designed to

2

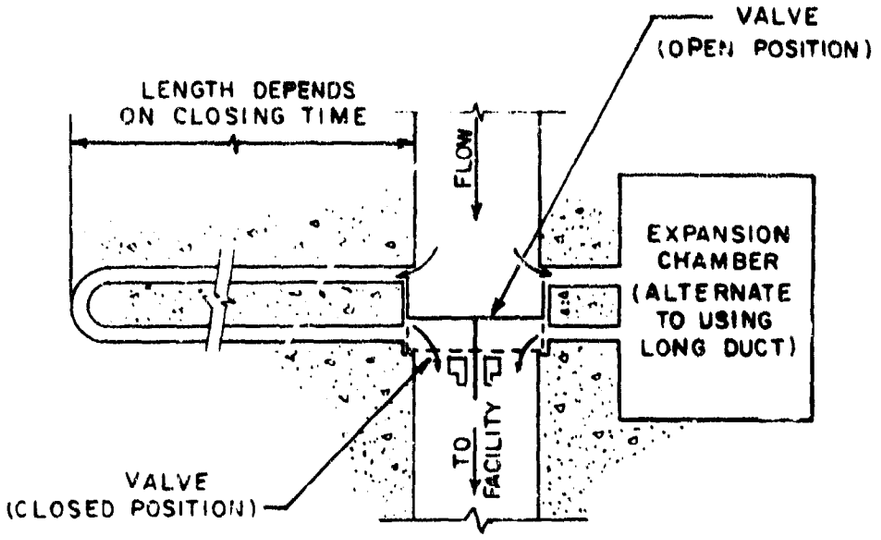


Figure 10–25. Time-delay path.

avoid a buildup of interior pressure which would impede closing of the valve. The ratio of the area of the chamber cross section to that of the valve outlet should be preferably greater than 4:1 so as to diffuse leakage flow as quickly as possible. A chamber which has the prescribed necessary volume but has little change in area would act like a tunnel wherein entering pressures would encounter little attenuation in the length provided.

k. Various blast valves have been developed during the past 15 years. For present designs, air flow rates from about 300 cfm to 35,000 cfm can be obtained. Some valve designs are available in more than one size. The pressure loss across the valve at the rated air flow is in most cases less than 1 inch of water.

l. The maximum incident pressure capability of available valves is above 50 psi and generally at least 100 psi. For shelter purposes, these valves may be overdesigned since the protection level for many shelters will be less than 50 psi. Except for cost factors, using a 100-psi valve for a 10-psi shelter design should not necessarily present technical problems since a valve must operate at all pressures below the maximum design level.

m. The best type of actuation (blast or remote) depends partly on the design pressure as previously discussed with regard to reaction time and operational considerations. For long arrival times (low pressure), a remote-actuated device can close the valve before the blast arrival whereas leakage may occur for a blast-actuated valve. At a high pressure (short arrival time), the closing time for the remote-actuated valve may be longer than the arrival time.

n. At low pressures in the order of several psi, it is feasible to adapt conventional components of ventilation systems to close off air-intake and exhaust openings and thereby prevent or limit the entrance of blast pressures. One example is the use of reinforced, opposing blade dampers which are closed by a hydraulic mechanism when triggered by a remote sensor. During normal operation, these dampers perform their conventional function of regulating the flow of air through the ventilation system.

o. Where blast resistant closures are not required to prevent pressure buildup within a shelter, conventional air distribution louvers are used to seal the interior of the shelter from the elements. In this situation, provisions must be made to insure that the interior of the structure is protected from debris resulting from the failure of the conventional closure due to the blast effects. One method of accomplishing the required protection is by offsetting the opening from the closure by means of a blast-resistant duct or tunnel, the design of which would prevent propagation of the debris to the shelter. Also, where exterior openings are connected to interior air distribution system ducts, provisions should be made to prevent pressure buildup in the ducts. A hinged door in the duct immediately adjacent to the opening, which is capable of being opened by the blast, will provide access for the pressures from the ducts to the interior of the structure. This leakage pressure should be held to a minimum.

p. Typical available blast-valve designs are given in table 10–2. Also tabulated are methods of actuating the valves, blast pressure capacity, closing time, air flow rates, and methods of testing. Pertinent publications and test reports which contain other information pertaining to the individual valves are contained in the Bibliography.

Section V. PROTECTION AGAINST STRUCTURE MOTIONS

10–9. Structure Motions

a. General. Motions of the structures (usually one- or two-story buildings) considered in this manual may be classified as: (1) those motions which are induced by the motion of the ground below the structure as a result of ground shock and (2) motions caused by the transient effects of the air-induced shock wave propagating across the structure. Except for very large quantities of explosives (above the upper limit considered in this manual), the motions produced by the ground shock will usually be small in comparison to the motions produced by the blast loads, and therefore may be neglected. However, a brief discussion is presented below to familiarize the reader with the mechanism by which ground motions occur.

b. Ground Shock Motions.

(1) Ground motions associated with large high-explosive detonations are considered to be induced by two distinct processes, air-induced ground shock, and direct-transmitted ground shock. Both vertical and horizontal ground motions are usually associated with ground shock, with the vertical motions generally being the larger of the two.

(2) The air-induced shock is caused by the blast wave traveling over the ground surface and generating

Table 10–2. Blast Valves

Name of valve		Type (Actuated)	Blast characteristics		Air flow rates (cfm)	Tested
			Pressure (psi)	Closing time (ms)		
U.S. Army Chemical Corps M-1		Blast	100		300	Field
U.S. Army Chemical Corps E191R1		Blast	50		600	Shock tube and field
Office of Civil Defense	12″ϕ	Blast	100		600	Field
	16″ϕ	and	50	50	1,200	
	24″ϕ	remote	50		2,500	
Office of Corps of Engineers		Blast and remote		20	5,000	Shock tube
Bureau of Yards and Docks		Remote		500	2,200 to 30,000	
Mosler Safe Company		Blast	100		550	Shock tube
Järn and Plat	4″ϕ		280		150	Field
	8″ϕ				600	
	14″ϕ				1,750	
Technical Facilities WS-107 A2		Remote			35,000	
American Machine Foundry		Blast	100		80	
Cohen-Ammann & Whitney		Blast and remote				
Suffield Experimental Stations		Blast	4 to 20			
New Naval Civil Engr. Lab.	Brechenridge	Blast	100		660	Compressed air
	Bayles-Denny		5 to 100		180	
	Stephenson		5 to 104		125	
Artos Machinery Co. (Sand Filted)		Blast	100		300	Field

stress waves into the ground which create the ground motions. The characteristics of air-blast waves are a function of charge weight, height of burst, and distance from the explosion. Also affecting the magnitude of these motions are the geological conditions including type of soil and depth below the surface.

(3) The direct-transmitted ground shock is a transmission of energy into the ground in the immediate vicinity of the explosion where it is then dispersed to areas of lower pressure level directly through the ground. The direct ground shock is usually of major importance only in very high-pressure regions and therefore would be of more importance with the effects of close-in detonations. However, because the weight of the explosive involved in the design of structures for the high-pressure design range is relatively small, the effects produced by direct-transmitted shock on the foundation of the structure will be significantly less than that produced by the blast loads on the exposed structure.

c. Motions Due to Blast Loads.

(1) As the blast wave propagates across a structure, relatively large unbalanced blast loads are produced which cause either side sway motions or sliding of the structure in the horizontal direction and gross vertical displacement of the structure as a result of the blast loads acting on the roof in combination with the soil displacement below the structure. Also, local displacements of the individual elements occur. Evaluation of these motions is required in order that protection for the structure's contents can be achieved.

(2) An estimate of the motions (velocities, accelerations, and displacements) for individual elements can be made from the equations of motion given in chapter 5, whereas for the determination of the overall motions of a building, the applied blast loads and the inertial resistance of the building in addition to the interaction of the structure and the soil support must be considered. In the latter, the effects produced by the soil on sliding and overturning of the structure must be included. Overall vertical motions of those structures located close-in to a detonation result primarily from the rotation effects, whereas horizontal motions usually are dependent upon both the sliding and side-sway action.

(3) In order to determine the input necessary to design equipment and their supports, a conservative estimate of the structure's motions can be made by adding the peak motions of the overall movement of the structure to those of the individual elements. However, the possibility of the occurrence of resonance should also be considered.

(4) For equipment which is attached to elements near their supports (e.g., floor slab near column and/or wall supports), the equipment can be considered to be subjected to the same intensities of the input motion as that of the structure. If this equipment is mounted on flexible supports (isolation systems), then these supports are designed for the equipment tolerance and the above intensities of the input. The above procedure can also be used for equipment which is rigidly attached to flexible interior elements. On the other hand, if the equipment is separated from a flexible interior element by an isolation system, then the total system (both the element and isolation system) must be considered in the analysis to determine the motion of the equipment. Interior elements usually can be designed for the motion associated with the overall movement of the structure.

10–10. Isolation Systems

a. Design of shelters to provide protection for personnel and/or equipment may require the use of flexible support systems to attenuate to tolerable levels the high accelerations associated with the structure motions. Effective methods of accomplishing this are: (1) a combination platform and spring support system and (2) individual spring mounts. The former is usually employed when a number of pieces of equipment require isolation and/or when personnel are to be protected, while the second method is used for the isolation of individual pieces of equipment.

b. In most cases, isolated platforms will have to be low-frequency systems in the order of 2 or 3 cps or less for personnel protection and slightly higher for protection of equipment. Frequencies of these magnitudes usually require flexible systems for horizontal motions of most protective structures and for the larger vertical motions associated with the ground shock effects produced by large explosions. Also, flexible systems may be required for structure motions resulting from large rotations of either individual elements or the entire structure.

c. Two methods are generally being used at this time to produce the required flexibility, i.e., (1) pendulum arrangements whereby the platforms are suspended from spring supports which, in turn, are attached to the roof or to the shell of the structure near the roof, and (2) base-mounted isolated platforms resting on spring supports which, in turn, are mounted on the base slab for vertical support and on the walls for horizontal support. The selection of the appropriate system for use in a specific design is dependent upon the design criteria (protection category, pressure level, site conditions, population, and amount of equipment and functional requirement) in addition to being interrelated with the required shape and dimensions of the structure.

d. Several different types of springs are available which lend themselves for use in isolation systems. They consist of (1) air springs, (2) liquid springs, (3) conical volute springs, (4) helical coil springs, and (5) beam springs. The use of any of these springs in a particular system is governed by the magnitude and direction of the accelerations and displacement associated with the structure motions, platform size (total load: dead load

plus dynamic load), method of supporting the platform, and reliability.

e. The use of air or liquid springs is generally associated with large loads and displacements (in the order of 2 feet or more) and therefore is uneconomical for use in most facility designs considered in this manual. Also, because the air and liquid springs require pumps to maintain the pressure necessary to cushion the loads resulting from the structure motions, operational costs increase. Because of the possibility of pressure leakage, the reliability of these springs during emergency conditions would be somewhat less than other spring systems. Beam and volute springs are useful when small structure motions are encountered. Beam springs usually suffice for displacements of 1 or 2 inches while volute springs can be used for displacements in the order of 4 to 6 inches. For larger displacements (up to approximately 24 inches), either compression or extension helical coil springs can be used (fig. 10–26).

f. The platforms used in protective shelters usually consist of structural steel framing with deck plates, steel gratings, or some other commonly used flooring material. The interior steel structure may consist of one, two or more stories, depending on the contents of the building (population and equipment) and the shape of the shell. In most cases, the use of one-story platforms is the most efficient and economical arrangement for use in explosive handling facilities.

g. Generally, pendulum-type support systems are used for the support of platforms. If base mounts are used, the large rocking effects resulting from the eccentricity of the platform load substantially increases the required spring capacity and probably increases somewhat the overall dimensions of the structure. Also, addition of horizontal springs to insure against collapse of the vertical springs may be required. In the case of the pendulum, the structure motions are applied first to steel rods, each of which is attached to the shell of the structure at the upper end and to a vertical acting spring at the lower end. The spring, in turn, is attached to the platform and thereby attenuates the vertical affects of the structure motions acting on the platform. The effects of the horizontal motion are attenuated by the pendulum action of the steel rods and the platform (hinge connections are provided at the top and bottom of each steel rod). Sufficient rattle space between the support platform and the shell of the structure must be provided to prevent impact of the platform against

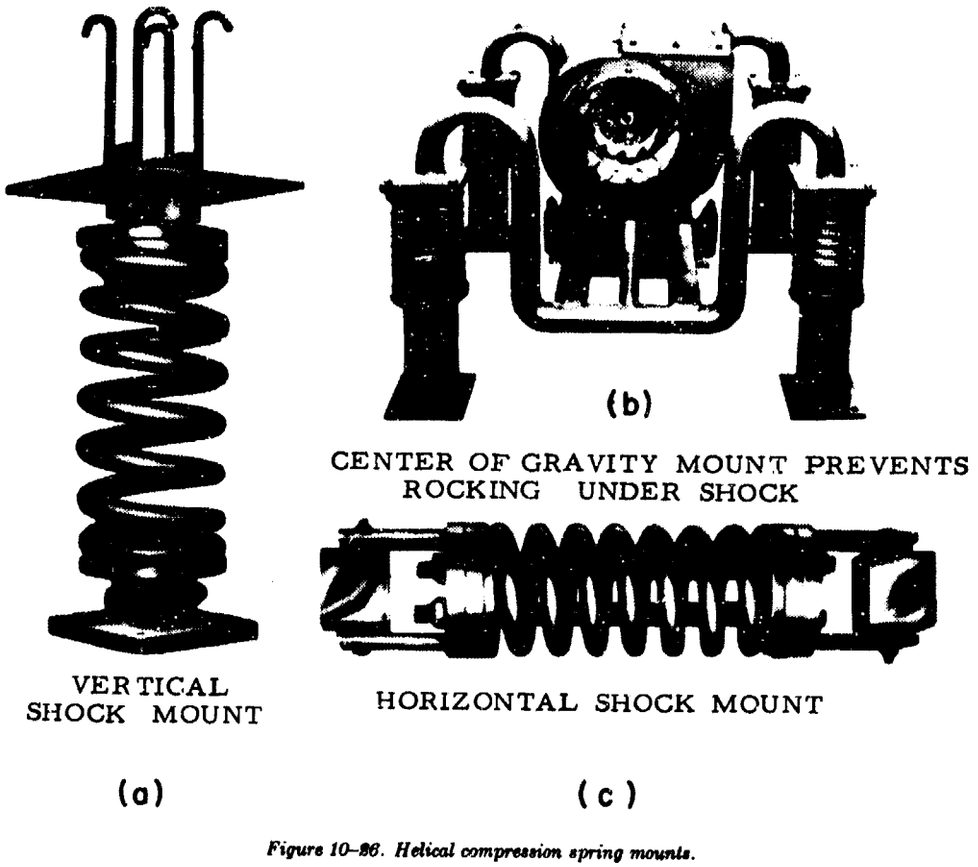
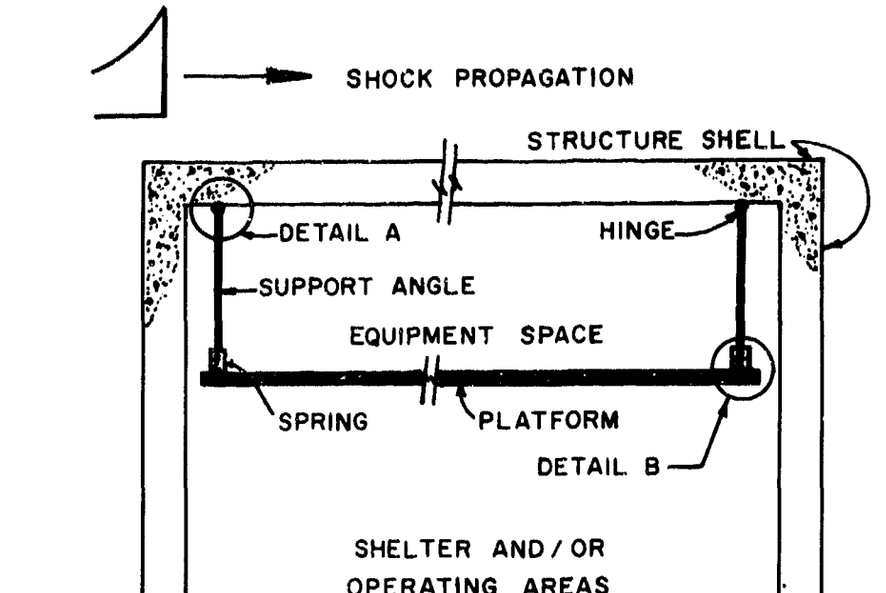


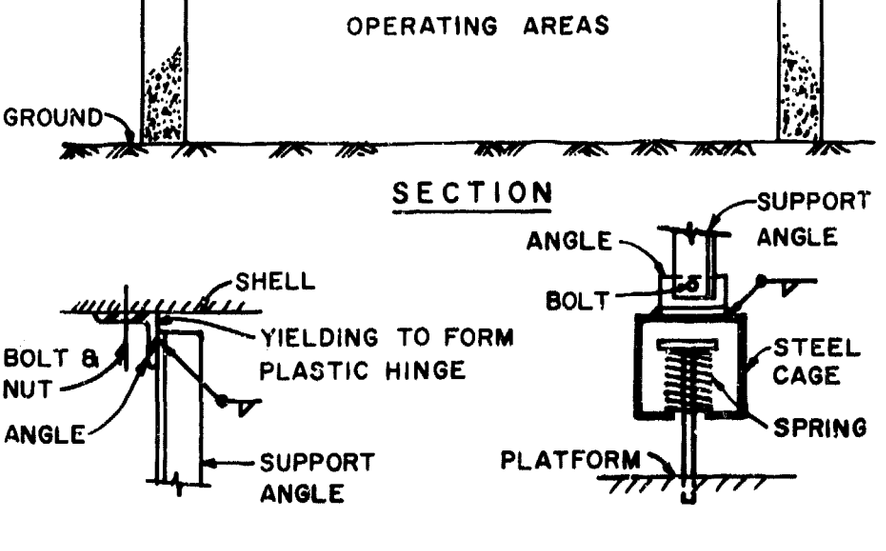
Figure 10–26. Helical compression spring mounts.

the walls. When the effects of the vertical motion are small, then the vertical springs may be eliminated and the rods attached directly to the platform.

h. To illustrate this latter condition, consider the hung ceiling of figure 10-27. The ceiling serves as the platform supporting the mechanical and electrical equipment (air ducts, piping, light fixtures, conduits, etc.) and the steel angle supports serve as the pendulum arms. The angles are designed to permit yielding at their connection to the structure and thereby form plastic hinges required for the pendulum system. In this illustration, the direction of the horizontal motion of the structure is assumed to be predominantly in the plane of the paper. If the blast load can occur from any direction, then the design would have to consider horizontal structure motions in all directions. Subsequently, the support arms would have to be designed to allow pendulum action of the platform consistent with that of the applied blast loads. In this case, the use of universal joints for the connection of the support rods both to the structure shell and the platform should be considered.



SECTION



DETAIL A DETAIL B

Figure 10-27 Typical suspended platform isolation system.

10–11. Protective Material, Clothing, and Restraining Devices

a. The protective methods discussed in this paragraph pertain primarily to the protection of personnel and include the use of (1) protective cushioning materials (energy-absorbing padding placed on interior surfaces of the structure), (2) protective clothing (helmets, padding, torso girdles, and protective shoes), (3) restraining devices (lap belts, shoulder belts, ankle and wrist restrainers, and secured seats), and (4) bracing devices (handholds and protective railings). These devices can provide a degree of protection against injuries caused by impact loads. The method chosen would be based on the degree of protection desired, the functional requirements, and the cost. It may be desirable to use several of these methods in a particular shelter.

b. Protective cushioning materials offer the advantage of providing protection without relying on the personnel in the shelter to perform any precautionary task. Effective use of protective clothing requires an element of control in assuring that the clothing is worn during normal operating conditions so that it will be effective during the emergency period. An important advantage in using protective clothing is that the dual-purpose function of the shelter area during the nonemergency period would not be affected. However, the clothing may be cumbersome and uncomfortable during prolonged use. Restraining devices are only useful in those facilities where continued movement by personnel is not required and therefore will only be of limited use in the operation of most explosive-handling facilities. Bracing devices are used to provide supplementary protection in conjunction with one or more of the other methods.

c. Protective cushioning material can be used as energy absorbing padding to protect personnel from injuries caused by impact and may be used on most potential impact surfaces such as walls, low ceilings, and interior furnishings, including flat surfaces as well as corners and edges.

d. Where protection against head injuries is of concern, cushioning is required on flat impact surfaces where impact may occur at velocities greater than 10 fps. Cushioning is also required to protect against injuries resulting from personnel falling over and striking a corner or edge. Although the properties of cushioning are quite different when used on a corner as compared to those of flat-surface cushioning, it has been shown that if the backup material has a radius of curvature greater than 2 inches, the impact effect is similar to that of a flat panel. Cushioning material on exterior walls of protective structures will provide protection against injuries which may be caused by compression waves transmitted by the blast loads. Also, equipment which is separated from floor slabs and other similar rigid supports by cushioning material will not respond to the high-frequency horizontal and vertical motions produced in these supports by the blast loads acting on the walls, or by direct propagation of the high-frequency motions to the interior floor slab by the blast loads acting on exterior extensions of the slab.

e. The use of cushioning materials on floors will result in difficulties in most operating facilities where large concentrated loads are common. To illustrate the effects of load concentration, none of the material available are capable of resisting without damage the effects produced by the concentrated loads produced by high-heeled shoes.

f. A list of materials which may be useful for cushioning and their safe-impact velocities are given in table 10–3.

g. Helmets have been found to be the most efficient protective clothing used for protecting the head. Efficient helmet designs incorporate a system that distributes the load over a large area of the skull and also includes energy-absorbing materials. Load distribution is accomplished by using a hard shell suspended by padding or support webbing at a distance of $\frac{5}{8}$ to $\frac{3}{4}$ inch from the head. In a proper design, high local impact forces are distributed over the entire side of the skull to which the blow is applied. In addition to the head, other areas of the body can be padded to protect against injuries which may result from impact. Such items as hip pads and pads to protect the back and spinal column are desirable. With impact or with high accelerations, the large gut mass may be displaced, resulting in rupture of the lungs or liver and fracture of the vertebral column. By enclosing the abdomen in a rigid girdle, this danger of injury can be considerably reduced.

h. As previously mentioned, restraining of personnel within chairs is not usually practical for operational facilities. However, in some testing operations, the job of the operator may require a minimum of motion throughout the shelter. In this latter case or similar situations, restraining devices may be of use. Seats to which personnel are restrained must be rigidly attached

Table 10–3. Safe Impact Velocities of the Human Head Using Protective Cushioning Materials

Cushioning material on hard flat surface	Limit of safe impact velocity
1-inch thick polystyrene foam: 1¼ lb/cu ft.	15 ft/sec
2-inch thick polystyrene foam: 1¼ lb/cu ft.	18 ft/sec
1-inch thick Ensolite* (polyvinyl chloride) 22266: 7 lb/cu ft.	17 ft/sec
2-inch thick foam rubber: 6 lb/cu ft.	11 ft/sec
2-inch thick polyurethane foam: Formulation A.	16 ft/sec

* Trade name of United States Rubber Co., Mishawaka, Indiana.

to the floor and must be designed to sustain the full acceleration loading applied by the personnel and the dead weight of the chair. Equipment which may be used for restraining include lap belts, shoulder straps, chest straps, thigh straps, ankle and wrist restrainers, and handholds.

i. As an aid in preventing personnel from falling over, handholds may be used along the structure walls and corridors. To prevent personnel from impacting with the walls, protective railings may also be used. These latter two methods of protection are only useful when used in combination with other methods of protection.

Section VI. EARTH-COVERED STEEL-ARCH MAGAZINES

10–12. General

a. In recent years, certain types of earth-covered steel-arch magazines have been approved and standardized for use by various government agencies involved with modern weapons and explosives. These magazines may provide definite advantages over other types of standard magazines. Among these advantages are:

(1) Less real estate per magazine is required because of the decreased intermagazine separations permitted when steel-arch magazines are used.

(2) An almost infinite number of storage situations

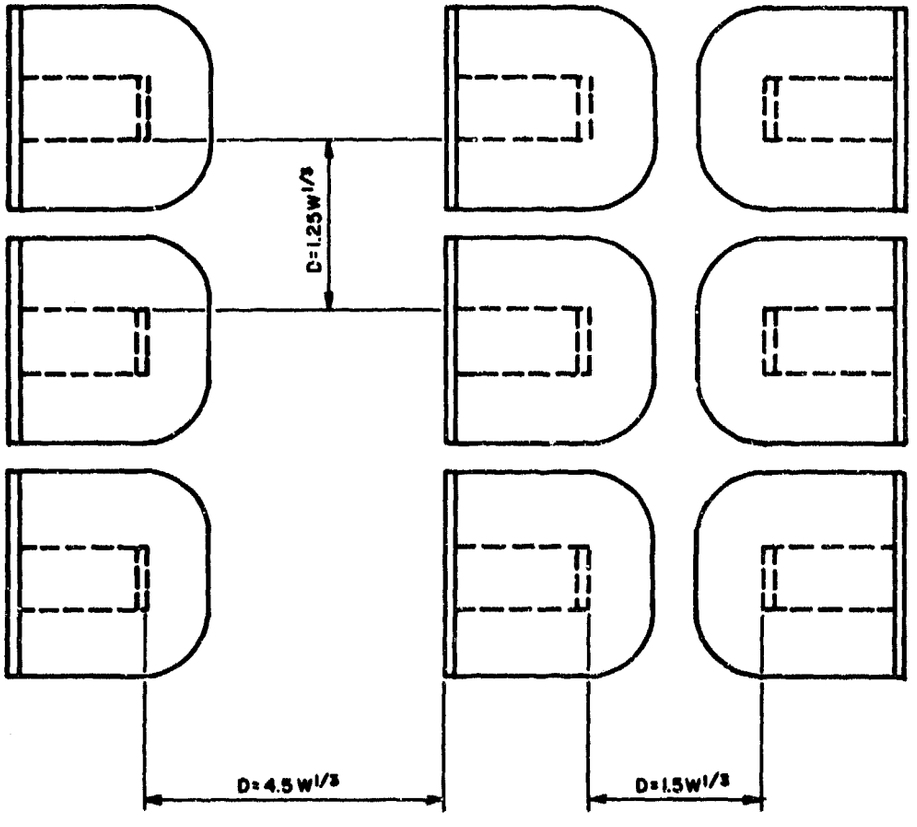


Figure 10–28. Minimum magazine separation distances.

exists
merely
and th
(3
usuall
(4
less ro
b. U

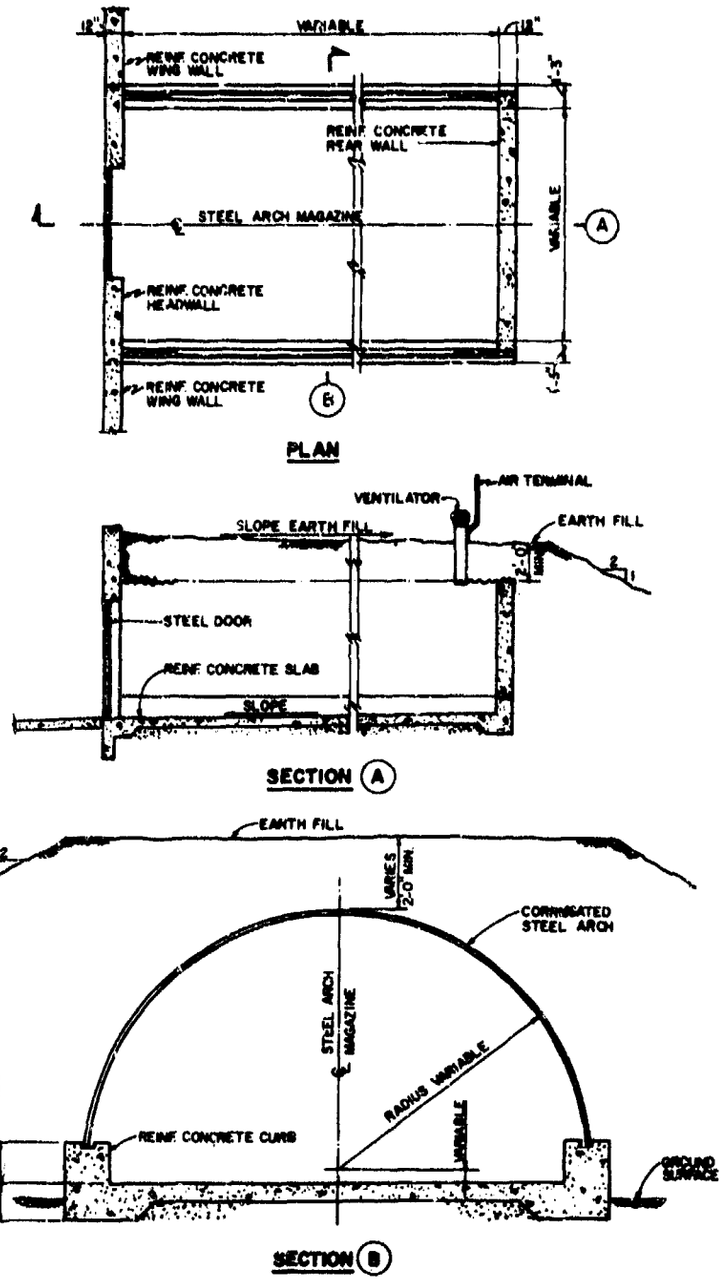


Figure 10–89. Typical earth-covered steel-arch magazine.

exists because magazines can be designed to any length merely by varying the number of steel-arch sections and their widths can be increased up to 30 feet.

(3) Steel-arch magazines can be more quickly and usually more economically constructed.

(4) Because of the reduced separation distances, less roads, fences, utilities, etc., are required.

b. Unlike the other structures discussed elsewhere in this manual, an earth-covered steel-arch magazine is not designed to resist the damaging effects of its exploding contents. It is accepted that the magazine will be demolished if an internal explosion occurs. During such an incident, the inside of a large-span arch might experience initial blast pressures considerably in excess of 10,000 psi. Less than 100 psi could lift the arch completely out of the ground; therefore, the major portion

of the protection is provided by the receiver magazines rather than the donor magazine.

c. Although steel-arch magazines are utilized primarily to prevent propagation of explosion, structures equivalent in strength to that described in paragraph 10–13 may be used for personnel protection and operating buildings if the requirements of the using service warrant it. In such cases, greater separation distances than those shown on figure 10–28 may be required for protection of personnel from the blast or ground shock. Special applications such as this require evaluation of the entrance of blast pressures into the protected space, availability of easily damaged or lightly supported accessories which may become hazardous debris, transmission of shock to persons through the steel-arch walls or floor, and overall movement of the magazine.

10–13. Description of Earth-Covered Steel-Arch Magazine

a. A typical earth-covered steel-arch magazine used for storing explosives is illustrated in figure 10 29 and has the following features:

(1) A semicircular corrugated steel arch forming roof and sides.

(2) A reinforced concrete floor slab with curbs along the sides for attaching the steel arch.

(3) A reinforced concrete rear wall that fits inside the arch.

(4) A reinforced concrete headwall that extends at least 2½ feet above the crown of the arch.

(5) Reinforced concrete wingwalls on either side of the headwall. The wingwalls may slope to the ground or may adjoin wingwalls from adjacent magazines. The wingwalls may be either monolithic or separated by expansion joints from the headwall.

(6) Heavy steel doors in the headwall.

(7) An optional gravity ventilation system.

(8) Earth covering at least 2 feet thick at the crown of the arch and covering the top, sides, and rear of the structure.

(9) Its own built-in lightning protection system.

b. It should be noted that for a specified magazine width the clear interior height can be increased by adjusting the height of the curbs along the sides of the magazine.

10–14. Investigations Performed

Investigational work with earth-covered steel-arch magazines has been concerned with the intrarelationships of magazine complexes for siting purposes. Numerous full-scale tests performed over a period of several years have established magazine separation formulae that will prevent magazine-to-magazine propagation of explosion. The arrangements which have been considered are magazines situated side-by-side, magazines situated back-to-front, and magazines situated back-to-back. Front-to-front exposure has not been considered. As a result of full-scale tests, steel-arch magazines constructed in conformance with present standard drawings of the cognizant construction agency can be sited in accordance with the minimum separation formulae shown in figure 10–28.

10–15. Design

a. Protection of magazines adjacent to a donor magazine is accomplished by combining the following factors:

(1) The intensity of the pressure front moving from the donor magazine to receiver magazines diminishes rapidly as the distance traveled increases.

(2) The earth cover over and around the donor magazine provides some confinement and tends to directionalize the explosive force both upward and outward from the door end of the magazine.

(3) The earth around and over receiver magazines resists fragment penetrations and provides mass to the steel arch to resist the blast pressures.

(4) The steel arch of receiver magazines is capable of resisting blast loads considerably in excess of the dead loads normally imposed on it.

b. Design of the presently used steel-arch magazine is essentially conventional except for two features, which are doors and thickness of steel-arch plate. The doors are designed to withstand the dynamic forces from an explosion in a nearby magazine if the siting is in accordance with figure 10–28. However, they provide almost no resistance to the effects of an explosion within the magazine. Also, the capacity of the doors to resist elastic rebound and negative phase pressures may be less than their capacity to resist positive phase pressures. Therefore, where personnel are concerned, all doors should be analyzed to determine their ultimate capacity to resist all the loadings involved. The thickness of steel-arch plate is the same as the steel thickness of the structures used in the full-scale tests that established magazine separation formulae. In general, it can be said that the steel thickness is roughly that required to support approximately 25 feet of earth fill and that the steel thickness increases with the span of the arch. Table 10–4 indicates the steel thicknesses specified for various magazine widths.

10–16. Construction

a. Effectiveness of earth-covered steel-arch magazines is largely determined by the quality of construction. A few of the construction details that could be sources for problems in this type of structure are discussed below.

b. Moisture proofing of any earth-covered structure is usually difficult. This difficulty is increased with a steel-arch structure because of the many lineal feet of joints available for introducing moisture. For example,

a small 14- by 25-foot steel-arch magazine contains approximately 190 feet of steel-plate edges that must be sealed. A large 26- by 80-foot magazine contains approximately 1,050 feet of edges. A sealant tape must be used that will not deteriorate or excessively deform under any anticipated environmental or structural condition.

Table 10–4. Required Steel Thicknesses for Various Magazine Widths

Width of magazine (ft.)	Steel thickness required	
	Gage No.	Inches
14 or less	8	0.1644
16	7	0.1838
18	5	0.2145
20	5	0.2145
22	3	0.2451
24	3	0.2451
26	1	0.2758
28	—	0.375
30	—	0.375

c. Earthfill material should be clean, cohesive, and free from large stones. A minimum earth cover of two feet must be maintained. Surface preparation of the fill is usually required to prevent erosion of the 2-foot cover. Restricting granular size of material reduces throwout of fragments in case of an accidental explosion and creates a more uniform energy absorbent over the top of the magazine.

d. Lightning protection is rather easily obtained in a steel-arch structure. All sections of steel-arch plate must be interconnected so that they become electrically continuous. In effect, a "cage" is created about the magazine contents. Probably the most critical point for lightning protection is the optional ventilator stack which projects above the surrounding earth cover.

10–17. Standard Design

Steel-arch structures for use as explosive storage or operating buildings must be at least equivalent in strength to those shown on Corps of Engineers Drawings Nos. AW 33-15-63 (5 Mar 1963), AW 33-15-64 (10 May 1963), AW 33-15-65 (10 Jan 1963), and the Corps of Engineers standard specifications cited thereon.

APPENDIX A

LIST OF SYMBOLS

α	(1) acceleration (in./ms^2) (2) depth of equivalent rectangular stress block (in.)
A	area (in.^{2})
A_d	area of diagonal bars at the support within a width b (in.^{2})
A_o	area of openings (ft^2)
A_s	area of tension reinforcement within a width b (in.^{2})
A_s'	area of compression reinforcement within a width b (in.^{2})
A_{sH}	area of flexural reinforcement within a width b in the horizontal direction on each face (in.^{2})*
A_{sV}	area of flexural reinforcement within a width b in the vertical direction on each face (in.^{2})*
A_v	total area of stirrups or lacing reinforcement in tension within a distance s_s or s_l and a width b_s or b_l (in.^{2})
b	(1) width of compression face of flexural member (in.) (2) width of concrete strip in which the direct shear stresses at the supports are resisted by diagonal bars (in.)
b_s	width of concrete strip in which the diagonal tension stresses are resisted by stirrups of area A_v (in.)
b_l	width of concrete strip in which the diagonal tension stresses are resisted by lacing of area A_v (in.)
B	(1) peak pressure of equivalent triangular loading function (psi) (2) constant defined in paragraph 4–22.
c	distance from the resultant applied load to the axis of rotation (in.)
c_I, c_{II}	distance from the resultant applied load to the axis of rotation for sectors I and II, respectively (in.)
c_o	dilatational velocity of concrete (ft/sec)
C	shear coefficient
C_d	shear coefficient for ultimate shear stress of one-way elements
C_f	post-failure fragment coefficient (lb^2-ms^4/in.^{8})
C_{rn}	peak reflected pressure coefficient at angle of incidence α
C_s	shear coefficient for ultimate support shear for one-way elements
C_{sH}	shear coefficient for ultimate support shear in horizontal direction for two-way elements*
C_{sV}	shear coefficient for ultimate support shear in vertical direction for two-way elements*
C_D	drag coefficient
C_{DQ}	drag pressure (psi)
C_{DQ_o}	peak drag pressure (psi)
C_E	equivalent load factor
C_H	shear coefficient for ultimate shear stress in horizontal direction for two-way elements*
C_L	leakage pressure coefficient
C_M	maximum shear coefficient
C_u	impulse coefficient at deflection X_u (psi-ms^2/in.^{2})
C_u'	impulse coefficient at deflection X_m (psi-ms^2/in.^{2})
C_V	shear coefficient for ultimate shear stress in vertical direction for two-way elements*
C_1	(1) impulse coefficient at deflection X_1 (psi-ms^2/in.^{2}) (2) parameter defined in figure 8–4
C_1'	impulse coefficient at deflection X_m (psi-ms^2/in.^{2})
d	distance from extreme compression fiber to centroid of tension reinforcement (in.)
d'	distance from extreme compression fiber to centroid of compression reinforcement (in.)
d_c	distance between the centroids of the
d_e	
d_i	
d_l	
d_{cc}	
d_1	
D	
D_o	
D_E	
DIF	
e	
$(2E')^{1/2}$	
E_c	
E_s	
f	
f_c'	
f_{dc}'	
f_{ds}	
f_{du}	
f_{dy}	
f_s	
f_u	
f_y	
F	
F_s	
F_E	
g	
h	
H	

* See note at end of symbols.

* See note at end of symbols.

* See note at end of

	compression and tension reinforcement (in.)
d_s	distance from support and equal to either d or d_c (in.)
d_t	inside diameter of cylindrical explosive container (in.)
d_l	distance between center lines of adjacent lacing bends measured normal to flexural reinforcement (in.)
d_{co}	diameter of steel core (in.)
d_1	diameter of cylindrical portion of primary fragment (in.)
D	(1) unit flexural rigidity (lb-in.)
	(2) location of shock front for maximum stress (ft)
	(3) minimum magazine separation distance (ft)
D_s	nominal diameter of reinforcing bar (in.)
D_E	equivalent loaded width of structure for non-planar wave front (ft)
DIF	dynamic increase factor
e	base of natural logarithms and equal to 2.71828 . . .
$(2E')^{1/3}$	Gurney Energy Constant (ft/sec)
E_c	modulus of elasticity of concrete (psi)
E_s	modulus of elasticity of reinforcement (psi)
f	unit external force (psi)
f_c'	static ultimate compressive strength of concrete at 28 days (psi)
f_{dc}'	dynamic ultimate compressive strength of concrete (psi)
f_{ds}	dynamic design stress for reinforcement (psi)
f_{du}	dynamic ultimate stress of reinforcement (psi)
f_{dy}	dynamic yield stress of reinforcement (psi)
f_s	static design stress for reinforcement (a function of f_y, f_u, and θ (psi)
f_u	static ultimate stress of reinforcement (psi)
f_y	static yield stress of reinforcement (psi)
F	(1) total external force (lbs)
	(2) coefficient for moment of inertia of cracked concrete section
F_s	force in the reinforcing bars (lbs)
F_E	equivalent external force (lbs)
g	variable defined in table 4–3
h	charge location parameter (ft)
H	(1) span height (in.)
	(2) distance between reflecting surface(s) and/or free edge(s) in vertical direction (ft)

H_c	height of charge above ground (ft)
$\bar{H}_c$	scaled height of charge above ground (ft/lb$^{1/3}$)
H_s	height of structure (ft)
$\bar{H}_T$	scaled height of triple point (ft/lb$^{1/3}$)
i	unit positive impulse (psi-ms)
i^-	unit negative impulse (psi-ms)
i_a	sum of scaled unit blast impulse capacity of receiver panel and scaled unit blast impulse attenuated through concrete and sand in a composite element (psi-ms/lb$^{1/3}$)
i_b	unit blast impulse (psi-ms)
$\bar{i}_b$	scaled unit blast impulse (psi-ms/lb$^{1/3}$)
$\bar{i}_{bt}$	total scaled unit blast impulse capacity of composite element (psi-ms/lb$^{1/3}$)
$\bar{i}_{bs}$	scaled unit blast impulse capacity of receiver panel of composite element (psi-ms/lb$^{1/3}$)
$\bar{i}_{bd}$	scaled unit blast impulse capacity of donor panel of composite element (psi-ms/lb$^{1/3}$)
i_e	unit excess blast impulse (psi-ms)
i_r	unit positive normal reflected impulse (psi-ms)
i_r^-	unit negative normal reflected impulse (psi-ms)
i_s	unit positive incident impulse (psi-ms)
i_s^-	unit negative incident impulse (psi-ms)
I	moment of inertia (in.^{4})
I_a	average of gross and cracked moments of inertia of width b (in.^{4})
I_c	moment of inertia of cracked concrete section of width b (in.^{4})
I_g	moment of inertia of gross concrete section of width b (in.^{4})
I_m	mass moment of inertia (lb-ms^2-in.)
j	ratio of distance between centroids of compression and tension forces to the depth d
k	constant defined in paragraph 8–5
K	(1) unit stiffness (psi/in.)
	(2) constant defined in paragragh 3–9
K_e	elastic unit stiffness (psi/in.)
K_{ep}	elasto-plastic unit stiffness (psi/in.)
K_E	equivalent elastic unit stiffness (psi/in.)
K_L	load factor
K_{LM}	load-mass factor
$(K_{LM})_e$	load-mass factor in the ultimate range
$(K_{LM})_{ep}$	load-mass factor in the post-ultimate range

* See note at end of symbols.

* See note at end of symbols.

K_M	mass factor
K_R	resistance factor
K_1	factor defined in paragraph 5–2
KE	kinetic energy
l	charge location parameter (ft)
l_p	spacing of same type of lacing bar (in.)
L	(1) span length (in.) except in chapter 4 (ft)*
	(2) distance between reflecting surface(s) and/or free edge(s) in horizontal direction (ft)
L_l	length of lacing bar required in distance s_l (in.)
L_e	embedment length of reinforcing bars (in.)
L_w	wave length of positive pressure phase (ft)
L_w^-	wave length of negative pressure phase (ft)
L_{wb}, L_{wd}	wave length of positive pressure phase at points b and d, respectively (ft)
L_1	total length of sector of element normal to axis of rotation (in.)
m	unit mass (psi-ms²/in.)
m_a	average of the effective elastic and plastic unit masses (psi-ms²/in.)
m_e	effective unit mass (psi-ms²/in.)
m_u	effective unit mass in the ultimate range (psi-ms²/in.)
m_{up}	effective unit mass in the post-ultimate range (psi-ms²/in.)
M	(1) unit bending moment (in-lbs/in.)
	(2) total mass (lb-ms²/in.)
M_e	effective total mass (lb-ms²/in.)
M_u	ultimate unit resisting moment (in-lbs/in.)
M_c	moment of concentrated loads about line of rotation of sector (in.-lbs)
M_A	fragment distribution parameter
M_E	equivalent total mass (lb-ms²/in.)
M_{HN}	ultimate unit negative moment capacity in horizontal direction (in.-lbs/in.)*
M_{HP}	ultimate unit positive moment capacity in horizontal direction (in.-lbs/in.)*
M_N	ultimate unit negative moment capacity at supports (in.-lbs/in.)
M_P	ultimate unit positive moment capacity at midspan (in.-lbs/in.)
M_{VN}	ultimate unit negative moment capacity in vertical direction (in.-lbs/in.)*
M_{VP}	ultimate unit positive moment capacity in vertical direction (in.-lbs/in.)*
n	(1) modular ratio
	(2) number of time intervals
N	number of adjacent reflecting surfaces
N_f	number of primary fragments larger than W_f
p	reinforcement ratio equal to $\frac{A_s}{bd}$ or $\frac{A_s}{bd_e}$
p'	reinforcement ratio equal to $\frac{A_s'}{bd}$ or $\frac{A_s'}{bd_e}$
p_b	reinforcement ratio producing balanced conditions at ultimate strength
p_m	mean pressure in a partially vented chamber (psi)
p_{mo}	peak mean pressure in a partially vented chamber (psi)
p_H	reinforcement ratio in horizontal direction on each face*
p_T	total reinforcement ratio equal to p_H+p_V
p_V	reinforcement ratio in vertical direction on each face*
P	pressure (psi)
P^-	negative pressure (psi)
P_i	interior pressure within structure (psi)
ΔP_i	interior pressure increment (psi)
P_f	fictitious peak pressure (psi)
P_o	peak pressure (psi)
P_r	peak positive normal reflected pressure (psi)
P_r^-	peak negative normal reflected pressure (psi)
$P_{r\alpha}$	peak reflected pressure at angle of incidence α (psi)
P_s	positive incident pressure (psi)
P_{sb}; P_{se}	positive incident pressure at points b and e, respectively (psi)
P_{so}	peak positive incident pressure (psi)
P_{so}^-	peak negative incident pressure (psi)
P_{sob}, P_{sod}, P_{soe}	peak positive incident pressure at points b, d, and e, respectively (psi)
q	dynamic pressure (psi)
q_b, q_e	dynamic pressure at points b and e, respectively (psi)
q_o	peak dynamic pressure (psi)
q_{ob}, q_{oe}	peak dynamic pressure at points b and e, respectively (psi)
r	(1) unit resistance (psi)
	(2) radius of spherical TNT (density equals 95 lb/ft³/charge (ft))
r^-	unit rebound resistance (psi)
Δr	
r_e	
r_{ep}	
r_u	
r_{up}	
r_1	
R	
R_f	
R_l	
R_A	
R_E	
R_G	
R_I, R_{II}	
s_e	
s_l	
S	
SE	
t	
Δt	
t_a	
t_b, t_e, t_f	
t_o	
t_o^-	
t_{of}	
t_{of}^-	
t_r	
t_u	
t_w	
t_A	
t_1	

* See note at end of symbols.

* See note at end of symbols.

* See note

Δr	change in unit resistance (psi)
r_e	elastic unit resistance (psi)
r_{ep}	elasto-plastic unit resistance (psi)
r_u	ultimate unit resistance (psi)
r_{up}	post-ultimate unit resistance (psi)
r_1	radius of hemispherical portion of primary fragment (in.)
R	(1) total internal resistance (lbs) (2) slant distance (ft)
R_f	distance traveled by primary fragment (ft)
R_l	radius of lacing bend (in.)
R_A	normal distance (ft)
R_E	equivalent total internal resistance (lbs)
R_G	ground distance (ft)
R_I, R_{II}	total internal resistance of sectors I and II, respectively (lbs)
s_s	spacing of stirrups in the direction parallel to the longitudinal reinforcement (in.)
s_l	spacing of lacing in the direction parallel to the longitudinal reinforcement (in.)
S	height of front wall or one-half its width, whichever is smaller (ft)
SE	strain energy
t	time (ms)
Δt	time increment (ms)
t_a	any time (ms)
t_b, t_e, t_f	time of arrival of blast wave at points b, e, and f, respectively (ms)
t_c	(1) clearing time for reflected pressures (ms) (2) container thickness of explosive charges (in.)
t_d	rise time (ms)
t_m	time at which maximum deflection occurs (ms)
t_o	duration of positive phase of blast pressure (ms)
t_o^-	duration of negative phase of blast pressure (ms)
t_{of}	fictitious positive phase pressure duration (ms)
t_{of}^-	fictitious negative phase pressure duration (ms)
t_r	fictitious reflected pressure duration (ms)
t_u	time at which ultimate deflection occurs (ms)
t_y	time to reach yield (ms)
t_A	time of arrival of blast wave (ms)
t_1	time at which partial failure occurs (ms)

* See note at end of symbols.

T	duration of equivalent triangular loading function (ms)
T_c	thickness of concrete section (in.)
$\bar{T}_c$	scaled thickness of concrete section (ft/lb$^{1/3}$)
T_N	effective natural period of vibration (ms)
T_s	thickness of sand fill (in.)
$\bar{T}_s$	scaled thickness of sand fill (ft/lb$^{1/3}$)
u	(1) particle velocity (ft/ms) (2) ductility ratio
u_u	ultimate flexural or anchorage bond stress (psi)
U	shock front velocity (ft/ms)
v	velocity (in./ms)
v_a	instantaneous velocity at any time (in./ms)
v_b	boundary velocity for primary fragments (ft/sec)
v_c	ultimate shear stress permitted on an unreinforced web (psi)
v_f	maximum post-failure fragment velocity (in./ms)
v_f (avg.)	average post-failure fragment velocity (in./ms)
v_i	velocity at incipient failure deflection (in./ms)
v_o	initial velocity of primary fragment (ft/sec)
v_r	residual velocity of primary fragment after perforation (ft/sec)
v_s	striking velocity of primary fragment (ft/sec)
v_u	ultimate shear stress (psi)
v_{uH}	ultimate shear stress at distance d_s from the vertical support (psi)*
v_{uV}	ultimate shear stress at distance d_s from the horizontal support (psi)*
V	volume of partially vented chamber (ft^3)
V_d	ultimate direct shear capacity of the concrete of width b (lbs)
V_{dH}	shear at distance d_s from the vertical support on a unit width (lbs/in.)*
V_{dV}	shear at distance d_s from the horizontal support on a unit width (lbs/in.)*
V_e	volume of structure (ft^3)
V_s	shear at the support on a unit width (lbs/in.)
V_{sH}	shear at the vertical support on a unit width (lbs/in.)*
V_{sV}	shear at the horizontal support on a unit width (lbs/in.)*
V_u	total shear on a width b (lbs)

* See note at end of symbols.

w	weight density of concrete (lbs/ft³)
w_s	weight density of sand (lbs/ft³)
W	charge weight (lbs)
W_c	total weight of explosive containers (lbs)
W_f	weight of primary fragment (oz)
W_{co}	total weight of steel core (lbs)
W_{c1}, W_{c2}	total weight of plates 1 and 2, respectively (lbs)
W_B	width of structure (ft)
WD	work done
x	yield line location in horizontal direction (in.)*
X	deflection (in.)
X_a	any deflection (in.)
X_e	elastic deflection (in.)
X_{ep}	elasto-plastic deflection (in.)
X_f	maximum penetration into concrete of armor-piercing fragments (in.)
X_f'	maximum penetration into concrete of fragments other than armor-piercing (in.)
X_m	maximum transient deflection (in.)
X_p	plastic deflection (in.)
X_s	maximum penetration into sand of armor-piercing fragments (in.)
X_u	ultimate deflection (in.)
X_E	equivalent elastic deflection (in.)
X_1	partial failure deflection (in.)
y	yield line location in vertical direction (in.)*
Z	scaled slant distance (ft/lb$^{1/3}$)
Z_A	scaled normal distance (ft/lb$^{1/3}$)
Z_G	scaled ground distance (ft/lb$^{1/3}$)
α	(1) angle formed by the plane of stirrups, lacing, or diagonal reinforcement and the plane of the longitudinal reinforcement (deg) (2) angle of incidence of the pressure front (deg)
β	(1) coefficient for determining elastic and elasto-plastic resistances (2) particular support rotation angle (deg)
γ	coefficient for determining elastic and elasto-plastic deflections
λ	increase in support rotation angle after partial failure (deg)
θ	support rotation angle (deg)
$\ddot{\theta}$	angular acceleration (rad/ms²)
θ_m	maximum support rotation angle (deg)
θ_H	horizontal rotation angle (deg)*
θ_V	vertical rotation angle (deg)*
Σo	effective perimeter of reinforcing bars (in.)
ΣM	summation of moments (in.-lbs)
ΣM_N	sum of the ultimate unit resisting moments acting along the negative yield lines (in.-lbs)
ΣM_P	sum of the ultimate unit resisting moments acting along the positive yield lines (in.-lbs)
μ	ductility factor
ν	Poisson's ratio
ϕ	(1) capacity reduction factor (2) bar diameter (in.)
———	free edge
═══	simple support
⧸⧸⧸⧸	fixed support
XXXX	either fixed, restrained, or simple support

* See note at end of symbols.

* *Note.* This symbol was developed for two-way elements which are used as walls. When roof slabs or other horizontal elements are under consideration, this symbol will also be applicable if the element is treated as being rotated into a vertical position.

APPENDIX B

BIBLIOGRAPHY

The listing in this bibliography is divided into subdivisions. The publications listed under "General" pertain to the overall manual, while the publications listed under chapter numbers pertain to the chapter in the manual under whose number they are listed.

General

1. *American Concrete Institute Standard Building Code Requirements for Reinforced Concrete*, ACI Committee 318–63, American Concrete Institute, Detroit, Michigan, June 1963.
2. *An Introduction to Protective Design for Nuclear Weapons*, PM 100-5, by Ammann & Whitney, Consulting Engineers, New York, New York, for the Office of Civil Defense, Department of the Army, Washington, D.C., April 1965.
3. *Annals of the New York Academy of Sciences, Volume 152, Art. 1, Conference on Prevention of and Protection Against Accidental Explosion of Munitions, Fuels and Other Hazardous Mixtures*, published by New York Academy of Sciences, October 1968.
4. *Design Manual, AEC Test Structures, Volumes I through III*, by Holmes and Narver Inc., under Contract AT (29-2)-20, for U.S. Atomic Energy Commission, Albuquerque Operations Office, Albuquerque, New Mexico, December 1961.
5. *Design of Structures to Resist the Effects of Nuclear Weapons*, Department of the Army Technical Manual TM5-856-1 thru 9, Washington, D.C.
6. *Minutes of the First Through Tenth Explosives Safety Seminar*, Sponsored by the Armed Services Explosives Safety Board, Washington, D.C., 1959 through 1968.
7. Newmark, N. M. and J. D. Haltiwanger, *Air Force Design Manual, Principles and Practices for Design of Hardened Structures*, Technical Documentary Report No. AFSWC-TDR-62-138, by Department of Civil Engineering, University of Illinois, Urbana, Illinois, under Contract AF29 (601)-2390, for Research Directorate, Air Force Special Weapons Center, Air Force Systems Command, Kirtland Air Force Base, New Mexico, December 1962.
8. Rindner, R. M., et al, *Establishment of Safety Design Criteria for Use in Engineering of Explosive Facilities and Operations, Reports No. 8, 9 and 11*, Technical Reports 3484, 3594 and 3712, Picatinny Arsenal, Dover, New Jersey, 1966 through 1968.

Chapter 3

1. *Study of Shock Isolation Methods for Civil Defense Shelters*, by Ammann & Whitney, Consulting Engineers, New York, New York, under Contract DA 49-129-ENG-506, for Department of the Army, Office of the Chief of Engineers, Washington, D.C., for the Office of Civil Defense, Work Order No. OCD-OS-62-159, OCD Research Sub Task 1152C, November 1963.
2. Cohen, E., and N. Dobbs, *The Design of More-Effective Cubicle-Type Protective Barriers for Explosive Storage and Manufacturing Facilities*, Ammann & Whitney, Consulting Engineers, New York, New York, Minutes of the Eighth Explosives Safety Seminar on High-Energy Propellants, sponsored by the Armed Services Explosives Safety Board, Washington, D.C., August 1966.
3. McLean, D. G. and D. S. Allan, *An Experimental Program to Determine the Sensitivity of Explosive Materials to Impact by Regular Fragments*, by Arthur D. Little, Inc., Cambridge, Massachusetts, under Contract DA-19-020-ORD-5617 for Commanding Officer, Picatinny Arsenal, Dover, New Jersey, December 1965.
4. Patton, L. M., *Investigation of Explosive Sensitivity to Multiple Fragment Impact*, Track Tests E-7101, U.S. Naval Weapon Center, China Lake, California, 1962.
5. Patton, L. M., *Investigation of Explosive Sensitivity to Multiple Fragment Impact*, Track Tests 7380, U.S. Naval Weapon Center, China Lake, California, 1963.
6. Richmond, D. R., et al, *The Relationship Between Selected Blast-Wave Parameters and the Response of Mammals Exposed to Air Blast*, Lovelace Foundation for Medical Education and Research, Albuquerque, New Mexico, Annals of the New York Academy of Sciences, Conference on Prevention of and Protection Against Accidental Explosion of Munitions, Fuels and Other Hazardous Mixtures, Volume 152, Art. 1, October 1966.
7. Rinder, R. M., *Establishment of Safety Design Criteria for Use in Engineering of Explosive Facilities and Operations, Report No. 8, Detonation by Fragment Impact*, Technical Report DB-TR: 6-59, Picatinny Arsenal, Dover, New Jersey, May 1959.
8. Rinder, R. M., *Response of Explosive to Fragment Impact*, Technical Report 3485, Picatinny Arsenal, Dover, New Jersey, December 1966.
9. Rinder, R. M., and S. Wachtell, *Safe Distances and Shielding for Prevention of Propagation of Detonation by Fragment Impact*, Technical Report DB-TR: 6-60, Picatinny Arsenal, Dover, New Jersey, December 1960.

Chapter 4

1. *Barricaded vs. Unbarricaded Blast Pressure—Distance Relationships*, Armed Services Explosives Safety Board, Department of Defense, Washington, D.C., July 1966.
2. *Effects of Impact and Explosion*, Volume 1, Office of Scientific Research and Development, National Defense Research Committee, Washington, D.C., 1946 (CONFIDENTIAL).

3. *Effects of Nuclear Weapons*, U.S. Department of Defense & U.S. Atomic Energy Commission, U.S. Government Printing Office, April 1962.
4. *Industrial Engineering Study to Establish Safety Design Criteria for Use in Engineering of Explosive Facilities and Operations*, by Ammann & Whitney, Consulting Engineers, New York, New York, under Contract DA-28-017-501-ORD-3889, for Process Engineering Branch, A.P.M.-E.D., Picatinny Arsenal, Dover, New Jersey, April 1963.
5. *Information Summary of Blast Patterns in Tunnels and Chambers*, Second Edition, Memorandum Report No. 1390, Ballistic Research Laboratories, Aberdeen Proving Ground, Maryland, March 1962.
6. *Summary of One-Third Scale Slab Tests and Scaled Bay Structure Tests*, by Ammann & Whitney, Consulting Engineers, New York, New York, under Contract DA-28-017-AMC-423(A) for Picatinny Arsenal, Dover, New Jersey, March 1969.
7. Altman, F. D., *Model Studies of Explosive Storage Cubicles*, NWL Report No. 1917, Warhead and Terminal Ballistics Laboratory, U.S. Naval Weapons Laboratory, Dahlgren, Virginia, May 1964.
8. Caudle, K. F., and H. A. Goertner, *Explosives-Effects and Properties*, NOLTR-65-218, Explosions Research Department, U.S. Naval Ordnance Laboratory, White Oak, Silver Spring, Maryland, February 1967 (CONFIDENTIAL).
9. Cohen, E., et. al., *Establishment of safety Design Criteria for Use in Engineering of Explosive Facilities and Operations, Report No. 10, Blast Pressures and Impulse Loads Produced by Explosions in Cubicle-Type Structures*, Technical Report 3604, by Ammann & Whitney, Consulting Engineers, New York, New York, and Picatinny Arsenal, Dover, New Jersey, under Contract DAAA-21-67-C-0217, May 1967.
10. Cohen, E., and N. Dobbs, *Design Procedures and Details for Reinforced Concrete Structures Utilized in Explosive Storage and Manufacturing Facilities*, Ammann & Whitney, Consulting Engineers, New York, New York, Annals of the New York Academy of Sciences, Conference on Prevention of and Protection Against Accidental Explosion of Munitions, Fuels and Other Hazardous Mixtures, Volume 152, Art. 1, October 1968.
11. Dobbs, N., et al, *Blast Pressures and Impulse Loads for Use in the Design and Analysis of Explosive Storage and Manufacturing Facilities*, Ammann & Whitney, Consulting Engineers, New York, New York, Annals of the New York Academy of Sciences, Conference on Prevention of and Protection Against Accidental Explosion of Munitions, Fuels and Other Hazardous Mixtures, Volume 152, Art. 1, October 1968.
12. Filler, W. S., et. al., *Barricade Effectiveness Evaluated from Records of Accidental Explosions*, Armed Services Explosives Safety Board, Department of Defense, Washington, D.C., July 1966.
13. Filler, W. S., *Post-Detonation Pressure and Thermal Studies of Solid High Explosives in a Closed Chamber*, U.S. Naval Ordnance Laboratory, Silver Springs, Maryland, a reprint from Sixth Symposium (International) on Combustion, The Combustion Institute, 1957.
14. Fletcher, R. F., *Characteristics of Liquid Propellant Explosions*, National Aeronautics and Space Administration, Manned Spacecraft Center, Houston, Texas, Annals of the New York Academy of Sciences, Conference on Prevention of and Protection Against Accidental Explosion of Munitions, Fuels and Other Hazardous Mixtures, Volume 152, Art. 1, October 1968.
15. Granstrom, S. A., *Loading Characteristics of Air Blast from Detonating Charges*, Transactions of the Royal Institute of Technology, Stockholm, Sweden, 1956.
16. Kaplan, K., and V. W. Davis, *Effectiveness of Barricades: Review of Basic Information*, URS 677-4R, DASA 2014, by United Research Systems Corporation, Burlingame, California, under Contract DASA 01-67-C-0046 for the Defense Atomic Support Agency, Washington, D.C., June 1968.
17. Kennedy, W. D., *The Effects of Air-Burst on the Blast from Bombs and Small Charges, II*, Analysis of Experimental Results, OSRD-4246, September 1944.
18. Kingery, C. N., *Air Blast Parameters Versus Distance For Hemispherical TNT Surface Bursts*, Report No. 1344, Ballistic Research Laboratories, Aberdeen Proving Ground, Maryland, September 1966.
19. Kingery, C. N. and B. F. Pannill, *Parametric Analysis of the Regular Reflection of Air Blast*, Report No. 1249, Ballistic Research Laboratories, Terminal Ballistics Laboratory, Aberdeen Proving Ground, Maryland, June 1964.
20. Richey, H. M., *Armed Forces Explosives Safety Board Wall Program, Phase C, Tests 1 through 13*, Technical Progress Report 346, U.S. Naval Weapon Center, China Lake, California, April 1964 (SECRET RESTRICTED DATA).
21. Rindner, R. M., *Establishment of Safety Design Criteria for Use in Engineering of Explosive Facilities and Operations, Report No. 2, Detonation by Fragment Impact*, Technical Report DB-TR: 0-59, Picatinny Arsenal, Dover, New Jersey, May 1959.
22. Rinder, R. M., and S. Wachtell, *Safe Distances Shielding for Prevention of Propagation of Detonation by Fragment Impact*, Technical Report DB-TR: 6-60, Picatinny Arsenal, Dover, New Jersey, December 1960.
23. Sound, A. R., *Summary Report of Earth-Covered, Steel-Arch Magazine Tests*, Technical Progress Report 401, U.S. Naval Weapon Center, China Lake, California, July 1965.
24. Sterne, T. E., *A Note on the Initial Velocities of Fragments From Warheads*, Report No. 648, Ballistic Research Laboratories, Aberdeen Proving Ground, Maryland, September 1947.
25. Weibull, H., *Pressures Recorded in Partially Closed Chambers at Explosion of TNT Charges*, Royal Swedish Fortifications Administration, Stockholm, Sweden, 1966.

Chapter 5

1. *American Concrete Institute Standard Building Code Requirements for Reinforced Concrete*, ACI Committee 318-63, American Concrete Institute, Detroit, Michigan, June 1963.
2. *Design of Structures to Resist Nuclear Weapons Effects*, ASCE Manual of Engineering Practice No. 42, American Society of Civil Engineers, New York, New York, 1961.
3. *Design of Structures to Resist the Effects of Nuclear Weapons*, Department of the Army Technical Manual TM 5-856-2, 3 and 4, Washington, D.C.
4. *Dynamic Tests of Concrete Reinforcing Steels*, Technical Report R 394, U.S. Naval Civil Engineering Laboratory, Port Hueneme, California, September 1965.
5. *Summary of One-Third Scale Slab Tests and Scaled Bay Structure Tests*, by Ammann & Whitney, Consulting Engineers, New York, New York, under Contract DA-28-017-AMC-423(A) for Picatinny Arsenal, Dover, New Jersey, March 1969.
6. *Ultimate Strength Design Handbook*, Volume No. 1, Special Publication No. 17, ACI Committee 340, American Concrete Institute, Detroit, Michigan, 1967.
7. *Ultimate Strength Design of Reinforced Concrete Columns*, Publication SP-7, Interim Report of ACI Committee 340, American Concrete Institute, Detroit, Michigan, 1964.

8. Cohen, E. and N. Dobbs, *Design Procedures and Details for Reinforced Concrete Structures Utilized in Explosive Storage and Manufacturing Facilities*, Ammann & Whitney, Consulting Engineers, New York, New York, Annals of the New York Academy of Sciences, Conference on Prevention of and Protection Against Accidental Explosion of Munitions, Fuels and Other Hazardous Mixtures, Volume 152, Art. 1, October 1968.
9. Cohen, E. and N. Dobbs, *Supporting Studies to Establish Safety Design Criteria for Storage and Processing of Explosive Materials-Interim Report No. 1, Summary of One-Third Scale Reinforced Concrete Slab Tests*, Technical Memorandum C-1, by Ammann & Whitney, Consulting Engineers, New York, New York, under Contract DA-28-017-AMC-423(A) for Picatinny Arsenal, Dover, New Jersey, June 1965.
10. Keenan, W. A., *Strength and behavior of Laced Reinforced Concrete Slabs under Static and Dynamic Load*, Technical Report R-620, U.S. Naval Civil Engineering Laboratory, Port Hueneme, California, April 1969.
11. Schwartz, A., et al, *Establishment of Safety Design Criteria for Use in Engineering of Explosive Facilities and Operations, Report No. 6, Test of One-Tenth Scale Bay Structure*, Technical Report 3439, by Picatinny Arsenal, Dover, New Jersey, and Ammann & Whitney, Consulting Engineers, New York, New York, under Contract DA-28-017-AMC-423(A), July 1966.
12. Timoshenko, S. and S. Woinowsky-Krieger, *Theory of Plates and Shells*, McGraw-Hill Book Co., New York, New York, 1959.
13. Whitney, C. S., and E. Cohen, *Guide for Ultimate Strength Design of Reinforced Concrete*, Ammann & Whitney, Consulting Engineers, New York, New York, Journal of the American Concrete Institute, November 1956.
14. Whitney, C. S., et al, *Design of Blast-Resistant Construction for Atomic Explosions*, Ammann & Whitney, Consulting Engineers, New York, New York, Journal of the American Concrete Institute, March 1955.
15. Wood, R. W., *Plastic and Elastic Design of Slabs and Plates*, The Ronald Press Company, New York, New York, 1961.

Chapter 6

1. *Design Manual, AEC Test Structures, Volumes II and III*, by Holmes and Narver, Inc., under Contract AT (29-2)-20, for U.S. Atomic Energy Commission, Albuquerque Operations Office, Albuquerque, New Mexico, December 1961.
2. *Design of Structures to Resist the Effects of Nuclear Weapons*, Department of the Army Technical Manual TM5-856-3 and 4, Washington, D.C.
3. *Summary of One-Third Scale Slab Tests and Scaled Bay Structure Tests*, by Ammann & Whitney, Consulting Engineers, New York, New York, under Contract DA-28-017-AMC-423(A) for Picatinny Arsenal, Dover, New Jersey, March 1969.
4. Cohen, E. and N. Dobbs, *Design Procedures and Details for Reinforced Concrete Structures Utilized in Explosive Storage and Manufacturing Facilities*, Ammann & Whitney, Consulting Engineers, New York, New York, Annals of the New York Academy of Sciences, Conference on Prevention of and Protection Against Accidental Explosion of Munitions, Fuels and Other Hazardous Mixtures, Volume 152, Art. 1, October 1968.
5. Keenan, W. A., *Strength and Behavior of Laced Reinforced Concrete Slabs under Static and Dynamic Load*, Technical Report R-620, U.S. Naval Civil Engineering Laboratory, Port Hueneme, California, April 1969.
6. Newmark, N. M. and J. D. Haltiwanger, *Air Force Design Manual, Principles and Practices for Design of Hardened Structures*, Technical Documentary Report No. AFSWC-TDR-62-138, by Department of Civil Engineering, University of Illinois, Urbana, Illinois, under Contract AF29 (601)-2390 for Research Directorate, Air Force Special Weapons Center, Air Force Systems Command, Kirtland Air Force Base, New Mexico, December 1962.
7. Whitney, C. S., et al, *Design of Blast-Resistant Construction for Atomic Explosions*, Ammann & Whitney, Consulting Engineers, New York, New York, Journal of the American Concrete Institute, March 1955.

Chapter 7

1. *Summary of One-Third Scale Slab Tests and Scaled Bay Structure Tests*, by Ammann & Whitney, Consulting Engineers, New York, New York, under Contract DA-28-017-AMC-423(A) for Picatinny Arsenal, Dover, New Jersey, March 1969.
2. Cohen, E. and N. Dobbs, *Design Procedures and Details for Reinforced Concrete Structures Utilized in Explosive Storage and Manufacturing Facilities*, Ammann & Whitney, Consulting Engineers, New York, New York, Annals of the New York Academy of Sciences, Conference on Prevention of and Protection Against Accidental Explosion of Munitions, Fuels and Other Hazardous Mixtures, Volume 152, Art. 1, October 1968.
3. Cohen, E. and N. Dobbs, *Supporting Studies to Establish Safety Design Criteria for Storage and Processing of Explosive Materials-Interim Report No. 1, Summary of One-Third Scale Reinforced Concrete Slab Tests*, Technical Memorandum C-1, by Ammann & Whitney, Consulting Engineers, New York New York, under Contract DA-28-017-AMC-423(A) for Picatinny Arsenal, Dover, New Jersey, June 1965.
4. Richey, H. M., *Armed Services Explosives Safety Board Dividing Wall Program, Phase C, Tests 1 through 13*, U.S. Naval Weapon Center, China Lake, California, 1964 (SECRET RESTRICTED DATA).
5. Schwartz, A., et al, *Establishment of Safety Design Criteria for Use in Engineering of Explosive Facilities and Operations, Report No. 6, Test of One-Tenth Scale Bay Structure*, Technical Report 3439, by Picatinny Arsenal, Dover, New Jersey and Ammann & Whitney, Consulting Engineers, New York, New York, under Contract DA-28-017-AMC-423(A), July 1966.
6. Williamson, G. R., *Response of Fibrous-Reinforced Concrete to Explosive Loadings*, Technical Report No. 2-48, Ohio River Division Laboratories, Corps of Engineers, Department of the Army, Cincinnati, Ohio, January 1966.

Chapter 8

1. *Effects of Impact and Explosion*, Volume 1, Office of Scientific Research and Development, National Defense Research Committee, Washington, D.C., 1946 (CONFIDENTIAL).
2. *Fundamentals of Protective Design (Non-Nuclear)*, Department of the Army Technical Manual TM5-855-1, Washington, D.C., July 1965.
3. *Industrial Engineering Study to Establish Safety Design Criteria for Use in Engineering of Explosive Facilities and Operations*, by Ammann & Whitney, Consulting Engineers, New York, New York, Under Contract DA-28-017-501-ORD-3889, for Process Engineering Branch, A.P.M.E.D., Picatinny Arsenal, Dover, New Jersey, April 1963.
4. Cohen, E. and N. Dobbs, *Design Procedures and Details for Reinforced Concrete Structures Utilized in Explosive Storage and Manufacturing Facilities*, Ammann & Whitney, Consulting Engineers, New York, New York, Annals of the New York Academy of Sciences, Conference on Prevention of and Protection Against Accidental Explosion of Muni-

tions, Fu
Art. 1, Oc

Chapter 9

1. *American C*
ments fo
Americar
1963.
2. *Manual of*
Structure
Institute
3. *Summary*
Structure
gineers,
017-AMC
Jersey, N
4. Cohen, E.
Reinforce
and Mar
sulting E
New Yo
tion of
Munitio
152, Art
5. Cohen, E.
of Reinfo
Whitney
Annals
on Prev
plosion
tures, V
6. Wachtell,
Size Co
Jersey,
Confere
cidental
ous Mix

Chapter 10

1. *American*
ments f
Americ
1963.
2. *Anti-Blas*
Little,
of Defe
Septem
3. *Army Mo*
Depart
1961.
4. *Care, Har*
Depart
206, W
5. *Investigat*
a Blast
Co., C
for U.S
D.C.
6. *Quantity-*
and Sto
DoD I
ington,
7. *Shock Tu*
Inform
Branch
Groun
8. *Shock Tu*
II, Bl

tions, Fuels and Other Hazardous Mixtures, Volume 152, Art. 1, October 1968.

Chapter 9

1. *American Concrete Institute Standard Building Code Requirements for Reinforced Concrete*, ACI Committee 318-63, American Concrete Institute, Detroit, Michigan, June 1963.
2. *Manual of Standard Practice for Detailing Reinforced Concrete Structures*, ACI Committee 315-65, American Concrete Institute, Detroit, Michigan, 1965.
3. *Summary of One-Third Scale Slab Tests and Scaled Bay Structure Tests*, by Ammann & Whitney, Consulting Engineers, New York, New Yorks, under Contract DA-28-017-AMC-423(A) for Picatinny Arsenal, Dover, New Jersey, March 1969.
4. Cohen, E. and N. Dobbs, *Design Procedures and Details for Reinforced Concrete Structures Utilized in Explosive Storage and Manufacturing Facilities*, Ammann & Whitney, Consulting Engineers, New York, New York, Annals of the New York Academy of Sciences, Conference on Prevention of and Protection Against Accidental Explosion of Munitions, Fuels, and Other Hazardous Mixtures, Volume 152, Art. 1, October 1968.
5. Cohen, E. and N. Dobbs, *Models for Determining the Response of Reinforced Concrete Structures to Blast Loads*, Ammann & Whitney, Consulting Engineers, New York, New York, Annals of the New York Academy of Sciences, Conference on Prevention of and Protection Against Accidental Explosion of Munitions, Fuels and Other Hazardous Mixtures, Volume 152, Art. 1, October 1968.
6. Wachtell, S., *Comparison of Blast Response-Scaled vs. Full-Size Concrete Structures*, Picatinny Arsenal, Dover, New Jersey, Annals of the New York Academy of Sciences, Conference on Prevention of and Protection Against Accidental Explosion of Munitions, Fuels and Other Hazardous Mixtures, Volume 152, Art. 1, October 1968.

Chapter 10

1. *American Concrete Institute Standard Building Code Requirements for Reinforced Concrete*, ACI Committee 318-63, American Concrete Institute, Detroit, Michigan, June 1963.
2. *Anti-Blast Value Development, 1960–1964*, by Arthur D. Little, Inc., Cambridge, Massachusetts, for Department of Defense, Office of Civil Defense, Washington, D.C., September 1964.
3. *Army Material Command Safety Manual*, AMCR 385-224, Department of the Army, Washington, D.C., February 1961.
4. *Care, Handling, Preservation and Destruction of Ammunition*, Department of the Army Technical Manual TM9-1300-206, Washington, D.C.
5. *Investigations Concerning Feasibility of Various Designs for a Blast Closure Device*, by American Machine and Foundry Co., Chicago, Illinois, under Contract No. NBy-13030, for U.S. Navy, Bureau of Yards and Docks, Washington, D.C.
6. *Quantity-Distance Standards for Manufacturing, Handling and Storage of Mass-Detonating Explosives and Ammunition*, DoD Instruction 4145.22, Department of Defense, Washington, D.C., January 1966.
7. *Shock Tube Test of Mosler Safe Company Blast Valve*, BRL Information Memorandum No. 20, Explosion Kinetics Branch, Ballistic Research Laboratories, Aberdeen Proving Ground, Maryland, August 1959.
8. *Shock Tube Test of Mosler Safe Company Blast Valve, Phase II*, BRL Information Memorandum No. 25, Explosion Kinetics Branch, Ballistic Research Laboratories, Aberdeen Proving Ground, Maryland, August 1959.
9. *Study of Blast-Closure Devices*, AFSWC-TDR-62-10, by American Machine and Foundry Co., Chicago, Illinois for Air Force Special Weapons Center, Kirtland Air Force Base, New Mexico, February 1962.
10. *Study of Shock Isolation Methods for Civil Defense Shelters*, by Ammann & Whitney, Consulting Engineers, New York, New York, under Contract DA 49-129-ENG-506, for Department of the Army, Office of the Chief of Engineers, Washington, D.C., for the Office of Civil Defense, Work Order No. OCD-OS-62-159, OCD Research Sub-Task 1152C, November 1963.
11. Allen, F. C., et. al. *Test and Evaluation of Anti-Blast Valves for Protective Ventilating Systems*, WT-1460, Operation Plumbbob, Project 31.5, available from the Office of Technical Services, Department of Commerce, Washington, D.C.
12. Bayles, J. J., *Development of the B-D Blast-Closure Valve*, Technical Note N-546, U.S. Naval Civil Engineering Laboratory, Port Hueneme, California, December 1963.
13. Bergman, S. and B. Staffors, *Blast Tests on Rapid-Closing Anti-Blast Valves*, Royal Swedish Fortification Administration, Stockholm, Sweden, November 1963.
14. Birnbaum, H. and E. Laing, *Evaluation of Various Types of Personnel Shelters Exposed to an Atomic Explosion*, WT-1218, Ammann & Whitney, Consulting Engineers, New York, New York, Operation Teapot, Projects 34.1 and 34.3, available from the Office of Technical Services, Department of Commerce, Washington, D.C., 1958.
15. Breckenridge, T. A., *Preliminary Development and Tests of a Blast-Closure Valve*, Technical Note N-460, U.S. Naval Civil Engineering Laboratory, Port Hueneme, California, September 1962.
16. Chapler, R. S., *Evaluation of Four Blast Closure Valves*, Technical Report R 347, DASA-13.154, U.S. Naval Civil Engineering Laboratory, Port Hueneme, California, January 1965 (Official Use Only).
17. Cohen, E., *Blast Vulnerability of Deep Underground Facilities as Affected by Access and Ventilation Openings*, Ammann & Whitney, Consulting Engineers, New York, New York, Proceedings of the Second Protective Construction Symposium, R-341, Volume I, The RAND Corporation, Santa Monica, California, 1959.
18. Cohen, E., et. al, *Response of Protective Vaults to Blast Loadings*, Ammann & Whitney, Consulting Engineers, New York, New York, WT-1451, Operation Plumbbob, Project 30.4, available from the Office of Technical Services, Department of Commerce, Washington, D.C., 1962.
19. Cohen, E. and A. Bottenhoffer, *Test of German Underground Personnel Shelters*, WT-1454, Ammann & Whitney, Consulting Engineers, New York, New York, Operation Plumbbob, Project 30.7, available from the Office of Technical Services, Department of Commerce, Washington, D.C., June 1962.
20. Cohen, E., and N. Dobbs, *Application of New Design Techniques for High Capacity Protective Barriers—Case Studies*, Ammann & Whitney, Consulting Engineers, New York, New York, Minutes of the Tenth Explosives Safety Seminar, sponsored by the Armed Services Explosives Safety Board, Washington, D.C., August 1968.
21. Cohen, E., and N. Dobbs, *Cost Effectiveness Studies of Facilities for High-Hazard Explosive Material*, Ammann & Whitney, Consulting Engineers, New York, New York, Minutes of the Ninth Explosives Safety Seminar, sponsored by the Armed Services Explosives Safety Board, Washington, D.C., August 1967.
22. Cohen, E. and S. Weissman, *Blast Closure Systems*, Ammann

& Whitney, Consulting Engineers, New York, New York, Proceedings of the Symposium on Protective Structures for Civil Populations, Subcommittee on Protective Structures, Advisory Committee on Civil Defense, National Academy of Sciences and National Research Council, April 1965.

23. Flathou, W. J., et. al. *Blast Loading and Response of Underground Concrete-Arch Protective Structures*, WT-1420, U.S. Waterways Experiment Station, Jackson, Mississippi, Operation Plumbbob, Project 3.1, Chief, Defense Atomic Support Agency, Washington, D.C.
24. Hassman, M. and E. Cohen, *Review of Blast Closure Systems*, Ammann & Whitney, Consulting Engineers, New York, New York, 29th Symposium on Shock, Vibration and Associated Environments, Part III, Bulletin No. 29, U.S. Naval Research Laboratory, Washington, D.C., July 1961, available from the Office of Technical Services, Department of Commerce, Washington, D.C.
25. Hellberg, E. N. *Performance of the Swedish Rapid-Closing Anti-Blast Valve*, Technical Note 439, Task Y-F 008-10-11, U.S. Naval Civil Engineering Laboratory, Port Hueneme, California, May 1962.
26. Jones, W. A., et. al. *A Simple Blast Valve*, Suffield Technical Note No. 113, Suffield Experimental Station, Ralston, Alberta, Canada, Defense Research Board, Department of National Defense, Canada, DRB Project No. D89-16-01-09, February 1963.
27. Kaplan, K., and V. W. Davis, *Effectiveness of Barricades: Review of Basic Information*, URS 677-4R, DASA 2014, by United Research Systems Corporation, Burlingame, California, under Contract DASA 01-67-C-0046 for the Defense Atomic Support Agency, Washington, D.C., June 1968.
28. Means, R. S., *Building Construction Cost Data, 26th Annual Edition*, Robert Snow Means Co., Duxtury, Massachusetts, 1968.
29. Miller, P., *Report of Dividing Wall Test, Phase A, No. 4*, U.S. Naval Weapon Center, China Lake, California, September 1964.
30. Neidhardt, G. L., et. al., *Field Test of Reinforced Concrete Shelters and Prototype Door*, WT-1448, Operation Plumbbob, Project 30.1, available from the Office of Technical Services, Department of Commerce, Washington, D.C.
31. Newmark, N. M., and J. D. Haltiwanger, *Air Force Design Manual, Principles and Practices for Design of Hardened Structures*, Technical Documentary Report No. AFSWC-TDR-62-138, by Department of Civil Engineering, University of Illinois, Urbana, Illinois, under Contract AF29 (601)-2390 for Research Directorate, Air Force Special Weapons Center, Air Force Systems Command, Kirtland Air Force Base, New Mexico, December 1962.
32. Ort, F. G. and M. D. Mears, *Development of the Closure, Protective Shelter, Anti-Blast, 600 cfm, E19R1*, Technical Report CWLR-2269, Chemical Warfare Labs., U.S. Army Chemical Center, Edgewood, Maryland, January 1959.
33. Ort, F.G., and M. D. Mears, *Scientific Director's Report of Atomic Weapon Tests at Eniwetok*, 1951, Annex 6.10 Operation Greenhouse, Evaluation of Collective-Protective Equipment, U.S. Army Chemical Center, Edgewood, Maryland, March 1952.
34. Rindner, R., *Case Studies on Application of New Design Methods for High Capacity Protective Barriers*, Picatinny Arsenal, Dover, New Jersey, Minutes of the Ninth Explosive Safety Seminar, sponsored by the Armed Services Explosive Safety Board, Washington D.C., August 1967.
35. Sound, A. R., *Summary Report of Earth-Covered, Steel-Arch Magazine Tests*, Technical Progress Report 401, U.S. Naval Weapon Center, China Lake, California, July 1965.
36. Stephenson, J. M., *Preliminary Tests of the Stephenson Valve*, 2nd Report, Technical Note N-619, U.S. Naval Civil Engineering Laboratory, Port Hueneme, California, July 1964.
37. Stephenson, J. M., *Test of German Sand-Type Filter*, Technical Report R263, U.S. Naval Civil Engineering Laboratory, Port Hueneme, California, November 1963.
38. Weals, F. H., *Tests to Determine Separation Distances of Earth-Covered Magazines*, U.S. Naval Weapon Center, China Lake, California, Annals of the New York Academy of Sciences, Conference on Prevention of and Protection Against Accidental Explosion of Munitions, Fuels and Other Hazardous Mistures, Volume 152, Art. 1, October 1968.

GLOSSARY

Acceleration—The change of velocity as a function of time.

Acceptor explosive—The explosive charge which requires protection. See *Receiver System*.

Admixture—The addition of either chopped steel wire or nylon fibers to reinforced concrete.

Ambient pressure—The atmospheric pressure acting at a given altitude. See *Duration*.

Angle of incidence—The angle formed by the line which defines the normal distance between the piont of detonation and the surface of a protective element and the line which defines the path of shock propagation between the center of the explosion and any other point on the element.

Angle of obliquity—The angle formed by the trajectory path of a primary fragment and the surface of an element.

Attenuation—The decrease in intensity of a blast wave as a result of absorption of energy.

Barricade—A mound, a single revetted barricade, or another type of artificial or natural obstruction which provides protection at least equivalent to that of a mound.

Barrier—A protective structure where one or more sides and/or the roof are of frangible construction or open to the atmosphere. Barriers include operating buildings and magazines used in explosive facilities.

Blast door—A protective closure for personnel and/or vehicular access or egress openings.

Blast effects (or blast output)—The blast pressures and impulse loads produced by an explosion.

Blast loads—The forces, associated with the pressure output, acting on an element or structure.

Blast pressures—See *Pressures*.

Blast-resistant design—The design of a protective structure to resist the blast output of an explosion.

Blast shield—A protective closure device for ventilation openings consisting of structural steel plates and support angles.

Blast valve—A mechanical and electrical protective closure device for ventilation openings.

Blast wave—A pulse of air in which the pressure increases sharply at the front, accompanied by winds, progagated continuously from an explosion. See *Shock Wave*.

Brittle mode—The response of a structural element which is associated with fragments formed by partial or total failure.

Bundled bars—A grouping together of several reinforcing bars at one or more locations.

Burst (See *Unconfined Explosion*)—

- *Air*—An explosion which is located at a distance away from and above the protective structure so that ground reflections of the initial blast wave occur before the wave arrives at the structure.
- *Free-air*—An explosion which is located adjacent to and above a protective structure so that no intermediate amplification of the initial blast wave occurs between the center of the explosion and the structure.
- *Surface*—An explosion which is located on or close to the ground surface so that the initial blast wave is amplified at the point of detonation due to ground reflections.

Capacity reduction factor—A safety factor utilized in design to insure against a shear failure in the structural element.

Casing (or container)—A metal covering which partially or fully encloses an explosive.

Charge weight (or charge)—

- *Actual*—The total weight of an explosive including that portion which is not involved in the detonation process.
- *Effective*—The weight of an explosive involved in the detonation process.
- *Equivalent*—The weight of a spherical TNT charge (hemispherical charge for surface bursts) which will produce the same blast effects as the explosive under consideration.

Composite construction—Walls composed of two concrete panels (donor and receiver) separated by a sand-filled cavity.

Cubicle—An area which is partially or fully enclosed by blast-resistant walls and roof. See *Barrier*.

Deflection—

- *Elastic*—The maximum deflection in the elastic range, that is, the deflection at the formation of the first yield line.
- *Elasto-plastic*—The deflection at the formation of the second yield line.
- *Equivalent maximum elastic*—A fictitious deflection calculated in order to idealize the elastic and elasto-plastic portions of the resistance-deflection variation of an element's response.
- *Large*—The maximum deflection corresponding to a support rotation angle of greater than five degrees.
- *Limited*—The maximum deflection corresponding to a support rotation angle of five degrees or less.
- *Maximum*—The largest deflection sustained by an element in the direction of and as a result of a given loading condition.
- *Partial failure*—The deflection where one or more of the supports of a two-way element fail; all further flexural action conforms to that of a one-way element.
- *Plastic*—The deflection at the formation of the last yield line.
- *Ultimate*—The deflection at incipient failure.

Deflagration—Rapid and violent burning.

Degree of freedom—The number of independent displacement variables needed to completely specify the configuration of a dynamic system.

Degree of protection—A scale which is used to measure the required protection, in any one protection category, relative to the sensitivity of the receiver system.

Detonation (See *Explosion*)—

- *Mass*—Similar to a simultaneous detonation except that a much larger quantity of explosives is involved.
- *Simultaneous*—A detonation of separated quantities of explosives or ammunition occurring so nearly at the same time that the effect on the surroundings is the same as if the several quantities were not separated and were detonated en masse.

Diagonal bars—Reinforcing bars which are used to resist the high support shears in a structural element produced by high intensity blast loads.

Direct spalling—The dynamic disengagement of the concrete surface of an element, resulting from a tension failure in the concrete normal to its free surface, caused by shock presures of an impinging blast wave being transmitted through the element. See *Scabbing*.

Donor explosive—The explosive contained in the donor system.

Donor system—The portion of an explosion protection system which produces the damaging output.

Drag coefficient—A coefficient which is equal to the drag pressure divided by the dynamic pressure and is dependent upon the shape (or geometry) of the structure or element.

Drag loading (or drag pressure)—The force on an object or structure due to the transient winds accompanying the passage of a blast wave. The drag pressure is the product of the dynamic pressure and the drag coefficient.

Ductile mode—The response of a structural element which is characterized by the element's ability to attain relatively large inelastic deflections without complete collapse.

Ductility factor—The ratio of the maximum deflection to the equivalent maximum elastic deflection of an element.

Duration—The interval between the time of arrival of the blast wave at a given location and the time for the magnitude of the blast pressures to return to ambient pressure at the location in question See *Phase*.

Dynamic increase factor—The ratio of the dynamic to static stresses of a material.

Dynamic similarity—The requirement that the work done, kinetic energy, and strain energy of the equivalent dynamic system must be identical, respectively, with those of the given structure.

Earth-covered magazine (or igloo)—An arch-type, earth-covered magazine which may be constructed of concrete, metal or wood. See *Magazine*.

Effective mass—The mass of an equivalent single-degree-of-freedom system. The value of the effective mass differs for the elastic, elasto-plastic, and plastic ranges of behavior.

Elastic range—The response range of an element in which its deflections will essentially return to zero after removal of the load.

Elastic rebound—The elastic displacement of an element occurring in a direction oppostie from that of the blast load and as a result of the removal of the load.

Elasto-plastic range—The response range of an element which occurs after the formation of the first yield line but before the last yield line.

Element (or member)—A component of a structure including walls, panels, slabs or beams.

Equivalent dynamic system—A system which consits of a number of concentrated masses joined together by weightless springs and subjected to concentrated loads which vary with time. These concentrated masses replace the distributed masses of a given structure in order to simplify the dynamic analysis of the structure.

Explosion (See *Detonation*)—

Multiple—Two or more explosions whose initiation time is such as to cause the blast effects of the various explosions to be cumulative on the response of a structure.

Partially confined—An explosion occurring within or immediately adjacent to a structure. In addition, partially confined explosions may be subdivided into fully vented explosions where the pressures produced by the accumulation of gases from the explosion are quickly released, and partially vented explosions where the gas accumulation will exert pressures in addition to those produced by the shock pressures.

Unconfined—An explosion occurring exterior to a structure such that the blast loads acting on the structure may be classified as a free-air burst, an air burst or a surface burst. See *Burst*.

Explosive (or high-explosive)—A chemical compound or mechanical mixture which, when subjected to heat, friction, detonation or other suitable initiation, undergoes a very rapid chemical change with the evolution of large volumes of highly heated gases which exert pressures in the surrounding medium.

Explosive protection system—A storage or manufacturing facility containing potentially explosive material, for which some specified degree of protection against the effects of accidental explosions is provided.

Flexural reinforcement—The reinforcing steel which is used to resist the flexural stresses (compression or tension) developed in a reinforced concrete element.

Fragment shield—A device which is composed of steel plates or other mass material which can be attached to or placed a short distance from a protective barrier and will provide protection for personnel or other portions of a receiver system from the effects of primary and/or secondary fragments.

Frangible construction—Those elements of a protective structure whose strength and mass are such as to minimize the amplification of shock front and/or gas pressures produced by a partially confined explosion.

Ground shock—

Air-induced—Ground motions induced by a blast wave traveling over the ground surface and generating stress waves into the ground.

Direct-transmitted—Ground motions induced by a transmission of energy into the ground in the immediate vicinity of the explosion where it is then dispersed to areas of lower pressure level directly through the ground.

Haunch—A concrete fillet between two intersecting structural elements.

Impulse—

Excess—The portion of the impulse resulting from the blast wave which exceeds the flexural impulse capacity of the structural element.

Total—The product of the force from the blast wave of an explosion and the time during which it acts on a structural element. It is the integral with respect to time of the force, the integration being between the time of arrival of the blast wave and the time at which the force returns to zero on the element.

Unit—The product of the pressure from the blast wave of an explosion and the time during which it acts on a structural element. It is the area under the pressure-time curve between the time of arrival of the blast wave and the time at which the pressure returns to zero on the element. The pressure can be incident, reflected or dynamic.

Impulse capacity—The flexural impulse capacity (area under the resistance-time curve) of an element which responds in the ductile mode is equal to the amount of blast impulse corresponding to the kinetic energy, produced by the blast loads, which is numerically equal to the potential energy of the element developed during a specified response range. If the element responds in the brittle mode, then the impulse capacity (momentum) of the post-failure fragments must be added to the flexural impulse capacity of the element to obtain the total impusle capacity.

Incipient failure—The point at which the ultimate deflection of a structural element is reached. Any further increase in deflection beyond this point results in total collapse.

Inhabited building distance—The minimum permissible distance used to separate an inhabited building and an ammunition or explosives location. An inhabited building denotes a building or structure, other than an operating building or magazine, occupied in whole or part as a habitation for human beings.

Interior pressures—The pressures from an explosion that are

reflected and reinforced within a structure. The explosion is located within a barrier-type structure and the blast pressures are amplified due to their multiple reflections by the structure as a result of the proximity of the structure to the explosion.

Intraline distance—The minimum permissible distance used to separate any two operating buildings and/or sites within an operating line, at least one of which contains or is designed to contain explosives.

Isolation system—A flexible support system used to provide protection for personnel and/or equipment against the effects of structural motions. An isolation system attenuates to tolerable levels the high accelerations associated with these structural motions.

Kinetic energy—The energy an object or structural element has by virtue of its motion which is translational and/or rotational.

Lacing reinforcement—Continuous, bent diagonal bars which tie together the straight flexural reinforcing bars on each face of an element and thereby confine the intervening concrete. This system of lacing is absolutely necessary for elements designed to resist high, nonuniform blast loads as well as those designed to achieve large deflections.

Load factor—The design factor by which the total load applied to a structural element is multiplied to obtain the equivalent concentrated load for the equivalent single-degree-of-freedom system. The load factor is numerically equal to the resistance factor.

Load-mass factor—The factor formed by combining two basic equivalent design factors, that is, the mass factor divided by the load factor.

Mach front—See *Mach Stem*.

Mach stem—The shock front formed by the interaction of the incident and reflected shock fronts accompanying an air burst. The Mach stem is also called the Mach front. See *Triple Point*.

Magazine—Any building or structure, except an operating building, designed or specifically designated for the storage of explosives, ammunition, or loaded ammunition components.

Mass—The weight of an object or structural element divided by the acceleration due to gravity.

Mass factor—The design factor by which the total distributed mass of a structural element is multiplied to obtain the equivalent lumped mass of the equivalent single-degree-of-freedom system.

Mode of vibration—The vibratory deflection shape of an element produced by a specified loading.

Modular ratio—The ratio of the modulus of elasticity of structural steel to that of concrete.

Modulus of elasticity—The ratio of stress to strain in the elastic range of response of an element.

Moment of inertia—The summation of the second moment of the area of an element about its neutral axis. The specific terms below are for reinforced concrete elements.

- *Average*—A numerical average of the magnitudes of the gross and cracked moments of inertia.
- *Cracked*—A summation of the second moment of the concrete area, which resists the compression stresses, and the transformed area of the reinforcement, which resists the tensile stresses, about the neutral axis.
- *Gross*—A summation of the second moment of the total concrete area about the neutral axis.

Momentum—The product of the mass and velocity of an object or structural element.

Multiple reflections—The amplification of the blast wave pressures, produced by a partially confined explosion, due to the impact of the shock front on various interior surfaces of a structure.

Natural frequency—The number of vibrations in one second an element completes in its fundamental mode of vibration.

Natural period of vibration—The time interval during which a vibrating body completes one vibration in its fundamental mode.

Neutral axis—The lonitudinal section in a structural element where zero bending strain, and therefore, zero stress exists.

Normal distance—The distance measured between the center of an explosion and a given location of the surface of an element. In this case, the plane of the element is perpendicular to the path of propagation of the blast wave.

Optimum reinforcement ratio—The ratio of the percentage of vertical reinforcement to that of the horizontal reinforcement in a two-way element, which for a given total quantity of flexural reinforcement will provide the maximum impulse capacity to the element.

Partial failure—The failure of one or more supports of a structural element resulting in a loss of strength and a reduction in the resistance. This point denotes the deflection after which all further flexural action conforms to that of a one-way element.

Phase (See *Duration*)—

- *Positive*—A period which begins when the shock wave arrives at a particular location and ends when the positive shock pressures reduce to the ambient pressure.
- *Negative*—A period which begins when the positive shock pressures reduce to the ambient pressure and ends when the negative shock pressures return to the ambient value.

Plane wave—A wave in which the pressures acting over the full height of the shock front are approximately equal. See *Mach Stem*.

Plastic hinge—A section in a concrete element where any additional rotation beyond a particular rotation (at yield stress) will not be accompanied by an increase in the moment capacity at the section. See *Yield Line*.

Plastic range—The response of an element occurring after the formation of the last yield line.

Poisson's ratio—The ratio of the transverse to longitudinal strain occurring in an element.

Post-failure fragments—Concrete fragments formed upon failure of a structural element.

Post-ultimate range—The response range occurring between partial and incipient failure of a two-way element.

Potential energy—The strain energy which results from the straining of an element produced by the blast loads; and which is numerically equal to the area under the resistance-deflection curve.

Pressures (*or overpressures*)—

- *Dynamic*—The air pressure which results from the mass air flow (or winds) behind the shock front of a blast wave.
- *Incident*—The pressure acting in the initial or incident blast (or shock) wave from an explosion.
- *Leakage*—The pressure produced by a partially confined explosion within a structure which spills out onto the exterior ground surface.
- *Reflected*—The total pressure which results instantaneously at the surface when a blast (or shock) wave traveling in one medium strikes another medium.

Pressure design range—

- *High*—This design range is associated with those protective structures and/or elements which are designed for high intensity blast pressures whose durations are short in comparison to the response time of the structure. The structure responds primarily to the impulse of the blast load.
- *Intermediate*—This design range is associated with those protective structures and/or elements which are designed for pressures which are less than those of the high pressure range, however, the durations of the pressures are in the order of the response time of the structure. The structure responds to the pressure-time history of the blast load.
- *Low*—This design range is associated with those protective

structures and/or elements which are designed for pressures less than those of the intermediate range but whose durations are long in comparison to the response time of the structure. The structure responds primarily to the peak pressure of the blast load.

Primary fragments—Fragments formed from casings, containers, or other metal objects located in the immediate vicinity of an explosion.

Propagation of explosion—The detonation of an acceptor explosive by; the blast pressures or primary fragment effects of the donor system, the motions of the structure, or the debris resulting from partial or total failure of either the structure or its contents.

Protective structure—A structure which is designed to provide protection for either personnel, valuable equipment and/or acceptor explosives against the damaging output of an explosion of the donor charge.

Receiver sensitivity—The degree to which the components of the receiver system are sensitive to the output of the donor system.

Receiver system—The portion of a explosion protective system which requires protection.

Reflection factor—The ratio of the peak reflected pressure to its corresponding incident pressure.

Resistance—The sum of the internal forces in a structural element whose function is to resist movement of the mass produced by the blast loads.

Elastic—The resistance which is developed during the elastic response range.

Elasto-plastic—The resistance which is developed during the elasto-plastic response range.

Post-ultimate—The resistance which is developed during the post-ultimate range.

Rebound—The resistance which is developed during the rebound phase of response.

Ultimate—The resistance which is developed at the formation of the last yield line.

Resistance factor—The design factor by which the resistance of an element is multiplied to obtain the resistance of the equivalent single-degree-of-freedom system. The resistance factor is numerically equal to the load factor.

Safety distance—An empirical distance related to the quantity of explosives which is the minimum permitted for separation of facilities within a hazardous area of possible explosions, and for separation of the explosive hazard from inhabited buildings, passenger railroads and public highways, in order to control the magnitude of damage, loss of life and serious injuries.

Safety factor—A factor used in design to account for unknown factors which in turn may lead to an overestimate of the protective capabilities of an element.

Scabbing—The dynamic disengagement of the concrete surface of an element, resulting from a tension failure in the concrete normal to its free surface, caused by large strains in the flexural reinforcement. See *Direct Spalling*.

Separation distance—A minimum distance between possible explosions and a facility providing protection for the receiver system; the magnitude of which will depend upon the degree of protection required.

Shear reinforcement—See *Lacing* and/or *Stirrups*

Shelter—A structure which encloses or nearly encloses the receiver system and is used to provide full protection for personnel and other items.

Shock front—The fairly sharp boundary between the pressure disturbance created by an explosion (in air, water, or earth) and the ambient atmosphere, water, or earth, respectively. It constitutes the front of the shock (or blast) wave.

Shock wave—A continuously propagated pressure pulse (or wave) in the surrounding medium which may be air, water, or earth, initiated by the expansion of the hot gases produced by an explosion. A shock wave in air is generally referred to as a blast wave, because it resembles and is accompanied by strong, but trasient, winds. See *Blast Wave*.

Slant distance—The distance measured between the center of an explosion and a given location on the surface of an element. In this case, the plane of the element is other than perpendicular to the path of propagation of the blast wave.

Spalling—See *Direct Spalling or Scabbing*.

Stiffness—The slope of the resistance-deflection curve in a given range of response of an element (elastic or elasto-plastic ranges). The equivalent elastic stiffness is defined as the slope of the resistance-deflection curve used to idealize the elastic and elasto-plastic response ranges of the element.

Stirrups—Web reinforcement used to resist excessive diagonal tension stresses in a reinforced concrete element produced by load intensities consistent with the intermediate or low pressure design ranges and where support rotations are equal to or less than 2 degrees. See *Lacing*.

Strain energy—See *Potential Energy*.

Structural motions—The motions of a structure caused by the impact of the blast wave and/or the ground motions below the structure.

Support condition—The type of support which exists at ends of one-way elements and around the periphery of two-way elements.

Fixed—Where there is complete resistance to both translation, perpendicular and parallel to the axis of the element, and rotation.

Free edge—Where there is no resistance to either translation, perpendicular or parallel to the axis of the element, or to rotation.

Restrained—Where there is complete resistance to translation, perpendicular and parallel to the axis of the element, but only partial resistance to rotation.

Simple—Where there is complete resistance to translation, perpendicular and parallel to the axis of the element, but not to rotation. In special cases, such as, the design of blast doors, translation parallel to the door's axis may be permitted.

Support rotation—The angle formed at a support between the plane of an element prior to being loaded (undeflected position) and the plane in which some specified deflection occurs.

Time—

Arrival—The finite time interval required for the blast wave to travel from the center of an explosion to any particular location.

Clearing—The finite time interval required for the blast presures acting on an element to reduce to some specified intensity.

Response—The finite time interval required for the maximum deflection of an element to occur.

Rise—The finite time interval required for the blast pressures acting on an element to increase from zero to a maximum value.

TNT equivalent—A measure of the energy released in the explosion of a given quantity of material, expressed in terms of the weight of TNT which would release the same amount of energy when exploded.

Total collapse—The condition of a structural element in which it completely loses its ability to resist the applied blast loads, that is, the element has exceeded the incipient failure condition.

Triple point—The intersection of the incident, reflected, and Mach shock fronts accompanying an air burst. The height of triple point above the ground surface, that is, the height of the Mach stem, increases with increasing distance from a given explosion. See *Mach Stem*.

Velocity—

Boundary (or minimum)—The velocity of a primary frag-

ment with a given weight which will result in propagation of explosion to the acceptor charge with a given casing thickness.

Dilatatinal--The velocity at which the longitudinal (or compression) wave travels through a given material.

Residual—The velocity of a primary fragment after it perforates an element.

Shock front—The velocity of the shock front in a medium at a particular time after an explosion. For a shock front in air, the velocity of the wave is referred to as the blast wave velocity.

Striking—The velocity at which a primary fragment strikes an elemnt.

Wave length—The length of the shock wave measured at a finite time interval after an explosion at which time the shock wave has propagated a specific distance from the center of the explosion depending upon the explosive quantity involved. A wave length exists for both the positive and negative phases of the shock wave.

Yield line—A series of tension cracks formed by the initiation of yielding in the tensile steel along a line of maximum moment. Positive yield lines are formed at the interior of slabs where positive moments are developed while negative yield lines occur at the supports where negative moments are developed. See *Plastic Hinge*.

Yield Stress—The stress produced in a structural element at which yielding of the material occurs.

INDEX

	Paragraph	Page
Acceleration	6–3*e*, 6–6*g*, 6–6*i*	6–3, 6–5
Acceptor explosive	3–9	3–4
Admixture	7–5*c*	7–2
Ambient pressure	4–5*b*, 4–13*c*	4–2, 4–60
Anchorage, laced elements	9–6*a*(2)	9–6
Angle of incidence	4–6*d*, 4–6*e*	4–3
Angle of obliquity	8–1, 8–2	8–2
Barricade	2–4*c*	2–1
Barrier	2–4*c*, 3–6, 6–2*d*(3)	2–1, 3–2, 6–1
Blast door	10–7	10–8
Blast lock	2–4*b*, 10–7*e*	2–1, 10–8
Blast Mat	7–5*e*(2)	7–3
Blast Pressures	*See* Pressure	
Blast Shield	10–8	10–10
Blast Valve	10–8	10–10
Blast Wave	4–5*a*	4–2
Bond Stress, Flexural & anchorage	5–4	5–8
Bottom-up Period	10–6*c*	10–8
Brittle Mode	3–10, 3–11*d*	3–5
Bundled Bars	9–3*c*	9–1
Burst:		
Air	4–4*a*(1)(*b*), 4–7	4–1, 4–3
Free-air	4–4*a*(1)(*a*), 4–6	4–1, 4–3
Surface	4–4*a*(1)(*c*), 4–8	4–1, 4–7
Capacity Reduction Factor	5–1*g*, 5–3*a*(2)	5–1, 5–2
Charge Reflection Factor	4–8*b*	4–7
Charge Weight:		
Actual	1–5*b*	1–1
Effective	1–5*b*, 4–3*b*, 4–3*c*(1)	1–1, 4–1
Equivalent	4–3*c*(2)	4–1
Composite construction	6–12, 6–13, 7–5*d*, 8–7, 8–8, 9–7	6–21, 6–40, 7–2, 8–3, 9–8
Conservation of energy	6–3*c*	6–3
Construction joint	9–2*d*, 9–9*c*, 9–9*d*	9–1, 9–11
Corner effects	5–10*c*(3)	5–7
Cost effectiveness	10–4, 10–5	10–4, 10–5
Cross sections,		
Reinforced concrete	5–1*a*	5–1
Type I	5–1*b*	5–1
Type II	5–1*c*, 5–1*d*	5–1
Type III	5–1*e*	5–1
Deflagration	4–3*b*(3)	4–1
Deflection:		
Elastic	5–14*a*	5–16
Elasto-Plastic	5–14	5–14
Equivalent Maximum Elastic	5–16	5–19
Large	5–17, 6–9*a*(4)	5–20, 6–10
Limited	5–16, 6–2*d*(1)(*b*), 6–9*c*(5)	5–19, 6–1, 6–10
Maximum	3–11	3–7
Partial Failure	5–12, 6–9*a*(4), 7–5*e*	5–13, 6–10, 7–6
Ultimate	5–12	5–13
Degree of Freedom	6–5*d*	6–4
Degree of Protection	1–2*a*, 6–2*e*	1–1, 6–3
Detonation:		
High-Order	2–2*c*	2–1
Low-Order	2–2*c*	2–1
Simultaneous	10–2*d*	10–1
Delay Path	10–8*i*	10–14
Diagonal Bars	5–3*b*(3), 5–3*b*(4), 9–6*a*(5)	5–2, 9–6
Diagonal Tension	5–3*a*	5–2
Direct Shear	5–3*b*	5–2
Direct Spalling	3–11*d*(2), 7–3	3–7, 7–1
Donor System	2–1, 2–2	2–1
Donor Explosive	3–1	3–1
Door Openings	5–10*d*(3)	5–8
Drag Coefficient	4–14*b*(1), 4–14*c*(4)	4–61, 4–62
Drag Pressure	4–14*b*(1)	4–61
Ductile Mode	3–10, 3–11*b*, 3–11*c*	3–5, 3–6
Ductility Factor	6–2*j*, 6–7*b*, 6–8*b*	6–3, 6–7, 6–7
Duration	4–5*b*, 4–10*a*(10), 4–13*d*, 4–13*e*, 4–14*b*(2)	4–2, 4–9, 4–60, 4–60, 4–61
Dynamic increase factor	5–5*c*	5–3
Dynamic similarity	6–4*c*	6–4
Eardrum rupture	3–7*a*(2)	3–2
Effectiveness mass	6–6	6–4
Elastic Rebound	6–8*c*(4)(*a*)	6–10
Equivalent dynamic system	6–4*b*	6–4
Excess shear stress	5–3*a*(5)(*a*)	5–2
Excess Impulse	7–7*a*	7–4
Expansion Joint	9–9*e*	9–11
Explosion,		
Fully vented	4–10	4–9
Partially confined	4–9	4–9
Partially vented	4–11	4–59
Multiple	4–17, 4–18, 4–19	4–65
Unconfined	4–4*a*(1)	4–1
Explosive Materials	4–3*b*	4–1
Exterior or Leakage Pressure Load	4–4*a*(2)(*a*), 4–10*b*	4–1, 4–59
Flexural Rigidity	5–14*c*	5–16
Fragility Level	3–3*b*(2)	3–4
Fragment Shield	7–5*e*	7–2
Frangible Elements	2–4*c*, 4–9*b*, 4–9*c*	2–1, 4–9

This Document Contains Page/s
Reproduced From
Best Available Copy

	Paragraph	Page
Ground shock:		
Air-induced	10-9b(2)	10-15
Direct-transmitted	10-9b(3)	10-15
Gurney energy constant	4-21a	4-66
Haunch	9-5	9-5
High Explosive	4-3b	4-1
Igloo	2-4c, 4-10b(7)	2-1, 4-59
Impulse, Average	4-10a	4-9
Impulse Capacity	6-14a, 7-8	6-40, 7-6
Impulse Coefficient	6-9c(1), 6-9c(2)	6-11, 6-13
Inhabited Building Distance	10-3b(4)	10-3
Interior or High Pressure Load	4-4a(2)(b)	4-1
Interior or shock front Pressure	4-9a	4-9
Intraline distance	10-3b(1)	10-2
Isolation system	10-10	10-16
Kinetic energy	6-3f, 6-4a	6-4, 6-4
Lacing Reinforcement	3-11b, 5-3a(4), 9-4	3-5, 5-2 9-1
Lightweight Concrete	5-1h	5-1
Line loads	5-10d(3)	5-8
Laod Factor	6-6d	6-4
Load-Mass Factor	6-6c, 6-6i, 6-6j, 6-6k	6-4, 6-5
Loop Bars	9-6c	9-8
Lung Damage	3-7a(2)	3-2
Mach Front	4-7a, 4-7b	4-3, 4-5
Mass Factor	6-6f	6-5
Mode of Vibration	6-6h	6-5
Modular Ratio	5-7c	5-7
Modulus of Elasticity:		
Concrete	5-7a	5-5
Steel	5-7b	5-5
Moment capacity, ultimate static	5-2	5-1
Moment of Inertia:		
Average	5-8b	5-5
Cracked	5-8b	5-5
Gross	5-8b	5-5
Monolithic	9-7a	9-8
Multi-Cubicle Structure	9-8	9-10
Natural period of vibration	6-8c(2)	6-7
Optimum reinforcement ratio	6-9c(3), 7-8j, 10-5m, 10-5n	6-13, 7-7, 10-7, 10-8
Partial Failure	5-9c	5-6
Personnel Protection	6-2d(1)	6-1
Plane Wave	4-12b	4-60
Plane Hinge	5-9b	5-6
Plenum Chamber	10-8b, 10-8e, 10-8j	10-11, 10-13, 10-14
Poisson's ratio	5-14c	5-16
Post-Failure Fragments	3-11d(1), 7-6	3-7
Potential Energy	6-3c	6-3
Pouring sequence, for concrete	9-9b	9-1
Pressure:		
Dynamic	4-13b	4-60
Incident	4-5a	4-2
Maximal effective	3-7a(3)	3-2
Maximum mean	4-11a(2), 4-11a(3), 4-18b	4-59, 4-65
Reflected	4-5c	4-2
Pressure Design Range	3-2a, 6-2g	3-1, 6-3
High	3-2b	3-1
Intermediate	3-2c	3-1
Low	3-2d	3-1
Primary Fragments:		
Largest	4-22c	4-66
Number	4-22b	4-66
Propagation of explosion	1-2b	1-1
Protective Structure	2-1, 2-4	2-1
Protection Category	3-4, 6-2d	3-2, 6-1
Quantity-distance relationship	10-2m	10-2
Rate of Strain	5-5c	5-3
Rattle Space	10-10g	10-16
Receiver System	2-1, 2-3	2-1
Resistance	5-9a	5-6
Elastic	5-13a	5-14
Elasto-plastic	5-13	5-14
Post-ultimate	5-11	5-12
Rebound	6-8c(4)	6-6
Ultimate	5-10	5-6
Resistance Factor	6-6e	6-5
Safety Factor	1-5b	1-1
Scabbing	3-11d(2), 7-4	3-7, 7-2
Separation distance	4-10a(12), 4-10a(13)	4-12 10-14 10-19
Shear stress, ultimate	5-18, 5-19, 5-20, 6-12	5-20, 5-21, 6-21
Shear Key	9-8b	9-10
Shelter	2-4b, 3-5, 6-2d(2)	2-1, 3-2, 6-1
Shock Front	4-3a, 4-5a	4-1, 4-2
Single-degree-of-freedom system	6-5d	6-4
Slump, of Concrete	9-2c	9-1
Spalling	3-11d(1)	3-7
Splices, of Reinforcement:		
Flexural	9-3d, 9-3e	9-1
Lacing	9-4f, 9-4g	9-5
Stiffness		
Elastic	5-14	5-14
Elasto-plastic	5-14	5-14
Equivalent elastic	5-16, 6-8c(2)(c)	5-19, 6-7
Stirrups	5-3a(4)	5-2
Strain Energy	6-3f, 6-4a	6-4
Structural Motions	3-7b, 3-8b	3-3, 3-4
Support Rotation	5-6d	5-4
Time:		
Arrival	4-5b, 4-10a(10)	4-2, 4-9
Clearing	4-14b(1)	4-61
Closure	10-8e	10-13
Response	3-2b, 6-8c(1), 6-9b, 7-8f	3-1, 6-6, 6-10, 7-6
Rise	4-13e	4-60

2

This Document Contains Page/s
Reproduced From
Best Available Copy

	Paragraph	Page
TNT Equivalent	1-5*b*, 4-3*c*	1-1, 4-1
Tramway	10-2*c*, 10-3*a*	10-1, 10-2
Tremies	9-9*d*	9-11
Triple Point	4-7*c*, 9-7d	4-5, 9-8
Velocity:		
Boundary or Minimum	3-9*d*(2), 3-9*d*(4)	3-5
Dilatational	8-4*d*	8-2
Initial	4-20*b*, 4-21*a*	4-66, 4-66
Instantaneous	6-9*a*(2)	6-10
Residual	8-4*e*, 8-8*b*	8-1, 8-3
Shock Front	4-5*a*	4-2
Striking	4-20*c*, 4-24*a*	4-66, 4-67
Wave Length	4-5*e*, 4-14*c*(1)	4-2, 4-62
Yield Line Location Ratio	5-10*c*(13)	5-7

This document contains
blank pages that were
not filmed

This Document Contains Page/s
Reproduced From
Best Available Copy

By Order of the Secretaries of the Army, the Navy, and the Air Force:

W. C. WESTMORELAND,
General, United States Army,
Chief of Staff.

Official:
KENNETH G. WICKHAM,
Major General, United States Army,
The Adjutant General.

W. A. WALLS,
Captain, CEC, United States Navy
Assistant Commander for
Engineering and Design

J. P. McCONNELL, *General, USAF*
Chief of Staff

Official:
JOHN F. RASH, *Colonel, USAF*
Director of Administrative Services

Distribution:
Active Army
USAMC Log Intern Tng Cen
Red River Army Dep (200)
MUCOM
ATTN: AMSMU-SS-SD (100)
AMC Fld Safety Agcy
Charleston IN 47111 (25)
Army Dep (3)
MICOM
ATTN: AMSMI-ON (25)
TECOM
ATTN: AMSTE-AD-S (25)
WECOM
ATTN: AMSWE-SF (10)
HQ USAMC
ATTN: AMCSF-D (165)
NG: State AG (3)
USAR: None
For explanation of abbreviations used, see AR 320-50

Navy:
SNDL Part I (one copy each unless otherwise specified):
21 (CINCPACFLT, CINCLANTFLT only); 24J (Atlantic only); 27G (COMNAVSUPPFORANTARCTICA only); 39B; 39D; 39E; 5CD (COMUSNAVSO only).
SNDL PART II (one copy each unless otherwise specified):
A3; A4A; A6; B1; B2 (JCS, DASA only); B3; B5; C3; E3A; FF1; FF3; FF4; FF7; FA6; FA7 (less Argentia, Bermuda, Iceland, Mayport, Roosevelt Roads, Philadelphia); FA10; FA12; FA18; FA23 (Nantucket, Cape Hatteras, Antigua, Barbados, San Salvador, Eleuthera, Grand Turk only); FB4; FB6; FB7; FB8; FB10; FB13; FB17; FB21; FB29 (Guam only); FB34; FG1; FJ27; FJ28; FJ35; FJ36; FKA1A; FKA1B; FKA1D; FKA1E; FKA1F; FKA6A2; FKA6A3A; FKA6A8; FKA6A9; FKA6A12; FKA6B1; FKA6B2; FKL1; FKM8; FKM9; FKM10; FKN1 (less Atlantic, Western-3 copies each); FKN1 (Atlantic, Western only—5 copies each); FKN2; FKN3; FKN4; FKN5; FKP1A; FKP1B; FKP1E; FKP1J; FKP4D; FKR1A; FKR3A; FKR3C; FKR3H; FKR3J; FT6; V3; V9; V12; V16.
Additional copies may be obtained from:
U.S. Naval Publications and Forms Center, 5801 Tabor Avenue, Philadelphia, Pa. 19120.
Air Force: F.

This document contains blank pages that were not filmed

☆ U.S. GOVERNMENT PRINTING OFFICE: 354-516